

**Faculty of Engineering and Computing
Department of Civil Engineering**

**Characterisations of Base Course Materials
in Western Australia Pavements**

Komsun Siripun

**This thesis is presented for the Degree of
Doctor of Philosophy
of
Curtin University of Technology**

July 2010

DECLARATION

This thesis contains no material which has been accepted for the award of any other degree or diploma in any university.

To the best of my knowledge and belief, this thesis contains no material previously published by any other person except where due acknowledgment has been made.

The following publications have resulted from the work carried out for this degree.

Refereed Journal Papers:

1. Jitsangiam, P., Nikraz, H., **Siripun, K.**, (2009). “Characterization of Cement-Modified Base Course Materials for Western Australia Roads”, Journal of the Southeast Asian Geotechnical Society, accepted (GEJ168).
2. Jitsangiam, P., Nikraz, H., **Siripun, K.**, (2009). “Evaluation of a Stabilized Sand Residue for Use as Roadway Materials”, Journal of the Southeast Asian Geotechnical Society, accepted (GEJ169).
3. Jitsangiam, P., Nikraz, H., **Siripun, K.**, (2009). “Characterization, Analysis and Design of Hydrated Cement Treated Crushed Rock Base as a Road Base Material in Western Australia”, Journal of Civil Engineering and Architecture, accepted (A- -level classified).
4. Jitsangiam, P., Nikraz, H., **Siripun, K.**, (2009). “Construction and Demolition (C&D) Waste as a Road Base Material for Western Australia

Roads”, Australian Geomechanics, Journal of the Australian Geomechanics Society, 44 (3): p. 57-62.

5. **Siripun, K.**, Jitsangiam, P., Nikraz, H., (2009). “Characterization, Analysis and Design of Hydrated Cement Treated Crushed Rock Base as a Road Base Material in Western Australia”, International Journal of Pavement Research and Technology, 2 (6): p. 257-263.
6. **Siripun, K.**, Nikraz, H., Jitsangiam, P., (2009). “Mechanical Behaviour of Hydrated Cement Treated Crushed Rock Base (HCTCRB) Under Repeated Cyclic Loads”, Australian Geomechanics, Journal of the Australian Geomechanics Society, 44 (4): p. 53-64.

Refereed Conference Papers:

1. Jitsangiam, P., Nikraz, H., **Siripun, K.**, (2008). "Construction and demolition (C&D) waste as a highway material" 3rd International Geo-Chiangmai Conference, Chiang Mai, Thailand, 10th-12th December, pp. 179-186.
2. Jitsangiam, P., Nikraz, H., **Siripun, K.**, (2008). “Sustainable use of Residue Sand as Highway Material" 3rd International Geo-Chiangmai Conference, Chiang Mai, Thailand, 10th-12th December, pp. 187-193.
3. Jitsangiam, P., Nikraz, H., and **Siripun, K.**, (2009). “Utilisation of Alumina By-Products as Construction Materials(GEO-05)” 6th Regional Symposium on Infrastructure Development, Bangkok, Thailand, 12th-13th January, CD-ROM.

4. Jitsangiam, P., Nikraz, H., and **Siripun, K.**, (2009). “Characterisation of Cement Treated Crushed Rock for Western Australia Roads (GEO-06)” 6th Regional Symposium on Infrastructure Development, Bangkok, Thailand, 12th-13th January, CD-ROM.
5. Jitsangiam, P., Nikraz, H., and **Siripun, K.**, (2009). “Characterization of Hydrated Cement Treated Crushed Rock Base (HCTCRB) as a Road Base Material in Western Australia” International Conference on 2009 Geohunan : Challenges and Recent Advances in Pavement Technologies and Transportation Geotechnic, Hunan, China, 3rd-9th August.
6. **Siripun, K.**, Nikraz, H., Jitsangiam, P., (2010). “Deformation Behaviour of Unsaturated Soil as Crushed Rock Base (CRB) Layer”, 3rd International Conference on Problematic Soils, 7th-9th April, p.311-318.
7. **Siripun, K.**, Nikraz, H., Jitsangiam, P., (2010). “Permanent deformation evaluation of Unbound Granular Materials (UGMs) layer”, The Seventeenth Southeast Asian Geotechnical Conference, 10th-13th May, CD-ROM.
8. **Siripun, K.**, Nikraz, H., Jitsangiam, P., (2010). “Mechanical Characteristics of Cement Treated Base Course under Repeated Loads”, Twin Int'l Conferences on Geotechnical and Geo-Environmental Engineering, 23th-25th June.
9. **Siripun, K.**, Nikraz, H., Jitsangiam, P., (2010). “Permanent deformation behaviour of Crushed Rock Base (CRB) as Highway Base Course Material”, the 11th International Conference on Asphalt Pavements, Accepted.

10. **Siripun, K.**, Nikraz, H., Jitsangiam, P., (2011). “Failure Criterion of Unsaturated Soil as Crushed Rock Base (CRB) Layer under Dynamic Loads”, The 14th Asian Regional Conference on Soil Mechanics and Geotechnical Engineering, Accepted.

Signature:.....

Date:.....

Characterisations of Base Course Materials in Western Australia Pavements

ABSTRACT

Western Australia (WA) has a road network of approximately 177,700 km, including a 17,800 km stage highway system (Main Roads Western Australia 2009). This infrastructure supports a population of only about two million, and road funds always have to be carefully considered when allocated to highway authorities or other organisations. Pavement design is a process intended to find the most economical combination of suitable materials and layer thicknesses for construction. The pavement must have a carefully-specified unbound granular base to further reduce construction costs, and must be surfaced with an approximately 30 mm asphalt surface in WA. High quality aggregates are therefore required for the base course layer of a pavement because of its proximity to the road surface. Traffic loads on the road surface result in high stress levels on the base course layer. Consequently, Hydrated Cement Treated Crushed Rock Base (HCTCRB) was developed.

Current pavement analysis and design in WA is thought to be sub-standard. A number of highways and roads in WA are exhibiting extensive surface damage as a result of the increasing numbers of vehicles in use. Since pavement analysis and design in WA relies predominantly on empirical design, experience and basic experimentation, explanations for the damage occurring under present conditions are difficult to determine and assess.

In most areas of the USA and Europe, pavement design and analysis has entered a new era with mechanistic design replacing empirical design. Unlike the empirical

approach, a mechanistic approach seeks to explain pavement characteristics under real operational pavement conditions (loads, material properties of the pavement structure, and environments), and is based on design parameters derived from sophisticated tests which can simulate real pavement conditions in the test protocol (WSDOT 2008). The mechanistic approach to pavement design produces more relevant and useful results and these procedures, along with linear elastic analysis, were introduced into Australia by the 1987 NAASRA Guide (NAASRA 1987), of which the revised version became the AUSTROADS Guide (Austroads 2004) to the Structural Design of Road Pavements. AUSTROADS published a National Pavement Research Strategy which has been the keystone for the national co-ordination of pavement research, both within government and industry.

Adaptation of the Cement Modified Crushed Rock Base concept has brought about an excellent road base material for Western Australia (WA) by the addition of a small amount of cement (1-2% by mass) to a fresh crushed rock material. The mix is stockpiled for a hydration period, and after that retreated before construction, unlike the traditional concept for cement modified/stabilised materials. This material is usually called Hydrated Cement Treated Crushed Rock Base (HCTCRB), a name established by Western Australia Mainroads (MRWA). More than 250,000 tonnes of HCTCRB has been used at a cost in excess of \$10 million over the last eight years.

Recently, as a result of early damage on new highways and roads in WA, MRWA and its contractors and organisations have attempted to identify the cause of this damage. HCTCRB, which is currently the best option for base course materials in WA, and Crushed Road Base (CRB), the original road base material, need to be re-examined to overcome the shortcomings in terms of analysis, design, and application. All of the factors involved in HCTCRB and CRB for today's

pavement conditions have been extrapolated far beyond the bounds of the original data, and current experience shows these require detailed re-investigation.

This research aimed to study on the characteristics of CRB and HCTCRB and to determine reliable mathematical material models for the improvement in the current pavement design criteria. This study also investigated both elastic and plastic behaviour of CRB and HCTCRB. In this study, there were two relevant factors of both pavement materials which are considered in order to fulfil a lack of understanding in realistic conditions in pavements of the current pavement design.

1) *The material strength* which indicates the limitation and stability of pavement materials under traffic loads. This study employed the Mohr-Coulomb failure envelope to define the limitation of material implementation and also brought in the resilient modulus of materials to be the significant input parameter for multi-layer finite element analysis to characterise the stress distribution in pavements.

2) *The pavement failure* of long term road performance relating to the design life of pavements. The permanent deformation behaviour and the shakedown concept under various stress conditions, simulated from repeated load triaxial (RLT) tests, therefore, were taken into account to investigate such long-term performance of HCTCRB and CRB and then the implementation of the findings was made to the current pavement analysis and design. Furthermore, more reliable mathematic models of base course materials for short and long term performance during their service life were established based on the laboratory test results of this study.

ACKNOWLEDGEMENTS

This thesis is part of a research project on the characterisations of base course materials in Western Australia pavements. The research has been carried out at Curtin University of Technology. Many individuals and organisations have significantly contributed to the work during the project and although it is not possible to name them all, the contributions of the following individuals should be pointed out.

The most significant persons who have wholeheartedly supported my doctoral thesis are my supervisor, Professor Hamid Nikraz and my co-supervisor, Dr. Peerapong Jitsangiam at Curtin University of Technology. I wish to express my deepest gratitude to them for their generous efforts, helpful advice and comments.

I never thought I would have such enormous and magnificent support from anyone however the way Professor Hamid and Dr. Peerapong guided my work was exemplary. I would like to thank them for progressively building up my self-assurance in the scholarly field, for looking after my family in every way throughout my study and the provision of financial assistance. I also would like to thank them for continuously encouraging me to publish my research in journal and conference papers. This would not have been achieved without their wonderful support and confidence in my ability. I am very proud to be their student and also a member of their fantastic team.

I also wish to thank my undergraduate students for their assistance in performing laboratory experiments as part of their work on their final year projects. Mr. Mark Whittaker for supplying materials, Mr. Kenneth Whitbread for his meticulous proof-reading and other faculty members of the Civil Engineering Department for their excellent collaborative work.

I am also deeply indebted to my parents who taught me the value of hard work and to groups of Thai companions for their assistance to my wife and I for the duration of our time in Perth. I must also say how grateful I am to my wife, Supawadee, for her encouragement, wonderful support and patience.

Finally, I am deeply indebted to all whose direct and indirect support, encouragement and more importantly, understanding and patience, have contributed to my doctoral studies.

TABLE OF CONTENTS

Contents	Page
DECLARATION	ii
ABSTRACT	vi
ACKNOWLEDGEMENTS	ix
TABLE OF CONTENTS	xi
LIST OF FIGURES	xvi
LIST OF TABLES	xxii
LIST OF NOTATIONS	xxiii
1. INTRODUCTION	25
1.1 Objective and scope	25
1.2 Background	26
1.3 Significance	28
1.4 Research approach	28
1.5 Thesis outline	31
2. BACKGROUND AND LITERATURE REVIEW	33
2.1 Definition and function of pavement	33
2.1.1 Pavement material	33
2.1.2 Flexible pavements	34
2.1.3 Rigid pavements	35
2.2 Flexible pavement analysis and design	36
2.2.1 Pavement layers and materials	37
2.2.2 Pavement distress and failure criteria	42
2.2.3 Pavement response models	46

2.2.4 Current methods of pavement analysis and design	47
2.2.5 CIRCLY (MINCAD Systems 2004)	59
2.3 Unbound granular materials (UGMs)	61
2.3.1 Introduction	61
2.3.2 Mineralogy	65
2.3.3 Soil structure	70
2.3.4 Particle size distribution	75
2.3.5 Moisture content	78
2.3.6 Compaction	80
2.3.6 Soil strength improvement	84
2.3.7 Failure criteria and response model	86
2.4 Mechanical behaviours of granular materials under repeated loading	94
2.4.1 Stress-strain behaviour under traffic loads	94
2.4.2 Repeated loading behaviours	101
2.4.2.1 Resilient modulus	102
2.4.2.2 Permanent deformation behaviour	105
2.4.2.3 Factors affecting repeated loading properties	107
2.4.3 The shakedown concept	122
2.4.3.1 Introduction	122
2.4.3.2 Permanent strain under a number of load cycles models	127
3. RESEARCH METHODOLOGY AND EXPERIMENTAL PROGRAM	132
3.1 Overview	132
3.2 Main materials in this study	134
3.2.1 Crushed Rock Base (CRB)	134
3.2.2 Hydrated cemented treated crushed rock base (HCTCRB)	136
3.2.3 Cement	136
3.3 Non-mechanical characterization	137
3.3.1 Particle size distribution	138

3.3.2 Particle shape and surface of CRB and HCTCRB	141
3.3.3 Compaction	143
3.4 Mechanical characterization	145
3.4.1 The California Bearing Ratio (CBR)	146
3.4.2 Static and repeated cyclic triaxial tests	148
3.4.2.1 Specimen preparation	149
3.4.2.2 Static triaxial tests	154
3.4.2.3 The resilient modulus	155
3.4.2.4 Permanent deformation	158
3.4.2.5 The shakedown limit evaluation	160
3.4.2.6 The pavement analysis and design implementation	161
4. RESULTS AND DISCUSSION	162
4.1 Non-mechanical behaviour	162
4.1.1 Particle size distribution	162
4.1.2 Particle shape and surface	166
4.1.3 Compaction	169
4.2 Mechanical behaviour	171
4.2.1 California Bearing Ratio (CBR)	172
4.2.2 Shear strength parameters	173
4.2.3 The resilient modulus	179
4.2.3.1 Resilient modulus results and modelling	181
4.2.3.2 The effects of hydration periods and water content	184
4.2.4 Permanent deformation	191
4.2.4.1 Permanent deformation results and modelling	191
4.2.4.2 The effects of hydration periods and water content	193
4.2.5 Shakedown behaviour	197
4.2.5.1 Range A – Plastic shakedown range	200
4.2.5.2 Range B – Intermediate response – Plastic creep	202

4.2.5.3 Range C – Incremental collapse	205
4.3 Summary	210
4.3.1 Non-mechanical characterisation	210
4.3.2 Mechanical characterisation	211
 5. IMPLEMENTATION OF EMPIRICAL - MECHANISTIC PAVEMENT ANALYSIS AND DESIGN	 215
5.1 Overview	215
5.2 Pavement analysis and design	218
5.3 Pavement structure model	223
5.4 Multi-layer analysis of pavement structure	227
5.4.1 The stress distribution with various asphalt layer thicknesses	232
5.4.2 The stress distribution with various base layer thicknesses	234
5.4.3 The stress distribution with various asphalt layer modulus	235
5.4.4 The stress distribution with various base layer modulus	237
5.5 Response model and criteria of unbound granular material (UGM) layer	238
5.5.1 Ultimate strength failure criteria of UGM layers	239
5.5.2 The resilient modulus model	240
5.5.3 The permanent deformation model	241
5.6 Ultimate strength pavement design	245
5.6.1 Thickness and performance evaluation	246
5.6.1.1 Bearing capacity estimation and pavement thickness design	247
5.6.1.2 Multi-layer strength and performance evaluation	250
5.6.1.3 The acceptable plastic strain of the unbound granular material (UGM) base layer	251
5.7 Conclusion and discussion	253
 6. CONCLUSIONS AND RECOMMENDATIONS	 256

6.1 Conclusions	256
6.1.1 CRB and HCTCRB characterisations	256
6.1.2 Pavement analysis and design for CRB and HCTCRB	259
6.2 Recommendations for future study	261
REFERENCES	263
APPENDIX: MATERIAL RESULTS AND ANALYSIS	274

LIST OF FIGURES

Figure No.	Title	Page
Figure 1.1	Diagram of Research Approach	29
Figure 2.1	Schematic of a flexible pavement structure (FHWA 2004)	35
Figure 2.2	Stress distribution of flexible pavement layers (Hirsigner 2005)	35
Figure 2.3	Schematic of a rigid pavement structure (FHWA 2004)	36
Figure 2.4	Concept of load spreading and the ideal pavement	37
Figure 2.5	Components of flexible pavement structures	38
Figure 2.6	The possibility range for the various types of flexible pavements	40
Figure 2.7	Illustration of fatigue cracking	43
Figure 2.8	Illustration of the development of permanent deformation	44
Figure 2.9	Design chart for granular pavements (Austroads 2004)	50
Figure 2.10	Strains induced in a layer pavement system (Austroads 2004)	53
Figure 2.11	Mechanistic design framework and component (Cement Association of Canada 2005)	55
Figure 2.12	The tetrahedral skeleton of silicate minerals (David Barthelmy 2009)	67
Figure 2.13	Soil structure	72
Figure 2.14	The three-phase soil system	73
Figure 2.15	Three physical states of soil-aggregate mixtures	77
Figure 2.16	Crushed rock gradation	78
Figure 2.17	CRB and HCTCRB compaction curve	82
Figure 2.18	The Mohr-Coulomb failure envelope	90
Figure 2.19	The p-q diagram of HCTCRB and CRB	93
Figure 2.20	Stress components acting on an element (Lekarp 97)	94
Figure 2.21	Stresses under a rolling wheel load (Lekarp and Dawson 1998)	95
Figure 2.22	Stresses in motion of a rolling wheel load	

(Lekarp and Dawson 1998)	96
Figure 2.23 The stress-strain behaviour of UGMs (Lekarp and Dawson 1998)	97
Figure 2.24 A hysteresis loop for viscous-elastic permanent behaviour	97
Figure 2.25 The stress-strain behaviour of unbound material under repeated loading (Dawson A R and F 1999)	98
Figure 2.26 The dependence between the contact force F and displacement d between two particles (Kolisoja 1997)	99
Figure 2.27 Basic strains in granular materials during each load cycle	102
Figure 2.28 The effect of density on permanent strain (Barksdale and Itani 1989)	109
Figure 2.29 The effect of grading and compaction on plastic strain (Barksdale and Itani 1989)	110
Figure 2.30 The effect of grain size distribution on the aggregate's susceptibility to permanent deformations (Kolisoja 1997)	112
Figure 2.31 Influence of drainage on permanent deformation development (Dawson A R and F 1999)	114
Figure 2.32 Triaxial test results with CCP and VCP (Allen 1973)	117
Figure 2.33 The effect of stress history on permanent strain (Brown and Hyde 1975)	120
Figure 2.34 An example of the effect of the number of load repetitions on the permanent axial strain of a RLT test specimen (Kolisoja 1997)	122
Figure 2.35 Elastic/permanent behaviour under repeated cyclic pressure and tensile load (Johnson 1996)	125
Figure 2.36 Permanent deformation behaviour at low stress levels (stable conditions)	125
Figure 2.37 Permanent deformation behaviour at high stress levels (unstable conditions)	126
Figure 3.1 The overall research diagram of the study	133
Figure 3.2 The CRB sample used in this study	135

Figure 3.3 Particle sieves and a sieve shaker machine	141
Figure 3.4 The scanning electron microscope used in this study	143
Figure 3.5 The compaction equipment	144
Figure 3.6 The soaked CBR and HCTCRB setup in the soaking container	147
Figure 3.7 The penetration stage of CBR and HCTCRB tests setup	147
Figure 3.8 The triaxial test machine used in this study	149
Figure 3.9 All mixtures in the mixing machine	150
Figure 3.10 Crushed rock after mixing with cement	151
Figure 3.11 HCTCRB hydration in a plastic bag for 7 days	151
Figure 3.12 The HCTCRB remixed after a 7-day hydration process	152
Figure 3.13 Testing material and compaction equipment	152
Figure 3.14 CRB after compaction	153
Figure 3.15 A wrapped mould of HCTCRB after compaction	153
Figure 3.16 Testing sample setup before triaxial testing	154
Figure 3.17 Illustration of the vertical force waveform	157
Figure 3.18 Permanent deformation testing setup	157
Figure 3.19 The vertical loading waveform	161
Figure 4.1 Gradation of CRB and HCTCRB with uncompacted conditions	163
Figure 4.2 CRB's gradation under compacted and uncompacted conditions	164
Figure 4.3 HCTCRB's gradation under compacted and uncompacted conditions	164
Figure 4.4 HCTCRB's uncompacted gradation for various hydration periods	165
Figure 4.5 HCTCRB's compacted gradation with various hydration periods	165
Figure 4.6 Surface of CRB	166
Figure 4.7 The surface of HCTCRB uncompacted	167
Figure 4.8 The surface of HCTCRB 7 day compacted	167
Figure 4.9 Spectrum of CRB	168
Figure 4.10 Spectrum of HCTCRB	169
Figure 4.11 Compaction test results of CRB and HCTCRB	170

Figure 4.12 Compaction curves of HCRCRB over various hydration periods	171
Figure 4.13 CBR results of CRB and HCTCRB	172
Figure 4.14 The stress-strain relations of CRB	175
Figure 4.15 The stress-strain relations of HCTCRB	176
Figure 4.16 CRB Mohr's circles and the Mohr-Coulomb failure envelope	177
Figure 4.17 HCTCRB Mohr's circles and the Mohr-Coulomb failure envelope	178
Figure 4.18 p-q diagrams of CRB and HCTCRB	178
Figure 4.19 Applied stress conditions of resilient modulus tests following Austroads-APRG 00/33 standard in the p-q diagram	180
Figure 4.20 Resilient modulus results of CRB and HCTCRB	182
Figure 4.21 The CRB and HCTCRB resilient modulus models and the measurements	183
Figure 4.22 The resilient modulus of CRB at various moisture contents	185
Figure 4.23 The resilient modulus at 100%OMC over various hydration Periods	187
Figure 4.24 The resilient modulus at 90%OMC for various hydration Periods	187
Figure 4.25 The resilient modulus at 80%OMC for various hydration Periods	188
Figure 4.26 The resilient modulus results of HCTCRB type A (no additional water)	189
Figure 4.27 The resilient modulus results of HCTCRB type B (8% additional water)	190
Figure 4.28 The resilient modulus results of HCTCRB type C (%OMC additional water)	190
Figure 4.29 CRB permanent deformation predictions	192
Figure 4.30 HCTCRB permanent deformation predictions	193
Figure 4.31 CRB permanent deformations with various %OMC	194
Figure 4.32 Comparison of permanent deformations between	

CRB and HCTCRB	194
Figure 4.33 Permanent deformations of HCTCRB type A (no additional water)	196
Figure 4.34 Permanent deformations of HCTCRB type B (8% additional water)	196
Figure 4.35 Permanent deformations of HCTCRB type C (%OMC additional water)	197
Figure 4.36 CRB vertical permanent deformations versus number of load cycles	198
Figure 4.37 HCTCRB permanent deformations versus number of load cycles (N)	198
Figure 4.38 CRB vertical permanent strain rate versus vertical permanent strain	199
Figure 4.39 HCTCRB permanent strain rate versus vertical permanent strain	199
Figure 4.40 CRB Range A vertical permanent strains versus number of load cycles compared with the strain model	201
Figure 4.41 HCTCRB Ranges A and B vertical permanent strain compared with the strain model	202
Figure 4.42 CRB vertical permanent strain rate versus number of load cycles	204
Figure 4.43 CRB Range B vertical permanent strain versus number of load cycles compared with the model	204
Figure 4.44 Vertical permanent strain rates versus number of load cycles	206
Figure 4.45 CRB Range C vertical permanent strain versus number of load cycles compared with the strain model	206
Figure 4.46 HCTCRB Range C vertical permanent strain compared with the strain model	207
Figure 5.1 Pavement design diagram for CRB and HCTCRB as a base layer	217
Figure 5.2 Data input for CIRCLY	222

Figure 5.3 Standard pavement diagram	225
Figure 5.4 Finite element diagram of pavement	225
Figure 5.5 Stress distribution under low loading traffic	228
Figure 5.6 Stress distribution under high loading traffic	228
Figure 5.7 Vertical stress distribution of pavement structure	229
Figure 5.8 Horizontal stress of pavement structure	230
Figure 5.9 Shear stress of pavement structure	230
Figure 5.10 Maximum principal stress of pavement structure	231
Figure 5.11 Asphalt layer stress versus asphalt layer thickness	233
Figure 5.12 Base layer stress versus asphalt layer thickness	233
Figure 5.13 Asphalt layer stress versus base layer thickness	234
Figure 5.14 Base layer stress versus base layer thickness	235
Figure 5.15 Asphalt layer stress versus asphalt layer modulus	236
Figure 5.16 Base layer stress versus asphalt layer modulus	236
Figure 5.17 Asphalt layer stress versus base layer modulus	237
Figure 5.18 Base layer stress versus base layer modulus	238
Figure 5.19 Static failure criteria of CRB and HCTCRB compared with finite element analysis	240
Figure 5.20 The resilient modulus predictions	241
Figure 5.21 CRB permanent deformation predictions	242
Figure 5.22 HCTCRB permanent deformation predictions	242
Figure 5.23 Ranges A, B and C of CRB	243
Figure 5.24 Ranges A, B and C of HCTCRB	244
Figure 5.25 Number of traffic compared with plastic strain	245
Figure 5.26 Ultimate strength design method	246
Figure 5.27 Bearing estimation of unbound granular subgrade	249

LIST OF TABLES

Table No.	Title	Page
Table 2.1	Pavement material categories and characteristics (Austroad, 1992)	41
Table 2.2	The main minerals of soil	66
Table 2.3	Typical states of soil-aggregates	76
Table 3.1	Characterisation tests (Main Roads Western Australia 2007)	135
Table 3.2	General specifications of the cement (COCKBURN CEMENT 2006)	137
Table 3.3	HCTCRB classification	144
Table 3.4	Stress levels following Austroad-APRG 00/33 standard	158
Table 3.5	Stress levels for permanent deformation of base materials following Austroad-APRG 00/33 standard	159
Table 4.1	California Bearing Ratio (CBR) results and specifications	173
Table 4.2	Peak deviator stresses and confining pressures from static triaxial tests	175
Table 4.3	Shear strength parameters (c and ϕ) for CRB and HCTCRB using the results of static triaxial shear tests	177
Table 4.4	Resilient modulus models for CRB and HCTCRB	184
Table 4.5	Model coefficients for Range A	201
Table 4.6	Model coefficients for Range B	203
Table 4.7	Summary of non-mechanical test results of CRB and HCTCRB	214
Table 5.1	Pavement material parameters	226
Table 5.2	The meaning of notation	232
Table 5.3	Bearing capacity based on CBR test results	250
Table 5.4	Pavement layer analysis	252

LIST OF NOTATIONS

e	=	Void ratio
k	=	A factor used in the calculation of N ($k=280$ for $E=2000$ MPa; $k=200$ for $E=5000$ MPa; $k=150$ for $E=10000$ MPa)
m	=	Moisture content (%)
ν	=	Poisson's ratio
A_v	=	Air void (%)
C_c	=	Coefficient of curvature
C_u	=	Coefficient of uniformity
CBR	=	California bearing ratio
CH	=	refer to unified soil classification chart of Unified Soil Classification
CL	=	refer to unified soil classification chart of Unified Soil Classification
CGF	=	Cumulative growth factor
D_{10}	=	Particle size at 10% passing
D_{30}	=	Particle size at 30% passing
D_{60}	=	Particle size at 60% passing
G_s	=	Specific gravity
H_v	=	Heavy vehicle (%)
MDD	=	Maximum dry density
M_r	=	Resilient modulus
OMC	=	Optimum moisture content
SiO_2	=	Silica oxide
TiO_2	=	Titanium oxide
V	=	Total soil volume (solid, water and air voids)

V_a	=	Volume of air void
V_B	=	percentage by volume of bitumen in the asphalt
V_s	=	Volume of solid
V_w	=	Volume of water
γ_d	=	Dry density
γ_w	=	Density of water at room temperature
ρ_w	=	Water density
ρ_s	=	Solid density
σ_1	=	Normal stress
σ_3	=	Confining stress
SEM	=	Scanning electron microscope

CHAPTER 1

INTRODUCTION

1.1 Objective and scope

The objectives of this research are to report non-mechanical and mechanical aspects of Crushed Rock Base (CRB) and Hydrated Cement Treated Crushed Rock Base (HCTCRB) as a base course material in Western Australia. In particular, this research aims to:

- i) Study the non-mechanical and index aspects of CRB and HCTCRB in order to explain the mechanical, chemical and environmental effects on basecourse layers;
- ii) Report on mechanical material responses and models (bearing capacity, shear strength, resilient and permanent deformation) of CRB and HCTCRB under different conditions in order to improve the current pavement analysis and design;
- iii) Compare the specific non-mechanical and mechanical characteristics of virgin material (CRB) and modified material (HCTCRB) under various conditions in order to clarify the understanding of HCTCRB;
- iv) Study the limits of allowable working criteria of CRB and HCTCRB under both static and cyclic loads in terms of various stress levels and environmental conditions based on laboratory test results; and

v) Study stress-strain distribution of selected pavement structure using the multi-layer finite element analysis with the material models of CRB and HCTCRB to be considerable criteria for an implementation of the current pavement analysis and design.

1.2 Background

Flexible pavements composed of unbound granular materials (UGMs) as a base course layer with thin bituminous surfacings are widely used in Western Australian pavements and other states. The principle function of base course layers in a flexible pavement is to transfer and reduce the stresses and strains induced by wheel loading to underneath layers without unacceptable damage of in-situ soils (subgrade).

In Western Australia, Crushed Rock Base (CRB) and Hydrated Cement Treated Crushed Rock Base (HCTCRB) are the commonly used as base course materials. Understanding the actual behaviour of both materials under traffic loads is very important in the advanced pavement analysis and design and is more significant in the development of novel pavement engineering knowledge than the conventional approach. Conventional pavement design procedure relies on experience and the results of simple tests such as the California Bearing Ratio (CBR) and material index properties. Such results cannot embrace the consideration of materials in multidimensional geometry, realistic behaviour, and distribution of displacements during cyclic loading, stress and strain in multilayered pavement design. Consequently, the use of empirical approaches seems to be far behind the realistic conditions of pavements today.

The performance of a base course material is strongly dependent upon its strength and deformation while subjected to traffic loads. A large deformation of a base course layer causes rutting on a bituminous surface. Thus, in practice, pavement construction is designed to provide sufficient depths over the sub layer so that shear failures and excessive permanent deformation would not take place in each layer.

The shakedown concept is the theoretical approach in explaining the unbound granular materials (UGMs) permanent deformation characteristics under repeated cyclic load conditions. For the original concept of the shakedown concept, there are four ranges of a material response under repeated loading.

- Purely elastic for low loading levels, in which no permanent strain accumulation occurs;
- Elastic shakedown. The applied stress is slightly below the plastic shakedown limit. The material exhibits a plastic response for a finite number of cycles, although the ultimate response is in an elastic regime;
- Plastic shakedown. The applied stress is in the level at avoiding a rapid incremental collapse. The material achieves a long-term steady state response with no accumulation of plastic strains, but hysteresis in the stress-strain plot; and
- Incremental collapse. The repeated stress is relatively large, therefore the plastic strain accumulates rapidly with failure occurring in the relatively short-term.

The original use of the shakedown concept in pavement design was first introduced by Sharp and Booker (1984) and Sharp (1983). They justify the

application of the shakedown concept from the results of the AASHTO road tests (Kent 1962) when in some cases, distress was reported to stabilise after a finite number of load applications. More recently, studies have been made to obtain upper-bound (Collins and Boulbibane 1998) and lower-bound (Yu and Hossain 1998) solutions for the shakedown load capacity of simple pavement structures.

1.3 Significance

The result of our work will then specifically yield:

- a new understanding of the behaviour of CRB and HCTCRB under real traffic load conditions based on mechanistic characterisation and the shakedown concept that will not only determine the proper capacity of their uses, but will also contribute to a complete understanding of how to fit both materials into a new analysis and design approach;
- specific response models and distress models for CRB and HCTCRB for particular use in mechanistic-empirical design.

When the results are applied, they will:

- improve pavement analysis and design methods for Western Australia;
- improve highway and road construction methods relating to CRB and HCTCRB;
- improve the quality of highways and roads in service for Western Australia.

1.4 Research approach

To achieve the objectives of this research, the study was carried out using the methodology shown in Figure 1.1.

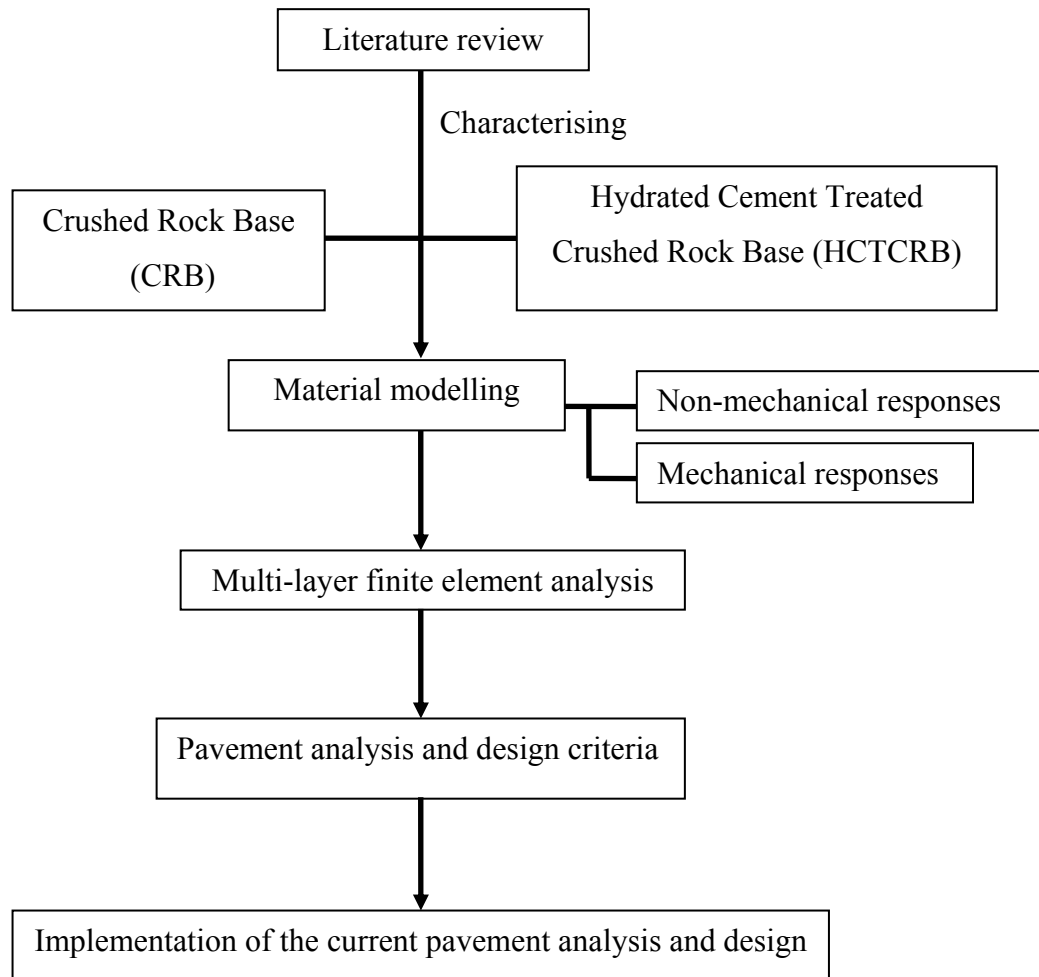


Figure 1.1 : Diagram of Research Approach

Literature review

For the first stage of the research, a detailed review of the literature relevant to comprehensive characteristics of CRB and HCTCRB, including the study of shakedown concept and the current pavement analysis and design, was carried out in order to assess the current stage of knowledge available.

The characterisation of Crushed Rock Base (CRB) and Hydrated Cement Treated Crushed Rock Base (HCTCRB)

In the second stage, both elasticity and plasticity of CRB and HCTCRB were investigated with respect to non-mechanical and mechanical properties such as index properties, shear strength parameters, resilient and permanent deformation under various load and environmental conditions.

Material modelling

The third stage was to analyse all laboratory test results and determine suitable material models using existing concepts. The limit use and response models of CRB and HCTCRB were defined based on sophisticated test results under various selected conditions.

Multi-layer finite element analysis

The fourth stage was to employ the finite element method analysing multi-layer pavement structure using input parameters from laboratory test results. Stress-strain distributions of selected pavement structure configurations were studied and more details in Chapter 5.

Pavement analysis and design criteria

The fifth stage was to combine the stress-strain distribution of the selected pavement structure based on the finite element method with material models to

determine the appropriated criteria of CRB and HCTCRB as basecourse materials. Bearing capacity and shear strength parameter were used to define suitable pavement layer thickness and material limit use for short term performance. For long term performance, the permanent deformation and the shakedown concept are employed to predict the number of vehicles during the service life.

Implementation of the current pavement analysis and design

The last stage was to introduce the pavement model and criteria with the multi-layer finite element method of CRB and HCTCRB as a mechanistic approach for Western Australia based on the laboratory test results.

1.5 Thesis outline

This thesis has six chapters, including an introduction.

Chapter 1 consists of an introduction into the entire research study and highlights the objective, scope, methodology and organisation of the study.

Chapter 2 reviews the pavement materials and theoretical concepts used in this study. The physical, chemical, and mechanical characteristics of CRB and HCTCRB in terms of unbound granular material are described. An overview of the fundamental knowledge of the road base analysis and design which are suggested to be used are presented.

Chapter 3 introduces the experimental program in which the test materials, test methods, and the procedures are described.

Chapter 4 discusses and summarises the results of all tests conducted in the research, including basecourse characterisation, analysis, and design criteria for CRB and HCTCRB.

Chapter 5 implements the results of this study to the empirical-mechanistic application of the design and construction of road bases. Design and construction aspects with relevant comments on those structures are introduced.

Chapter 6 presents the conclusion drawn from this study in conjunction with the recommendation for further research.

CHAPTER 2

BACKGROUND AND LITERATURE REVIEW

2.1 Definition and function of pavement

2.1.1 Pavement material

The vital objectives of pavement material layers are to resist the anticipated traffic capacity with convenient services for road users. These facilitations reduce to suitably low mechanical applications as no outcome in excessive deterioration and settlement of themselves and the foundation layer. Other qualities of the pavement materials are that they should also be able to endure environmental effects such as moisture, frost, and temperature.

Natural soil is usually not strong enough to carry repeated application of traffic loads without significant deterioration, hence a particular structure above the natural subgrade to improve the strength of the in-situ condition. This is called a pavement and is usually multi-layered. Traditionally pavements have been classified in the past as flexible and rigid. A flexible pavement consists of compacted granular material below a bituminous surfacing and the latter uses a concrete slab laid either directly on the in-situ soil or on a shallow granular base. However, the use of these terms is now rather confusing since there is a rising use of stiff cemented or bituminous bases which replace crushed rock bases in flexible pavements.

Supplies for the pavement are local sources to avoid high effective cost and if these are not suitably strong, they should be modified or stabilised through natural

granular material or treated with cement, fly ash, lime or any chemical additions. Multiple layers may be utilised for economic purposes whereby a cheaper, weaker material is used for the majority of the base courses, with an overlaying stronger layer. As stated, the two regular pavement categories are flexible and rigid pavements. Flexible pavement differs in terms of the pavement structure in the use of asphaltic surfacing materials for a flexible road and reinforced concrete for a rigid road. All load resistance of a rigid pavement derived from only the stiff surface other than the flexible system will contribute with composite layers. In the flexible pavement, the base layer underneath the surface is usually natural, modified or recycled materials. They should be inexpensive and have a fine adequate potency and stiffness for distributing the applied traffic loads in an acceptable magnitude to the subgrade layer (in-situ or modified soils) so the concentrated traffic load will not damage the subgrade during service life.

2.1.2 Flexible pavements

There are normally two materials below the asphaltic surface system that comprise the road base, natural granular materials and modified materials. Diverse materials are employed for technical, environmental or economic purposes. These layers always deform under traffic loads and distribute stress to the top of in-situ layers. With most flexible pavements, the quality and thickness of each layer is different from the other layers within the pavement. Generally, it can be noted that the thickness is inversely proportional to the quality, therefore for the layers closer to the surface, the quality of the soil increases to better withstand traffic loads. Figures 2.1 and 2.2 illustrates the regular diagram and the stress distribution of the flexible pavement system, respectively.

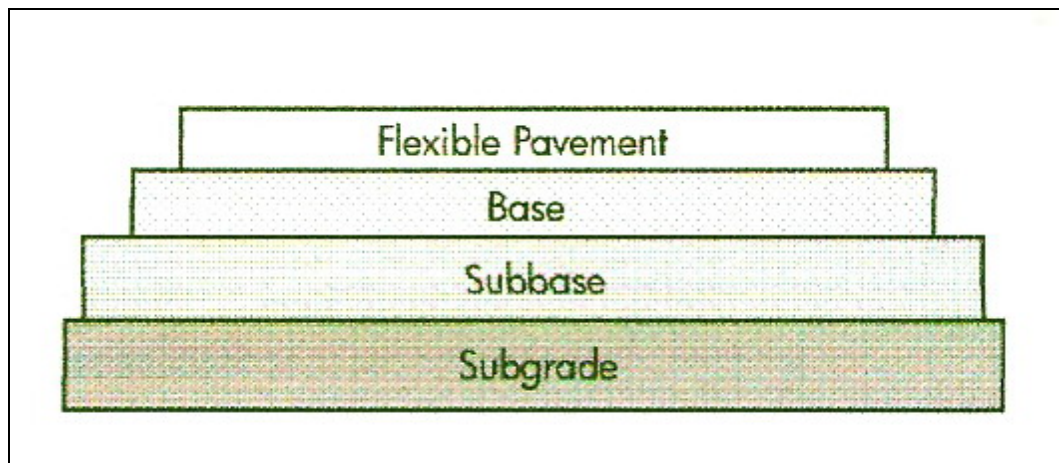


Figure 2.1 Schematic of a flexible pavement structure (FHWA 2004)

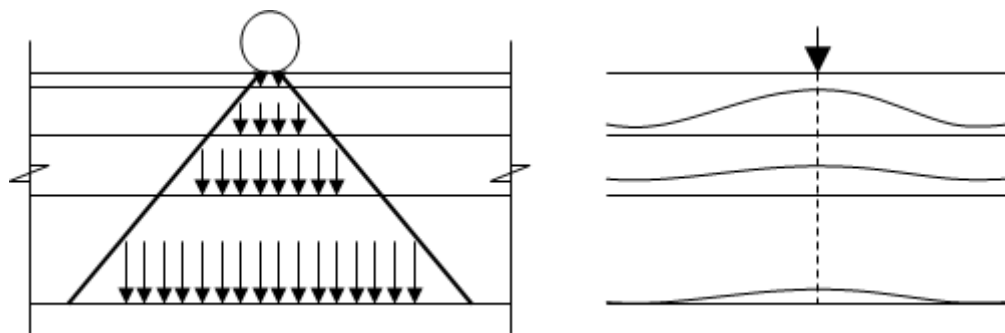


Figure 2.2 Stress distribution of flexible pavement layers (Hirsinger 2005)

2.1.3 Rigid pavements

In contrast to flexible pavements, rigid pavements are typically placed on a single layer of natural granular or stabilised road base material as shown in Figure 2.3. As there is one layer under the surface and over the subgrade, it can be called either a base or a subbase. The assortment of a stabilised base course or a granular base course depends on the traffic load and subgrade characterisation. Rigid pavements are able to resist a large number of very heavy wheel loads and cement-treated, asphalt-treated, or a pozzolanic stabilised mixture (PSM) base are

used. Granular materials, however, may erode when heavy traffic induces pumping in wet climates (FHWA 2004).

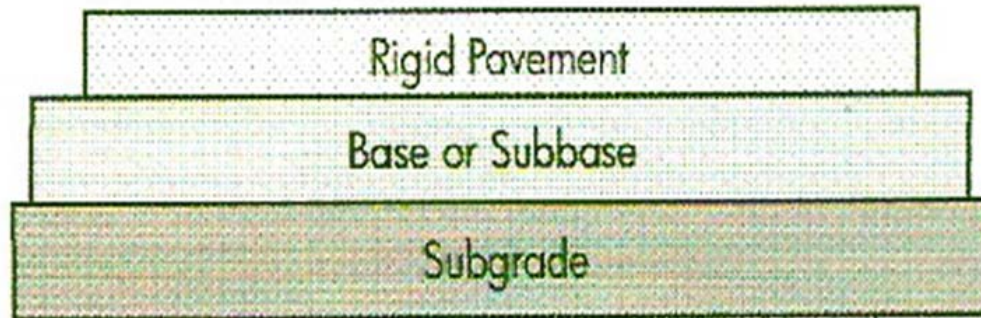


Figure 2.3 Schematic of a rigid pavement structure (FHWA 2004)

2.2 Flexible pavement analysis and design

It should be noted at this point that as almost all Western Australian pavements are flexible with thin bituminous surfacing, this thesis focuses on this section of pavement. Asphalt pavements may hold stiffness as firm as Portland cement concrete pavements, when relatively thick asphaltic concrete surface layers are used at specific temperatures. It should be obvious that the definitions of flexible and rigid are arbitrary and were established in an attempt to distinguish between asphalt and Portland cement concrete pavements. A main function of the pavement is to distribute the wheel loads over an area of subgrade much larger than the contact area of the tyre with the pavement and thus reduce the maximum subgrade stress to a level which the soil can tolerate without unacceptable deformation during the life of the pavement. This is demonstrated in Figure 2.4.

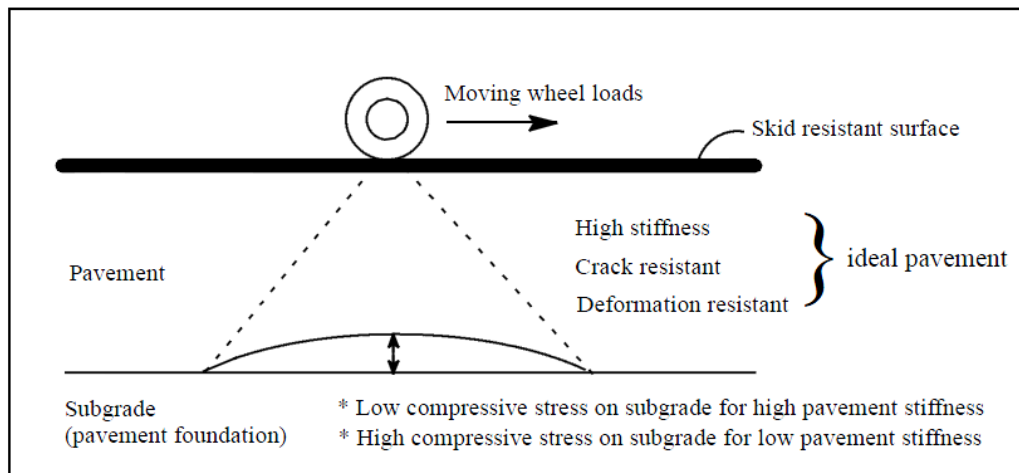


Figure 2.4 Concept of load spreading and the ideal pavement

In summary, the basic principles of pavement design are to provide a structural layer or layers with sufficient stiffness and thickness to protect the subgrade, while ensuring that the layer itself does not crack or deform plastically during the design life (Brown and Selig, 1991). Pavements are usually designed for 20 years or longer and over this period, they may be subjected to millions of load repetitions.

2.2.1 Pavement layers and materials

Current flexible pavements usually consist of three major layers, bituminous surfacing, base and subbase. The soil foundation for flexible pavements is termed the subgrade and the surface of which is generally referred to as the design subgrade level as shown Figure 2.5.

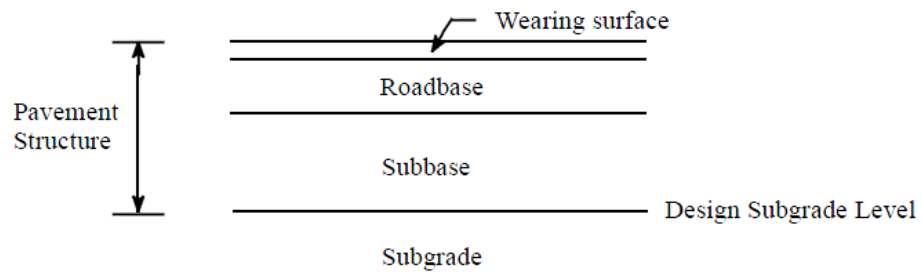


Figure 2.5 Components of flexible pavement structures

In general, the unit cost of materials increases from the bottom to the top of the pavement layers and the design of a pavement structure entails the selection of the most economical combination of pavement layers, with respect to both thicknesses and material types (Croney, 1977).

The surface course is purposely designed to withstand cyclic traffic loads as well as providing a protective seal against excess water penetrating the lower courses from above (Wright 1996) and to provide a safe and smooth riding surface. The surface must also possess skid resistance in wet weather and usually consists of multiple bituminous layers either spray sealed or of an asphalt consistency. The wearing surface can range from 25 mm of bitumen for low-volume traffic areas to 150 mm in thickness or more or asphalt concrete for high-volume traffic areas. However, if the pavement is for rural low-volume use, it may be unsealed with the top surface coat forming part of the base course.

The base course is located next to the surface and provides most of the load carrying capabilities of the pavement. Its principle purpose is to supply sufficient wrap to limit the stresses and strains of wheel loading so that unacceptable failure and deformation do not take place. It can be composed of one or more types of

materials, natural gravel, fine crushed rock, broken stone and modified soil (Nikraz 2004). A base course is defined as the layer of material that lies immediately below the wearing surface of a pavement, and the subbase is a layer of material between the base and subgrade. The roadbase is the main structural layer for distributing traffic loads so that the stresses and strains developed by them in the subgrade and the sub-base are within the capacity of the materials in these layers. It may be constructed of stone fragments, slag, soil-aggregate mixtures, cement-treated granular materials or bituminous-aggregate mixtures of several types. The subbase is also a load-distributing layer but is of weaker material than the roadbase. It provides a suitable work platform for construction operations above as well as to permit the building of relatively thick pavements at low cost. Subbases may consist of selected materials, such as natural gravels and can be lower quality material as long as the thickness design criteria are fulfilled. To ensure a satisfactory design, the thickness of base and subbase should be sufficient to prevent overstressing to the subgrade. In most flexible pavement structures, the stiffness of each layer is greater than the layer below and smaller than the layer above. Layers consisting of some types of cementitious roadbase materials may be exceptions to this general rule. The overall thickness of the pavement, as well as the individual layers, depends on the traffic it is carrying, the climate, the quality of the subgrade, and the mechanical properties of the materials in the pavement layers. In summary, base courses and subbases are used under flexible pavements to provide a stress-distributing medium which will spread the load applied at the surface. This is the prime requirement of the base course, although it may also provide drainage and give added protection against frost action when necessary.

The subgrade is commonly the foundation of the existing natural earth but it may also be composed of selected compacted fill placed during earthwork operations

(Nikraz 2004). If the subgrade contains unsuitable characteristics, it may be stabilised to improve properties. Conversely when this does occur, the section of stabilised sub-grade is generally considered a lower sub-base section, hence part of the pavement and not part of the subgrade (Nikraz 2004).

The pavement foundation has two roles. It must, firstly, provide a short-term pavement to carry construction traffic and provide an adequate platform for the construction. Subsequently, it must perform in the longer term as a support system to the completed pavement for the required design life (Brown and Selig, 1991).

<div style="text-align: center;"> <hr/> Granular <hr/> Natural Soil </div> <p style="text-align: center;">(a) Gravel road</p>	<div style="text-align: center;"> <hr/> Bitumen seal <hr/> Granular <hr/> Natural Soil </div> <p style="text-align: center;">(b) Sealed granular road</p>
<div style="text-align: center;"> <hr/> Asphaltic <hr/> Granular <hr/> Natural Soil </div> <p style="text-align: center;">(c) Asphalt pavement</p>	<div style="text-align: center;"> <hr/> Asphaltic <hr/> Cement treated <hr/> Granular <hr/> Natural Soil </div> <p style="text-align: center;">(d) Composite pavement</p>

Figure 2.6 The possibility range for the various types of flexible pavements

These range from low-volume unsurfaced roads through to heavy-duty asphalt pavements for highways and airports. The feature common to all is one or more granular layers placed on the soil foundation. These layers embrace materials whose engineering properties are the most complex and variable.

Characteristics	Unbound Granular	Cemented	Asphalt
Material Type	Crushed rock Gravel Soil aggregate Mechanically stabilised materials Chemically modified materials	Lime stabilised materials Cement stabilised materials Lime/flyash stabilised materials Slag stabilised materials	Asphalt Asphalt Concrete
Behaviour Characteristics	Development of shear strength through particle interlock. No significant tensile strength.	Development of shear strength through particle interlock and chemical bonding. Significant tensile strength.	Development of shear strength through particle interlock and cohesion. Significant tensile strength. Properties are temperature sensitive.
Distress Modes	Deformation through shear and densification Disintegration through breakdown.	Cracking developed through shrinkage, fatigue and overstressing. Erosion and pumping in the presence of moisture	Cracking developed through fatigue, overloading. Permanent deformation

Table 2.1 Pavement material categories and characteristics (Austroad, 1992)

As can be seen from Figure 2.6, flexible pavement materials can be essentially classified into three main categories according to their fundamental behaviour under the applied loadings. They are: (a) Unbound granular materials; (b) Cemented materials; and (c) Asphalt. These pavement material categories and their characteristics are summarized in Table 2.1. In general it can be observed that the quality of the materials decreases with depth.

2.2.2 Pavement distress and failure criteria

It is essential to comprehend the types of pavement distress as to ascertain whether typical types of pavement distress are progressive, leading to the eventual deterioration of the road, or are non progressive. Distinction will be made here between two different major types of failure. The first, structural failure includes a collapse of the pavement structure or a breakdown of one or more of the pavement components to make the pavement incapable of sustaining the loads imposed upon its surface. The second, classified as functional failure which may or may not be accompanied by structural failure, occurs due to its roughness causing discomfort to passengers (Yorder and Witczak, 1975). Since pavement damage generally results from the accumulation of very small irreversible deformations for each load cycle, the word failure in pavement engineering seems to be inadequate. Instead, the term well-designed pavement will fail at the end of its design life becomes more acceptable. A road pavement suffers progressive structural deterioration from the day it is opened to traffic.

The objective of engineering design is to ensure that a degree of deterioration necessitating reconstruction or major structural repair is reached only towards the end of the design life which has been selected for the pavement. Roads very seldom become redundant. Engineers normally carry out structural repairs or provide an overlay to extend the life beyond that envisaged in the original design, before the terminal condition is reached. In view of this, the engineer who is responsible for maintaining the road needs a method of judging how far the pavement has progressed towards the failure condition. In general, a performance criterion is usually set for this purpose. Structural deterioration manifests itself in terms of deformation and cracking, thus the failure criteria are best expressed in terms of these two factors. The main features of pavement distress are cracking

and permanent deformation resulting from the repeated application of traffic loads. Deformation and cracking induced by traffic loading are the criteria most commonly used for assessing the state of serviceability of a pavement and hence for deciding when maintenance is necessary.

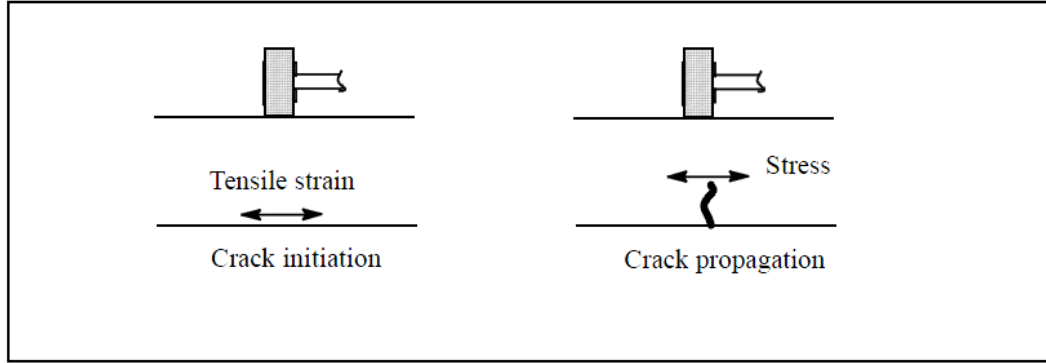


Figure 2.7 Illustration of fatigue cracking

Surface cracking unaccompanied by any deformation in the pavement structure is attributed to fatigue failure in the bituminous layers and is said to be the most common mode of distress in flexible pavements (Monismith, 1973). Investigations of such phenomena in flexible pavements have shown that strain is a good indicator of fatigue performance. Fatigue manifests itself as cracking of the surfacing layer. It has been found that cracking is commonly the result of repeated horizontal tensile strains at the bottom of the stiffer surfaces or cemented layers as shown in Figure 2.7. The relationship between the number of load applications (N) causing the initiation of cracking and the tensile strain ϵ is:

$$N = C \cdot \left(\frac{1}{\epsilon} \right)^m \quad (2.1)$$

where: C and m are constants whose values depend on the type and composition of the bituminous mix asphalt. When assessing the fatigue performance of flexible pavements in structural design, layered elastic analysis is used to determine the

maximum value of the tensile strain. The results of the analysis depend on the elastic modulus assumed for the pavement layers based on typical conditions. For instance, the general case of bituminous layers always depends upon temperature. Permanent deformation provides the principal indication of deterioration in flexible pavements. It develops mainly in the wheel-tracks of the left-hand traffic lanes on which commercial traffic concentrates. It increases with time, or more precisely, with the cumulative amount of commercial traffic which the pavement has carried. Figure 2.8 shows such a development of maximum deformation with time. This type of curve is widely used to characterize the performance of flexible roads. The total deformation found by measurements on the surface of a pavement is the result of component deformations in the pavement layers and the soil foundation. These deformations may arise from shear, viscous flow, and compaction or consolidation process. All flexible pavements exhibit an initial rapid increase in deformation due to traffic compaction of the pavement layers. A well-designed pavement will thereafter show only a small increase of deformation with time.

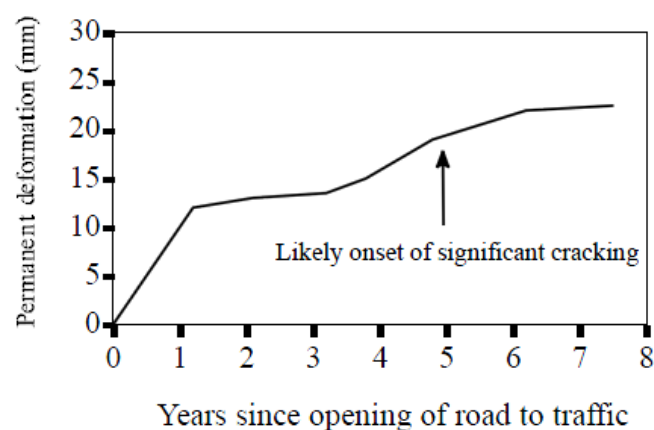


Figure 2.8 Illustration of the development of permanent deformation

Severe transverse deformation is generally accompanied by cracking in the wheel-cracks (Croney, 1977). Such cracking, particularly in areas liable to potholes of water, permits moisture to enter the road structure. For this reason, once obvious deformation has occurred, rapid deterioration is likely to follow on roads subjected to heavy traffic. Observations made on experimental roads carrying normal traffic and on other in-service roads show that once pavement deformation has reached 25 mm (measured from the original surface level) in the nearside wheel-tracks, the subsequent stages of deterioration are likely to be rapid.

In the UK and other European countries, the predominant mode of distress in flexible pavements is permanent deformation appearing at the road surface in the form of ruts (Peattie, 1978). The permanent displacement that appears at the surface of a pavement is the sum of the deformation of each of the pavement layers together with that in the subgrade. The distribution of this deformation is not fully known but measurements in different parts of the world have shown that the proportions vary from road to road. This factor is used as a criterion of performance, and once a rut depth of 10mm measured under a 1.8m straight edge (this corresponds to a value of 15 mm measured from the original level) has been reached the pavement is considered to have reached a critical condition. Maintenance is then required if satisfactory performance is to be obtained in the future (Norman et al, 1973). It was also reported that cracking in the nearside wheel-tracks is first observed when the permanent deformation measured from the original surface of the pavement is about 15-20mm. Once a rut depth of 20 mm has developed, the pavement is considered to have failed (Croney, 1977).

2.2.3 Pavement response models

This section provides a brief description of the subset of the field of continuum mechanics as it relates to pavement engineering and the modelling of pavement materials. The definition of a pavement response model is that it is a model that predicts the response of a pavement structure subjected to the single application of a tyre/wheel assembly/axle/vehicle. These models calculate the distribution of the stress and strain in the pavement due to the applied load. The loading can either be static and monotonic or static and cyclic moving with constant amplitude or moving with varying amplitude. The last case is the most realistic of an actual pavement structure but the most complicated to model. The models that incorporate cyclic loading are best suited to modelling materials that have either time dependent and/or non-elastic properties. The equations that model the response of the material to an external load are called the constitutive laws/equations/models. The constitutive model can be based on either physical theories or the analysis of laboratory or field measurements. In order for any proposed constitutive model to be scientifically robust, it should obey the fundamental laws of Newtonian physics which cover the conservation of mass, momentum, moment of momentum and energy and the laws of thermodynamics. From a practical engineering viewpoint, the benefits that might be gained from the use of a complex constitutive model may not be realized if the parameters of the model cannot be readily or easily determined. A typical pavement structure will be composed of two or more layers of different materials, with each material having its own constitutive model. If the pavement structure is modelled using these different constitutive models, the only practical and readily available way to compare the modelled pavement with the actual pavement is to compare the surface deflection under an applied load. Since only one response is measured to test the validity of two or more components of the system, it is difficult to assess

the accuracy or relative contribution of each component to the total system response. There are generally two types of response models, analytical and numerical. Analytical models use established principles from the field of solid mechanics in order to model the complete system, whilst numerical models are based on an assemblage of small analytical models that are solved simultaneously to achieve overall system equilibrium.

2.2.4 Current methods of pavement analysis and design

Analysis and design methods for flexible pavements have been developed since the early part of the last century. Traditional design systems are still being used in numerous countries and must be developed to replace the mechanistic empirical approaches currently in use. Empirical methods with or without a strength test were the early methods employed in the design of flexible pavements and refers to the soil classification system (Hogentogler and Terzaghi 1929; AASHTO 1986). In the past, most pavement structures were natural earth or gravel roads and the load carrying capacity of the pavement solely depended on the shear strength parameters of the selected materials. Currently almost 65% of the global road network still consists of earth and gravel roads (Molenaar 2007). It is clear that the design procedure observed only stresses induced in the pavement and the shear failure allowable of the pavement surface. Vehicles run into problems because of the lack of bearing capacity of the pavement material. From this example, precise knowledge of the load pressures applied to the pavement and the strength of the materials used is essential in order to be able to design pavements that can sustain millions of load repetitions.

The empirical design systems were, not surprisingly, based on determining the required thickness of good quality layers on top of the subgrade to prevent shear

failure to occur in the subgrade. Certainly, the required thickness was dependent on the shear resistance of the subgrade and the amount of traffic. Furthermore, the quality of the covering layers has to be such that shear failure will not occur in these layers. This was the basis for the California Bearing Ratio (CBR) thickness design method. In the CBR design charts, the traffic load was characterised by means of a number of vehicles per day and the shear resistance of the materials was characterized by means of their CBR value. The charts were used in the following way. First of all, the number of commercial vehicles had to be determined. When this number was known, the appropriate curve had to be selected. Next the CBR value of the subgrade needed to be determined and the required layer thickness on top of the subgrade estimated. Finally, in the CBR test, a plunger was inserted into the soil sample with a specific displacement rate and the load was obtained. The load – displacement curve was plotted in this way and compared with reference material along with the CBR value. The CBR design method results in thin asphalt layers are mostly required to provide a smooth driving surface and sufficient skid resistance. Design curves based on road material tests became available in the 1960s and a guide introduced the structural design of roads under various conditions of climate, materials and traffic loading. Experience and simple knowledge of index properties (such as the CBR) are the key input factors of the empirical approach which limits in shear failure and in deflections (Huang 1993).

The empirical nature of traditional pavement design procedure is based on experience and the results of simple tests such as the California Bearing Ratio (CBR), particle size distribution, moisture sensitivity, aggregate durability, angle of shearing resistance and deflection. Such results are all static parameters and simple index parameters rather than any consideration of multidimensional geometry, realistic material behaviour and displacement distribution during cyclic

loading, stresses and strain distribution in multilayered pavement design. Consequently, the use of empirical approaches is considered to the sub-standard and can be evaluated only in a limited capacity. Traditional, this design procedure has been criticized by Wolff who argued that it is too simplistic and does not take into account the non-linear behaviour of UGMs (Wolff and Visser 1994).

Flexible pavement design is a process whereby the optimum arrangement of materials is chosen, taking into consideration suitable strength, serviceability and economics for a given application. It can be achieved by either the empirical or mechanistic method. The empirical method is suitable for pavements composed of granular material or those containing an asphaltic surface layer of less than 30 mm in thickness. Pavements containing bound or cemented material or asphalt thicknesses of 30 mm or more require the mechanistic design method to be used instead (Nikraz 1998). This is because the empirical method uses an estimated approach to serviceability and fatigue analysis that limits its use to low trafficked applications, whereas the mechanistic approach takes a closer look at the mechanics of the pavement. Empirical pavement design procedures rely to some extent on the engineer's knowledge and experience of flexible pavements. The design procedure is based on main components such as design traffic, material's CBR assessment, elastic parameters, determination of pavement thickness from Figure 2.9, and the determination of pavement composition (Nikraz 1998).

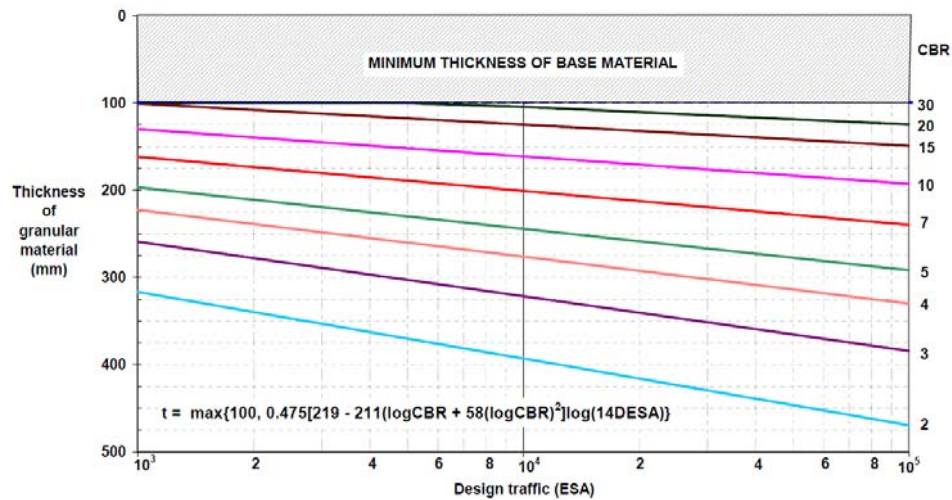


Figure 2.9 Design chart for granular pavements (Austroads 2004)

The use of empirical design as a reliable pavement method is limited for it does not consider variances in fatigue, material behaviour and climate. Instead it provides a general solution to these aspects. To increase the reliability of the design, an analytical approach known as mechanistic design was developed. Design procedures in Australia remained relatively primitive until 1979 when the National Association of Australian State Road Authorities (NAASRA 1975) produced its Interim Guide to Pavement Thickness Design. Subsequently, it was largely adopted by individual road authorities. The guide's approach is similar to the Shell method, although a number of modifications are included.

The traditional design method (empirical design) is no longer acceptable because the test protocols only obtain the design parameters from static loading tests and do not reveal the shortcoming of mechanical fundamentals. A mechanistic design attempts to explain pavement characteristics under real pavement conditions such as loads, material properties of the structure and environments based on design parameters from sophisticated tests which can simulate real pavement conditions

into the test protocol (Collins, Wang et al. 1993). The key point of the success of this analytical method is the experimental measurement and appropriate pavement analysis and design approach. A pavement structural model, stress and strain conditions are preliminary requirements of this study in assessing, the structural contributions of wearing, base, subbase, subgrade to the carrying capacity of the pavement structure while using different layer thicknesses/or different materials (elastic modulus).

The mechanistic-empirical (M-E) approach is based on limitations in the use of the principles of mechanics, such as elasticity, plasticity, and visco-elasticity. It consists of two stages: the first is an analysis of the pavement layer system using a mechanistic model such as the multi-layered concept and finite element (FE) procedure that includes elastic, nonlinear elastic (such as resilient modulus model), or elastoplastic models such as Von Mises, Mohr-Coulomb, and hardening or continuous yielding (Vermeer 1982). In the second stage, the stresses and strains from the wheel load, computed from the first stage, are usually used in empirical formulas to determine rutting, damage, cracking, and amount of traffic. Generally, uniaxial quantities of the tensile strain, ϵ_t , at the bottom of the asphalt layer, and the vertical compressive strain, ϵ_c , at the top of the subgrade layer are used to calculate various deteriorations using empirical formulas as shown in Figure 2.10. This approach can initiate improvements in design in comparison to the empirical approach. However empirical formulas to calculate distress may not provide accurate predictions as they do not account for multidimensional geometry, nonhomogenities, anisotropy, and nonlinear material responses, which are strongly dependent on stress, strain, time, environmental factors, and load repetitions (Chandrakant 2007). The full mechanistic approach can allow for all factors lacking in the empirical formulas in stage two of the M-E approach, in a unified method for all layers. As a result,

distresses are evaluated as a part of the solution (e.g., finite element) procedure, without the requirement of empirical formulas.

The M-E approach relies on two main parameters, resilient modulus and permanent strain. This is where the non-linear elasticity and plasticity of the pavement materials are established in relation to vehicle – pavement interaction. The design is centred on the structural analysis of pavements with multiple layers and steps for mechanistic pavement design as follows (Nikraz 1998);

1. Evaluate the multiple input considerations namely, construction and maintenance parameters, environmental aspects, subgrade, materials, traffic and performance criteria.
2. Choose a test pavement.
3. Analyse the test pavement to determine acceptable traffic.
4. Evaluate the acceptable traffic with the design traffic. From a comparison, the pavement is either accepted or rejected. If the test pavement is rejected, a new test pavement is chosen, and the procedure is repeated until a suitable pavement is achieved.

The two main modes of failure met with in the mechanistic approach are failure by excessive deformation and fatigue. For flexible pavements, fatigue occurs mainly at the bottom of the surface, asphalt layer and is caused by the tensile strain in the horizontal axis induced by traffic loading as shown in Figure 2.10.

The resilient modulus (M_r), the equivalent modulus of elasticity of the materials in the pavement is established on the recoverable quantity of strain, after axial stress

is removed. It is defined as the ratio of deviator axial stress (σ_d) to the resilient axial strain (ϵ_r).

$$M_r = \frac{\sigma_d}{\epsilon_r} \quad (2.2)$$

where:

M_r = Resilient modulus

σ_d = Axial stress

ϵ_r = Resilient axial strain

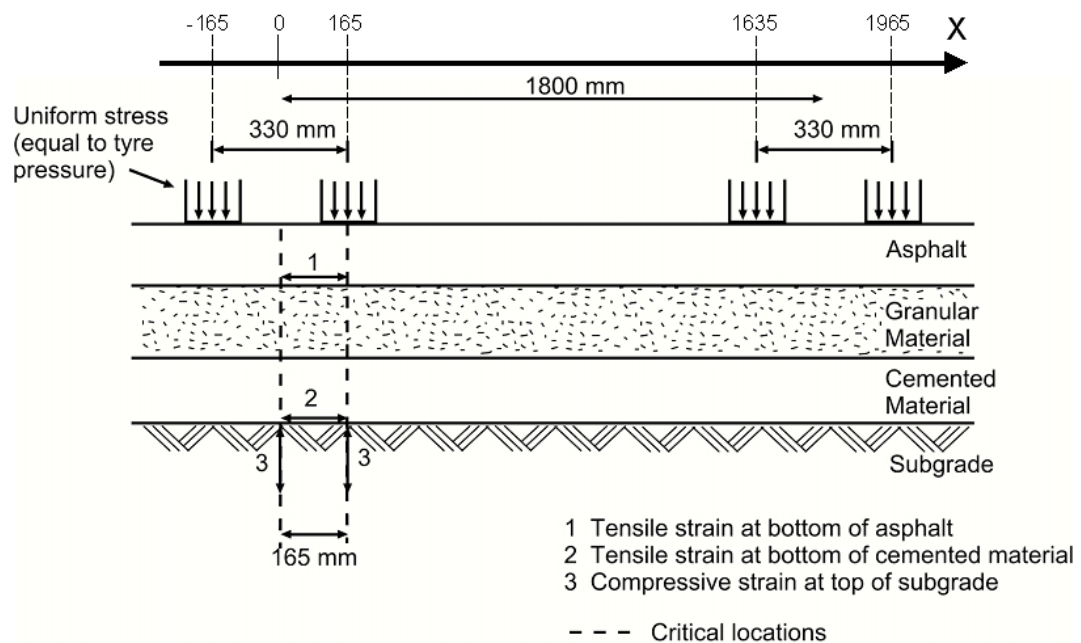


Figure 2.10 Strains induced in a layer pavement system (Austroads 2004)

The resilient modulus can be found through Repeated Load Triaxial (RLT) Test conducted in laboratories. This method of analysing pavements is becoming popular in Australia because of its ability to better analyse the pavement. However, there are still problems with sample end effects, system deflection and noise, sample bending and friction and compaction method effects. Technology in this field is advancing, allowing for the evolution of data analysis and standardisation of test procedures to increase accuracy.

With pavement aspects such as the resilient modulus, Poisson's ratio and shear modulus known, mechanistic analysis and pavement design can be performed using computer programs such as CIRCLY. CIRCLY (MINCAD Systems 2004) is a commonly used pavement analysis program in Australia and forms an important part of the Austroads Design Guide (Austroads 2004). The mechanistic design is known in Figure 2.11 and consists of:

- evaluating the input parameters (structure, material, traffic, and climate),
- selecting a trial pavement,
- analysing the trial pavement to determine its responses in terms of stresses, strains, and deflection induced,
- determining the performance prediction, and
- comparing the performance with failure criteria.

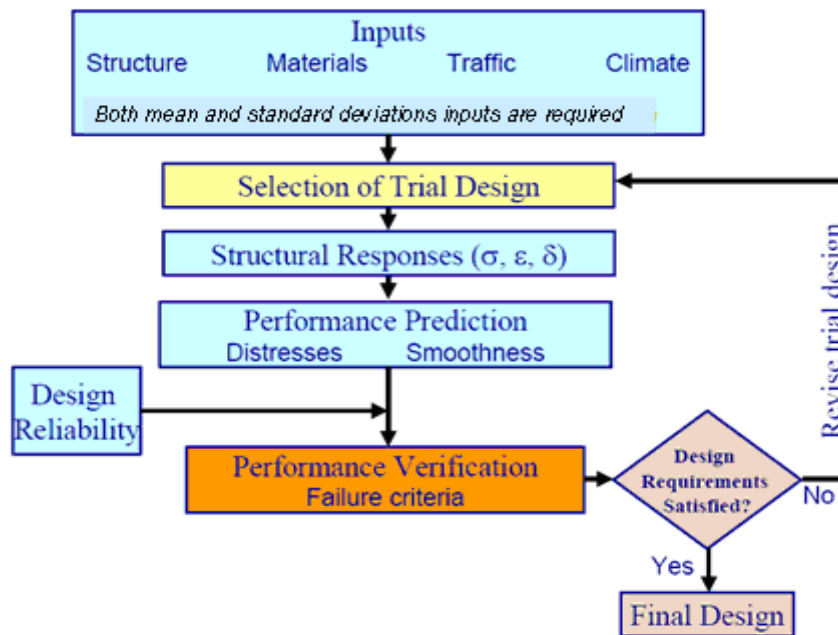


Figure 2.11 Mechanistic design framework and component (Cement Association of Canada 2005)

The first version of the Austroads Design Guide is based on the philosophy that an engineer must have a good understanding of the process and the mechanics of pavement behaviour. The engineer is encouraged to develop the design from first principles with the use of a computer program (e.g. CIRCLY, Wardle 1980) for calculating stresses and strains in a multi-layered elastic medium. Thus, the guide promotes a preliminary mechanistic based design method in which the performance of the pavement structure can be determined from the application of an analytical process. Strain is used as an input into a performance relationship that relate to the critical response of the allowable amount of design axles/traffic. Jameson (1996) documented the history of the design method of which the origins can be traced back to the Californian State Highways Department design method

(Porter 1942). The performance relationship given in the Austroad Design Guide for unbound granular pavements is the subgrade strain criterion.

$$N_{\text{allowable}} = \frac{[9300]^7}{\epsilon_{\text{sg}}} \quad (2.3)$$

where

ϵ_{sg} = Vertical compressive strain at the top of the subgrade (microstrain)

$N_{\text{allowable}}$ = Allowable number of equivalent number of standard axles

The concept of the subgrade strain (initially stress) criteria was first proposed in the pavement design method developed by the Shell Oil Company (Peattie 1962) and was also intended to apply to the compressive stress at the top of the unbound granular layers. Peattie (1962) and Dorman (1962) briefly mentioned some work that indicated if the stress criterion of the subgrade was satisfied, then the stresses in the granular layers would be below the failure level for the granular material. The initial values of the coefficients for Equation 2.3 for the Shell Design method were based on the analysis of successful pavements design in accordance with the Californian State Highways Department design method (Dormon et al., 1964). Therefore, it would appear that the original analytical pavement design method initially had a performance requirement for the granular materials, but this was removed from the final version of the design method as the subgrade performance was usually the critical criteria compared to the granular criteria. The coefficients of Equation 2.3 were derived from the analysis of many pavements from NAASRA Design. A difficulty lies in the development of performance criteria for new materials, since Equation 2.3 was derived from an empirical design chart after many years of observations and changes had been made in the development of the base design chart. New material would most likely only have a limited amount of performance data from a laboratory and/or limited field tests. These

findings raised questions over the robustness or applicability of the analytical part of the empirical design to accurately model either materials or pavement structures.

The current pavement design method in Western Australia and Australia is provided by the AUSTROADS Pavement Design Guide (Austroads 2004). This has been promoted at the level of a mechanistic-empirical based design method where the performance of a pavement structure can be determined from the application of an analytical process. It uses this to determine the response of the pavement structure to a single load and a critical response is whether the horizontal tensile strain is at the bottom of an asphalt layer or the vertical compressive strain is at the top of the subgrade layer. The strain is used as an input into a performance relationship that relates the critical response to the allowable amount of design axles/traffic. Based on mechanistic pavement analysis and design, it was found that the stress dependency of the vertical modulus can be modelled using the elastic model by dividing the layers into several sub-layers. From the mechanistic design step, the pavement structure scenario was established initially from the generally used pavement cross-section in Western Australia which contains asphalt as a road surface, hydrated cement treated crushed rock base (HCTCRB) as a road base, crushed limestone as a road subbase, and Perth silty sand as a road subgrade. The pavement was analysed to find the vertical and the horizontal stresses occurring in the pavement material layer (Harichandran, R.S. et al. 1990). The suitable resilient modulus of materials for mechanistic design was determined from its resilient modulus model by relying on the laboratory results of the modulus tests. CIRCLY 5.0 was used to determine the traffic loading intensity of a pavement. This software uses state-of-the-art material properties and performance models and is continuously being developed and extended. The first mainframe version of CIRCLY was released in

1977, its version is CIRCLY 5.0 and is an integral component of the Austroads Pavement Design Guide widely used in Australia and New Zealand (CIRCLY 5 2004). The system calculates the cumulative damage induced by a traffic spectrum consisting of any combination of user-specified vehicle types and load configurations. As well as using the usual equivalent single wheel and axle load approximations, optionally the contribution, such as foundation engineering and settlement analysis, can also be analysed using CIRCLY. CIRCLY is based on integral transform techniques and offers significant advantages over linear elastic analysis techniques

Mechanistic-based procedures have been gradually replacing empirical methods in the design of both road and airfield pavements in Australia. Two main load-associated failure mechanisms are considered: the first produces fatigue cracking of bound materials and the second produces permanent deformation or rutting of the pavement surface. The maximum vertical compressive strain at subgrade level is related to the repetitions to cause surface rutting failure. The maximum horizontal tensile strain at the underside of the asphalt or cemented layers is related to repetitions to cause fatigue cracking of those layers. The mechanistic-based design method involves calculating pavement damage from these critical strains using empirical equations, called failure criteria or performance relationship, in the form:

$$N = \left(\frac{k}{\varepsilon} \right)^b \quad (2.4)$$

where N is the predicted life, k is a material constant, ε is the load-induced strain, and b is the damage exponent of the material. The empirical parameters k and b are determined by calibrating the design method against observed performance of test pavements or of pavements in service. Arrangements of different strains will

be induced when different load types exist. The Cumulative Damage Factor (CDF) concept is then needed to sum the damage. The Damage Factor for the i -th loading is defined as the number of repetitions (n_i) of a given strain divided by the allowable repetitions (N_i) of the strain that would cause failure. The CDF is obtained by summing the damage factors over all the loadings in the traffic spectrum using Miner's hypothesis:

$$\text{CumulativeDamageFactor} = \frac{n_i}{N_i} \quad (2.5)$$

The pavement is presumed to have reached its design life when the cumulative damage reaches 1.0. With the advance of computer software development, the incorporation of data bases for material properties and loadings and the user-friendly working environment within CIRCLY (1997), it has become one of the most popular tools in the design of pavement structures in Australia.

2.2.5 CIRCLY (MINCAD Systems 2004)

A large number of computer programs have been developed for calculating stresses, strains and deflections of layered elastic systems. The stresses and strains in these programs are checked against the defined failure criteria. In all these programs, pavement layers are considered as homogeneous, linear elastic. In real situations, the assumption of homogeneous, linear elastic pavement materials becomes invalid. Almost all pavement materials are not homogeneous, especially granular materials particulate in nature. The finite element method for the analysis of flexible pavements was first applied by Duncan (Duncan, Monismith et al. 1968). Many computer programs based on this method were later developed. Its use in determining the stresses, strains and deflections is becoming popular with the availability of high-speed computers. Furthermore, it can handle structures with non-linear materials. In all these programs, traffic loading is considered as

static loading whereas the incorporation of traffic loading as dynamic loading is still in its early stages of research.

Static analysis of multi-layered pavement subgrade systems using linear elastic pavement structure is characterised by its Young's Modulus and Poisson's ratio. In some programs, resilient modulus based on the recoverable strain under repeated loading is used instead of Young's Modulus. The stresses, strains and deflections at specified distances from the load are then theoretically calculated, assuming a semi-infinite subgrade and infinite lateral boundaries. These calculated responses are matched with defined failure criteria. Layer thicknesses and material properties are adjusted until the computed responses are lower than the failure criterion.

CIRCLY, software for the mechanistic analysis and design of road pavements, uses state-of the-art material properties and performance models and is continuously being developed and extended. The first mainframe version of CIRCLY was released in 1977 and the current Windows version is CIRCLY 5.0. It is an integral component of the Austroads Pavement Design Guide (Austroads 2004) widely used in Australia and New Zealand. The system calculates the cumulative damage induced by a traffic spectrum consisting of any combination of user-specified vehicle types and load configurations. As well as using the usual equivalent single wheel and axle load approximations, optionally the contribution, such as foundation engineering and settlement analysis, can also be analysed using CIRCLY. CIRCLY is based on integral transform techniques and offers significant advantages over linear elastic analysis techniques, such as the finite element method.

2.3 Unbound granular materials (UGMs)

2.3.1 Introduction

Basecourse unbound granular materials (UGMs) such as gravel and crushed rock are widely used in Western Australia nevertheless modified granular materials and stabilised granular materials are alternative materials for heavily trafficked roads. UGMs are the backbone of road and railway structures. Without proper attention to the base, road structures will fail within a short period of time. UGMs are complex materials since they have produced from rocks through weathering and hauling of the weathered material by environment effects. Consequently, it will be obvious that pavement design and analysis should have a basic understanding of the behaviour of these materials (Molenaar 2005). The key parameters of UGMs for the design and analysis of flexible pavements are their stiffness and strength characteristics which are strongly influenced by the stress conditions to which the material is subjected. Other important factors are the degree of compaction, the moisture content as well as characteristics of the material itself like gradation etc (Molenaar 2007).

UGMs that consist of gravels or crushed rock aggregates which have a particular grading that formulates mechanical strength, are practicable and able to be compacted. Their performance is largely governed by their shear strength, stiffness and resistance to material breakdown under construction and traffic loading. The most common modes of distress of granular base layers are rutting due to insufficient resistance to permanent deformation through shear and densification, and disintegration through particle breakdown (Austroads 2004). The basecourse's significant role is the load bearing layer of a pavement and takes part in the performance of that pavement. This section will describe the basis of

the selection of conventional UGMs for flexible pavements. The general requirements for such materials are given in the NAASRA (NAASRA 1975; NAASRA 1980; NAASRA 1982; NAASRA 1982).

UGMs are very significant pavement construction materials that are used in the base, subbase and subgrade. Understanding the characteristics and behaviour of UGM's and their response when subjected to applied loads is therefore necessary for practical work. Basically, UGMs are rather complicated and natural soils and gravels particular show varied behaviour as a consequence of geological history that had an influence on their mineralogical composition, particle shape and size distribution. Moreover the actual degree of compaction and moisture content are of enormous importance. The UGMs of some countries are not natural materials anymore but processed materials being the result of recycling of old concrete and masonry resulting from construction and demolition. Residues from refinery factories are also commonly used for road bases and subbases. All this means that there is a wide variety of materials available on the market nowadays that allow good quality road bases and subbases to be built.

UGMs consist of particles in contact and surrounding voids. The micromechanical behaviour of granular materials is therefore inherently discontinuous and heterogeneous. The macroscopic behaviour of granular materials is determined not only by how discrete grains are arranged in space, but also by what kinds of interactions are operating among them. In order to understand the mechanical behaviour of granular materials from a microscopic point of view, a study should start by specifying the spatial distribution and orientation of grains and their contact conditions. Some continuum mechanical concepts such as stress and strain tensors are necessary to formulate problems in a consistent manner, since the degree of freedom of contact forces and movements at grain level becomes

tremendously large. Special emphasis is placed on particle rotation and contact moments since there is some positive evidence supporting the idea that granular materials can be idealized as a polar (generalized) continuum. A tensor, called the fabric tensor, is also introduced to characterise, the UGM in a tensor form. A spatial application is also utilised to derive some phenomenological constitutive equations.

UGMs have mechanical properties that are stress-dependent and very sensitive to climatic and environmental conditions. Previous research has presented the stress-dependent permanent deformation behaviour of UGMs that are typically used in unbound pavement layers. This can best be illustrated by the difference in behaviour of dry sand when poured on a heap or poured into a bucket. It is a well-known fact that one can easily put a stick in the heap of sand. One also knows, however, that the stick will easily fall down. On the other hand, it is very difficult to put the stick in the sand when the sand is in the bucket. The penetration resistance in that case is much higher. The only difference between the two cases is the fact that the bucket of the sand is supported in a lateral direction and confined. This immediately shows that unbound granular materials gain in strength and stiffness when confinement is applied. The same mechanism occurs to explain why a pack vacuum packed coffee is stiff. The confinement in this case is provided by the atmospheric pressure on the outside of the pack. The pack, however, immediately loses its stiffness and strength as soon as the vacuum (the confinement) is released. In soil as well as in pavement engineering, it is common practice to use the triaxial test to determine the strength and stiffness of unbound granular and cohesive materials.

The design criteria applied in current (analytical) design methods are intended to guard against excessive permanent deformation originating within the subgrade

(rutting) and cracks initiating at the underside of the bound layers (fatigue). These criteria are usually expressed as a relationship between loads induced resilient stresses or strains and the permissible number of load applications expressed in terms of standard units of equivalent applied traffic axles. The criterion for the subgrade is normally observed by applying a permissible limiting value for the compressive vertical strain at the top of the subgrade that has been derived from analysis of data originating from the AASHO road test. These methods assume that rutting/permanent deformations occur only in the subgrade. The thickness of the Unbound Granular Layer (UGL) is determined from the subgrade condition (CBR and/or resilient modulus) and the design traffic. No practicable design criterion is known for the UGLs. These specifications for UGLs typically include criteria for durability, cleanliness, particle shape and grading, none of which is a direct measure of resistance against rutting/permanent deformation caused by repeated loading. The Repeated Load Triaxial (RLT) test has the ability to simulate dynamic pavement loading on UGLs as occurring in pavement constructions. These tests show a wide range of UGL performance even though all the materials comply with the same specifications (Tho, 1989). British accelerated pavement tests done by Little (Little, 1993) show the same results and indicate that, depending on the pavement structure, 30 % to 70 % of surface rutting is attributed to the UGLs. However, these effects could not be observed on pavements designed according to the Austroads pavement design guideline. The current specification for UGLs (e.g. grading, durability) is not suitable to determine the deformation performance of these materials. Thus, new analytical pavement design methods should incorporate repeated load deformation performance of the UGL. One practical goal of this investigation was to develop an approach to overcome the current limitations in design practice and to develop a simple design chart that can assist a pavement engineer in evaluating the risk of rutting within an UGL.

Regarding factors influencing the mechanical characteristics of unbound base materials, attention is paid to the principles with respect to the mechanical characteristics of unbound base materials. It has become quite clear that stress conditions have an enormous influence on the strength, stiffness and resistance to permanent deformation of unbound granular materials. Of course, there are also being many other factors that are of influence, some of the most important gradation, angularity, type of material, degree of compaction, and moisture content and will be discussed in following section.

2.3.2 Mineralogy

Firstly what is a mineral? The following definitions on what constitutes a mineral were taken from several different sources and are arranged by time. A mineral is an element or chemical compound that is normally crystalline and that has been formed as a result of geological processes. They are naturally occurring inorganic substances with a definite and predictable chemical composition and physical properties (Nickel 1995).

As well known, the inherent behaviours of rock and soil are mainly determined by the mineral aspect, the size and geometric arrangement of the mineral particles. The mineralogy of soils varies the grain properties and determines the influences of the soil. For instance, all coarse grained soil usually has individual particles with an aggregation of minerals. Unlikely finer grain, each particle consists of a single mineral. The total properties of the soil are also influenced by the way the individual particles arrangement with density and other interrelated factors. A number of the main minerals originating in soil are shown in Table 2.2. Soil minerals occur in various forms, but the most important group are silicates of one

form or another (Gerrard 2000) such as in silicates (quartz, feldspar, amphibole, pyroxene, mica and carbonates) dominating where soils are developed from limestone or dolomite parent material. The argument will therefore be restricted to the carbonates and silicates. Soil is a weathering product (mechanical or chemical) derived from a parent material. In many areas the soil is derived from limestone or dolomite bedrock or reefs. Soils exhibit cleavage hence they readily break-up into smaller sized particles. The cleavage, softness and solubility in acids give these minerals a rather low resistance to mechanical and acid weathering. They are found in areas where the water is alkaline and where the parent material is close enough to ensure the continuous supply of fresh material. Soils derived from igneous and metamorphic rocks are dominantly silicates.

Table 2.2 The main minerals of soil

Soil type	Minerals
Sand, Gravel	Quartz, Feldspar, Amphibole, Pyroxene, Calcite, Magnetite
Silt	Quartz, Mica, Calcite, Dolomite
Clay	Quartz, Mica

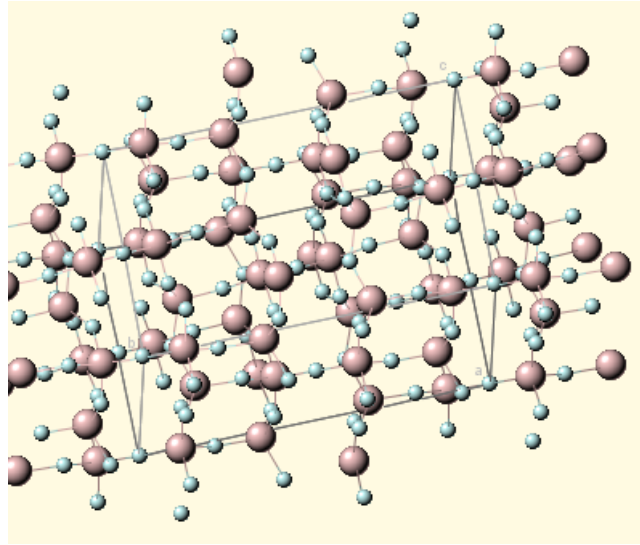


Figure 2.12 The tetrahedral skeleton of silicate minerals (David Barthelmy 2009)

Silicate minerals consist of silicon and oxygen (Si-O) with tetrahedral link in various forms. These tetrahedral units can be arranged into numerous configurations with themselves and with alkaline earths (Mg) and metals (Fe). The basic building unit of silicate minerals is the so called silica tetrahedron as shown in Figure 2.12. This skeleton consists of a silicon ion (Si^{4+}) core along with surrounding four oxygen ions (O^{2-}). This means that with silicon being a quadrivalent cation and oxygen a divalent anion, each silica tetrahedron must have negative charge of 4. The structure of silicate minerals can be explained by the way in which this negative charge requires to be balanced. One chain of the tetrahedron will share two molecules of oxygen with an adjacent tetrahedral and two with a neighbouring tetrahedral and two would remain unshared, resulting in a negative charge of 2. If three oxygens in each tetrahedron are shared this results in a sheet structure, and the overall charge on any one tetrahedron is reduced to 1. If all oxygens are shared with a neighbouring tetrahedral, a space networks and the positive charge in those minerals. In these minerals, the silicon tetrahedrons

are built into a network in all three directions and are characterized by hardness and resistance to chemical attack. The silicates exhibit a wide range in properties depending on the manner in which the basic building blocks are assembled. The various interlinking therefore fabricates four different types of silicate such as isolated tetradra (orthosilicates), chains (inosilicated), sheets (phyllosilicates) and three-dimensional networks (tektosilicates). In sheet silicates, the tetrahedrons build in two directions. The individual crystal units consist of thin sheets. The chemical bonds within a sheet are strong but the bonds between the sheets are weak. Hence, these minerals have excellent cleavage parallel to the sheets. They are softer than the space lattice silicates.

Unlike tektosilicates, most silicate groups have a residual negative charge that needs to be balanced by the addition of cation sections, so-called cation exchange. Mineral substitutions are related to environmental conditions and identification of the specific nature of the substitutions may therefore tell us something about the environment at the time of formation. These mechanism produce a wide variety of mineral types. The tektosilicate group includes some of the most important minerals, such as quartz and feldspars. Quartz is made up of silicon tetrahedral in which the silicon ion fits between four oxygen ions. The structure is compact and chemically strong, making it a significant resistant to weathering. The sheet silicates (phyllosilicates) possibly play the most important role in soils. Because they possess a sheet structure, many have a well-developed cleavage which aids the weathering main sheet structure.

Clay minerals are distinguished by both their mineralogy and their particle size. Most particles are less than 0.002 mm in diameter. Mineralogically, they are all silicates built of two basic building blocks, the silicate tetrahedron and the aluminium or magnesium octahedron. The sharing of the oxygen ions in the

tetrahedron sheet is done in such a way that the tetrahedrons all sit on a triangular base with their points in the same direction. The centres of the tetrahedrons generally contain a silicon ion (Si^{4+}) but occasionally this is replaced by an aluminium ion (Al^{3+}) which, although it has not the same electrical value, has almost the same size as the silicate ion. This phenomenon is called isomorphous substitution and will be discussed in greater detail later. Each oxygen ion at the base of the tetrahedron belongs to two tetrahedrons. The oxygen at the tips however is often linked with a hydrogen ion (H^+) to form a hydroxyl ion (OH^-). The tetrahedron sheet may, therefore, be considered as a layer of silicon ions between a layer of oxygen and a layer of hydroxyl ions. Clay minerals are formed by sandwiching tetrahedral and octahedral layers together to form sheets and sheets together to form particles. There are three common groups of clay minerals of main soil in pavement engineering, kaolinite, illite and montmorillonite. Kaolinite consists of a silica sheet and a gibbsite sheet. These sheets are tightly bonded together by common oxygen ions. The chemical bonds inside a sheet of kaolinite are covalent bonds and are very strong. The kaolinite sheets are locked together by weaker hydrogen bonds between the oxygens of the silica sheet and the hydroxyls of the alumina sheet. Hence the particles have well developed cleavage parallel to the sheets, hence, their property influences shrinking, swelling on drying and wetting conditions so that there is a group of clay minerals known as swelling clays.

A number of mixed layer minerals can also occur. These result from the interlayering of more than one sheet silicate mineral. They usually exist as intergrades when one mineral is being transformed into another during weathering. There are also a few non-silicate minerals in soils such as free oxides and hydroxides of iron, aluminium and magnesium. Other non-silicate minerals are carbonates, such as those of calcium, magnesium and amorphous silica, which

are often found in volcanic soils. Carbonates may not dominate a soil in terms of volume or weight, but they can exert a considerable influence on soil processes. The following are important properties of carbonates:

- They are easily soluble in water and therefore can be lost from or redistributed within the soil.
- Even small amounts of carbonate may raise the pH value of the soil and help to sustain a high level of biological activity.
- Carbonates, especially calcium carbonate, are the first substances to start accumulating when the climate becomes arid.

It seems that the main soil problems in pavements are associated with fine grained materials. It has been shown that if fine grained materials have a high LL and a high PI, they will show excessive swelling and shrinkage as well as a low bearing capacity when wet. The question now is why fine grained, cohesive soils are so different from sands and why is there such a large variation in behaviour when different types of fine grained cohesive soils are compared with each other. The reason for this is that cohesive soils are mainly composed of minerals.

2.3.3 Soil structure

Soil is a three-phase material consisting of solid particles, liquid and gas. The solid components of soils are the product of weathered rocks. The liquid component is usually water and the gas component is usually air. The gaps between the solid particles are called voids. As shown in Figure 2.13, the voids may contain air, water, or both. Its mechanical behaviour is largely dependent on the size of its solid particles and voids. As the solid particles are formed from physical and chemical weathering of rocks, it is important to have some

understanding of the nature of their formation. The total volume (V) and the total weight (W) of the specimen can be measured in the laboratory. In the idealized three phases, the solid particles are gathered in one region such that there are no voids in between, as shown in Figure 2.14. The volume of this component is V_s and its weight is W_s . The second component is water, whose volume is V_w and whose weight is W_w . The third component is air, which has a volume V_a and a very small weight that can be assumed to be zero. Note that the volume of voids (V_v) is the sum of V_a and V_w . The total volume is:

$$V = V_v + V_s = V_a + V_w + V_s \quad (2.3)$$

Also, the total weight

$$W = W_w + W_s \quad (2.4)$$

Definitions of several basic soil parameters that hold important physical meanings will now be discussed and their basic parameters used to obtain relationships that are useful in soil mechanics. The void ratio e is the proportion of the volume of voids with respect to the volume of solids:

$$e = \frac{V_v}{V_s} \quad (2.5)$$

The porosity n is given as

$$n = \frac{V_v}{V} \quad (2.6)$$

Note that

$$e = \frac{V_v}{V_s} = \frac{V_v}{V - V_v} = \frac{V_v / V}{V / V - V_v / V} = \frac{n}{1 - n} \quad (2.7)$$

The degree of saturation is defined as

$$S = \frac{V_w}{V_v} \quad (2.8)$$

Note that when the soil is fully saturated, all the voids are filled with water (no air). In that case we have $V_v = V_w$, Substituting this yields $S = 1$ (100% saturation). On the other hand, if the soil is totally dry, we have $V_w = 0$; therefore, $S = 0$ (or 0% saturation). The size and shape of the grains, the particle size distribution and the ratio between solid material, water and air determine the characteristics of the soil. Several parameters for this soil system are defined. Figure 2.14 shows an idealization of the soil system in which the three components are separated and represented by three volumes.

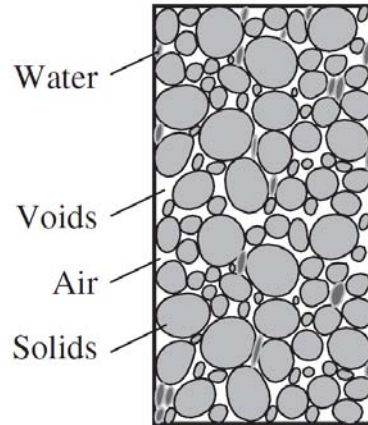


Figure 2.13 Soil structure

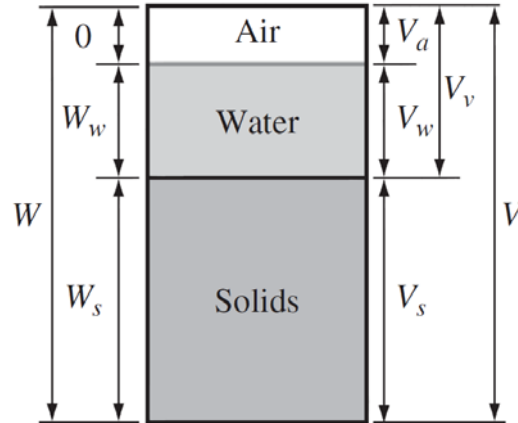


Figure 2.14 The three-phase soil system

The moisture content is the proportion of the weight of water with respect to the weight of solids:

$$\omega = \frac{W_w}{W_s} \quad (2.9)$$

The water content of a soil specimen is easily measured in the laboratory by weighing the soil specimen first to get its total weight (W). Then it is dried in an oven and weighed to get W_s . The weight of water is then calculated as:

$$W_w = W - W_s \quad (2.10)$$

W_w is divided by W_s to get the moisture content. Another useful parameter is the specific gravity G_s , defined as:

$$G_s = \frac{\gamma_s}{\gamma_w} = \frac{W_s / V_s}{\gamma_w} \quad (2.11)$$

where: γ_s is the unit weight of the soil solids and γ_w is the unit weight of water ($\gamma_w = 9.81 \text{ kN/m}^3$). Note that the specific gravity represents the relative unit

weight of solid particles with respect to water. Typical values of G_s range from 2.65 for sands to 2.75 for clays. The unit weight of soil is defined as:

$$\gamma = \frac{W}{V} \quad (2.12)$$

and the dry unit weight of soil is given as

$$\gamma_d = \frac{W_s}{V} \quad (2.13)$$

Dry density and the water content are of special importance because they strongly influence the structural behaviour of a given soil or granular material. For this reason, these parameters must be specified when a road has to be built. Compaction tests in the laboratory are therefore performed to establish the optimum values. The degree of saturation is strongly related with soil suction and pore pressure. Soil suction develops with lower degrees of saturation, especially in fine grained soils, and leads to higher stiffness due to extra induced compressive stresses, whereas pore pressures may develop if the degree of saturation reaches 100%, resulting in reduced effective stresses and possibly shear. The void ratio e and porosity n are related to each other as follows: Another important parameter is the specified gravity of the grains in some countries also called relative density. It is defined as the ratio between the mass of dry solids and the mass of distilled water displaced by the dry soil particles. As it is a ratio between two quantities with the same dimension, the specific gravity itself is dimensionless: Specific gravity is used in the calculation of the degree of saturation and in the calculation of the sedimentation speed of soil particles with a

diameter less than 0.075 mm. In the case of porous materials, it should be noted that enclosed pores in the material are supposed to be a part of the material.

2.3.4 Particle size distribution

Geotechnical engineering usually classifies soils to determine whether they are suitable for particular applications. Particle size distribution is another main influence on compaction and mechanical characteristics of pavement material. All pavement material specifications would need to confirm details about the grain size distribution and the consistency of each material. Subsequently, it can make comparisons with particular charts and tables that will give the specific type of each soil. Practically, specific charts are able to define which of these soils have the best compaction characteristics based on its classification. Most basic soil classification systems are based on the particle size distribution curve for a given soil. Particle size analysis is usually carried out a sieve on the coarse portion of the soil (more than 0.075 mm), and a hydrometer analysis on the fine portion of the soil (less than 0.075 mm) in diameter. As stated, granular materials consist of an arrangement of particles and between the particles there are voids which may be (partly) filled with moisture.

Table 2.3 Typical states of soil-aggregates

(a) Aggregate with no fines	(b) Aggregate with sufficient fines maximum density	(c) Aggregate with for great amount of fines
Grain-to-grain contact	Grain-to-grain contact With increased resistance Against deformation	Grain-to-grain contact destroyed, aggregate 'floating' in soil
Variable density	Increased density	Decreased density
Pervious	Practically impervious	Practically impervious
Non-frost-susceptible	Frost-susceptible	Frost-susceptible
High stability if Confined, low if Unconfined	High stability in confined or unconfined conditions	Low stability
Not affected by Adverse water condition	Not affected by adverse water conditions	Greatly affected by adverse water conditions
Very difficult to Compact	Moderately difficult to compact	Not difficult to compact

Figure 2.15 and Table 2.3 show the common three particles arrangement but another one should be identified as well, particle arrangement with even particles whether coarse or fine grains are presented. In Figure 2.15, the coarse particles are stones with a specific hardness which can be anything ranging from granite to siliceous river gravel. The fine particles are usually products of further deterioration or weathering of the parent material. Especially fine particles interact with water which means that their behaviour in relation to water is important. If the fine particles are e.g. clay, then structures b and c will be rather strong because clay is a hard and strong material when dry. On the other hand, structure c will

lose its strength when wet because clay has only limited strength when wet. Particle arrangement b is much less affected by wet conditions because in that case, the coarse particles will provide the transfer loads. What becomes clear from this picture is that one needs to know the particle size distribution and the behaviour of the fine material in relation with moisture. In this particular case, it is necessary not only to know the grain size distribution, but also the bulk density of the soil mass and the specific density of the grains. If the bulk density of the soil mass is much lower than the specific density of the grains, then it is evident that the soil mass must contain a large number of voids. If a material has a continuous grading following the Fuller curve, then the voids between the larger particles are filled with fine material resulting in dense packing. This immediately results in a larger number of contact points between the particles. The resistance to shear of the skeleton depends on the sum of the friction forces that are generated between the particles. When the number of contact points increases, the total friction in the skeleton increases which in turn results in a higher resistance to shear. Examples of particle size distribution curves are shown in Figure 2.16.

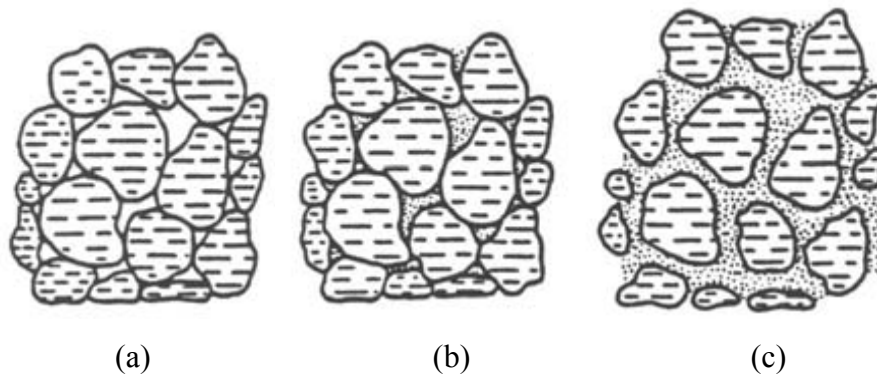


Figure 2.15 Three physical states of soil-aggregate mixtures

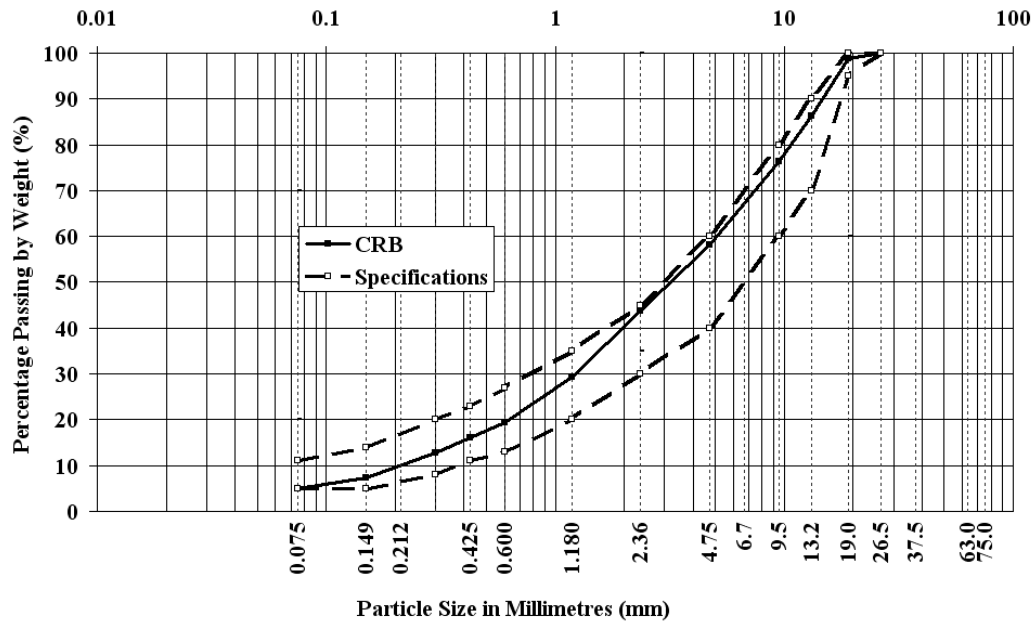


Figure 2.16 Crushed rock gradation

2.3.5 Moisture content

In road construction, water is used to contribute and lubricate individual particles to achieve high levels of compaction because it acts as a lubricant between the grains, allow slipping into the most effective packing. Without water, UGMs are unable to achieve the maximum density, however, it also presents a major contribution to the deterioration processes as it plays a major role interface with the material properties. Water in a pavement can come from many sources such as groundwater, stormwater, even the construction process of the road. In many low volume roads, the drainage system is not designed for large amounts of surface water so during a long rainy period, the water level in the drains may increase and penetrate the road structure. Water is a polar substance which means the particles have a definite positive and negative direction allowing molecules to dissolve with the minerals in the aggregate surface. Water also tends to migrate into the

pore system by capillary attraction if the pores are small enough, a factor which is related to the grain size distribution of the material and the amount of fine grains. Too much water on the road structure combined with repeated loading from traffic may cause reduced effective stress due to excessive pore pressure in the material. This is what happens in moisture susceptible materials during a wet climatic period. The consequences are reduced strength capacity and increased deformation in the base and subbase leading to cracking and rutting of the pavement. Traffic load in the pavement structure is transferred by grain-to-grain contacts. Eventually these may lead to deterioration by crushing and abrasion in the particle contact surfaces. The particles may then rearrange to form denser structures. The deformation behaviour of UGMs under repeated loading may be separated into two modes; resilient (recoverable) and permanent deformation mode. These types of deformation mechanisms are usually treated independently in the systematic approach. UGM deformation behaviour is known to be subject to many factors and moisture content.

Many researchers have studied the effect of water on resilient and permanent deformation. Hicks and Monismith (1971) reported an apparent increase in deformation with increasing water content (Hick and Monosmith 1971). Barksdale and Itani (1989) observed a significant decrease in the resilient modulus of soaking material. All samples were run under drained conditions. For well-graded materials, moisture seemed to be positive until optimum moisture content was achieved, after that the resilient modulus decreased towards complete saturation. Resistance to deformation is influenced by the changes in moisture content rather than the resilient modulus for UGMs. An UGM is susceptible to water allowing it to use into the pore structure. Water is unusual in the deformation of coarse single-sized particle materials significantly because it is not retained in the pore structure but is more or less on the surface of the particles.

The only effect of the water here would be as a lubricant. However, over time a uniformly graded material may be subjected to interparticular crushing. The accumulation of fine grains may change the grading of the material and make it more sensitive to water. By using strong materials the risk of this is reduced.

The water acts as a lubricant. A possible explanation for this behaviour is as follows. In the oven-dried condition, the surface ions are not completely hydrated. The actual mineral surfaces come close together and the bonding is strong. As water is introduced the ions hydrate and become less strongly attached to the mineral surfaces. Hence shear resistance drops as water is introduced.

It is important to contrast the role of the contaminants in the cases of very smooth and rough surfaces. With rough surfaces, the contaminants serve to weaken the crystalline bond and increasing the mobility of the contaminants with water helps get them out of the way and minimizes their adverse influence. With very smooth surfaces, the contaminants are actually part of the mineral, and increasing their mobility decreases the resistance. In the saturated conditions, the friction between sheet minerals can be low. Since clay minerals are always surrounded by water in practical situations, it is important to test these minerals in saturated conditions.

2.3.6 Compaction

Compaction involves applying mechanical energy to partially saturated soils for densification purposes. This process brings soil particles closer to each other, thus decreasing the size of the voids by replacing air pockets with soil solids. Theoretically, we can achieve 100% saturation by replacing all air pockets by soil solids if we apply enough mechanical energy (compaction), but that is practically impossible. With proper compaction, the soil becomes stronger (higher shear

strength), less compressible when subjected to external loads (less future settlement), and less permeable, making soil a good construction material for highway embankments, ramps, earth dams, dikes, backfill for retaining walls and bridge abutments, and many other applications. Soils are compacted in layers, with each layer being compacted to develop a final elevation and/or shape. Compaction machines such as smooth rollers, pneumatic rollers, and sheepfoot rollers are generally used for this purpose.

The type of material is important since soft particles may crush easily resulting in a less optimum gradation. Moisture content plays an important role depending on its amount because significant suction (capillary) forces may develop resulting in a material with a good resistance to shear. The compaction energy generated by a compactor is proportional to the pressure applied by the compactor, its speed of rolling, and the number of times it is rolled (number of passes). Usually, only a few passes are needed to achieve the proper dry unit weight, provided that the proper moisture content is used for a particular soil. The required field dry density is 90 to 95% of the maximum dry density that can be achieved in a laboratory compaction test whether standard Proctor test or modified Proctor test (Main Roads Western Australia 2007) carried out on the same soil. The standard proctor test is a laboratory test used to determine the maximum dry unit weight and the corresponding optimum moisture content for a given compaction energy and a given soil. The soil specimen is obtained from the borrow site which is usually earth cut close to the construction site. The soil is first dried, crushed and then mixed with a small amount of water in a uniform manner. The resulting moisture content should be well below the natural moisture content of the soil an example of which is shown in Figure 2.17.

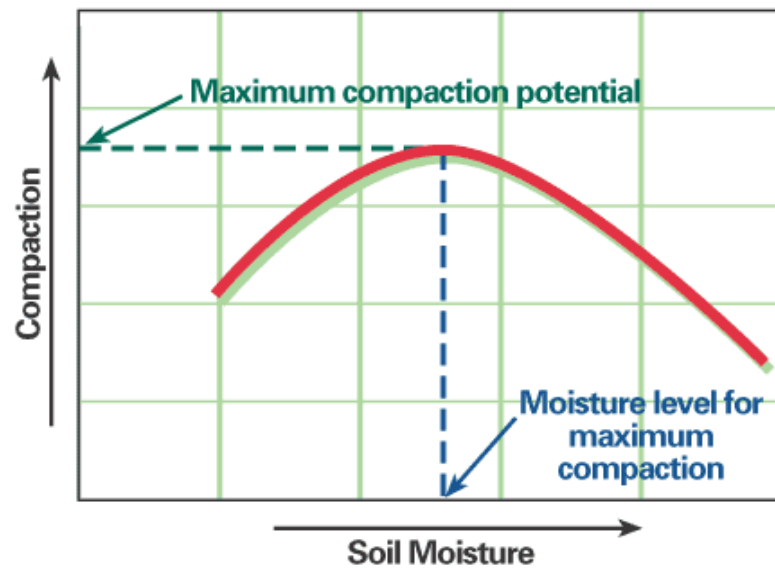


Figure 2.17 Compaction curve

This has to do with the fact that at a given moment, the granular skeleton has obtained its optimum compaction; the particles have reached their closest packing. If loading is continued, the particles will slide over each other resulting in a less dense packing and in an increase in volume. The moisture content associated with the maximum dry unit weight is called the optimum water content. As shown in the Figure 2.17, when the moisture content is increased beyond the optimum water content, the dry unit weight decreases. This is caused by the water that is now occupying many of the voids making it more difficult for the soil to compact further. Note that the degree of saturation corresponding to the optimum moisture content is 75 to 80% for most soils.

The compaction curve provides valuable information such as the maximum dry density (MDD) and the optimum water content (OMC). Usually, the required relative compaction is 90 to 95% because it is very difficult and costly to achieve a field dry unit weight that is equal to the maximum dry unit weight obtained from

the laboratory compaction test. We need to specify the corresponding moisture content that must be used in the field to achieve a specific MDD. In general, granular soils can be compacted in thicker layers than silt and clay. Granular soils are usually compacted using kneading, tamping, or vibratory compaction techniques. Cohesive soils usually need kneading, tamping, or impact. It is to be noted that soils vary in their compaction characteristics. Soils such as GW, GP, GM, GC, SW, SP, and SM (the Unified Soil Classification System) have good compaction characteristics. Other soils, such as SC, CL, and ML, are characterised as good to poor. Cohesive soils with high plasticity or organic contents are characterized as fair to poor.

When compacting in layers, the top surface is compacted as the next layer is rolled. Nonetheless, the difficulty of compacting close to the surface should be taken into account when carrying out compaction tests. All vibratory compactors are effective and economical on sand and gravel. Heavy to medium weight rollers will achieve compaction in thick layers. Light vibratory compactors will also achieve good compaction results on limited lift thicknesses. Dry compaction sand can also be compacted in a dry state, for example, in arid or semi-arid areas where watering of the material is either impractical or too costly. Self-propelled single-drum vibratory rollers have achieved very satisfactory results compacting 30-50 cm layers of uniformly graded dune sand with water content below 2%. Dry compaction has been applied with good results in road and airfield construction in Africa and the Middle East.

Sub-bases and bases normally consist of granular types of soil (gravel or crushed stone), although a relatively high content of fine grains is allowed in some countries. Densities are generally higher than those specified for embankments. Heavy vibratory rollers may be advantageous in the compaction of such semi-

cohesive types of subbase materials, while those consisting of clean sand and gravel can be effectively compacted in comparatively thick lifts with medium-heavy vibratory rollers. Compaction standards are normally very high, in the range 95-100% Modified Proctor. Vibratory compaction has been the standard compaction method on granular bases for many years. As there are normally high specifications for these courses, the lift thickness is usually lower than for subbase compaction. Medium-heavy rollers will normally compact satisfactorily in layers of up to 25 cm. Subbase and base layers may also consist of granular materials stabilized with cement, lime or bitumen to increase their strength. Vibratory rollers are also used to compact stabilized subbase and base layers, often in combination with pneumatic tyred rollers. If the materials show some self cementing action, the curing time is of importance.

2.3.6 Soil strength improvement

Insitu modifications and stabilisation is the proven technique for both new construction and the rehabilitation of existing roads. A lack of design details, poor specification clauses, poor construction practices by contractors with little knowledge of the process, quality control and materials may cause early the distress of roads. Also, one of the problems faced by contractors during tendering is the variation of specifications. For example, insitu stabilisation specifications are likely to change from one region to another region or State. It is frustrating to find that one council would specify binder content by volume and another by weight. This all leads to confusion and may lead to insufficient binder content in the pavement material.

During 1992, concerns were raised regarding the suitability and performance of the crushed rock base (CRB) used in Western Australia when the results of

Benkelman Beam testing on a section of the Kwinana Freeway between South Street and the Forrest/Yangebup Road were analysed by Cray (1992). High curvatures imply a lack of pavement stiffness in the upper layers which would lead to a reduced asphalt surfacing life due to premature fatigue cracking. As a result, a project was initiated to better understand the performance of pavement materials, by establishing the resilient modulus and strain characteristics of CRB. All of the CRB tested showed an unexpectedly high sensitivity to moisture, the importance of which had not been previously recognised. Various options for improving the performance of the CRB and reducing its sensitivity to moisture by using additives (e.g. Portland and blended cements, superplasticiser) and by modifying the particle size distribution were examined using the repeated load triaxial testing apparatus. Adding small amounts of cement significantly increased the strength and stiffness of the CRB while varying the particle size distribution curves did not appear to significantly improve the CRB performance. There was little difference in the test results between the different cement types used. The concern with adding cement, even with as little as 1%, is that the CRB could begin to behave as a bound material which could then lead to fatigue cracking problems. However, it was found that if a small quantity of cement was added to the CRB and the material was disturbed during hydration to prevent setting up, the CRB blend showed a marked improvement in strength and reduced sensitivity to moisture. This method of stabilisation was perceived as having great potential since the resultant material could be used without the risk of becoming too stiff and therefore prone to fatigue, and could also be used in the field without the time constraints normally associated with traditional cement stabilisation methods. The material became known as Hydrated Cement Treated Crushed Rock Base (HCTCRB). Over the years, HCTCRB has been widely used as a base course material in Western Australia. As it has a higher modulus value, it has been used in heavy traffic pavements. Further, there is a significant advantage in

manufacturing the Hydrated Cement Treated Crushed Rock Base (HCTCRB) as there is no time restraint in placement and there is a reduced risk of the material becoming too stiff and cracking. HCTCRB was re-treated before compaction in the construction site to avoid cracking that usually occurs with cementitious materials. This method of adding cement to a basecourse aggregate is used in stockpiling and then used as a basecourse with improved resistance to deformation/rutting. The HCTCRB in Western Australia is classified as a modified aggregate for high-volume roads as an economical alternative to structural asphalt.

2.3.7 Failure criteria and response model

The main failure criteria of unbound granular materials are shear failure from wheel loading. The shear strength of soil is the resistance offered by the soil to overcome applied stresses. High curvatures imply a lack of pavement stiffness in the upper layers which would lead to a reduced asphalt surfacing life due to premature rutting. To sustain a good service life, quality material must be placed in pavement layers. The failure criterion used to classify which material is suitable for designed road and will not present the functional failure before its life span. The shear strength of soil has to be determined accurately because it is crucial in the design of many geotechnical structures, such as natural or human-made slopes, retaining walls, foundations, and pavement. Shear strength parameters can also be measured in the laboratory using direct shear and/or triaxial compression testing methods on undisturbed or reconstituted soil samples.

The sliding between particles is the most important mechanism of deformation within a soil mass. Hence the resistance of soil to deformation is influenced strongly by the shear resistance at contacts between particles. Knowledge of the

possible magnitude of this resistance, and of the factors that influence this resistance, is basic to the mastery of soil mechanics. It must be emphasized that the shear resistance of a soil mass to shear or compression is also very important in the interlocking of particles, largely a function of packing density.

- The mechanism of shear resistance

The shear resistance between two particles is the force that must be applied to cause a relative movement between the particles. Its source is the attractive forces that act among the surface atoms of the particles. These attractive forces lead to chemical bond formation at points of contact of the surfaces. Thus the frictional resistance between two particles is fundamentally of the same nature as the shear resistance of a block of solid, intact material such as steel.

The strength and the number of bonds that form at the interface between two particles are influenced very much by the physical and chemical nature of the surfaces of the particles. Hence an understanding of the magnitude of the shear resistance between particles involves an understanding of the factors that influence the interaction between the two surfaces at their point of contact. However, the interaction effect can be summarised by saying that the total shear resistance (the product of the strength of each bond and the total number of bonds) is proportional to the normal force that is pushing the two particles together. If this normal force decreases, either the strength or the number of bonds decreases, and thus the total shear resistance decreases. Hence we say that interparticle shear resistance is frictional in nature.

There are situations in which part of the total shear resistance between particles is independent of the normal force pushing the particles together, and even if normal force is decreased to zero, there is still a measurable shear resistance. In such

cases, there is true cohesion between particles. This can develop between soil particles that have remained in stationary contact over a long period. In some cases this true cohesion can be very important, as when cementation turns sand into sandstone. Generally, however, the true cohesion magnitude of unbound material between particles is very small, and its contribution to the strength of a soil is also very small.

The shear resistance between two bodies is proportional to the normal force between the bodies and is independent of the dimensions of the two bodies. The law can be illustrated by pulling a brick over a flat surface. The various factors determine the shear resistance of granular soil. These factors fall into two general groups. The first group includes those factors that affect the shear resistance of a given soil, the void ratio of the soil, the confining stresses, and the rate of loading. It is necessary to understand the influence of these factors so that the strength appropriate for a practical problem can be measured. Of these factors, void ratio and confining stress are by far the most important. The second group includes those factors that cause the strength of one soil to differ from the strength of another, even for the same confining stress and void ratio, the size, shape, and gradation of the particles making up the soil. Knowledge of the effects of these factors is important when selecting soils for embankments, dams, pavement materials.

- The effect of confining stress

A typical program of triaxial tests to establish the influence of confining stress on strength involves the following steps. Two or more cylindrical specimens of a given soil are made, all having the same void ratio. The specimens are placed within triaxial cells and subjected to different confining stresses and loads axially. The resulting vertical strains and volume changes are recorded. In order to clarify the influence of the stress, the stress-strain curves have been normalized with regard to the confining stress and the value of q at any strain has been divided by σ_v . The normalized curves for these two tests are very similar in shape and magnitude. However, some important trends should be noted.

First, granular soil is frictional. The resistance to sliding at each contact point is proportional to the normal force at that contact, and hence the overall resistance increases as the confining stress increases.

Second, interlocking also contributes to the overall resistance as it decreases as the confining stress increases because the particles become flattened at contact points, sharp corners are crushed, and particles break. Even though these actions result in a denser specimen, they make it easier for shear deformations to occur.

Granular soil is a frictional material but deviates from purely frictional behaviour because of the effect of confining stress upon interlocking. The deviation behaviour is decreased by using confining stresses which are only slightly different from each other and increased by using one small and one very large confining stress.

- The Mohr-Coulomb failure criterion

The strength of unbound material is usually defined in terms of the stress developed at the peak of the stress-strain curve. Figure 2.18 shows the data from triaxial tests, each at a different confining stress. First, Mohr circles are drawn to represent the states-of-stress at the peak point of the stress-strain curves. The subscript f in the equation denotes that this is the failure condition. The physical meaning of the Mohr envelope may be understood from the following statements.

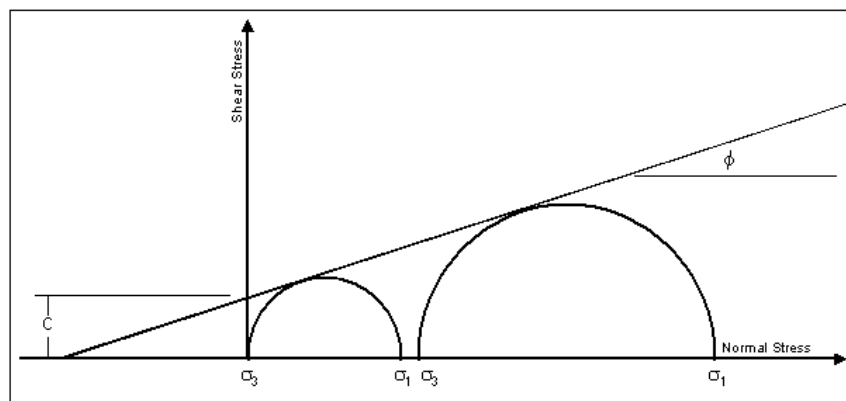


Figure 2.18 The Mohr-Coulomb failure envelope

- If the Mohr circle for a given state of stress lies entirely below the Mohr envelope for a soil, then the soil will be stable for that state of stress.
- If the Mohr circle is tangent to the Mohr envelope, then the full strength of the soil has been reached on some plane through the soil. The limiting stress condition occurs on a plane inclined at an angle of ϕ to the plane on which the major principle stress is acting. This plane is written as σ_{ff} and the normal stress on the failure plane at failure.

- It is not possible to have within a soil a state-of-stress whose Mohr circle intersects the Mohr envelope for that soil. Any attempt to impose such a state-of-stress would result in unlimited failures.

This is generally true for granular soils tests using a wide range of confining stresses. However, for most calculations regarding the stability of a soil mass, it is necessary to use a failure relationship, a straight line. Thus the strength is expressed by the Mohr-Coulomb failure law.

$$\tau_{ff} = c + \sigma_{ff} \tan \phi \quad (2.14)$$

where c is called the cohesion or cohesion intercept, and ϕ is called the friction angle or angle of shearing resistance. The way in which a straight line is fitted to a Mohr envelope in Figure 2.18 might be fitted by a straight line. The actual Mohr envelope for soil passes through the origin of the Mohr diagram; the soil will not stand as a cylinder if the confining pressure is zero. In order to employ the equation over a large range of stresses, it is necessary to use a cohesion intercept. If the Mohr envelope for a soil were a straight line through the origin rather than a curve, then the failure law could be simplified. The curvature of the Mohr envelope is greatest for dense granular soils and decreases as a soil becomes looser. The Mohr envelope for the strength in the ultimate condition apparently is quite straight over a large range of stresses. For most engineering problems, the stresses are small enough to make use of the equation. However, there are many problems such as high earth dams where the strength of a dry granular soil can be satisfactorily represented only by either a curved Mohr envelope or by an equation. Another way to represent the true nonlinear strength relation is to treat ϕ as a variable that depends upon confining pressure. Thus ϕ is computed from the

slope of the straight line drawn through the origin and tangent to the Mohr circle representing the stresses at failure. This method of representing strength is not particularly useful when making stability calculations, but does make it easy to see just to what degree the strength is nonlinear with respect to confining stress.

This method generally used for granular soils and at the same time is one of the most widely used and most controversial equations encountered in soil mechanics. The equations are useful approximations. This validity is a simple consequence of the way in which c and ϕ were defined. However, the failure plane as defined previously, following the original suggestion of Mohr, may or may not be the plane upon which shear strains become concentrated when the soil fails. The difference between these two planes has occupied the attention of Rowe (1963). A theoretical failure plane, or slip line, by definition lies at an angle $(45+\phi/2)$ to the plane upon which the major principal stress acts. Failure often occurs along a curved surface rather than along a plane, and this is often called a theoretical failure surface (or slip surface) and an observed failure surface. Moreover triaxial test results are able to use p-q diagram as an alternative way to plot the results of a series of triaxial strength tests. The point gives the values of p and q corresponding to the peak points of the stress-strain curves. The curve drawn through these points is called the K-line the same as the Mohr envelope as shown in Figure 2.19.

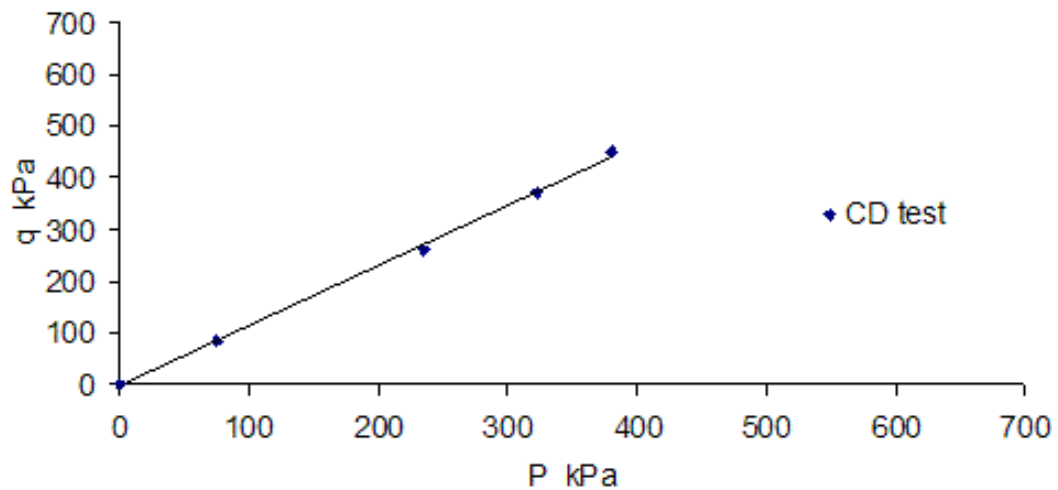


Figure 2.19 The p-q diagram of HCTCRB and CRB

There are diverse responses modelling for unbound granular materials, nonetheless the most accepted modellings are elastic, visco-elastic and elastoplastic models. Basically, the elastic concept predicts material response by using a linear line that material is always presented fully as a recovery deformation. Subsequently, two other types of mechanism are considered more like real conditions. The first involves time-dependent deformation due to viscosity and the second energy dissipation due to sliding between particles. A brief review is given of these models. In visco-elastic models, many granular materials consist of a visco-elastic binder between particles. In this case, the time dependent deformation of the binder leads to visco-elastic behaviour of the assembly. Along this line, a contact law has been developed for compression and tangential compliance and for rolling and twisting compliance of two elastic particles connected by the binder. The contact law for two particles with a visco-elastic binder has been applied to the derivation of a rheological constitutive relationship for a granular assembly viewed as a discrete system of particles connected with equivalent springs and dashpots. For elastoplastic models under a loading

condition of high deviator stress, large shear deformation occurs accompanied by a significant amount of particle sliding. The contact law is of elastoplastic type which again leads to elastoplastic behaviour of the assembly. The strain exhibits non-uniformity of strain in the modelling.

2.4 Mechanical behaviours of granular materials under repeated loading

2.4.1 Stress-strain behaviour under traffic loads

The stresses acting on a given element in a material can be defined by its normal and shear stress components, as shown in Figure 2.20. It can be proven that for any general state of stress through any point in a body, three mutually perpendicular planes exist on which no shear stresses act. The resulting stresses on these planes are thus represented by a set of three normal stresses; called principal stresses σ_1 , σ_2 and σ_3 (Figure 2.20).

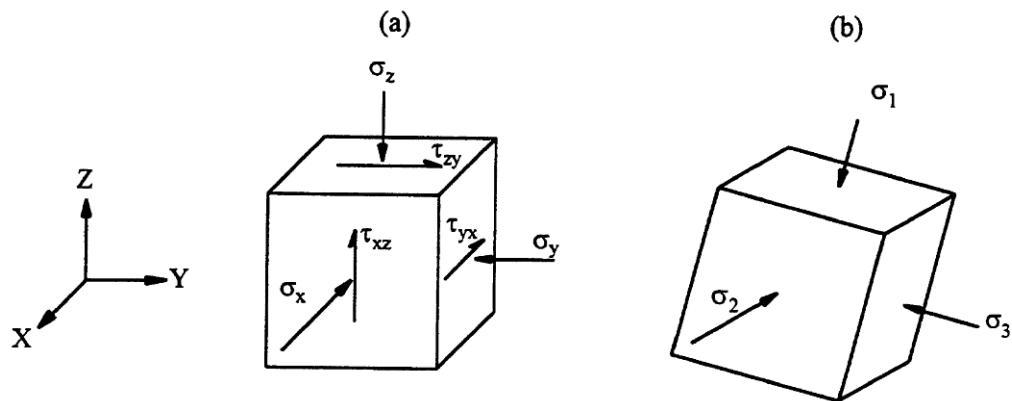


Figure 2.20 Stress components acting on an element (Lekarb 97)

The principal stresses (σ_1 , σ_2 , σ_3) are physical invariants that are independent of the choice of co-ordinate systems (X, Y, Z). The pavement in the field is usually

loaded by moving wheel loads, which at any time impose varying magnitudes of vertical, horizontal, and shear stresses in the UGM layer. As a result, rotation of the principal stress occurs. Figures 2.21 and 2.22 show that the principal stresses act vertically and horizontally only when the shear stresses are zero, i.e. directly beneath the centre of the wheel load. For laboratory testing, the RLT apparatus is the type most commonly used for UGM characterization. Combinations of the vertical and horizontal stresses can be reproduced in a RLT test. This type of loading, however, does not provide for the shear reversal or the change in the direction of principal stresses can only be simulated with new RLT equipment. The stresses applied in a RLT test are equivalent to the in-situ principal stresses directly beneath the centre line of the wheel load. If the in situ stress condition below the centre of a single wheel load is considered, then $\sigma_1 = \sigma_z =$ vertical stress, and $\sigma_2 = \sigma_3 = \sigma_r =$ horizontal stress (Lekarp and Dawson 1998).

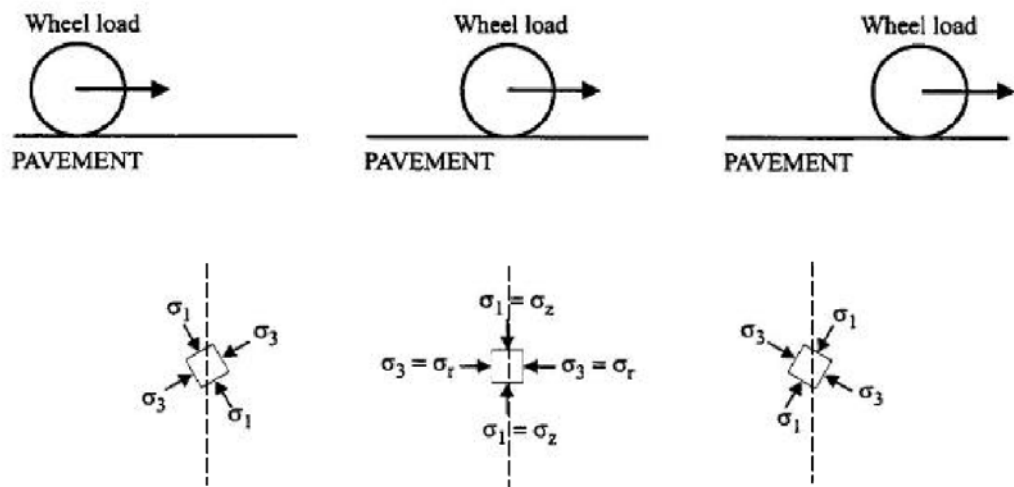


Figure 2.21 Stresses under a rolling wheel load (Lekarp and Dawson 1998)

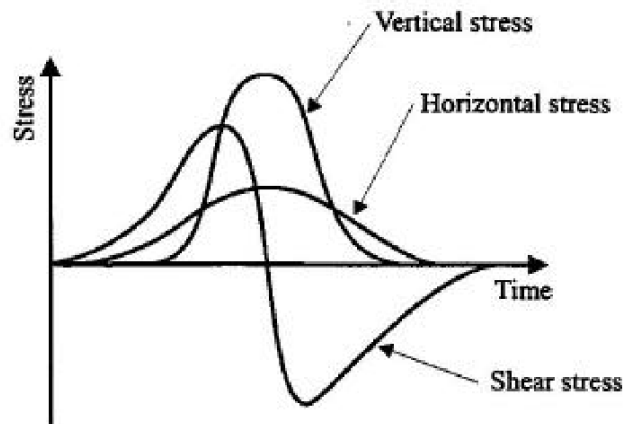


Figure 2.22 Stresses in motion of a rolling wheel load (Lekarp and Dawson 1998)

The strain resistance of an UGM depends on the applied stresses. The behaviour shown in Figure 2.23 is typical for UGMs i.e. as the stress increases, the material's resistance to further strain diminishes. At low levels of stress, the stiffness of the material increases with rising magnitudes of load (strain hardening). The compacted UGM becomes even more closely packed and harder to move as its components (particles) are forced into new interlocked positions. As the stress increases further (near to failure) the stiffness of the material decreases (strain softening). Eventually the material achieves failure. UGM are different from soils in their physical characteristics and also in their response to applied cyclic loads. An UGM is an assembly of a large number of individual particles with different shapes and sizes. These materials carry only a very small amount of tensile stress.

UGMs layers in a pavement are subjected to a large number of load cycles during their service life. These layers exhibit a combination of resilient strains which are recovered after each load cycle, and permanent strains, which accumulate with

every load cycle. Even at small stresses, resilient and permanent strains can arise. The stress-strain relationship for UGM is given by a non-linear curve which is not retraced on the removal of stresses but forms a hysteresis loop. Evaluation of a particular hysteresis loop will produce the values for the permanent and resilient strains per load cycle. Figure 2.24 gives the general idea of a single hysteresis loop.

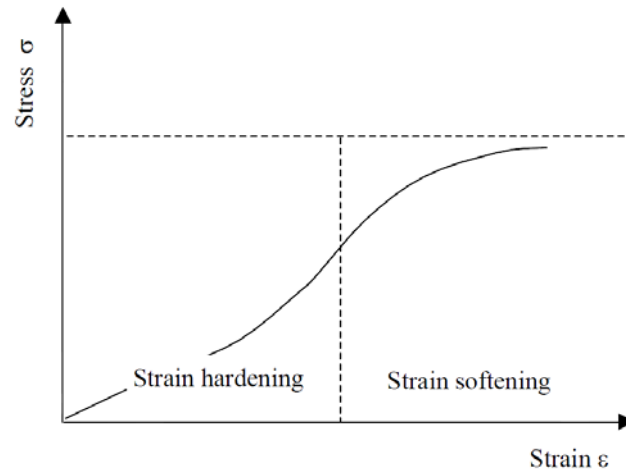


Figure 2.23 The stress-strain behaviour of UGMs (Lekarp and Dawson 1998)

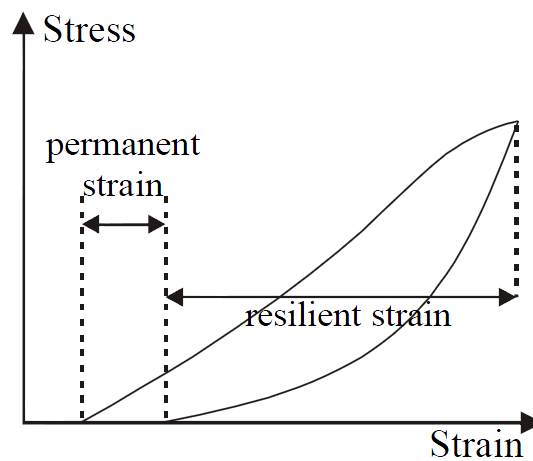


Figure 2.24 A hysteresis loop for viscous-elastic permanent behaviour

The area of the hysteresis loop corresponds to the strain work per volume element.

$$W = \int s de \quad (2.15)$$

where

s [N/mm²] stress

e [-] strain

The greatest part of this work is transformed into heat energy which changes material properties which finally leading to damage. Only a small part of this work will be accumulated. A typical example (RLT test result) of the behaviour of UGMs under dynamic loading is shown in Figure 2.25. By comparing the hysteresis loops in Figures 2.24 and 2.25, the loops in Figure 2.25 are much narrower at the bottom part, but they must still be open (as the permanent strain per load cycle is not zero) because there is a gap between the loops of the cycles for 20,000 and 80,000 load repetitions. This indicates a small amount of permanent strain at every load cycle.

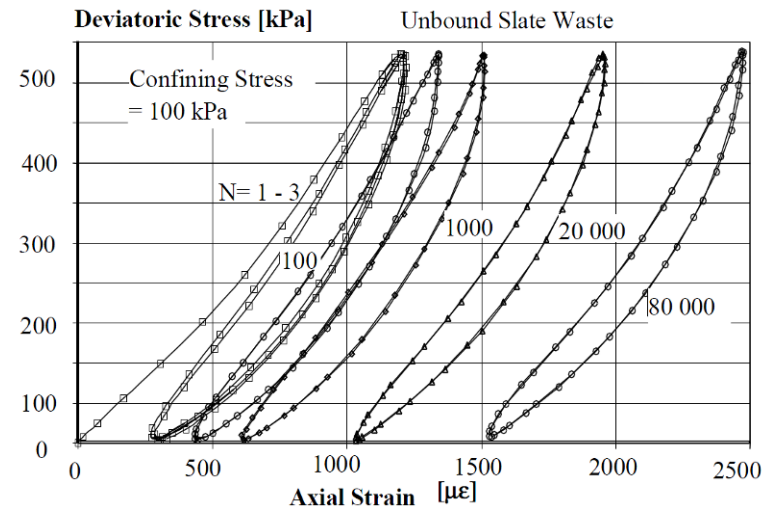


Figure 2.25 The stress-strain behaviour of unbound material under repeated loading (Dawson A R and F 1999)

Despite many years of research, the deformation mechanisms of UGMs are not yet fully understood. The non-linearity of the stress-strain relationship is affected by the structure of the grain assembly (the Hertz contact theory (Hertz 1982)). The deformation of UGMs under dynamic loading is the result of different mechanisms (Thom and Brown 1988). The resilient deformation is mainly caused by the deformations of the individual grains. In a stress-less state, the grains touch punctual (number 0 in Figure 2.26). When the force F , transmitted by the inter-particle contacts, is increased, the size of the inter-particle contact areas must increase due to the compression of those contacts - the resistance of the centres of individual aggregate particles approaching each other also increase. As illustrated in Figure 2.26, the displacement D_d between the particles (resilient deformation of the particles) decreases with the increase of the contact force DF .

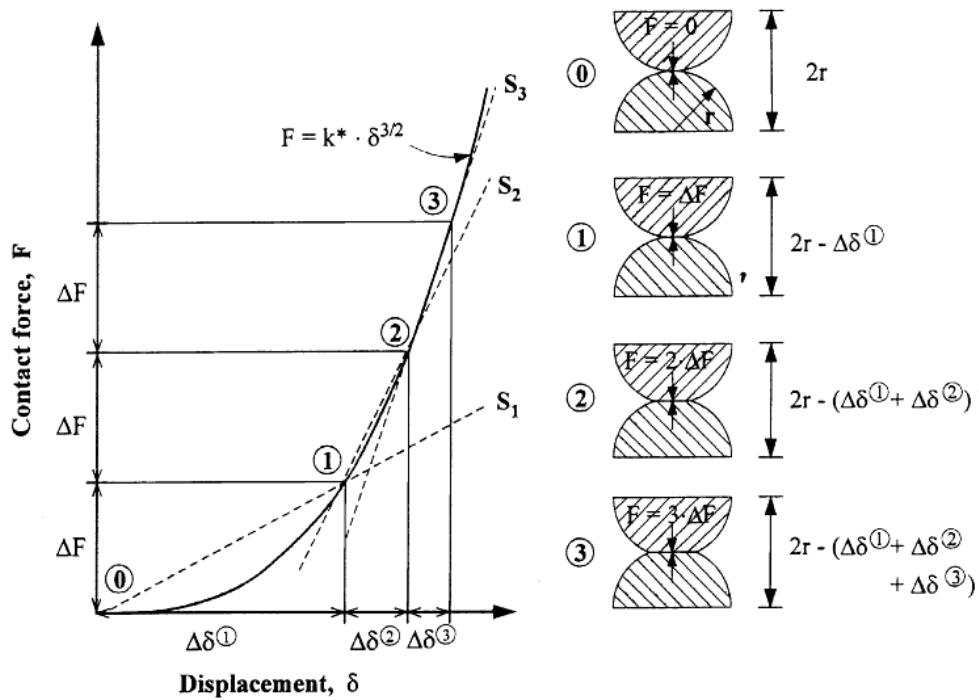


Figure 2.26 The dependence between the contact force F and displacement d between two particles (Kolisoja 1997)

However, at high stress levels, additional effects will probably affect the non-linear resilient deformation behaviour. In a densely compacted granular material, the particles are packed closely together leaving relatively small pores between the grains. Shear strain forces the particles to climb on each other and the volume increases. If the expansion is restricted, the dilatation will result in increased stiffness. Permanent deformation is mainly caused by a mechanism of re-orientation. The re-orientation mechanism is characterized by rotation and sliding of the individual particles. The resistance to particle sliding and rotation is dependent on inter particle friction. Grain breakage/crushing occurs if the contact stresses between the grains exceeds the strength of the grains and is governed by grain size, magnitude of applied stresses, mineralogy and strength of the individual particles (Lekarb 1997). Grain abrasion is defined as the spalling of small particles from the grain surfaces and this occurs even at low stress levels. Spalling occurs at the contact points between the grains once the local strength of the grains has been exceeded. Loading of the grains during the laying and compaction process is much more severe than under traffic loading. For this reason grain fragmentation is of minor importance during the service conditions of the pavement.

Thom and Brown (Thom and Brown 1988) used RLT tests to assess elastic stiffness, shear strength and susceptibility to permanent deformation. They recognized that elastic stiffness correlates among other things with frictional resistance at particle contact points which is dependent on the microscopic properties. The shear strength and the resistance against permanent deformation were found to be a function of visible roughness. The ranking of resistance against permanent deformation showed some similarity to those for shear strength, however, notable differences were recognized. The reason was argued to be that

the shear strength is influenced by the overall particle shape as well as its roughness. It was also argued that the loading, (whether dynamic or static) and the stress levels between the individual grains must be different. This was reflected by the fact that a direct dependency between the shear strength and the resistance against permanent deformation was not observed. For this reason, different micromechanical processes must be in play. However, to confirm these results further investigations are necessary.

2.4.2 Repeated loading behaviours

Granular materials always experience some non-recoverable deformation after each load application. After the first few load applications, the resilient (recoverable) deformation increases more than the non-recoverable deformation. If the load is small compared to the strength of the material and is repeated a large number of times, the deformation under each application is nearly completely recoverable and proportional to the load and can be considered elastic. This behaviour of granular materials is characterized by the resilient modulus. The term 'resilient' refers to that portion of the energy that is put into a material while it is being loaded and recovered when it unloaded. The rest of the energy that is not recovered when loaded is capable of doing work on the material. This work results in the accumulation of strain on repeated loading and unloading. This accumulated permanent strain in an aggregate base causes rutting. The deformational response of granular layers under traffic loading is characterized by a recoverable (resilient) deformation and a residual (permanent) deformation which is illustrated in Figure 2.27.

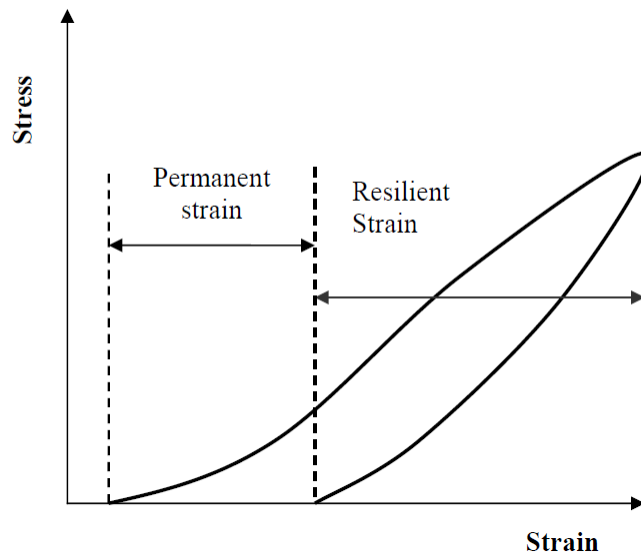


Figure 2.27 Basic strains in granular materials during each load cycle

Previous research indicates that repeated loading properties of granular materials like resilient modulus and permanent deformation accumulation are major factors that influence the structural response and performance of conventional permanent strain. These parameters are typically determined in a repeated load triaxial test which is performed by placing a specimen in a triaxial cell and applying repeated axial loads. After subjecting the specimen to a confining pressure, measurements are taken of the recoverable axial deformation and the applied load. Both resilient (recoverable) and permanent axial deformation responses of the specimen are recorded and used to calculate the resilient modulus and the permanent deformation, respectively.

2.4.2.1 Resilient modulus

The theory of elasticity traditionally defines the elastic properties of a material by the modulus of elasticity, E , and the Poisson ratio, ν . Dealing with unbound

aggregates in base layers, the elastic modulus E is replaced by the resilient modulus, M_r , to describe the elastic, recoverable behaviour of a material subjected to cyclic loading in a triaxial apparatus. The resilient modulus is known to be nonlinear and stress dependent. For repeated load triaxial tests with constant confining stress, the resilient modulus is defined as the ratio of the peak axial repeated deviator stress to the peak recoverable axial strain of the specimen. The resilient modulus of a material under constant confining pressure is expressed as:

$$M_r = \frac{(\sigma_1 - \sigma_3)}{\varepsilon_1} = \frac{\sigma_d}{\varepsilon_a^r} \quad (2.16)$$

where

M_r = resilient modulus,

σ_1 = major principal or axial stress,

σ_3 = minor principal or confining stress,

σ_d = deviator stress,

ε_1 = major principal or axial resilient strain, and

ε_a^r = axial resilient strain.

A resilient modulus test is in principle non-destructive, as most of the deformations are recovered. For these types of tests the same sample may be used several times. For high stress levels however, some permanent deformations will occur. In these cases the resilient modulus may sometimes be dependent on how large the permanent deformations are and the effect of changes in the structure of the material. In most cases, however when the initial phase of development of permanent deformations is over, the resilient modulus is independent of the permanent deformations. Lekarp (1999) presented a “state-of-the-art” on the research on the resilient modulus behaviour of unbound granular materials. Most of the research conducted on the response of unbound granular materials to cyclic

loading in a triaxial apparatus has concentrated on the resilient part of the deformation. By studying the literature on earlier research, Lekarp (1999) found that the resilient behaviour of unbound granular materials was affected by several factors, like; stress, density, moisture content, fines content, grading, aggregate type, number of load applications, stress history, load duration, frequency and load sequence. A great deal of effort has been made to develop models that can describe and predict the non-linear resilient behaviour of unbound granular materials. In this chapter, two of the oldest and most used models are discussed. More advanced models exist, taking the anisotropic behaviour or the resilient dilatancy into account (Hoff et al., 1999). However, these models have not been accepted into common use.

The k- θ model

The k- θ model is a non-linear, stress-dependent power function model first described by Seed et al. (1962). This curve-fitting model is based on the sum of principal stresses or bulk stress. It is the commonly used model to account for the stress dependency of a resilient modulus. In its dimensionless form, the model is given as follows:

$$M_r = k_1 \cdot \sigma_a \left(\frac{\theta}{\sigma_a} \right)^{k_2} \quad (2.17)$$

where

θ = bulk stress; $\theta = \sigma_1 + \sigma_2 + \sigma_3 = \sigma_1 + 2 \cdot \sigma_3$

k_1 and k_2 = model parameters from regression analyses of triaxial test results;

σ_a = reference pressure (100 kPa).

The original k- θ model has several shortcomings (Hicks and Monismith, 1971; Uzan, 1985). It considers the all-around bulk stress to represent triaxial stress states and does not account for the confining pressure and deviator (or shear) stress individually. Stress level is only accounted for by the bulk stress in this model. This means that all combinations of principal stresses giving the same sum will have the same effect on the resilient modulus.

The Uzans model

Uzan (1985) developed a new non-linear model from the k- θ model to account for the shortcomings of the earlier models. The effect of shear strain was taken into account, one of the serious shortcomings of the k- θ model. The model was first presented as follows;

$$M_r = k_1 \cdot \sigma_a \left(\frac{\theta}{\sigma_a} \right)^{k_2} \cdot \left(\frac{\sigma_d}{\sigma_a} \right)^{k_3} \quad (2.18)$$

where,

σ_d = deviator stress.

k_1 , k_2 and k_3 = model parameters from regression analyses of triaxial test results.

This model seems to fit well with results obtained from cyclic load triaxial testing and has been used by many researchers. It proved to be superior to the k- θ model (Kolisoja, 1997) and has been further developed for the three-dimensional case where deviator stress is replaced with octahedral shear stress.

2.4.2.2 Permanent deformation behaviour

Permanent deformations represent the non-recoverable part of the deformations. The plastic strain accumulates as the loading continues until the material is either rearranged into a stronger structure or failure occurs. Rutting is the most common

damage caused by permanent deformations in unbound granular layers. As mentioned earlier, most of the research work done on the deformation behaviour of unbound granular materials is concentrated on the resilient behaviour. Lekarp (1999) summarized the research on permanent deformations in a “state-of-the-art”. He found that the development of permanent strain was affected by several factors, like; stress level, principal stress reorientation, number of load applications, moisture content, stress history, density, fines content, grading and aggregate type. Lekarp (1999) also stated that there is a need for developing computational models for the prediction of permanent strain response in unbound granular materials. The existing models are mostly based on the effect of the number of load applications.

One of the main important aspects of the design philosophy for flexible pavements is the limitation of ruts in the pavement structure. Measuring rut development is relatively simple, but the prediction of rut development is extremely complex. The problem cannot be solved solely by accurate characterization of the pavement layers (e.g. asphalt layers, UGLs, subgrade); an assessment of the impact of environmental conditions and calculations of the appropriate stress distribution during the entire life of the pavement are also required. Although the largest amount of permanent deformation results from the asphalt layers, this deals with the different factors influencing the permanent deformation behaviour of UGMs. A number of summaries of the factors that influence the permanent deformation behaviour of UGMs can be found in the literature and one of the most recent reviews was presented by Lekarp (Lekarp 97).

2.4.2.3 Factors affecting repeated loading properties

Many factors simultaneously affect both the resilient modulus and permanent deformation properties of granular materials. However, their influence on the resilient modulus was not the same as on permanent deformation properties. In this section a brief overview of the factors influencing both the resilient modulus and permanent deformation is presented. The variation in the influence of these properties is also described.

- Aggregate type and particle shape

Previous research has shown that gravel has a higher resilient modulus than crushed limestone (Lekarp, Isacsson et al. 2000). However, many researchers have reported that crushed aggregate, having angular to subangular shaped particles, provides better load spreading properties and a higher resilient modulus than uncrushed gravel with subrounded or rounded particles. A rough particle is also said to result in a higher resilient modulus. Allen argued that angular materials, such as crushed stone undergo smaller plastic deformations compared to materials with rounded particles (Allen 1973). This behaviour was said to be the result of a higher angle of shear resistance in angular materials due to better particle interlock. Barksdale and Itani investigated the influence of aggregate shape and surface characteristics on aggregate rutting (Barksdale and Itani 1989). They concluded that a blade shaped crushed aggregate is slightly more susceptible to rutting than other types of crushed aggregate. Moreover, cube-shaped, rounded river gravel with smooth surfaces is much more susceptible to rutting than crushed aggregates (Lekarp, Isacsson et al. 2000).

- Compaction Method and density

Generally, two compaction methods are recommended for the preparation of test specimens: kneading or impact and static. The resilient modulus is directly related to the stiffness, which increases with an increase in compactive effort. This increase in stiffness varies with different materials and depends on the water content of which there was an increase in stiffness when going from standard Proctor energy up to a modified Proctor compaction energy.

Hicks and Monismith found the effect of density to be greater for partially crushed than for fully crushed aggregates (Hick and Monosmith 1971). They found that the resilient modulus increased with relative density for the partially crushed aggregate tested, whereas it remained almost unchanged when the aggregate was fully crushed. They further reported that the significance of changes in density decreased as the fine grains content of the granular material increased. Barksdale and Itani reported that the resilient modulus increased markedly with increasing density only at low values of mean normal stress (Barksdale and Itani 1989). At high stress levels, the effect of density was found to be less distinct. Vuong reported test results showing that at densities above the optimum value, the resilient modulus is not very sensitive to density (Vuong and Brimble 2000). Resistance to permanent deformation in granular materials under repetitive loading appears to be highly improved as a result of increased density. Barksdale studied the behaviour of several granular materials and observed an average of 185% more permanent axial strain when the material was compacted at 95% instead of 100% of maximum compaction density. Allen reported an 80% reduction in total plastic strain in crushed limestone and a 22% reduction in gravel as the specimen density was increased from Proctor to modified Proctor density (Allen 1973). For rounded aggregates, this decrease in strain with increasing

density is not considered to be significant, as these aggregates are initially of a higher relative density than angular aggregates for the same compactive effort (2).

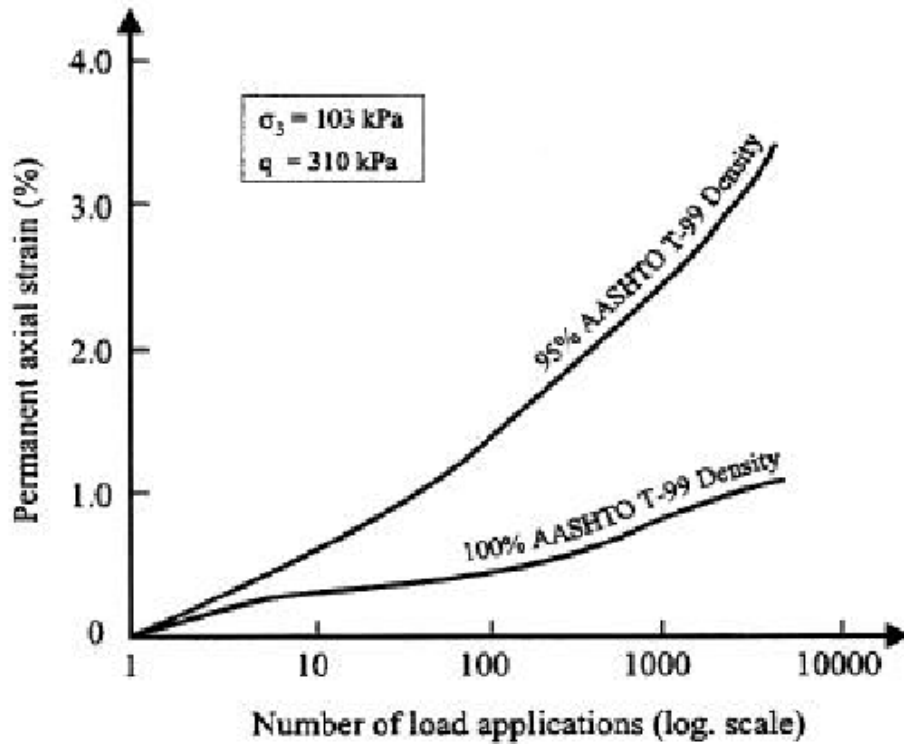


Figure 2.28 The effect of density on permanent strain (Barksdale and Itani 1989)

- Fine particle content

Studies demonstrating the variation in response of granular materials subjected to repeated axial stresses indicate that the fines content (percent passing No.200 sieve) can also affect the resilient behaviour (Hick and Monosmith 1971). Hicks and Monismith observed some reduction in the resilient modulus with increasing fines content for the partially crushed aggregates tested, whereas the effect was reported to be the opposite when the aggregates were fully crushed. The variation of fines content in the range of 2-10% was reported by Hicks to have a minor

influence on resilient modulus. Yet, a dramatic drop of about 60% in resilient modulus was noted by Barksdale and Itani when the amount of fines increased from 0 to 10%. An initially increasing stiffness and then a considerable reduction as clayey fines were added to a crushed aggregate. The effect of the fine content was investigated and it was noted permanent deformation resistance deformation in granular materials is reduced as the fines content increases as shown in Figure 2.29.

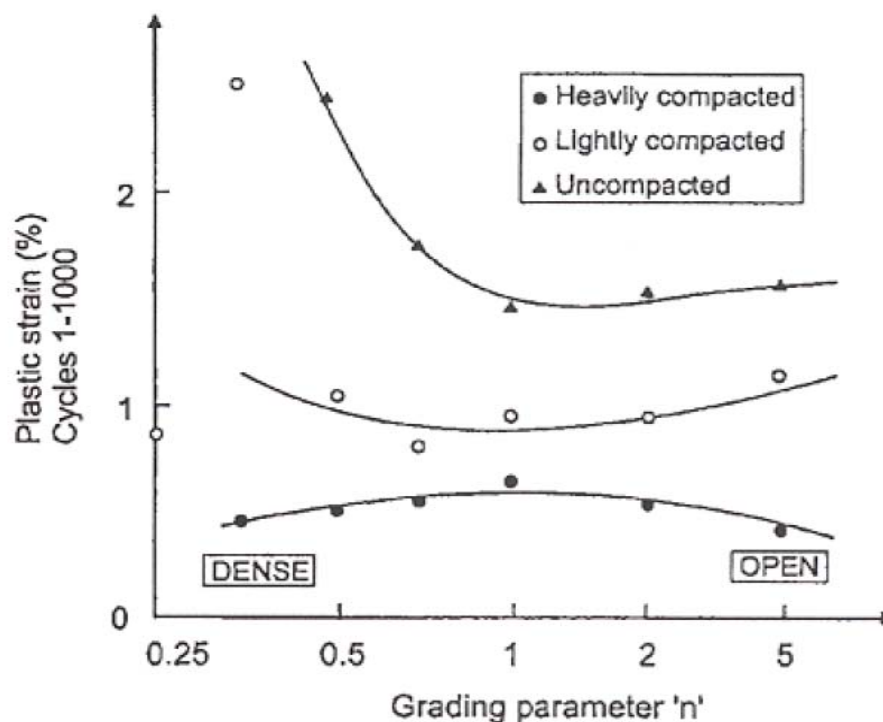


Figure 2.29 Effect of grading and compaction on plastic strain
(Barksdale and Itani 1989)

- Gradation and physical properties of grain

Kolisoja showed that for aggregates with similar grain size distribution and the same fines content, the resilient modulus increased with increasing maximum

particle size (Kolisoja 1997). As the size of the particle increases, the particle to particle contact decreases resulting in less total deformation and consequently higher stiffness. Thom and Brown concluded that uniformly graded aggregates were only slightly stiffer than well-graded aggregates (Thom and Brown 1988). They further indicated that the influence of gradation on the permanent deformation depends on the level of compaction. The effect of gradation on permanent deformation was more significant than the degree of compaction, with the highest plastic strain resistance for the densest mix.

If the grading is changed in such a way that relative density increases, then resistance to permanent deformation will rise. Significantly higher permanent strains may be expected for aggregates containing extremely high fines content ($d < 0.074 \text{ mm} > 15 \%$) or at a low content of fine as shown in Figure 2.30. This could be explained by the assumption that the entire fines fraction does not necessarily fit into the pore spaces between the large particles. Therefore a skeleton of larger particles in full contact does not exist. As a result the resistance against permanent deformation and stiffness decreases.

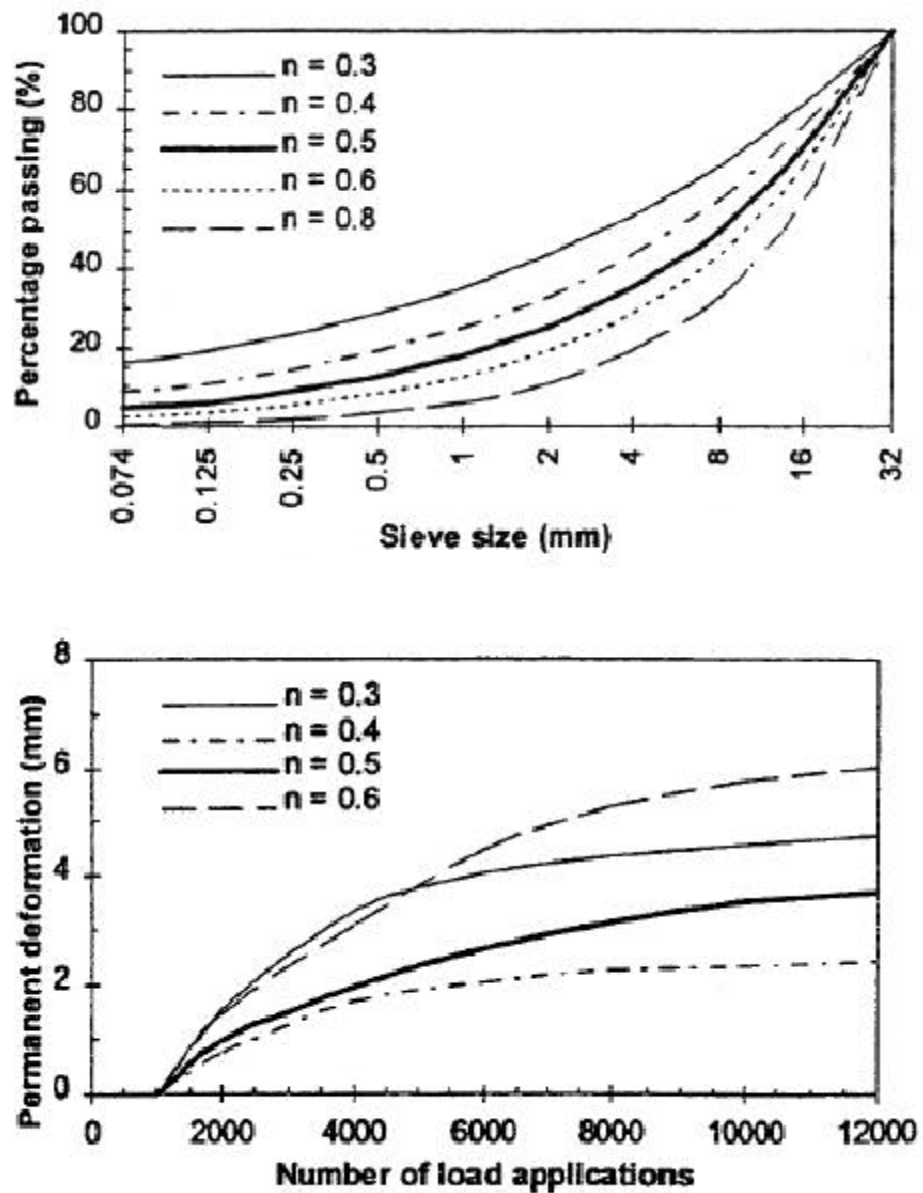


Figure 2.30 The effect of grain size distribution on the aggregate's susceptibility to permanent deformations (Kolisoja 1997)

A significant factor influencing the grain shape of coarse-grained aggregates is the mineralogical composition of the aggregate particles. The crushing technique used to produce the aggregates affects the grain shape of the crushed materials. With respect to grain shape, two general groups can be formed; the first group is composed of natural sands and gravels and the second group of crushed materials. In this group, particle contact is between two smooth surfaces, whilst in the second group (i.e. crushed aggregates) the particle edges can be very sharp. This difference between the natural aggregate having rounded grains and crushed aggregate having sharp-edged grains is of most significance in long term and permanent deformation behaviour. The crushed material is likely to have more grain abrasion than the natural aggregate, especially at high stresses.

Many investigations have addressed the effect of macro and micro roughness of the particles on the deformation behaviour (Thom and Brown 1988; Kolisoja 1997). The surface friction angle can be measured using a sliding type test performed by pulling a representative specimen of aggregate loaded on a rough test surface. The surface friction at the contact points of particles can be assumed to affect the resilient deformation behaviour, especially when the external load reaches the value, which makes the particles slide.

- Moisture content

In practice there is always water within an UGM later. The water film on the surface of the grains influences the shear resistance. The occurrence of a moderate amount of moisture benefits the strength and the stress and strain behaviour of UGMs. Having achieved total saturation, repeated load applications may lead to the development of positive pore water pressure with any further increases in the water content. Excessive pore water pressure reduces the effective stress, resulting in diminishing permanent deformation resistance of the material. Thus a high

water content within an UGL causes a reduction in stiffness and hence deformation resistance of the layer. Figure 2.31 shows RLT test results whereby both samples started at the same moisture content but one was allowed to drain, like a real UGM layer in pavements, (so it became dryer) while the other one stayed at the same moisture content and experienced a much larger amount of permanent deformation.

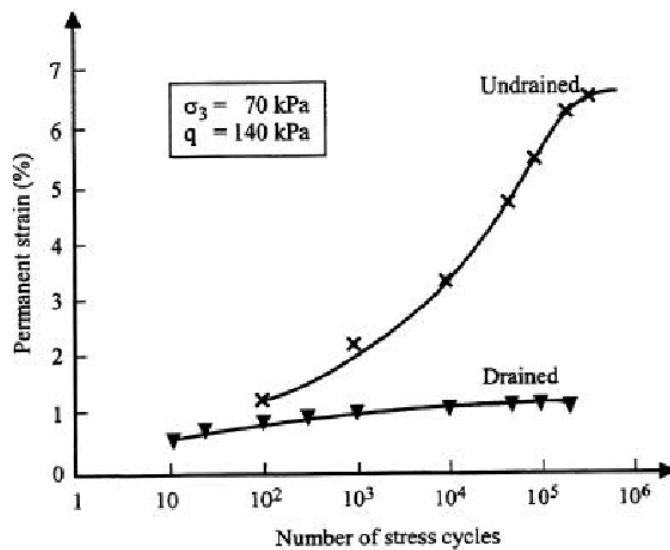


Figure 2.31 Influence of drainage on permanent deformation development
(Dawson A R and F 1999)

The moisture content of most untreated granular materials has been found to affect the resilient response characteristics of the material in both laboratory and in situ conditions. Many researchers who studied the behaviour of granular materials at high degrees of saturation have all reported a notable dependence of resilient modulus on moisture content, with the modulus decreasing with growing saturation level (Lekarp, Isacsson et al. 2000). Research has shown that the effect of moisture also depends on the analysis. Hicks stated that a decrease in the resilient modulus due to saturation is obtained only if the analysis is based on total

stresses (Hick and Monosmith 1971). At below the optimum moisture content stiffness tends to increase with increasing moisture level, apparently due to development of suction. Beyond the optimum moisture content, as the material becomes more saturated and excess pore water pressure is developed, the effect changes to the opposite and stiffness starts to decline fairly rapidly. As moisture content increases and saturation is approached, positive pore pressure may develop under rapid applied loads. Excessive pore pressure reduces the effective stress, resulting in diminishing permanent deformation resistance of the material. The literature available suggests that the combination of a high degree of saturation and low permeability due to poor drainage leads to high pore pressure, low effective stress, and consequently, low stiffness and low deformation resistance. In a study conducted by Haynes and Yoder (Haynes and Yoder 1963), the total permanent axial strain rose by more than 100% as the degree of saturation increased from 60 to 80%. Barksdale observed up to 68% greater permanent axial strain in soaked samples compared with those tested in a partially soaked condition (Barksdale 1972). Thompson reported results of repeated load triaxial tests on the crushed stone from the AASHTO Road Test at varying degrees of saturation (Thompson M. R. and Naumann 1993). In all cases, the samples experienced a substantial increase in permanent deformation after soaking. It was suggested that one reason for the observed increase was the development of transient pore pressures in the soaked samples.

Holubec performed RLT tests and studied the deformation behaviour of drained crushed aggregates at a range of water contents (Holubec 1969). The test results showed that increasing the water content led to higher permanent deformations. At 1,000 load cycles, the total permanent axial strain of a waterbound macadam pavement rose by about 300 % as the water content increased from 3.1% to 5.7%. Similarly, the total permanent axial strain of gravel sand grew up to 200 % as the

water content increased from 3 % to 6.6 %. Thom and Brown studied the impact of the water content on the permanent deformation behaviour of Dolomite-material (Thom and Brown 1988). The outcome of the investigation showed a serious increase of permanent deformations resulting from the rise in water content of the specimens. Furthermore, it became clear that a relatively small increment of water content had a disproportionate effect on the increase in permanent deformation. This tendency was also observed without the creation of pore water pressure. It was stated that this behaviour could be attributed to the fact that the existence of water within granular assemblies partly lubricated the particles and consequently resilient as well as permanent deformations rose.

- Specimen size

Austroad and AASHTO specifies that the diameter of the specimen is a function of the maximum size of the aggregate used in the base material. Further, it specifies that the diameter to height ratio is 1:2 (Voung and Brimble 2000; AASHTO 2002). Thus, according to this for a maximum aggregate size of 19 mm, the size of the specimen is 100 mm in diameter with a height of 200 mm. Reliable results could be obtained with soil specimens having regular ends provided the slenderness (height to diameter ratio, l/d) is in the range of 1.5 to 3.0. Since then, many researchers have studied end restraint effects on the shear strength of soils and concluded that sample slenderness can be reduced to 1.0 if frictionless platens are used (Adu-Osei 2000). Adu-Osei et al. changed the specimen size from a l/d ratio of 2:1 to 1:1. They found that specimens with l/d ratio of 2:1 gave reliable results when the end platens were lubricated. These specimens were also more stable and practical.

- Stress state

Previous investigations and studies show that stress state has the most significant impact on the resilient and permanent properties of granular materials and that duration and frequency have very little effect. Hicks conducted tests at stress durations of 0.1, 0.15, and 0.25 s and found no change in the resilient modulus (Hick and Monismith 1971). However, the resilient modulus increases considerably with an increase in confining pressure and sum of principal stresses. Monismith et al. reported an increase as great as 500% in the resilient modulus for a change in confining pressure from 20 kPa to 29 200 kPa (Monismith, H. B. Seed et al. 1967). An increase of about 50% in the resilient modulus was observed by Smith and Nair when the sum of principal stresses increased from 70 kPa to 140 kPa (Smith and Nair 1973). Allen and Thompson compared the test results obtained from both constant confining pressure tests (CCP) and variable confining pressure tests (VCP) (Allen 1973) as shown in Figure 2.32. They reported higher values of the resilient modulus computed from the CCP test data. They showed that the CCP tests resulted in larger lateral deformations. Brown and Hyde suggested later that VCP and CCP tests yield the same values of resilient modulus provided that the confining pressure in the CCP test is equal to the mean value of the pressure used in the VCP test (Brown and Hyde 1975).

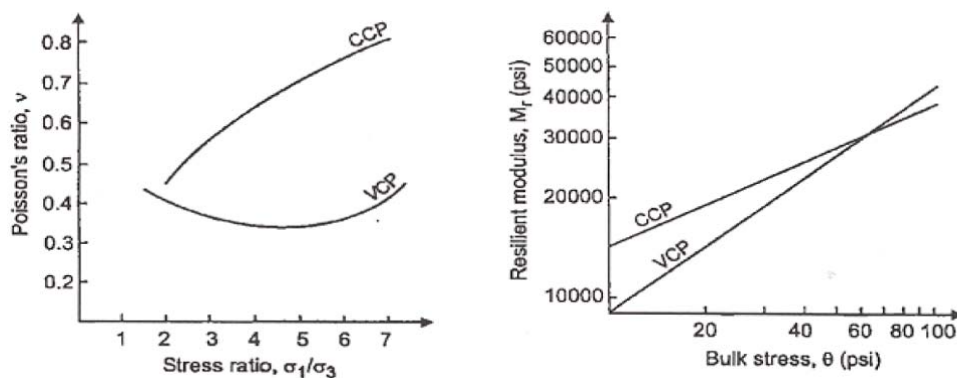


Figure 2.32 Triaxial test results with CCP and VCP (Allen 1973)

Many studies have indicated a high degree of dependence on confining pressure and the first stress invariant (sum of principal stresses) for the resilient modulus of untreated granular materials. The resilient modulus is said to increase considerably with an increase in confining pressure and the sum of principal stresses, while permanent deformation decreases with an increase in confining pressure. Compared to confining pressure, deviator or shear stress is said to be much less influential on the resilient modulus of the material. In laboratory triaxial testing, both constant confining pressure and variable confining pressure are used.

Brown and Hyde suggested that variable confining pressure and constant confining pressure tests yield the same values of resilient modulus, provided that the confining pressure in the constant confining pressure test is equal to the mean value of the pressure used in the variable confining pressure test (Brown and Hyde 1975). The accumulation of axial permanent strain is directly related to deviator stress and inversely related to confining pressure. Several researchers have reported that permanent deformation in granular materials is principally governed by some form of stress ratio consisting of both deviator and confining stresses. Lekarp and Dawson argued that failure in granular materials under repeated loading is a gradual process and not a sudden collapse as in static failure tests (Lekarp, Isacsson et al. 2000). Therefore, ultimate shear strength and stress levels that cause sudden failure are of no great interest for analysis of material behaviour when the increase in permanent strain is incremental. The magnitude of permanent deformations developed strongly depends on the stress level and increases with rising deviator stress and decreasing confining stress. Morgan studied the behaviour of sand under repeated loading with an increasing number of load cycles and observed the impact of deviator stress and confining stress on the cumulative permanent deformations (Morgan J R 1966). A direct dependency

between the sum of permanent strains, number of load cycles applied and deviator stress was found at a particular level of confining stress. By maintaining the deviator stress at a steady level, the permanent axial strains were inversely proportional to confining stress levels. Barksdale conducted numerous RLT tests on UGMs at constant confining pressures and up to 100,000 load cycles (Barksdale 1972). He drew the conclusion that permanent deformations were highly dependent on the applied load and increased when confining pressure decreased and deviator stress rose. Pappin studied a limestone of good grading with RLT tests (Pappin J W 1979). He recognised the permanent strains to be a function of the length of the stress path and the stress ratio (deviator stress/confining stress). The resistance to permanent deformation decreased when the applied stress approached the failure curve, i.e. the accumulated permanent strains increased at rising deviator stress.

- Stress history

Studies have indicated that stress history may have some impact on the resilient behaviour of granular materials. Repeated load triaxial tests on samples of a well-graded crushed limestone were studied, all compacted to the same density in a dry state (Brown and Hyde 1975). The results showed that the material was subjected to stress history effects, but these could be reduced by preloading with a few cycles of the current loading regime and avoiding high stress ratios in tests for resilient response. Hicks reported that the effect of stress history is almost eliminated and a steady and stable resilient response is achieved after the application of approximately 100 cycles of the same stress amplitude (Hick and Monosmith 1971). Allen suggested that specimens should be conditioned for approximately 1,000 cycles prior to repeated load resilient tests (Allen 1973). The resilient characteristics of unbound granular materials are basically insensitive to stress history, provided the applied stresses are kept low enough to prevent

substantial permanent deformation in the material. Therefore, large numbers of resilient tests can be carried out sequentially on the specimen to determine the resilient parameters of the material. Permanent deformation behaviour of granular materials is directly related to the stress history. Brown and Hyde showed that the higher the stress level, the higher is the permanent deformation as shown in Figure 2.33 (Brown and Hyde 1975). They also indicated that permanent strain resulting from a successive increase in the stress level is considerably smaller than the strain that occurs when the highest stress is applied immediately.

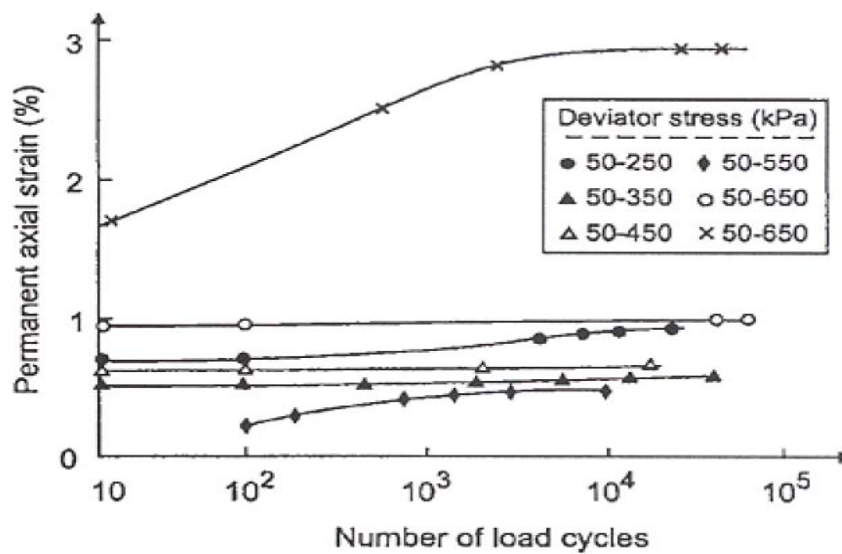


Figure 2.33 The effect of stress history on permanent strain
(Brown and Hyde 1975)

The number of load repetitions does not only affect the permanent strain response but always has to be considered as a combination of the number of load repetitions and the stress condition. If the intensity of the applied loading is not too high, the accumulation of permanent deformations on a certain stress path is normally assumed to stabilise as the number of load repetitions increases. The

curve representing the accumulated permanent deformation asymptotically approaching a limiting value, i.e. the permanent deformation rate per load cycle tends towards zero. Increasing stress ratios lead to a progressive rise of the accumulating permanent deformations. The number of load repetitions required while investigating the permanent deformation behaviour in RLT tests is of great importance from a practical point of view (time required for completing the tests and hence overall experimental costs). Sometimes this number of load repetitions is not adequate. Kolisoja found that specimens can apparently stabilize after 80,000 load cycles (degressive curve linearity) (Kolisoja 1997) as shown in Figure 2.34.

Morgan studied the behaviour of two types of sand under a repeated vertical load at both constant and varying confining pressures using a RLT apparatus (Morgan J R 1966). He applied up to 2 million load cycles and recognized that even towards the end of the tests the permanent deformations still increased. Barksdale investigated the behaviour of UGMs using RLT tests at constant confining pressure and dynamic deviator stress (Barksdale 1972). After applying 100,000 load cycles, he reasoned that permanent axial deformations rise linearly with the logarithm of the number of load cycles. Furthermore he discovered that the increase in permanent deformations under very small deviator stresses slowed down for growing numbers of load repetitions. By exceeding a certain level of deviator stress the permanent deformation development increased with a growing number of load cycles. Barksdale's test results showed a possible sudden rise of the increment of permanent deformations after a relatively high number of load repetitions.

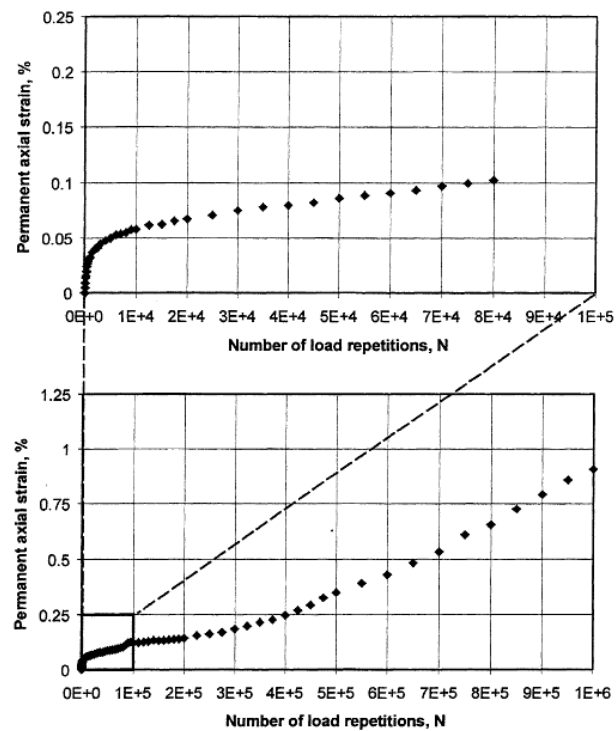


Figure 2.34 An example of the effect of the number of load repetitions on the permanent axial strain of a RLT test specimen (Kolisoja 1997)

Even though the effect of stress history on permanent deformation behaviour is recognized, very limited research appears to have been carried out to study this effect. In current laboratory permanent deformation tests, the effect of stress history is normally eliminated by using a new specimen for each stress path applied.

2.4.3 The shakedown concept

2.4.3.1 Introduction

The shakedown concept has been used to explain the behaviour of conventional engineering structures under repeated cyclic loading. Basically, it was originally

developed to analyse the behaviour of pressure vessels subjected to cyclic thermal loading. Subsequently, it was improved to analyse the behaviour of metal surfaces under repeated rolling or sliding loads. For the theoretical approach of the UGMs permanent deformation used to describe the behaviour of tested materials under repeated cyclic loading, triaxial tests under macro-mechanical observations of the material response and the distribution of the plastic deformation in the tested material were investigated. They can predict progressive accumulations of plastic strains under repeated loading and whether the amount of the applied loads exceeds a certain limited-value called the shakedown limit or limit load (SAMARIS 2004).

Firstly, the possible employment of the shakedown concept in pavement design was introduced by Sharp and Booker (1984) and Sharp (1983). They explained the application of the concept based on the tested results of the AASHO road tests (AASHTO 1986) where in some cases, deterioration was reported due to stiffening or post-compaction after a number of load cycles (Kent 1962). Moreover, studies have been produced to obtain upper-bound (Collins and Boulbibane 1998) and lower-bound (Yu and Hossain 1998) for the shakedown limit of UGMs in simple pavement structures. At low stress levels, the mechanism of permanent deformation has an initial post compaction or re-arrange phase, while the permanent strain rate is relatively high although this is reduced with increasing numbers of load cycles. A stable state may be maintained for a period of time unless the states change. Maree reported the behaviour of gravel and crushed stone and that under constant confining stress, the specimens stabilised under a certain threshold of repeated deviator stress and developed a design procedure, based on a failure model (Maree et al. 1982). Numerous investigations have been conducted regarding the behaviour of UGMs used in flexible pavements. Lekarp summarized the main findings regarding the effects of

different material parameters on the permanent strain response of UGMs and the maximum applied stress in UGM layers is within the maximum repeated deviator stress limit (Lekarp, Isacsson et al. 2000). The original shakedown concept maintains that there are three ranges of permanent deformation response under repeated loading as shown in Figure 2.35.

- Plastic shakedown range (Range A). The loading levels apply below the plastic creep range and the material response indicates plastic in a few initial cycles, although the ultimate response is elastic after Post-compaction. The deformation is completely resilient and does not develop any permanent deformations when it reaches a state of stability as shown in Figure 2.36.
- Plastic creep range (Range B). The applied loading level is low enough to avoid a quick incremental collapse. The material achieves a long-term stable state response with any accumulation of plastic strain (Post-compaction) however, the material will show failure with a large number of load cycles after a stable state.
- Incremental collapse range (Range C). The repeated loading is relatively large so that plastic strain accumulates rapidly with failure occurring in a small number of load cycles after stiffening as shown in Figure 2.37.

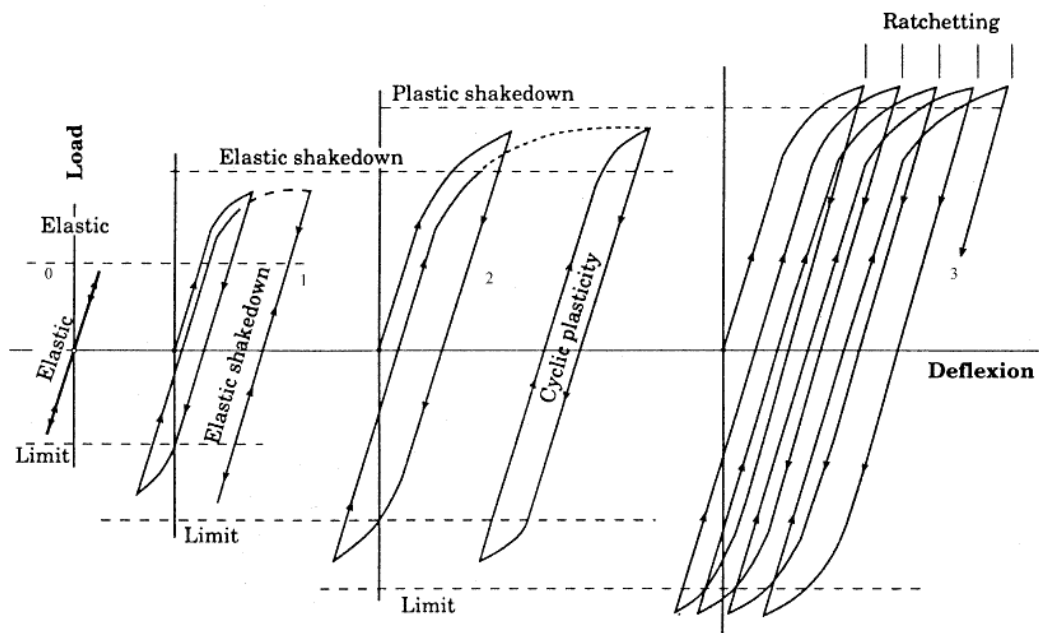


Figure 2.35 Elastic/permanent behaviour under repeated cyclic pressure and tensile load (Johnson 1996)

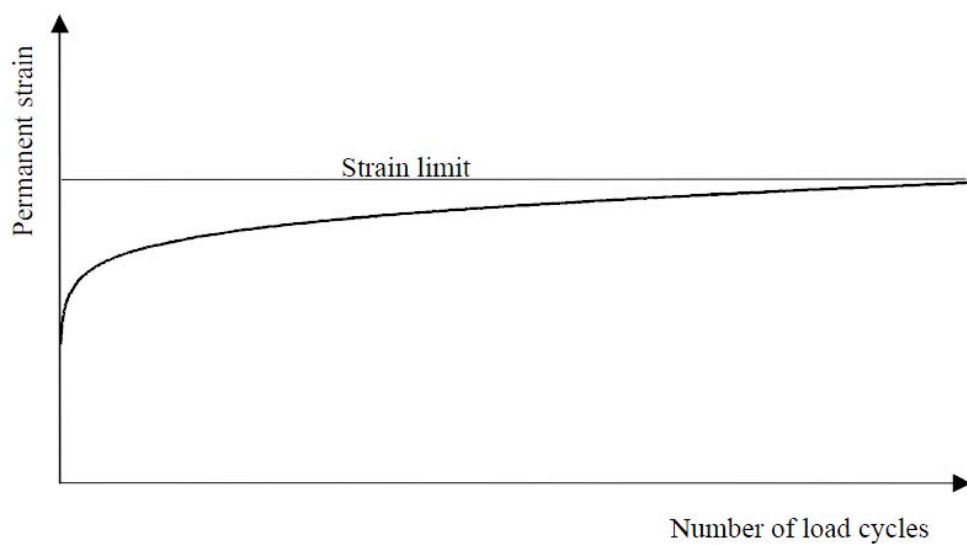


Figure 2.36 Permanent deformation behaviour at low stress level (stable conditions)

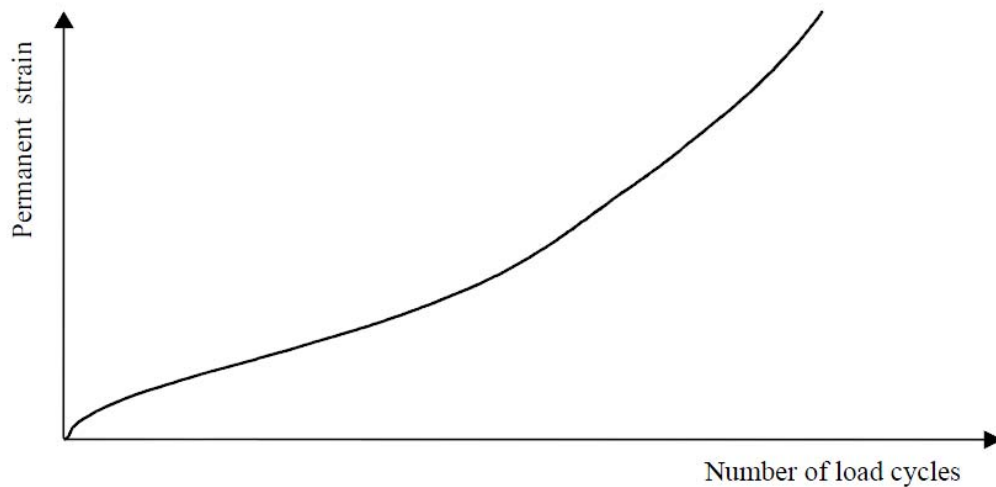


Figure 2.37 Permanent deformation behaviour at high stress level (unstable conditions)

A pavement is likely to show progressive accumulation of permanent strains (rutting) under repeated traffic loading if the magnitude of the applied loads exceeds the limiting value (Range C). If the applied traffic loads are lower than this limit, after any post-compaction stabilisation, the permanent strains will level off and the pavement will achieve a stable state of “shakedown” (Ranges A and B) presenting only resilient deformation under additional traffic loading (Sharp 1985). This implies an adaptation by the pavement subjected to the working load. This could be due to a change in material response (compaction degree), due to a change in stress state or due to a combination of both effects. With this understanding of the components of material behaviour, the shakedown concept typically then adopts classical upper and/or lower bound limit theorems. These incorporate the appropriate shakedown limit stress states (rather than the higher stress state associated with static failure) to compute the load carrying capacity of the structure if it is not to reach excessive permanent strain. Multilayer systems

such as pavements are subjected to repeated traffic loads of various magnitudes and number of load cycles. For performance prediction, it is of great importance to know whether a given pavement will experience progressive accumulation of permanent deformation leading to state of incremental collapse or if the increase in permanent deformation will cease, resulting in a stable response (shakedown state).

2.4.3.2 Permanent strain under a number of load cycles models

In the long-term behaviour model of pavements, it is essential to take into account the accumulation of permanent strain with the number of load cycles and stress levels that play an important role. Hence the main research purpose focussing on long-term behaviour should be to establish a constitutive model which predicts the amount of permanent strain at any number of cycles at a given stress ratio. The constitutive models of the permanent strain behaviour of UGMs are much less developed than models of the resilient strain behaviour. In the past, the permanent deformation of aggregates for pavement applications has been modelled in a variety of ways. Some of these are logarithmic with respect to the number of loading cycles (Barksdale 1972; Sweere 1990) whilst others are hyperbolic, tending towards an asymptotic value of deformation with increasing numbers of load cycles (Wolff and Visser 1994; Paute, Horny et al. 1996). A recent review of permanent behaviour referred to many different models and some of which will now be presented. The first type is that due to this approach, the permanent axial strain of a RLT test specimen is supposed to accumulate in a linear relation to the logarithms of the number of the load cycles (Barksdale 1972) as follows Equation (2.19):

$$\epsilon^p = a + b \log(N) \quad (2.19)$$

where ε^p is permanent deformation in Micrometers; a and b are regression constants; and N is the number of loading cycles. The long-term deformation behaviour of UGMs was also investigated by Sweere in a series of RLT tests. He suggested that for a large number of load cycles the following approach should be employed:

$$\varepsilon^p = A \cdot N^B \quad (2.20)$$

where:

ε^p	[10 ⁻³] % permanent strain
A, B	[-] regression parameters
N	[-] number of load cycles.

To implement the RLT measured permanent strain development in the computation of permanent strain development in a pavement structure, the strain in the material under consideration has to be known as a function of both the number of load cycles and the stresses in the materials. Furthermore the shakedown approach should be considered. Lekarp and Dawson (Lekarp and Dawson 1998) suggested that the shakedown approach might also be employed in explaining the permanent deformation behaviour of UGM. By carrying out RLT tests on different UGMs, they defined a relationship between the accumulated permanent strain after a defined number of load cycles, the stress path length and the maximum shear normal stress ratio.

Comparisons of measured and model predicted values displayed close similarities to the shakedown concept. In conclusion, they pointed out that more research is required to determine this shakedown limit. However, for FE calculations of UGM as part of a FE based pavement design, the prerequisite is a stress and load cycles dependent model for the permanent deformation behaviour of UGM. Some

stress dependent models are available (Barksdale 1972) but two, the Theyse-Model and the Huurman-Model, use the shakedown approach, in particular modelling the stable and unstable permanent deformation behaviour to model the permanent deformation behaviour of UGM as a function of the number of load cycles. Similar to what Sweere (1990) found for his laboratory test results, the log-log approach was also used by Huurman (Huurman 1997) to describe the permanent strain development (axial and radial) in UGM in pavements under traffic by Equation (2.21). Huurman used a RLT apparatus to determine the permanent deformation behaviour of different sands.

$$\varepsilon^p = A \cdot \left[\frac{N}{1000} \right]^B + C \left[e^{\frac{D \cdot N}{100}} - 1 \right] \quad (2.21)$$

where:

- ε^p [%] permanent strain
- e [-] base of the natural logarithm (= 2.17828....)
- N [-] number of load cycles.

The first term of the model describes a linear increase of permanent strain with N on a $\log(\varepsilon^p)$ - $\log(N)$ scales. Parameter A gives the ε^p at 1,000 load cycles and B gives the subsequent slope of ε^p with the rising number of load cycles. In the case of stable behaviour, model parameters C and D are equal to zero. It is clear that the unstable behaviour at high stress levels can not be described by the first term alone because an exponential rather than linear increase of ε^p with N on the same $\log(\varepsilon^p)$ - $\log(N)$ scales is observed. To implement the RLT, measured permanent strain development in the computation of permanent strain in a pavement structure, the permanent strains in the materials have to be determined as a function of the applied stresses and the number of load cycles. However, the determination of parameters A, B, C and D for the model proposed by Huurman

depends on σ_1 = major principal stress and $\sigma_{1,f}$ = major principal stress at failure. In this investigation it was found from tests that $\sigma_{1,f}$ could not be obtained for the crushed UGMs, as already explained. In this research the plastic Dresden-Model as developed at the Dresden University of Technology has been used to determine parameters A and B as a function of the principal stresses σ_1 and σ_3 for Range A (Equations (2.22) and (2.23)) and for Range B (Equations (2.24) and (2.25)):

$$A = (a_1 \cdot e^{a_2 \sigma_3}) \sigma_1^2 + (a_3 \cdot \sigma_3^{a_4}) \sigma_1 \quad (2.22)$$

$$B = (b_1 \cdot e^{b_2 \sigma_3}) \sigma_1 + (b_3 \cdot \sigma_3^{b_4}) \quad (2.23)$$

$$A = (a_1 \cdot \sigma_3^{a_2}) \left(\frac{\sigma_1}{\sigma_3} \right)^2 + (a_3 \cdot \sigma_3^{a_4}) \frac{\sigma_1}{\sigma_3} \quad (2.24)$$

$$B = (b_1 \cdot \sigma_3^{b_2}) \left(\frac{\sigma_1}{\sigma_3} \right) + (b_3 \cdot \sigma_3^{b_4}) \quad (2.25)$$

where:

σ_3 [kPa] minor principal stress (absolute value)

σ_1 [kPa] major principal stress (absolute value)

a_2, a_3, b_2, b_3 model parameters

a_1, a_4, b_1, b_4 model parameters.

As already mentioned, the behaviour observed for the higher stress level cannot be described by means of Equations (2.22)-(2.25). A second term was therefore, added to Equation (2.21). The model parameters C and D are again stress dependent. By analysing the test results, parameters C and D become available to recognise collapse. In this research, parameters A, B, C and D were also determined. Finally, it was realised that it is possible to model the permanent

deformation behaviour of UGMs in a stress dependent way. However, it is necessary to model each behaviour range separately. As already described, several other researchers in the past have attempted to correlate repeated and static failure load test results. This approach has received mixed support because the deformation behaviour of UGM is regarded as very complex and the repeated and static load tests do not necessarily induce the same structural responses. For this reason it is necessary to develop an empirical model that is dependent on the number of load cycles and stresses σ_1 and σ_3 . However, the HUURMAN-Model described earlier should form the basis for further investigations on the permanent deformation behaviour of UGMs. This model uses one simple equation with few parameters only to describe the permanent deformation behaviour in the stable range as well as in the unstable range.

CHAPTER 3

RESEARCH METHODOLOGY AND EXPERIMENTAL PROGRAM

3.1 Overview

This chapter shows the research methodology and the experimental program followed in this study, the main objective of which is to evaluate the comprehensive characterisation of conventional road base materials of Western Australia, based on sophisticated laboratory test results, inherent responses, numerical and mechanistic approaches in order to implement effectively current pavement analysis and design. The study focuses on crushed rock base (CRB) and hydrated cement treated crushed rock base (HCTCRB) which are extensively used as unbound granular road base materials in Western Australia. The research plan was designed to facilitate sophisticated laboratory works as shown in Figure 3.1 to which indicates the pathway to project destination. Firstly, the basic characteristics of CRB and HCTCRB were investigated in order to expose their appearance and physical characteristics. Subsequently, more complicated responses were determined of their performances for improving knowledge of mechanical behaviour under various environmental conditions. Once the experiment programs had been completed, analysing the laboratory test results and numerical procedures were carried out then the application of the results to implement pavement analysis and design would be addressed. Finally, conclusions and recommendations were drawn.

This chapter describes the materials tested within the Geomechanics laboratory at Curtin University of Technology. The methodology and the experiment program including methods and testing procedures are presented as follows:

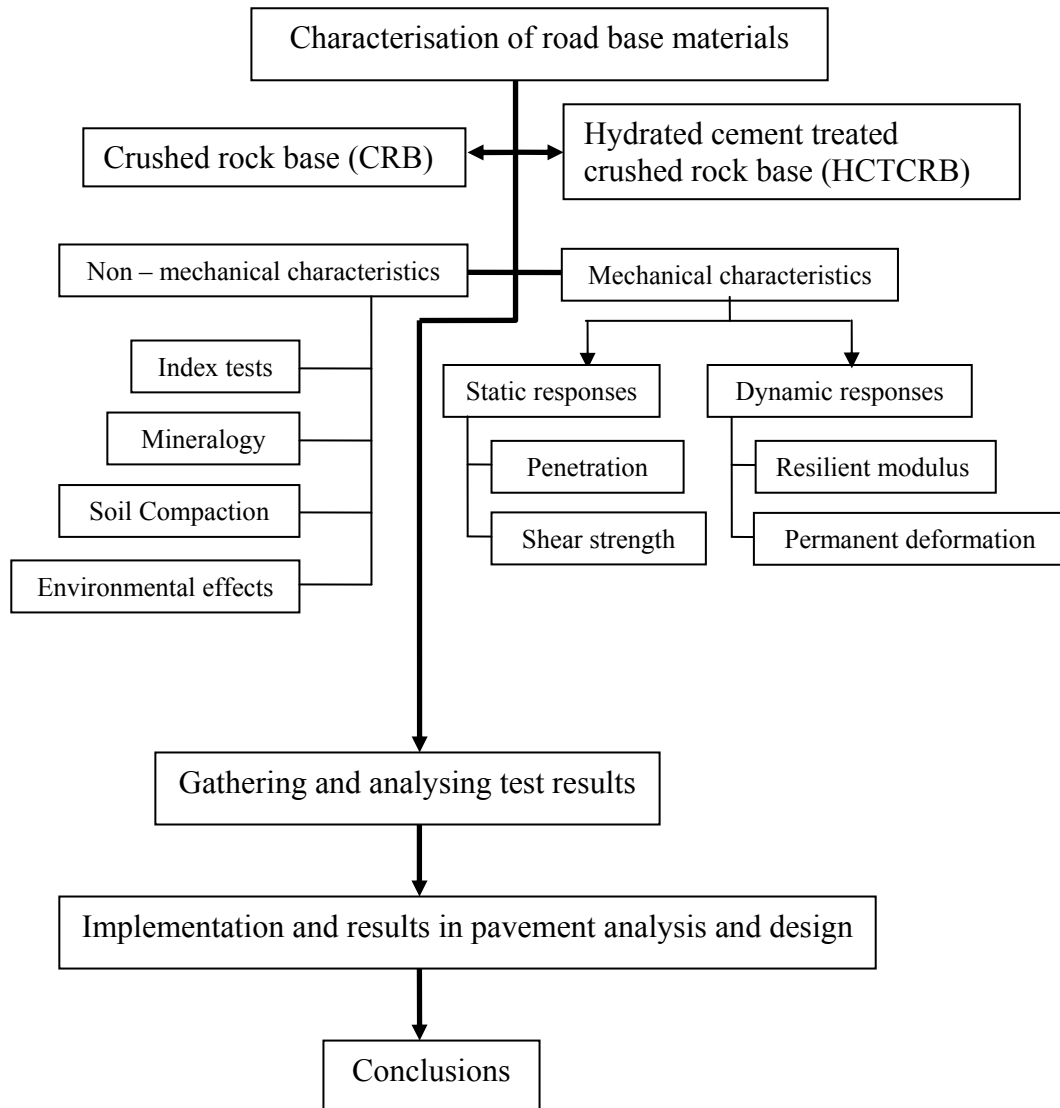


Figure 3.1 The overall research diagram of the study

3.2 Main materials in this study

3.2.1 Crushed Rock Base (CRB)

Crushed rock is composed of rock fragments produced by the crushing and screening of igneous, metamorphic or sedimentary source rock which conforms to specification requirements (Main Roads Western Australia 2006) that source rock for the production of crushed rock and aggregates, with or without additions, produced in a controlled manner to achieve standards for grading, plasticity etc. Despite CRB and HCTCRB are usually used for road base material, a number of responses are still unknown on complex and dynamic parameters including moisture sensitivity, cohesion internal friction and resilient modulus and permanent deformation discussed in this study.

The crushed rock samples used in this study were collected from a local stockpile of a Gosnells quarry as shown in Figure 3.2 and kept in sealed containers. For the previous test results, the local stockpile passed the basic standard and material properties of base course specifications (Main Roads Western Australia 2003) as shown in Table 3.1.



Figure 3.2 The CRB sample used in this study

Table 3.1 Characterisation tests (Main Roads Western Australia 2007)

Tests*	Results	Tests*	Results
Liquid Limit, LL	22.4%	Coefficient of uniformity, Cu	22.4
Plastic Limit, PL	17.6%	Coefficient of curvature (Cc)	1.4
Plastic Index, PI	4.8%	% fines	5 %
Linear Shrinkage, LS	1.5%	Flakiness Index, FI	22.5%

* Test methods in accordance with MRWA Test Method (MAIN ROADS Western Australia 2006)

** Drained triaxial compression tests at 100% OMC.

3.2.2 Hydrated cemented treated crushed rock base (HCTCRB)

Presently, traffic growth has raised both magnitude and quantity resulting natural and existing pavement materials are unable to cope with any premature deterioration. Local road authorities are attempting to seek a higher potential material than currently existing. Stabilisation and modification were found as alternative methods to improve material properties of natural material. Hydrated cemented treated crushed rock base (HCTCRB), an alternative material, is manufactured by blending 2 % cement with a standard dry weight crushed rock base (Main Roads Western Australia 2003). It is mixed and stockpiled in the range of -1.0% to +2.0% of the optimum moisture content of the untreated crushed rock base as obtained by MRWA Test Method WA 133.1 (Main Roads Western Australia 1997) during the initial hydration 7-day period based on MRWA specification (Main Roads Western Australia 2007). Subsequently, stockpiled material was retreated to break chemical bonding for keeping HCTCRB as a modified material then placed as a pavement base course. HCTCRB clearly presents more strength improvement but there is doubt about its water susceptibility and mechanical responses for long term performance.

3.2.3 Cement

The cement used in this study was the bagged product of Cockburn Cement (Cockburn Cement 2006) of General Purpose Portland Cement -type GP following the standard of AS 3972-1977 (Australian Standard 1997) as shown in Table 3.2.

Table 3.2 General specifications of the cement (COCKBURN CEMENT 2006)

Parameter	Method	Units	Typical	Range	AS3972-1977 limits
Chemical Analysis					
SiO ₂	XRF	%	20.7	19.5-21.6	-
Al ₂ O ₃	XRF	%	4.8	4.5-5.3	-
Fe ₂ O ₃	XRF	%	2.7	2.3-3.1	-
CaO	XRF	%	63.8	62.2-65.5	-
MgO	XRF	%	2.1	1.5-2.8	-
SO ₃	XRF	%	2.5	2.0-3.2	3.5% max
LOI	AS2350.2	%	1.8	0.5-2.7	-
Chloride	ASTM C114	%	0.01	0.01-0.02	-
Na ₂ O equiv.	ASTM C114	%	0.50	0.45-0.65	-
Fineness Index	AS2350.8	m ² /kg	400	350-450	-
Normal Consistency	AS2350.3	%	29.5	28.0-30.0	-
Setting Times	AS2350.4				
Initial		mins	120	90-150	45mins min
Final		mins	190	135-210	10 hrs max
Soundness	AS2350.5	mm	1	0-2	5 mm max
Compressive Strength	AS2350.11				
3 days		MPa	38	33-40	-
7 days		MPa	48	41-52	25MPa min
28 days		MPa	60	53-68	40MPa min

3.3 Non-mechanical characterization

The non-mechanical behaviour of soil is the primary characteristics of materials that is indicated and classified for road construction or any other purpose. The characteristics of pavement materials usually are required to classify types, sources, arrangement, physical appearance and index properties of such material.

Consequently, the non-mechanical properties of test materials have to be preliminary evaluated regarding the likelihood of their use. The laboratory tests investigated the non-mechanical properties of CRB and HCTCRB as follow:

- Particle size distribution
- Particle shape and surface
- Compaction

Laboratory procedures carried out to detect these characteristics were mostly performed in accordance with Australian Standard Methods of testing soils for engineering purposes-AS 1289 (Australian Standard 2000).

3.3.1 Particle size distribution

Particle size distribution of CRB and HCTCRB were determined by using a sieve analysis test procedure in accordance with the Australian standard-AS1289.3.6.1 (Australian Standard 1995). Following this standard, particle size distribution was carried out in two separate stages, the coarse (nominal size of 20 mm to 6 mm), and fine particles (nominal size of 6 mm to 2 mm). To find the gradation of testing materials, a particle size distribution must be undertaken. This was carried out in accordance with Main Road test method WA 115.1 (Main Roads WA 2006). The required outcome from the performance of this test is the characterisation of the particle size distribution of the test samples. Hence the largest sieve used in the coarse sieving should approximate the nominal particle size of the test sample (Main Roads Western Australia 2006). This test also used the method in conjunction with Australian Standard 1289.3.6.1 (Standards Australia 1995), which also provides extra guidance on top of that provided by

WA 115.1. It should be noted that WA 115.1 breaks the sieving procedure into two sections, coarse and fine, whilst AS 1289.3.6.1-1995 breaks it into three sections, coarse, intermediate and fine. These breakdowns are for convenience only and do not affect the mechanics of the test in anyway. The following procedure was accepted from WA 115.1, due to the grading characteristics of the CRB and HCTCRB. Hence only two stages were required.

In this study, the procedure (obtained from WA 115.1 with additional information from AS 1289.3.6.1-1995) was performed as follows:

1. A test sample was taken in accordance with Test Method WA 100.1.
2. From the test sample, a test portion was prepared in accordance with Test Method WA 105.1. and the initial mass (mint.) of the test portion to 0.1 of a gram was recorded.
3. Coarse Sieving
 - a. Nest sieves in order of decreasing size of opening from top to bottom were selected. The aperture of the largest sieve selected approximated the size of the largest particle in the sample being tested. For particle sizes greater than 19.0 mm appropriate sieves are generally 75.0, 53.0 and 37.5 mm, however other, larger or intermediate sieve sizes should be used as appropriate for the nominal size of the test sample. The smallest sieve was 2.36 mm and a retainer was placed underneath.
 - b. The test portion was placed in the top sieve.
 - c. The sieves were agitated. Note (AS 1289.3.6.1): Sieving needs to continue until the mass passing the sieve in 1 minute is less than 1 percent of the mass of the material retained in the sieve.

- d. The mass was determined and recorded, to 0.1 of a gram, of material retained on each sieve including any material cleaned from the mesh or perforated plate. If the sieve portion was divided into test increments, the particles retained from each sieving were combined and considered as single sieve fractions.
- e. A representative test increment, of at least 30 g, from the material passing the 2.36 mm sieve was obtained and the hygroscopic moisture content (w) in accordance with Test Method WA 110.1 or WA 110.2 was determined.

4. Fine Sieving

- a. The nest from 1.18 mm to 0.075 mm were placed in order of decreasing size of opening from top to bottom, with a retainer under the bottom sieve and sediment in the top sieve. Note that unless otherwise directed the following fine sieves should be used for the particle size distributions: 1.18 mm, 0.600 mm, 0.425 mm, 0.300 mm, 0.150 mm and 0.075 mm.
- b. The sieves were agitated.
- c. The mass, to 0.01 of a gram, of materials retained on each sieve including any material cleaned from the mesh were determined and recorded.

Firstly, the CRB and HCTCRB were prepared on the sieve as shown in Figure 3.3, and the set shaken on a mechanical sieve shaker for 15 minutes, approximately. The retaining masses of the particles in each sieve were determined.

In this study, several sieve analyses were performed on samples prepared in different conditions such as uncompacted, compacted, and various hydration

periods to investigate the environmental effects to the gradation characteristics. For both CRB and HCTCRB, the sieve tests were carried out on CRB and HCTCRB at 3, 7, 15, 30 and 45 day hydration periods for uncompacted and compacted conditions. The test results would exhibit the gradation curves and hydration period effect of their gradation. The sieve analysis results were then averaged to give a representative gradation of test material under different conditions.



Figure 3.3 Particle sieves and a sieve shaker machine

3.3.2 Particle shape and surface of CRB and HCTCRB

The particle shape and surface of CRB and HCTCRB were investigated into their physical appearance and mineral compound. The test material samples were subjected to microscopic examination in order to characterise their particle shape, surface roughness and compound element. A modern optical microscope which

has a digital camera was utilised. A scanning electron microscope (Carl Zeiss EVO SEM) at the Centre for Material Research (CMR) of the Department of Physics, Curtin University of Technology, was used to examine the materials. This microscope has a significant advantage of digital image capture allowing data transfer and the added convenience of further analysis using image processing software installed in the microscope computer. Several imaging modes in transmitted and reflected light are available. This method focused on pictures for CRB and HCTCRB to make comparisons.

For each condition, compacted and uncompacted samples were mounted on specimen stubs. They were then coated in a carbon (graphite) coating to provide an electrical conductance. Two types of images were taken for each sample, backscatter electron and secondary electrons. The backscatter electron picture shows heavier elements more brightly and is used for finding areas of different composition, as they will have different contrasts. The secondary electron pictures show more of the surface of the sample as the secondary electrons come from close to the surface, rather than the backscatter, from where the electrons come from deeper in the sample. The test results also presented the element spectrum of CRB and HCTCRB.

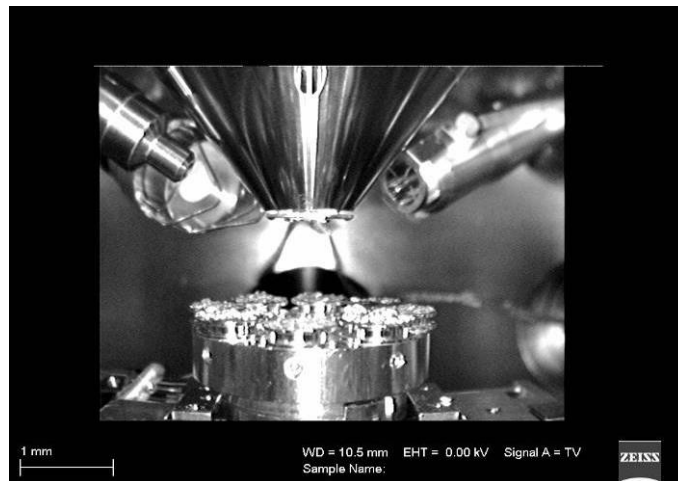


Figure 3.4 The scanning electron microscope used in this study

3.3.3 Compaction

Two general methods of compaction tests are used for engineering purposes; a standard and a modified one. The test procedures are mainly different in the number of blows delivered to soil layers. This study investigated the compaction characteristics of conventional road base materials by using modified compactive effort in accordance with Australian Standard AS 1289.5.2.1 (Australian Standard 2003). The modified compaction method has a 50 mm diameter hammer which has a mass of 4.9 kg. On a total of five layers of soil, the rammer drops from a height of 450 mm delivering a compactive effort of 21.62 Joules per impact. Twenty five blows for each layer were delivered at 2703 kJ/m^3 , approximately four times the applied load on the standard test. The top 5mm of every layer was scrapped to ensure good bonding between layers. The mould used the same mould as the standard compaction. Veinier calliper measurements showed slight variations in mould dimensions due to manufacturing inconsistency.

The compaction processes were carried out to define 100 % maximum dry density (MDD) and 100% optimum moisture content (OMC) of CRB and HCTCRB. The HCTCRB sample tests were conduct at 5, 7, 15, 30 and 45 day hydration periods to determine suitable %OMC for each hydration period. In this section, HCTCRB has to be defined in 3 types by the amount of water contents during compaction process in order to observe the moisture sensitivity of HCTCRB as shown in Table 3.3. The test results would be used to established compaction curves, a suitable OMC for each hydration period, and the moisture sensitivity of HCTCRB and hydration period effects.

Table 3.3 HCTCRB classification

	Description
Type A	No additional water
Type B	Suitable %OMC for each hydration period
Type C	8% water content (HCTCRB OMC)



Figure 3.5 The compaction equipment

3.4 Mechanical characterization

For pavement materials, the mechanical characteristics which usually affect the main function in pavement structures, quality service and long term performance are required better understanding to maintain satisfied performance during a service life. The mechanical responses of pavement materials, therefore, have to be determined to assess the service level of their uses. A series of laboratory tests was performed to determine the important mechanical properties of CRB and HCTCRB. In traditional practice, pavement materials rely on the California Bearing Ratio (CBR) test result hence the laboratory procedure would start investigate at CBR tests. This study would improved the conventional approach by using sophisticated laboratory results such as shear strength parameters, the resilient modulus and permanent deformation which was investigated. It consisted of:

- California Bearing Ratio (CBR)
- Shear strength parameters
- Resilient modulus
- Permanent deformation

Laboratory procedures carried out to investigate these mechanical characteristics were mostly performed in accordance with Australian Standard and Main Roads Western Australia Methods of testing aggregates for engineering purposes-AS 1289 (Australian Standard 2000) and (Main Roads Western Australia 2007).

3.4.1 The California Bearing Ratio (CBR)

The CBR tests were performed on CRB and HCTCRB in accordance with Australian Standard-AS1289.1.1 (Australian Standard 1998) for un-soaked and soaked methods. The CBR test generally starts from the compaction stage. The hammer weight used was the same as in the modified compaction test, 4.9 kg. A total of 5 soil layers with the given number of blows per layer dropping from a height of 450 mm were compacted. The number of blows applied the same energy as a modified compaction test and depended on the appropriate target dry density of soils. For both CRB and HCTCRB, the compaction processes were carried out to achieve 100 % maximum dry density (MDD) and 100% optimum moisture content (OMC) of their compaction test results. Fifty six blows per layer were performed on each specimen. A spacer disk was first inserted before the first layer of a test material was added into the mould to temporarily fill the space under the soil so when the mould was flipped (spacer disk on top), a stem and plate and two metal surcharges were placed in position replacing the spacer disk. A metal surcharge was applied on the compacted testing material to simulate the surcharge of the pavement in a real situation. After the compaction, the unsoaked CBR and HCTCRB tests were straight away carried out. For the soaked test, a dial gauge was placed at the top of the stem and plate. The CBR and HCTCRB mould and the gauge were then soaked entirely in water (see Figure 3.6) for four days. The gauge was in position to measure the amount of swell in the test materials which would occur when they were soaked in water.

The test was conducted on equipment with a steel penetration piston with a 49.6 ± 0.1 mm diameter. The stem and plate were removed to slot the piston between the surcharge disks. This stage of the test was performed on both the soaked and the unsoaked samples. The concept of CBR test was to push the driven plunger

into the soil sample and to obtain a measurement of the sample deformation from a gauge built onto the machine. Figure 3.7 shows the penetration stage setup on the Universal testing machine.



Figure 3.6 The soaked CBR and HCTCRB setup in the soaking container



Figure 3.7 The penetration stage of CBR and HCTCRB tests setup

3.4.2 Static and repeated cyclic triaxial tests

Static and repeated cyclic tests were carried out with a triaxial apparatus consisting of main set consisting of the load actuator and a removable chamber cell. The specimens were placed in the triaxial cell between the base platen and the crosshead of the testing machine as shown in Figure 3.8. Controllers were used to manage the chamber, as well as the air pressure. The analogue signals detected by the transducers and load cell were received by a module where they were transformed to digital signals. A computer converts modules of the digital signals sent from the system. The system was located in the main set and facilitates the transmission of the orders to the actuator controller. User and triaxial apparatus communication were controlled by a computer which used convenient and precise software. This makes it possible to select the type of test to be performed as well as all the parameters, stress levels, data to be stored. The load cell, the confining pressure and the externally linear variable differential transducer (LVDT) on the top of the triaxial cell, used to measure deformations over the entire length of the specimens, were measured by the control and data acquisition system (CDAS) which provided the control signals, signal conditioning, data acquisition. The CDAS was networked with the computer which provided the interfacing with the testing software and stored the raw test data. These enabled the resultant stress and strain in the sample to be determined.

This apparatus however, is limited to laboratory samples with a maximum diameter of 100 mm and a height of 200 mm based on the standard method of Austroads APRG 00/33-2000 (Voung and Brimble 2000). Moreover, the apparatus allows the laboratory sample to be subject to static and cyclic axial deviator stresses but it is not feasible to vary the confining radial stresses at the

same time. Confining pressure was generated to simulate the lateral pressure acting on the surrounding materials as occurring in a pavement layer. The pressure was applied and stresses were found at different points in the granular material. The results were expressed in terms of deviator stress $q = \sigma_1 - \sigma_3$, and mean normal stress $p = (\sigma_1 + 2\sigma_3)/3$. The static and dynamic axial stresses came from a high pressure air actuator capable of accurately applying a stress pulse following the stress level.

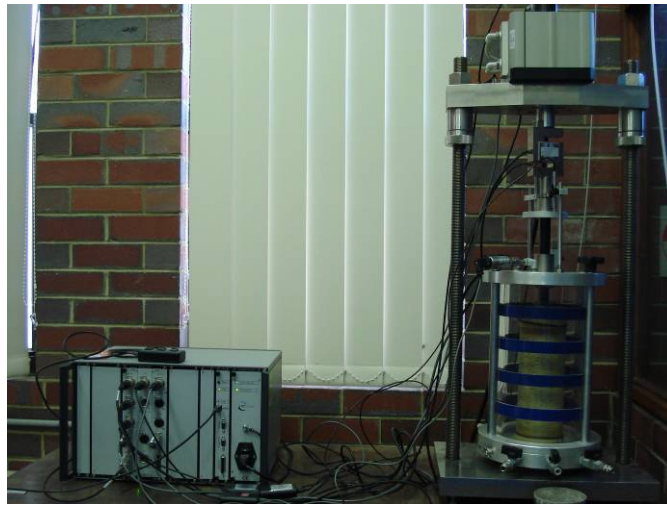


Figure 3.8 The triaxial test machine used in this study

3.4.2.1 Specimen preparation

All tested CRB and HCTCRB samples were prepared varieties of %OMC and MDD to observe enviromental effects. However, the HCTCRB procedure entailed adding 2% GP cement (dry masses) to the wet crushed rock and each mixture was placed in the mixing machine for at least 10 minutes or until it became uniform in color and texture as shown in Figures 3.9 and 3.10. The mixtures were then kept at room temperature in sealed plastic bags for periods of the time as shown in Figure 3.11. In Figure 3.12, a mixture of a particular OMC and hydration period,

it was then re-mixed in the machine for at least 10 minutes in accordance with MRWA specifications (Main Roads Western Australia 2007). Compaction processes were then carried out using a modified compaction method in a standard mould 100 mm in diameter and 200 mm in height as shown in Figures 3.13 and 3.14. Sample preparations were carried out by using a standard cylinder mould 100 mm in diameter and 200 mm in height by the modified compaction method (Main Roads Western Australia 2007). Compaction was accomplished on 8 layers with 25 blows of a 4.9 kg rammer at a 450 mm drop height for each layer. Fully bonding conduction between the layers of each layer had to be scarified to a depth of 6 mm before for the next layer was compacted. After compaction, the specimens were kept in moulds wrapped to prevent loss of moisture for 28 days for cemented materials as shown in Figure 3.15. The basic properties of each specimen were determined and specimens were carefully removed from the moulds. A crosshead and stone disc were placed on the specimen and it wrapped in two platens by a rubber membrane and finally sealed with o-rings at both ends as shown in Figure 3.16. Finally, it was carefully carried to the base platen set of the chamber triaxial cell.



Figure 3.9 All mixtures in the mixing machine



Figure 3.10 Crushed rock after mixing with cement



Figure 3.11 HCTCRB hydration in a plastic bag for 7 days



Figure 3.12 The HCTCRB remixed after a 7-day hydration process



Figure 3.13 Testing material and compaction equipment



Figure 3.14 CRB after compaction



Figure 3.15 A wrapped mould of HCTCRB after compaction

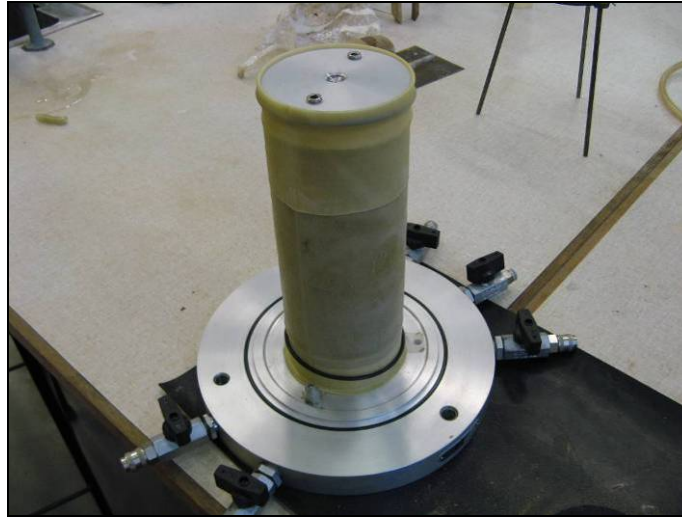


Figure 3.16 Testing sample setup before triaxial testing

3.4.2.2 Static triaxial tests

The fresh crushed rock and HCTCRB (fresh crushed rock with 2% cement by dry weight) were initially tested in terms of the compaction test in accordance with Main Roads Western Australia (MRWA) Test Method WA 133.1 (Main Roads Western Australia 2007) to establish the compaction curves for determining their optimum moisture content (OMC). For both CRB and HCTCRB, the compaction processes were carried out to achieve 100 % maximum dry density (MDD) and 100% optimum moisture content (OMC) of its compaction test results. Drained triaxial compression tests were conducted to establish the cohesion (c) and the internal friction angle (ϕ) of CRB and HCTCRB at 7 hydration periods and 28 days curing time including establishing the Mohr-Coulomb failure envelope. CRB samples were tested immediately and cemented specimens at 100%OMC and 100%MDD of the 7-day hydration period and the 28-day curing time were tested under unsaturated conditions based on the pavement material standard and suctions were not measured. In these tests, the specimen response was measured

at three different constant confining pressures. As stated, current pavement analysis and design use only a CBR value to classify suitable base course material without any failure criteria and long term performance by assuming the pavement structure will never fail at the base course, which is only for load transfer. This study will define static pavement failure criterion by using the Mohr-Coulomb failure envelope in terms of p-q diagrams to fulfil any lack of base course failure criterion.

3.4.2.3 The resilient modulus

The standard method of Austroads APRG 00/33-2000 (Voung and Brimble 2000) of repeated load triaxial test (RLT) Method was followed for the resilient modulus tests in this study. The UTM-14P digital servo control testing apparatus in the Geomechanics Laboratory, Department of Civil Engineering, Curtin University of Technology was used. New specimens were prepared as described in the previous section.

Basically, the specimens were placed within the triaxial cell and positioned between the base plate and crosshead of the testing machine. The dynamic axial stress came from a feedback-controlled high pressure air actuator capable of accurately applying a stress pulse following the acting stress of the standard. A confining pressure was generated by a closed loop controlled actuator to simulate the lateral pressure acting on surrounding materials as would occur in a road. The confining pressure was applied by air pressure. The machine conveyed a vertical dynamic force of rectangular waveform with a period of 3 secs and a load pulse of 1 sec duration, in accordance with the standard requirements and is demonstrated in Figure 3.17. Resilient modulus testing was performed during which, the specimens were loaded with various stress stages at the ratios of the dynamic

deviator stress (σ_d) with frequency of 0.33 Hz to the static confining stress (σ_3) based on Austroads APRG 00/33-2000 (Voung and Brimble 2000), each stress stage was simulated from the particular condition in the pavement structure.

The load cell, the confining pressure, and the external linear variable differential transducer (LVDT) on the top of the triaxial cell, which was used to measure deformations over the entire length of the specimen, were measured by a control and data acquisition system (CDAS) which provided control signals, signal conditioning, and data acquisition. The CDAS communicated with the computer which provided interfacing with the testing software and stored the raw test data. These enabled the resultant stress and strain in the sample to be determined.

For both CRB and HCTCRB, the compaction processes were carried out to achieve 100 % maximum dry density (MDD) and 100% optimum moisture content (OMC) of its compaction test results and then attempted to dry back to 80% and 60%OMC to observe the moisture effect. Drained triaxial conditions were conducted on CRB and HCTCRB at 3, 7, 15, 30 and 45 day hydration periods with 28 days of the curing time under unsaturated conditions based on the pavement material standard and the suctions were not measured. The test established the resilient modulus model, moisture and hydration period effects. After compaction, in accordance with this standard (Voung and Brimble 2000), the specimens were applied sequentially by the difference of the 65 stress stages straightaway to conduct the resilient modulus test to check the elastic condition of each specimen throughout the multiple loading stress stages as shown in Table 3.4. This process simulates the complicated traffic loading acting on pavement. Before performing the resilient modulus process, a pre-conditioning stage was carried out to allow the end caps to bed into the specimen and the applied stresses and resilient strains to stabilise under the imposed stress condition, thus 1000

loading cycles of pre-conditioning were used and for each stress stage after pre-conditioning, 200 loading cycles were applied to the specimens. This process simulates complicated traffic loading acting on a pavement.

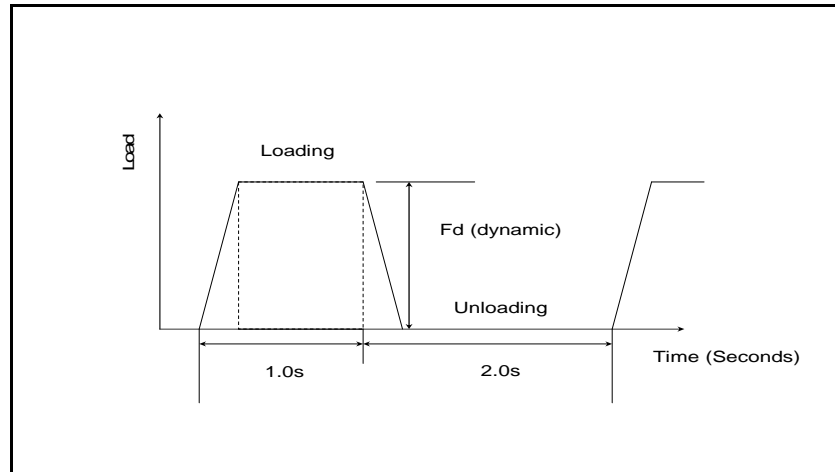


Figure 3.17 Illustration of the vertical force waveform



Figure 3.18 Permanent deformation testing setup

Table 3.4 Stress levels following Austroad-APRG 00/33 standard

Resilient Modulus Stress Levels								
Stress Stage Number	σ_3 (kPa)	σ_d (kPa)	Stress Stage Number	σ_3 (kPa)	σ_d (kPa)	Stress Stage Number	σ_3 (kPa)	σ_d (kPa)
0	50	100	22	30	150	44	20	185
1	75	150	23	40	200	45	30	275
2	100	200	24	50	250	46	40	370
3	125	250	25	75	375	47	50	450
4	150	300	26	100	500	48	30	275
5	100	200	27	50	250	49	20	225
6	50	150	28	30	180	50	30	335
7	75	225	29	50	300	51	40	450
8	100	300	30	75	450	52	50	550
9	125	375	31	50	300	53	20	250
10	150	450	32	30	180	54	30	375
11	75	225	33	40	250	55	40	500
12	40	125	34	30	210	56	20	300
13	30	100	35	40	280	57	30	450
14	40	150	36	50	350	58	40	600
15	50	200	37	75	525	59	30	500
16	75	300	38	40	280	60	20	350
17	100	400	39	20	150	61	30	550
18	125	500	40	30	245	62	20	375
19	75	300	41	40	325	63	30	575
20	30	125	42	50	400	64	20	400
21	20	100	43	30	245	65	20	500

3.4.2.4 Permanent deformation

New specimens were prepared following the same method as the resilient modulus specimen, described in the sample preparation item. CRB and HCTCRB were carried out to achieve 100 % maximum dry density (MDD) and 100% optimum moisture content (OMC) of its compaction test results and then dried to

80% and 60% OMC to observe the moisture effect. Drained triaxial condition tests were conducted on CRB and HCTCRB at 3, 7, 15, 30 and 45 day hydration periods with 28 days of curing time under unsaturated conditions based on the pavement material standard and suctions were not measured. The test results would establish the permanent deformation model, moisture and hydration period effects.

Permanent deformation testing was calculated in accordance with Austroads – APRG 00/33 standard. In this testing, the specimens were loaded with three stress stages, each involving 10,000 cycles at a stress condition of specific dynamic deviator stress and static confining pressure as shown in Table 3.5.

Table 3.5 Stress levels for permanent deformation of base materials following Austroad-APRG 00/33 standard

Permanent Deformation Stress Levels		
Stress Stage Number	Base	
	Confining pressure, σ_3	Cyclic deviator stress, σ_d
	kPa	kPa
1	50	350
2	50	450
3	50	550

3.4.2.5 The shakedown limit evaluation

Shakedown limit tests were carried out with a cyclic triaxial apparatus consisting of a main set containing the load actuator, a removable chamber cell. Specimens were placed in the triaxial cell of the testing machine as stated. Laboratory samples with a diameter of 100 mm and a height of 200 mm based on the standard method of Austroads APRG 00/33-2000 (Voung and Brimble 2000). CRB and HCTCRB were carried out to achieve 100 % maximum dry density (MDD) and 100% optimum moisture content (OMC) of its compaction test results. Drained triaxial condition tests were conducted on CRB and HCTCRB at 7 day hydration periods with 28 day curing time. The test results would be established the shakedown limit ranges and dynamic failure criteria of CRB and HCTCRB.

Confining pressure was generated by air to simulate the lateral pressure acting on the surrounding materials as occurs in a pavement layer with different depths. The pressure was applied based on stresses were found at different points in the granular material. The results were expressed in terms of deviator stress $q = \sigma_1 - \sigma_3$, mean normal stress $p = (\sigma_1 + 2\sigma_3)/3$ and the confining pressure was simulated from the thickness of pavement base course layer commonly use in Western Australia. For this reason, it was decided to test the laboratory samples to a number of different stress levels and the particular confining pressure was 40 kPa. After the confining pressure had been applied, additional dynamic vertical stress was applied. Triaxial tests were carried out with axial stress pulses reaching stress ratios of $\sigma_1/\sigma_3 = 5-26$. The cyclic axial stress came from a high pressure air actuator capable of accurately applying a stress pulse following the stress level. In this test, there was a haversine waveform frequency of 1 Hz over a period of 1.0 sec and a load pulse of 0.1 sec duration, as illustrated in Figure 3.19. The series

was planned to find the limit range of road base material in term of dynamic approach and presented deformation of pavement material in different conditions. However, in case the stress level could not achieve the sample failure, the test terminations were the strain rate of 0.01 microstrain/cycle or at least 200,000 cycles.

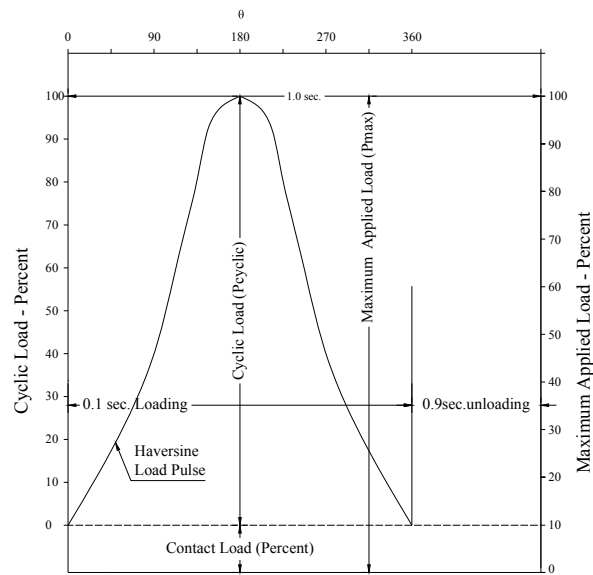


Figure 3.19 The vertical loading waveform

3.4.2.6 The pavement analysis and design implementation

This section discusses the implementation of pavement analysis and design based on CRB and HCTCRB test results. Multi-layer finite element analysis of selected pavement structure was carried out with the material models of CRB and HCTCRB to investigate responses of such pavement structure. The objective of the application is to introduce and discuss pavement analysis and design aspects with details shown in Chapter 5.

CHAPTER 4

RESULTS AND DISCUSSION

This chapter presents the results and discussion of laboratory experiments performed on CRB and HCTCRB following the methodology and experimental program of Chapter 3. Firstly, the basic characteristics of CRB and HCTCRB were described based on non-mechanical test results. These exposed the appearance and physical characteristics influencing their responses. Subsequently, more complicated responses of CRB and HCTCRB were described under various simulating conditions. Afterwards the results were gathered and analysed using a numerical procedure.

4.1 Non-mechanical behaviour

4.1.1 Particle size distribution

The particle size distribution characteristic of soils is usually a part in pavement material specifications which normally depict the upper and the lower limits of the particle size distribution of a suitable material to be used for a particular construction purpose. Main Roads Western Australia has established particle size distribution specifications of base course, subbase course, and earthwork materials. In this study, the sieve analysis of the CRB and HCTCRB with various hydration periods were performed to observe the particle size distribution characteristic of material.

Generally, a sieve analysis test result is represented in terms of a gradation chart which shows the relative sieve sizes and percentages of soil masses passing

through the sieve set. The particle size distributions for CRB derived from the tests in this study are shown in Figure 4.1. It was found that the majority of the fractions lies within the specification requirements (Main Roads Western Australia 2006). From this result, CRB could be suitable as a base course material. A comparison of the gradations between both CRB and HCTCRB is also illustrated in Figure 4.1. It is visible that HCTCRB's gradation curve shifts to the right hand side from CRB curve because amount of cement added reacts with CRB particles, which have the grain size smaller than 6.70 mm, resulting in bigger grains. Cement and water existing in fresh crushed rock formed new bigger particles with fine grain but course grains were unable to maintain cement bonding after the retreated process.

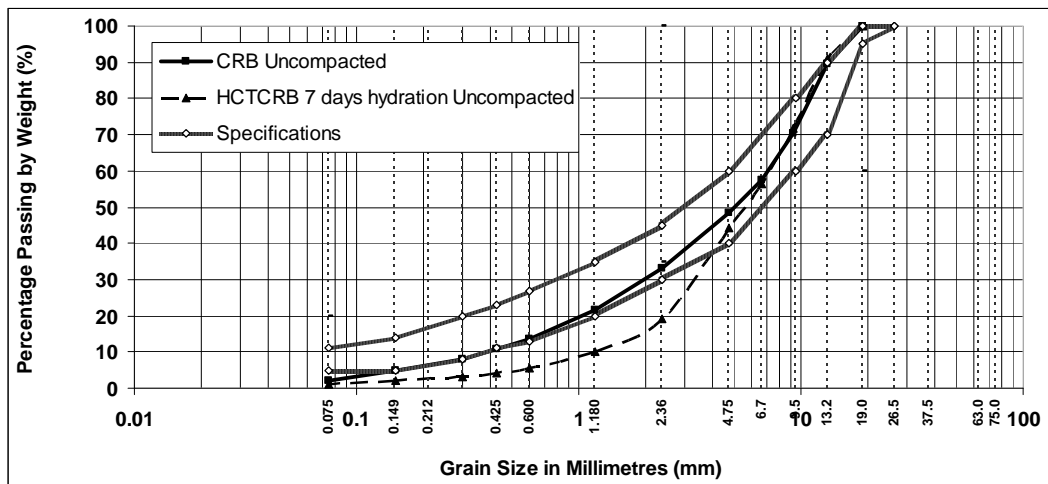


Figure 4.1 Gradation of CRB and HCTCRB with uncompacted conditions

The study also focused on the effect of compaction and hydration periods of CRB and HCTCRB to gradation. Firstly, Figures 4.2 and 4.3 present CRB and HCTCRB gradation at compacted and uncompacted conditions. After compaction, individual particles of CRB break down to smaller particles but its gradation still lies in the specification.

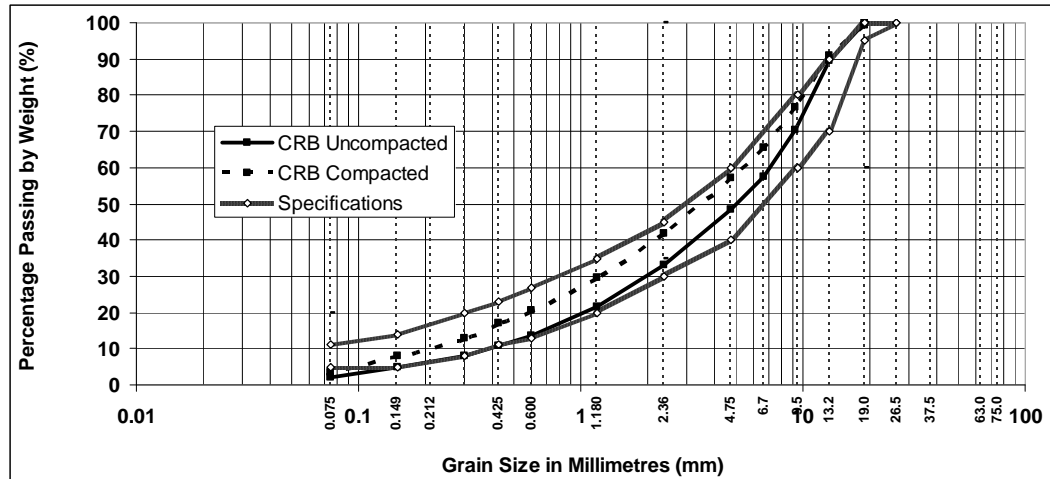


Figure 4.2 CRB's gradation under compacted and uncompacted conditions

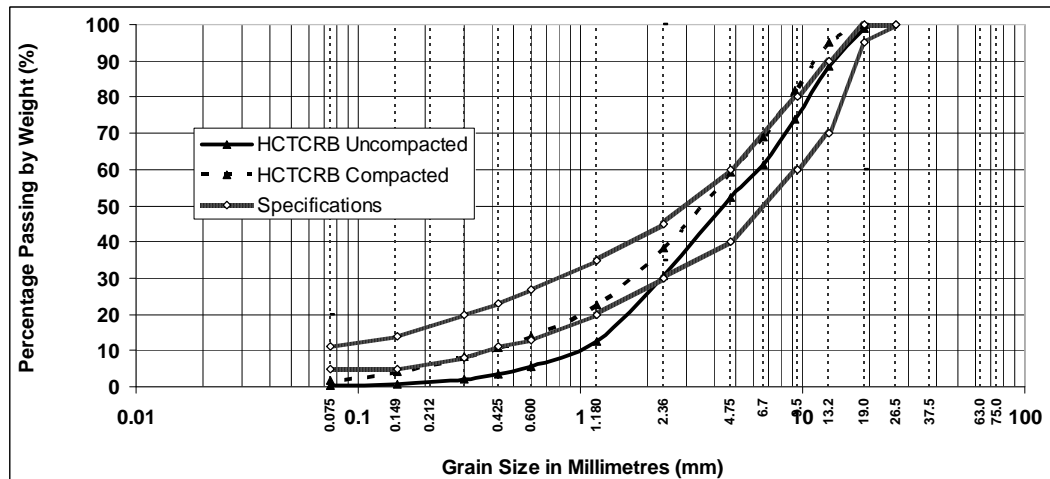


Figure 4.3 HCTCRB's gradation under compacted and uncompacted conditions

Although HCTCRB was not complying with the specifications at uncompacted conditions, but it eventually presented a related trend with CRB gradation in terms of a compacted state. Unlike HCTCRB which was investigated about the effect of hydration periods on gradation. It does not show any significant difference and suitable hydration periods should be more than 3 days because their all gradations lie in the specifications as shown in Figures 4.4 and 4.5.

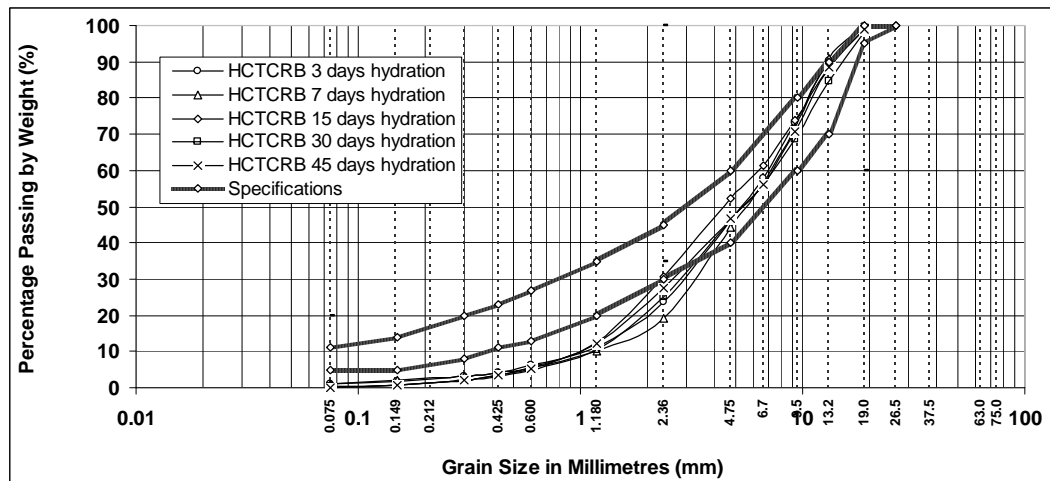


Figure 4.4 HCTCRB's uncompacted gradation for various hydration periods

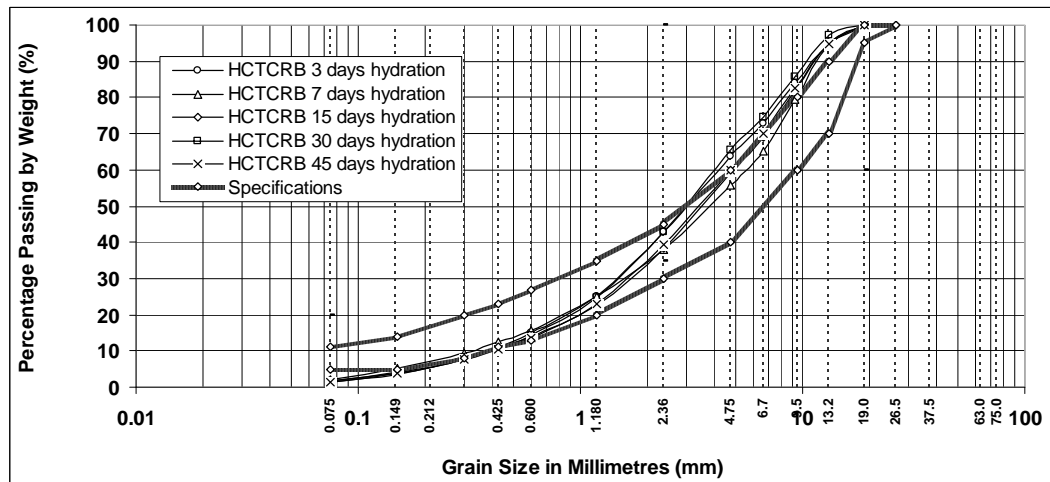


Figure 4.5 HCTCRB's compacted gradation with various hydration periods

4.1.2 Particle shape and surface

To study the particle shape of CRB and HCTCRB in this study, a scanning electron microscope (SEM) with a digital camera was used. Figures 4.6 and 4.7 show the magnified images of CRB compared to HCTCRB. The figures show individual surfaces, shape and different features of particle appearance between CRB and HCTCRB particle appearance. In Figure 4.6, CRB presents a rougher surface than HCTCRB, as it was formed by crushing large mineral chunks with sharp edges and corners. In contrast, the HCTCRB surface was filled with cement paste as shown in Figure 4.7. Despite efforts during the compaction process in the field, it was unable to restore the roughness of HCTCRB's surface back to its original surface as CRB (see Figure 4.6). The surface roughness of compacted HCTCRB locates between CRB and uncompacted HCTCRB as shown in Figure 4.8. From this point, HCTCRB must have a less internal friction value than HCTCRB even if in a compacted condition.

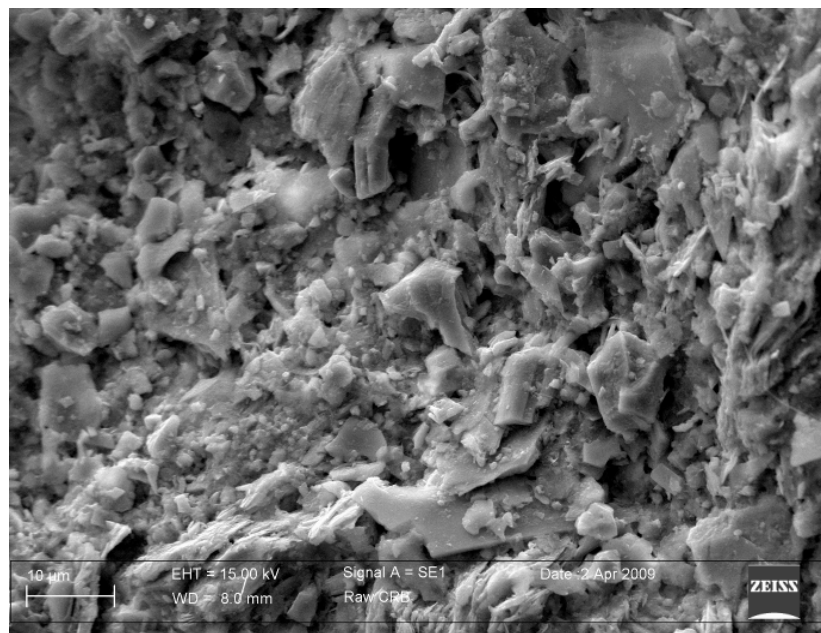


Figure 4.6 Surface of CRB

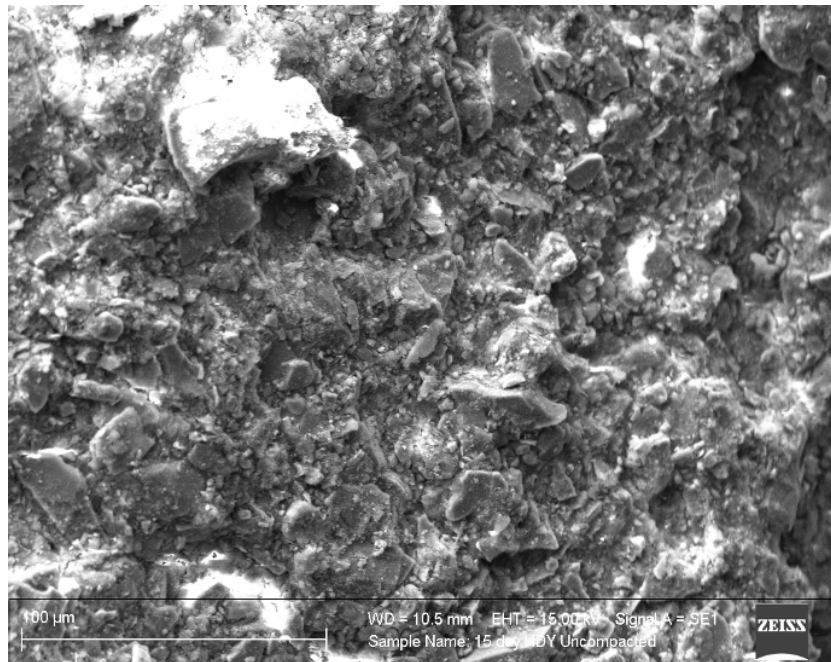


Figure 4.7 The surface of HCTCRB uncompact

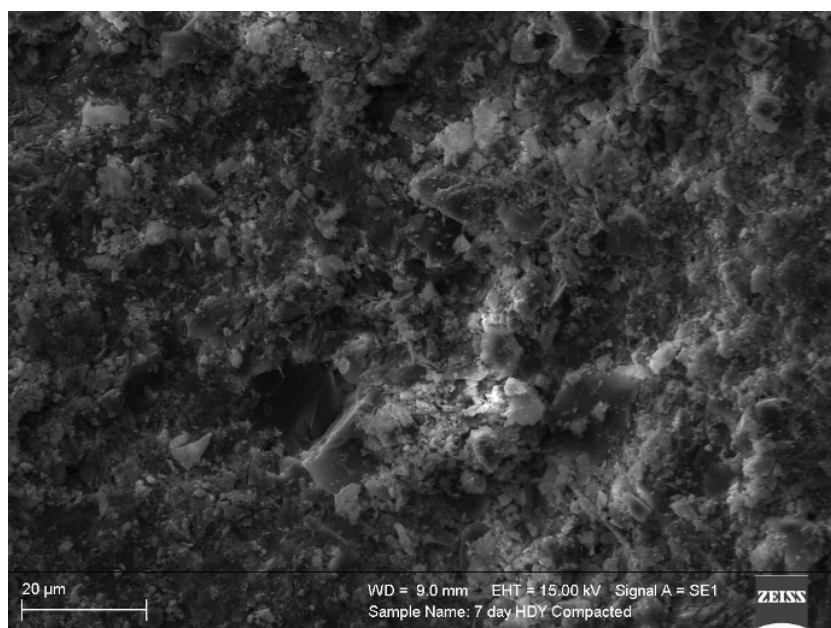


Figure 4.8 The surface of HCTCRB compacted

Moreover, HCTCRB would have more cohesion between particles than raw CRB in terms of shear strength parameters. The test results show that cement treated material would have a particle surface smoother and of more cohesive potency than its parent material. On the other hand, internal friction of the contacting surface would be less because such material does not have much confining stress response. More details about cement treated effects of shear strength parameters will be discussed in static triaxial test results. Other results from scanning electron microscope (SEM) were the element spectrum of CRB and HCTCRB as shown in Figures 4.9 and 4.10, respectively. The spectrum results show significant main element compounds of CRB's parent material that consists of SiO_2 and 2% cement content as added.

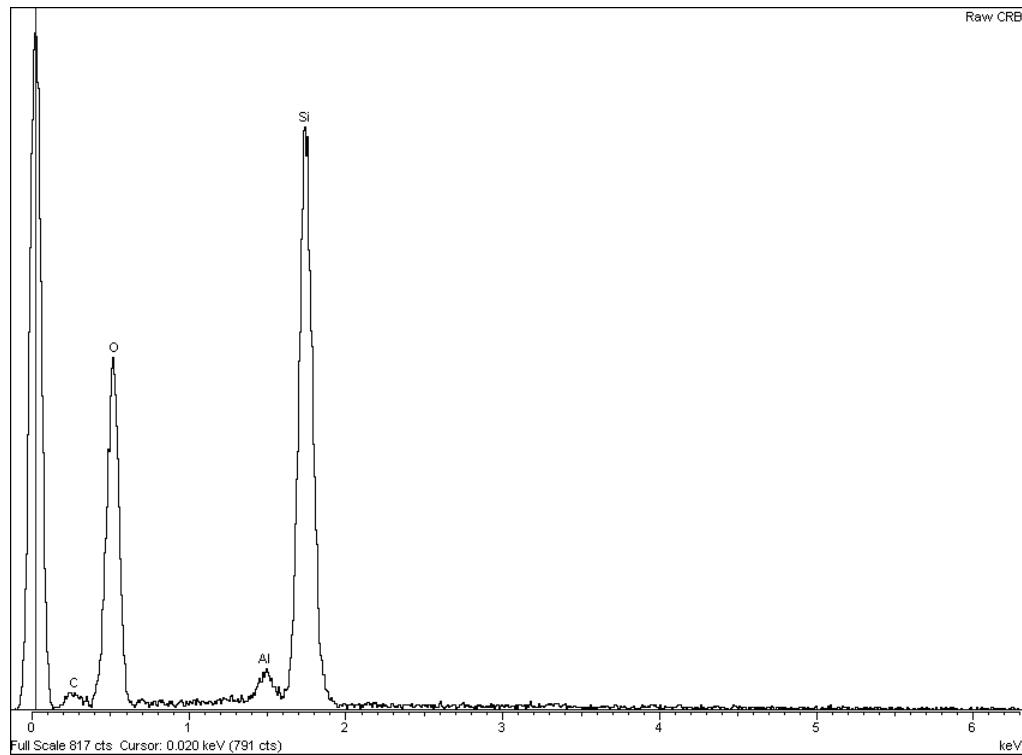


Figure 4.9 Spectrum of CRB

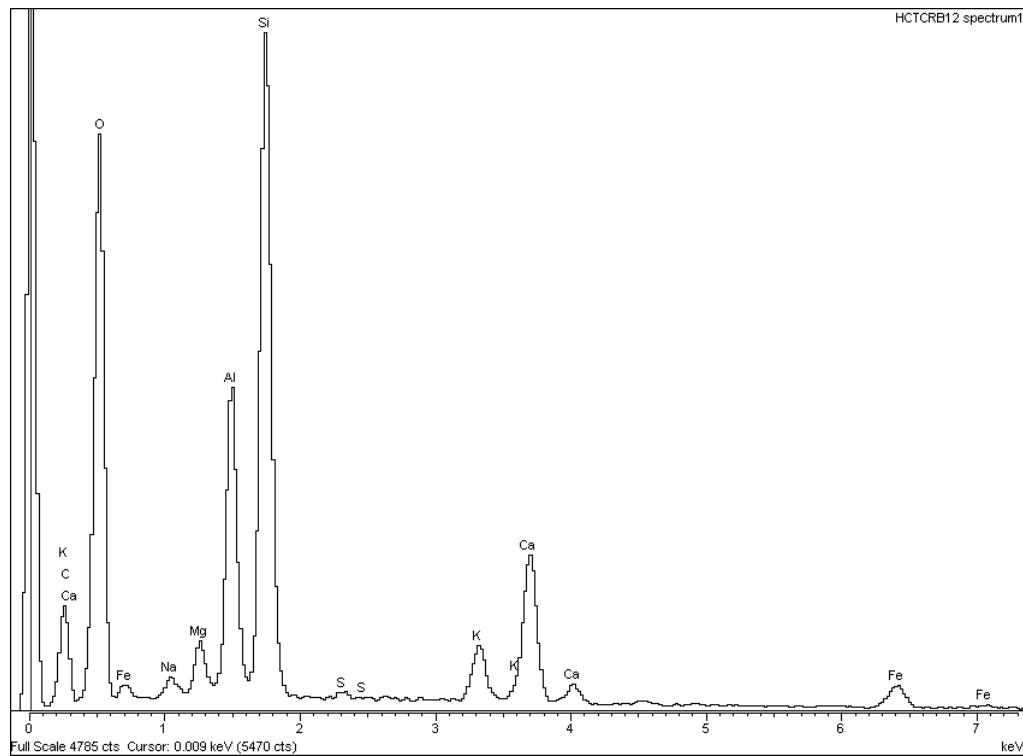


Figure 4.10 Spectrum of HCTCRB

4.1.3 Compaction

Figure 4.11 shows the compaction test results of CRB and HCTCRB over a 7 day hydration period in the form of compaction charts. For the tests on CRB, the maximum dry densities (MDD) are 2.27 tons/m³ and 2.12 tons/m³ on HCTCRB. The optimum moisture contents (OMC) are 5.5 % CRB and 8 % HCTCRB.

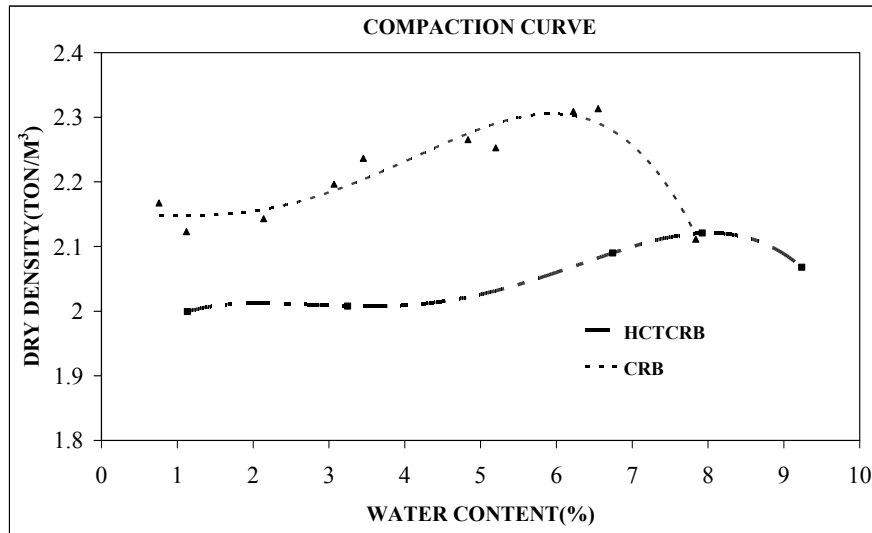


Figure 4.11 Compaction test results of CRB and HCTCRB

This section also discusses the effects of cement contents and hydration periods to MDD and OMC of test materials. From the results, cement content of the mixture increases OMC and reduces MDD. The main purpose of the moisture content in the compaction process is to lubricate each particle as close as zero voids. When the parent material deals with cement, some moisture in lubrication was absorbed by the cement for hydration reaction. This is why cemented material usually uses extra water to achieve MDD. Cement content also affects MDD by mixing fine grain and water to form new material gradation as stated in the gradation section. Thus, different hydration periods also present specific gradation and compaction curve. There are many arguments about suitable hydration periods of HCTCRB and a compaction curve is necessary to determine particular hydration periods for road construction. This study recommends 15 and 30 day hydration periods that show maximum dry density and suitable OMC should be between 7% and 8 % from compaction test result perspectives.

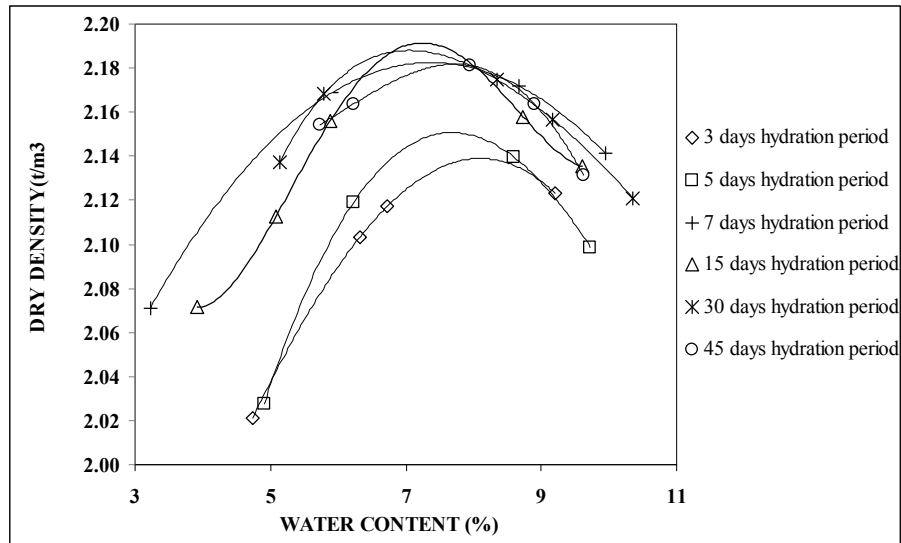


Figure 4.12 Compaction curves of HCTCRB over various hydration periods

4.2 Mechanical behaviour

This section covers the mechanical behaviour of CRB and HCTCRB as a Western Australia road base material in order to evaluate and define material responses. Firstly, California Bearing ratio (CBR), the traditional test for road design, was used to determine material capacity in term of penetrated resistance. Although mechanistic analysis and design have been introduced for a new pavement approach, it is unable to fully replace all empirical methods because the approach is ongoing based on sophisticated testing almost all pavement engineers must spend time to become familiar with it. CBR discussed the basic capable classification of pavement material. Subsequently, triaxial tests such as static shear tests, resilient modulus tests and permanent deformation tests were performed on CRB and HCTCRB. The resilient modulus or stiffness of pavement structures is also a critical factor in determining the thickness and composition of pavement layers. It performs reliably on the pavement behaviour under repeated

loading condition which simulate the real conditions of traffic loading in laboratory testing.

Permanent deformation of pavement materials is manifested as rutting and shoving, visible damage on the road from excess deformation of the pavement because the material does not have the stability to cope with the prevailing loading and environmental conditions. Consequently, both resilient modulus and permanent deformation characteristics would be parameters to examine CRB and HCTCRB as road base materials. The models of failure criteria, resilient modulus and permanent deformation of both materials have been established and comparisons of the results are given at the end of this section.

4.2.1 California Bearing Ratio (CBR)

Table 4.1 and Figure 4.13 show the results of the California Bearing Ratio (CBR) from this study and the specifications of Austroads (Austroads 2004).

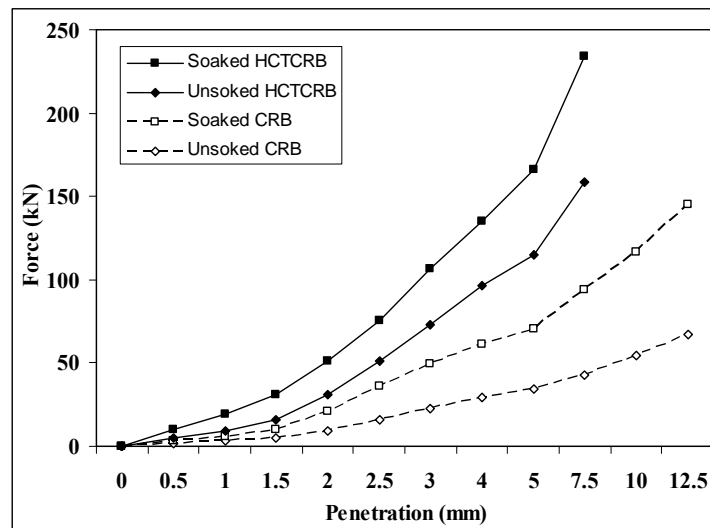


Figure 4.13 CBR results of CRB and HCTCRB

Table 4.1 California Bearing Ratio (CBR) results and specifications

California Bearing Ratio (CBR) results (%)		
Testing material	Soaked	Un-soaked
CRB	180	170
HCTCRB	250	220
CBR values (%) for Austroads minimum specification (Austroads 2004)		
Recycled concrete subbase	50	N/A
Recycled concrete base course	100	N/A
Gravel base course	80	N/A
Ferricate base course	80	N/A
Crushed rock base course	100	N/A

It should be noted that based on results and specifications, both CRB and HCTCRB comply with the specifications of road base materials.

4.2.2 Shear strength parameters

This section presents the results and discusses the static triaxial shear tests operated on CRB and HCTCRB for a 7 day hydration period at the compaction of 100% maximum dry density and 100% optimum moisture content derived from the compaction curve. The purpose of the tests was to examine the strength characteristic and to determine the ultimate shear strength parameters of test materials under the triaxial shear test. Static triaxial tests by means of the drained triaxial compression tests were performed to obtain information on the cohesion (c) and the internal friction angle (ϕ) of CRB and HCTCRB. These tests also established the failure envelope line of such CRB and HCTCRB to determine the maximum stress level of these materials so that the limited uses of testing material

could be indicated. Various confining pressures were applied on the test specimens in each test. The CRB and HCTCRB specimens were prepared as detailed in section 3.4.2.2.

The peak deviator stresses from the stress-strain curves can be seen in Table 4.2. Moreover, Figures 4.14 and 4.15 exhibit a series of graphs of the stress strain relationship from these tests. The Figures 4.14 and 4.15 also depict the relationship between the deviator stress and the axial strain of the three selected confining pressures. For the stress-strain curves, it also can be observed that the static deviator stress initially increases with greater axial strain until it reaches peak strength. For a higher confining pressure, apparently, the peak strength becomes higher and the strain corresponding to the peak strength also becomes higher. All three curves in Figures 4.14 and 4.15 exhibit that after the peak strength, there is the post peak regime which the stress reduces with increasing strain. This characteristic is similar to that of dense granular materials and is normally described as strain softening. The strain-softening process is concomitant with the generation of large deformations, which cause geometrically non-linear effects to become important (Suiker et al. 2005). It should be noted that for cemented stabilised materials, their stress-strain relationships usually perform as brittle materials so that the stress-strain curve drops dramatically after reaching peak stress but HCTCRB shows strain softening which would be a suitable characteristic for a flexible road base material with respect to stress strain relations. This means that HCTCRB exhibits as unbound granular material even though 2% cement was added. The peak strength and the confinement of CRB and HCTCRB in these tests was interpreted using a Mohr-Coulomb failure law in which the cohesion (c) and the internal friction angle (ϕ) are considered in a

failure relationship, a straight line fitted to a Mohr envelope (Lamb and Whitman 1979).

Table 4.2 Peak deviator stresses and confining pressures from static triaxial tests

Test no.	CRB		HCTCRB	
	Confining pressure, (σ_3) kPa	Deviator stress, (σ_d) kPa	Confining pressure, (σ_3) kPa	Deviator stress, (σ_d) kPa
1	40	750	50	1100
2	60	1020	100	1300
3	80	1200	150	1600

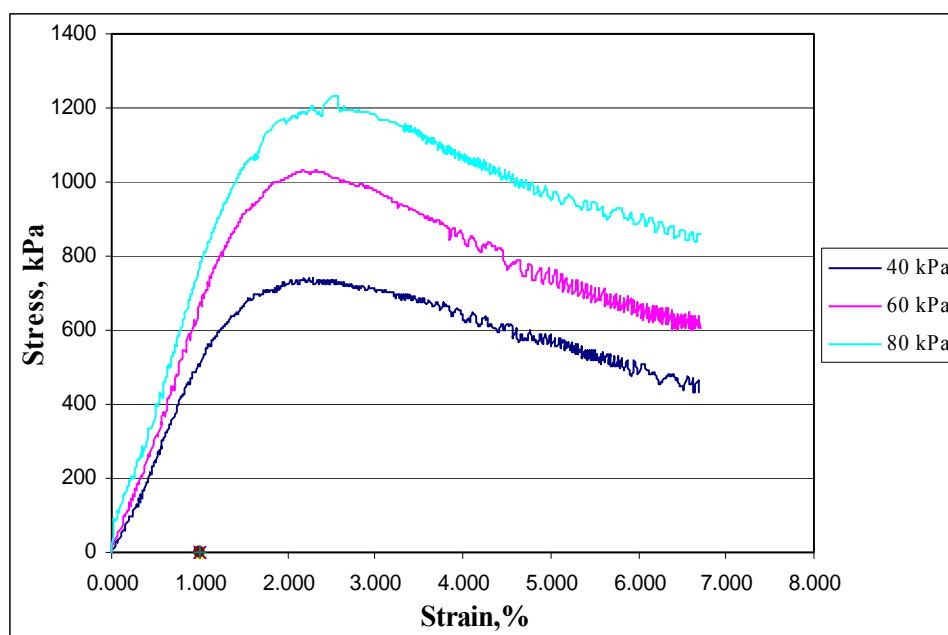


Figure 4.14 The stress-strain relations of CRB

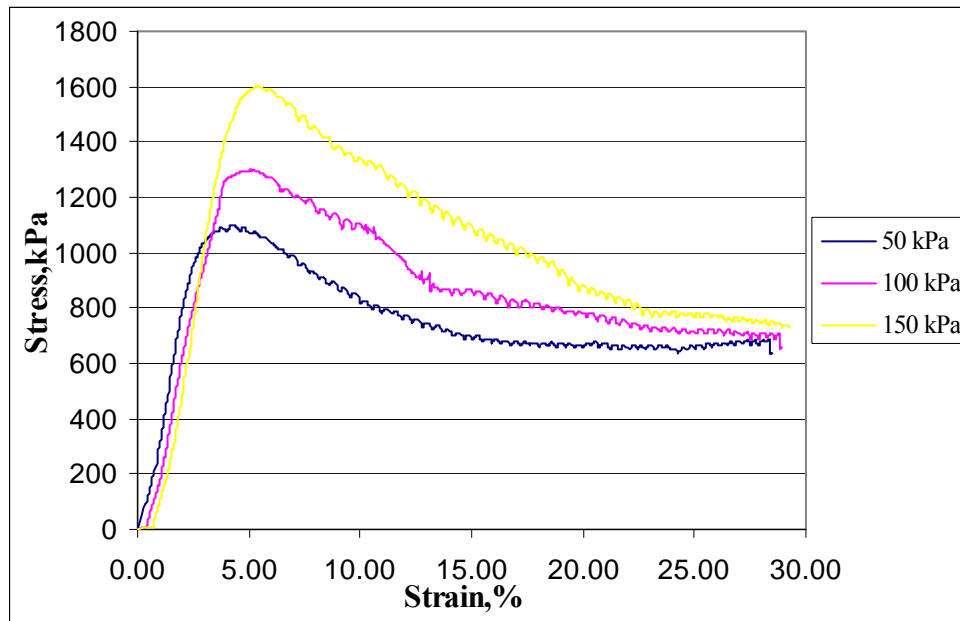


Figure 4.15 The stress-strain relations of HCTCRB

Figures 4.16 and 4.17 are the relative graphs of shear stresses plotted against normal stresses. A straight line was fitted through the data to form a Mohr-Coulomb failure envelope to obtain shear strength parameters (c and ϕ). Figures 4.16 and 4.17 also show Mohr's circles and the Mohr-Coulomb failure envelope of these tests. The results show that the envelope (corresponding to the peak stresses) is linear for the stress range tested and in the conventional Mohr-Coulomb stress space, thus the proper failures correspond to an internal friction angle (ϕ) and apparent cohesion (c) as shown in Table 4.3. The cement content of HCTCRB has modified shear strength characteristics of CRB by increasing its cohesive strength and decreasing internal friction. As stated, cement content with water and fine grain in a soil skeleton of CRB produces new gradations in fine particle area of their grading curve. It also covers the rough surfaces and sharp edges of CRB along with hydrated bonding between individual particles.

Table 4.3 Shear strength parameters (c and ϕ) for CRB and HCTCRB using the results of static triaxial shear tests

CRB		HCTCRB	
Modified compaction		Modified compaction	
Cohesion (c)	Friction angle, ϕ (degree)	Cohesion (c)	Friction angle, ϕ (degree)
32 kPa	59°	168 kPa	43°

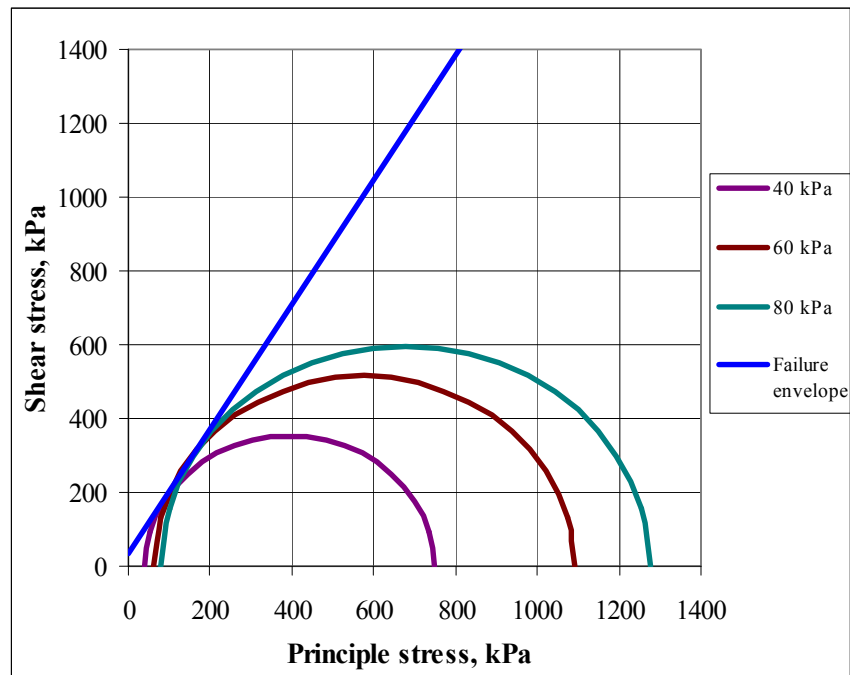


Figure 4.16 CRB Mohr's circles and the Mohr-Coulomb failure envelope

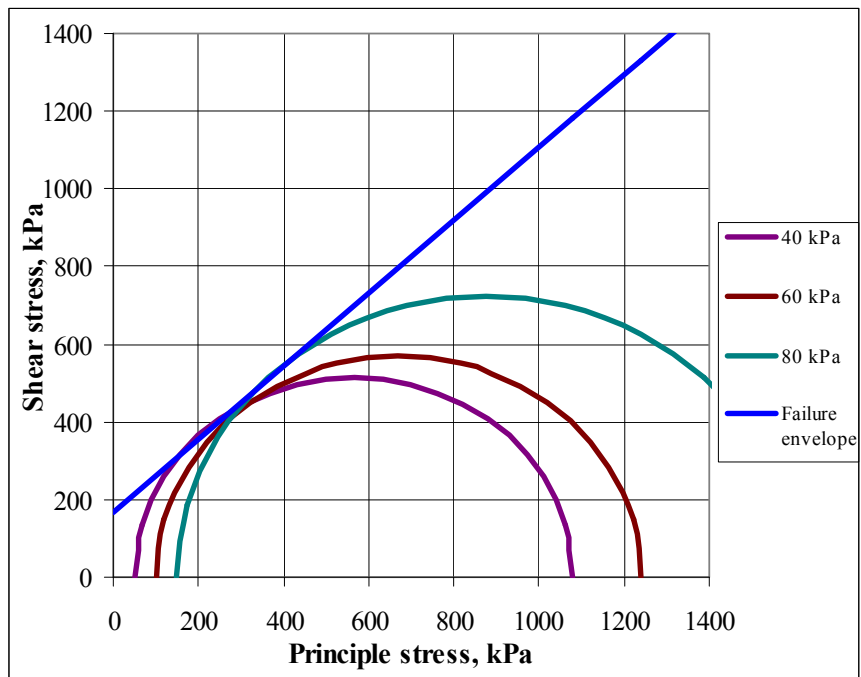


Figure 4.17 HCTCRB Mohr's circles and the Mohr-Coulomb failure envelope

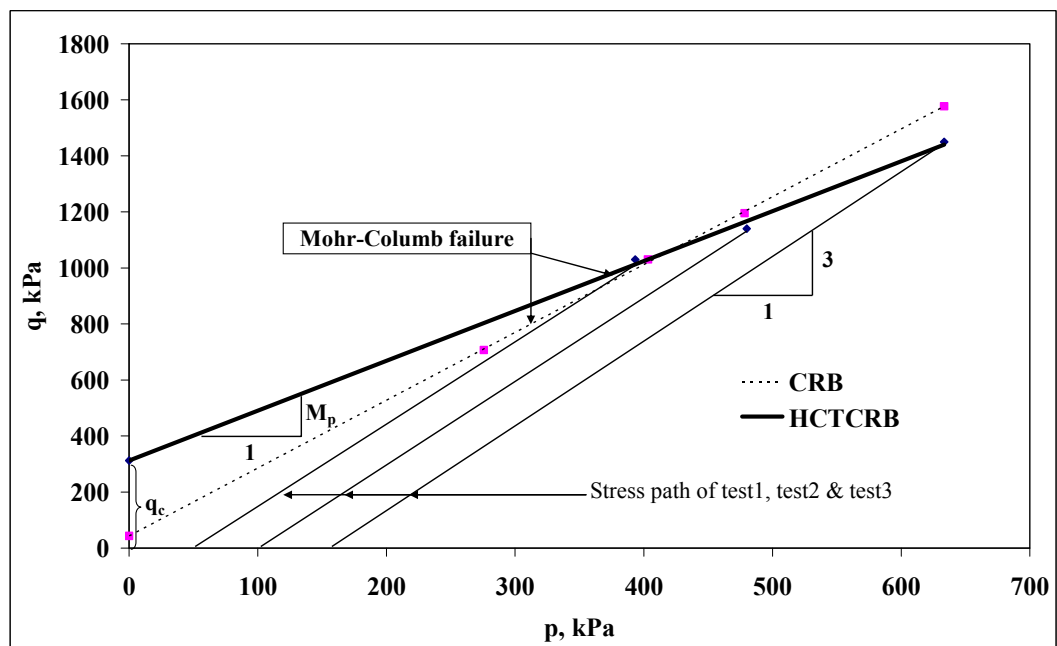


Figure 4.18 p-q diagrams of CRB and HCTCRB

The shear strength characteristics of a base course material are also significant as they provide valuable information on the material quality of resisting external loads. The failure envelope of such material is relevant to evaluate maximum capacity of materials in withstanding the applied loads and this envelope is based on, shear strength parameters (c and ϕ). In this study, the ultimate shear strength parameters of CRB and HCTCRB were determined by means of the p-q diagram as shown in Figure 4.18.

4.2.3 The resilient modulus

Effective pavement layers must exhibit high resilient modulus in order to distribute loads adequately to underneath layers without excessive deformation and reduce resilient deformation of upper bituminous layers. The pavement must withstand deformation which might contribute to surface rutting (Dawson A.R. 1993).

The resilient modulus is an important material aspect of flexible pavement materials and is the input parameter in modern pavement design. From the tests, it is based on the recoverable strains taking place from a series of combinations of confining and dynamic deviator stresses in triaxial tests applied to soil specimens to take into account the non-linear behaviour of base course materials under cyclic loading condition. Because the resilient modulus is the elastic behaviour of pavement materials, its behaviour could be considered under the elastic loading regime. Following the standard test method of Austroads-APRG 00/33 (Young and Brimble 2000), it allows a suite of 65 stress conditions having various stress levels applied to a tested specimen to characterise the vertical resilient (recoverable) strain under a combination of applied dynamic vertical and static

confining stresses. From Figure 4.19, 65 stress conditions were plotted in term of p-q diagram to compare with the failure envelop of CRB and HCTCRB as stated in the previous section. All applied stress conditions were under their Mohr-Coulomb failure envelopes in the p-q diagram. It means that the test specimens were not damaged during such testing under the given loading conditions because all test conditions was within their Mohr-Coulomb failure criteria. However few applied stresses were positioned on the failure line of CRB which means there was a possible risk of early failure.

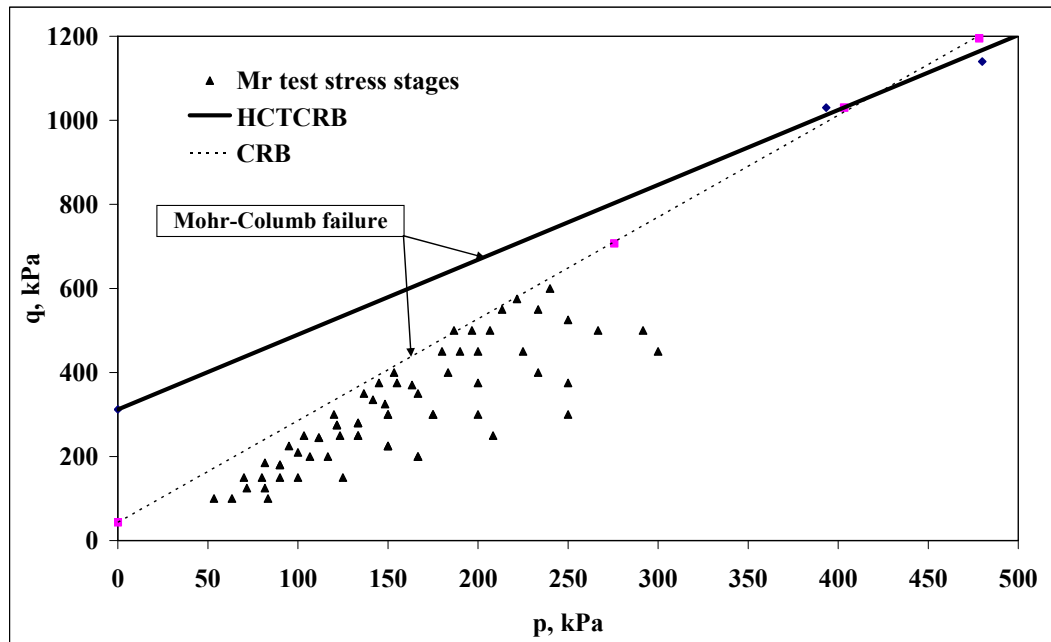


Figure 4.19 Applied stress conditions of resilient modulus tests following Austroads-APRG 00/33 standard in the p-q diagram

The resilient modulus determined from the RLT test is defined as the ratio of the repeated deviator stress to the recoverable or resilient axial strain as shown in Equation (4.1):

$$M_r = \frac{\sigma_d}{\varepsilon_r} \quad (4.1)$$

where: M_r is the resilient modulus, σ_d is the repeated deviator stress (cyclic stress in excess of confining pressure), and ε_r is the recoverable strain in a vertical direction. Based on the specifications of CRB and HCTCRB, the laboratory test results in the condition of 100% MDD at 100% OMC show its characteristics and determine suitable mathematical models of the resilient modulus of CRB and HCTCRB.

4.2.3.1 Resilient modulus results and modelling

The laboratory test for determining the resilient modulus is expensive, time-consuming, meriting suitable numbers and quality specimens to be prepared and tested for reliable results. The resilient tests are therefore mostly conducted in research and review of the test complexity perspective. It is desirable to find a suitable resilient modulus model based on laboratory results to estimate resilient modulus values. Furthermore in recent years, computer programs are new relevant to pavement analysis and design so resilient modulus is an important input parameter for the analysis and design program. Generally, the resilient modulus is the non-linear relationship with respect to the magnitude of applied stresses. The K-Theta (K- θ) model (Hick and Monosmith 1971) is the significant model for the non-linear behaviour of the granular materials and it is taken into account for the resilient modulus behaviour of CRB and HCTCRB in this study.

Figure 4.20 shows the results of the resilient modulus test plotted versus loading sequences, revealing that the CRB resilient modulus is between 100 and 300 MPa and the values of HCTCRB over a 7 day hydration period are at a minimum of 300 MPa and a maximum of 950 MPa. Cement added in CRB with an appropriate

amount of water, producing HCTCRB, gains more resilient modulus values than that of original CRB of 3 times.

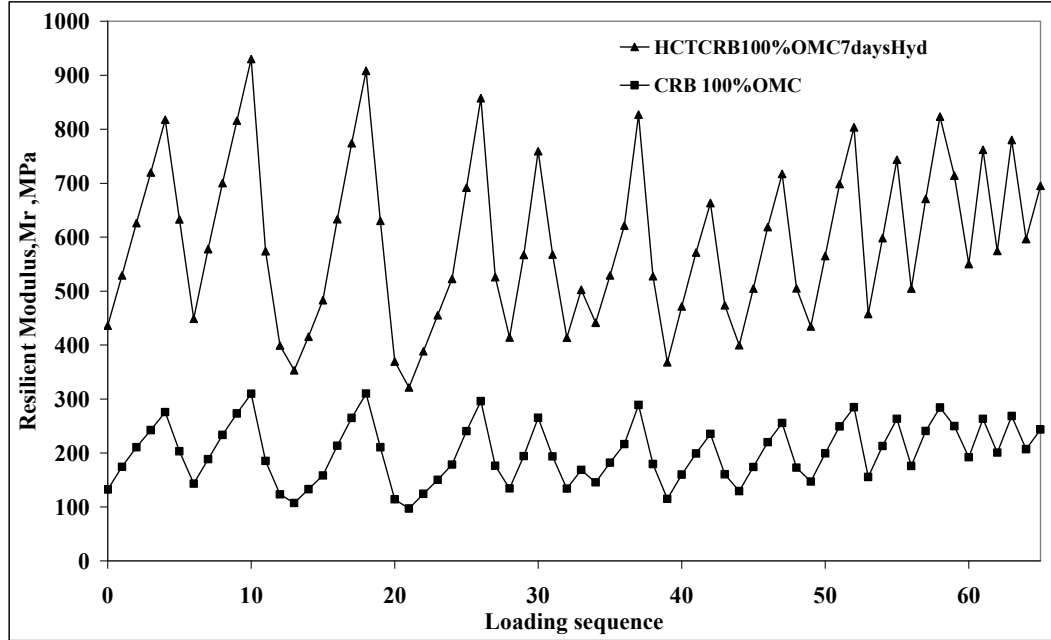


Figure 4.20 Resilient modulus results of CRB and HCTCRB

Generally, resilient modulus results are non-linear with respect to the magnitude of applied stresses. The results of the resilient modulus of CRB and HCTCRB can be modelled reasonably by using The K-Theta ($K-\theta$) model (Hick and Monosmith 1971). Figure 4.20 shows the results of the test plotted versus the loading sequences. The representative $K-\theta$ model of CRB and HCTCRB are exhibited in Equations (4.2) and (4.3) respectively.

$$M_r = k_1 \cdot \theta^{k_2} = 1.8604\theta^{0.7606} \text{ for CRB} \quad (4.2)$$

$$M_r = k_1 \cdot \theta^{k_2} = 8.9102\theta^{0.6817} \text{ for HCTCRB} \quad (4.3)$$

where M_r is the resilient modulus, MPa; θ is bulk stress ($\sigma_1 + \sigma_2 + \sigma_3$) where ($\sigma_2 = \sigma_3$); σ_1 is the major principal stress (vertical axial stress); σ_3 is the minor principal stress (confining stress); k_1 and k_2 are regression coefficients as shown in Table 4.4.

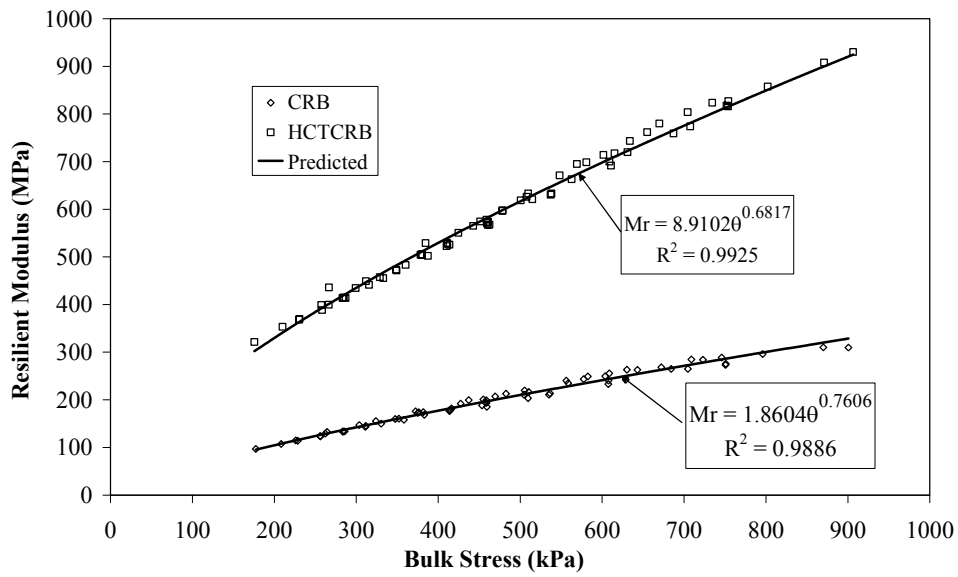


Figure 4.21 The CRB and HCTCRB resilient modulus models and the measurements

Table 4.4 and Figure 4.21 show the results of modelling resilient modulus values of CRB and HCTCRB based on the resilient modulus tests in this study. From Figure 4.21, it can be seen that the K-Theta model used in this study is a suitable resilient model for unbound granular materials in this study. The application of this resilient modulus model will be discussed in the next chapter.

Table 4.4 Resilient modulus models for CRB and HCTCRB

Model	Equation	The regression coefficients		Symbols
K-Theta (K- θ)	$M_r = k_1 \theta^{k_2}$	k_1	k_2	M_r = Resilient modulus, MPa θ = Bulk Stress = $(\sigma_1 + \sigma_2 + \sigma_3)$
CRB		1.8604	0.7606	k_1, k_2 = Regression coefficients
HCTCRB		8.9102	0.6817	

4.2.3.2 The effects of hydration periods and water content

To investigate the moisture content effects of CRB and HCTCRB, the results of 100%, 80% and 60% OMC were represented to show their characteristics. Figure 4.22 shows the results of the resilient modulus test plotted against the bulk stress $(\sigma_1 + \sigma_2 + \sigma_3)$ for CRB at different %OMC. It was found that:

- All crushed rock samples exhibit the stress-dependency behaviour.
- There is a significant improvement of resilient modulus and permanent deformation between 100%OMC and 80%OMC after a dry back process. However, the results present slight differences of resilient modulus and permanent deformation characteristics between 80%OMC and 60%OMC. It means that the moisture content does greatly affect the performance of CRB at unsaturated conditions in terms of the resilient modulus. During the 100%OMC, the pore pressure inside soil skeleton reduced crushed rock stiffness and the cohesive bonding was broken up during the loading process.

- Based on 65 stress levels of loading of the RLT test, the resilient modulus values of all crushed rock samples of these conditions are between 150 MPa and 550 MPa at 60%OMC.
- To minimise the effect of moisture content, CRB should be achieved at least 80% OMC of the dry back process to improve performance before bituminous surface overlaying.

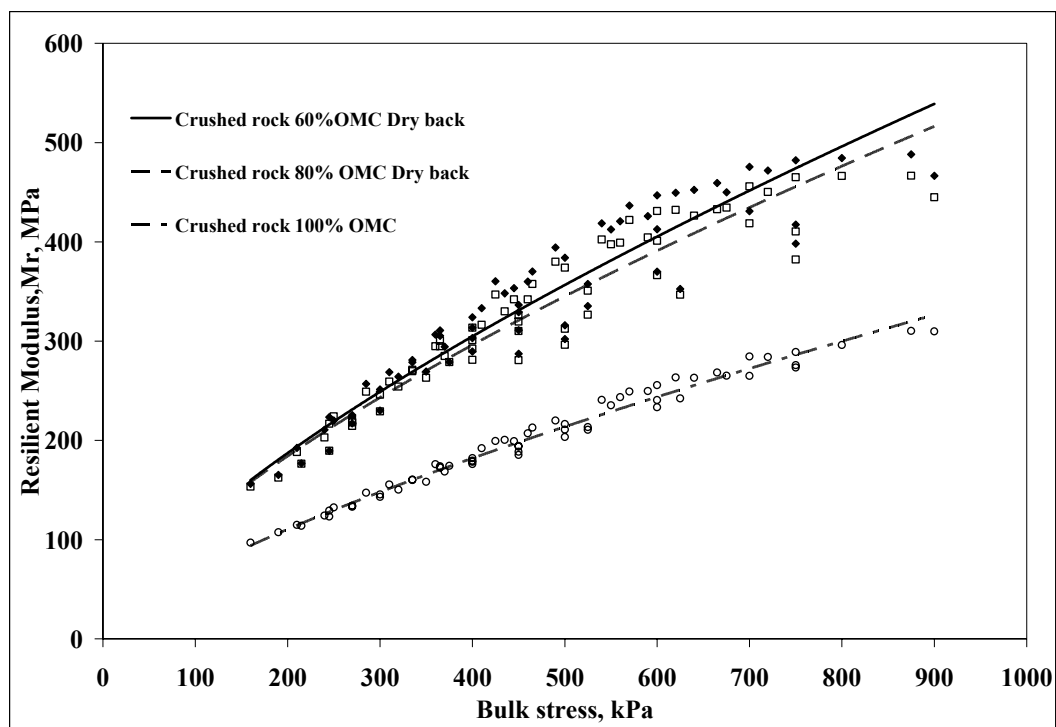


Figure 4.22 The resilient modulus of CRB at various moisture contents

Figures 4.23, 4.24 and 4.25 show the resilient modulus results of HCTCRB samples of 100%OMC, 90%OMC, and 80%OMC at 7, 14, and 30-day hydration periods. Resilient modulus values are plotted against loading sequences. All HCTCRB samples show significantly higher resilient modulus values than CRB.

indicating CRB can improve its resilient modulus characteristic by using the HCTCRB technique.

- There is a slight difference in resilient modulus characteristics of HCTCRB at all percentages of OMC over 7, 14, and 30-day periods. That means the hydration period and added water in this investigation do not affect the performance of HCTCRB in terms of the resilient modulus characteristics very much. This is a result of the re-treating before compaction in HCTCRB producing processes. During the hydration period, the chemical reaction between cement and water generates cementitious bonding. The bonding is broken up in the re-treating process. Although a compaction process is performed directly after re-treating, the chemical bonding, which is significant to the strength, is hard to generate further. The mixture is only compacted from the same energy effort thus the resilient modulus characteristics of all samples with different conditions of water and hydration periods are slightly different.
- All HCTCRB samples exhibit the stress-dependency behaviour.
- Based on 65 stress levels, the resilient modulus values of all HCTCRB samples of these conditions are between 300 MPa and 1100 MPa.

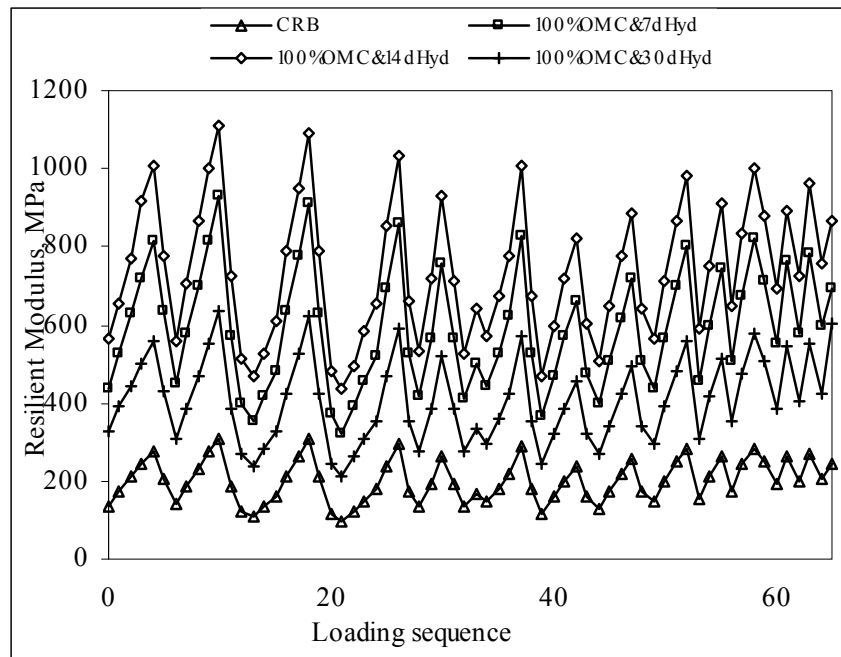


Figure 4.23 The resilient modulus at 100%OMC over various hydration periods

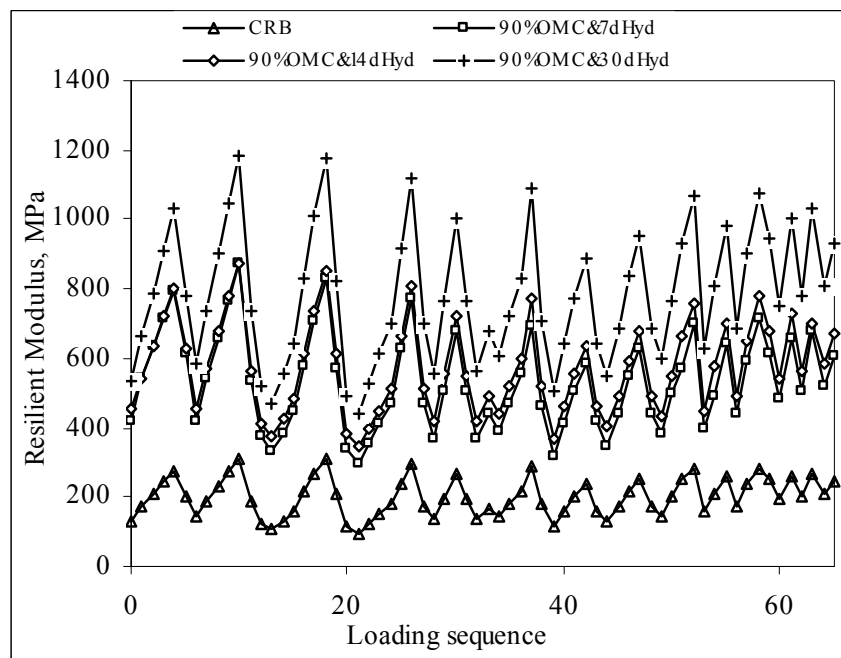


Figure 4.24 The resilient modulus at 90%OMC for various hydration periods

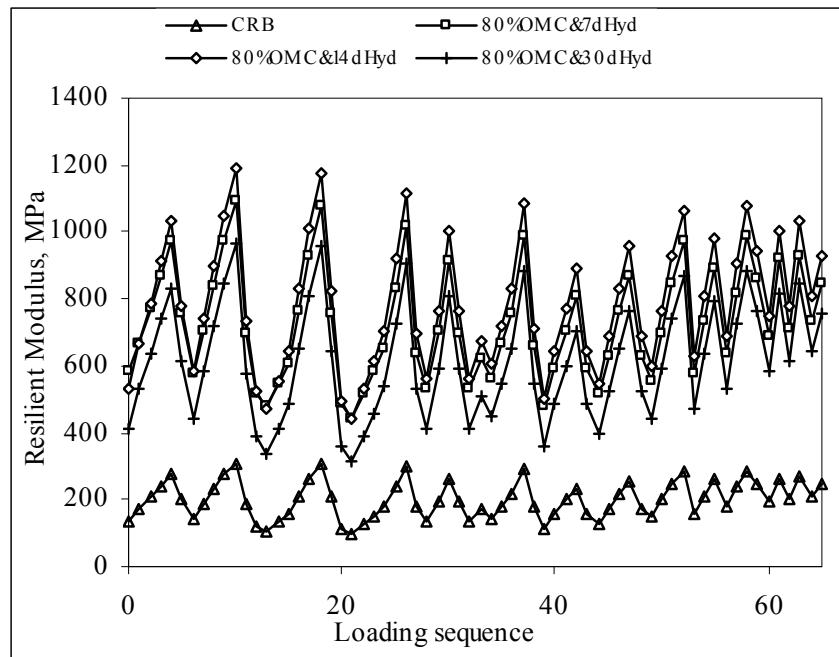


Figure 4.25 The resilient modulus at 80%OMC for various hydration periods

As there are some doubts about the suitable moisture content and hydration period of HCTCRB, a series of tests was performed on 5, 7, 15, 30 and 45 day hydration periods with 3 OMC types (A, B and C) of HCTCRB as stated in Chapter 3.

- It found all hydration periods exhibit relatively similar resilient modulus curve tending on HCTCRB type A as shown in Figure 4.26.
- HCTCRB after a hydration period without additional water does not present significant response at various hydration periods, unlike HCTCRB types B and C as shown in Figures 4.27 and 4.28, where resilient modulus results present inconsistent results between particular hydration periods but the resilient modulus results of type C tend to increase with a hydration period of more than 7 days, higher than type A and B.

- If HCTCRB behaves at its individual %OMC, then it will present high performance in terms of resilient modulus. Consequently, HCTCRB is significantly more moisture susceptibility than CRB.
- The compaction process at a construction site should be started after a 7 day hydration period of stockpiled HCTCRB and be compacted without additional water or less than a water content of 8%. If HCTCRB is compacted as wet side, the compacted layer can not begin surface overlaying unless is achieved 80% of dry back.

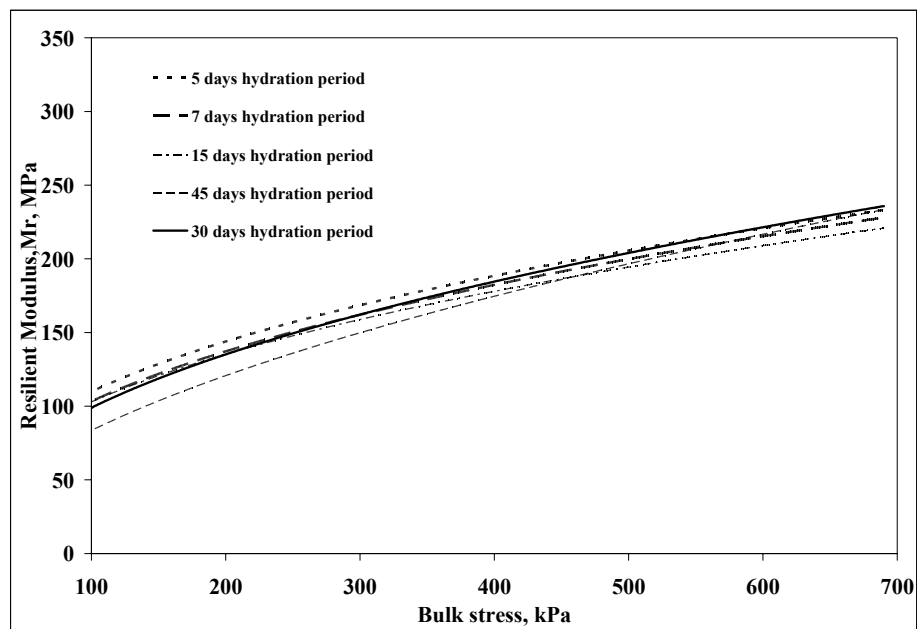


Figure 4.26 The resilient modulus results of HCTCRB type A
(no additional water)

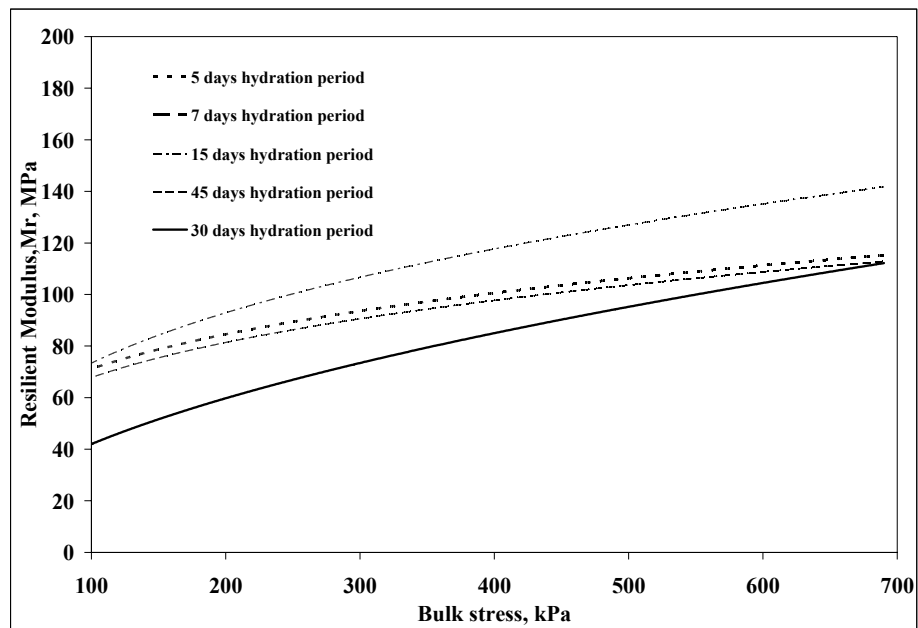


Figure 4.27 The resilient modulus results of HCTCRB type B
(8% additional water)

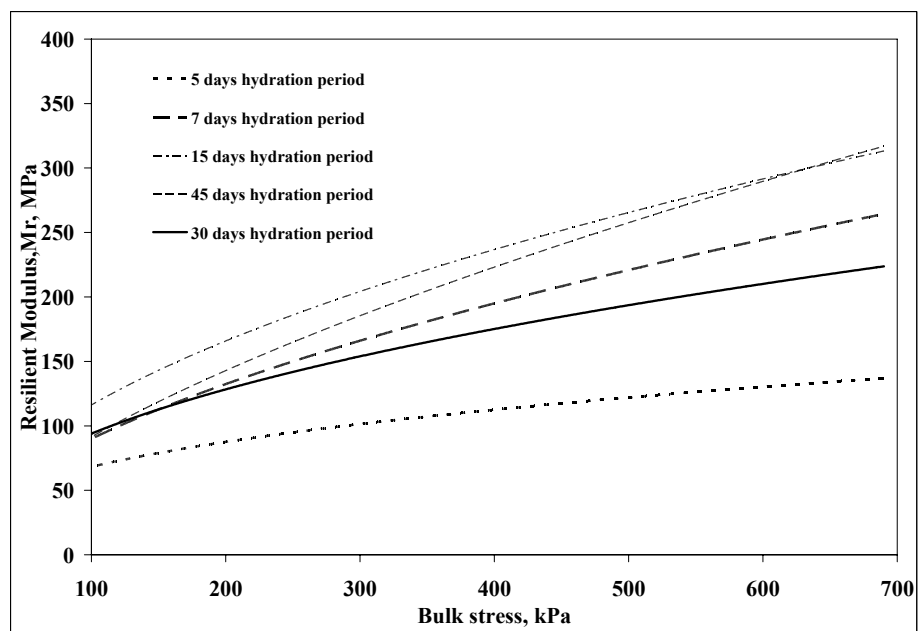


Figure 4.28 The resilient modulus results of HCTCRB type C
(%OMC additional water)

4.2.4 Permanent deformation

Permanent deformation of pavement materials, manifest as rutting and shoving, particularly along the outer wheel path near the pavement shoulder, results from the material having insufficient stability to cope with the prevailing loading and environmental conditions (Austroads 2004). It is necessary to understand pavement performance in terms of permanent deformation characteristics under traffic loading. Normally, permanent deformation at the top of the base course is not taken as a design criterion unlike the tensile strain at the bottom of the asphalt layer and the vertical compressive strain or the permanent deformation at the top of the subgrade. At the moment, there is no suitable model which reliably describes rutting development in the base course under traffic. However, to estimate rutting characteristics of stabilised red sand, the test procedure of the Austroads-APRG 00/33 standard (Voung and Brimble 2000) was used in this study.

4.2.4.1 Permanent deformation results and modelling

This section presents the permanent deformation behaviour of CRB and HCTCRB. Figures 4.29 and 4.30 illustrate the typical results of the deformation tests in terms of the relationship between permanent deformation and loading cycles for CRB and HCTCRB respectively. The various test values can be extracted from Figures 4.29 and 4.30 for assessing the potential for deformation under real conditions. Furthermore, it can be noted that the deformations of CRB and HCTCRB are dominated by the applied load in the testing range because when they increase from loading stage 1 to loading stage 3, the deformation of such material increases significantly. Similarly, the number of loading cycles also seems to be influenced by the permanent deformation values.

Figures 4.29 and 4.30 also indicate that deformation can be modelled quite reasonably by using the model suggested by Sweere, G.T.H from SAMARIS (SAMARIS 2004). Sweere suggested for the long-term deformation behaviour of unbound granular materials (UGMs) under a large number of load cycles the approach to employ as the proposed deformation model of CRB and HCTCRB is shown in Equations (4.4) and (4.5) respectively.

$$\varepsilon^p = A \cdot N^B = 0.7168 \cdot N^{0.1095} \text{ for CRB} \quad (4.4)$$

$$\varepsilon^p = A \cdot N^B = 0.0231 \cdot N^{0.1841} \text{ for HCTCRB} \quad (4.5)$$

where ε^p is permanent deformation in millimeters; A and B are regression constants; and N is the number of loading cycles.

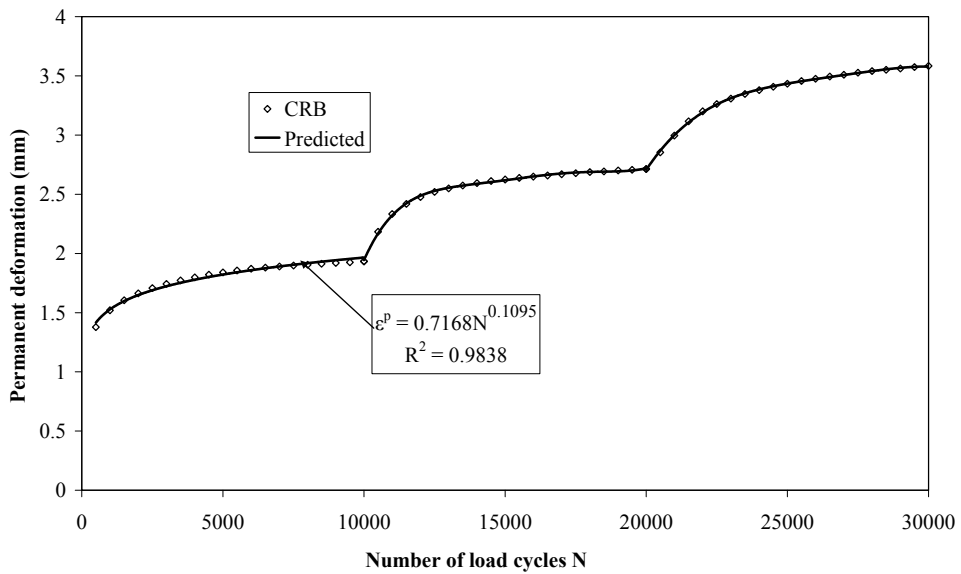


Figure 4.29 CRB permanent deformation predictions

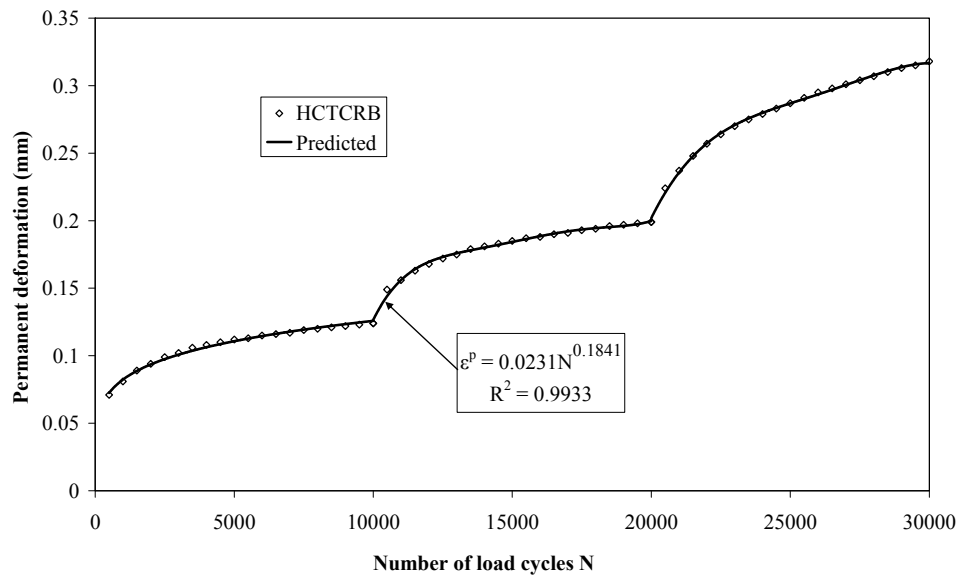


Figure 4.30 HCTCRB permanent deformation predictions

4.2.4.2 The effects of hydration periods and water content

From Figure 4.31, there is a significant difference of permanent deformation between 100%OMC and 80%OMC after the dry back process of CRB.

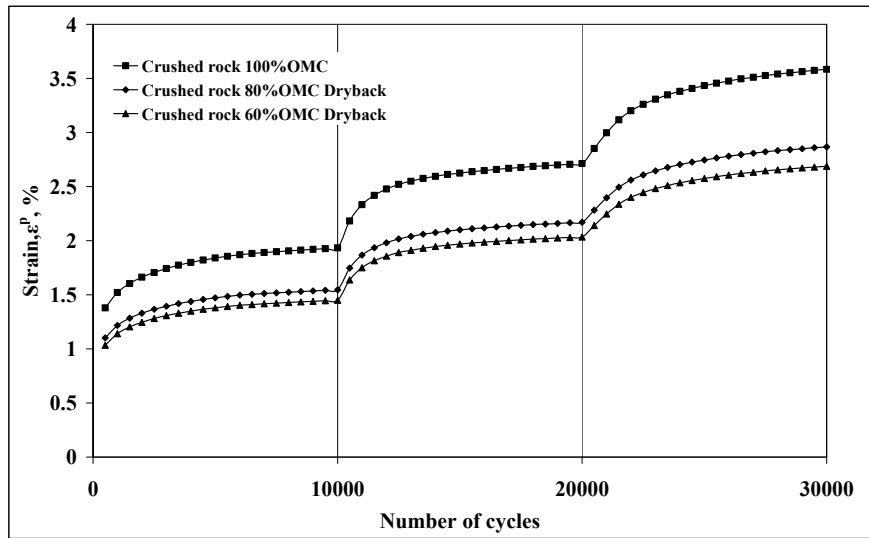


Figure 4.31 CRB permanent deformations with various %OMC

However, the results reveal a small difference of permanent deformation characteristics between 80%OMC and 60%OMC relative to the resilient modulus. Permanent deformation of CRB was greatly improved by the addition of 2% cement content as shown in Figure 4.32.

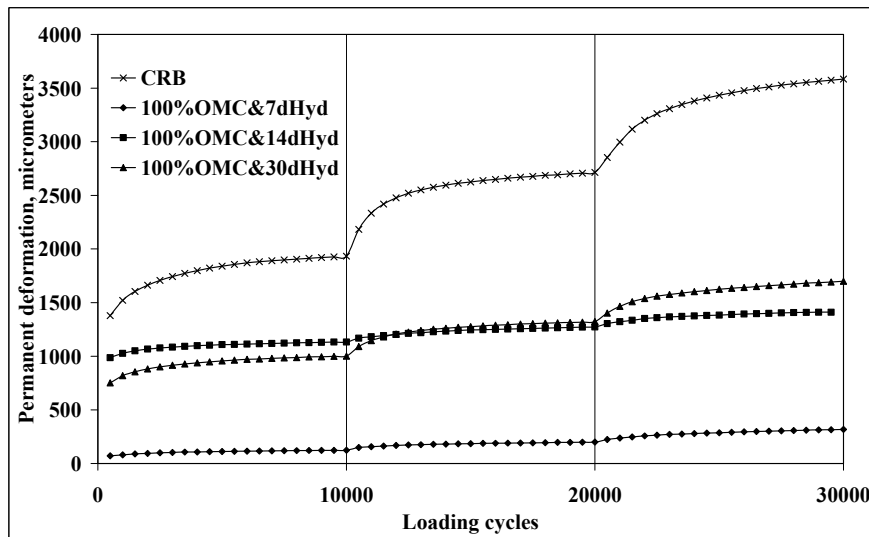


Figure 4.32 Comparison of permanent deformations between CRB and HCTCRB

As main interest regarding water and hydration effects should be which moisture content and hydration periods are suitable for HCTCRB, a series of tests was performed on 5, 7, 15, 30 and 45 day hydration periods with 3 OMC types (A, B and C) of HCTCRB. All the periods present a moderate trend of curves and very low permanent deformation on HCTCRB type A as shown in Figure 4.33, unlike HCTCRB type B as shown in Figures 4.34, where permanent deformation scattering results between particular hydration periods and there were extremely high permanent deformations. Remarkably, this type is unable to withstand a full load sequence without premature failure. It means that the HCTCRB hydration periods do not present a significant response at various hydration periods unless water is added. Permanent deformation results of type C were very low, similar to type A except that HCTCRB at a 5 day hydration period shows the highest value. Thus if HCTCRB conducts at its individual %OMC and without additional water, then it will present an acceptable permanent deformation. Compaction should therefore be started after a 5-7 day hydration period of stockpiled HCTCRB and compacted without additional water or less than a water content of 8%. If HCTCRB is compacted with high moisture content, surface overlaying is not allowed to begin unless it achieves a suitable OMC or less.

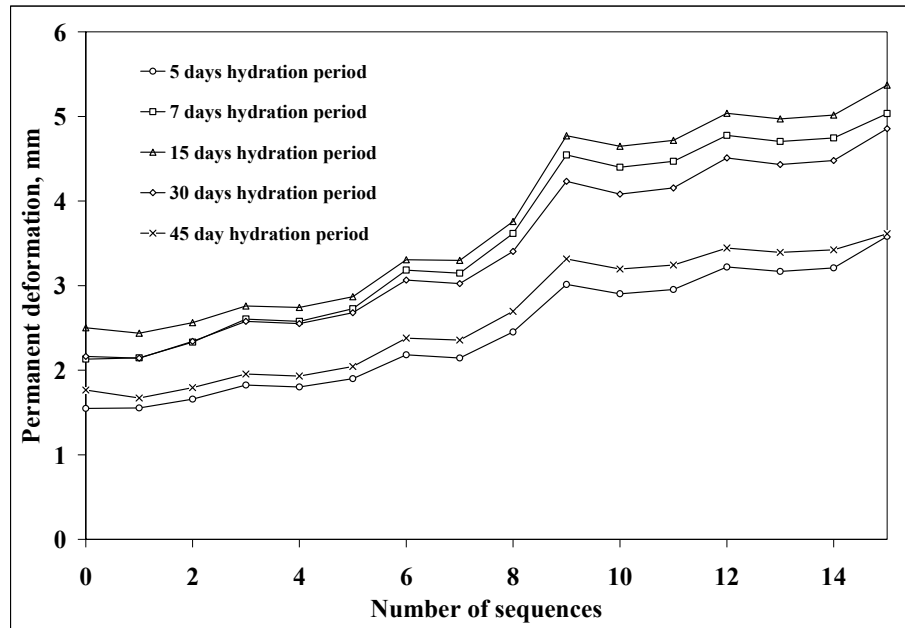


Figure 4.33 Permanent deformations of HCTCRB type A (no additional water)

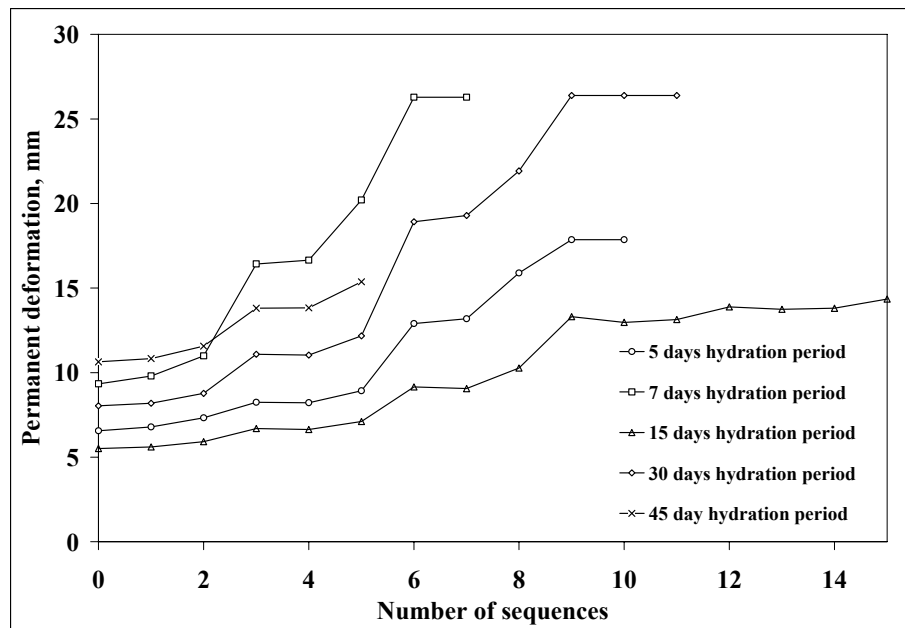


Figure 4.34 Permanent deformations of HCTCRB type B (8% additional water)

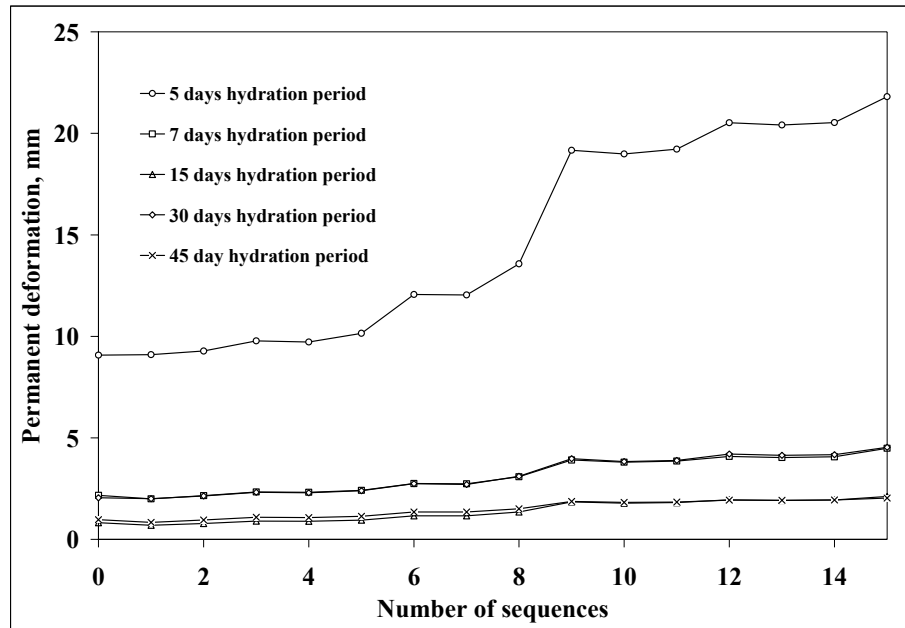


Figure 4.35 Permanent deformations of HCTCRB type C
(%OMC additional water)

4.2.5 Shakedown behaviour

According to the test results, three ranges of permanent deformation characteristics are illustrated in Figures 4.36 and 4.37. As the test results show CRB and HCTCRB responses always produce permanent deformation during cyclic loading and they show no purely elastic behaviour under repeated cyclic loads same as that in common base course materials (Werkmeister, Dawson et al. 2001). For the results of the plastic behaviour of CRB and HCTCRB, it can be noticed that the multi-layer linear elastic theory would not be suitable to analyse precisely the CRB layer in a pavement structure. Permanent deformation behaviour is described on the basis of internal friction between grains, particle shape, compaction, consolidation, distortion, etc and test results can be explained separately into three ranges (Ranges A, B and C) in according with the shakedown concept.

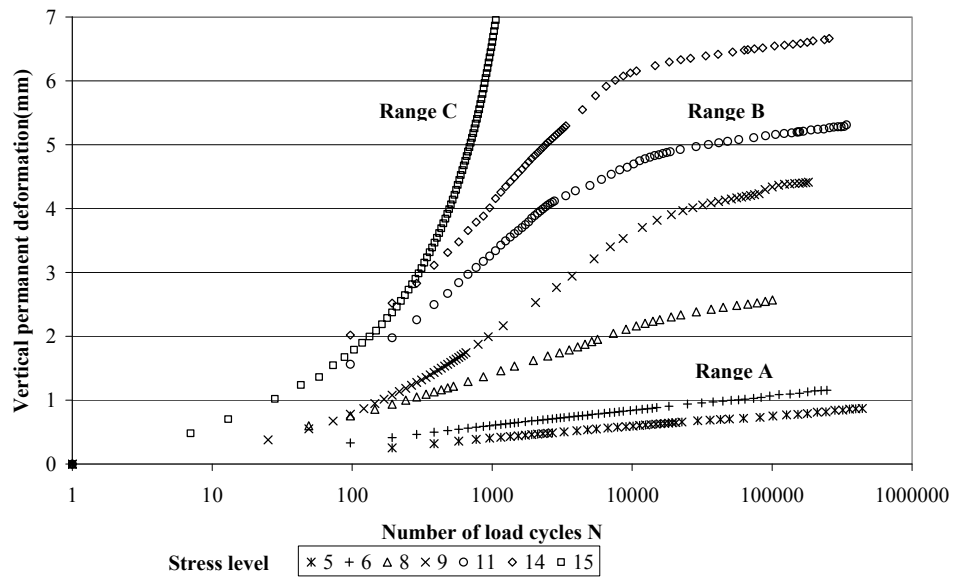


Figure 4.36 CRB vertical permanent deformations versus number of load cycles

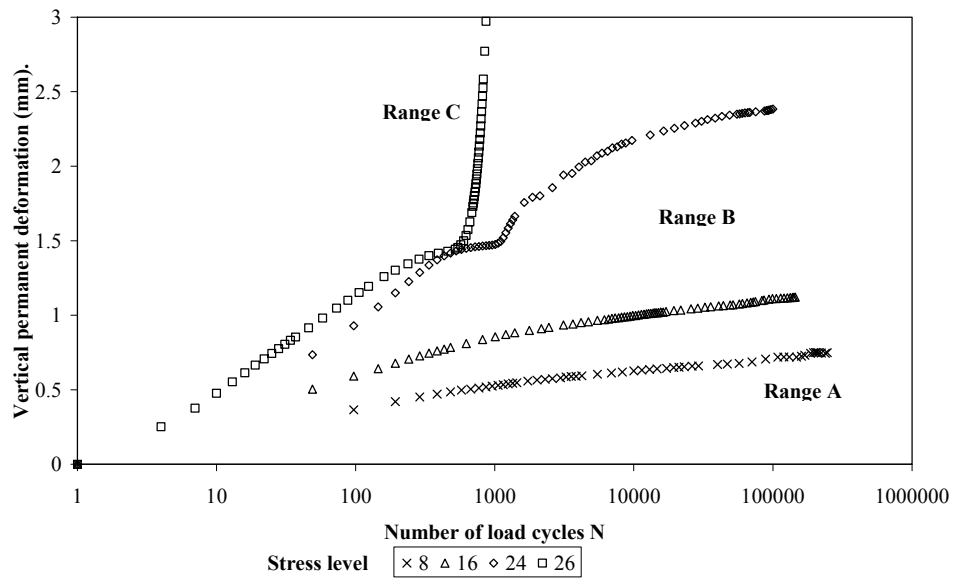


Figure 4.37 HCTCRB permanent deformations versus number of load cycles (N)

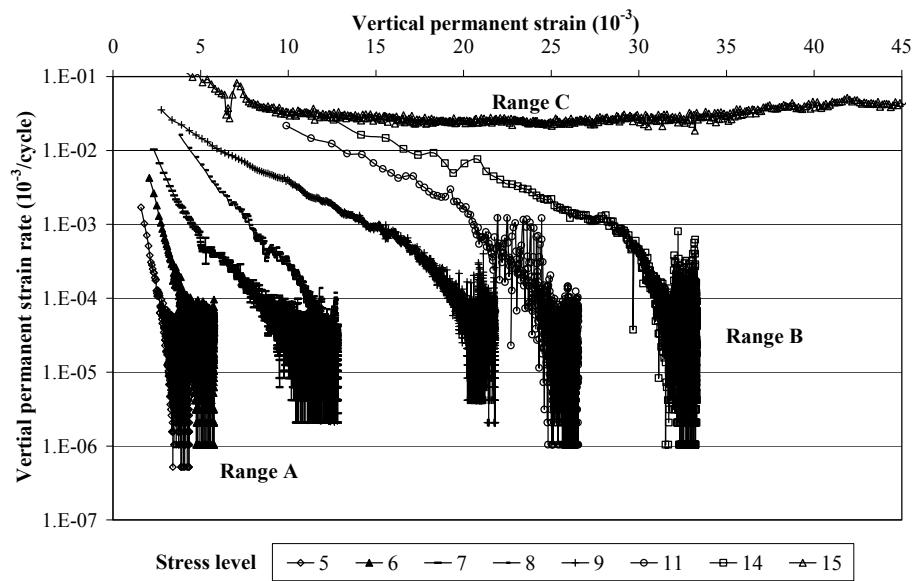


Figure 4.38 CRB vertical permanent strain rate versus vertical permanent strain

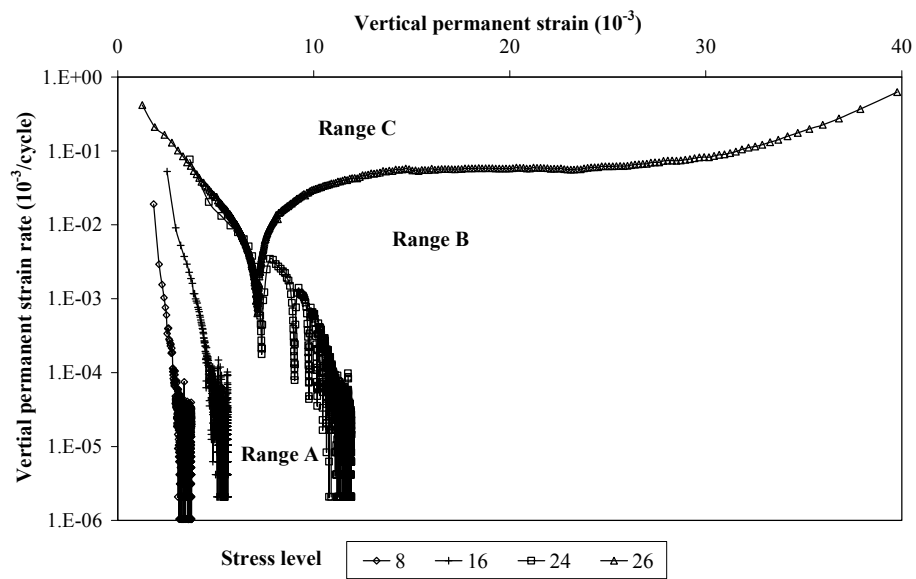


Figure 4.39 HCTCRB permanent strain rate versus vertical permanent strain

4.2.5.1 Range A – Plastic shakedown range

The lower group of lines (Stress levels of 5 to 9) in Figure 4.36 indicate the response of Range A of CRB. The behaviour is entirely plastic for a number of cyclic load cycles until it reaches a stable state after the post-compaction period, the response becomes completely resilient (no further vertical permanent displacement) as shown in Figures 4.36 and 4.38. Figure 4.37 shows Range A of HCTCRB at stress levels 8-16 is more than CRB twice and HCTCRB working state of stress level 11 achieved Range A. Figures 4.38 and 4.39 indicate that the vertical permanent strain rate decreases rapidly until it reaches a state of equilibrium. Figures 4.40 and 4.41 demonstrate strain model under the given stress levels by using the model coefficients as shown in Table 4.5. In an observation of each stress level, a number of load cycles are required before a stable condition of the test material exhibits. It could be concluded that CRB behaviour of the stress levels of 5 to 9 and HCTCRB behaviour of the stress levels of 8 to 16 become stable after the post-compaction stage under service load at the given stress level. Also, Range A of the shakedown behaviour can be allowed in pavements, an adequately small accumulated displacement, as acceptable permanent deformation would be seen in a course base layer and this would terminate after a set number of load cycles. CRB and HCTCRB do not reach failure.

Table 4.5 Model coefficients for Range A

Type	CRB	HCTCRB
parameter	Range A	Range A
a_1 [-]	0.000115	0.00185
a_2 [kPa ⁻¹]	-0.02000	-0.11000
a_3 [kPa ⁻¹]	0.000001	0.0000013
a_4 [-]	1.7600	1.8500
b_1 [-]	0.00050	0.00030
b_2 [kPa ⁻¹]	-0.00800	-0.01200
b_3 [kPa ⁻¹]	0.00590	0.00200
b_4 [-]	0.55000	0.12000

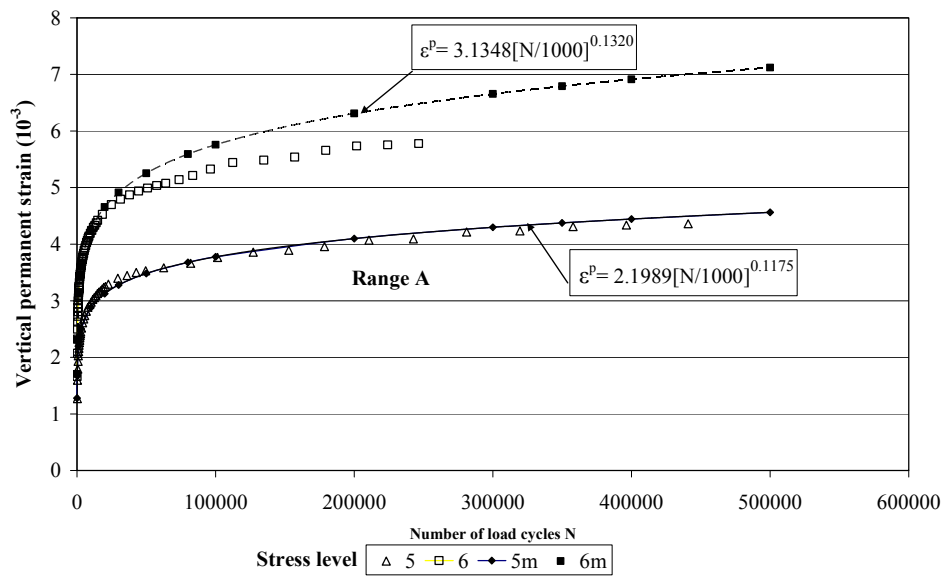


Figure 4.40 CRB Range A vertical permanent strains versus number of load cycles compared with the strain model

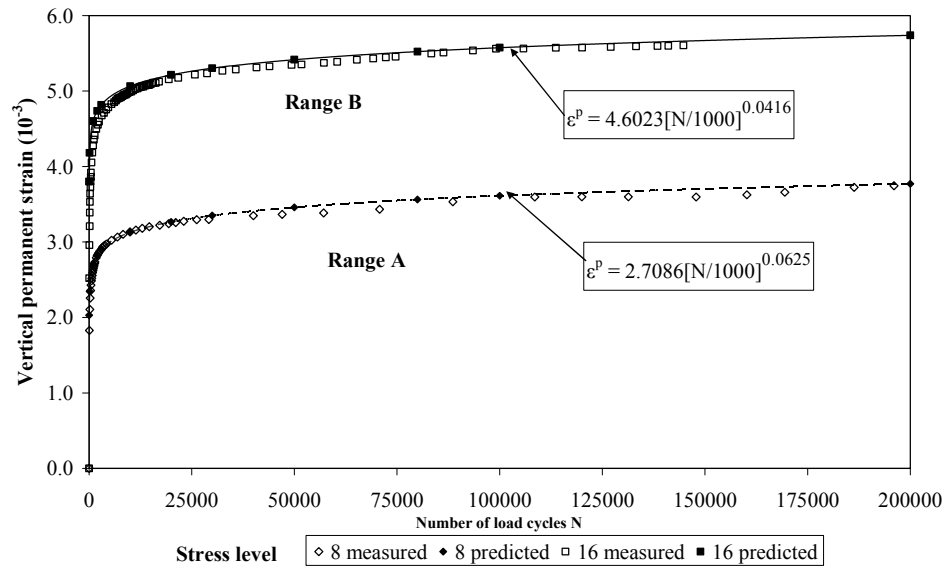


Figure 4.41 HCTCRB Ranges A and B vertical permanent strain compared with the strain model

4.2.5.2 Range B – Intermediate response – Plastic creep

Figures 4.36 and 4.37 show the response of Range B (stress levels of 10 to 14 for CRB and stress levels of 16 to 24 for HCTCRB) which are intermediate responses of all observations in this study. Their characteristics can be described that at the early stage of the load cycles, the level of permanent strain rates decreases significantly but they are lower than that of Range A as shown in Figures 4.38 and 4.39. The degree of an increase in the permanent strain rate of the early stage of loading cycles can be observed from the slope of the graphs in Figures 4.38 and 4.39. It is clear that the slope of the Range A response graph is steeper than the graph of Range B response. That means the Range A response exhibits higher permanent strain rates. In Figure 4.42, the example of the Range B response graph between permanent strain rates and numbers of loading cycles is illustrated and

the end of the post-compaction stage can be defined roughly as the point that the permanent strain rate becomes constant or the response graph starts to flat which is at the loading cycle of 70,000. In Figure 4.43, the comparison of the measured vertical permanent strains and the strain model which is derived from model coefficients as shown in Table 4.6 is illustrated. However, it can be predicted that an excessive permanent strain would not occur while an unbound pavement material is in this Range B response but this characteristic could maintain for a number of load repetitions until the material starts to exhibit the larger permanent deformation at which the material is going to Range C of a failure characteristic.

Table 4.6 Model coefficients for Range B

Type	CRB	HCTCRB
parameter	Range B	Range B
$a_1 [-]$	0.00050	0.00011
$a_2 [\text{kPa}^{-1}]$	1.44000	1.45000
$a_3 [\text{kPa}^{-1}]$	-0.00150	-0.00040
$a_4 [-]$	1.3550	1.4450
$b_1 [-]$	0.00735	0.00350
$b_2 [\text{kPa}^{-1}]$	0.00010	-0.08550
$b_3 [\text{kPa}^{-1}]$	0.00010	0.00010
$b_4 [-]$	0.000001	0.55000

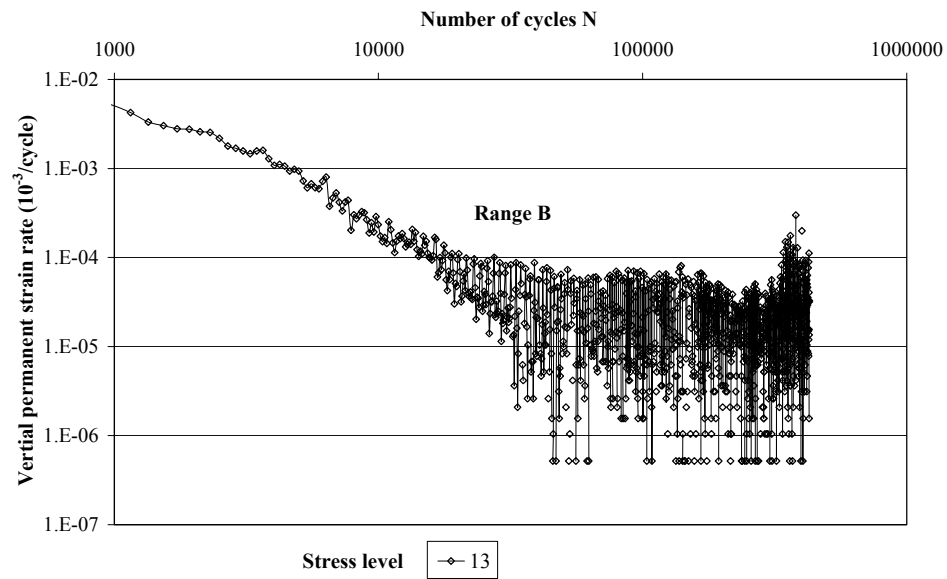


Figure 4.42 CRB vertical permanent strain rate versus number of load cycles

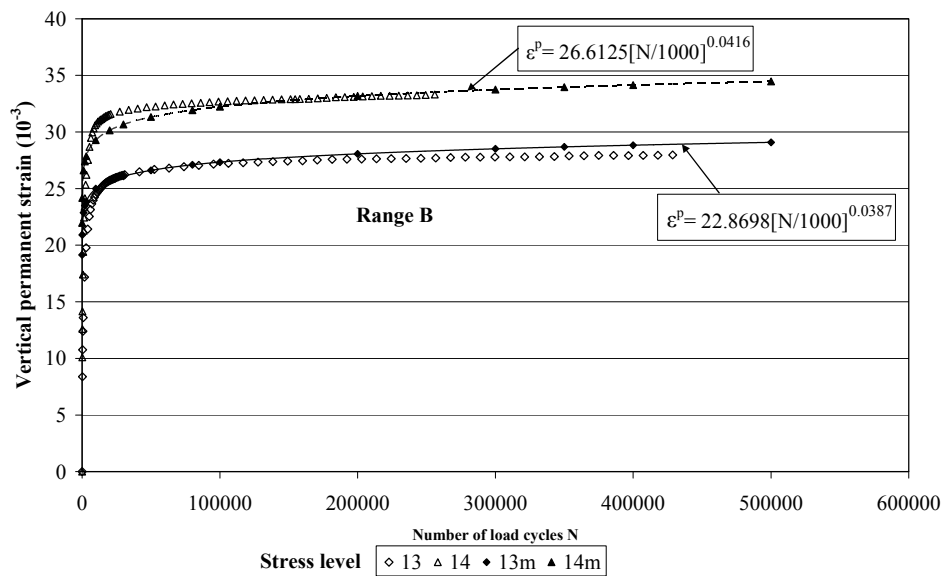


Figure 4.43 CRB Range B vertical permanent strain versus number of load cycles compared with the model

4.2.5.3 Range C – Incremental collapse

In Figures 4.36 and 4.37, at stress level of 15 for CRB and stress level of 26 for HCTCRB, Range C response exhibits. The response graph of Range A is unique when compared with others. It is observed that from the graphs of the stress level of 15 for CRB and stress level of 26 for HCTCRB, the permanent strain rate decreases slowly from the beginning and then becomes nearly constant. While the permanent strain rate is constant, it means excessively large amounts of permanent deformation occur in every consecutive loading cycle; and this characteristic refers to the failure of materials taking place. At the Range C stress level of the particular material, the failure occurs at a relatively small number of loading cycles when the cumulative permanent strain rate becomes almost constant at the particular permanent strain as shown in Figure 4.44. The test materials at this stress level cannot maintain a stable state. Range C response of CRB and HCTCRB would cause failures in pavements from excessive deformation in the base layer which this lead to rutting exhibits in a pavement surface. In practice, it could indicate that CRB and HCTCRB as base course materials are absolutely not suitable for the pavement which has the stress level of 15 and 26, respectively taking place in the base course layer. Figures 4.45 and 4.46 illustrate the permanent strain model compared to the measured values.

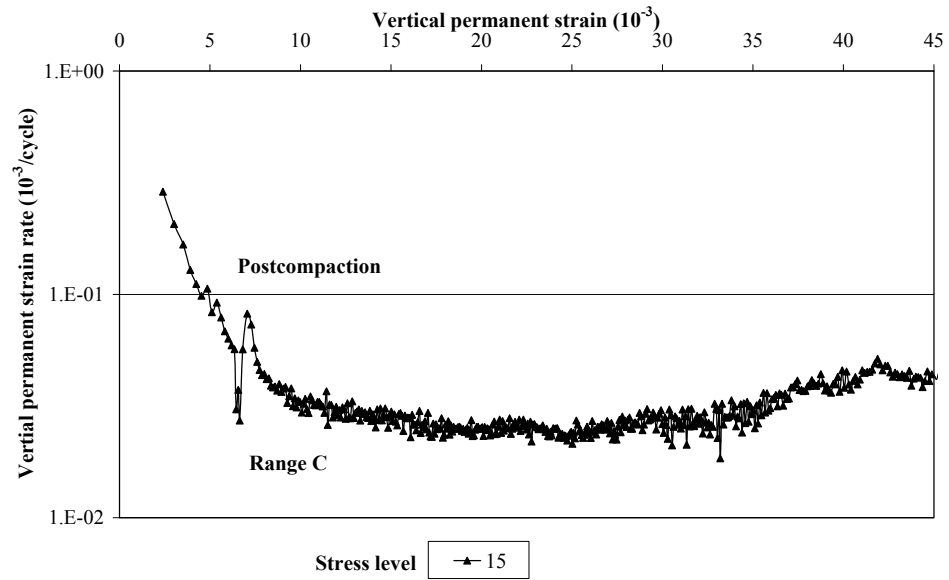


Figure 4.44 Vertical permanent strain rates versus number of load cycles

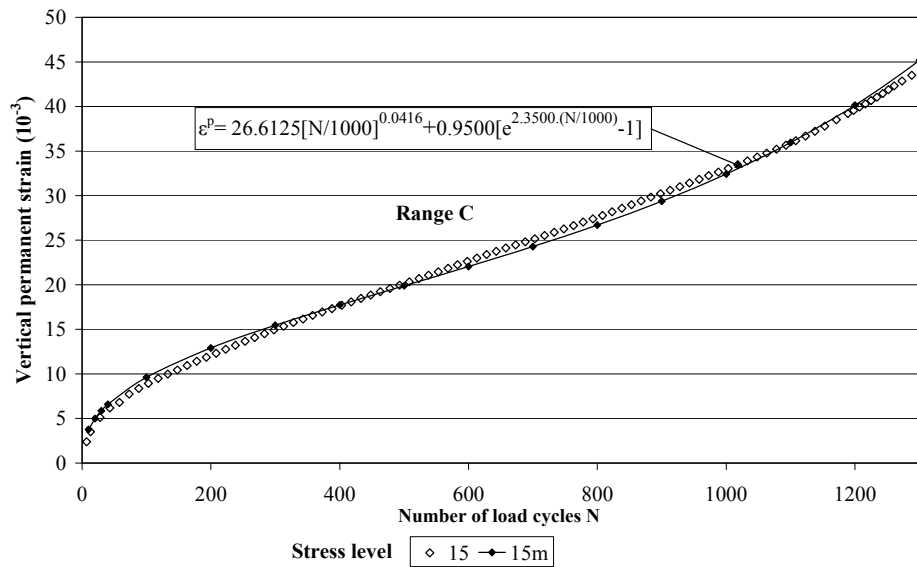


Figure 4.45 CRB Range C vertical permanent strain versus number of load cycles compared with the strain model

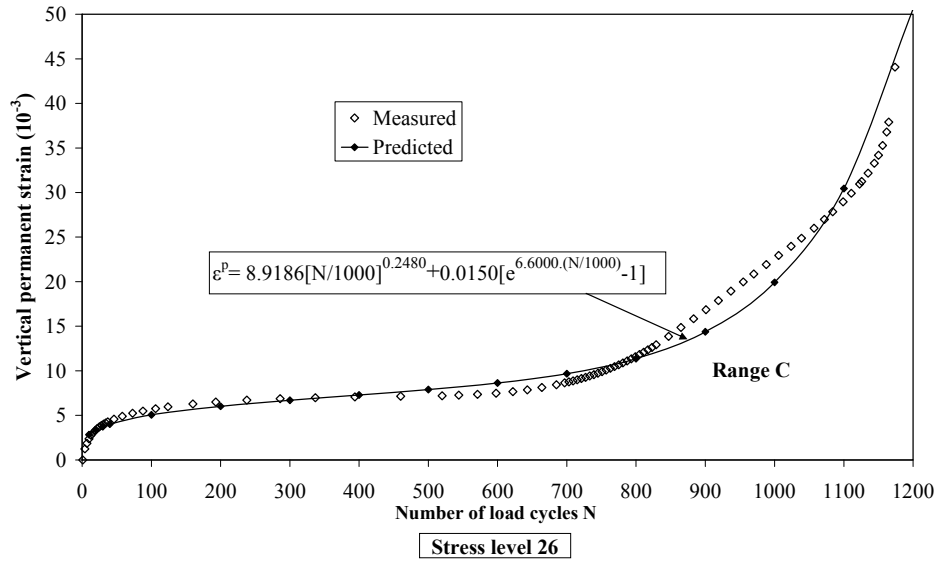


Figure 4.46 HCTCRB Range C vertical permanent strain compared with the strain model

It can be concluded that the use of the shakedown concept to explain the behaviour of CRB and HCTCRB under cyclic loading conditions from RLT test is applicable, although the adaptation of this concept has established to allow for particular responses of solid materials subjected to repeated loading. The shakedown ranges defined in this paper, Ranges A, B, and C, also occurs in all UGMs as observed by other researchers. CRB and HCTCRB under designed stress level conditions show a relationship between permanent strains and a number of loading cycles. When a number of cyclic loads are applied, the permanent deformation occurs accumulatively. For CRB and HCTCRB as Unbound Granular Materials, UGMs, these materials comprise of the discrete particles of coarse grains and fine grains. All discrete particles need to rearrange and adjust themselves by getting closer while subjected to cyclic loads to gain more stable resistant from an externally applied load and the material becomes denser under the externally cyclic load. By getting closer of CRB and HCTCRB

particles, the plastic deformation takes place. This behaviour of CRB and HCTCRB or UGMs under cyclic loading conditions lead to that the use of a purely elastic approach in pavement analysis is not appropriate as no purely elastic response is found in the CRB and the HCTCRB during repeated cyclic loading tests.

For low stress levels, the CRB behaves corresponding to Range A at stress levels of 5 to 9 and at stress levels of 8 to 16 for HCTCRB. After some cycles from the beginning, the particles can reach a stable state because some energy can dissipate because of viscosity of a material. At this range of stress levels, the dissipated energy is independent of the loading and does not change from one cycle to another. The pavement will reach a shakedown limit after post-compaction deformation, with no further permanent deformation developing, and the vertical strain rate rapidly increases and the material subsequently responds elastically. Hence Range A of CRB and HCTCRB would be accepted for pavement construction when the accumulated strains before the development of fully resilient behaviour is sufficiently small (a stable state of materials). The other step of this study is to examine the application of material in the pavement that responds to Range B. For higher loadings at stress levels of 10 to 14 for CRB and at stress levels of 16 to 24 for HCTCRB, the energy input is first quickly dissipated by re-arrangement from the sliding of internal contacts of material particles, the so-called post-compaction. The dissipated energy per cycle relaxes then to a stationary value, therefore the vertical strain rate decreases up to a constant rate. This characteristic depends on magnitude and frequency of cyclic loads and also on the friction and the stiffness of contact points of soil grains. A deep investigation of the size dependence would help to identify if the material is evolving on a much longer time scale to a final shakedown state in which all the energy supplied to the system is dissipated. It seems that the material in Range B

does not shake down, rather it would fail due to excessive deformation at a very high number of load repetitions. It is important to know the acceptable maximum number of load cycles at a failure. That would prevent distress rapidly occur in the pavement after Range B ends. Further tests with load applications up to 1,000,000 load cycles may be necessary to find the point of failure. For many low-volume road pavements where the total number of vehicles carried is small and maintenance is probably required to correct inadequacies other than traffic-induced rutting, Range B behaviour would also be acceptable for pavements. Range C behaviour at stress level 15 for CRB and 26 for HCTCRB would not be allowed to occur in pavements. If the stress levels imposed are high enough, there is no possibility for a material to re-arrange to the new state and post-compaction leads to an incremental collapse. The material is not able to dissipate enough energy without changing its configuration so it needs to modify its shape.

The Range A limit (plastic shakedown limit) can be used to predict whether or not a stable state occurs in the UGM layer of the road structure. The plastic shakedown limit of CRB and HCTCRB should be used in the Western Australian pavement design guidelines. It can be suggested that the maximum stresses occurring in UGM layers would be within Range A. Based on a current pavement design guideline, the approximated working stress of Western Australian road is around the level of 11 at the base layer indicating that CRB reacts corresponding to Range B behaviour and possibly deterioration at a number of load repetitions. As noticed for Range B response of UGMs, the acceptable maximum number of traffic loads is required to predict the service life of the CRB base course road and a suitable maintenance plan of pavements could be designed. Unlike HCTCRB which achieves Range A behaviour and will achieve a stable state with the same amount of traffic without rutting failure. This matter is necessary to remake in a pavement design guideline. It has been shown that the permanent strain

characteristics of CRB and HCTCRB could be modelled using the Dresden-model for each behaviour range separately.

4.3 Summary

CRB and HCTCRB are extensively used in Western Australia as base courses. However, there are no suitable laboratory results enabling comprehensive responses of these materials as building materials for a road base. The results obtained from laboratory study are summarised as follows:

4.3.1 Non-mechanical characterisation

The summarised results from CRB and HCTCRB are:

- Both CRB and HCTCRB have particle size characteristics suitable for a road base even if the gradation of stockpiled HCTCRB does not fit specification requirements. However, compacted HCTCRB does finally meet the specifications.
- The particle shape characterisation illustrates the different features of CRB and HCTCRB. CRB presents a rougher surface than HCTCRB, whereas CRB, formed by crushing large mineral chunks, has sharp edges and corners but the HCTCRB surface was filled with cement paste. The surface roughness of compacted HCTCRB locates between CRB and uncompacted HCTCRB. From this point, HCTCRB must have a lower internal friction value than HCTCRB (even in a compacted condition). The main compound elements of CRB and HCTCRB is SiO_2 .

- For the modified compaction test on CRB, the maximum dry densities (MDD) were 2.27 tons/m³ and 2.12 tons/m³ of HCTCRB. The optimum moisture contents (OMC) were 5.5 % for CRB and 8 % for HCTCRB.

4.3.2 Mechanical characterisation

The mechanical behaviours of CRB and HCTCRB were investigated by repeated load triaxial (RLT) tests. These were carried out in terms of the CBR test, static triaxial tests, resilient modulus tests and the permanent deformation tests to obtain an understanding of the static capable strength, resilient and permanent deformation characteristics of those materials under real conditions of traffic loading and environmental effects simulated in the tests. The summarised results from CRB and HCTCRB are shown in Table 4.7 and:

- The shear strength parameters could be modelled by using the Mohr-Columb failure envelope.
- The resilient modulus characteristics could be modelled using the following K- θ model (Hick and Monosmith 1971):

$$M_r = k_1 \cdot \theta^{k_2} = 1.8604\theta^{0.7606} \text{ for CRB} \quad (4.2)$$

$$M_r = k_1 \cdot \theta^{k_2} = 8.9102\theta^{0.6817} \text{ for HCTCRB} \quad (4.3)$$

where M_r is resilient modulus in MPa; θ is bulk stress ($\sigma_1 + \sigma_2 + \sigma_3$) where ($\sigma_2 = \sigma_3$); σ_1 is major principal stress (vertical axial stress); σ_3 is minor principal stress (confining stress); k_1 and k_2 are regression coefficients

- the long-term permanent deformation characteristics could be modelled using the Sweere's model (Sweere 1990):

$$\varepsilon^p = A \cdot N^B = 0.7168 \cdot N^{0.1095} \text{ for CRB} \quad (4.4)$$

$$\varepsilon^p = A \cdot N^B = 0.0231 \cdot N^{0.1841} \text{ for HCTCRB} \quad (4.5)$$

where ε^p is permanent deformation in millimeters; A and B are regression constants; and N is the number of loading cycles.

- Three ranges of permanent deformation accumulation were observed and the test results can be separated into three ranges (A, B and C) based on the shakedown concept.

Range A – Plastic shakedown range

Stress levels 5-9 indicate the response of Range A of CRB. The behaviour is entirely plastic for a number of cyclic load cycles although when it reaches a stable state after the post-compaction period, the response becomes completely resilient and no further vertical permanent displacement takes place. Range A of HCTCRB at stress levels 8-16 is more than twice CRB and HCTCRB working at a state of stress level 11 achieved Range A. UGMs behaviour in these stress levels would become stable after post-compaction under service loading. Also, Range A of the shakedown behaviour is allowed in the pavement, acceptable small accumulated displacement, as an acceptable permanent deformation would be seen in a course base layer and this would terminate after a set number of load cycles.

Range B – Intermediate response – Plastic creep

Stress levels 10-14 of CRB and levels 16-24 of HCTCRB present Range B. At the beginning of the load cycles, the level of permanent strain rate decreases rapidly but is less than Range A at the same time at a lower rate. Test results showed that although the deformation is not completely resilient, permanent deformation is acceptable for the first period of the cycles. CRB reacts corresponding to Range B and a great number of failures could occur if the condition does not change and if it is maintained long enough, it deteriorate in the end as Range C.

Range C – Incremental collapse

Stress levels 15 for CRB and 26 for HCTCRB indicate Range C behaviour and the permanent strain rate decreases during the first period of load cycles then its becomes lower, nearly constant. Failure occurs with a relatively small number of load cycles when the cumulative permanent strain rate increases very rapidly after which the strain rate does not decrease again. Range C behaviour in UGMs would result in the failure of the pavement by shear deformation in the base layer experienced as rutting at the road pavement surface. This range should not be employed in a designed pavement standard.

Table 4.7 Summary of non-mechanical test results of CRB and HCTCRB

Properties	CRB		HCTCRB	
CBR	Soaked (%)	Unsoaked (%)	Soaked(%)	Unsoaked (%)
	180	170	250	220
Shear Strength	Cohesion (c)	Internal friction (ø)	Cohesion (c)	Internal friction (ø)
	32 kPa	59°	168 kPa	43°
Resilient modulus	100-300 MPa		300-900 MPa	
Permanent deformation	3 mm		0.3 mm	
Shakedown	Range B		Range A	

CHAPTER 5

IMPLEMENTATION OF EMPIRICAL - MECHANISTIC PAVEMENT ANALYSIS AND DESIGN

5.1 Overview

Flexible pavement with thin bituminous surfacing is widely used in the Australian road network. Over the past few years, roads have been subjected to a variety of growing loading situations in terms of numbers and scales resulting in the main factors contributing to pavement failures before the design life of pavements. Basically, flexible pavements with bituminous surfacing is a complex structure consisting of a number of materials with different properties, hence an ideal mathematical model of a pavement structure may not yet be completely available. Most numerical response models based on an analytical multi-layered theory do consider a linear elastic theory in which the material in each layer is assumed to be homogenous, isotropic, and linear. Such material can be characterised by two elastic parameters such as the modulus of elasticity and Poisson's ratio. In pavement design methods widely used in the analysis of layered pavement systems under traffic loads, pavement layers are considered as homogenous, linear elastic and isotropic materials and under static loading. The application of the multi-layer elastic theory with static loading is a reasonable approach compared with empirical pavement design methods. Nonetheless, the failure criteria derived such approach are still trustworthy to the tensile strains at the bottom of the asphalt layer and the compressive strains at the top of the subgrade. The use of tensile strain values for flexible pavements would be justified if the thickness of the stiff asphalt layer subjected to traffic loads is relatively thick. These approach

methods terminate the pavement base, subbase, and subgrade elastoplastic behaviour and subsequently work as stress transmitters (CIRCLY 5 2004).

In practice, base and subbase courses indicate possible deterioration if unsuitable materials are placed in the pavement structure. As traffic passes, the top and bottom of a pavement changes from tension to compression and tension again before it returns to its original contour (Akbulut and Aslantas 2005). There are two important criteria to classify the ultimate allowable carrying capacity of pavement. The first is the vertical strain on the top of the subgrade and the second is the maximum permissible horizontal strain at the bottom of the stiff asphaltic layer (Austroads 2004). As stated, the current design criteria of base and subbase courses are solely subjected to compressive ($\sigma_{y,y}$) distribution with multi-layers along with the magnitude of stress induced in sub layers depending on each elastic stiffness of the road base for a given layer thickness, unlikely in realistic conditions. Hence, pavement analysis and design inevitably involve additional base and subbase attributes. From the analysis and design point of view, there are doubts in responses relative to their performance. This study aims to simulate a particular multi-layered pavement structure employing the finite element approach combined with laboratory results of materials to introduce a pavement analysis and design based on mechanistic pavement design approach so that a better understanding of this approach will be gained. To improve pavement analysis and design more precisely than in the past, the realistic responses during the service life of a road need to be investigated so that the most economical and suitable layer thickness for the pavement can be determined.

This chapter discusses the applications of CRB and HCTCRB as pavement materials for road bases based on the results of the laboratory work of this study.

The objective of the application is to introduce and discuss pavement analysis and design aspects as shown in Figure 5.1. Implementation of pavement analysis and design guidelines and general comments on CRB and HCTCRB for pavement unbound granular road base also are suggested as ultimate strength design.

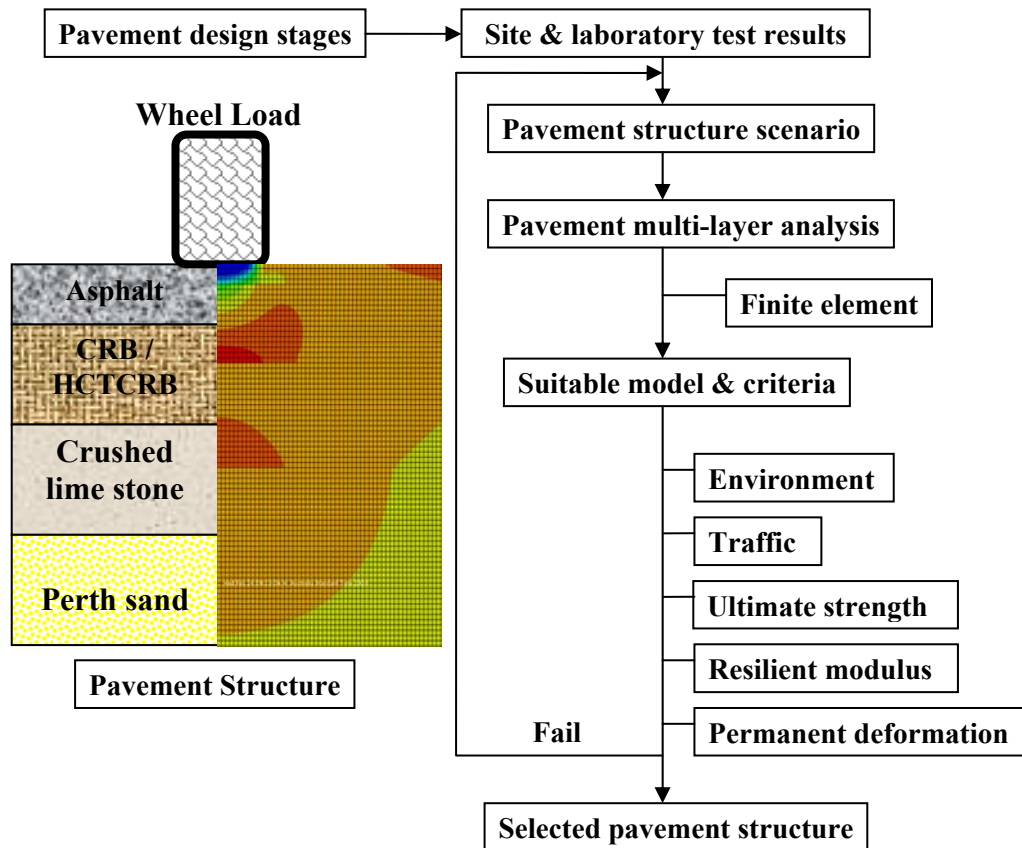


Figure 5.1 Pavement design diagram for CRB and HCTCRB as a base layer

5.2 Pavement analysis and design

The traditional design method (empirical design) becomes sub-standard because the test protocols do obtain the design parameters from static loading tests and the shortcoming of mechanical fundamentals. A mechanistic design attempts to explain pavement characteristics under real pavement conditions such as loads, material properties of the structure and environments based on design parameters from sophisticated tests which can simulate real pavement conditions into the test protocol (Collins et al. 1993). The key point of this analytical method is the experimental measurement and appropriate pavement analysis and design approach. The pavement structural model, stress and strain conditions will be used in this study to assess the structural contribution of wearing, base, subbase, subgrade to the carrying capacity of the pavement structure using different layer thicknesses/or different materials (elastic modulus).

Analysis and design methods for flexible pavements have been used since early in the last century. Traditional design systems still being used however reveal that design systems must be developed to include current mechanistic empirical approaches. Empirical methods with or without a strength test were the early methods employed in the design of flexible pavements referring to the soil classification system (Hogentogler and Terzaghi 1929; AASHTO 1986). In the past, most pavement structures were natural earth or gravel roads and the load carrying capacity of the pavement solely depended on the shear strength parameters of the selected materials. It should be remembered that currently almost 65% of the global road network still consists of earth and gravel roads (Molenaar 2007). It is clear that design procedure observes only stresses induced in the pavement and the shear failure allowance of the pavement surface. Vehicles

run into problems because of the lack of the bearing capacity of the pavement material. From this example, precise knowledge of the load pressures applied to the pavement and the strength of the materials used is essential to be able to design pavements that can sustain millions of load repetitions.

The empirical design systems were, not surprisingly, based on determining the required thickness of good quality layers on top of the subgrade to prevent shear failure to occur in the subgrade. Certainly, the required thickness was dependent on the shear resistance of the subgrade and the amount of traffic. Furthermore, the quality of the covering layers has to be such that shear failure will not occur in these layers. This was the basis for the California Bearing Ratio (CBR) thickness design method. In the CBR design charts, the traffic load was characterised by the number of vehicles per day and the shear resistance of the materials was characterized by their CBR value. The charts were used in the following way. First, the number of commercial vehicles had to be determined and when this number was known, the appropriate curve was to be selected. Next the CBR value of the subgrade needed to be determined and the required layer thickness on top of the subgrade will be estimated. A summary of the CBR test, a plunger was inserted into the soil sample with a specific displacement rate and the load was obtained during specific displacement rate. A load – displacement curve was provided in this way and compared with reference to material with the CBR value. The CBR design method results in thin asphalt layers to provide a smooth driving surface and sufficient skid resistance. Design curves based on road material tests became available in the 1960s detailing the structural design of roads under various conditions of climate, materials and traffic loading. Experience and simple knowledge of index properties (such as the CBR) are the key input factors of the empirical approach which limits shear failure and deflections (Huang 1993).

The empirical nature of traditional pavement design procedure is based on experience and the results of simple tests such as the California Bearing Ratio (CBR), particle size distribution, moisture sensitivity, aggregate durability, angle of shearing resistance and deflection. Such results are all static parameters and simple index parameters rather than any consideration of multidimensional geometry, realistic material behaviour and displacement distribution during cyclic loading, stresses and strain distribution in multilayered pavement design. Consequently, the use of an empirical approach becomes sub-standard and can be evaluated only in a limited capacity. Traditional design procedure has been criticized by Wolff who argues that it is too simplistic and does not take into account the non-linear behaviour of UGMs (Wolff and Visser 1994).

The mechanistic-empirical (M-E) approach is based on limitations in the use of the principals of mechanics, such as elasticity, plasticity, and visco-elasticity. It consists of two stages: the first is an analysis of the pavement layer system using a mechanistic model such as the multi-layered concept and finite element (FE) procedure that includes elastic, nonlinear elastic (such as resilient modulus model), or elastoplastic models such as Von Mises, Mohr-Coulomb, and hardening or continuous yielding (Vermeer 1982). In the second stage, the stresses and strains from the wheel load, computed from the first stage, are usually used in empirical formulas to determine rutting, damage, cracking, and amount of traffic. Generally, uniaxial quantities of the tensile strain, ϵ_t , at the bottom of the asphalt layer, and the vertical compressive strain, ϵ_c , at the top of the subgrade layer are used to calculate various deteriorations using empirical formulas. This approach can make improvements in design compared to the empirical approach. Whose formulas to calculate distress may not provide accurate predictions as they do not account for multidimensional geometry, nonhomogenieties, anisotropy, and nonlinear material responses, which are strongly dependent on stress, strain,

time, environmental factors, and load repetitions (Chandrakant 2007). The full mechanistic (M) approach can allow for all factors not considered in the empirical formulas in stage two of the M-E approach, in a unified method for all layers. As a result, the distresses are evaluated as a part of the solution (e.g., finite element) procedure, without the requirement of empirical formulas.

The current pavement design method in WA and Australia is provided by the AUSTROADS Pavement Design Guide (Austroads 2004), which has been promoted at the level of a mechanistic-empirical based design method, where the performance of a pavement structure can be determined from the application of an analytical process. It uses this to determine the response of the pavement structure to a single load and a critical response whether the horizontal tensile strain at the bottom of an asphalt layer or the vertical compressive strain at the top of the subgrade layer. The strain is used as an input into a performance relationship that relates the critical response to the allowable amount of design axles/traffic. Based on the mechanistic pavement analysis and design, it was found that the stress dependency of vertical modulus can be modelled by using the elastic model by dividing the layers into several sub-layers. From the mechanistic design step, the pavement structure scenario was established first from the generally used pavement cross-section in Western Australia which contains asphalt as a road surface, hydrated cement treated crushed rock base (HCTCRB) as a road base, crushed limestone as a road subbase, and Perth silty sand as a road subgrade. The pavement was analysed to find the vertical and the horizontal stresses occurring in the pavement material layer (Harichandran, R.S. et al. 1990). The suitable resilient modulus of materials for mechanistic design was determined from its resilient modulus model by relying on the laboratory results of the modulus tests. CIRCLY 5.0 was used for mechanistic pavement design to determine the traffic loading intensity of a pavement. This software uses state-of-the-art material properties and

performance models and is continuously being developed and extended. The first mainframe version of CIRCLY was released in 1977 and the current Windows version is CIRCLY 5.0. It is an integral component of the Austroads Pavement Design Guide widely used in Australia and New Zealand (CIRCLY 5 2004). The system calculates the cumulative damage induced by a traffic spectrum consisting of any combination of user-specified vehicle types and load configurations. As well as using the usual equivalent single wheel and axle load approximations, optionally the contribution, such as foundation engineering and settlement analysis, can also be analysed using CIRCLY which is based on integral transform techniques and offers significant advantages over linear elastic analysis techniques. Figure 5.2 shows example of data input for CIRCLY.

Data input for CIRCLY

Aggregate pavement		Design traffic load = 1.0×10^7 ESA		
Layer No.	Material ID	Isotropy	Modulus (MPa)	Layer thickness (mm)
1	Asphalt	Isotropic	3000	40
2	CRB/HCTCRB	Anisotropic	750-1000	150-350
3	Crushed limestone	Anisotropic	350	200
4	Subgrade CBR 15	Anisotropic	150	Infinite

Pavement Cross-section

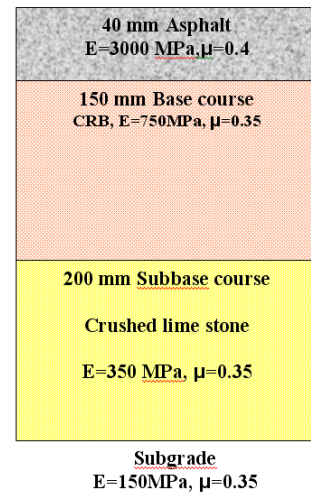


Figure 5.2 Data input for CIRCLY

A large number of computer programs have been developed for calculating stresses, strains and deflections of layered elastic system which are checked against the defined failure criteria. In all these programs pavement layers are

considered as homogeneous, linear elastic. In real situations, however, the assumption of homogeneous, linear elastic pavement materials becomes invalid. Almost all pavement materials are not homogeneous, especially granular materials particulate in nature. The finite element method for the analysis of flexible pavements was first applied by Duncan (Duncan et al. 1968). Many computer programs based on this finite element method were later developed and its use in determining stresses, strains and deflections is becoming popular, with the availability of high-speed computers. Furthermore, this method can handle structures with non-linear materials. In all these programs, the traffic loading is considered as static loading.

Static analysis of multi-layered pavement subgrade systems using linear elastic pavement structure is characterised by its Young's Modulus and Poisson's ratio. In some programs, resilient modulus based on the recoverable strain under repeated loading is used instead of Young's Modulus. The stresses, strains and deflections at specified distances from the load are then theoretically calculated, assuming a semi-infinite subgrade and infinite lateral boundaries. These calculated responses are matched with defined failure criteria. Layer thicknesses and material properties are adjusted until the computed responses are lower than the failure criterion.

5.3 Pavement structure model

This study was undertaken to incorporate realistic material properties of the pavement layers in the analysis of flexible pavements using the finite element method and an elastoplastic model. As a preliminary step, pavement materials within Western Australia were subjected to a static and loading, selected and modelled as a finite element model. An analysis was carried out using the finite

element computer package ABAQUS/STANDARD (ABAQUS Version 6.9 2009), when this pavement model was subjected to static loading while considering the linear and non-linear material properties of the pavement layers. The results of RLT tests under cyclic loading were considered in pavement analysis and design.

In the modelling of the problem, the finite element program used eight nodes of isometric elements as a solid continuum. The problems were simplified under the plain strain condition and material properties of each layer on the pavement were used. Dimensional parameters used in the modelling are illustrated in Figure 5.3 and Figure 5.4 shows the finite element meshes of the problem and the type of boundary conditions of the particular structure. The normal contact pressure of 750 kPa based on the Austroads design protocol (Austroads 2004) was assumed to be uniformly distributed over the contact area. All pavement structures were modelled consisting of four layers, wearing, base course, subbase and sub-grade as shown in Figure 5.3. Finite elements were unified by nodes at their common edges. The interfaces between layers are considered as fully bonded and rough. Boundary conditions were considered in the finite element modelling and rotation was allowed at all supports. The following conditions are applied with reference to Figure 5.4, when defining the boundary conditions. The vertical displacements of the bottom plane of the model are pinned. The side planes were released in vertically but were fixed horizontally. FE analysis provided an approximate solution for an engineering structure with various types of boundary conditions and under various types of loading using a stiffness or energy formulation. In the derivation of the stiffness matrix for elements, three factors such as the geometry of elements, the degrees of freedom allowed for the nodes to displace and the material properties of elements are considered. This solution provides displacements at the nodal periods and stresses and strains at integration points.

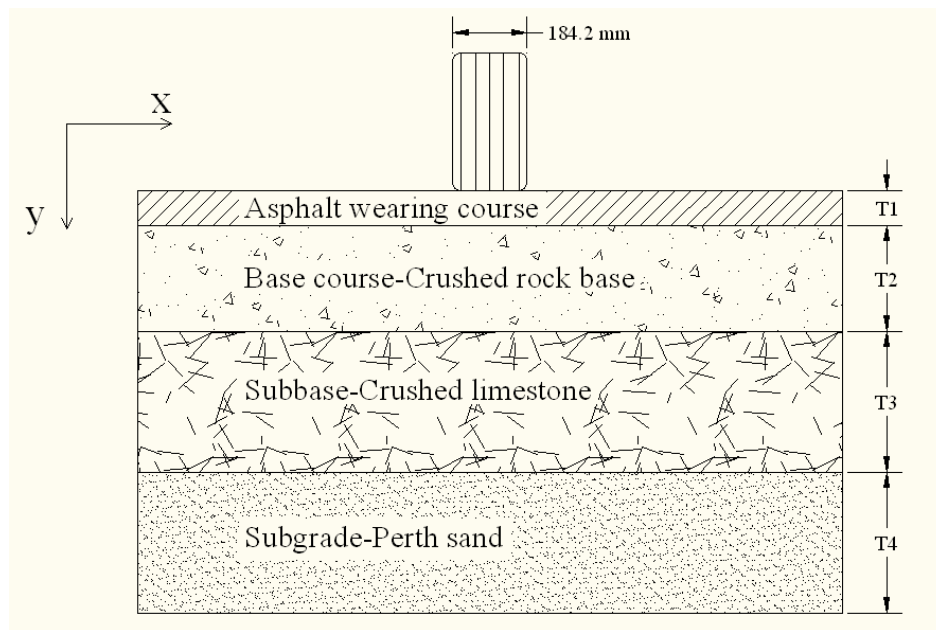


Figure 5.3 Standard pavement diagram

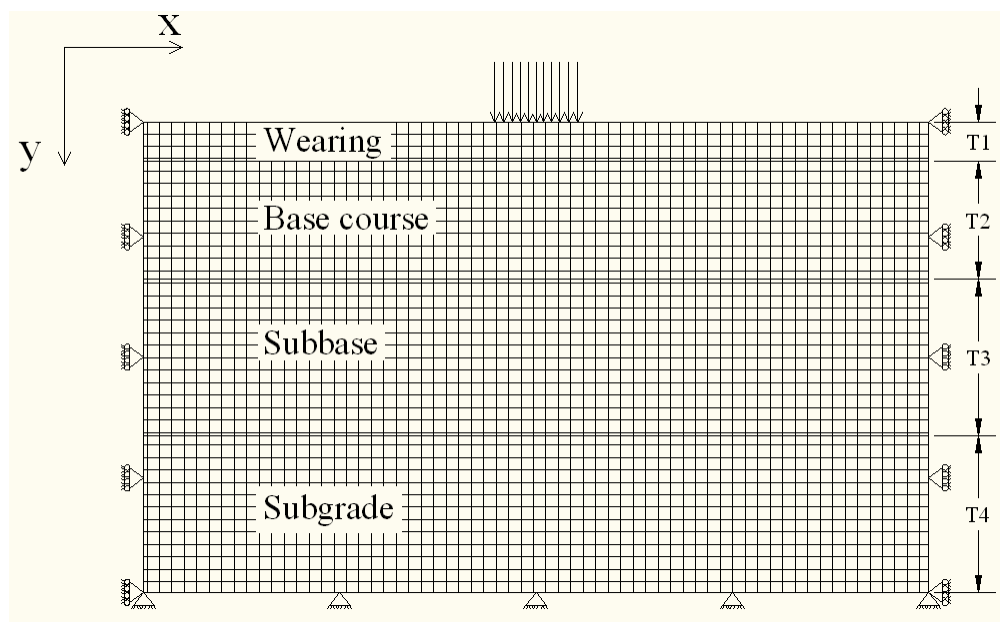


Figure 5.4 Finite element diagram of pavement

The Western Australian pavement selected for this study consists of a 30 mm thick asphalt layer as the surfacing course, a 150 mm thick HCTCRB layer as the basecourse, a 200 mm thick crushed limestone (CLS) as the subbase course, and Perth sand (PS) as the subgrade. The pavement layer configuration, thicknesses, material properties are given in Table 5.1. This pavement was subjected to a static pressure equal to 750 kPa, applied through a single wheel radius of 92.1 mm. In estimating, the linear elastic properties of pavement materials, the test results were used with the AUSTROAD and AASHTO Road Guide (AASHTO 1986; Austroads 2004) from previous chapter. This study also presents the elastoplastic of Mohr-Coulomb failure envelope and the results of RLT tests carried out on UGMs (Voung and Brimble 2000) as a method to determine the static and dynamic characteristics of granular materials under traffic conditions. Moreover, resilient and permanent deformation models were used to fulfil the absence of long term failure of pavement design in this study. The stress–strain relationships of granular layers are assumed to be in elastoplastic theory. The layer elastic concept was used to analyse the stress and strain within layers in which the asphalt layer was considered as homogeneous, linear elastic and isotropic, while UGM layers and the subgrade were considered as linear elastic at the initial stage for vertical load distribution, later changed to plastic.

Table 5.1 Assumption of conventional pavement material parameters

Layer	Material	Modulus (MPa)	Poisson ratio	Thickness (mm)
Wearing	Asphalt	3000	0.30	30
Base	HCTCTB	750	0.35	150
Subbase	Crushed lime stone	350	0.35	200
Subgrade	Perth sand	150	0.35	vary

5.4 Multi-layer analysis of pavement structure

The most important component in pavement analysis is the stress-strain distribution in pavement structure. In pavement engineering, there are various analysis and design method of pavements. The pavement structural model, stress and strain conditions were the preliminary purpose of this study. The structural involvement of wearing, base, subbase, subgrade to the pavement carrying capacity in terms of different layer thicknesses/or different materials (elastic modulus) was established. Various thicknesses and materials were used in the pavement modelling and the load magnitude effects of the stress distribution are presented in this section. The main layers of this study are the wearing and base courses which were evaluated with different thicknesses and the elastic modulus.

The preliminary behaviour of stress distribution study should be the effects of traffic loads on pavement structure. As well known, current pavement design established two key criteria on the horizontal tensile strain at the bottom of an asphalt layer and the vertical compressive stress at the top of a subgrade layer by not considering base and subbase responses. Base and subbase layer are as a function of a load transfer purpose. Figure 5.5 presents the assumption using finite element analysis which shows maximum stress always occurs at the asphalt layer and at the top of subgrade. It seems this hypothesis is correct for pavement analysis but the pavement structure in Figure 5.5 was only subjected to traffic stress of 7.5 kPa. However if the traffic stress increased beyond 7.5 kPa, the pavement responses will show more complicated responses as shown in Figure 5.6. The stress distribution does not uniformly distribute as expected through underneath layers. The high stress areas always take place in asphalt and base layers. It would interpret from Figure 5.6 that the pavement which is subjected to the traffic stress more than 7.50 kPa is failed at the asphalt and the base course.

Definitely, for 750 kPa of the design load of the current pavement design protocol, the pavement structure response is the same as that in Figure 5.6. It needs to be noted that based on the current design load (750 kPa), pavement does not behave following the assumption leading to the wrong design criteria based on the presentation of Figure 5.6.

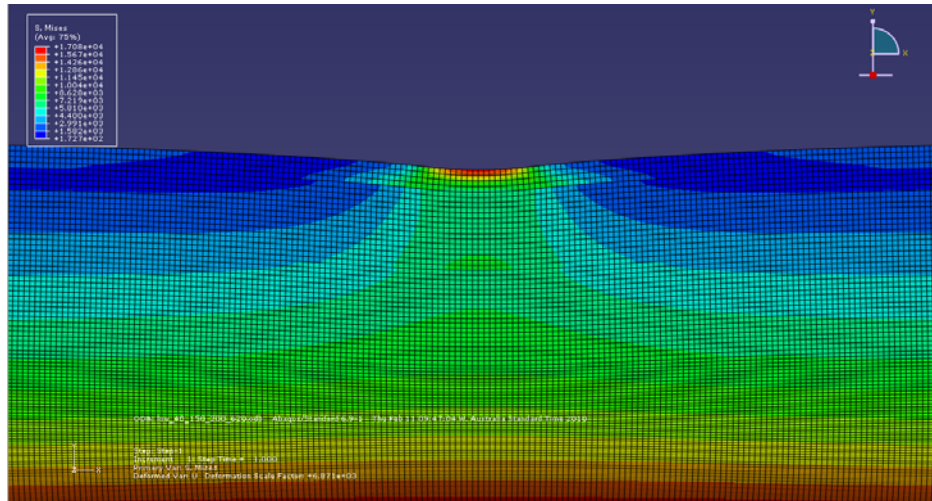


Figure 5.5 Stress distribution under low loading traffic

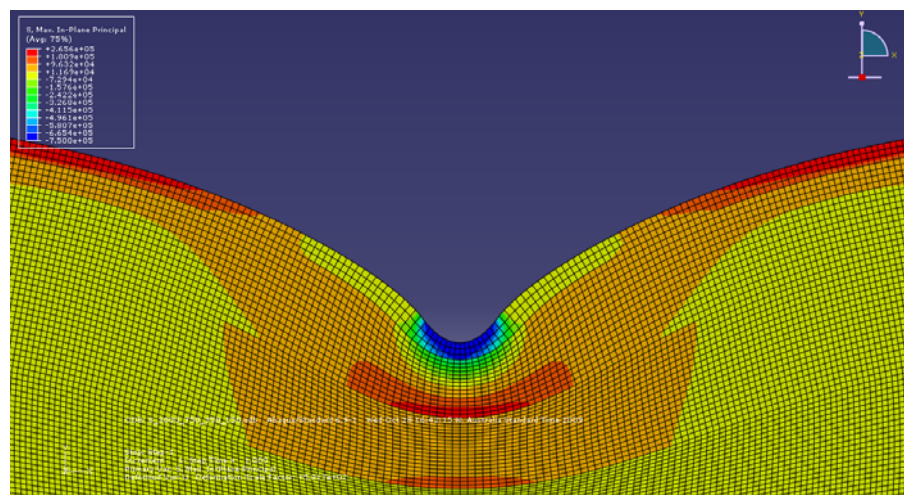


Figure 5.6 Stress distribution under high loading traffic

Figures 5.7 to 5.10 illustrate the various types of stress distribution of the particular pavement under a selected load of 750 kPa and having material parameters as shown in Table 5.1. Figure 5.7 shows the vertical stress distribution that stresses concentrate at the top of the pavement surface and then are distributed from top to bottom of the layer thicknesses. In this study, vertical stress values were used to determine design stress of each pavement layer compared with failure criteria for pavement design. On the other hand, the horizontal stress, it does not appropriately transfer through the underneath layers and only affects the wearing course at the top of the base course as shown in Figure 5.8. Although vertical and horizontal stresses present a significant difference of the stress distribution characteristic, their maximum stress values take place underneath of the wheel path. In contrast, the shear stress does not indicate the greatest value at the middle wheel path as shown in Figure 5.9.

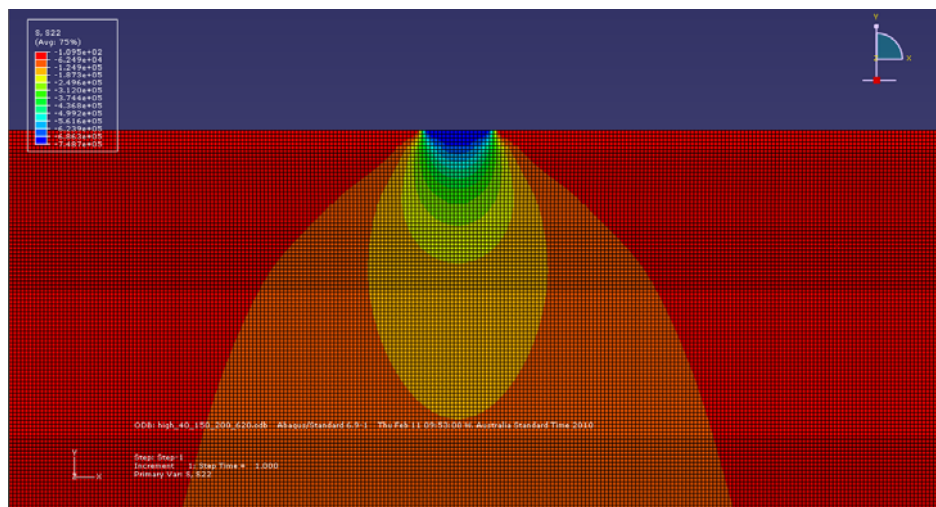


Figure 5.7 The vertical stress distribution of pavement structure

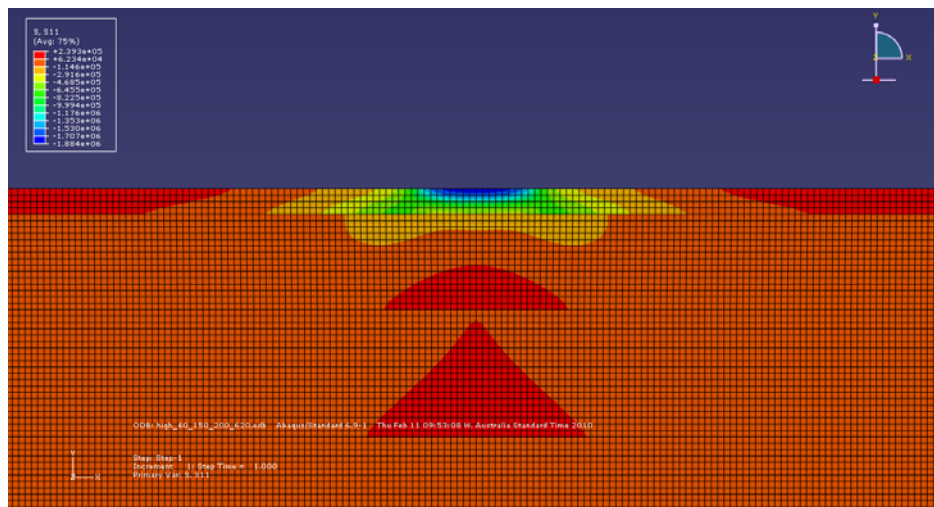


Figure 5.8 Horizontal stress of pavement structure

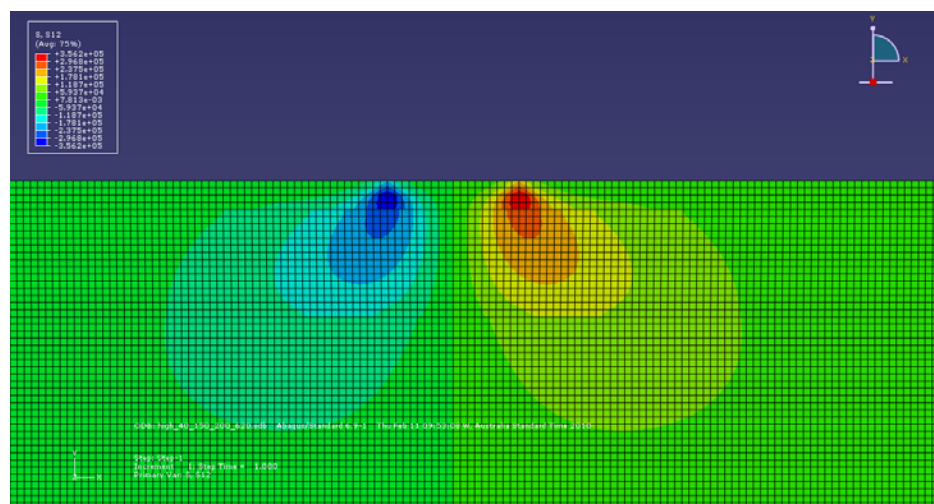


Figure 5.9 Shear stress of pavement structure

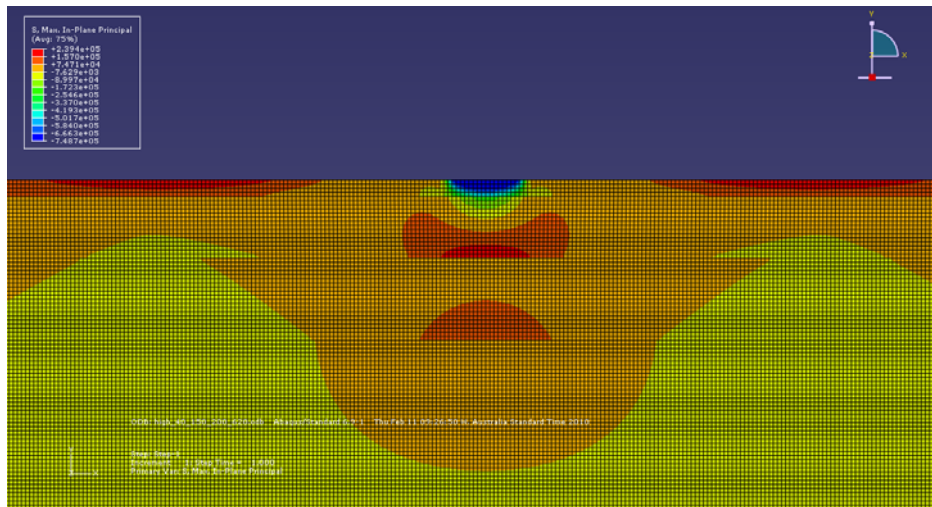


Figure 5.10 Maximum principal stress of pavement structure

In Figure 5.10, all stress components in the pavement are able to combine as the maximum principal stress. The compressive stress usually shows within the asphalt layers as well as on the top of the base course underneath the wheel path, moreover the tensile stress was evident at the lower and surrounding surface of the tyre. It can be seen from Figure 5.10 that the surface of the pavement is in tension over the front and back area on the edge of the wheels in a longitudinal direction. It can be note that the pavement behaviour under traffic loads has never shown tensile strain at the bottom of an asphalt layer as a conventional design criterion. On the other hands, an asphalt layer must resist vertical tensile stress and the compressive stress in the short time when a vehicle passes, it is not the horizontal tensile stress at all based on this analysis.

In Figures 5.11 to 5.18 illustrate the stress distributions of selected pavement structure with various material properties and layer thicknesses and the meaning of notation in Figures 5.11 to 5.18 as shown in Table 5.2.

Table 5.2 The meaning of notation

	Stress direction	Pavement layer	Position
xx AC top	Horizontal	Asphalt layer	At the top of layer
xx AC bottom	Horizontal	Asphalt layer	At the bottom of layer
yy AC top	Vertical	Asphalt layer	At the top of layer
yy AC bottom	Vertical	Asphalt layer	At the bottom of layer
xx Base top	Horizontal	Base layer	At the top of layer
xx Base bottom	Horizontal	Base layer	At the bottom of layer
yy Base top	Vertical	Base layer	At the top of layer
yy Base bottom	Vertical	Base layer	At the bottom of layer

5.4.1 The stress distribution with various asphalt layer thicknesses

Figures 5.11 and 5.12 show the stress taking place in the pavement system when a vehicle travels over layers of various asphalt thicknesses. In this part, the stress variation with varying the asphalt layer thicknesses was considered based on the pavement material properties as shown in Table 5.1. For design criterion, the maximum compressive stress occurs on the top surface and a considerable amount of tensile strain occurs underneath which may be the main cause of fatigue phenomena on the pavement layers (Austroads 2004). As already stated, an asphalt layer did not exhibit the horizontal tensile stress at the bottom of a thickness of 30 mm. On the other hands, vertically, compression is reduced by depth and turns to be tension at the bottom an asphalt layer when the thickness is more than 55 mm as shown in Figure 5.11. It needs to be noted that the maximum tensile stress taking place in an asphalt layer is not the horizontal tensile stress at the bottom of the layer as understood for long time in the basic design criteria but is at the top of the layer, the horizontal compressive stress which has a more magnitude twice than the horizontal tensile one. It is clear that the top layer and the bottom layer are critically important to meet induced strains causing

premature structure failure. Figure 5.12 shows the stress distribution of base layers compared with asphalt layer thicknesses.

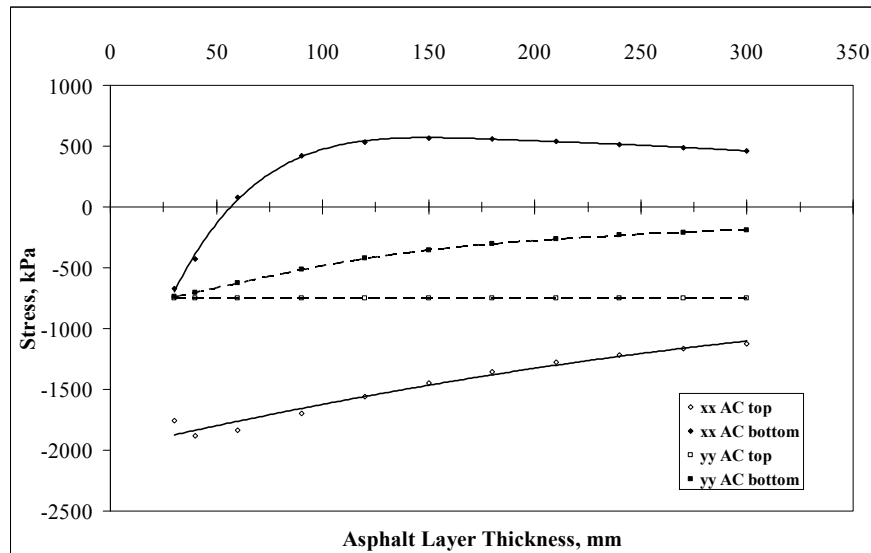


Figure 5.11 Asphalt layer stress versus asphalt layer thickness

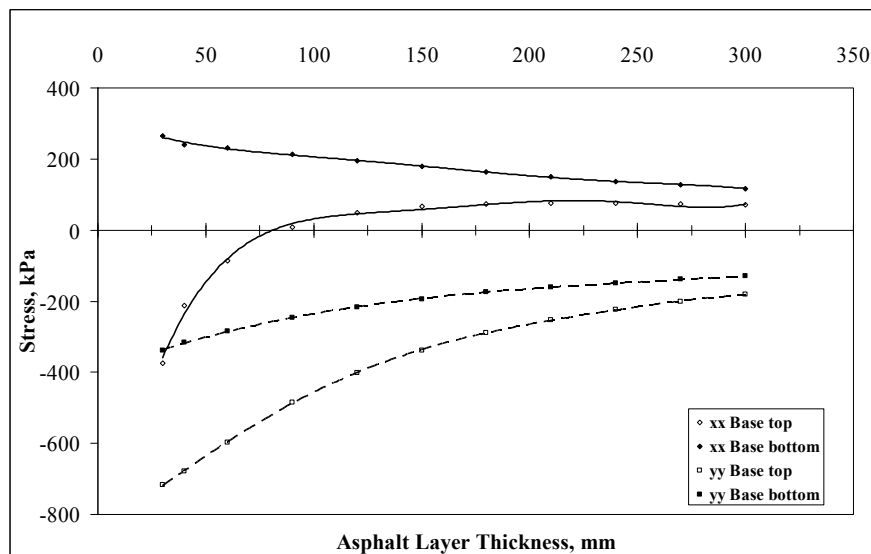


Figure 5.12 Base layer stress versus asphalt layer thickness

5.4.2 The stress distribution with various base layer thicknesses

Figures 5.13 and 5.14 show the stress taking place in the pavement system with varying base layer thickness and pavement material parameters as in Table 5.1 under the load design over the layers. There are no significant stress responses with various base thicknesses only stress transferring to the subbase if the compressive vertical stress of the layer is excessive, unacceptable permanent deformation could occur at the top of the lower layer and this would cause deterioration of the pavement.

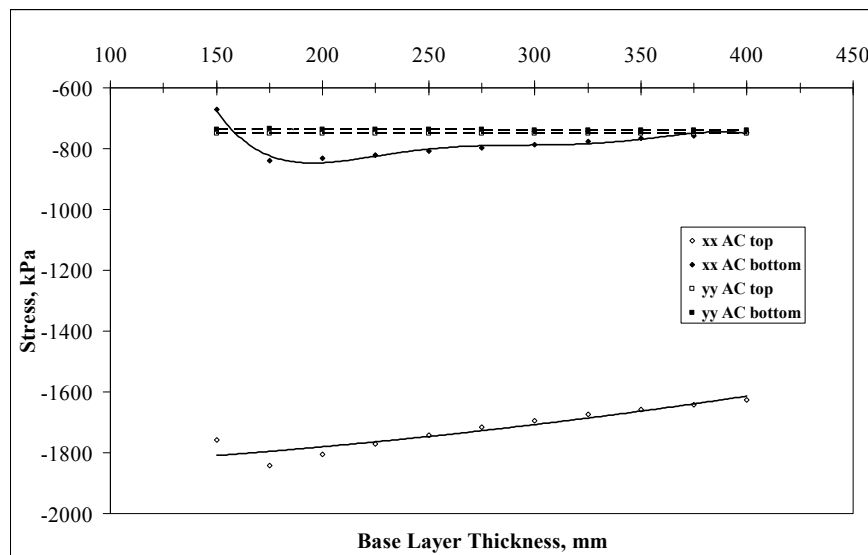


Figure 5.13 Asphalt layer stress versus base layer thickness

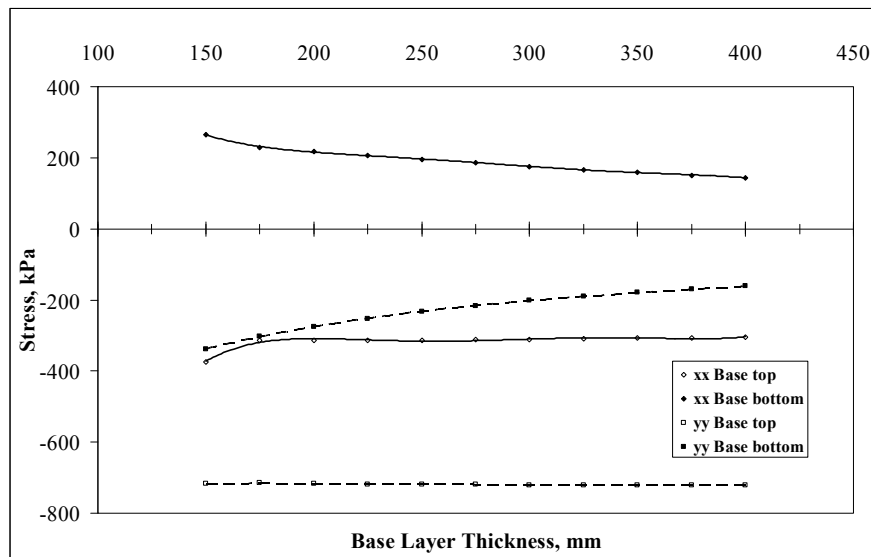


Figure 5.14 Base layer stress versus base layer thickness

5.4.3 The stress distribution with various asphalt layer modulus

There are no significant vertical stress responses and the vertical compressive stress constantly occurs in the wearing and base course layers and subbase base with various asphalt layer modulus. The horizontal stress only affects the top and the bottom of wearing course and the top of base course as shown in Figures 5.15 and 5.16. It seems that an increase of asphalt layer modulus elasticity leads to an increase of only the horizontal direction on the wearing surface.

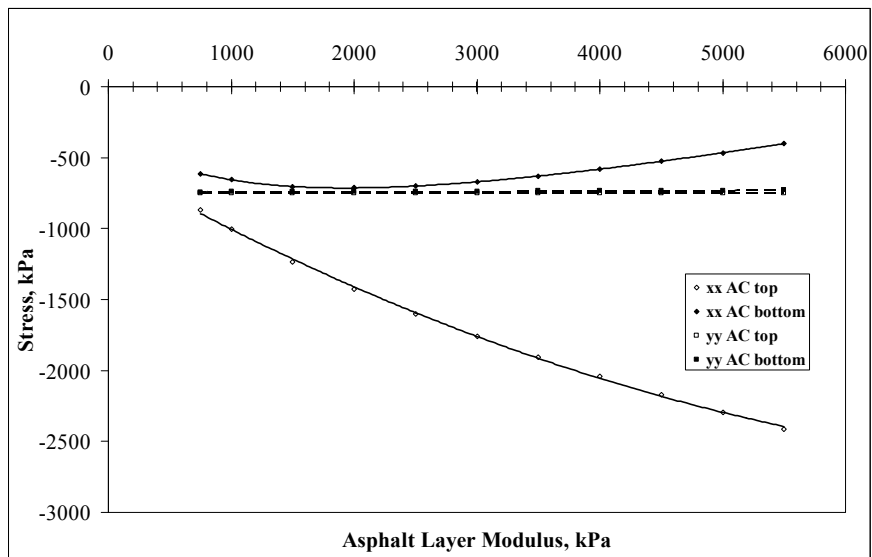


Figure 5.15 Asphalt layer stress versus asphalt layer modulus

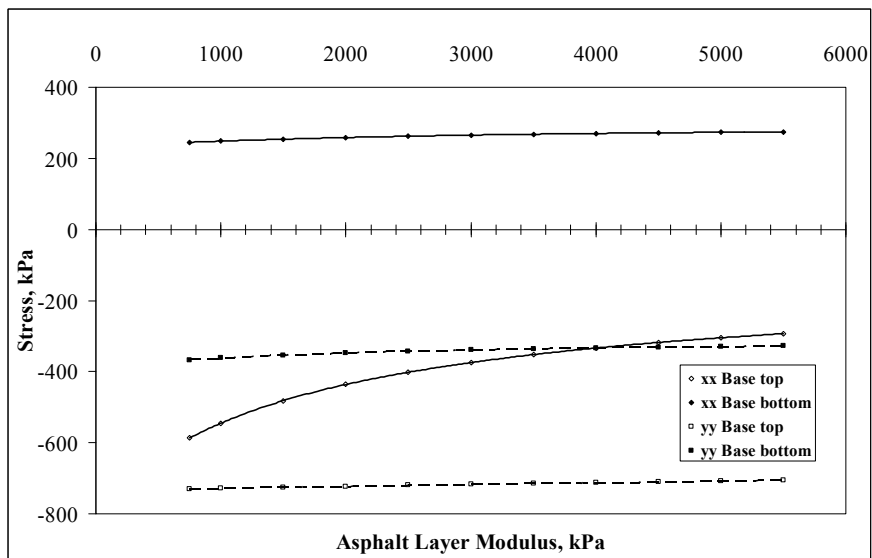


Figure 5.16 Base layer stress versus asphalt layer modulus

5.4.4 The stress distribution with various base layer modulus

Figures 5.17 and 5.18 show insignificant vertical stress responses and the vertical compressive stress constantly occurs in the wearing and base course layers with various base layer modulus. However the results present the changes of the stresses in the asphalt layer occurring with different elastic moduli of the base course. Increasing the elastic modulus of the base course causes an increase in the horizontal compressive stress at the bottom and a reduction in that at the top of the wearing course. Consequently, a variation of the elastic modulus of the base course does not dramatically affect to the change of the stress distribution of the vertical stress in the asphalt layer.

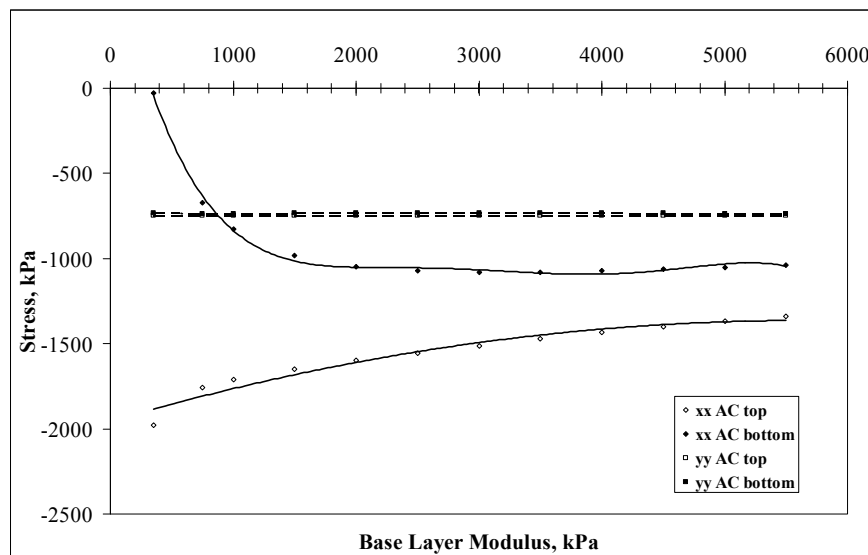


Figure 5.17 Asphalt layer stress versus base layer modulus

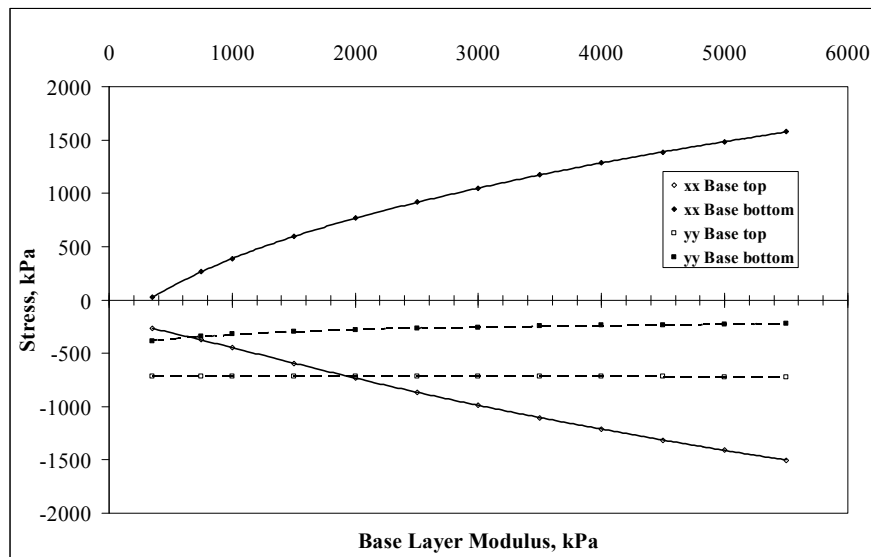


Figure 5.18 Base layer stress versus base layer modulus

5.5 Response model and criteria of unbound granular material (UGM) layer

CRB and HCTCRB widely used as base course materials in Western Australia, can be classified as unbound granular materials (UGMs). For the pavement analysis and design, pavement material responses are based on material parameters of which the bound material is normally relied on the linear elastic theory. Unlikely, unbound materials (such as CRB and HCTCRB) have the more complicated performance of the elastoplastic behaviour. Hence, it is necessary to clarify the real performance of UGMs under traffic loading. This section shows the inherent behaviour of UGMs in order to apply to the analytical approach of current pavement design. The most important characteristics for pavement design are static failure criteria, resilient modulus and permanent deformation. Firstly, the failure domains were defined by static triaxial tests.

5.5.1 Ultimate strength failure criteria of UGM layers

This study presents an alternative approach of the UGM failure for pavement design. In this session, the static failure criteria of the UGMs layer was determined by using a p-q stress diagram. Figure 5.19 shows the static triaxial test results of CRB and HCTCRB on the p-q diagram where the Mohr-Coulomb failure was defined in terms of principal stresses. The deviator stress, $q = (\sigma_1 - \sigma_3)$, was plotted against the mean applied stress, $p = (\sigma_1 + 2\sigma_3)/3$. The results shown in Figure 5.19, indicate the Mohr-Coulomb failure envelope (corresponding to the maximum stresses) is linear for the stress range tested and has a characteristic in p-q stress space: $M_p = q/p = 1.723$ with a deviator stress intercept, $q_c = 339$ kPa. In the conventional Mohr-Coulomb stress space, the properties failure correspond to an internal friction angle (ϕ) at a peak strength of 43° and an apparent cohesion (c) of 168 kPa compared to 59° and 32 kPa respectively of CRB results.

Based on the failure envelopes of CRB and HCTCRB, the stress distribution of UGMs layers from previous finite element analysis with various layer thicknesses and modulus were plotted in a comparison with the both failure envelopes. In Figure 5.19, all stress levels of various pavement conditions were fitted within HCTCRB failure envelope of the p-q stress diagram. It seems that HCTCRB is suitable to be placed in the pavement structure in terms of the static shear strength criterion for particular pavement layers in this study. However, CRB is able to resist the applied load unless the wearing thickness is thick enough to achieve the acceptable vertical stress on the top of base course because the stress levels of thin wearing course do not fit the CRB failure envelope as shown in Figure 5.19.

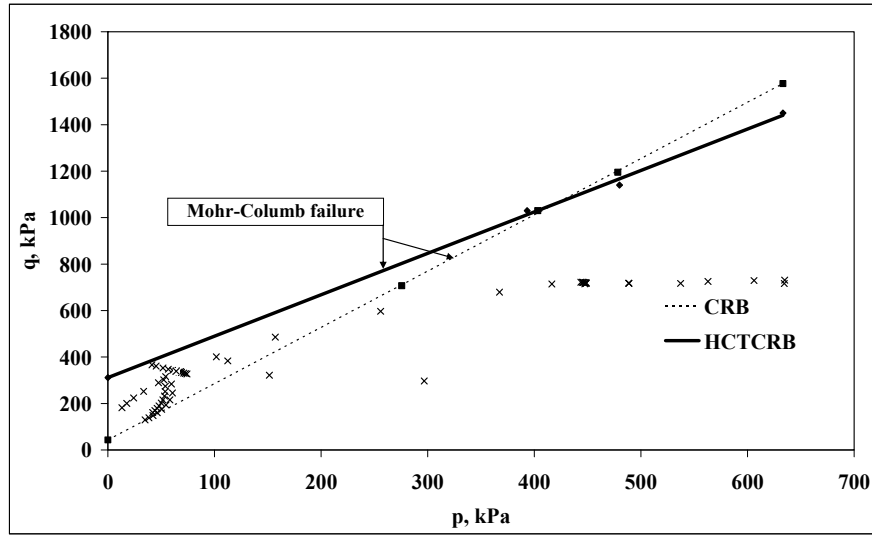


Figure 5.19 Static failure criteria of CRB and HCTCRB compared with stress distribution using finite element analysis

5.5.2 The resilient modulus model

The resilient modulus determined from the repeated load triaxial (RLT) test is defined as the ratio of the repeated deviator stress to the recoverable or resilient axial strain:

$$M_r = \frac{\sigma_d}{\varepsilon_r} \quad (5.1)$$

where M_r is the resilient modulus, σ_d is the repeated deviator stress, and ε_r is the recoverable strain in a vertical direction. The results of CRB and HCTCRB at 100% maximum dry density (MDD) at 100% optimum moisture content (OMC) are represented to show its characteristics and to determine suitable mathematical models of resilient modulus of CRB and HCTCRB. Figure 5.20 shows the results of resilient modulus of CRB and HCTCRB and the K-Theta (K- θ) model. The

representative K- θ model of CRB and HCTCRB are able to define resilient modulus in different pavement conditions for the input of finite element analysis.

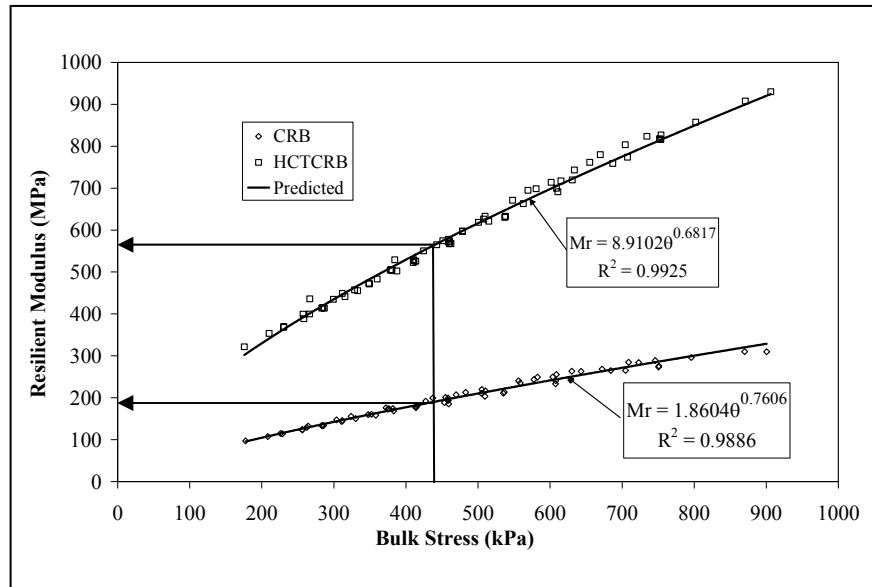


Figure 5.20 The resilient modulus predictions

5.5.3 The permanent deformation model

The permanent deformation of pavement material must be considered in pavement design parameters because CRB and HCTCRB have never performed as pure elastic materials. Figures 5.21 and 5.22 show the typical results of the permanent deformation tests (Voung and Brimble 2000) in terms of the relationship between permanent deformation and loading cycles for CRB and HCTCRB respectively, to exhibit the comparison of the measured and permanent deformation values and the predicted values for proposed permanent deformation models. Figure 5.21 and 5.22 also indicate that permanent deformation can be modelled quite reasonably by using the model suggested by Sweere (Sweere 1990).

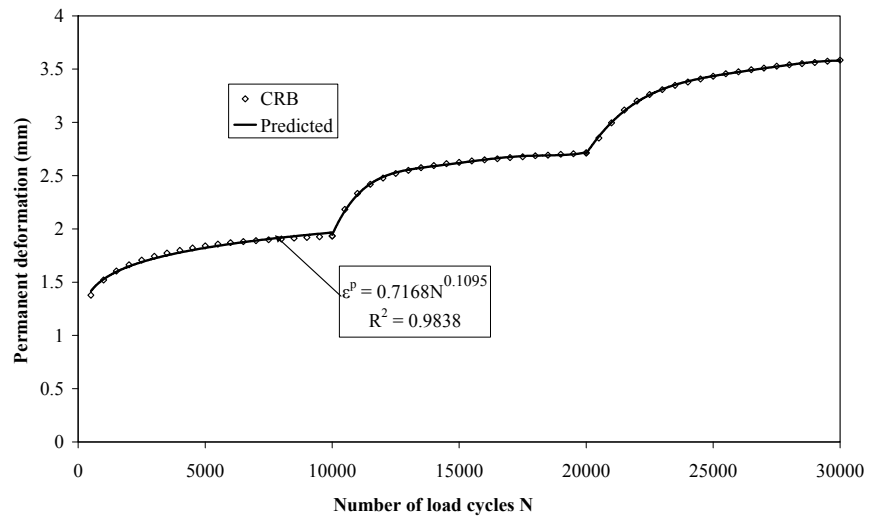


Figure 5.21 CRB permanent deformation predictions

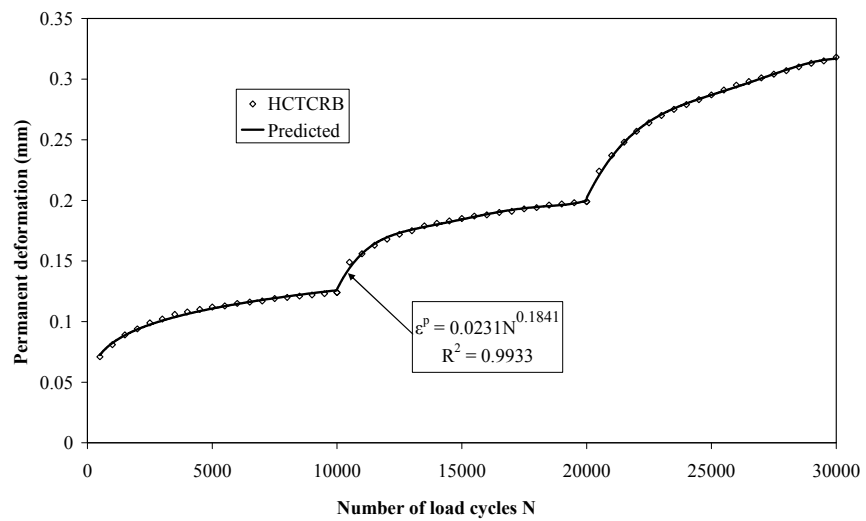


Figure 5.22 HCTCRB permanent deformation predictions

To implement the permanent deformation result from Repeated Load Triaxial (RLT) to the strain computation in a pavement structure, the computed strain has to be known as a function of both the number of load cycles and the stresses in the materials. Furthermore the shakedown approach should be taken into account in explaining the permanent strain behaviour of UGM and classified its behaviour into 3 ranges of RLT tests (Range A, Range B, and Range C). Figure 5.23 and 5.24 show the limited ranges of CRB and HCTCRB, each stress ratio and defines the limited use as Range C.

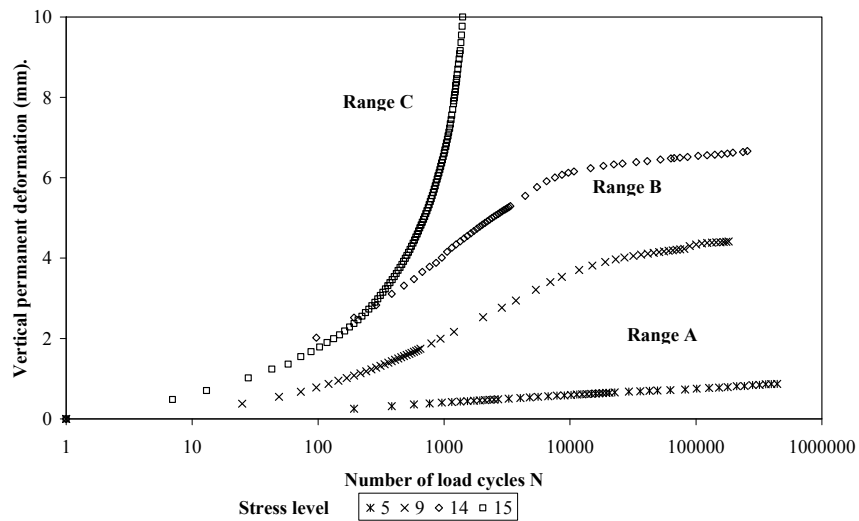


Figure 5.23 Ranges A, B and C of CRB

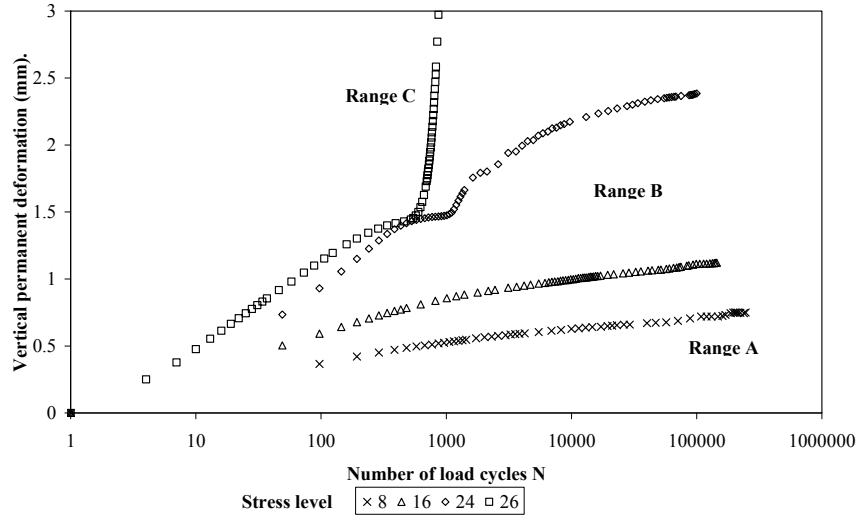


Figure 5.24 Ranges A, B and C of HCTCRB

The plastic strain of UGMs was also discussed in order to find the number of vehicles using RLT test results. From Figures 5.23 and 5.24 show the responses of plastic strain for CRB and HCTCRB each stress ratio respectively. The limited range of CRB and HCTCRB were stress levels of 14 and 25 respectively. The representative plastic strain model of CRB and HCTCRB limited stages are exhibited in Equations (5.2) and (5.3) respectively. Static failure criteria used to determine the acceptable amount of permanent deformation in an UGM was defined at 2% strain based on a triaxial shear test (Molenaar and Houben 2002). This means that a permanent deformation of 2% was substituted in Equations (5.2) and (5.3) to establish the suitable number of vehicles. Consequently, the number of vehicles that CRB and HCTCRB are able to sustain without any deterioration based on the limited range of material is shown in Figure 5.25.

$$\varepsilon^p = 26.6125 \cdot \left[\frac{N}{1000} \right]^{0.0416} \quad \text{for CRB} \quad (5.2)$$

$$\varepsilon^p = 12.3978 \cdot \left[\frac{N}{1000} \right]^{0.0646} \quad \text{for HCTCRB} \quad (5.3)$$

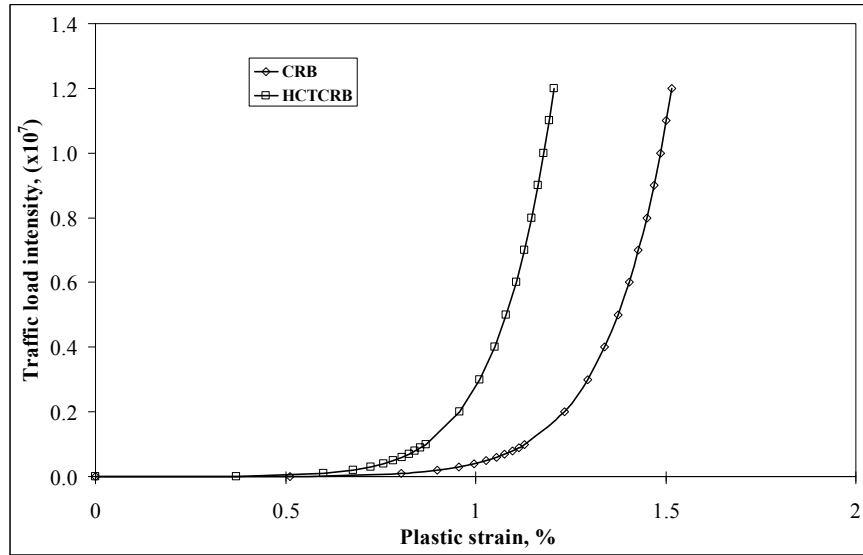


Figure 5.25 Number of traffic compared with plastic strain

5.6 Ultimate strength pavement design

This study introduces an alternative pavement design by using static analysis of multi-layered pavement and linear elastic with the Poisson ratio, resilient modulus and permanent deformation. Resilient modulus based on the recoverable strain under repeated loading is used instead of Young's modulus. The stresses, strains and deflections at specified distances from the load are then theoretically calculated, assuming finite subgrade and finite lateral boundaries. These calculated responses are matched with defined failure criteria. Layer thicknesses and material properties are adjusted until the computed responses are lower than the failure criterion as shown in Figure 5.26.

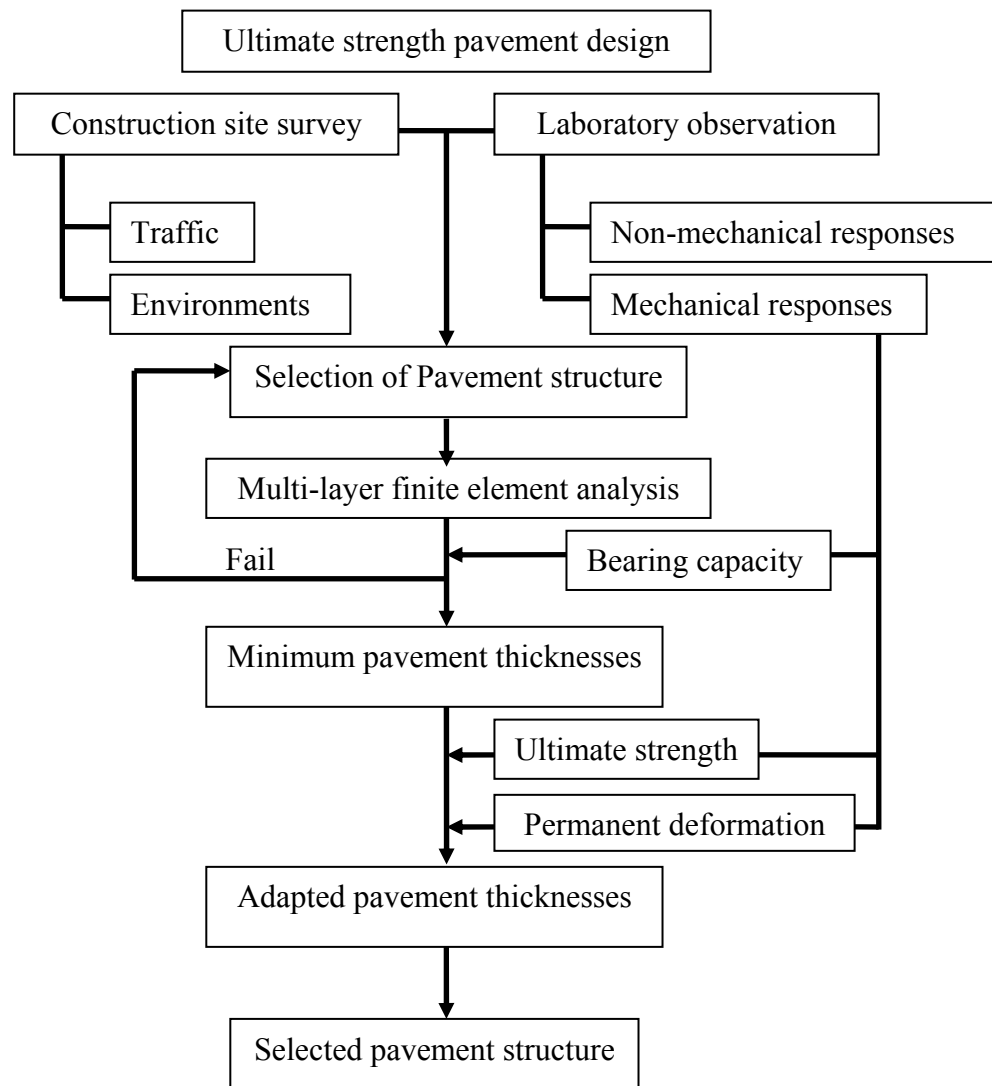


Figure 5.26 : Ultimate strength design method

5.6.1 Thickness and performance evaluation

Elastic theory with laboratory test results are employed for bound materials, such as asphalt and stabilised granular material, in order to evaluate their ultimate strength and thickness by using compressive and tensile parameters. This study

also presents the elastoplasticity of bearing and shear capacity and permanent deformation for unbound granular pavement material. As is well known in the early stages, flexible pavement risks rutting premature deterioration at road completion because of insufficient carrying load ability on pavement layers. It seems vital that a designer should select an appropriate traffic load and materials for a pavement design. An over design would impact project budget although under design comes with expensive maintenance. A pavement design that considers the ultimate strength of each layer would terminate unexpected rutting. This proposed design starts at the determination of the bearing capacity of pavement materials including punching and contacting resistance consideration and then the results are compared with those derived from the multi-layer finite element analysis. From this point, the thickness of the pavement layers including asphalt, base and subgrade are determined based on the bearing capacity of subgrade layer complying with the vertical strain equation at the top of subgrade as designed traffic. The latter, minimum thickness of asphalt layer was defined based on the assumption that no unacceptable permanent deformation occurs in base and subbase layers using permanent deformation test results. Finally, each layer was then analysed to indicate stress-strain results as an example in Section 5.4 and compared with the design allowance. The procedure shows whether the calculated responses matched defined failure criteria on particular layer thicknesses and then material properties have to be adjusted again to find matching points with the failure criteria as shown in Figure 5.26.

5.6.1.1 Bearing capacity estimation and pavement thickness design

The unbound granular pavement material layer in this study used California bearing ratio (CBR) test results to determine its bearing capacity from the concept of the shallow foundation bearing capacity as shown in Table 5.3. The CBR test is

still widely used in the design and analysis of pavements and this proposed design employed for bearing failure criteria complies with the multi-layer finite element analysis. The study presents an alternative method using the analytical approach with the drained shear strength parameters (cohesion, internal friction angle) of unbound granular materials for pavement thickness design. This approach is based on the shallow foundation-bearing capacity theory and the configuration of the CBR test can be closely modelled in bearing capacity theory as a circular foundation with a surcharge as shown in Figure 5.27. The ultimate bearing capacity of a circular traffic load is calculated from an equation that incorporates appropriate soil parameters (e.g. shear strength, unit weight) and details about the size, shape and founding depth of the footing. Terzaghi (1943) stated the ultimate bearing capacity of a strip footing as a three-term expression incorporating the bearing capacity factors: N_c , N_q and N_γ in Equation (5.4) which are related to the angle of friction. Eventually, the ultimate bearing capacity of subgrade material has to be assessed with design stress based on analysis of the results. The pavement thickness would be defined by using Equation (5.7) with a safety factor of 2.5. Subsequently, the allowable vertical compressive strain of particular pavement thickness conforms to Equation (5.8) (Austroads 2004) for traffic design evaluation.

$$\frac{Q_{ult}}{(\pi/4).D^2} = (1.3).C.N_c + (0.3).\gamma.D.N_\gamma + \gamma.H.N_q \quad (5.4)$$

$$S.F = 2.5 = \frac{q_{ult}}{q_s} \quad (5.5)$$

$$D = d + H \quad (5.6)$$

$$H = \left[\frac{q_s.(2.5) - (1.3).C.N_c - (0.3).\gamma.d.N_\gamma}{(0.3).\gamma.N_\gamma + \gamma.N_q} \right] \quad (5.7)$$

$$N = \left[\frac{9300}{\mu\varepsilon} \right]^7 \quad (5.8)$$

where :

- Q_{ult} [kN] ultimate bearing load
- q_{ult} [kPa] ultimate bearing capacity
- q_s [kPa] stress at the top of subgrade
- D [m] load diameter at the subgrade
- d [m] load diameter at the surface
- γ [kN/m³] average unit weight of the pavement layers
- H [m] pavement thickness
- S.F safety of factor
- N_C, N_q and N_γ dimensionless factors based on the friction angle
- N number of standard axle repetitions (SAR)
- $\mu\epsilon$ [-] micro strain at the top of subgrade

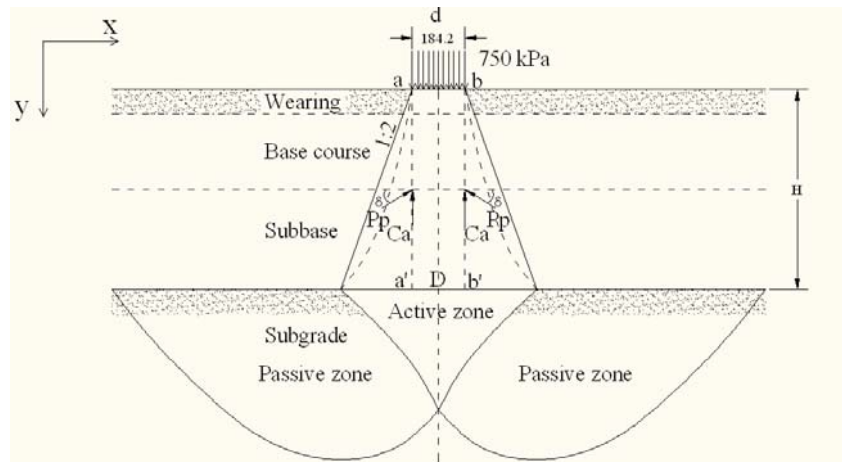


Figure 5.27 : Bearing estimation of unbound granular subgrade

Table 5.3 : Bearing capacity based on CBR test results

% CBR	Ultimate bearing capacity (kPa) at 2.5 mm	Allowable bearing capacity (safety factor 2.5) (kPa)
5%	336	134
10%	672	269
15%	1008	403
20%	1344	538
30%	2016	806
40%	2688	1075
50%	3360	1344
60%	4032	1613
70%	4704	1882
80%	5376	2150
90%	6048	2419
100%	6720	2688

5.6.1.2 Multi-layer strength and performance evaluation

At this stage of this proposed analysis, all premature deteriorations of pavement structures were terminated in terms of the ultimate strength of each layer. Following thickness determination, ultimate strength parameters are used to define the suitable stiffness of pavement structure. Design stresses of certain pavement layers were selected from maximum stresses. As is well known, the asphalt strength requirement is only based on Marshall test results and this study also presents asphalt capacity in terms of compressive strength. Base, subbase and subgrade as unbound granular material have two main criteria. The first is bearing

capacity under a single wheel load and the second is shear resistance surrounding the wheel load that can be determined by materials' shear strength parameters using Equation (5.9). Table 5.4 presents the material capacities compared with analysing stresses.

$$S.F. = \frac{\tau_{ult}}{\tau_s} = \frac{C + \sigma_n \tan \phi}{\tau_s} \quad (5.9)$$

where :

τ_{ult}	[kN] ultimate shearing load
τ_s	[kPa] maximum shear stress
C	[kPa] cohesion
σ_n	[kPa] normal stress
ϕ	[°] internal friction angle

5.6.1.3 The acceptable plastic strain of the unbound granular material (UGM) base layer

The plastic strain of unbound granular material (UGM) was also discussed in order to find the acceptable plastic strain of the base course using repeated load triaxial (RLT) test results. From Section 5.5.3, Figures 5.23 and 5.24 show the responses of plastic strain for CRB and HCTCRB, each stress ratio respectively and the minimum thickness of asphalt would be defined under this limited stage. The representative plastic strain model of CRB and HCTCRB limited stage is exhibited in Equations (5.2) and (5.3), respectively. Static failure criteria used to determine the acceptable amount of permanent deformation in an UGM was located at 2% strain based on a triaxial shear test (Molenaar and Houben 2002). This means that a permanent deformation of 2% was substituted in the Equation to establish the suitable number of vehicles. Consequently, the number of vehicles

that CRB and HCTCRB are able to sustain without any deterioration based on the limited range of materials.

Table 5.4 : Pavement layer analysis

5.4 (a)	Maximum stress (kPa) Under wheel load	Stress capacity (kPa)	Safety factor	Layer thickness (mm)
Asphalt	1759	6000	3.41	30
5.4 (b)	Vertical stress (kPa) Under wheel load	Bearing capacity (kPa)	Safety factor	Layer thickness (mm)
Base	717	6720	9.4	150
Subbase	324	3360	10.4	200
subgrade	179	445	2.5	-
5.4 (c)	Shear stress (kPa) front&behind load	Shear capacity (kPa)	Safety factor	Layer thickness (mm)
Base	265	464	1.7	150
Subbase	121	257	2.1	200
subgrade	40	93	2.3	-

5.7 Conclusion and discussion

Flexible pavements exhibit the elastoplastic behaviour and can be more accurately modelled by the finite element program. From the results, the following conclusions can be drawn based on the general design assumption that maximum horizontal tensile stress occurs at the bottom of the bond layers and the maximum horizontal compressive stress occurs at the surface of the pavement. The horizontal tensile stress is mainly effective on the bottom of the wearing course and at the top of the base course. However, the horizontal tensile stress under the wheel path was significantly high compared to other regions. This may be the cause of crack propagation in the layers. Horizontal tensile stress is also effective on the bottom of the pavement (subgrade) compared to the middle layers (UGMs). It may be concluded that the top and the bottom of the pavement are critical for failure phenomena. Vertical compressive stress, which is mainly the reason for the rutting failure, is effective on the wearing and base courses. The stress does not have the same on the granular layers. Increasing the elastic modulus of the wearing course tends to increase horizontal stress at the surface of the pavement. Consequently, as bitumen bound layers are vitally important in the design procedure.

The thickness of pavements should provide appropriate stresses and strains on the top of subgrade and can be determined by shallow foundation analytical approach with multi-layer finite element analysis. From the results, the following conclusions can be drawn as a general design assumption that the maximum stress for asphalt layer should focus on both horizontal and vertical directions. In particular, the horizontal compressive stress on the top and the tensile stress on the bottom of the asphalt layer that usually presents more critical values than the vertical one, unlike current design criteria that focuses only on horizontal tensile

stress at the bottom. Horizontal stress may affect top down fatigue cracking related failures, a different outline to vertical stress. However, the vertical and horizontal stresses under the wheel path were significantly high compared to other regions. Vertical compressive and shear stress are the two main effects on base, subbase and subgrade different from current design criteria that require an acceptable strain on the top of the subgrade. Based on the results, the UGM layers including subgrade are always affected by shear stress at surrounding wheel loads compared to compressive stress. The base course, especially, tends to fail with shear stress although its compressive capacity is very high. From this point, unbound granular base course should achieve high internal friction or high shear resistance to cope rutting and shoving failures. The following conclusions were drawn:

- The minimum pavement thickness should be more than 350 mm to prevent the excessive strain at the top of subgrade based on bearing capacity and multi-layer finite element analysis.
- The most critical strength of unbound granular material is shear stress surrounding wheel contact area rather than compressive strength.
- Ultimate strength and permanent deformation analysis using finite elements constitutes a powerful and versatile approach that should be developed in future. In particular, this type of analysis can serve as a guide to more rational design and analysis on a whole range of pavement structures.
- The failure criterion of the thin asphalt layer should be considered with the maximum horizontal compressive strain and the effects of stress change under traffic load.

- The elastic modulus of pavement material is only related with the horizontal stress at participating layers but the main thickness layer is mainly linked to vertical stress distribution.
- The finite element program, by incorporating an elastictoplastic relationship of laboratory test results in conjunction with an approach for verification of failure criteria, leads to acceptable solutions and reliability with the material properties and the amount of traffic intensity.
- Based on the existing empirical approach, it is possible to include suitable UGM layer parameters that can describe the real behaviour of the pavement.

Elastoplastic analysis using finite elements constitutes a powerful and versatile approach that should be developed in future. In particular, this type of analysis can serve as a guide to more rational design and analysis on a whole range of pavement structures.

CHAPTER 6

CONCLUSIONS AND RECOMMENDATIONS

6.1 Conclusions

This study aimed to evaluate the non-mechanical and mechanical characteristics of CRB and HCTCRB as road base materials for implementing to the current pavement analysis and design. A number of CRB samples collected from a stockpile in Western Australia were extensively performed in the laboratory for the non-mechanical and mechanical characteristics of both CRB and HCTCRB. Based upon the significant parameters of these materials found in the study, they were applied to the pavement structure analysis, design aspects, and some construction guidelines were introduced. The following conclusions are drawn from this study.

6.1.1 CRB and HCTCRB characterisations

The findings of CRB and HCTCRB characterizations are:

- 1) The analysis of the particle size distribution of CRB and HCTCRB demonstrates that most CRB and HCTCRB fractions lie within road base specifications (Main Roads Western Australia 2007). The hydration period does not significantly affect to the HCTCRB gradation characteristic, especially at the compacted stage, all gradations with various hydration periods return to the requirements again. Cement content also changes gradation by increasing fine grain fractions.

- 2) Observation of the scanning electron microscope (SEM) pictures of CRB and HCTCRB revealed that the CRB was well crushed and has sharp edges and a rougher surface, while the particles of HCTCRB covered by cement paste have smooth surfaces even in a compacted condition.
- 3) For the compaction test on CRB, the maximum dry densities (MDD) were 2.27 tons/m³ and 2.12 tons/m³ of HCTCRB. The optimum moisture contents (OMC) were 5.5 % of CRB and 8 % of HCTCRB over a 7 day hydration period. Although various hydration periods of HCTCRB present specific optimum moisture contents, all moisture contents are lower than 8%. From this point, cement treated material will have an OMC higher than their raw material as CRB.
- 4) The CBR results of both materials were, for soaked CBR, 180 % of CRB and 250% of HCTCRB and, for un-soaked CBR, 170% and 220% of CRB and HCTCRB, respectively. Both CRB and HCTCRB comply with the specifications for road base materials (Austroads 2004).
- 5) The shear strength parameters, c and ϕ , from static triaxial tests on both CRB and HCTCRB at modified compaction density indicate that c values were 32 kPa and 168 kPa and ϕ values were 59° and 43°, respectively. CRB shows higher internal friction angles than HCTCRB and shows more cohesive response than CRB. Both materials attain very high strength parameters.

- 6) The resilient modulus characteristics can be modelled using the K- θ model based on the test result. It presents that CRB resilient modulus was between 100 and 300 MPa and values of HCTCRB locates at a minimum of 300 MPa and a maximum of 900 MPa. The cement contents added in CRB improving its stiffness more than three times of that at the original material in terms of the resilient modulus. All materials exhibit stress-dependency behaviour. To minimise the effect of moisture content, CRB and HCTCRB should achieve at least 80% OMC of the dry back process. HCTCRB should have significantly more moisture susceptibility than CRB. The compaction process on a construction site should be started after 7 day hydration period of stockpiled HCTCRB and be compacted without additional water or less than 8%.
- 7) The long-term permanent deformation characteristics can be modelled using Sweere's model based on the test result. The results show that CRB permanent deformation was 3 mm and HCTCRB was 0.3 mm. If HCTCRB was conducted at its individual %OMC or without additional water, then it presented an acceptable permanent deformation. The compaction should be started after a 5-7 day hydration period of the HCTCRB stockpile and be without additional water or less than 8%. CRB and HCTCRB can be separated into three ranges based on the shakedown concept. Range A of HCTCRB at stress levels 8-16 is more than twice that of CRB and the HCTCRB working state of stress level 11 achieved Range A. CRB reacts corresponding to Range B, a great number of failures could occur if the stress condition does not change and if it is maintained long enough, it will deteriorate at the end. Stress levels 15 for CRB and level 26 for HCTCRB indicate Range C behaviour and the permanent strain rate decreases during the first period of load cycles then becomes lower, nearly

constant. Failure occurs with a relatively small number of load cycles when the cumulative permanent strain rate increases very rapidly after which the strain rate does not decrease again. Range C behaviour in unbound granular materials (UGMs) would result in the failure of the pavement.

6.1.2 Pavement analysis and design for CRB and HCTCRB

The findings of CRB and HCTCRB for pavement analysis and design are:

- 1) Index test results are used to explain and classify the basic characteristics of pavement materials for construction guidance and design criteria of each material. The covered testing will ensure potential and suitable use of such material for any purposes.
- 2) Selected materials were examined on non-mechanical characteristics and complied with the specification requirements as a good quality. Sophisticated tests were performed to discover their mechanical characteristics and failure criterion. This study employed three main aspects (shear strength parameters, resilient modulus and permanent deformation) of CRB and HCTCRB as design criterion. Their failure criterion indicates the limited use of pavement materials for design purposes in this study.
- 3) The finite element program can simulate suitably model pavement structure in multi-layer and requires particular parameters based on laboratory results. The effects of various structure physicals, traffic loads and material properties were assessed by the finite element method and the

analysis results of selected pavement structure verified with material models to confirm pavement performance.

- 4) After preliminary bearing strength classifications using CBR values, the shear strength parameters (c and ϕ) in p - q diagrams were used to determine the maximum carrying load capacity of the pavement structure in terms of ultimate strength of CRB and HCTCRB. This process was terminated by any premature failure and early rutting on the pavement through the lack of the shear strength resistance.
- 5) The resilient modulus was accounted as elastic parameter requirements to establish designed stress and strain of the pavement in the finite element. It is also used to determine stress distribution of adjacent layers in multi-layer analysis.
- 6) This study presents alternative pavement analysis and design of CRB and HCTCRB for road bases based on the static shear strength and the resilient modulus model derived from the laboratory results. These are used for pavement strength design at the early stage of a pavement life. To accomplish long term performance, the permanent deformation was considered to predict a number of vehicles for the selected pavement structure. The results revealed that CRB and HCTCRB could carry traffic loads of more than 1×10^6 times at 2% strain. Permanent deformation is also used to terminate the unexpected responses of the pavement material in terms of the shakedown concept.

6.2 Recommendations for future study

- 1) The laboratory investigation in this study has indicated that CRB and HCTCRB appear to be suitable for use in the construction of roads but several environmental effects still need to be further investigated. HCTCRB has been developed to avoid cracking in a cementitious base layer but it presents high moisture susceptibility. It is recommended that these materials not be available under actual service conditions. Further research desires to focus on the correlation of the laboratory results and modelling to full scale and field performance.
- 2) For the failure criteria and model for road bases, the further investigation of exact failure modes is recommended because the actual behaviour of road materials is complicated. Stress-dependency, water sensitivity, pore pressure and suction of unsaturated soil are the main factors that should be examined further to improve reliability of modelling under real conditions. Moreover, the effects of anisotropic, visco-elastic, plastic, 3-dimension, particle breakdown behaviour for pavement analysis require to be investigated in terms of micro and macro observations.
- 3) To fulfil the overall pavement design, further study should investigate other pavement layers such as asphalt, subbase and subgrade and traffic behaviour.
- 4) Based on stress distribution analysis, a flexible pavement using thin bituminous surface needs to be revised the failure criterion of tensile stress at the bottom of the asphalt layer and the compressive stress at the top of the subgrade.

- 5) Stress in motion and types of stress should be observed in further work to study the effects of traffic loads on pavement structure in order to develop suitable laboratory tests.
- 6) The laboratory test for the shakedown limit determination should be improved to reduce a number, time and complication of the test procedures and should consider volume change for the 3-dimensional approach.

REFERENCES

- AASHTO (1986). Guide for the design of pavement structures. Washington D.C., Association of State Highways and Transportation Officials.
- AASHTO (2002). Standard Method of Test for Resilient Modulus of Subgrade Soils and Untreated Base/Subbase Materials.
- ABAQUS Version 6.9 (2009). User's Manual. Providence, RI, USA, Dassault Systèmes Simulia Corp.
- Adu-Osei (2000). Characterization of Unbound Granular Materials. Department of Civil Engineering. Texas A&M University.
- Akbulut, H. and K. Aslantas (2005). "Finite element analysis of stress distribution on bituminous pavement and failure mechanism." **26**(4): 383-387.
- Allen, J. (1973). The Effect of Non-Constant Lateral Pressures of the Resilient Response of Granular Materials. Department of Civil and Environmental Engineering. Illinois, University of Illinois at Urbana-Champaign.
- Australian Standard. (1995). "AS 1289.3.6.1- Soil classification tests- Determination of the particle size distribution of a soil-Standard method of analysis by sieving." 2007, from <http://www.saiglobal.com>.
- Australian Standard (1997). Portland and Blended Cements. Australia, Australian Standard: pp. 1-10.

- Australian Standard. (1998). "AS 1289.6.1.1- Soil strength and consolidation tests- Determination of the California Bearing Ratio of a soil- Standard laboratory method for a remoulded specimen." 2007, from <http://www.saiglobal.com>.
- Australian Standard. (2000). "AS 1289.0-Method of testing soils for engineering purposes." 2007, from <http://www.saiglobal.com>.
- Australian Standard. (2003). "AS 1289.5.2.1- Soil compaction and density tests- Determination of the dry density/moisture content relation of a soil using modified compactive effort." 2007, from <http://www.saiglobal.com>.
- Austroroads (2004). Pavement Design-A Guide to the Structural Design of Road Pavements, Austroroad Inc.2004.
- Barksdale, R. D. (1972). Laboratory Evaluation of Rutting in Base Course Materials. 3rd International Conference on the Structural Design of Asphalt Pavements, London.
- Barksdale, R. D. and S. Y. Itani (1989). Influence of aggregate shape on base behaviour. Washington, D.C., Transportation Research Board.
- Brown, S. F. and A. F. L. Hyde (1975). "Significance of Cyclic Confining Stress in Repeated Load Triaxial Testing of Granular Material." Transportation Research Board Transportation Research 113 Record 537: pp. 49-58.
- Cement Association of Canada. (2005). "Overview of mechanistic-empirical pavement design." Retrieved 9th May, 2007, from www.cement.ca.

- Chandrakant, S. D. (2007). "Unified DSC Constitutive Model for Pavement Materials with Numerical Implementation." International Journal of Geomechanics 7(2): 83-101.
- CIRCLY 5 (2004). User Manual. Australia, MINCAD Systems.
- COCKBURN CEMENT. (2006). "General Specification (COCKBURN GERNERAL PURPOSE PORTLAND CEMENT-TYPE GP)." Retrieved November, 2006, from <http://www.cockburncement.com.au/productinfo/range/specifications/Cockburn%20GP.pdf>.
- Cockburn Cement. (2006). "General Specification (Cockburn General Purpose Portland Cement Type GP)." Retrieved November, 2006, from <http://www.cockburncement.com.au/productinfo/range/specifications/Cockburn%20GP.pdf>.
- Collins, I. F. and M. Boulbibane (1998). "The application of shakedown theory to pavement design." Metals Mat 4(4): 832-837.
- Collins, I. F., A. P. Wang, et al. (1993). "Shakedown theory and the design of unbound pavements." Road Transp. Res 2(4): 28-39.
- David Barthelmy. (2009). "Mineralogy Database." Retrieved December, 2009, from <http://webmineral.com/data/Coesite.shtml>.
- Dawson A R and W. F (1999). Plastic Behaviour of Granular Materials. Department of Civil Engineering, University of Nottingham.

- Dawson A.R. , T., A.R., and Paute, J.L. (1993). Mechanical characteristics of unbound granulare materials as a function of condition. Proceedings of The European Symposium Euroflex, Lisbon, Protugal, A.A. Balkema/ Rotterdam/ Brookfield.
- Duncan, J., C. Monismith, et al. (1968). "Finite element analysis of pavements." Highway Research Board Highway Research Record 228: 18–33.
- FHWA (2004). Foundry sand facts for civil engineers, US. Department of Transportation: Federal Highway Administration.
- Gerrard, J. (2000). Fundamentals of Soils. New York, Routledge.
- Harichandran, M. S. Y. R.S., et al. (1990). "MICH-PAVE: A nonlinear finite element Transportation Research Record." program for the analysis of flexible pavement 1286: 123-131.
- Haynes, J. G. and E. J. Yoder (1963). "Effects of Repeated Loading on Gravel and Crushed Stone Base Course Materials Used in the AASHTO Road Test." Highway Research Record 39.
- Hick, R. G. and C. L. Monosmith (1971). "Factors influencing the resilient response of granular materials." Highway Research Recond No. 345: 15-31.
- Hick, R. G. and C. L. Monosmith (1971). "Factors influencing the resilient response of granular materials." Highway Research Record 345: 15-31.

- Hirsigner, J. M. (2005). Stabilisation of red sand using fly ash and kiln dust for use in rigid pavement design. Civil Engineering. Perth, Western Australia, Curtin University of Technology.
- Hogentogler, C. and C. Terzaghi (1929). "Interrelationship of load, road and subgrade." Public Road(May): 37–64.
- Holubec (1969). "Cyclic Creep of Granular materials." Department of Highways Ontario, Report No. RR147.
- Huang, Y. H. (1993). Pavement analysis and design. N.J, Prentice-Hall, Englewood Cliffs.
- Huurman, M. (1997). Permanent deformation in concrete block pavements. PhD Thesis, Delft University of Technology: 119 –125.
- Kent, M. F. (1962). "Road test vehicle operating costs related to gross weight." Highway Research Board Special Rep 73(Washington, D.C.): 149-165.
- Kolisoja, P. (1997). Resilient Deformation Characteristics of Granular Materials. Tampere, Finland, Tampere University of Technology.
- Lamb, T. W. and R. W. Whitman (1979). Soil Mechanics, SI Version, John Wiley & Sons.
- Lekarp, F. and A. R. Dawson (1998). "Some Influences on the Permanent Deformation Behaviour of Unbound Ggranular Materials." US Transportation Research Board.

- Lekarp, F., U. Isacsson, et al. (2000). "State of the Art. II: Permanent strain response of unbound aggregates." *Transp. Eng* **126**(1): 76-84.
- Main Roads Western Australia. (1997). "Dry density/moisture content relationship: modified compaction fine and medium grained soils." Retrieved December, 2006, from <http://www.mainroads.wa.gov.au/>.
- Main Roads Western Australia. (2003). "Crushed Rock Base Basecourse." Retrieved December, 2006, from <http://www.mainroads.wa.gov.au/>.
- Main Roads Western Australia. (2003). "A guide to the selection and use of naturally occurring materials as base and subbase in roads in Western Australia " Retrieved September, 2008, from <http://standards.mainroads.wa.gov.au/NR/mrwa/frames/standards/standards.asp?G={E582C897-FF5E-4C02-8B46-51E88C1E5DD8}>.
- Main Roads Western Australia. (2006). "A guide to the selection and use of naturally occurring materials as base and subbase in roads in Western Australia " Retrieved September, 2008, from <http://standards.mainroads.wa.gov.au/NR/mrwa/frames/standards/standards.asp?G={E582C897-FF5E-4C02-8B46-51E88C1E5DD8}>.
- MAIN ROADS Western Australia. (2006). "Test Method (Aggregate)." Retrieved September, 2006, from <http://www.mainroads.wa.gov.au/NR/mrwa/frames/standards/standards.asp?G={1532D87F-C1AC-4386-9968-5E5F4FD002E5}>.

Main Roads Western Australia. (2007). "Dry density/moisture content relationship: modified compaction fine and medium grained soils." Retrieved September, 2008, from <http://standards.mainroads.wa.gov.au/NR/mrwa/frames/standards/standards.asp?G={E582C897-FF5E-4C02-8B46-51E88C1E5DD8}>.

Main Roads Western Australia. (2007). "Test Method (Aggregate)." Retrieved September, 2008, from <http://standards.mainroads.wa.gov.au/NR/mrwa/frames/standards/standards.asp?G={E582C897-FF5E-4C02-8B46-51E88C1E5DD8}>.

Main Roads Western Australia. (2009). "Stat Road Network." Retrieved April 15,, 2009, from <http://www.mainroads.wa.gov.au/UsingRoads/TouringWAMaps/Pages/StateRoadNetworkMaps.aspx>.

Maree, J. H., C. R. Freeme, et al. (1982). The permanent deformation of pavements with untreated crushed stone bases and measured in Heavy Vehicle Simulator tests. 10th Australian Research Board Conference Part 2.

MINCAD Systems (2004). CIRCLY 5 User Manual. Australia.

Molenaar, A. A. A. (2005). Cohesive and non-cohesive soils and unbound granular materials for bases and sub-bases in roads. Nederland, Delft University of Technology.

Molenaar, A. A. A. (2007). Design of Flexible Pavements. Nederland, Delft University of Technology.

Molenaar, A. A. A. and L. J. M. Houben (2002). Estimation of maximum strains in road bases and pavement performance predictions. International Institute for Infrastructural, Environmental and Hydraulic Engineering. Delft, Delft University of Technology.

Monismith, C. L., H. B. Seed, et al. (1967). Prediction of Pavement Deflections from Laboratory Tests. Proceedings of the 2nd International Conference on Structural Design of Asphalt Pavements.

Morgan J R (1966). The Response of Granular Materials to Repeated Loading. Proceedings, 3rd Australian Road Board Conference, Sydney.

NAASRA (1975). Pavement Materials Part 3 - Crushed Rock. Australia.

NAASRA (1980). Pavement Materials Part 2 - Natural Gravel, Sand-Clay, Soft Fissile Rock. Australia.

NAASRA (1982). Pavement Materials Part 1-Search. Australia.

NAASRA (1982). Pavement Materials Part 4 - Aggregates. Australia.

NAASRA (1987). PAVEMENT DESIGN: A Guide to the Structural Design of Road Pavements, NATIONAL ASSOCIATION OF AUSTRALIAN STATE ROAD AUTHORITIES (NAASRA).

- Nickel, E. H. (1995). "The definition of a mineral." The Canadian Mineralogist **33**: 689-690.
- Nikraz, H. (1998). Pavement design. Curtin University of Technology. Perth, Western Australia.
- Nikraz, H. (2004). Geotechnical Engineering 262: Lecture notes: Curtin University of Technology. Perth, Western Australia.
- Pappin J W (1979). Characteristics of a Granular Material for Pavement Analysis. Department of Civil Engineering, University of Nottingham.
- Paute, J. L., P. Horny, et al. (1996). Repeated load triaxial testing of granular materials in the French Network of Laboratories des Ponts et Chaussées. European Symposium on Flexible Pavements, Balkema, Rotterdam.
- SAMARIS (2004). Selection and evaluation of models for prediction of permanent deformations of unbound granular materials in road pavement, SAM-05-DE10., Sustainable and Advanced Materials for Road Infrastructure.
- Sharp, R. W. (1985). Pavement Design Based on Shakedown Analysis. Washington, D.C., Transportation Research Board.
- Smith, W. S. and K. Nair (1973). "Development of Procedures for Characterization of Untreated Granular Base Coarse and Asphalt Treated Base Course Materials." Federal Highway Administration Report No. FHWA-RD-74-61.

- Suiker, A. J., E. Selig, et al. (2005). "Static and Cyclic Triaxial Testing of Ballast and Subballast." Journal of Geotechnical and Geoenvironmental Engineering **131**(6): 771-782.
- Sweere, G. T. H. (1990). Unbound granular bases for roads. PhD Thesis, Delft University of Technology.
- Thom, N. H. and S. F. Brown (1988). The Effect of Grading and Density on the Mechanical Properties of a Crushed Dolomitic Limestone. Proceedings of the 14th Australian Road Research Board Conference.
- Thompson M. R. and D. Naumann (1993). "Rutting Rate Analyses of the AASHO Road Test Flexible Pavements." Transportation Research Record **1384**.
- Vermeer, P. A. (1982). A five-constant model unifying well-established concepts. International Workshop on Constitutive Relations for Soils. Grenoble, France.
- Young, B. T. and R. Brimble (2000). Austroads Repeated Load Triaxial Test Method-Determination of Permanent Deformation and Resilient Modulus Characteristics of Unbound Granular Materials Under Drained Conditions. APRG DOCUMENT APRG 00/33(MA), Austroads.
- Werkmeister, S., A. R. Dawson, et al. (2001). "Permanent deformation behaviour of unbound granular materials and the shakedown theory." Transp. Res. Board **1757**: 75-81

Wolff, H. and A. T. Visser (1994). "Incorporating elasto-plasticity in granular layer pavement design." Transp. Eng.

Wright, H. (1996). Highway Engineering. New York, John Wiley&Sons.

WSDOT. (2008). "WSDOT Pavement Guide." Retrieved October 15,, 2008, from <http://training.ce.washington.edu/WSDOT/>.

Yu, H.-S. and M. Z. Hossain (1998). "Lower bound shakedown analysis of layered pavements using discontinuous stress fields." Comput. Method Appl. Mech. Eng. **167**: 209-222.

APPENDIX:

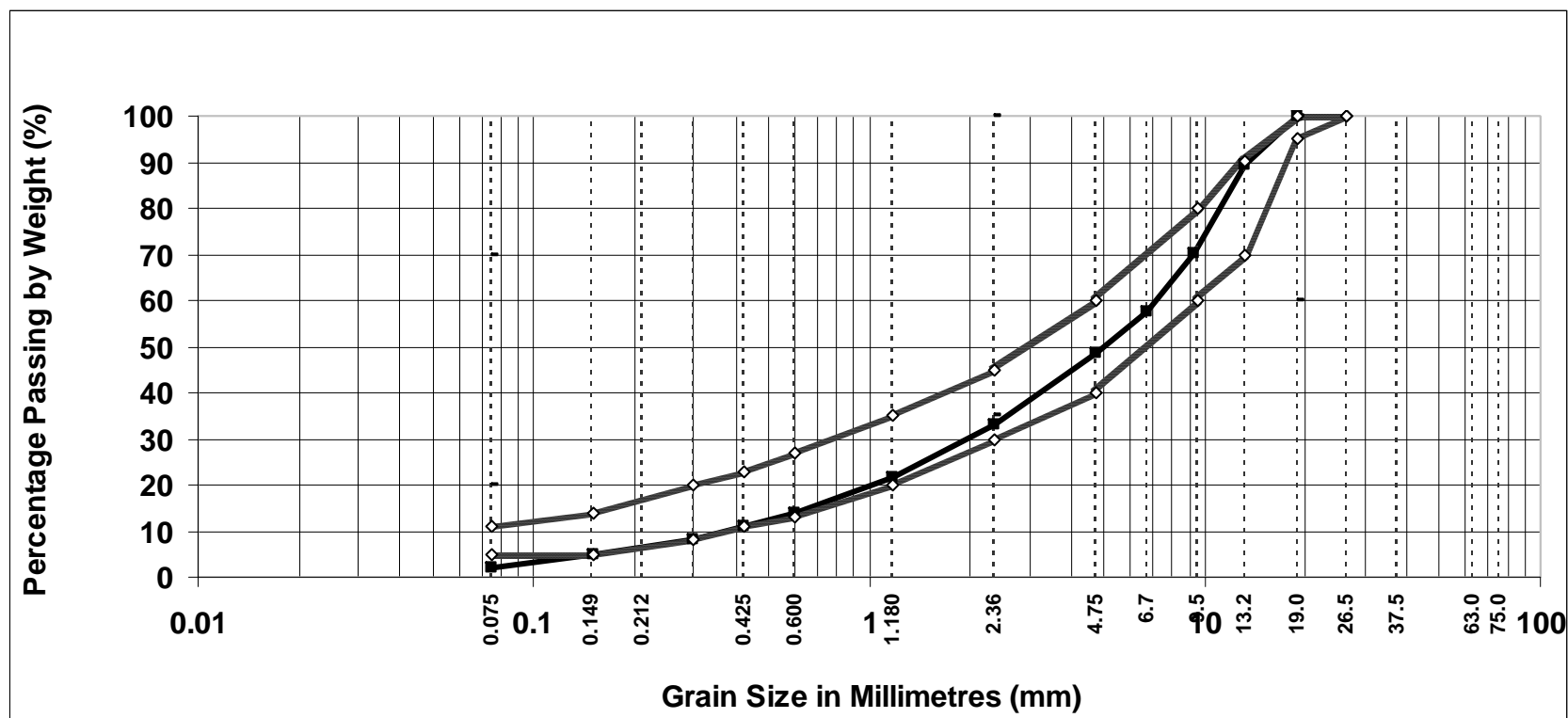
APPENDIX: MATERIAL RESULTS AND ANALYSIS

APPENDIX A: NON-MECHANICAL CHARACTERISATIONS

APPENDIX A
(Non-Mechanical Characterisations)
Particle Size Distribution

CRB Uncompacted											
		Test 1	1118	g	Test 2	1094	g	Test 3	1171	g	Avg.
	Sieve Size	Wt Rtn (g)	Ret %	Pass. %	Wt Rtn (g)	Ret %	Pass. %	Wt Rtn (g)	Ret %	Pass. %	Pass. %
	19	0	0.00	100.00	0	0.00	100.00	0	0.00	100.00	100.00
	13.2	78.36	7.01	92.99	159.7	14.60	85.40	119.8	10.23	89.77	89.39
	9.3	198.9	17.79	75.20	254	23.22	62.18	188	16.05	73.71	70.37
	6.7	127.4	11.40	63.81	154.6	14.13	48.05	152.3	13.01	60.71	57.52
	4.75	100.2	8.96	54.84	95.2	8.70	39.35	108.5	9.27	51.44	48.55
	2.36	180.7	16.16	38.68	156.6	14.31	25.04	191.5	16.35	35.09	32.94
	1.18	152.37	13.63	25.05	95.7	8.75	16.29	139.4	11.90	23.19	21.51
	0.6	112.9	10.10	14.95	56	5.12	11.17	96.7	8.26	14.93	13.68
	0.425	36.9	3.30	11.65	23.23	2.12	9.05	35.7	3.05	11.88	10.86
	0.3	32.8	2.93	8.72	22.9	2.09	6.95	36.31	3.10	8.78	8.15
	0.15	40.6	3.63	5.09	29	2.65	4.30	43.23	3.69	5.09	4.83
	0.075	29.45	2.63	2.45	28	2.56	1.74	31.6	2.70	2.39	2.19
	0	29.25	2.62	-0.16	18.8	1.72	0.02	28.8	2.46	-0.07	-0.07

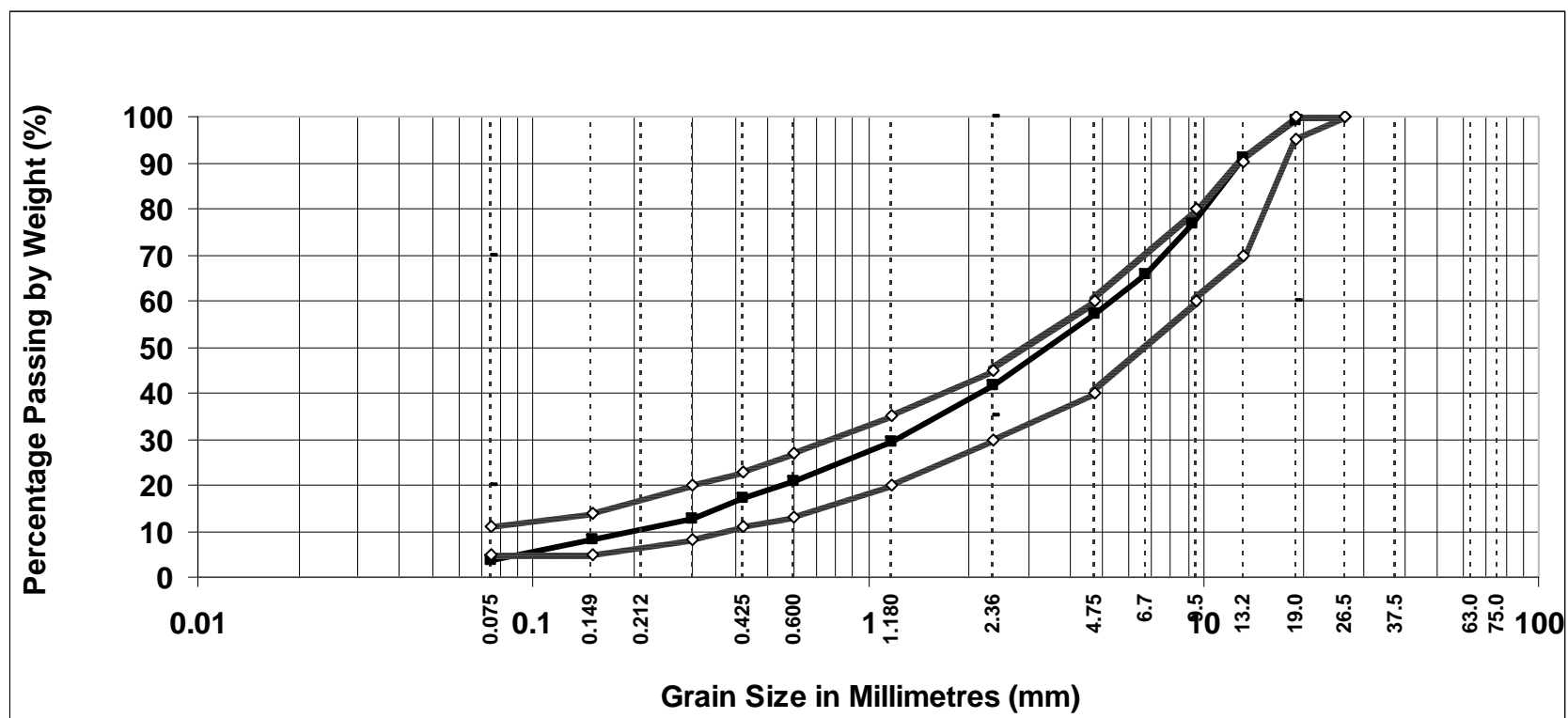
Appendix A: Non-Mechanical Characterisations



Appendix A: Non-Mechanical Characterisations

CRB Compacted											
		Test 1	1077	g	Test 2	1100	g				Avg.
	Sieve Size	Wt Rtn (g)	Ret %	Pass. %	Wt Rtn (g)	Ret %	Pass. %				Pass. %
	19	17.14	1.59	98.41	0	0.00	100.00				99.20
	13.2	63.5	5.90	92.51	114.75	10.43	89.57				91.04
	9.3	152.5	14.16	78.35	161.72	14.70	74.87				76.61
	6.7	110.1	10.22	68.13	131.52	11.96	62.91				65.52
	4.75	93.1	8.64	59.49	88.34	8.03	54.88				57.18
	2.36	174.1	16.17	43.32	162.72	14.79	40.09				41.70
	1.18	137.8	12.79	30.53	128	11.64	28.45				29.49
	0.6	97.24	9.03	21.50	95.4	8.67	19.78				20.64
	0.425	40.7	3.78	17.72	37.7	3.43	16.35				17.03
	0.3	50.8	4.72	13.00	42.7	3.88	12.47				12.73
	0.15	49.3	4.58	8.42	50.7	4.61	7.86				8.14
	0.075	48.9	4.54	3.88	51.6	4.69	3.17				3.53
	0	44.4	4.12	-0.24	33.7	3.06	0.10				-0.07

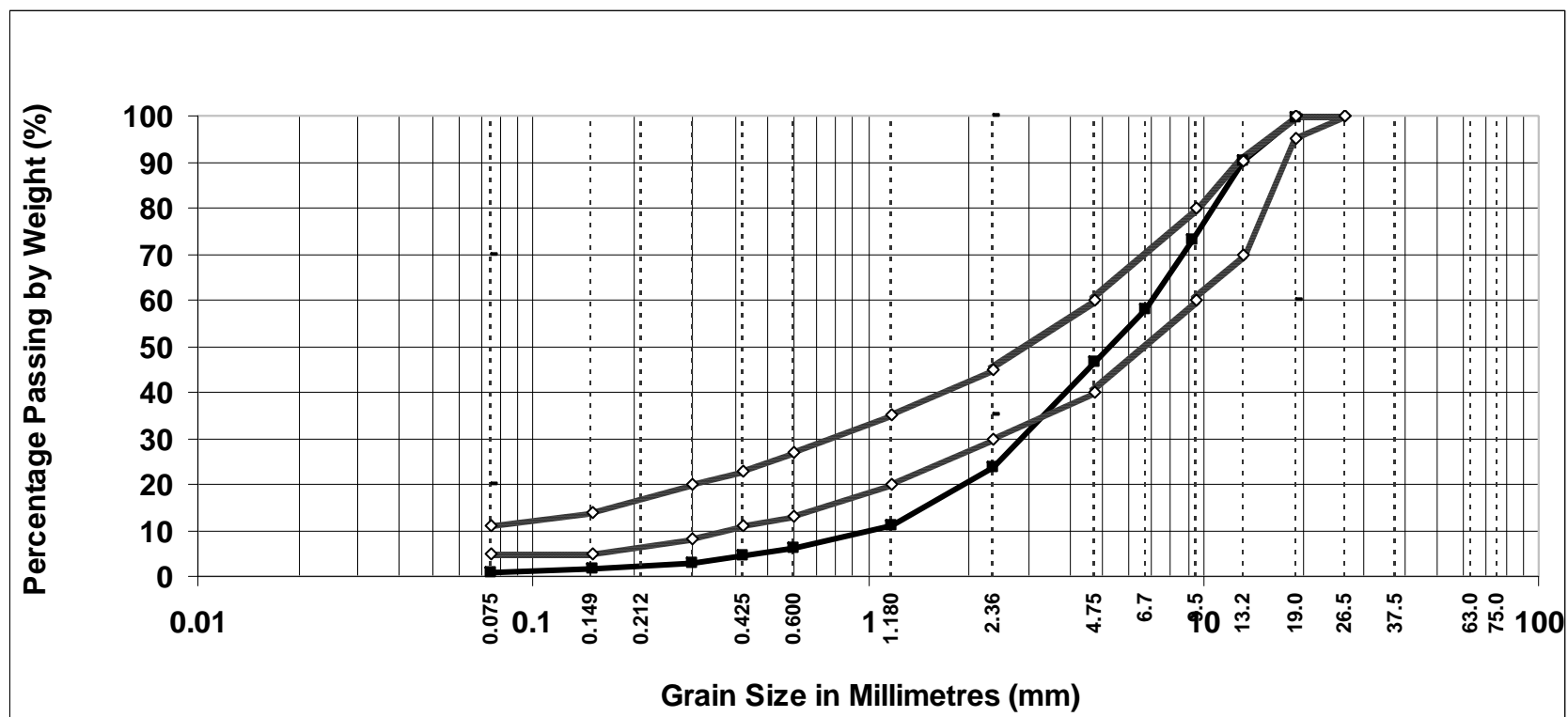
Appendix A: Non-Mechanical Characterisations



Appendix A: Non-Mechanical Characterisations

3 day Uncompacted											
		Test 1	1008	g	Test 2	1031	g	Test 3	1018	g	Avg.
	Sieve Size	Wt Rtn (g)	Ret %	Pass. %	Wt Rtn (g)	Ret %	Pass. %	Wt Rtn (g)	Ret %	Pass. %	Pass. %
	19	9	0.89	99.11	0	0.00	100.00	0	0.00	100.00	99.70
	13.2	78	7.74	91.37	122	11.83	88.17	94	9.23	90.77	90.10
	9.3	155	15.38	75.99	185	17.94	70.22	178	17.49	73.28	73.17
	6.7	137	13.59	62.40	167	16.20	54.03	166	16.31	56.97	57.80
	4.75	118	11.71	50.69	115	11.15	42.87	117	11.49	45.48	46.35
	2.36	236	23.41	27.28	224	21.73	21.14	230	22.59	22.89	23.77
	1.18	143	14.19	13.10	114	11.06	10.09	128	12.57	10.31	11.17
	0.6	55	5.46	7.64	48	4.66	5.43	50	4.91	5.40	6.16
	0.425	21	2.08	5.56	19	1.84	3.59	17	1.67	3.73	4.29
	0.3	15	1.49	4.07	13	1.26	2.33	12	1.18	2.55	2.98
	0.15	19	1.88	2.18	12	1.16	1.16	12	1.18	1.38	1.57
	0.075	11	1.09	1.09	4	0.39	0.78	6	0.59	0.79	0.88
	0	18	1.79	-0.69	8	0.78	0.00	9	0.88	-0.10	-0.26

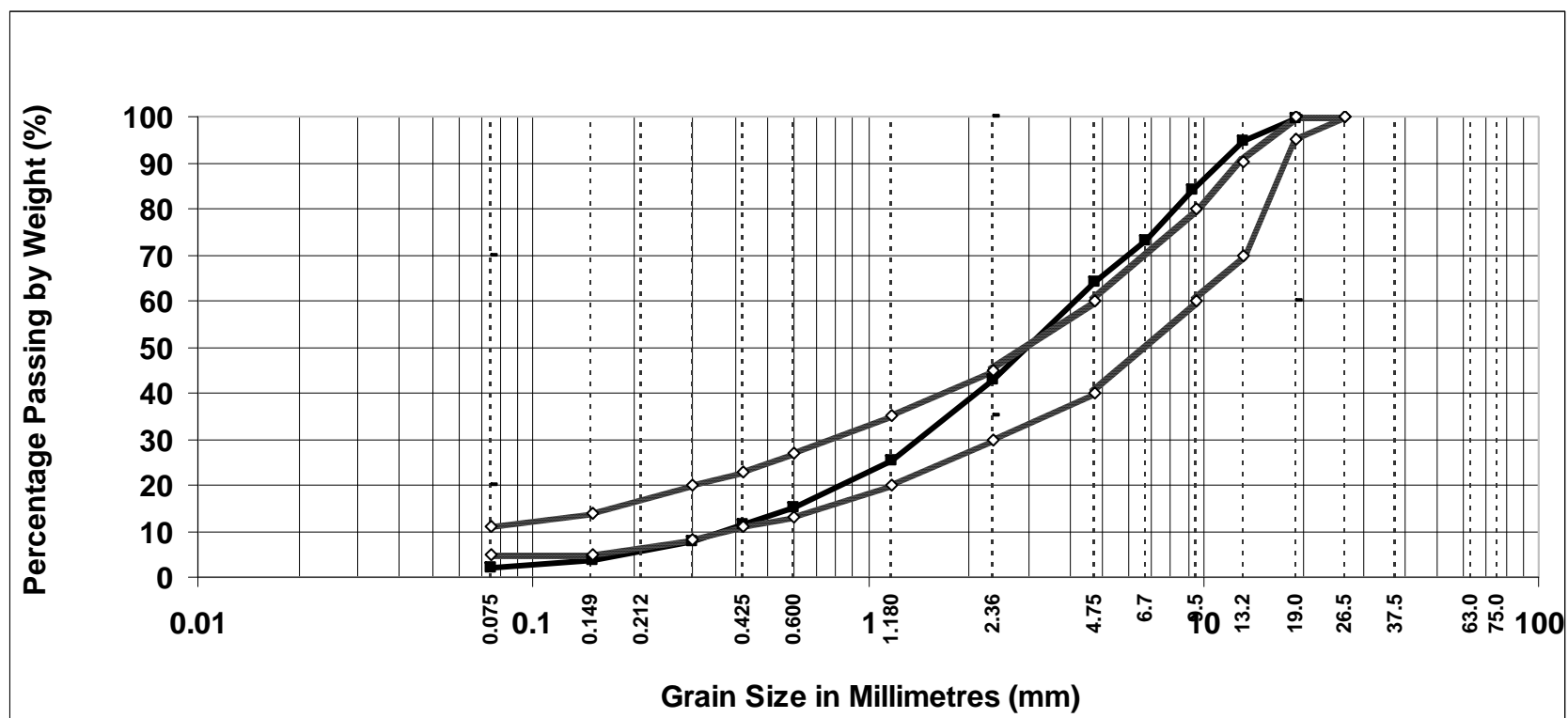
Appendix A: Non-Mechanical Characterisations



Appendix A: Non-Mechanical Characterisations

3 day Compacted											
		Test 1	1030	g	Test 2	1066	g	Test 3	1036	g	Avg.
	Sieve Size	Wt Rtn (g)	Ret %	Pass. %	Wt Rtn (g)	Ret %	Pass. %	Wt Rtn (g)	Ret %	Pass. %	Pass. %
	19	9	0.87	99.13	0	0.00	100.00	0	0.00	100.00	99.71
	13.2	56	5.44	93.69	83	7.79	92.21	21	2.03	97.97	94.63
	9.3	89	8.64	85.05	127	11.91	80.30	113	10.91	87.07	84.14
	6.7	120	11.65	73.40	117	10.98	69.32	115	11.10	75.97	72.90
	4.75	103	10.00	63.40	95	8.91	60.41	84	8.11	67.86	63.89
	2.36	220	21.36	42.04	202	18.95	41.46	237	22.88	44.98	42.83
	1.18	178	17.28	24.76	180	16.89	24.58	194	18.73	26.25	25.20
	0.6	99	9.61	15.15	108	10.13	14.45	111	10.71	15.54	15.04
	0.425	39	3.79	11.36	39	3.66	10.79	41	3.96	11.58	11.24
	0.3	40	3.88	7.48	36	3.38	7.41	35	3.38	8.20	7.70
	0.15	41	3.98	3.50	39	3.66	3.75	41	3.96	4.25	3.83
	0.075	20	1.94	1.55	21	1.97	1.78	21	2.03	2.22	1.85
	0	18	1.75	-0.19	22	2.06	-0.28	22	2.12	0.10	-0.13

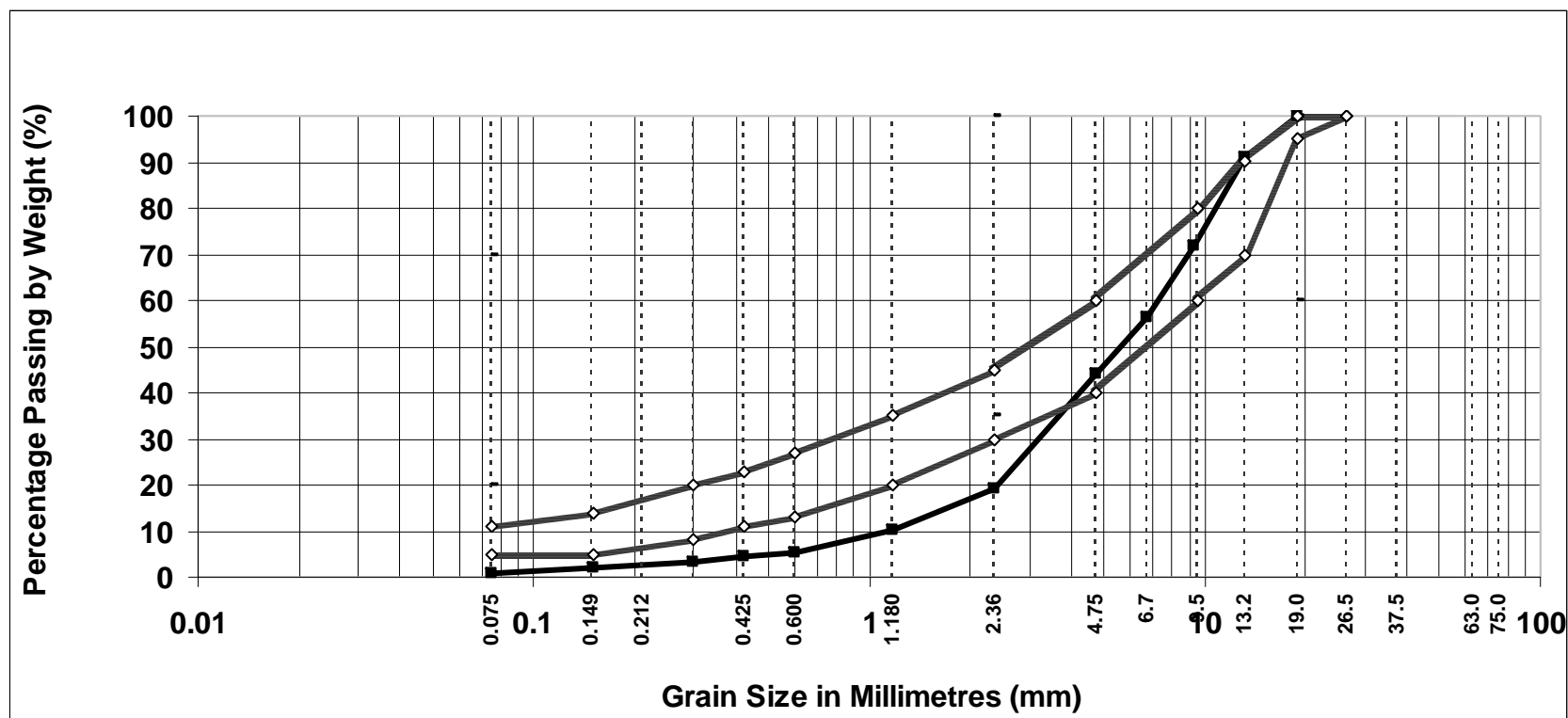
Appendix A: Non-Mechanical Characterisations



Appendix A: Non-Mechanical Characterisations

7 day Uncompacted											
		Test 1	1038	g	Test 2	1018	g	Test 3	1196	g	Avg.
	Sieve Size	Wt Rtn (g)	Ret %	Pass. %	Wt Rtn (g)	Ret %	Pass. %	Wt Rtn (g)	Ret %	Pass. %	Pass. %
	19	0	0.00	100.00	0	0	100	0	0.00	100.00	100.00
	13.2	89.3	8.60	91.40	55.6	5.46	94.54	150.9	12.62	87.38	91.11
	9.3	231.3	22.28	69.11	196.6	19.31	75.23	198.5	16.60	70.79	71.71
	6.7	170.3	16.41	52.71	146.1	14.35	60.87	184	15.38	55.40	56.33
	4.75	132.7	12.78	39.92	125.4	12.32	48.56	137.9	11.53	43.87	44.12
	2.36	238.2	22.95	16.97	272	26.72	21.84	295.5	24.71	19.16	19.33
	1.18	82.9	7.99	8.99	111.2	10.92	10.91	106.8	8.93	10.23	10.05
	0.6	43.7	4.21	4.78	53.8	5.28	5.63	52.1	4.36	5.88	5.43
	0.425	10.2	0.98	3.80	11.96	1.17	4.45	13.7	1.15	4.73	4.33
	0.3	9.7	0.93	2.86	11.2	1.10	3.35	12.9	1.08	3.65	3.29
	0.15	11.7	1.13	1.73	11.7	1.15	2.20	15.8	1.32	2.33	2.09
	0.075	9.7	0.93	0.80	12.1	1.19	1.02	13.7	1.15	1.19	1.00
	0	7.52	0.72	0.08	10.9	1.07	-0.06	14.2	1.19	0.00	0.01

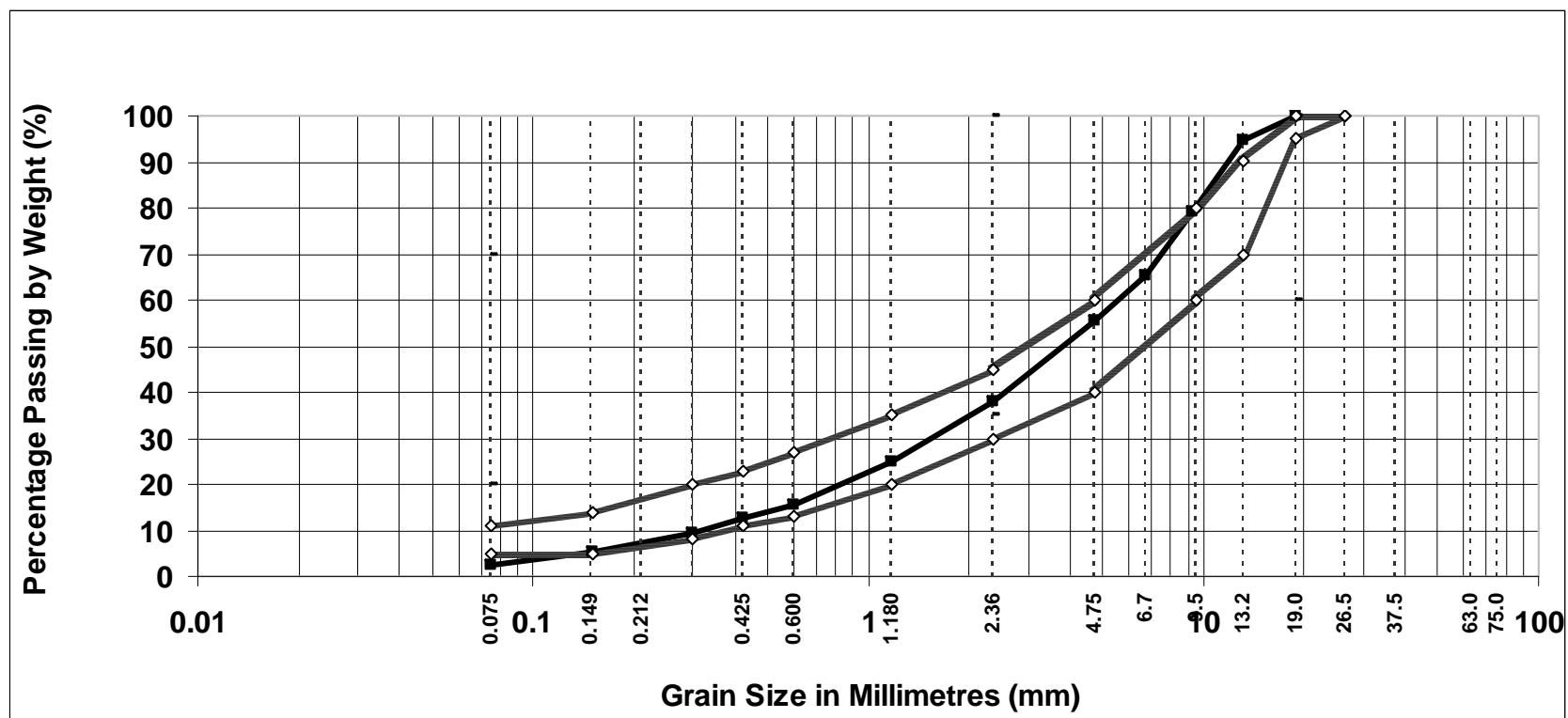
Appendix A: Non-Mechanical Characterisations



Appendix A: Non-Mechanical Characterisations

7 day Compacted											
		Test 1	961	g	Test 2	1050	g	Test 3	992	g	Avg.
	Sieve Size	Wt Rtn (g)	Ret %	Pass. %	Wt Rtn (g)	Ret %	Pass. %	Wt Rtn (g)	Ret %	Pass. %	Pass. %
	19	0	0.00	100.00	0	0.00	100.00	0	0.00	100.00	100.00
	13.2	39.8	4.14	95.86	73.6	7.01	92.99	46.8	4.72	95.28	94.71
	9.3	152.8	15.90	79.96	173.2	16.50	76.50	136.2	13.73	81.55	79.34
	6.7	145	15.09	64.87	153.3	14.60	61.90	123.4	12.44	69.11	65.29
	4.75	98.7	10.27	54.60	99.54	9.48	52.42	93	9.38	59.74	55.58
	2.36	163	16.96	37.64	175.4	16.70	35.71	186.7	18.82	40.92	38.09
	1.18	121.7	12.66	24.97	125.1	11.91	23.80	147.7	14.89	26.03	24.93
	0.6	86.5	9.00	15.97	89.5	8.52	15.27	102.3	10.31	15.72	15.65
	0.425	28.4	2.96	13.02	30.8	2.93	12.34	31.4	3.17	12.55	12.64
	0.3	30.86	3.21	9.81	32.9	3.13	9.21	32	3.23	9.32	9.45
	0.15	40.3	4.19	5.61	43.2	4.11	5.09	42.2	4.25	5.07	5.26
	0.075	28.7	2.99	2.63	31.6	3.01	2.08	29.8	3.00	2.07	2.26
	0	22.7	2.36	0.26	24.3	2.31	-0.23	20.2	2.04	0.03	0.02

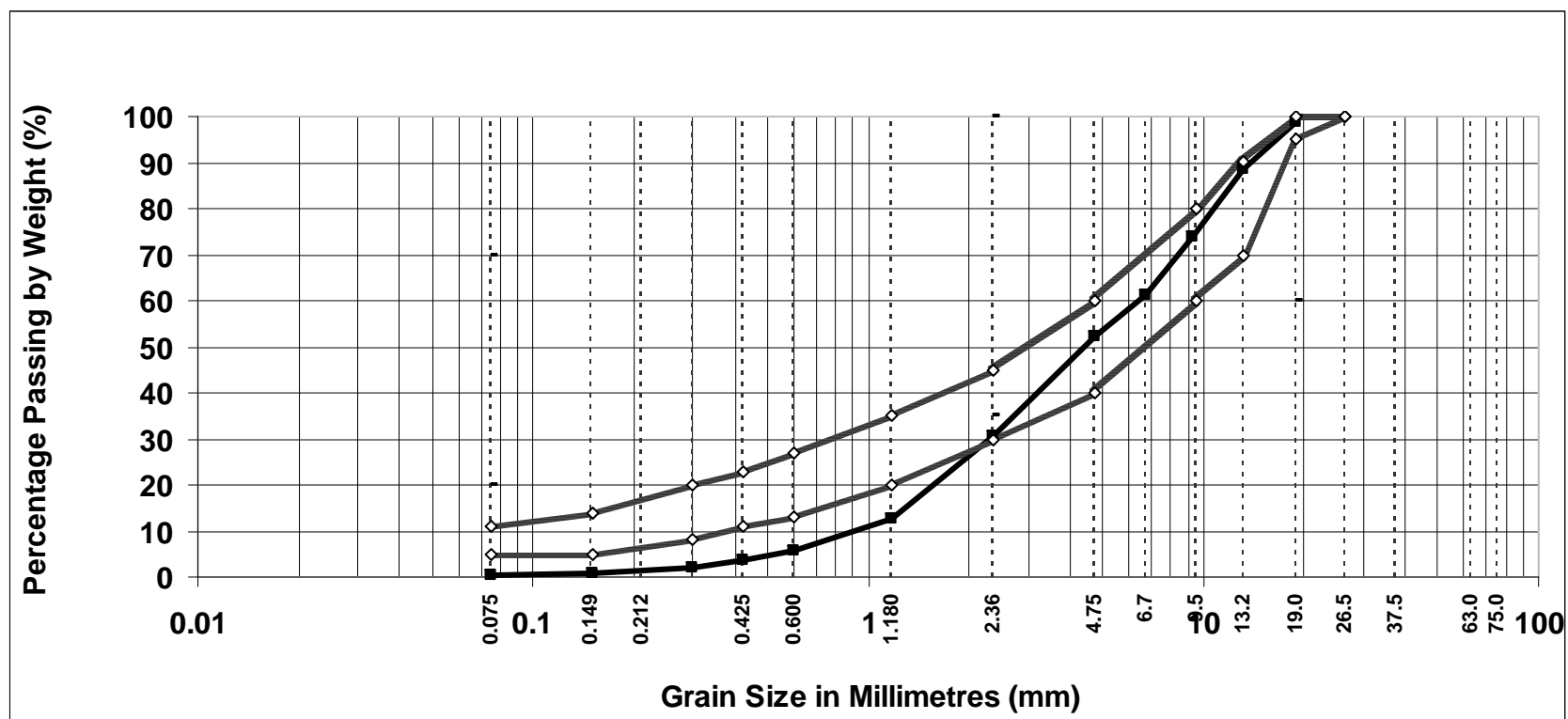
Appendix A: Non-Mechanical Characterisations



Appendix A: Non-Mechanical Characterisations

15 day Uncompacted											
		Test 1	1070	g	Test 2	1028	g	Test 3	1086	g	Avg.
	Sieve Size	Wt Rtn (g)	Ret %	Pass. %	Wt Rtn (g)	Ret %	Pass. %	Wt Rtn (g)	Ret %	Pass. %	Pass. %
	19	26.2	2.45	97.55	0	0.00	100.00	9.8	0.90	99.10	98.88
	13.2	135.7	12.68	84.87	63.2	6.15	93.85	131.4	12.10	87.00	88.57
	9.3	212.3	19.84	65.03	103.5	10.07	83.78	156.9	14.45	72.55	73.79
	6.7	141.4	13.21	51.81	105.2	10.23	73.55	150.7	13.88	58.67	61.35
	4.75	83.8	7.83	43.98	103.28	10.05	63.50	96.45	8.88	49.79	52.43
	2.36	195.43	18.26	25.72	264.7	25.75	37.75	234.2	21.57	28.23	30.57
	1.18	151.8	14.19	11.53	232.4	22.61	15.15	182.7	16.82	11.40	12.69
	0.6	67.4	6.30	5.23	87.25	8.49	6.66	69.1	6.36	5.04	5.64
	0.425	20.5	1.92	3.31	26	2.53	4.13	22	2.03	3.02	3.49
	0.3	13.5	1.26	2.05	18.2	1.77	2.36	13.8	1.27	1.74	2.05
	0.15	12.9	1.21	0.85	17.75	1.73	0.63	13.3	1.22	0.52	0.67
	0.075	4	0.37	0.47	4.45	0.43	0.20	3.8	0.35	0.17	0.28
	0	4.4	0.41	0.06	3.5	0.34	-0.14	3	0.28	-0.11	-0.06

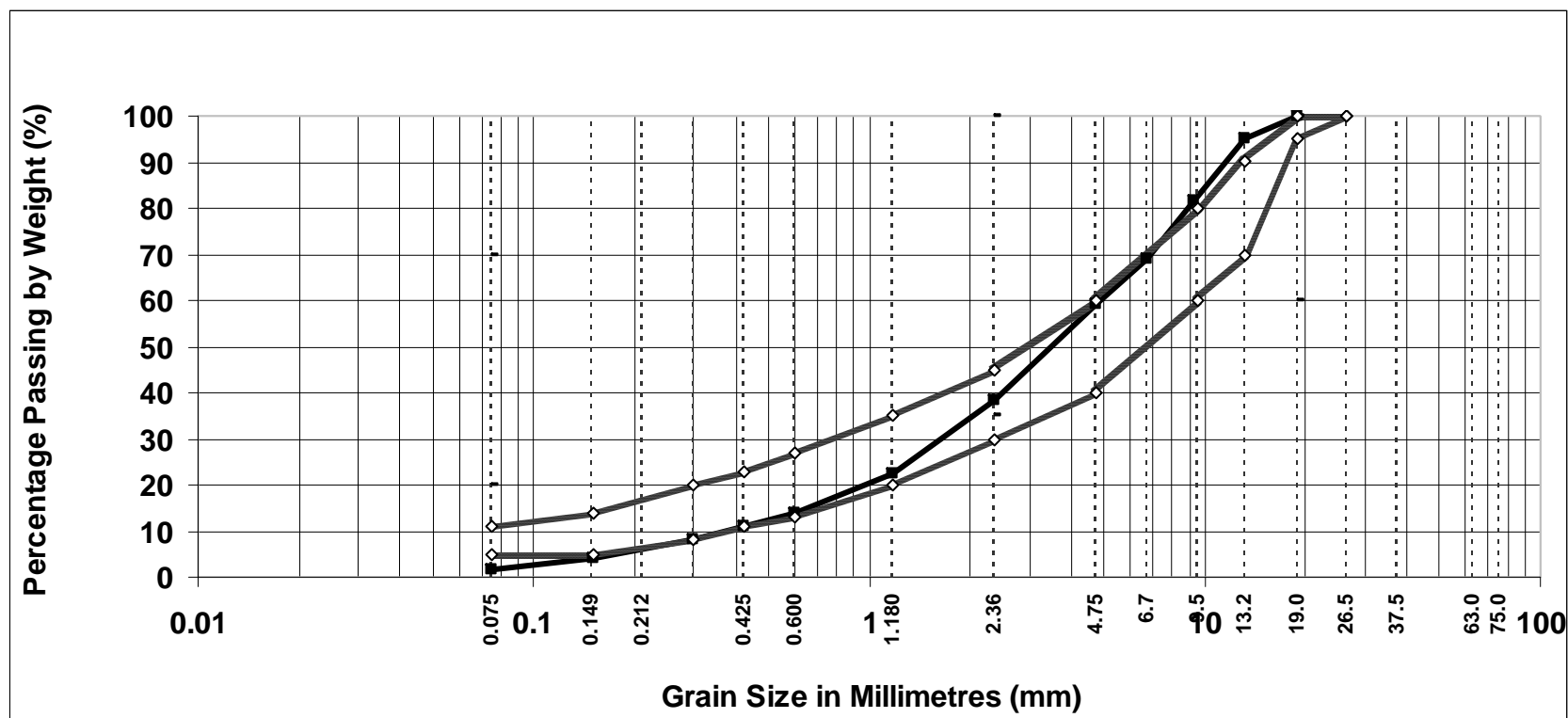
Appendix A: Non-Mechanical Characterisations



Appendix A: Non-Mechanical Characterisations

15 day Compacted											
		Test 1	824	g	Test 2	1004	g	Test 3	1035	g	Avg.
	Sieve Size	Wt Rtn (g)	Ret %	Pass. %	Wt Rtn (g)	Ret %	Pass. %	Wt Rtn (g)	Ret %	Pass. %	Pass. %
	19	0	0.00	100.00	0	0.00	100.00	0	0.00	100.00	100.00
	13.2	42	5.10	94.90	37.3	3.72	96.28	61.3	5.92	94.08	95.09
	9.3	121	14.68	80.22	127.5	12.70	83.59	131.3	12.69	81.39	81.73
	6.7	131	15.90	64.32	127	12.65	70.94	98.7	9.54	71.86	69.04
	4.75	93.3	11.32	53.00	93.3	9.29	61.64	92.1	8.90	62.96	59.20
	2.36	173.4	21.04	31.95	209.8	20.90	40.75	211.5	20.43	42.52	38.41
	1.18	113.5	13.77	18.18	167.5	16.68	24.06	176.2	17.02	25.50	22.58
	0.6	57.1	6.93	11.25	91.8	9.14	14.92	100.8	9.74	15.76	13.98
	0.425	20.1	2.44	8.81	34.8	3.47	11.45	35.9	3.47	12.29	10.85
	0.3	16.8	2.04	6.77	27.4	2.73	8.73	31.4	3.03	9.26	8.25
	0.15	26.2	3.18	3.59	43.6	4.34	4.38	46	4.44	4.81	4.26
	0.075	16.6	2.01	1.58	30.7	3.06	1.32	30	2.90	1.91	1.61
	0	13.3	1.61	-0.04	12.8	1.27	0.05	19.8	1.91	0.00	0.00

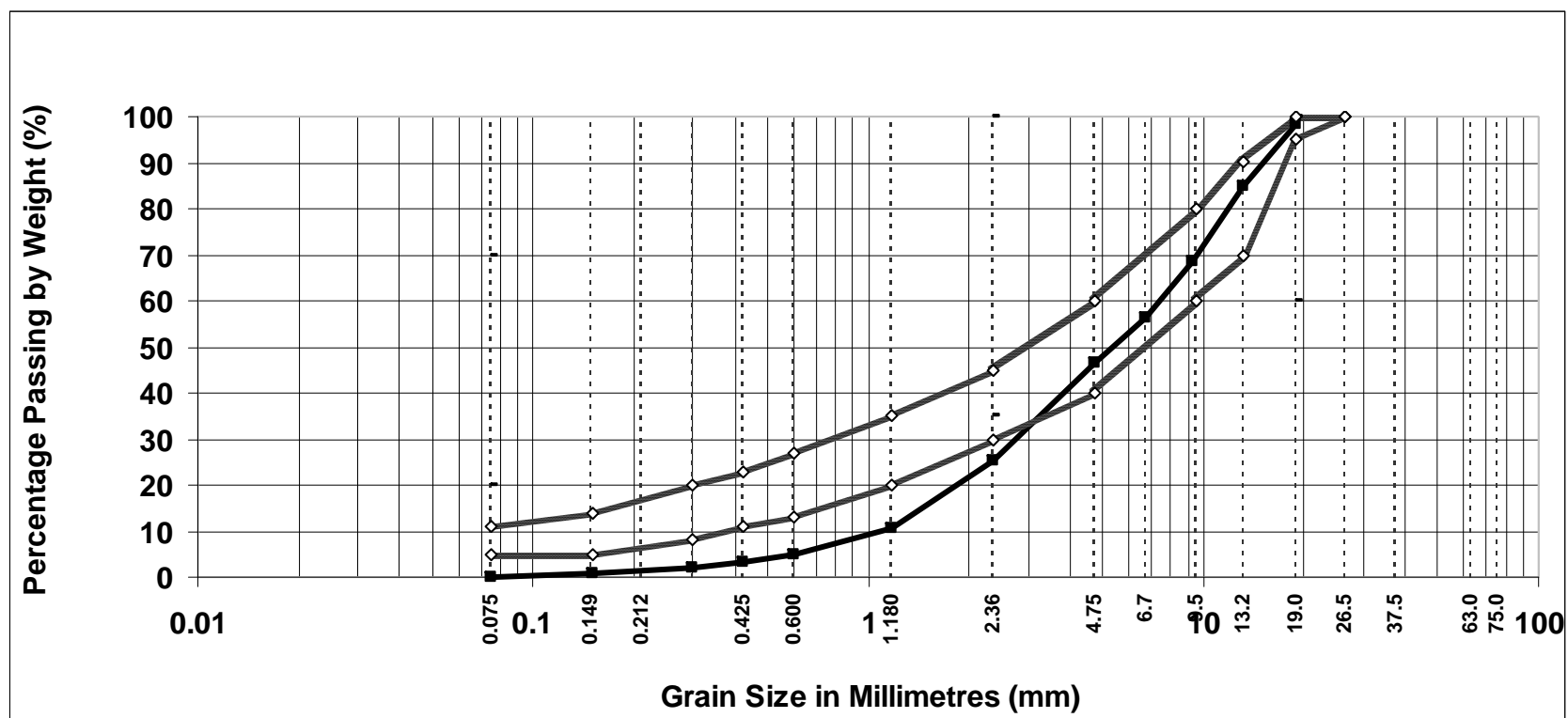
Appendix A: Non-Mechanical Characterisations



Appendix A: Non-Mechanical Characterisations

30 day Uncompacted											
		Test 1	1041	g	Test 2	1039	g	Test 3	1021	g	Avg.
	Sieve Size	Wt Rtn (g)	Ret %	Pass. %	Wt Rtn (g)	Ret %	Pass. %	Wt Rtn (g)	Ret %	Pass. %	Pass. %
	19	21.3	2.05	97.95	22.45	2.16	97.84	13.25	1.30	98.70	98.17
	13.2	147.5	14.17	83.78	108.5	10.44	87.40	160.1	15.68	83.02	84.73
	9.3	193	18.54	65.24	156	15.01	72.38	150.7	14.76	68.26	68.63
	6.7	135.2	12.99	52.26	132.8	12.78	59.60	116.3	11.39	56.87	56.24
	4.75	102.9	9.88	42.37	94.9	9.13	50.47	105.3	10.31	46.56	46.47
	2.36	200.5	19.26	23.11	241.7	23.26	27.20	216.2	21.18	25.38	25.23
	1.18	137.7	13.23	9.88	169	16.27	10.94	149.3	14.62	10.76	10.53
	0.6	54.9	5.27	4.61	64.2	6.18	4.76	60.4	5.92	4.84	4.74
	0.425	16	1.54	3.07	15.7	1.51	3.25	15.9	1.56	3.29	3.20
	0.3	11.7	1.12	1.95	11.5	1.11	2.14	11.5	1.13	2.16	2.08
	0.15	13.9	1.34	0.61	14.6	1.41	0.74	14.4	1.41	0.75	0.70
	0.075	4.94	0.47	0.14	5.3	0.51	0.23	5.27	0.52	0.23	0.20
	0	3.1	0.30	-0.16	3.2	0.31	-0.08	2.4	0.24	0.00	-0.08

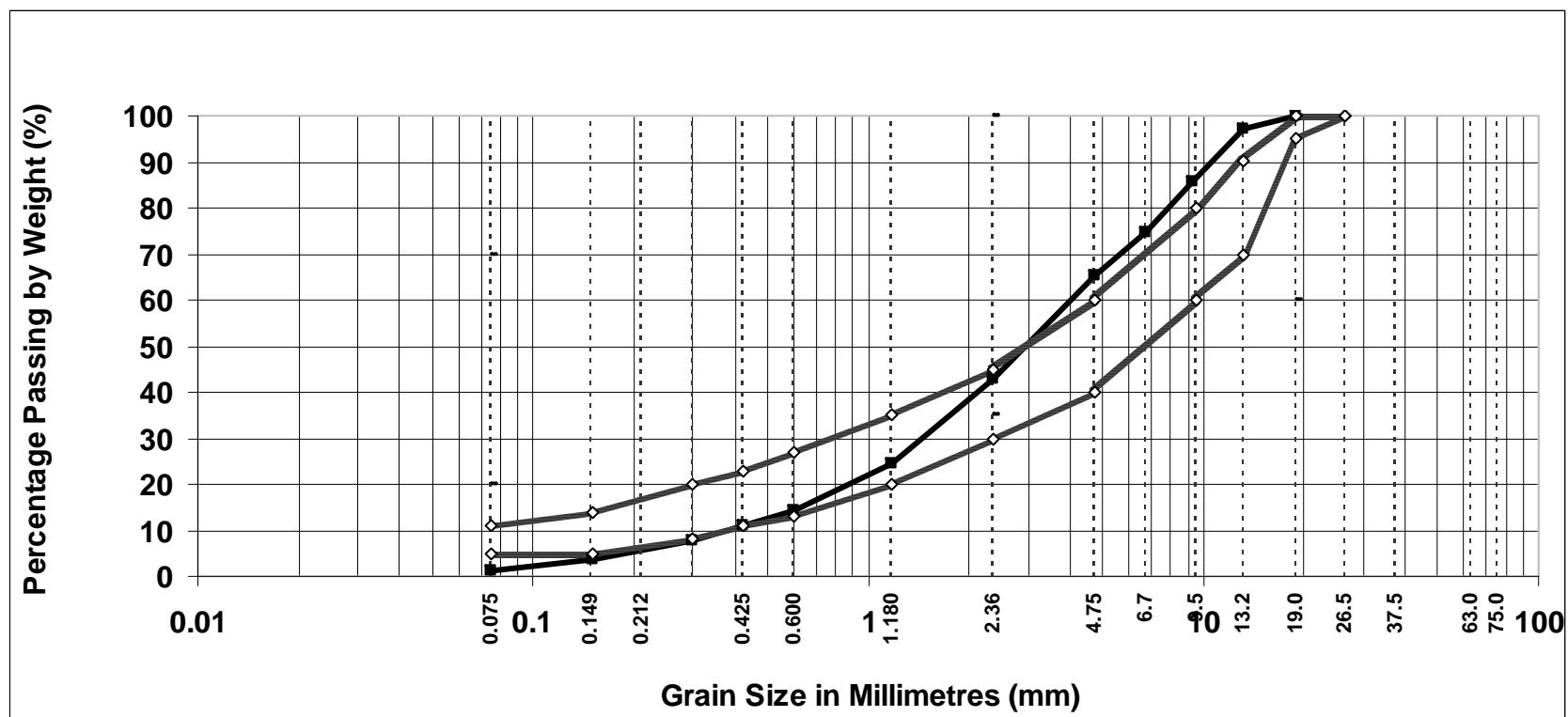
Appendix A: Non-Mechanical Characterisations



Appendix A: Non-Mechanical Characterisations

30 day Compacted											
		Test 1	1052	g	Test 2	1042	g	Test 3	1174	g	Avg.
	Sieve Size	Wt Rtn (g)	Ret %	Pass. %	Wt Rtn (g)	Ret %	Pass. %	Wt Rtn (g)	Ret %	Pass. %	Pass. %
	19	0	0.00	100.00	0	0.00	100.00	0	0.00	100.00	100.00
	13.2	25.2	2.40	97.60	33.5	3.21	96.79	38.4	3.27	96.73	97.04
	9.3	128.1	12.18	85.43	91.1	8.74	88.04	153.2	13.05	83.68	85.72
	6.7	131.3	12.48	72.95	99.2	9.52	78.52	132.9	11.32	72.36	74.61
	4.75	97.8	9.30	63.65	92.9	8.92	69.61	107.8	9.18	63.18	65.48
	2.36	231.7	22.02	41.63	254	24.38	45.23	246.1	20.96	42.21	43.02
	1.18	192.5	18.30	23.33	208	19.96	25.27	198.1	16.87	25.34	24.65
	0.6	106.3	10.10	13.22	110.5	10.60	14.66	120.7	10.28	15.06	14.32
	0.425	34.1	3.24	9.98	36.1	3.46	11.20	41	3.49	11.57	10.92
	0.3	31.7	3.01	6.97	31.8	3.05	8.15	34.1	2.90	8.66	7.93
	0.15	42.8	4.07	2.90	46	4.41	3.73	51.6	4.40	4.27	3.63
	0.075	23.5	2.23	0.67	24.9	2.39	1.34	29.2	2.49	1.78	1.26
	0	17.3	1.64	-0.98	18.6	1.79	-0.44	21.6	1.84	-0.06	-0.49

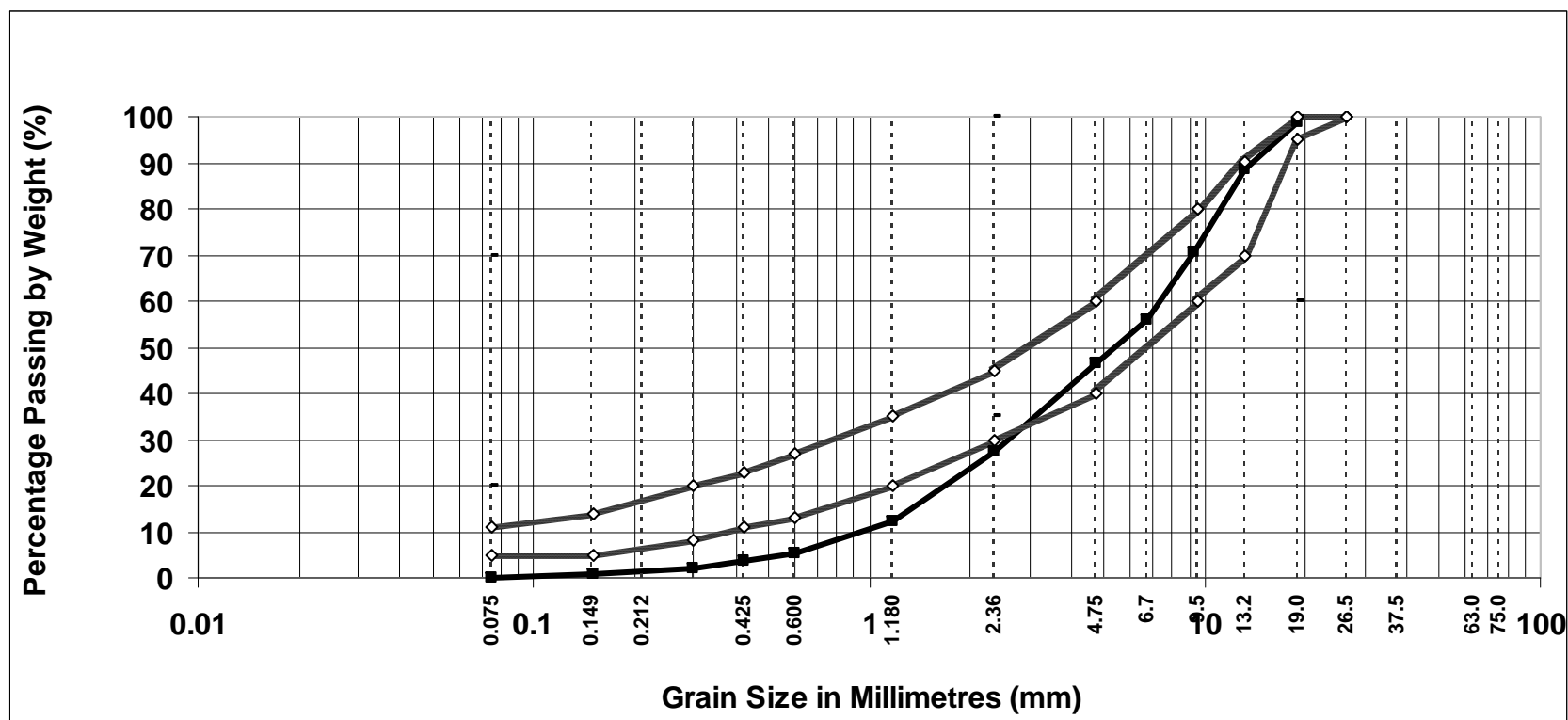
Appendix A: Non-Mechanical Characterisations



Appendix A: Non-Mechanical Characterisations

45 day Uncompacted											
		Test 1	1142	g	Test 2	1063	g	Test 3	1079	g	Avg.
	Sieve Size	Wt Rtn (g)	Ret %	Pass. %	Wt Rtn (g)	Ret %	Pass. %	Wt Rtn (g)	Ret %	Pass. %	Pass. %
	19	0	0.00	100.00	13.5	1.27	98.73	20.85	1.93	98.07	98.93
	13.2	76.7	6.72	93.28	142.9	13.44	85.29	123.2	11.42	86.65	88.41
	9.3	174	15.24	78.05	165.5	15.57	69.72	241.9	22.42	64.23	70.67
	6.7	174	15.24	62.81	141.9	13.35	56.37	163.4	15.14	49.09	56.09
	4.75	126.5	11.08	51.73	87.5	8.23	48.14	99.6	9.23	39.86	46.58
	2.36	254	22.24	29.49	203.1	19.11	29.03	176	16.31	23.54	27.36
	1.18	189.8	16.62	12.87	176.5	16.60	12.43	136.9	12.69	10.86	12.05
	0.6	80.5	7.05	5.82	75.7	7.12	5.31	63.7	5.90	4.95	5.36
	0.425	23.4	2.05	3.77	20	1.88	3.42	18.5	1.71	3.24	3.48
	0.3	15.8	1.38	2.39	13.9	1.31	2.12	12.8	1.19	2.05	2.19
	0.15	19.2	1.68	0.71	16.2	1.52	0.59	14.7	1.36	0.69	0.66
	0.075	6.5	0.57	0.14	5.4	0.51	0.08	4.4	0.41	0.28	0.17
	0	3.7	0.32	-0.18	3.9	0.37	-0.28	3	0.28	0.00	-0.15

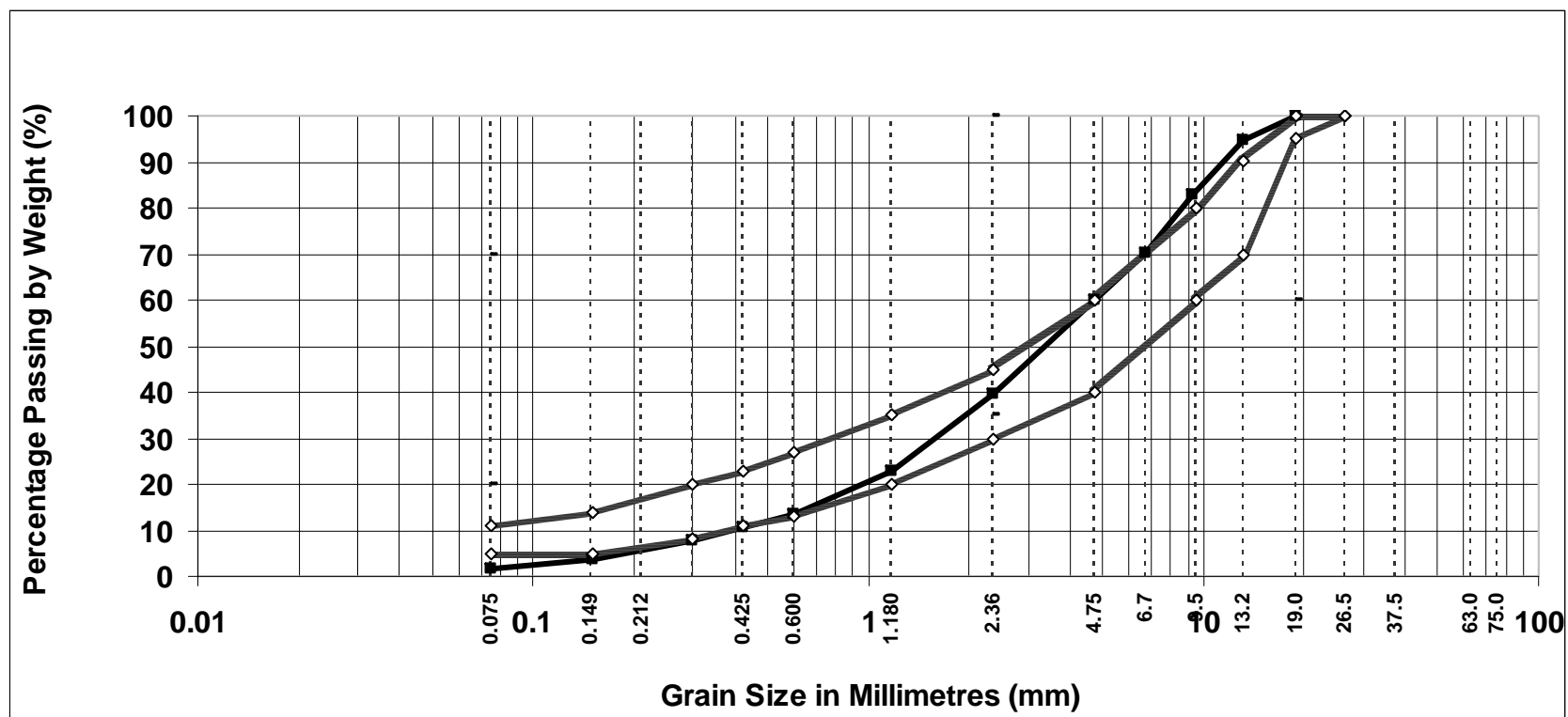
Appendix A: Non-Mechanical Characterisations



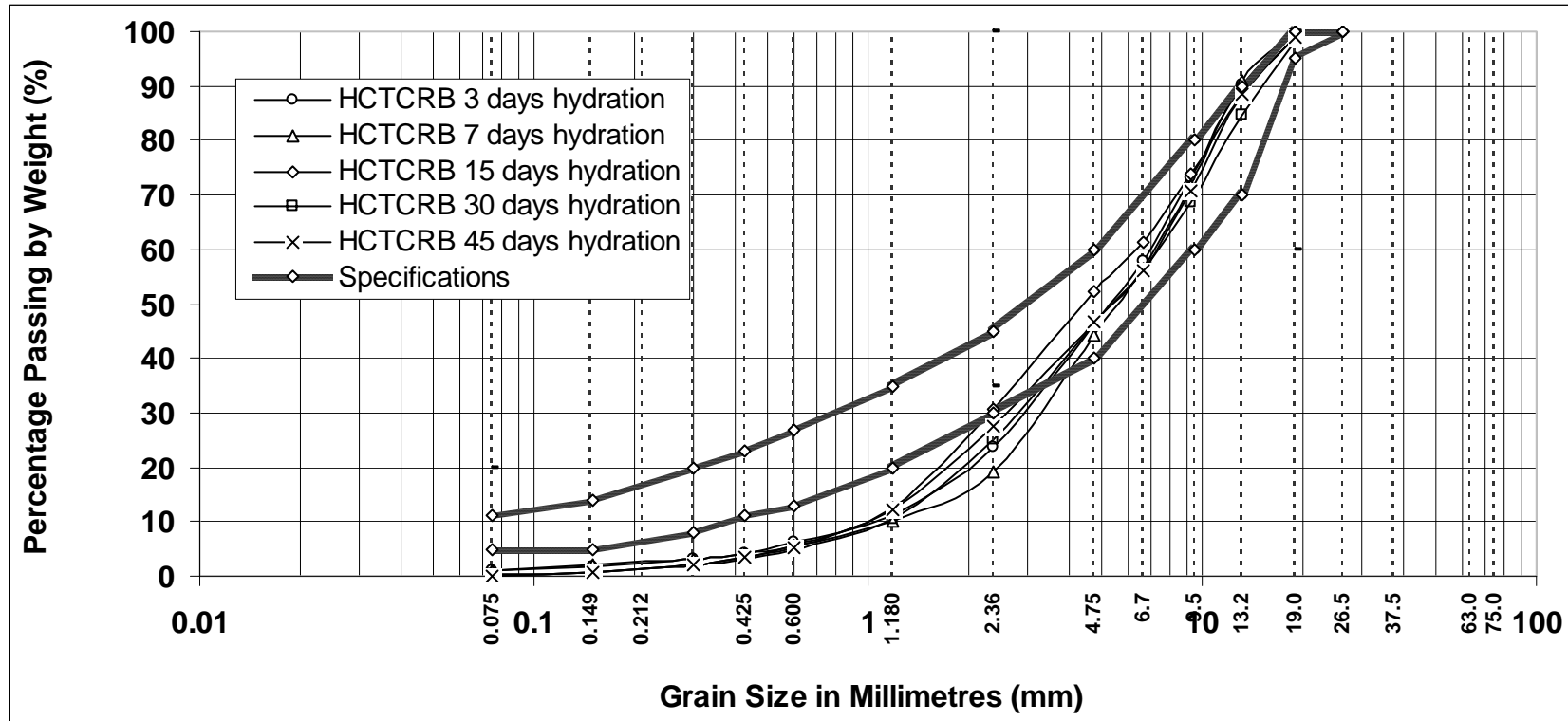
Appendix A: Non-Mechanical Characterisations

45 day Compacted											
		Test 1	1064	g	Test 2	1061	g	Test 3	1055	g	Avg.
	Sieve Size	Wt Rtn (g)	Ret %	Pass. %	Wt Rtn (g)	Ret %	Pass. %	Wt Rtn (g)	Ret %	Pass. %	Pass. %
	19	0	0.00	100.00	0	0.00	100.00	0	0.00	100.00	100.00
	13.2	66.9	6.29	93.71	43.7	4.12	95.88	56.5	5.36	94.64	94.75
	9.3	105.1	9.88	83.83	143.5	13.52	82.36	135.6	12.85	81.79	82.66
	6.7	111.5	10.48	73.36	144.9	13.66	68.70	139.7	13.24	68.55	70.20
	4.75	116.7	10.97	62.39	111.3	10.49	58.21	99.2	9.40	59.15	59.91
	2.36	227.2	21.35	41.03	214.1	20.18	38.03	208.3	19.74	39.40	39.49
	1.18	187.5	17.62	23.41	163.1	15.37	22.66	178.1	16.88	22.52	22.86
	0.6	101.7	9.56	13.85	95.4	8.99	13.67	95.7	9.07	13.45	13.66
	0.425	33.2	3.12	10.73	31.1	2.93	10.74	33.8	3.20	10.25	10.57
	0.3	30.5	2.87	7.87	30	2.83	7.91	27.9	2.64	7.60	7.79
	0.15	44.1	4.14	3.72	42.9	4.04	3.86	43.4	4.11	3.49	3.69
	0.075	25.6	2.41	1.32	24.1	2.27	1.59	21.6	2.05	1.44	1.45
	0	17.9	1.68	-0.37	17.7	1.67	-0.08	16.5	1.56	-0.12	-0.19

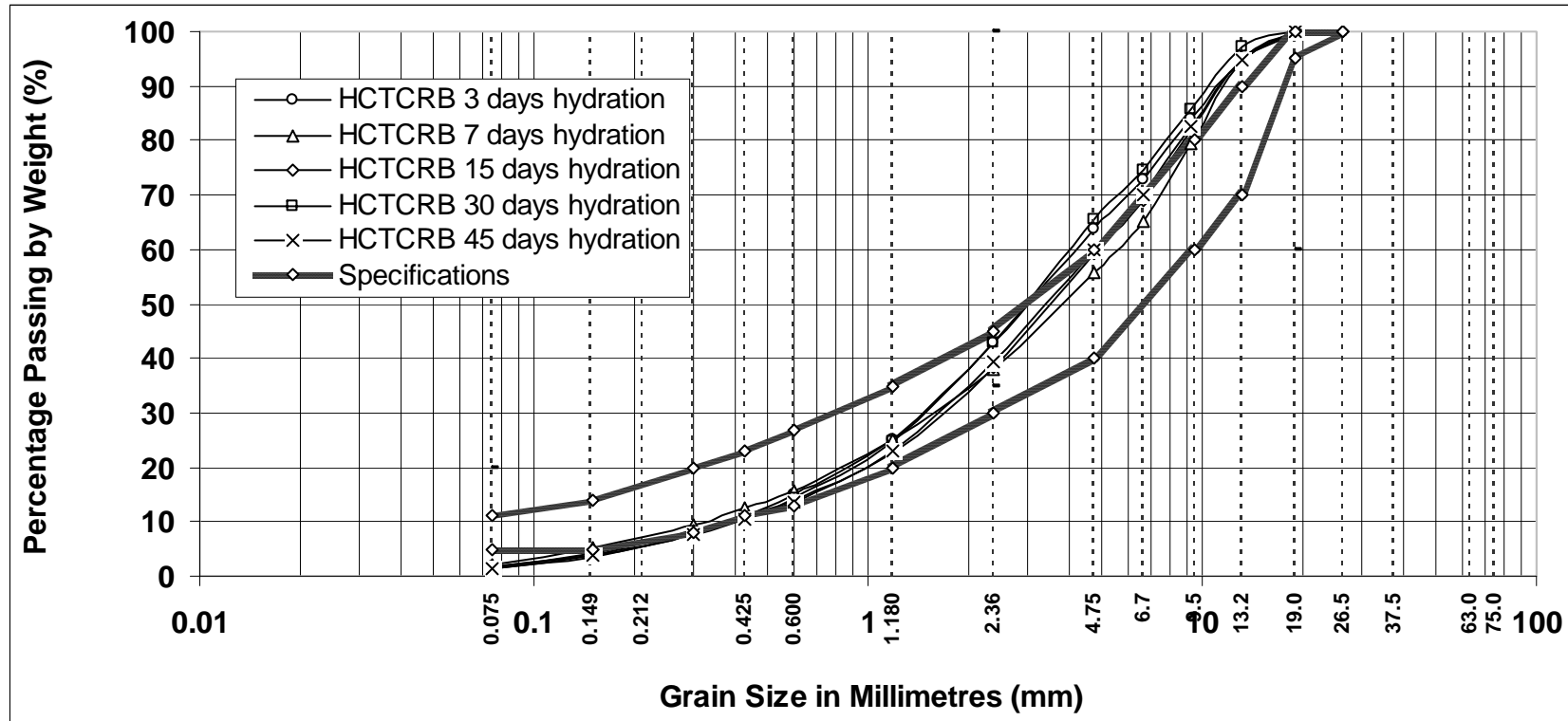
Appendix A: Non-Mechanical Characterisations



Appendix A: Non-Mechanical Characterisations



Appendix A: Non-Mechanical Characterisations



Appendix A: Non-Mechanical Characterisations

APPENDIX A (Non-Mechanical Characterisations) Moisture Content

	7 Day Material Samples			28/05/2008					
Sample #	1	2	3	4	5	6	7	8	9
Tare	5316	5327	5443	5266	5452	5418	5269	5310	5448
Gross	8821	8789	8919	8821	8941	8860	8754	8777	8979
Nett	3505	3462	3476	3555	3489	3442	3485	3467	3531
Density	2.09	2.06	2.07	2.12	2.08	2.05	2.08	2.06	2.10
Target for 85%	8782	8751	8880	8782	8902	8822	8715	8739	8940
Target for 65%	8730	8699	8829	8729	8851	8771	8664	8687	8888
% MDD	97.08	95.89	96.28	98.47	96.64	95.34	96.53	96.03	97.80
Notes		Sample Discarded	Sample Discarded	Tested as 7-OMC-28		Sample Discarded		Tested as 7-OMC-7	Laminated, used for moisture

Appendix A: Non-Mechanical Characterisations

Location:	Curtin Soil Mechanic Lab				tested Date:				
Soil Description:					Test By:				
			Dry back	80			60		
			Sample No.	1	2	3	1	2	3
WATER CONTENT									
Weight of Wet Soil + Container			g	301.15	345.24	307.51	295.78	302.14	314.87
Weight of Dry Soil + Container			g	279.11	318.45	284.57	274.35	280.15	291.68
Weight of Water			g	22.04	26.79	22.94	21.43	21.99	23.19
Weight of Container			g	85.78	85.78	85.78	86.21	86.21	86.21
Weight of Dry Soil			g	193.33	232.67	198.79	188.14	193.94	205.47
Water Content,w			%	11.40	11.51	11.54	11.39	11.34	11.29
Volume of mould			cm3	1570.80	1570.80	1570.80	1570.80	1570.80	1570.80
Preparation of soil (Wd)			g	3078.76	3078.76	3078.76	3078.76	3078.76	3078.76
Water			g	350.98	354.49	355.28	350.68	349.09	347.48
Weight of mould			g	5069.00	5160.00	5131.00	5239.00	5072.00	5229.00
Target weight at 100%OMC			g	8498.75	8593.25	8565.04	8668.45	8499.85	8655.24
Final weight at particular OMC			g	8428.55	8522.36	8493.99	8528.17	8360.21	8516.25
Actual water			g	280.79	283.59	284.23	210.41	209.45	208.49
%actual water content			%	80.71	81.52	81.70	60.48	60.20	59.93

Appendix A: Non-Mechanical Characterisations

Location:	Curtin Soil Mechanic Lab			tested Date:					
Soil Description:				Test By:					
			Dry back	80			60		
			Sample No.	1	2	3	1	2	3
WATER CONTENT									
Weight of Wet Soil + Container			g	300.25	352.47	308.86	307.54	301.23	302.22
Weight of Dry Soil + Container			g	278.35	325.74	285.67	284.63	279.11	280.23
Weight of Water			g	21.9	26.73	23.19	22.91	22.12	21.99
Weight of Container			g	85.78	85.78	85.78	86.21	86.21	86.21
Weight of Dry Soil			g	192.57	239.96	199.89	198.42	192.9	194.02
Water Content,w			%	11.37	11.14	11.60	11.55	11.47	11.33
Volume of mould			cm3	1570.80	1570.80	1570.80	1570.80	1570.80	1570.80
Preparation of soil (Wd)			g	3000.22	3000.22	3000.22	3000.22	3000.22	3000.22
Water			g	341.20	334.21	348.07	346.41	344.04	340.04
Weight of mould			g	5069.00	5160.00	5131.00	5239.00	5072.00	5229.00
Target weight at 100%OMC			g	8410.42	8494.43	8479.29	8585.63	8416.26	8569.26
Final weight at particular OMC			g	8342.18	8427.59	8409.67	8447.07	8278.64	8433.25
Actual water			g	272.96	267.36	278.45	207.85	206.42	204.02
%actual water content			%	80.51	78.86	82.13	61.31	60.89	60.18

Appendix A: Non-Mechanical Characterisations

Location:	Curtin Soil Mechanic Lab			tested Date:								
			Dry back	80			60			60		
			Sample No.	1	2	3	1	2	3	1 day	7 days	28 days
WATER CONTENT												
Weight of Wet Soil + Container			g	224.15	305.25	234.56	315.36	306.14	306.35	326.23	301.25	314.32
Weight of Dry Soil + Container			g	210.5	284.12	220.13	293.26	284.39	284.96	302.95	280.15	292.24
Weight of Water			g	13.65	21.13	14.43	22.1	21.75	21.39	23.28	21.1	22.08
Weight of Container			g	85.78	85.78	85.78	86.21	86.21	86.21	85.25	85.25	85.25
Weight of Dry Soil			g	124.72	198.34	134.35	207.05	198.18	198.75	217.7	194.9	206.99
Water Content,w			%	10.94	10.65	10.74	10.67	10.97	10.76	10.69	10.83	10.67
Volume of mould			cm3	1570.80	1570.80	1570.80	1570.80	1570.80	1570.80	1570.80	1570.80	1570.80
Preparation of soil (Wd)			g	2921.68	2921.68	2921.68	2921.68	2921.68	2921.68	2921.68	2921.68	2921.68
Water			g	319.76	311.26	313.81	311.85	320.65	314.44	312.43	316.30	311.66
Weight of mould			g	5069.00	5160.00	5131.00	5239.00	5072.00	5229.00	5239.00	5072.00	5229.00
Target weight at 100%OMC			g	8310.45	8392.94	8366.49	8472.53	8314.33	8465.12	8473.11	8309.98	8462.34
Final weight at particular OMC			g	8246.49	8330.69	8303.73	8347.79	8186.07	8339.34	8348.14	8183.46	8337.68
Actual water			g	255.81	249.01	251.04	187.11	192.39	188.66	187.46	189.78	187.00
%actual water content			%	80.33	78.19	78.83	58.75	60.41	59.24	58.86	59.59	58.72

Appendix A: Non-Mechanical Characterisations

Location:	Curtin Soil Mechanic Lab													
Weight of Wet Soil + Container		g	330.1 2	304.3 9	312.0 3	295.2 6	306.8 7	301.1 2	302.1 5	314.8 7	311.0 2	307.9 8	306.6 4	314.8 5
Weight of Dry Soil + Container		g	306.2 5	282.7 4	290.3 1	275.1 5	285.1 8	280.2 3	281.3 9	292.6 8	289.2 4	286.4 7	285.3 1	292.7 4
Weight of Water		g	23.87	21.65	21.72	20.11	21.69	20.89	20.76	22.19	21.78	21.51	21.33	22.11
Weight of Container		g	85.78	85.78	85.78	85.78	85.78	85.78	85.78	85.78	85.78	85.78	85.78	85.78
Weight of Dry Soil		g	220.4 7	196.9 6	204.5 3	189.3 7	199.4	194.4 5	195.6 1	206.9	203.4 6	200.6 9	199.5 3	206.9 6
Water Content,w		%	10.83	10.99	10.62	10.62	10.88	10.74	10.61	10.72	10.70	10.72	10.69	10.68
Volume of mould		cm3	1570. 80	1570. 80	1570. 80	1570. 80	1570. 80	1570. 80	1570. 80	1570. 80	1570. 80	1570. 80	1570. 80	1570. 80
Preparation of soil (Wd)		g	2921. 68	2921. 68	2921. 68	2921. 68	2921. 68	2921. 68	2921. 68	2921. 68	2921. 68	2921. 68	2921. 68	2921. 68
Water		g	316.3 3	321.1 5	310.2 7	310.2 7	317.8 1	313.8 8	310.0 8	313.3 5	312.7 6	313.1 5	312.3 3	312.1 3
Weight of mould		g	5229. 00	5131. 00	5245. 00	5245. 00	5245. 00	5245. 00	5245. 00	5245. 00	5245. 00	5245. 00	5245. 00	5245. 00
Target weight at 100%OMC		g	8467. 01	8373. 83	8476. 95	8476. 95	8484. 49	8480. 56	8476. 76	8480. 03	8479. 44	8479. 83	8479. 01	8478. 81
Final weight at particular OMC		g	8340. 48	8245. 37	8352. 84	8352. 84	8357. 37	8355. 01	8352. 73	8354. 69	8354. 34	8354. 57	8354. 08	8353. 96
Actual water		g	189.8 0	192.6 9	186.1 6	186.1 6	190.6 9	188.3 3	186.0 5	188.0 1	187.6 6	187.8 9	187.4 0	187.2 8
%actual water content		%	59.60	60.51	58.46	58.46	59.88	59.14	58.42	59.04	58.93	59.00	58.84	58.81

Appendix A: Non-Mechanical Characterisations

Location:	Curtin Soil Mechanic Lab								
			Dry back	UCS		60			
			Sample No.	1	2	3	1	2	3
				1 day			28 days		
WATER CONTENT									
Weight of Wet Soil + Container			g	311.14	301.95	304.21	302.51	303.14	310.12
Weight of Dry Soil + Container			g	287.65	280.2	281.34	280.32	280.32	287.14
Weight of Water			g	23.49	21.75	22.87	22.19	22.82	22.98
Weight of Container			g	85.78	85.78	85.78	85.78	85.78	85.78
Weight of Dry Soil			g	201.87	194.42	195.56	194.54	194.54	201.36
Water Content,w			%	11.64	11.19	11.69	11.41	11.73	11.41
Volume of mould			cm ³	1570.80	1570.80	1570.80	1570.80	1570.80	1570.80
Preparation of soil (Wd)			g	3000.22	3000.22	3000.22	3000.22	3000.22	3000.22
Water			g	349.11	335.64	350.86	342.22	351.93	342.40
Weight of mould			g	5229.00	5229.00	5229.00	5229.00	5131.00	5245.00
Target weight at 100%OMC			g	8578.33	8564.86	8580.09	8571.44	8483.15	8587.62
Final weight at particular OMC			g	8438.69	8430.60	8439.74	8434.55	8342.38	8450.66
Actual water			g	209.47	201.38	210.52	205.33	211.16	205.44
%actual water content			%	61.79	59.40	62.10	60.56	62.28	60.60

Appendix A: Non-Mechanical Characterisations

Location:	Curtin Soil Mechanic Lab								
			Dry back	UCS		60			
			Sample No.	1	2	3	1	2	3
				1 day			28 days		
WATER CONTENT									
Weight of Wet Soil + Container			g	321.32	305.65	301.41	303.33	306.21	302.35
Weight of Dry Soil + Container			g	297.45	283.24	279.24	281.32	283.26	280.34
Weight of Water			g	23.87	22.41	22.17	22.01	22.95	22.01
Weight of Container			g	85.78	85.78	85.78	85.78	85.78	85.78
Weight of Dry Soil			g	211.67	197.46	193.46	195.54	197.48	194.56
Water Content,w			%	11.28	11.35	11.46	11.26	11.62	11.31
Volume of mould			cm ³	1570.80	1570.80	1570.80	1570.80	1570.80	1570.80
Preparation of soil (Wd)			g	3078.76	3078.76	3078.76	3078.76	3078.76	3078.76
Water			g	347.19	349.41	352.82	346.55	357.80	348.29
Weight of mould			g	5229.00	5229.00	5229.00	5229.00	5131.00	5245.00
Target weight at 100%OMC			g	8654.95	8657.17	8660.58	8654.31	8567.56	8672.05
Final weight at particular OMC			g	8516.08	8517.41	8519.45	8515.69	8424.44	8532.74
Actual water			g	208.31	209.65	211.69	207.93	214.68	208.97
%actual water content			%	59.88	60.26	60.85	59.77	61.71	60.07

Appendix A: Non-Mechanical Characterisation

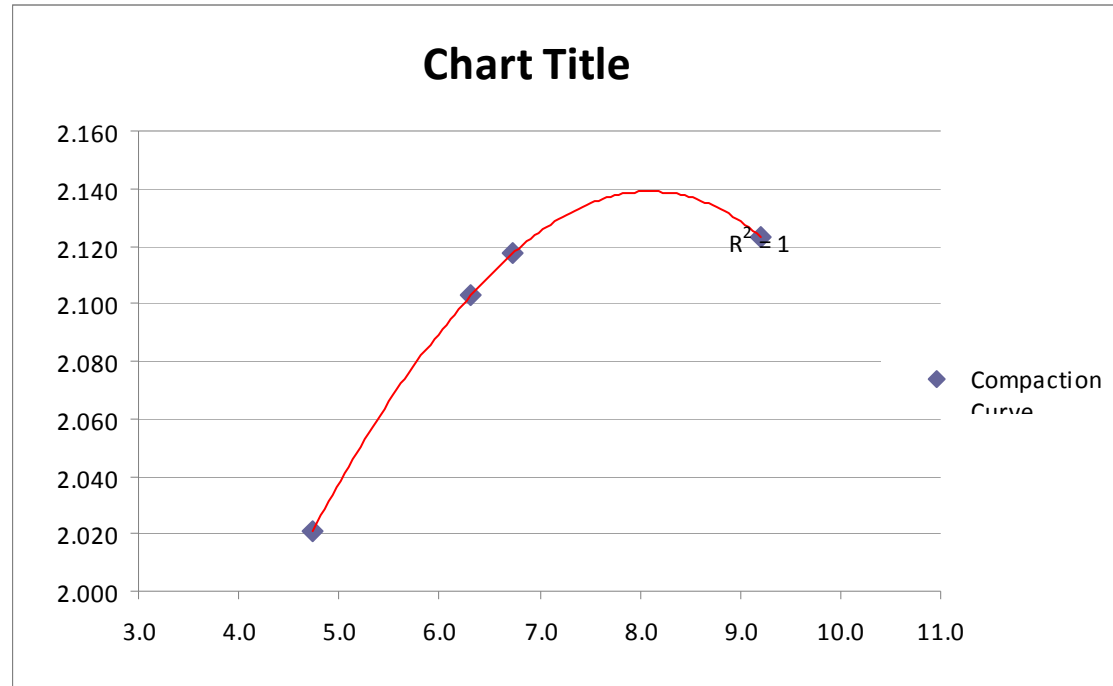
APPENDIX A (Non-Mechanical Characterisations) Compaction Test

SOIL MECHANIC LABORATORY CURTIN UNIVERSITY OF TECHNOLOGY								
Project:		Hydration of HCTCRB			Source of Soil:		Gosnell Quarry	
Location:		Curtin Soil Mechanic Lab			tested Date:		30-03-2009	
Soil Description:		HCTCRB+2%cement+8%water			Test By:			
Compaction Method:Modified				Mold Dimension:		105.27x115.61mm		
Hammer weight			4.9	Kg	Dropped Height		450	mm
No. of Layer			5		No. of Blow		25	blows/layer
COMPACTION				test no.	1	2	3	4
Assumed Water Content				%	dry	8	9.37	11.37
Weight of Air Dry Soil Use				g	2500	2500	2500	2500
Water Content of Air Dry Soil				%	0	0	0	0
Amount of Water Added				cm ³	0	0	30	86.7
Weight of Wet Soil + Mould				g	6132	6252	6276	6335
Weight of Mould				g	4002	4002	4002	4002

Appendix A: Non-Mechanical Characterisation

Weight of Wet Soil, W				g	2130	2250	2274	2333
Wet Density,	$r_{(total)} =$	W/V		g/cm^3	2.12	2.24	2.26	2.32
Dry Soil Density	$r_{(dry)} =$	$100r_{(total)}$		g/cm^3	2.021	2.103	2.117	2.123
		(100+w)						
WATER CONTENT			container number					
Weight of Wet Soil + Container				g	213.81	399.6	95.76	208.19
Weight of Dry Soil + Container				g	208.12	381.2	91.45	198.06
Weight of Water				g	5.69	18.4	4.31	10.13
Weight of Container				g	87.98	89.98	27.41	87.98
Weight of Dry Soil				g	120.14	291.22	64.04	110.08
Water Content, w				%	4.74	6.32	6.73	9.20
RESULT OF SOIL COMPACTION TEST								
Test Number			1	2	3	4		
Dry Density,	$r_{(dry)}$	ton/m^3	2.021	2.103	2.117	2.123		
Water Content, w		%	4.74	6.32	6.73	9.20		

Appendix A: Non-Mechanical Characterisation



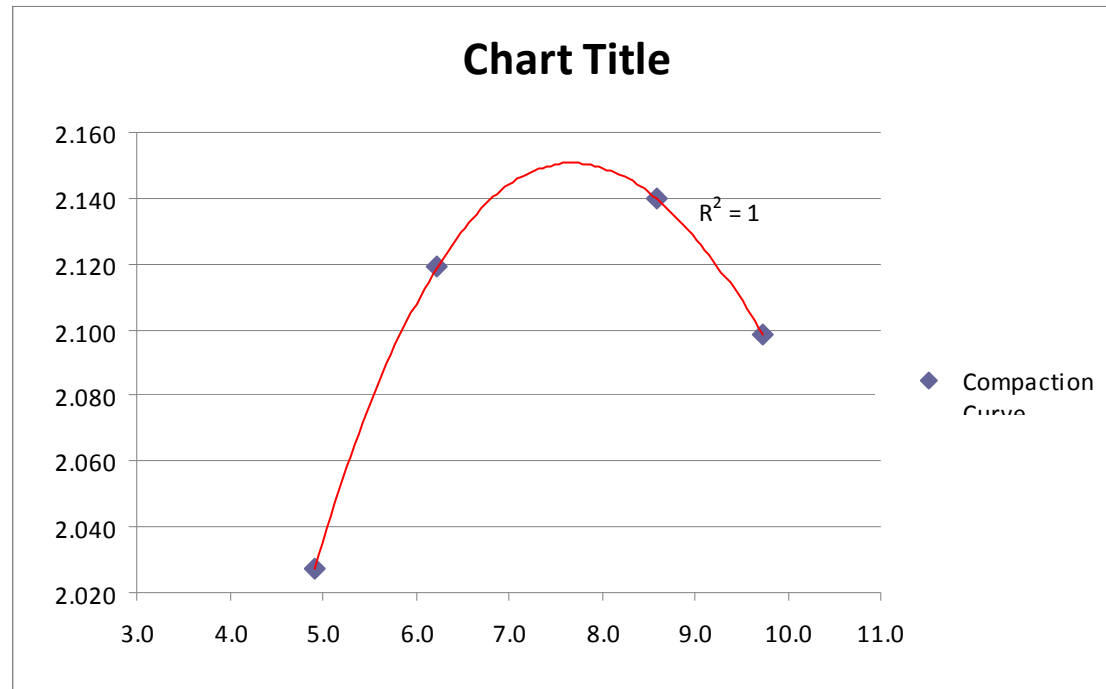
Appendix A: Non-Mechanical Characterisation

SOIL MECHANIC LABORATORY CURTIN UNIVERSITY OF TECHNOLOGY								
Project:		5 days Hydration of HCTCRB			Source of Soil:		Gosnell Quarry	
Location:		Curtin Soil Mechanic Lab			tested Date:		2/4/2009	
Soil Description:		HCTCRB+2% cement+8% water			Test By:			
Compaction Method: Modified				Mold Dimension:		105.27x115.61mm		
Hammer weight			4.9	Kg	Dropped Height		450	mm
No. of Layer			5		No. of Blow		25	blows/layer
COMPACTION				test no.	1	2	3	4
Assumed Water Content				%	dry	8	9.37	11.37
Weight of Air Dry Soil Use				g	2500	2500	2500	2500
Water Content of Air Dry Soil				%	0	0	0	0
Amount of Water Added				cm ³	0	0	30	86.7
Weight of Wet Soil + Mould				g	6142	6267	6319	6340
Weight of Mould				g	4002	4002	4002	4002
Weight of Wet Soil, W				g	2140	2265	2317	2338
Wet Density,		$r_{(total)} =$	W/V	g/cm ³	2.13	2.25	2.30	2.32

Appendix A: Non-Mechanical Characterisation

Dry Soil Density		$r_{(dry)} =$	$100r_{(total)}$	g/cm^3	2.027	2.119	2.099	2.140
			$(100+w)$					
WATER CONTENT			container number					
Weight of Wet Soil + Container				g	219.96	208.53	207	246.27
Weight of Dry Soil + Container				g	213.79	201	195.75	233.13
Weight of Water				g	6.17	7.53	11.25	13.14
Weight of Container				g	87.98	80.10	80.10	80.10
Weight of Dry Soil				g	125.81	120.9	115.65	153.03
Water Content, w				%	4.90	6.23	9.73	8.59
RESULT OF SOIL COMPACTION TEST								
Test Number			1	2	3	4		
Dry Density,		$r_{(dry)}$	ton/m^3	2.027	2.119	2.099	2.140	
Water Content, w		%	4.90	6.23	9.73	8.59		

Appendix A: Non-Mechanical Characterisation



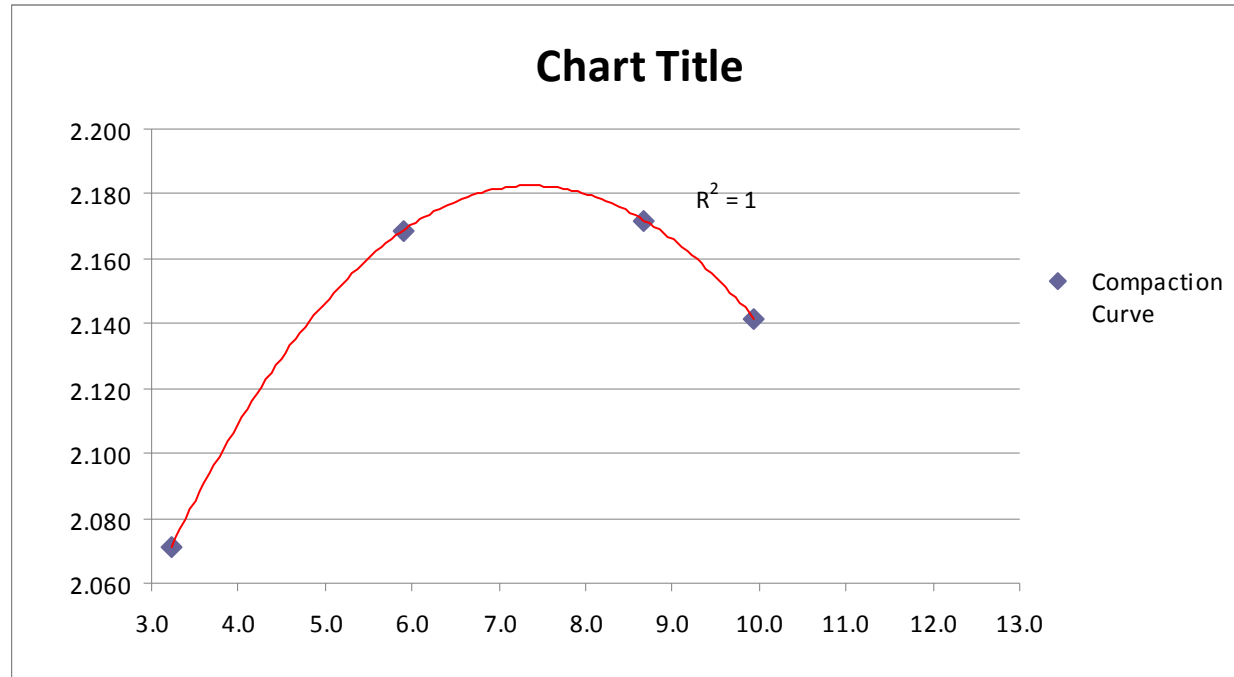
Appendix A: Non-Mechanical Characterisation

SOIL MECHANIC LABORATORY CURTIN UNIVERSITY OF TECHNOLOGY							
Project:		7days Hydration of HCTCRB			Source of Soil:		Gosnell Quarry
Location:		Curtin Soil Mechanic Lab			tested Date:	12/4/2009	
Soil Description:		HCTCRB+2%cement+8%water			Test By:		
Compaction Method:Modified				Mold Dimension:	105.27x115.61mm		
Hammer weight		4.9	Kg	Dropped Height	450	mm	
No. of Layer		5		No. of Blow	25	blows/layer	
COMPACTION			test no.		1	2	3
Assumed Water Content			%	8	8	9.37	11.37
Weight of Air Dry Soil Use			g	2500	2500	2500	2500
Water Content of Air Dry Soil			%	0	0	0	0
Amount of Water Added			cm ³	0	0	30	86.7
Weight of Wet Soil + Mould			g	6848	6912	6906	6688
Weight of Mould			g	4537	4537	4537	4537
Weight of Wet Soil, W			g	2311	2375	2369	2151
Wet Density,		$r_{(total)} =$	W/V	g/cm ³	2.30	2.36	2.35
Dry Soil Density		$r_{(dry)} =$	100 $r_{(total)}$	g/cm ³	2.169	2.172	2.141

Appendix A: Non-Mechanical Characterisation

			(100+w)					
WATER CONTENT			container number					
Weight of Wet Soil + Container				g	265.19	278.35	242	222.34
Weight of Dry Soil + Container				g	255.84	264.36	228.92	218.62
Weight of Water				g	9.35	13.99	13.08	3.72
Weight of Container				g	97.38	103.16	97.38	103.16
Weight of Dry Soil				g	158.46	161.2	131.54	115.46
Water Content, w				%	5.90	8.68	9.94	3.22
RESULT OF SOIL COMPACTION TEST								
Test Number			1	2	3	4	5	
Dry Density,		$\Gamma_{(dry)}$	ton/m ³	2.169	2.172	2.141	2.071	0.000
Water Content, w			%	5.90	8.68	9.94	3.22	0.00

Appendix A: Non-Mechanical Characterisation



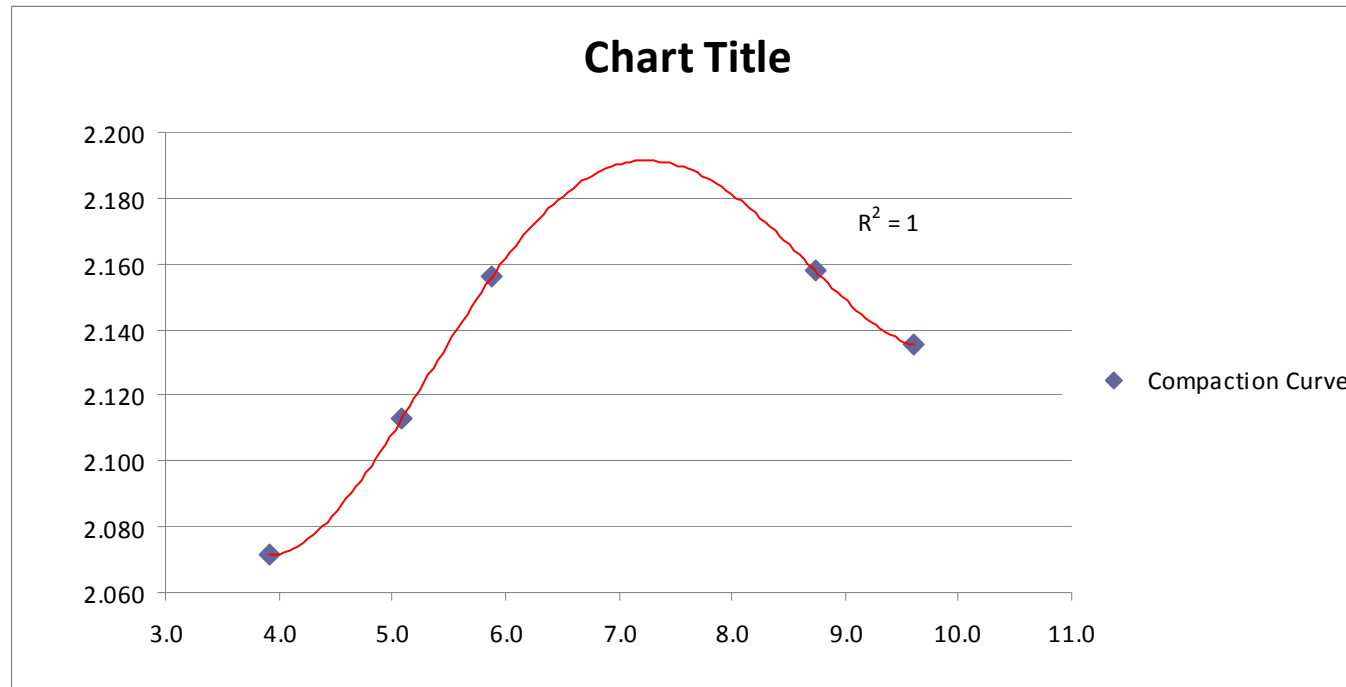
Appendix A: Non-Mechanical Characterisation

SOIL MECHANIC LABORATORY CURTIN UNIVERSITY OF TECHNOLOGY									
Project:	15days Hydration of HCTCRB			Source of Soil:		Gosnell Quarry			
Location:	Curtin Soil Mechanic Lab			tested Date:		5/2/2009			
Soil Description:	HCTCRB+2%cement+8%water			Test By:					
Compaction Method:Modified				Mold Dimension:		105.27x115.61mm			
Hammer weight		4.9	Kg	Dropped Height		450	mm		
No. of Layer		5		No. of Blow		25	blows/layer		
COMPACTION			test no.		1	2	3	4	5
Assumed Water Content			%		dry	original	9.37	11.37	11.37
Weight of Air Dry Soil Use			g		2500	2500	2500	2500	2500
Water Content of Air Dry Soil			%		0	0	0	0	0
Amount of Water Added			cm ³		0	0	30	86.7	86.7
Weight of Wet Soil + Mould			g		6770	6833	6897	6891	6702
Weight of Mould			g		4536	4536	4536	4536	4536
Weight of Wet Soil,W			g		2234	2297	2361	2355	2166
Wet Density,	$r_{(total)}=$	W/V	g/cm ³		2.22	2.28	2.35	2.34	2.15
Dry Soil Density	$r_{(dry)}=$	100r _(total)	g/cm ³		2.113	2.156	2.158	2.135	2.071

Appendix A: Non-Mechanical Characterisation

			(100+w)						
WATER CONTENT			container number						
Weight of Wet Soil + Container				g	198.8	198.21	217.3	256	269.4
Weight of Dry Soil + Container				g	193.06	191.65	206.28	240.58	262.3
Weight of Water				g	5.74	6.56	11.02	15.42	7.1
Weight of Container				g	80.11	80.11	80.11	80.11	81.11
Weight of Dry Soil				g	112.95	111.54	126.17	160.47	181.19
Water Content,w				%	5.08	5.88	8.73	9.61	3.92
RESULT OF SOIL COMPACTION TEST									
Test Number			1	2	3	4	5		
Dry Density,		r _(dry)	ton/m ³	2.113	2.156	2.158	2.135	2.071	
Water Content,w			%	5.08	5.88	8.73	9.61	3.92	

Appendix A: Non-Mechanical Characterisation



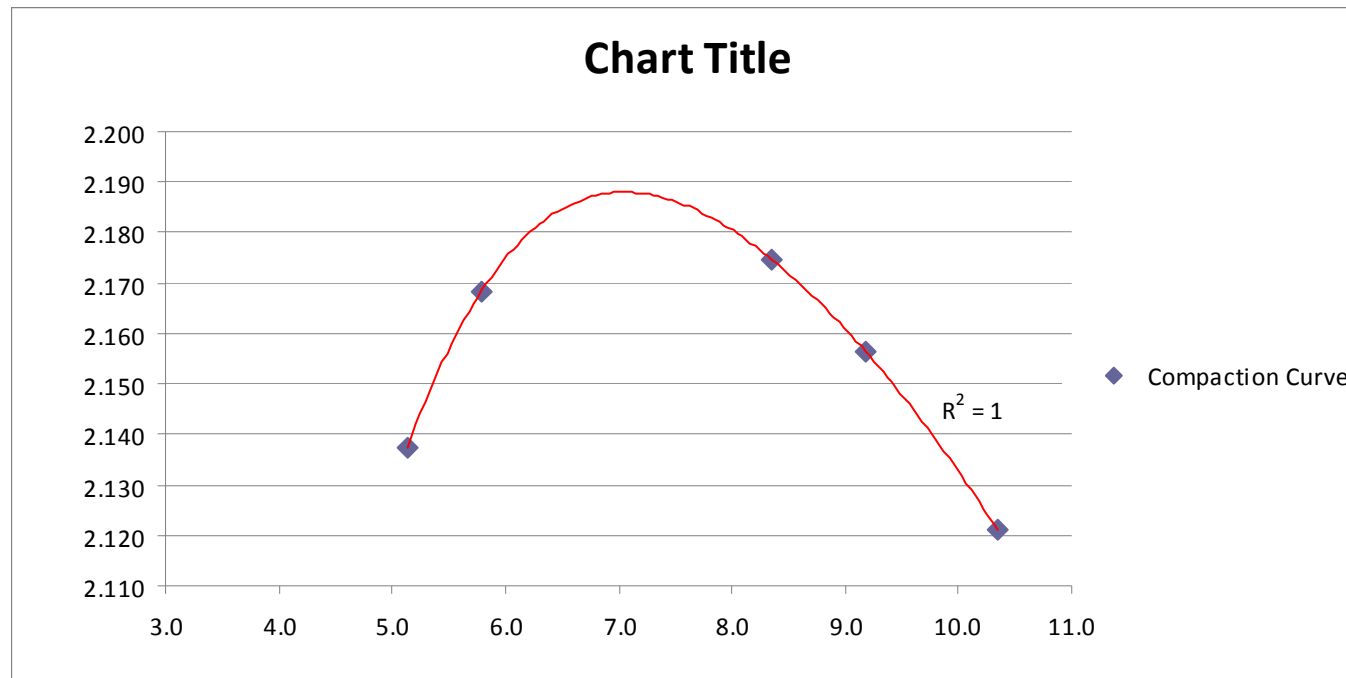
Appendix A: Non-Mechanical Characterisation

SOIL MECHANIC LABORATORY CURTIN UNIVERSITY OF TECHNOLOGY									
Project:	30days Hydration of HCTCRB			Source of Soil:		Gosnell Quarry			
Location:	Curtin Soil Mechanic Lab			tested Date:		19/05/2009			
Soil Description:	HCTCRB+2%cement+8%water			Test By:					
Compaction Method:Modified				Mold Dimension:		105.27x115.61mm			
Hammer weight		4.9	Kg	Dropped Height		450		mm	
No. of Layer		5		No. of Blow		25		blows/layer	
COMPACTION			test no.		1	2	3	4	5
Assumed Water Content			%	original	8		9.37	11.37	
Weight of Air Dry Soil Use			g	2500	2500		2500	2500	
Water Content of Air Dry Soil			%	0	0		0	0	
Amount of Water Added			cm ³	0	0		30	86.7	
Weight of Wet Soil + Mould			g	6844	6907		6891	6905	6797
Weight of Mould			g	4536	4536		4536	4536	4536
Weight of Wet Soil, W			g	2308	2371		2355	2369	2261
Wet Density,	$r_{(total)} =$	W/V	g/cm ³	2.29	2.36		2.34	2.35	2.25

Appendix A: Non-Mechanical Characterisation

Dry Soil Density		$r_{(dry)} =$	$100r_{(total)}$	g/cm^3	2.168	2.175	2.121	2.156	2.137
			(100+w)						
WATER CONTENT			container number						
Weight of Wet Soil + Container				g	254.88	265.5	417.35	342.38	295.76
Weight of Dry Soil + Container				g	247.12	253.75	388.1	323.1	286.46
Weight of Water				g	7.76	11.75	29.25	19.28	9.3
Weight of Container				g	112.98	112.98	105.28	112.98	105.29
Weight of Dry Soil				g	134.14	140.77	282.82	210.12	181.17
Water Content, w				%	5.79	8.35	10.34	9.18	5.13
RESULT OF SOIL COMPACTION TEST									
Test Number			1	2	3	4	5		
Dry Density,		$r_{(dry)}$	ton/m^3	2.168	2.175	2.121	2.156	2.137	
Water Content, w		%	5.79	8.35	10.34	9.18	5.13		

Appendix A: Non-Mechanical Characterisation



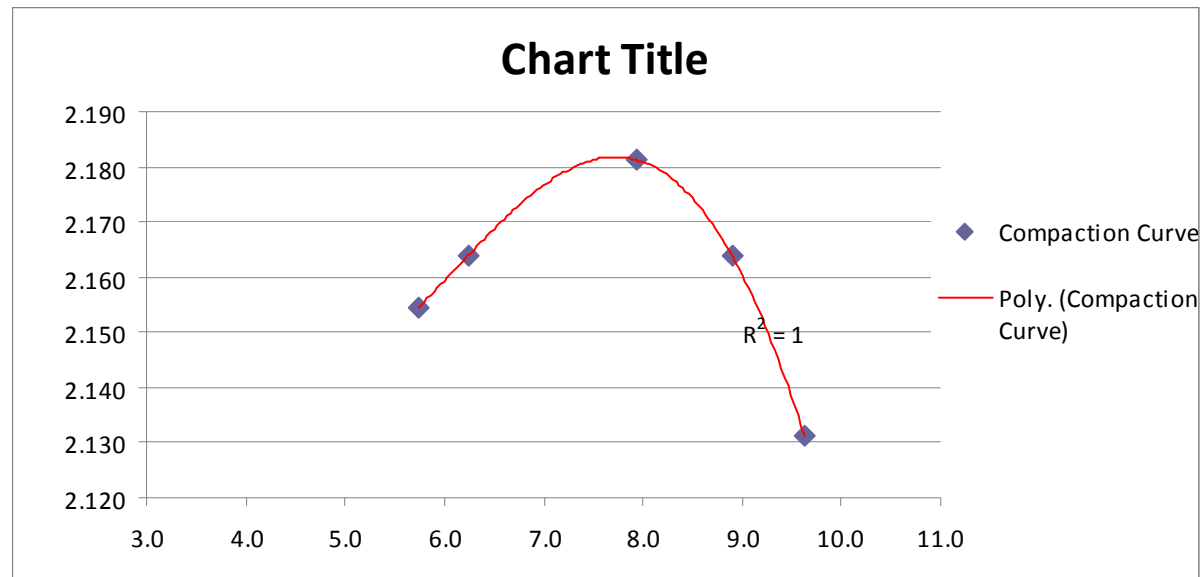
Appendix A: Non-Mechanical Characterisation

SOIL MECHANIC LABORATORY CURTIN UNIVERSITY OF TECHNOLOGY									
Project:		45days Hydration of HCTCRB			Source of Soil:		Gosnell Quarry		
Location:		Curtin Soil Mechanic Lab			tested Date:		24/06/09		
Soil Description:		HCTCRB+2%cement+8%water			Test By:		Chanh Do		
Compaction Method:Modified				Mold Dimension:		105.27x115.61mm			
Hammer weight			4.9	Kg	Dropped Height	450	mm		
No. of Layer			5		No. of Blow	25	blows/layer		
COMPACTION				test no.	1	2	3	4	5
Assumed Water Content				%	original	8	9.37	11.37	
Weight of Air Dry Soil Use				g	2500	2500	2500	2500	
Water Content of Air Dry Soil				%	0	0	0	0	
Amount of Water Added				cm ³	0	0	30	86.7	
Weight of Wet Soil + Mould				g	6828	6905	6907	6887	6849
Weight of Mould				g	4536	4536	4536	4536	4536
Weight of Wet Soil,W				g	2292	2369	2371	2351	2313

Appendix A: Non-Mechanical Characterisation

Wet Density,		$r_{(total)}=$	W/V	g/cm^3	2.28	2.35	2.36	2.34	2.30
Dry Soil Density		$r_{(dry)}=$	$100r_{(total)}$	g/cm^3	2.154	2.181	2.164	2.131	2.164
			(100+w)						
WATER CONTENT			container number						
Weight of Wet Soil + Container				g	224.15	234.56	247.97	308.12	352.63
Weight of Dry Soil + Container				g	216.65	223.62	234.72	288.59	336.97
Weight of Water				g	7.5	10.94	13.25	19.53	15.66
Weight of Container				g	85.78	85.78	85.78	85.78	85.78
Weight of Dry Soil				g	130.87	137.84	148.94	202.81	251.19
Water Content,w				%	5.73	7.94	8.90	9.63	6.23
RESULT OF SOIL COMPACTION TEST									
Test Number			1	2	3	4	5		
Dry Density,	$r_{(dry)}$	ton/m^3	2.154	2.181	2.164	2.131	2.164		
Water Content,w		%	5.73	7.94	8.90	9.63	6.23		

Appendix A: Non-Mechanical Characterisation

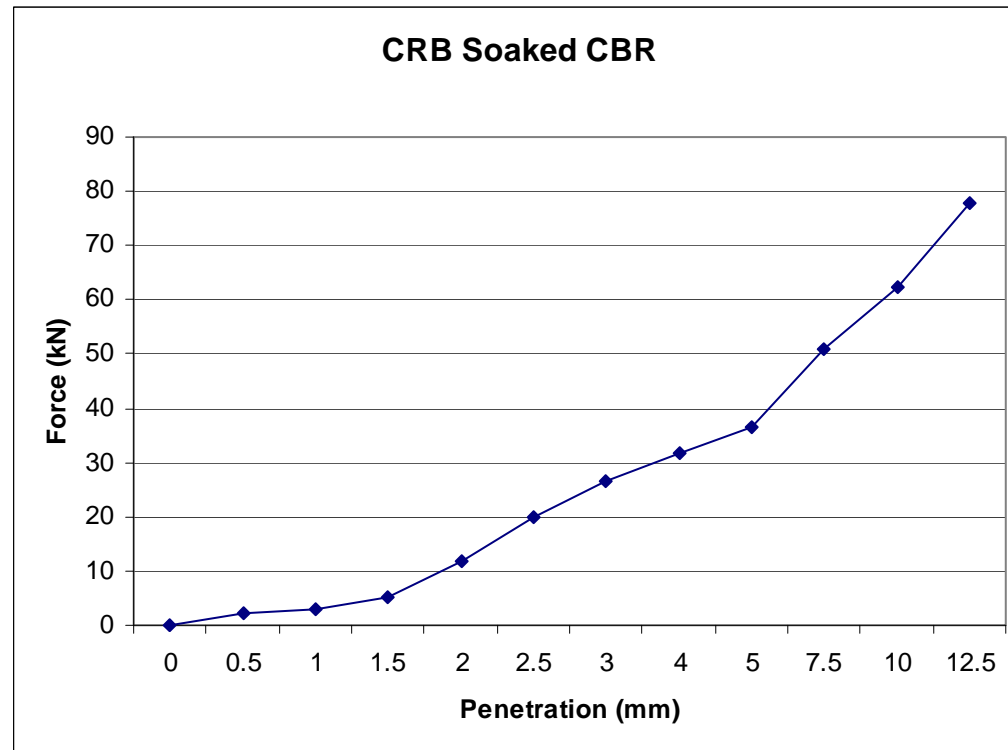


APPENDIX B: MECHANICAL CHARACTERISATIONS

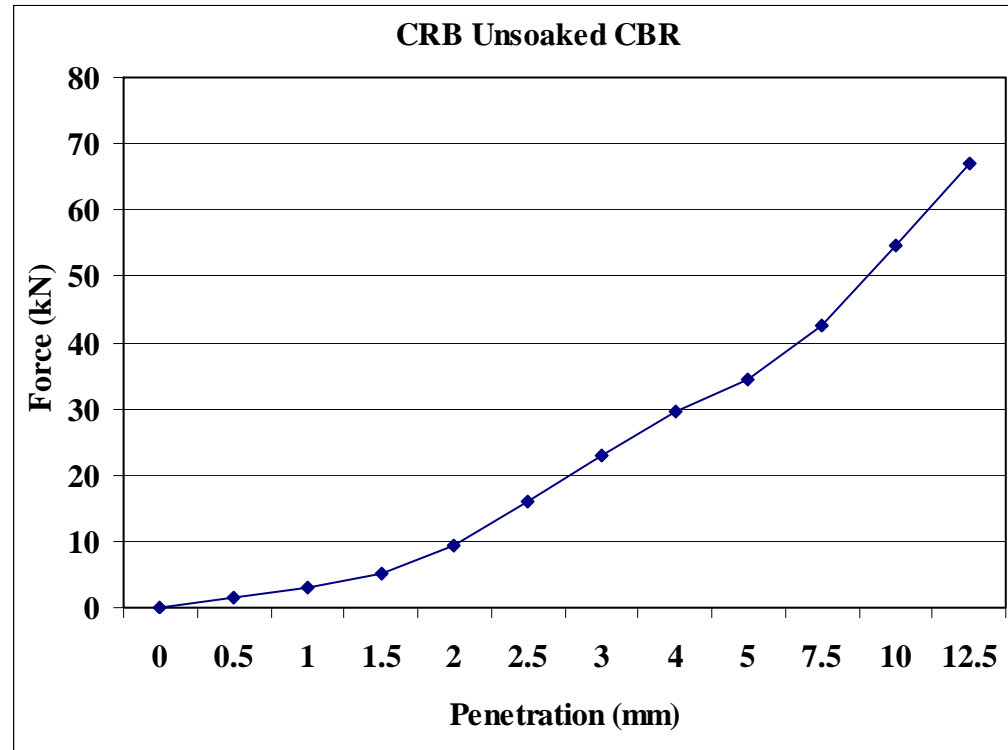
APPENDIX B
(Mechanical Characterisations)
CBR Test

Crushed Rock Soaked CBR		Crushed Rock Unsoaked CBR		HCTCRB Soaked CBR		Crushed Rock Unsoaked CBR	
Penetration (mm)	Force (kN)	Penetration (mm)	Force (kN)	Penetration (mm)	Force (kN)	Penetration (mm)	Force (kN)
0	0.09	0	0.03	0	0	0	0
0.5	2.08	0.5	1.56	0.5	4.68	0.5	1.56
1	3.12	1	3.12	1	9.88	1	3.12
1.5	5.2	1.5	5.2	1.5	15.6	1.5	5.2
2	11.96	2	9.36	2	20.8	2	9.36
2.5	19.76	2.5	16.12	2.5	24.96	2.5	15.08
3	26.52	3	22.88	3	33.8	3	23.4
4	31.72	4	29.64	4	39	4	34.84
5	36.4	5	34.32	5	50.96	5	44.2
7.5	50.96	7.5	42.64	7.5	75.4	7.5	65
10	62.4	10	54.6	10		10	
12.5	78	12.5	67.08	12.5		12.5	

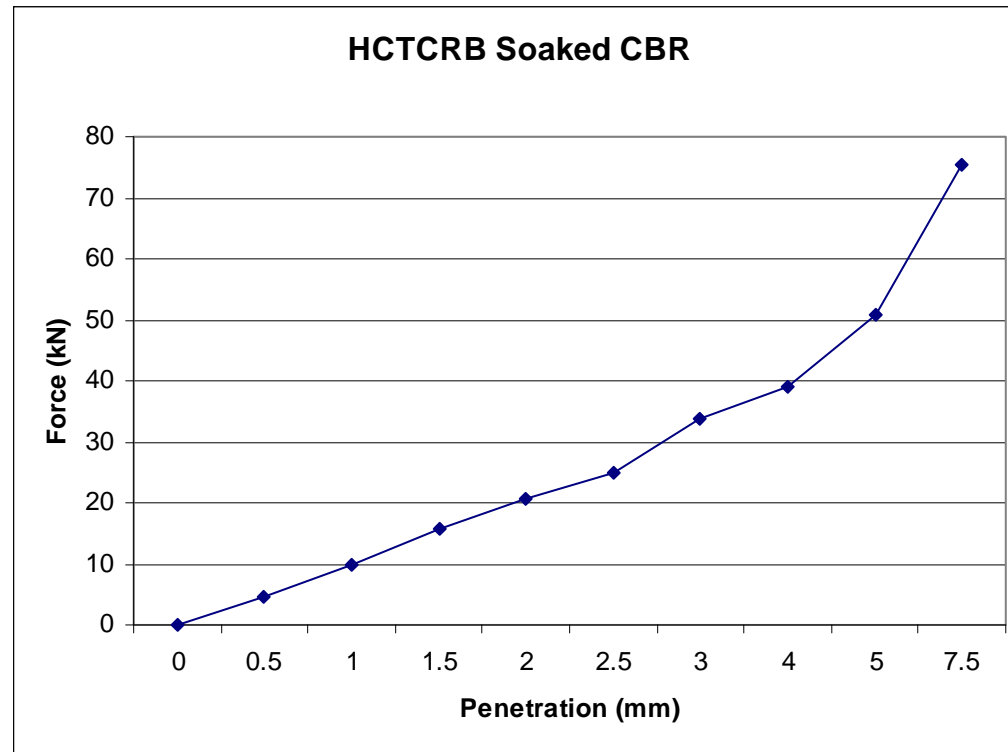
Appendix B: Mechanical Characteristics



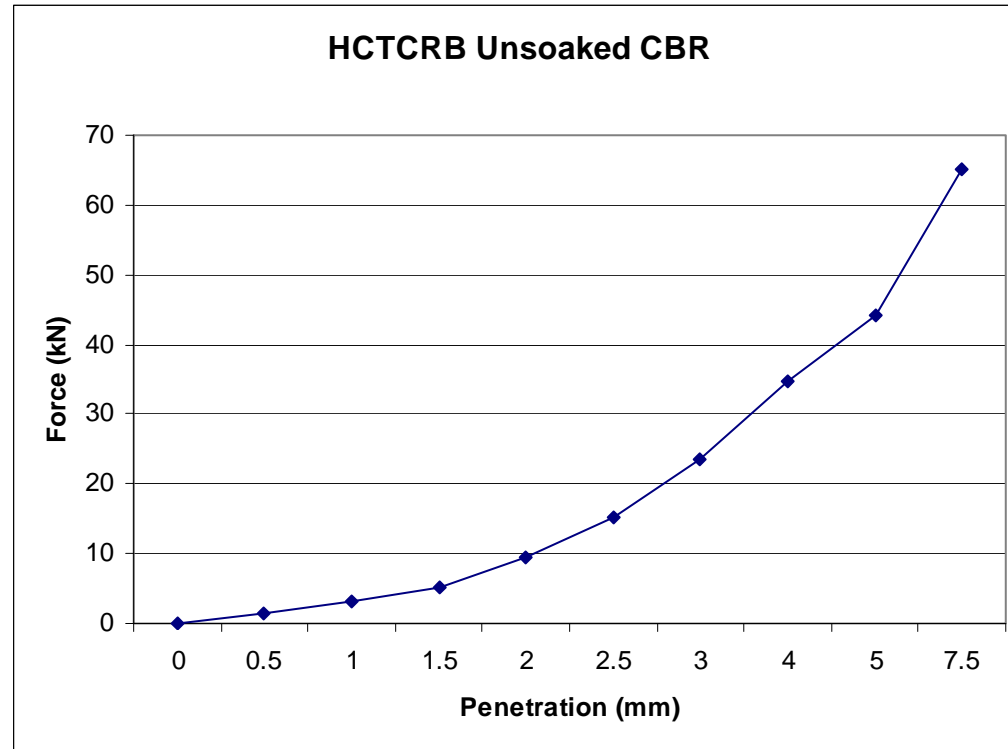
Appendix B: Mechanical Characteristics



Appendix B: Mechanical Characteristics



Appendix B: Mechanical Characteristics



Appendix B: Mechanical Characteristics

APPENDIX B (Mechanical Characterisations) Static Triaxial Test

UTS009 1.21 Unbound Material Resilient Modulus and Shear Test					
Date	10/06/2008 12:44:24 PM				
Archive File	C:\IPCglobal UTS\009 Resilient Modulus Test\Data\CRB_Tri_40kPa_Daniel_1.D009				
Template File	C:\IPCglobal UTS\009 Resilient Modulus Test\Templates\CRB Triaxial.P009				
Project	Final year and PhD projects				
Operator	Kom&Daniel				
Comments	compacted CRB at 100%OMC and MDD				
Specimen Information:					
Identification	CRB				
Dimensions	Point 1	Point 2	Point 3	Point 4	Point 5
Length (mm)	200				
Diameter (mm)	100				
X-Section area	7854				
Remarks	10062008				
Loading program	User defined stress program				
Load duration (ms)	100				
Cycle duration (ms)	1000				
Conditioning cycle count	20				

Appendix B: Mechanical Characteristics

Cycles per sequence	20				
Loading rod diameter (mm)	25				
Seating stress correction	No				
Axial Lvdt gauge length (mm)	200				
Shear stage confining stress (kPa)	40				
Shear loading rate (% strain/min)	0.125				
Shear stage termination strain (%)	15				
Modulus test Mean and Std. Deviation data:					
Sequence	Deviator stress (kPa)			Deviator force (kN)	
0	0.063	0.001		0.001	0
1	0.056	0		0.001	0

CRB 40 kPa		60 kPa		80 kPa	
Strain (%)	Stress(kPa)	Strain,%	stress,kPa	strain,%	stress,kPa
0.000	0	0.000	0.00	0.000	0.93
0.010	5.69	0.009	13.89	0.001	0.96
0.022	11.04	0.022	20.56	0.002	5.02
0.036	20.44	0.029	24.35	0.004	9.99
0.047	24.17	0.045	37.15	0.004	3.58
0.058	30.85	0.056	43.56	0.006	10.20
0.064	29.12	0.067	50.38	0.006	4.83
0.074	31.40	0.079	58.41	0.008	13.39
0.087	37.00	0.086	61.62	0.008	2.29
0.101	47.34	0.093	58.43	0.010	15.95
0.109	49.06	0.104	64.46	0.011	6.92
0.117	47.31	0.121	80.94	0.012	11.98

Appendix B: Mechanical Characteristics

0.130	58.39	0.126	79.21	0.013	19.69
0.144	65.78	0.137	84.12	0.013	8.46
0.151	61.47	0.155	104.11	0.015	23.78
0.160	65.75	0.157	95.04	0.016	25.15
0.174	78.53	0.172	110.16	0.017	23.07
0.186	85.37	0.181	115.23	0.019	41.58
0.197	90.29	0.190	114.59	0.020	37.53
0.208	95.36	0.206	133.89	0.020	33.97
0.218	98.69	0.211	126.18	0.022	54.01
0.226	99.34	0.228	145.55	0.023	51.84
0.235	98.46	0.232	140.85	0.023	46.03
0.247	102.78	0.248	156.87	0.024	53.17
0.261	119.92	0.254	153.63	0.026	66.86
0.268	117.48	0.269	170.33	0.027	69.76
0.281	122.86	0.276	167.05	0.028	62.64
0.291	131.98	0.287	176.92	0.029	67.48
0.299	127.02	0.300	187.94	0.030	80.09
0.314	145.83	0.307	182.49	0.032	93.94
0.319	134.23	0.321	200.79	0.032	92.11
0.336	158.19	0.333	207.27	0.033	88.57
0.342	148.61	0.341	202.71	0.034	102.78
0.357	169.47	0.349	203.29	0.036	114.73
0.367	168.90	0.360	212.49	0.037	115.42
0.374	166.46	0.371	215.86	0.037	110.20
0.387	182.47	0.382	233.11	0.038	116.63
0.399	190.28	0.393	241.59	0.039	127.70
0.408	190.33	0.409	257.67	0.041	144.67
0.417	190.38	0.420	262.38	0.042	150.99
0.430	209.06	0.428	261.47	0.043	155.01
0.442	213.55	0.436	257.42	0.044	157.98

Appendix B: Mechanical Characteristics

0.450	212.47	0.447	266.24	0.045	164.36
0.461	224.89	0.458	282.46	0.046	168.85
0.473	231.45	0.473	298.36	0.047	176.01
0.481	230.85	0.481	296.17	0.048	180.92
0.495	247.44	0.489	295.50	0.050	189.20
0.502	245.53	0.502	315.12	0.051	196.92
0.516	260.50	0.514	321.42	0.052	198.55
0.523	257.21	0.522	313.22	0.052	203.82
0.537	273.76	0.531	319.94	0.053	206.29
0.545	267.47	0.542	331.42	0.054	200.43
0.558	284.84	0.558	353.67	0.056	214.32
0.566	278.91	0.565	345.96	0.057	232.64
0.579	295.21	0.574	350.86	0.058	241.20
0.590	304.28	0.590	377.27	0.059	248.71
0.599	304.35	0.600	379.01	0.060	254.36
0.611	311.26	0.607	369.11	0.061	256.11
0.623	323.49	0.617	372.70	0.062	256.74
0.631	322.80	0.627	384.61	0.063	274.95
0.641	325.61	0.644	417.90	0.065	286.12
0.654	335.55	0.654	414.17	0.065	261.96
0.665	344.45	0.671	436.16	0.066	278.67
0.675	345.37	0.677	437.20	0.067	285.10
0.686	353.65	0.688	443.19	0.069	294.12
0.696	359.80	0.699	450.35	0.069	307.56
0.706	363.65	0.705	442.45	0.071	329.53
0.716	366.78	0.713	439.98	0.072	336.02
0.727	373.96	0.725	460.31	0.073	336.42
0.738	379.91	0.739	479.15	0.074	332.92
0.748	386.59	0.748	473.21	0.075	337.64
0.762	402.28	0.763	482.74	0.076	342.23

Appendix B: Mechanical Characteristics

0.772	406.61	0.776	509.49	0.077	352.03
0.783	414.49	0.786	518.57	0.078	369.10
0.794	419.87	0.798	530.29	0.080	392.61
0.804	423.82	0.806	532.42	0.081	397.68
0.814	426.02	0.817	541.40	0.081	397.00
0.823	427.80	0.828	546.70	0.082	397.32
0.834	432.02	0.835	544.40	0.083	406.59
0.847	447.60	0.844	540.45	0.085	431.72
0.858	453.67	0.852	541.95	0.086	427.99
0.868	454.91	0.862	552.61	0.086	429.43
0.878	457.79	0.881	587.91	0.087	415.41
0.887	456.44	0.888	581.52	0.089	451.88
0.898	464.09	0.896	573.21	0.090	460.30
0.909	472.20	0.905	579.62	0.091	462.35
0.921	480.74	0.919	601.68	0.092	475.42
0.932	485.44	0.934	625.08	0.093	489.36
0.942	485.16	0.943	623.63	0.094	505.99
0.952	487.76	0.949	609.80	0.095	496.99
0.962	488.70	0.959	616.74	0.096	501.22
0.975	503.95	0.975	648.22	0.097	510.51
0.985	506.06	0.984	643.49	0.099	538.24
0.995	507.94	0.991	641.41	0.099	530.11
1.004	503.81	1.007	674.11	0.100	538.83
1.015	510.72	1.019	677.53	0.102	563.35
1.027	521.58	1.024	667.43	0.103	556.97
1.038	528.89	1.035	680.65	0.104	569.85
1.049	533.26	1.049	698.06	0.105	590.18
1.061	536.72	1.056	688.69	0.106	582.51
1.070	539.00	1.070	709.22	0.107	601.80
1.082	549.27	1.079	707.32	0.108	602.24

Appendix B: Mechanical Characteristics

1.092	552.75	1.087	706.64	0.109	611.71
1.102	555.01	1.102	728.24	0.110	623.44
1.112	559.77	1.109	720.98	0.111	632.58
1.123	563.57	1.125	746.75	0.112	639.29
1.132	559.17	1.133	740.98	0.113	651.45
1.144	569.35	1.142	745.99	0.114	656.44
1.155	573.13	1.155	758.24	0.115	658.75
1.166	576.15	1.163	754.88	0.117	679.25
1.176	578.16	1.177	774.10	0.118	678.43
1.187	582.79	1.185	767.93	0.119	689.79
1.197	581.43	1.197	784.43	0.120	699.20
1.210	588.39	1.207	788.15	0.121	707.07
1.219	595.92	1.218	790.53	0.122	714.82
1.230	598.81	1.229	794.82	0.123	723.33
1.240	599.80	1.239	798.74	0.124	730.10
1.251	604.64	1.250	805.45	0.125	736.16
1.261	605.35	1.262	813.14	0.126	745.72
1.271	606.77	1.268	797.43	0.127	754.44
1.282	609.60	1.284	828.98	0.128	752.55
1.292	610.69	1.292	822.88	0.129	766.67
1.304	617.38	1.303	828.95	0.130	775.79
1.313	615.50	1.314	833.31	0.132	781.99
1.325	623.13	1.324	836.60	0.133	788.01
1.336	621.11	1.337	842.85	0.134	797.87
1.348	630.03	1.348	848.20	0.135	803.71
1.359	634.11	1.358	852.71	0.136	811.48
1.370	637.39	1.369	857.41	0.137	818.40
1.381	637.54	1.380	863.67	0.138	822.15
1.391	640.23	1.390	867.18	0.139	829.95
1.402	643.45	1.401	868.80	0.140	836.90

Appendix B: Mechanical Characteristics

1.411	642.32	1.412	876.07	0.141	843.67
1.423	648.43	1.422	879.68	0.142	851.16
1.432	641.16	1.433	882.48	0.143	858.23
1.442	645.71	1.443	885.36	0.144	863.00
1.455	654.91	1.454	889.24	0.146	871.60
1.466	658.75	1.465	894.69	0.147	876.03
1.477	661.42	1.476	901.21	0.148	881.52
1.487	664.98	1.486	904.56	0.149	889.28
1.497	663.78	1.497	906.91	0.150	895.55
1.507	663.90	1.507	911.58	0.151	903.81
1.517	663.67	1.518	914.26	0.152	909.81
1.529	673.18	1.529	918.57	0.153	914.65
1.542	686.30	1.540	921.92	0.154	922.25
1.552	684.45	1.551	923.90	0.155	926.83
1.562	684.96	1.561	924.02	0.156	934.47
1.571	682.32	1.572	926.85	0.157	938.01
1.583	685.20	1.582	931.65	0.158	943.71
1.592	680.18	1.593	932.11	0.159	948.47
1.602	680.69	1.604	935.62	0.160	953.99
1.613	684.41	1.614	938.39	0.162	958.25
1.626	696.45	1.625	935.37	0.163	964.45
1.637	696.34	1.636	939.26	0.164	969.08
1.647	697.19	1.646	942.81	0.165	974.10
1.658	697.13	1.657	944.87	0.166	981.29
1.668	697.84	1.668	948.41	0.167	986.16
1.678	697.73	1.679	950.86	0.168	992.10
1.687	690.44	1.690	954.25	0.169	996.70
1.699	695.26	1.698	958.72	0.170	1001.27
1.709	696.42	1.709	958.69	0.171	1006.88
1.720	699.61	1.722	964.49	0.172	1012.12

Appendix B: Mechanical Characteristics

1.732	707.93	1.732	969.75	0.173	1015.27
1.741	703.34	1.743	972.77	0.174	1019.44
1.752	704.99	1.753	975.73	0.175	1022.95
1.763	706.63	1.764	977.84	0.176	1027.09
1.773	705.05	1.774	979.56	0.177	1031.14
1.784	709.59	1.785	982.87	0.179	1035.64
1.793	705.18	1.796	987.31	0.180	1039.66
1.805	709.00	1.807	990.62	0.181	1042.38
1.816	710.69	1.817	994.51	0.182	1047.66
1.827	709.13	1.828	997.24	0.183	1051.80
1.837	704.61	1.839	999.79	0.184	1055.89
1.848	705.15	1.849	1001.54	0.185	1058.34
1.860	710.87	1.860	998.80	0.186	1061.72
1.869	701.54	1.871	999.59	0.187	1064.67
1.882	717.39	1.881	1000.69	0.188	1066.31
1.893	720.73	1.892	1000.92	0.189	1065.38
1.902	715.06	1.902	1000.49	0.190	1065.44
1.911	710.53	1.913	1000.62	0.190	1063.74
1.923	713.76	1.924	1002.89	0.191	1063.39
1.934	719.22	1.934	1004.95	0.191	1060.77
1.944	720.01	1.945	1006.39	0.191	1059.28
1.955	722.67	1.956	1002.97	0.192	1066.68
1.968	729.90	1.967	1007.09	0.193	1074.13
1.975	718.38	1.978	1009.36	0.193	1074.27
1.987	721.70	1.988	1010.88	0.194	1071.29
1.998	722.68	1.999	1009.84	0.194	1067.77
2.009	724.34	2.009	1012.38	0.194	1065.16
2.019	726.04	2.020	1009.19	0.194	1062.85
2.031	729.88	2.031	1013.63	0.194	1061.97
2.042	732.93	2.042	1015.76	0.195	1067.10

Appendix B: Mechanical Characteristics

2.052	733.80	2.052	1017.73	0.195	1068.43
2.061	727.07	2.063	1019.17	0.195	1069.14
2.071	723.56	2.074	1019.77	0.196	1069.55
2.082	725.65	2.084	1021.20	0.196	1068.10
2.094	731.88	2.095	1022.99	0.196	1066.42
2.105	734.35	2.106	1027.49	0.197	1073.38
2.115	733.00	2.116	1024.51	0.197	1081.96
2.125	726.38	2.127	1027.21	0.198	1092.10
2.136	726.11	2.138	1027.95	0.199	1101.90
2.148	732.73	2.148	1029.59	0.200	1111.06
2.158	733.08	2.159	1025.53	0.202	1119.47
2.170	734.79	2.170	1027.79	0.203	1127.48
2.180	737.06	2.180	1030.23	0.206	1135.04
2.191	737.89	2.191	1030.01	0.208	1142.39
2.200	733.77	2.202	1029.11	0.210	1149.36
2.209	727.43	2.212	1029.13	0.213	1155.27
2.221	730.57	2.223	1029.11	0.216	1160.75
2.233	733.66	2.234	1029.28	0.219	1165.40
2.244	735.19	2.244	1027.79	0.221	1169.14
2.255	737.84	2.255	1023.99	0.224	1172.19
2.263	729.88	2.266	1022.88	0.226	1174.32
2.274	728.77	2.276	1022.86	0.228	1159.34
2.287	735.49	2.287	1024.46	0.229	1159.39
2.298	739.67	2.298	1026.49	0.230	1165.54
2.306	729.87	2.308	1028.63	0.231	1167.55
2.317	726.64	2.319	1029.58	0.232	1168.90
2.329	733.66	2.330	1029.95	0.233	1172.05
2.340	737.52	2.340	1029.08	0.234	1174.75
2.351	735.65	2.351	1027.71	0.235	1177.01
2.359	724.84	2.362	1028.15	0.236	1178.97

Appendix B: Mechanical Characteristics

2.370	728.14	2.372	1028.08	0.237	1177.83
2.383	735.12	2.383	1028.78	0.238	1177.84
2.393	734.68	2.394	1028.58	0.239	1178.56
2.402	724.40	2.404	1028.66	0.240	1175.06
2.414	728.16	2.415	1027.17	0.241	1178.97
2.426	732.80	2.426	1028.67	0.243	1186.84
2.434	724.76	2.436	1023.58	0.244	1184.68
2.445	724.01	2.447	1021.15	0.245	1186.08
2.457	732.96	2.458	1019.58	0.246	1186.93
2.469	737.71	2.468	1019.59	0.247	1187.93
2.476	724.72	2.479	1018.66	0.248	1189.79
2.487	726.62	2.490	1015.13	0.249	1189.17
2.500	734.14	2.500	1014.43	0.250	1186.52
2.511	734.81	2.511	1013.00	0.250	1183.92
2.520	728.30	2.522	1013.19	0.251	1183.59
2.532	734.82	2.533	1012.52	0.252	1184.59
2.540	724.89	2.543	1011.70	0.253	1184.92
2.552	726.33	2.554	1010.69	0.254	1192.24
2.564	734.14	2.564	1011.21	0.255	1200.00
2.572	725.20	2.575	1008.96	0.257	1207.60
2.584	727.77	2.587	1008.87	0.258	1206.72
2.596	731.65	2.596	1003.95	0.260	1200.18
2.604	722.85	2.607	1003.14	0.261	1196.81
2.617	728.78	2.618	1002.64	0.261	1192.67
2.627	729.40	2.628	1003.29	0.262	1191.99
2.637	719.29	2.639	1002.06	0.263	1190.10
2.649	728.29	2.650	1002.74	0.263	1188.45
2.658	721.51	2.661	1002.22	0.264	1188.47
2.671	719.71	2.674	1000.80	0.264	1184.78
2.684	726.85	2.685	999.96	0.265	1183.25

Appendix B: Mechanical Characteristics

2.693	723.42	2.696	999.60	0.265	1186.75
2.703	717.32	2.706	997.45	0.266	1184.84
2.716	725.51	2.717	996.11	0.266	1183.79
2.725	716.66	2.727	995.47	0.267	1184.46
2.738	723.39	2.738	994.46	0.267	1184.33
2.746	712.09	2.749	994.03	0.268	1185.11
2.758	720.83	2.759	992.18	0.268	1183.64
2.767	711.30	2.770	991.49	0.269	1181.42
2.779	717.58	2.781	991.32	0.269	1180.98
2.788	712.74	2.791	990.86	0.270	1188.90
2.801	717.97	2.802	991.02	0.270	1198.89
2.810	707.86	2.813	991.63	0.272	1208.54
2.822	718.17	2.823	992.51	0.273	1217.21
2.831	712.56	2.834	992.89	0.275	1224.26
2.843	716.40	2.845	992.90	0.278	1230.57
2.853	717.14	2.855	993.41	0.281	1234.77
2.864	716.63	2.866	991.11	0.285	1234.56
2.875	714.76	2.877	988.31	0.288	1207.49
2.886	715.71	2.887	986.03	0.289	1195.68
2.896	711.83	2.899	988.90	0.290	1189.69
2.905	709.26	2.909	986.11	0.291	1195.46
2.919	717.63	2.919	986.72	0.292	1194.40
2.929	716.64	2.930	985.37	0.293	1195.86
2.939	715.05	2.941	982.75	0.294	1203.00
2.950	715.79	2.951	981.55	0.295	1197.07
2.960	715.36	2.963	982.16	0.296	1196.21
2.971	712.29	2.973	979.77	0.297	1193.89
2.981	712.41	2.984	979.82	0.298	1192.97
2.992	711.29	2.994	977.93	0.300	1194.57
3.003	712.19	3.005	977.17	0.301	1194.12

Appendix B: Mechanical Characteristics

3.014	705.27	3.016	975.97	0.302	1194.25
3.023	703.61	3.026	973.80	0.303	1193.15
3.032	706.33	3.037	973.71	0.304	1193.10
3.045	708.78	3.048	972.40	0.305	1193.16
3.055	706.13	3.058	970.45	0.306	1191.32
3.066	706.66	3.069	967.84	0.307	1190.86
3.077	707.03	3.080	968.37	0.308	1191.08
3.088	706.66	3.090	966.56	0.309	1191.77
3.097	702.61	3.101	963.69	0.310	1193.57
3.109	706.46	3.112	964.82	0.311	1191.06
3.120	706.24	3.122	963.61	0.312	1191.86
3.130	704.95	3.133	963.69	0.313	1191.29
3.141	704.51	3.144	960.24	0.314	1191.77
3.152	703.31	3.155	958.16	0.316	1189.68
3.162	702.72	3.165	956.08	0.317	1188.74
3.173	703.03	3.176	954.14	0.318	1187.49
3.184	701.40	3.187	955.07	0.319	1187.60
3.195	701.83	3.197	951.90	0.320	1188.89
3.206	701.00	3.208	945.95	0.321	1189.24
3.215	690.66	3.219	946.48	0.322	1187.53
3.227	698.14	3.229	945.99	0.323	1183.95
3.238	696.75	3.240	944.95	0.324	1183.50
3.246	683.95	3.250	945.15	0.325	1184.09
3.260	697.09	3.260	931.80	0.326	1183.57
3.269	690.10	3.272	937.51	0.327	1183.08
3.278	685.39	3.283	940.30	0.328	1182.35
3.292	695.01	3.293	938.38	0.329	1181.14
3.300	685.88	3.304	938.77	0.330	1178.60
3.310	681.42	3.315	937.24	0.332	1177.52
3.324	694.70	3.325	935.44	0.333	1172.53

Appendix B: Mechanical Characteristics

3.333	691.83	3.336	937.03	0.334	1167.36
3.342	683.24	3.347	935.97	0.335	1169.08
3.354	691.43	3.357	934.57	0.336	1169.45
3.366	694.69	3.368	932.63	0.337	1166.62
3.374	684.47	3.379	931.66	0.338	1168.14
3.385	686.72	3.389	927.00	0.339	1168.29
3.399	697.92	3.400	927.94	0.340	1166.90
3.408	692.32	3.411	928.60	0.341	1166.95
3.417	681.68	3.421	926.69	0.342	1168.97
3.427	680.97	3.432	924.84	0.343	1167.03
3.440	690.94	3.443	925.16	0.344	1166.75
3.452	693.79	3.454	925.22	0.345	1164.25
3.462	692.11	3.464	922.64	0.346	1163.58
3.471	681.61	3.475	920.77	0.348	1163.19
3.481	678.23	3.485	919.16	0.349	1161.45
3.491	677.76	3.496	917.12	0.350	1161.98
3.505	688.86	3.507	915.25	0.351	1161.20
3.515	684.97	3.517	916.02	0.352	1161.97
3.524	676.94	3.528	914.67	0.353	1157.22
3.534	677.09	3.539	914.62	0.354	1156.00
3.546	680.50	3.550	914.16	0.355	1154.51
3.558	684.81	3.560	907.12	0.356	1152.04
3.568	680.00	3.570	901.74	0.357	1150.99
3.577	670.15	3.581	901.12	0.358	1153.41
3.587	668.61	3.592	905.69	0.359	1150.89
3.600	677.42	3.603	905.70	0.360	1150.19
3.612	681.88	3.613	897.56	0.362	1153.28
3.622	674.97	3.624	897.32	0.362	1136.87
3.632	675.21	3.635	898.45	0.364	1158.01
3.642	667.83	3.646	900.43	0.365	1146.09

Appendix B: Mechanical Characteristics

3.652	665.32	3.656	897.86	0.366	1146.91
3.662	664.92	3.667	895.35	0.367	1150.08
3.672	662.27	3.677	894.09	0.368	1137.23
3.684	669.91	3.688	893.53	0.369	1151.89
3.697	675.44	3.699	896.60	0.370	1135.77
3.708	674.98	3.710	896.40	0.371	1151.69
3.719	672.54	3.721	895.59	0.372	1134.92
3.728	666.23	3.731	898.62	0.373	1144.56
3.737	656.90	3.741	890.47	0.374	1142.26
3.746	654.77	3.752	888.15	0.375	1130.37
3.758	658.85	3.764	889.35	0.377	1141.60
3.772	674.07	3.774	885.04	0.377	1124.78
3.783	671.25	3.784	886.63	0.379	1142.35
3.793	665.89	3.795	882.02	0.380	1128.07
3.804	668.13	3.805	881.00	0.380	1122.42
3.815	666.06	3.818	883.28	0.382	1133.89
3.826	665.87	3.827	881.01	0.383	1114.99
3.836	665.91	3.836	875.30	0.384	1130.67
3.847	665.14	3.848	876.70	0.385	1118.16
3.857	658.72	3.856	845.15	0.386	1119.01
3.865	648.60	3.867	855.35	0.387	1122.90
3.875	642.08	3.879	870.55	0.388	1105.08
3.885	638.41	3.893	878.35	0.390	1120.45
3.896	643.81	3.903	872.22	0.390	1106.50
3.908	647.39	3.913	866.30	0.391	1118.27
3.919	649.49	3.922	856.95	0.392	1115.28
3.933	657.02	3.930	854.50	0.393	1100.15
3.943	657.28	3.941	854.59	0.395	1120.95
3.954	655.21	3.955	865.41	0.395	1100.36
3.965	653.00	3.968	871.83	0.397	1118.96

Appendix B: Mechanical Characteristics

3.975	651.48	3.979	867.68	0.398	1106.51
3.985	645.02	3.989	860.42	0.399	1105.94
3.995	644.83	4.000	857.56	0.400	1103.45
4.003	632.48	4.010	853.64	0.401	1087.83
4.013	626.45	4.019	843.96	0.402	1107.56
4.024	622.85	4.028	832.64	0.403	1089.93
4.034	620.80	4.038	832.09	0.404	1091.12
4.045	623.45	4.048	829.38	0.405	1101.24
4.057	634.94	4.058	828.12	0.406	1079.76
4.068	631.55	4.069	831.82	0.407	1096.75
4.077	622.66	4.084	848.56	0.408	1089.67
4.089	630.78	4.096	853.62	0.409	1077.00
4.103	644.25	4.107	852.72	0.411	1097.09
4.115	647.66	4.118	850.41	0.411	1077.88
4.124	642.67	4.128	848.71	0.413	1095.07
4.135	641.68	4.139	846.31	0.414	1089.59
4.145	636.61	4.148	840.35	0.415	1073.54
4.154	626.51	4.157	829.96	0.416	1094.52
4.164	622.70	4.166	824.09	0.417	1073.76
4.173	616.98	4.177	816.57	0.418	1079.06
4.183	613.11	4.187	815.77	0.419	1084.69
4.194	613.35	4.198	811.99	0.420	1065.46
4.205	616.55	4.208	812.98	0.421	1088.75
4.215	618.11	4.219	820.20	0.422	1077.00
4.229	633.37	4.234	833.50	0.423	1061.22
4.240	631.51	4.243	830.67	0.425	1083.16
4.252	635.98	4.253	823.39	0.425	1065.68
4.262	626.54	4.264	824.40	0.426	1062.98
4.274	630.90	4.277	832.06	0.428	1077.69
4.284	629.13	4.288	835.29	0.428	1057.04

Appendix B: Mechanical Characteristics

4.291	613.85	4.300	838.26	0.430	1065.20
4.302	611.88	4.311	835.98	0.431	1075.23
4.312	608.45	4.321	834.23	0.432	1056.25
4.324	615.43	4.333	829.68	0.433	1059.98
4.335	613.73	4.343	827.28	0.434	1068.29
4.344	606.94	4.353	826.12	0.435	1049.83
4.354	603.68	4.365	827.75	0.436	1065.65
4.366	607.60	4.374	820.00	0.437	1064.73
4.376	603.07	4.385	818.65	0.438	1046.26
4.387	602.40	4.396	820.52	0.439	1052.27
4.397	597.66	4.406	819.25	0.441	1060.45
4.407	593.64	4.418	821.14	0.441	1041.00
4.419	598.35	4.429	819.24	0.443	1062.52
4.432	610.55	4.440	815.57	0.444	1057.31
4.443	611.28	4.450	813.63	0.444	1043.02
4.454	614.98	4.460	811.00	0.446	1063.58
4.463	606.40	4.468	801.81	0.447	1048.87
4.473	602.08	4.475	783.63	0.448	1037.48
4.485	608.05	4.485	777.12	0.449	1059.22
4.498	617.36	4.496	772.24	0.450	1041.67
4.509	618.74	4.506	763.55	0.451	1034.53
4.519	617.68	4.517	768.99	0.452	1056.85
4.529	611.92	4.529	770.95	0.453	1044.83
4.540	614.27	4.540	773.72	0.454	1031.24
4.551	615.19	4.552	778.15	0.456	1051.71
4.561	608.59	4.563	779.94	0.457	1044.35
4.567	578.34	4.574	785.85	0.457	1029.77
4.578	585.87	4.585	783.77	0.459	1050.22
4.590	588.79	4.597	779.93	0.460	1042.47
4.603	600.58	4.609	784.39	0.460	1021.44

Appendix B: Mechanical Characteristics

4.615	606.84	4.621	785.79	0.461	1021.00
4.623	593.68	4.632	787.99	0.463	1042.12
4.630	565.40	4.643	787.19	0.464	1031.72
4.641	568.45	4.653	787.40	0.465	1019.76
4.652	574.61	4.660	770.28	0.466	1033.86
4.666	590.07	4.667	751.82	0.467	1039.54
4.676	589.15	4.677	746.31	0.468	1024.51
4.685	578.78	4.688	745.07	0.469	1017.79
4.694	572.79	4.700	747.60	0.471	1038.11
4.706	575.22	4.711	748.29	0.472	1032.28
4.717	579.91	4.723	755.33	0.472	1018.92
4.728	578.45	4.736	763.91	0.473	1006.62
4.737	570.67	4.749	774.11	0.474	1012.97
4.751	585.93	4.761	775.99	0.476	1031.32
4.764	593.86	4.771	777.08	0.477	1025.92
4.775	598.15	4.779	770.41	0.478	1013.74
4.782	586.22	4.786	756.19	0.479	1003.85
4.791	571.02	4.795	739.73	0.480	1007.74
4.802	570.87	4.805	734.26	0.481	1025.39
4.819	583.70	4.816	733.63	0.482	1019.68
4.823	568.63	4.828	735.94	0.483	1003.70
4.834	573.33	4.840	745.70	0.484	998.34
4.843	566.56	4.854	755.84	0.485	1021.36
4.854	563.51	4.866	764.12	0.487	1015.76
4.867	575.36	4.878	768.88	0.487	1001.70
4.882	589.22	4.889	769.18	0.488	990.45
4.892	591.14	4.895	756.42	0.489	996.09
4.899	576.83	4.902	740.63	0.491	1010.97
4.908	564.44	4.912	725.72	0.492	1001.37
4.921	571.83	4.923	728.83	0.493	986.17

Appendix B: Mechanical Characteristics

4.934	584.38	4.937	738.55	0.494	989.10
4.946	591.18	4.950	751.57	0.495	1003.91
4.953	575.49	4.962	758.44	0.496	1007.15
4.961	559.53	4.974	761.15	0.497	998.39
4.973	565.49	4.985	765.50	0.498	984.93
4.987	580.78	4.987	732.60	0.499	981.63
4.999	586.50	4.997	723.94	0.500	1002.39
5.005	565.66	5.009	725.10	0.502	1003.14
5.014	559.09	5.022	731.01	0.503	997.08
5.027	566.52	5.035	741.35	0.503	981.73
5.041	580.50	5.047	751.64	0.504	977.86
5.050	575.88	5.059	756.95	0.505	990.77
5.057	555.44	5.070	759.87	0.507	1000.78
5.068	557.53	5.074	734.06	0.508	997.54
5.083	572.62	5.083	713.49	0.509	990.86
5.095	579.85	5.095	718.47	0.510	978.29
5.105	577.21	5.110	735.15	0.511	970.59
5.110	550.26	5.123	747.36	0.512	967.72
5.122	553.88	5.134	752.17	0.513	982.05
5.137	573.46	5.135	702.90	0.514	990.15
5.148	574.11	5.150	713.19	0.515	986.54
5.154	555.49	5.165	729.99	0.516	975.01
5.164	544.83	5.176	737.47	0.517	966.50
5.179	565.76	5.187	739.50	0.518	963.25
5.186	551.58	5.192	719.26	0.519	963.84
5.200	561.06	5.200	700.81	0.520	970.87
5.212	568.58	5.212	702.09	0.522	988.04
5.217	545.86	5.227	719.71	0.523	986.08
5.228	545.17	5.241	733.40	0.524	984.58
5.244	565.85	5.249	730.50	0.525	979.59

Appendix B: Mechanical Characteristics

5.249	538.90	5.253	695.09	0.526	970.22
5.264	555.49	5.266	702.12	0.527	960.05
5.273	553.36	5.280	717.27	0.528	955.78
5.281	537.60	5.294	728.54	0.529	954.35
5.298	564.30	5.305	733.16	0.530	953.23
5.302	533.54	5.309	712.18	0.531	958.64
5.318	562.35	5.317	694.07	0.532	970.86
5.324	539.97	5.329	696.41	0.534	971.34
5.347	555.84	5.352	720.79	0.535	969.26
5.356	548.66	5.364	728.12	0.536	967.54
5.361	523.75	5.367	704.94	0.537	964.81
5.376	542.28	5.376	688.88	0.538	960.00
5.385	539.37	5.391	701.03	0.539	954.85
5.394	524.52	5.406	720.72	0.540	945.49
5.409	548.27	5.417	723.79	0.541	941.39
5.415	521.30	5.420	694.38	0.542	938.52
5.430	545.90	5.430	685.36	0.543	938.70
5.435	522.10	5.444	696.26	0.544	947.86
5.453	546.64	5.460	716.86	0.546	958.86
5.457	517.69	5.470	721.58	0.547	955.41
5.474	547.33	5.472	676.32	0.548	957.78
5.478	518.68	5.486	692.79	0.549	962.60
5.495	543.78	5.502	711.31	0.550	965.82
5.500	519.28	5.513	715.90	0.551	963.53
5.516	544.23	5.515	678.08	0.552	959.85
5.522	517.76	5.527	678.81	0.553	957.13
5.536	537.35	5.544	704.71	0.554	955.87
5.544	520.24	5.556	715.16	0.555	951.01
5.553	516.11	5.558	681.21	0.556	946.79
5.568	536.24	5.569	680.70	0.557	939.13

Appendix B: Mechanical Characteristics

5.573	510.24	5.583	687.78	0.558	934.50
5.591	541.61	5.598	705.28	0.559	933.22
5.597	518.62	5.609	710.87	0.560	933.73
5.608	529.88	5.611	666.02	0.561	932.60
5.621	531.40	5.629	682.12	0.562	928.91
5.627	512.20	5.640	699.73	0.563	927.91
5.643	536.79	5.643	667.87	0.564	926.25
5.653	527.43	5.656	670.43	0.566	934.06
5.659	509.33	5.672	696.33	0.567	942.02
5.676	537.79	5.682	697.56	0.568	953.01
5.686	529.10	5.685	658.18	0.569	950.71
5.691	501.57	5.699	668.61	0.570	944.64
5.701	504.22	5.716	691.17	0.571	942.55
5.717	530.03	5.724	689.83	0.572	931.89
5.728	524.52	5.728	657.16	0.573	924.70
5.736	508.53	5.745	671.34	0.574	940.26
5.744	502.12	5.759	695.08	0.576	947.40
5.761	529.59	5.761	662.50	0.577	948.27
5.770	519.97	5.772	656.70	0.578	948.21
5.776	502.01	5.789	684.04	0.579	947.57
5.790	517.97	5.801	691.06	0.580	944.55
5.798	499.29	5.803	652.34	0.581	942.96
5.815	525.36	5.817	662.01	0.582	939.45
5.824	514.01	5.833	684.62	0.583	929.16
5.831	498.62	5.839	676.19	0.584	922.29
5.840	491.59	5.846	650.42	0.585	922.30
5.852	502.33	5.863	669.97	0.586	927.39
5.865	507.13	5.876	689.48	0.587	933.86
5.879	517.65	5.879	660.05	0.588	933.33
5.886	503.02	5.890	652.77	0.589	914.47

Appendix B: Mechanical Characteristics

5.894	492.03	5.907	679.87	0.590	910.44
5.904	487.78	5.918	686.68	0.591	910.85
5.914	474.02	5.920	644.92	0.592	909.02
5.925	482.12	5.936	658.77	0.593	898.35
5.937	488.88	5.952	682.58	0.594	904.19
5.954	517.28	5.953	650.00	0.596	904.99
5.964	514.67	5.965	646.78	0.597	907.89
5.974	508.46	5.983	675.49	0.598	913.15
5.982	498.37	5.987	653.17	0.599	920.24
5.990	486.21	5.996	638.29	0.600	922.38
5.999	480.01	6.014	666.12	0.601	922.88
6.011	487.16	6.023	668.60	0.602	925.11
6.026	505.05	6.027	631.78	0.604	926.25
6.038	509.73	6.044	650.76	0.605	925.50
6.050	510.67	6.058	668.57	0.606	927.13
6.060	508.95	6.059	625.57	0.607	928.30
6.070	506.51	6.075	649.53	0.608	928.00
6.080	500.88	6.090	669.00	0.609	928.50
6.089	494.43	6.092	633.46	0.610	927.15
6.100	490.45	6.105	633.33	0.611	923.47
6.111	491.83	6.122	659.94	0.612	915.92
6.125	486.83	6.123	620.79	0.613	909.58
6.131	478.66	6.138	635.09	0.614	904.99
6.142	481.54	6.155	663.10	0.615	901.57
6.155	487.39	6.155	621.69	0.616	895.40
6.163	480.71	6.174	651.36	0.617	899.66
6.177	486.88	6.185	663.24	0.618	904.66
6.186	484.51	6.187	624.99	0.619	910.47
6.196	481.68	6.204	648.56	0.621	916.72
6.204	474.06	6.218	662.83	0.622	920.82

Appendix B: Mechanical Characteristics

6.215	472.36	6.219	625.34	0.623	909.69
6.224	464.13	6.236	640.83	0.623	895.90
6.234	458.50	6.250	662.05	0.624	886.94
6.244	453.34	6.252	619.77	0.625	885.23
6.256	456.34	6.269	645.44	0.626	885.32
6.267	457.61	6.282	659.69	0.628	885.96
6.278	460.84	6.284	618.57	0.629	887.36
6.292	469.88	6.301	644.59	0.630	890.99
6.303	471.27	6.314	657.70	0.631	900.46
6.314	472.89	6.315	618.57	0.632	907.28
6.325	475.89	6.332	640.06	0.633	910.90
6.336	474.77	6.345	657.46	0.635	913.95
6.347	481.14	6.348	617.66	0.636	914.29
6.358	481.05	6.364	637.01	0.636	899.90
6.369	479.36	6.379	655.32	0.637	881.34
6.380	477.97	6.380	601.71	0.638	883.39
6.391	479.43	6.400	645.63	0.639	884.51
6.401	478.53	6.400	602.83	0.641	889.62
6.410	475.32	6.419	629.83	0.642	899.17
6.421	472.23	6.426	629.31	0.643	903.13
6.431	466.72	6.435	607.79	0.644	904.60
6.442	468.19	6.455	645.34	0.645	903.79
6.451	463.69	6.454	602.48	0.646	895.86
6.460	456.42	6.472	633.01	0.647	886.60
6.470	451.47	6.483	641.61	0.648	872.21
6.479	448.81	6.488	607.73	0.649	865.79
6.490	447.94	6.506	640.44	0.650	869.09
6.501	448.77	6.510	627.70	0.651	873.07
6.512	450.64	6.520	611.05	0.653	885.70
6.521	436.59	6.538	642.50	0.654	890.23

Appendix B: Mechanical Characteristics

6.535	458.55	6.540	608.09	0.655	890.13
6.549	471.49	6.554	620.23	0.656	894.50
6.561	473.21	6.574	650.18	0.657	894.58
6.572	470.53	6.575	605.90	0.658	875.87
6.581	467.03	6.592	636.54	0.658	867.76
6.590	453.50	6.593	602.43	0.660	858.95
6.601	451.45	6.610	624.45	0.661	860.96
6.614	469.55	6.623	639.67	0.662	862.16
6.621	453.67	6.626	602.68	0.663	873.79
6.630	435.07	6.645	638.98	0.664	877.89
6.639	431.76	6.646	605.21	0.666	880.13
6.652	444.16	6.662	620.37	0.667	881.11
6.666	461.48	6.673	628.05	0.668	882.51
6.679	463.82	6.680	603.39	0.669	881.27
6.689	461.28	6.698	635.33	0.669	869.02
6.684	430.83	6.700	607.70	0.670	854.33

50kPa		100kPa		150kPa	
Strain %	Stress (kPa)	Strain %	Stress (kPa)	Strain %	Stress (kPa)
0.00	0.00	0.00	0.00	0.00	0.00
0.35	95.77	0.40	6.22	0.42	8.71
0.42	108.20	0.42	11.19	0.45	7.46
0.45	118.15	0.46	23.63	0.49	7.46
0.50	130.59	0.46	31.09	0.52	6.22
0.54	143.03	0.52	46.02	0.56	6.22
0.59	155.46	0.56	58.45	0.59	6.22
0.63	169.14	0.61	69.65	0.64	7.46
0.67	182.82	0.66	80.84	0.68	8.71

Appendix B: Mechanical Characteristics

0.72	197.75	0.70	92.03	0.70	17.41
0.75	212.67	0.75	104.47	0.75	29.85
0.80	226.35	0.79	114.42	0.78	39.80
0.87	248.74	0.82	123.13	0.82	52.24
0.89	259.93	0.86	134.32	0.86	64.67
0.93	277.35	0.91	149.24	0.91	77.11
0.97	294.76	0.95	160.44	0.95	88.30
1.01	312.17	1.00	172.87	1.00	100.74
1.05	328.34	1.03	187.80	1.05	113.18
1.08	345.75	1.07	201.48	1.08	119.40
1.13	365.65	1.11	216.40	1.11	130.59
1.16	383.06	1.16	233.82	1.16	141.78
1.20	402.96	1.19	249.98	1.19	151.73
1.25	421.62	1.23	263.66	1.23	164.17
1.28	440.27	1.27	282.32	1.27	176.61
1.33	460.17	1.31	298.49	1.32	191.53
1.36	478.83	1.36	315.90	1.37	207.70
1.40	501.21	1.38	332.07	1.40	220.14
1.44	521.11	1.42	349.48	1.44	235.06
1.45	537.28	1.47	369.38	1.48	246.25
1.52	560.91	1.50	384.30	1.52	262.42
1.56	584.54	1.55	406.69	1.55	278.59
1.60	603.20	1.58	424.10	1.60	292.27
1.63	620.61	1.61	441.51	1.64	305.95
1.68	639.26	1.66	462.66	1.68	320.88
1.71	656.67	1.69	480.07	1.71	335.80
1.75	675.33	1.74	498.72	1.75	351.97
1.78	692.74	1.78	517.38	1.78	370.62
1.82	710.15	1.82	534.79	1.83	390.52

Appendix B: Mechanical Characteristics

1.85	726.32	1.85	552.20	1.87	410.42
1.89	741.25	1.88	567.13	1.91	431.57
1.93	756.17	1.92	585.78	1.95	450.22
1.96	771.10	1.96	603.20	2.01	475.09
1.99	786.02	2.00	618.12	2.03	490.02
2.03	799.70	2.04	631.80	2.07	509.92
2.07	813.38	2.08	646.73	2.11	532.31
2.10	827.06	2.12	661.65	2.15	553.45
2.14	839.50	2.15	675.33	2.19	575.83
2.18	851.94	2.18	687.77	2.23	598.22
2.21	866.86	2.21	700.20	2.29	604.44
2.26	879.30	2.25	713.88	2.32	620.61
2.29	891.73	2.29	726.32	2.34	638.02
2.33	902.93	2.32	738.76	2.39	664.14
2.37	914.12	2.35	752.44	2.42	685.28
2.41	925.31	2.39	763.63	2.45	708.91
2.45	936.51	2.42	774.83	2.49	732.54
2.53	953.92	2.48	792.24	2.53	754.93
2.53	956.41	2.48	795.97	2.56	777.31
2.56	965.11	2.52	810.89	2.61	802.19
2.62	973.82	2.56	823.33	2.65	824.58
2.65	982.52	2.60	835.77	2.67	844.47
2.71	991.23	2.64	846.96	2.73	866.86
2.74	996.21	2.67	856.91	2.77	886.76
2.78	1004.91	2.73	867.5913	2.81	907.90
2.83	1009.89	2.73	867.5913	2.84	929.05
2.87	1018.59	2.78	883.9169	2.87	948.95
2.92	1026.05	2.82	897.9103	2.92	971.33
2.95	1032.27	2.86	909.5715	2.96	989.99

Appendix B: Mechanical Characteristics

3.00	1037.25	2.89	921.2326	2.99	1008.64
3.03	1042.22	2.94	935.226	3.03	1027.30
3.08	1047.20	2.97	946.8872	3.05	1044.71
3.12	1049.68	3.02	960.8806	3.09	1063.37
3.17	1054.66	3.05	972.5417	3.13	1080.78
3.22	1058.39	3.08	981.8707	3.16	1098.19
3.26	1062.12	3.12	993.5318	3.20	1115.60
3.31	1064.61	3.16	1007.525	3.25	1135.50
3.35	1065.85	3.19	1016.854	3.27	1149.18
3.38	1068.34	3.23	1028.515	3.31	1164.11
3.44	1073.32	3.28	1044.841	3.34	1179.03
3.48	1074.56	3.32	1056.502	3.38	1196.44
3.53	1075.80	3.36	1068.163	3.42	1211.37
3.57	1075.80	3.39	1079.824	3.45	1226.29
3.60	1077.05	3.44	1096.15	3.49	1242.46
3.64	1078.29	3.47	1105.479	3.53	1257.38
3.68	1080.78	3.52	1119.473	3.58	1274.80
3.69	1082.02	3.56	1133.466	3.60	1287.23
3.75	1089.48	3.60	1147.459	3.64	1302.16
3.81	1091.97	3.64	1159.121	3.67	1313.35
3.86	1087.00	3.68	1173.114	3.71	1328.27
3.90	1083.26	3.72	1184.775	3.75	1341.95
3.94	1080.78	3.79	1208.098	3.79	1355.64
3.99	1079.53	3.80	1210.43	3.82	1368.07
4.01	1078.29	3.85	1253.26	3.87	1380.51
4.04	1079.53	3.89	1255.75	3.90	1392.95
4.07	1084.51	3.93	1259.48	3.95	1405.38
4.10	1087.00	3.97	1263.21	3.98	1415.33
4.13	1090.73	4.01	1266.95	3.99	1422.80

Appendix B: Mechanical Characteristics

4.21	1099.43	4.06	1266.95	4.04	1436.48
4.23	1096.95	4.11	1269.43	4.10	1450.16
4.28	1099.43	4.15	1271.92	4.15	1457.62
4.33	1096.95	4.21	1275.65	4.21	1471.30
4.37	1095.70	4.23	1275.65	4.23	1476.27
4.40	1094.46	4.29	1280.63	4.27	1484.98
4.45	1090.73	4.32	1280.63	4.32	1494.93
4.50	1087.00	4.36	1280.63	4.36	1502.39
4.53	1083.26	4.41	1283.11	4.40	1509.85
4.57	1080.78	4.45	1284.36	4.44	1518.56
4.59	1078.29	4.48	1286.84	4.48	1524.78
4.63	1078.29	4.53	1288.09	4.53	1532.24
4.67	1082.02	4.56	1289.33	4.56	1538.46
4.70	1084.51	4.60	1290.58	4.61	1543.43
4.75	1089.48	4.64	1293.06	4.67	1550.90
4.79	1089.48	4.68	1293.06	4.70	1553.38
4.84	1088.24	4.73	1294.31	4.74	1558.36
4.89	1084.51	4.77	1294.31	4.78	1562.09
4.93	1079.53	4.81	1295.55	4.82	1565.82
4.97	1075.80	4.85	1295.55	4.87	1572.04
5.00	1072.07	4.91	1296.79	4.91	1574.53
5.04	1070.83	4.95	1296.79	4.95	1579.50
5.07	1068.34	4.99	1296.79	5.01	1583.23
5.10	1069.58	5.01	1294.31	5.04	1584.48
5.14	1070.83	5.07	1296.79	5.08	1586.96
5.17	1073.32	5.11	1298.04	5.13	1589.45
5.22	1075.80	5.14	1296.79	5.17	1591.94
5.27	1074.56	5.19	1298.04	5.22	1593.18
5.32	1072.07	5.25	1298.04	5.26	1596.91

Appendix B: Mechanical Characteristics

5.37	1070.83	5.29	1296.79	5.30	1599.40
5.41	1065.85	5.32	1294.31	5.35	1599.40
5.44	1063.37	5.38	1295.55	5.43	1605.62
5.48	1059.63	5.43	1294.31	5.44	1599.40
5.52	1058.39	5.48	1293.06	5.48	1599.40
5.52	1052.17	5.52	1289.33	5.53	1599.40
5.58	1054.66	5.57	1288.09	5.58	1594.43
5.61	1057.15	5.62	1284.36	5.62	1591.94
5.66	1058.39	5.66	1281.87	5.67	1589.45
5.71	1057.15	5.71	1280.63	5.71	1588.21
5.76	1054.66	5.75	1278.14	5.74	1586.96
5.80	1050.93	5.79	1275.65	5.77	1585.72
5.85	1047.20	5.80	1270.68	5.82	1585.72
5.88	1044.71	5.85	1270.68	5.85	1588.21
5.92	1039.74	5.89	1273.16	5.89	1590.70
5.95	1038.49	5.93	1274.41	5.93	1590.70
5.99	1037.25	5.96	1273.16	5.98	1588.21
6.01	1031.03	6.01	1271.92	6.02	1585.72
6.06	1032.27	6.06	1269.43	6.07	1581.99
6.10	1031.03	6.11	1265.70	6.12	1577.01
6.14	1028.54	6.16	1259.48	6.17	1573.28
6.20	1026.05	6.21	1255.75	6.18	1567.06
6.23	1019.84	6.26	1247.05	6.23	1565.82
6.27	1016.10	6.31	1245.00	6.26	1563.33
6.31	1012.37	6.35	1243.00	6.29	1559.60
6.34	1009.89	6.36	1240.00	6.32	1559.60
6.38	1008.64	6.41	1225.90	6.37	1560.85
6.42	1008.64	6.44	1223.42	6.41	1560.85
6.45	1008.64	6.48	1227.15	6.45	1560.85

Appendix B: Mechanical Characteristics

6.49	1011.13	6.49	1223.42	6.51	1559.60
6.54	1009.89	6.51	1223.42	6.55	1553.38
6.59	1006.16	6.56	1227.15	6.59	1548.41
6.64	1001.18	6.59	1228.39	6.65	1545.92
6.69	994.96	6.64	1229.63	6.67	1538.46
6.73	989.99	6.70	1229.63	6.70	1535.97
6.75	986.26	6.75	1225.90	6.73	1533.49
6.78	985.01	6.80	1220.93	6.76	1533.49
6.81	983.77	6.84	1215.95	6.80	1537.22
6.84	985.01	6.88	1210.98	6.84	1538.46
6.88	988.74	6.92	1207.25	6.89	1538.46
6.92	991.23	6.95	1204.76	6.95	1535.97
6.97	991.23	6.98	1203.52	7.00	1528.51
7.03	987.50	7.00	1201.03	7.05	1521.05
7.09	980.04	7.03	1202.27	7.11	1503.64
7.14	971.33	7.07	1203.52	7.15	1492.44
7.18	963.87	7.11	1204.76	7.19	1484.98
7.19	955.16	7.16	1206.00	7.20	1476.27
7.24	955.16	7.21	1204.76	7.22	1473.79
7.28	955.16	7.26	1201.03	7.25	1473.79
7.28	951.43	7.30	1197.30	7.27	1476.27
7.31	953.92	7.36	1194.81	7.30	1482.49
7.34	957.65	7.39	1189.84	7.33	1489.96
7.39	961.38	7.43	1187.35	7.37	1494.93
7.46	960.14	7.46	1184.86	7.44	1497.42
7.52	955.16	7.50	1183.62	7.50	1494.93
7.58	947.70	7.52	1181.13	7.56	1484.98
7.63	940.24	7.55	1183.62	7.60	1475.03
7.66	932.78	7.58	1186.10	7.65	1465.08

Appendix B: Mechanical Characteristics

7.68	929.05	7.60	1186.10	7.68	1456.38
7.70	925.31	7.67	1191.08	7.71	1451.40
7.72	925.31	7.71	1191.08	7.74	1448.91
7.75	927.80	7.77	1188.59	7.77	1448.91
7.78	931.53	7.82	1183.62	7.80	1447.67
7.82	932.78	7.88	1177.40	7.82	1450.16
7.90	934.02	7.92	1169.94	7.87	1453.89
7.94	927.80	7.96	1163.72	7.93	1460.11
8.00	922.83	8.01	1156.26	7.96	1456.38
8.04	917.85	8.04	1150.04	8.01	1455.13
8.09	914.12	8.10	1148.79	8.06	1447.67
8.11	909.15	8.10	1143.82	8.11	1443.94
8.13	906.66	8.12	1141.33	8.15	1437.72
8.18	906.66	8.15	1141.33	8.18	1431.50
8.20	905.42	8.18	1146.31	8.22	1425.28
8.21	902.93	8.20	1150.04	8.26	1420.31
8.28	909.15	8.23	1155.01	8.29	1416.58
8.32	910.39	8.29	1157.50	8.32	1415.33
8.37	909.15	8.36	1156.26	8.35	1415.33
8.43	905.42	8.42	1151.28	8.40	1416.58
8.48	899.20	8.48	1143.82	8.43	1417.82
8.51	890.49	8.53	1136.36	8.47	1417.82
8.56	889.25	8.57	1131.38	8.53	1417.82
8.59	885.52	8.60	1126.41	8.58	1414.09
8.62	884.27	8.64	1126.41	8.62	1407.87
8.64	883.03	8.64	1121.43	8.67	1401.65
8.66	886.76	8.67	1121.43	8.72	1395.43
8.70	890.49	8.68	1125.16	8.75	1387.97
8.75	895.47	8.71	1130.14	8.76	1376.78

Appendix B: Mechanical Characteristics

8.80	894.22	8.75	1136.36	8.81	1376.78
8.87	889.25	8.80	1138.84	8.84	1373.05
8.94	879.30	8.86	1140.09	8.86	1375.53
8.98	870.59	8.94	1133.87	8.89	1379.27
9.03	866.86	9.03	1121.43	8.94	1381.75
9.05	860.64	9.09	1110.24	8.97	1385.48
9.07	856.91	9.13	1101.53	9.03	1385.48
9.09	856.91	9.16	1095.31	9.09	1384.24
9.11	856.91	9.17	1090.34	9.14	1379.27
9.12	858.15	9.19	1087.85	9.19	1370.56
9.17	868.10	9.19	1086.61	9.23	1363.10
9.21	871.84	9.22	1091.58	9.26	1359.37
9.27	871.84	9.23	1096.56	9.30	1354.39
9.36	865.62	9.26	1106.51	9.32	1350.66
9.41	858.15	9.31	1118.94	9.34	1350.66
9.46	851.94	9.35	1122.68	9.38	1354.39
9.48	845.72	9.42	1120.19	9.41	1358.12
9.52	840.74	9.50	1113.97	9.46	1359.37
9.54	838.26	9.57	1105.26	9.52	1360.61
9.55	835.77	9.61	1097.80	9.57	1356.88
9.58	838.26	9.65	1091.58	9.63	1350.66
9.61	843.23	9.68	1087.85	9.67	1343.20
9.64	849.45	9.69	1085.36	9.69	1335.74
9.70	854.42	9.73	1087.85	9.73	1333.25
9.75	853.18	9.73	1087.85	9.76	1329.52
9.82	849.45	9.75	1091.58	9.79	1328.27
9.88	843.23	9.78	1096.56	9.82	1330.76
9.93	834.52	9.82	1104.02	9.85	1332.01
9.97	828.31	9.86	1104.02	9.88	1339.47

Appendix B: Mechanical Characteristics

10.00	823.33	9.95	1105.26	9.93	1341.95
10.03	819.60	10.03	1099.38	9.99	1343.20
10.05	817.11	10.09	1095.102	10.04	1339.47
10.07	815.87	10.13	1091.893	10.10	1335.74
10.10	818.36	10.18	1093	10.15	1330.76
10.12	822.09	10.20	1086	10.18	1325.79
10.15	824.57	10.21	1099	10.21	1320.81
10.21	827.06	10.24	1089	10.23	1313.35
10.29	825.82	10.26	1095.256	10.27	1314.59
10.36	817.11	10.29	1070	10.30	1315.84
10.40	810.89	10.29	1093.117	10.33	1319.57
10.45	809.65	10.34	1089.374	10.39	1328.27
10.48	800.94	10.40	1085.095	10.41	1328.27
10.50	797.21	10.46	1080.817	10.48	1328.27
10.52	794.73	10.53	1076.004	10.53	1324.54
10.55	795.97	10.58	1072.26	10.59	1320.81
10.56	798.46	10.63	1092	10.62	1313.35
10.59	802.19	10.66	1066.377	10.66	1308.38
10.64	808.41	10.70	1063.703	10.68	1303.40
10.70	810.89	10.70	1063.703	10.71	1302.16
10.77	807.16	10.73	1048	10.73	1299.67
10.83	802.19	10.76	1058.89	10.77	1307.13
10.89	797.21	10.79	1056.751	10.81	1310.86
10.91	789.75	10.84	1053.542	10.86	1313.35
10.95	787.26	10.89	1049.264	10.92	1312.11
10.95	781.05	10.95	1044.985	10.97	1308.38
10.98	781.05	11.02	1040.172	11.02	1300.91
11.02	784.78	11.06	1036.963	11.07	1293.45
11.05	788.51	11.10	1034.289	11.11	1287.23

Appendix B: Mechanical Characteristics

11.08	792.24	11.15	1030.546	11.14	1279.77
11.13	794.73	11.17	1028.941	11.16	1273.55
11.19	797.21	11.20	1026.802	11.21	1271.06
11.25	792.24	11.23	1024.663	11.22	1267.33
11.30	788.51	11.25	1023.059	11.25	1267.33
11.36	786.02	11.28	1020.919	11.28	1272.31
11.38	783.53	11.31	1018.78	11.31	1274.80
11.42	781.05	11.33	1017.711	11.37	1279.77
11.43	777.31	11.39	1012.897	11.42	1278.53
11.47	779.80	11.47	1007.549	11.49	1273.55
11.49	781.05	11.51	1004.341	11.55	1267.33
11.53	786.02	11.56	1000.597	11.58	1257.38
11.58	787.26	11.62	996.3186	11.63	1249.92
11.65	788.51	11.66	993.6446	11.65	1243.70
11.71	782.29	11.70	990.4359	11.68	1241.22
11.74	774.83	11.73	988.2967	11.70	1237.48
11.79	771.10	11.76	986.1575	11.73	1241.22
11.82	767.36	11.78	984.5531	11.77	1243.70
11.85	763.63	11.81	982.4139	11.79	1249.92
11.88	762.39	11.84	980.2747	11.85	1253.65
11.90	762.39	11.87	978.1355	11.90	1251.16
11.94	766.12	11.91	974.9267	11.97	1246.19
11.96	768.61	11.96	971.7179	12.04	1236.24
12.01	773.58	12.01	967.9743	12.09	1223.80
12.06	774.83	12.07	963.1612	12.13	1215.10
12.13	773.58	12.15	948.00	12.15	1207.64
12.19	767.36	12.15	943.00	12.18	1202.66
12.25	759.90	12.21	940.00	12.19	1198.93
12.29	756.17	12.24	937.00	12.21	1198.93

Appendix B: Mechanical Characteristics

12.31	749.95	12.27	932.00	12.23	1203.90
12.33	747.47	12.30	928.00	12.26	1211.37
12.36	748.71	12.32	930.00	12.29	1218.83
12.37	748.71	12.35	923.00	12.35	1225.05
12.40	752.44	12.40	924.00	12.42	1225.05
12.44	757.41	12.45	916.00	12.49	1218.83
12.48	761.15	12.51	913.00	12.54	1210.12
12.55	761.15	12.57	908.00	12.60	1200.17
12.62	757.41	12.63	912.00	12.63	1191.47
12.69	752.44	12.67	916.00	12.70	1188.98
12.73	743.73	12.69	907.00	12.69	1179.03
12.77	737.52	12.73	913.00	12.70	1174.06
12.78	732.54	12.75	927.00	12.74	1174.06
12.81	728.81	12.76	936.00	12.75	1175.30
12.84	731.30	12.79	925.00	12.78	1182.76
12.84	730.05	12.81	890.00	12.82	1190.22
12.87	735.03	12.84	896.00	12.88	1195.20
12.91	741.25	12.91	903.00	12.94	1193.95
12.95	744.98	12.97	907.00	13.01	1187.74
13.03	746.22	13.03	904.00	13.08	1175.30
13.09	740.00	13.08	925.00	13.13	1164.11
13.16	736.27	13.11	864.37	13.16	1157.89
13.19	730.05	13.15	863.13	13.19	1149.18
13.22	726.32	13.18	861.89	13.22	1145.45
13.24	722.59	13.20	863.13	13.22	1141.72
13.27	722.59	13.24	866.86	13.25	1141.72
13.29	723.83	13.27	890.00	13.27	1146.69
13.32	727.57	13.32	873.08	13.30	1155.40
13.35	731.30	13.38	874.32	13.33	1164.11

Appendix B: Mechanical Characteristics

13.40	735.03	13.44	873.08	13.40	1167.84
13.47	735.03	13.49	869.35	13.47	1164.11
13.53	732.54	13.54	865.62	13.54	1155.40
13.58	727.57	13.58	860.64	13.63	1150.42
13.63	723.83	13.60	859.40	13.64	1135.50
13.66	718.86	13.63	858.15	13.66	1128.04
13.69	715.13	13.66	861.89	13.68	1124.31
13.71	713.89	13.68	863.13	13.71	1125.55
13.74	712.64	13.69	860.64	13.72	1123.06
13.77	713.89	13.74	866.86	13.74	1128.04
13.81	717.62	13.79	870.59	13.77	1135.50
13.85	720.10	13.86	870.59	13.82	1144.21
13.90	722.59	13.92	865.62	13.88	1149.18
13.96	722.59	13.98	861.89	13.94	1146.69
14.03	718.86	14.03	856.91	14.02	1137.99
14.07	712.64	14.06	853.18	14.07	1126.79
14.11	707.67	14.09	850.69	14.12	1118.09
14.15	703.94	14.10	848.20	14.15	1109.38
14.18	700.20	14.13	850.69	14.17	1104.41
14.20	697.72	14.15	851.94	14.19	1101.92
14.22	697.72	14.18	856.91	14.21	1100.68
14.25	698.96	14.22	861.89	14.22	1103.16
14.28	703.94	14.27	865.62	14.26	1111.87
14.32	707.67	14.33	866.86	14.29	1116.84
14.36	710.15	14.40	865.62	14.35	1124.31
14.42	710.15	14.46	861.89	14.42	1125.55
14.49	708.91	14.51	856.91	14.48	1119.33
14.55	703.94	14.52	848.20	14.54	1110.63
14.60	697.72	14.56	846.96	14.58	1100.68

Appendix B: Mechanical Characteristics

14.63	693.99	14.58	845.72	14.64	1095.70
14.66	690.25	14.62	849.45	14.66	1088.24
14.67	687.77	14.64	849.45	14.68	1083.27
14.70	687.77	14.66	853.18	14.70	1082.02
14.72	690.25	14.69	856.91	14.73	1082.02
14.75	695.23	14.75	866.86	14.75	1087.00
14.79	700.20	14.79	866.86	14.77	1093.21
14.86	703.94	14.86	868.10	14.83	1103.16
14.92	698.96	14.92	865.62	14.87	1104.41
14.98	695.23	14.97	861.89	14.95	1105.65
15.02	690.25	15.02	856.91	15.01	1098.19
15.05	687.77	15.06	854.42	15.08	1087.00
15.08	686.52	15.08	850.69	15.12	1078.29
15.09	684.04	15.11	848.20	15.16	1073.32
15.12	687.77	15.14	849.45	15.17	1065.85
15.16	691.50	15.15	849.45	15.20	1064.61
15.19	695.23	15.19	853.18	15.22	1060.88
15.25	697.72	15.22	856.91	15.23	1062.12
15.32	696.47	15.26	860.64	15.27	1069.58
15.38	690.25	15.33	860.64	15.30	1075.80
15.43	686.52	15.40	859.40	15.35	1082.02
15.45	681.55	15.47	851.94	15.41	1082.02
15.49	680.31	15.52	845.72	15.49	1075.80
15.51	679.06	15.55	840.74	15.55	1064.61
15.53	679.06	15.56	834.52	15.60	1054.66
15.55	680.31	15.60	833.28	15.63	1049.69
15.58	686.52	15.61	833.28	15.65	1044.71
15.63	689.01	15.63	834.52	15.66	1042.22
15.68	689.01	15.66	838.26	15.71	1045.95

Appendix B: Mechanical Characteristics

15.75	689.01	15.69	844.47	15.70	1045.95
15.82	686.52	15.72	849.45	15.73	1053.42
15.85	680.31	15.78	853.18	15.77	1062.12
15.88	677.82	15.85	849.45	15.83	1067.10
15.91	675.33	15.94	843.23	15.90	1064.61
15.90	669.11	16.00	835.77	15.99	1059.63
15.96	677.82	16.05	827.06	16.02	1049.69
15.99	680.31	16.08	822.09	16.05	1039.74
16.06	689.01	16.10	818.36	16.09	1037.25
16.08	686.52	16.12	814.62	16.09	1031.03
16.15	686.52	16.15	817.11	16.12	1033.52
16.21	682.79	16.15	815.87	16.15	1036.00
16.25	677.82	16.15	817.11	16.18	1042.22
16.29	674.09	16.20	827.06	16.22	1049.69
16.32	671.60	16.22	833.28	16.28	1050.93
16.34	670.36	16.25	837.01	16.37	1047.20
16.36	671.60	16.36	844.47	16.42	1036.00
16.39	672.84	16.44	835.77	16.47	1026.05
16.43	679.06	16.51	828.31	16.50	1018.59
16.47	681.55	16.57	820.84	16.53	1014.86
16.52	682.79	16.59	814.62	16.55	1011.13
16.59	681.55	16.62	808.41	16.56	1011.13
16.66	676.57	16.63	805.92	16.59	1013.62
16.70	671.60	16.65	804.68	16.61	1022.32
16.73	667.87	16.67	805.92	16.67	1036.00
16.76	664.14	16.69	809.65	16.70	1034.76
16.78	662.89	16.71	817.11	16.78	1037.25
16.80	662.89	16.74	825.82	16.84	1026.05
16.82	666.62	16.79	832.04	16.92	1016.11

Appendix B: Mechanical Characteristics

16.86	671.60	16.84	832.04	16.95	1007.40
16.90	675.33	16.92	827.06	16.97	998.69
16.95	677.82	17.02	824.57	17.00	994.96
17.03	677.82	17.07	815.87	17.02	992.47
17.08	675.33	17.10	809.65	17.03	992.47
17.13	670.36	17.13	805.92	17.05	996.21
17.17	670.36	17.14	803.43	17.08	1004.91
17.18	664.14	17.16	803.43	17.10	1011.13
17.21	662.89	17.18	803.43	17.17	1019.84
17.23	664.14	17.20	807.16	17.25	1019.84
17.27	669.11	17.23	814.62	17.32	1011.13
17.30	670.36	17.27	820.84	17.38	1004.91
17.35	675.33	17.32	825.82	17.42	996.21
17.41	677.82	17.38	828.31	17.45	988.74
17.47	675.33	17.45	825.82	17.49	987.50
17.52	672.84	17.52	823.33	17.49	981.28
17.56	669.11	17.57	815.87	17.52	981.28
17.60	666.62	17.61	809.65	17.54	982.53
17.60	662.89	17.65	805.92	17.58	986.26
17.64	665.38	17.67	802.19	17.61	992.47
17.68	669.11	17.69	799.70	17.66	994.96
17.71	671.60	17.71	800.94	17.72	993.72
17.74	674.09	17.73	800.94	17.79	989.99
17.80	675.33	17.76	805.92	17.85	981.28
17.87	672.84	17.79	810.89	17.89	973.82
17.92	669.11	17.83	815.87	17.92	967.60
17.96	664.14	17.90	817.11	17.94	962.63
17.99	661.65	17.96	817.11	17.97	960.14
18.01	659.16	18.03	812.14	17.99	962.63

Appendix B: Mechanical Characteristics

18.04	659.16	18.08	808.41	18.01	965.11
18.06	660.41	18.12	804.68	18.04	972.58
18.10	666.62	18.15	800.94	18.07	976.31
18.14	671.60	18.17	798.46	18.15	982.53
18.19	672.84	18.22	802.19	18.21	977.55
18.25	671.60	18.22	798.46	18.28	971.33
18.31	671.60	18.25	800.94	18.34	965.11
18.34	667.87	18.29	805.92	18.37	956.41
18.37	665.38	18.32	808.41	18.40	952.68
18.40	664.14	18.38	812.14	18.41	946.46
18.43	665.38	18.45	810.89	18.43	946.46
18.47	667.87	18.51	805.92	18.45	950.19
18.45	662.89	18.56	800.94	18.48	955.16
18.59	679.06	18.60	795.97	18.51	963.87
18.61	674.09	18.63	792.24	18.57	968.84
18.67	672.84	18.63	784.78	18.64	967.60
18.72	667.87	18.68	788.51	18.72	960.14
18.74	661.65	18.71	790.99	18.78	948.95
18.79	660.41	18.73	790.99	18.84	936.51
18.81	659.16	18.76	794.73	18.86	927.80
18.83	659.16	18.80	797.21	18.87	917.85
18.86	662.89	18.85	800.94	18.90	915.37
18.89	667.87	18.92	800.94	18.97	922.83
18.93	671.60	18.97	798.46	18.94	915.37
18.97	671.60	19.02	794.73	18.96	920.34
19.05	672.84	19.07	790.99	18.98	929.05
19.11	666.62	19.11	788.51	19.05	940.24
19.15	664.14	19.13	783.53	19.12	935.26
19.19	662.89	19.16	783.53	19.20	921.58

Appendix B: Mechanical Characteristics

19.22	660.41	19.19	781.04	19.27	909.15
19.24	660.41	19.21	782.29	19.30	895.47
19.27	661.65	19.26	788.51	19.33	889.25
19.29	664.14	19.27	788.51	19.35	884.27
19.33	667.87	19.32	790.99	19.38	883.03
19.38	670.36	19.36	788.51	19.38	880.54
19.44	669.11	19.44	790.99	19.40	884.27
19.50	666.62	19.50	788.51	19.42	892.98
19.55	662.89	19.54	784.78	19.45	902.93
19.59	659.16	19.58	781.04	19.52	909.15
19.60	657.92	19.61	778.56	19.58	899.20
19.63	657.92	19.65	776.07	19.69	891.73
19.66	659.16	19.66	774.83	19.74	880.54
19.69	661.65	19.69	774.83	19.77	870.59
19.72	666.62	19.73	777.31	19.79	863.13
19.78	667.87	19.76	779.80	19.81	860.64
19.83	667.87	19.81	784.78	19.83	859.40
19.90	666.62	19.85	784.78	19.85	861.89
19.94	664.14	19.90	782.29	19.87	866.86
19.97	659.16	19.98	781.04	19.88	874.32
20.00	659.16	20.02	777.31	19.95	884.27
20.01	657.92	20.08	777.31	20.03	885.52
20.06	661.65	20.10	769.85	20.10	876.81
20.10	664.14	20.12	767.36	20.18	868.10
20.13	666.62	20.15	766.12	20.21	858.16
20.20	669.11	20.17	766.12	20.23	851.94
20.26	667.87	20.20	768.61	20.25	849.45
20.29	664.14	20.23	773.58	20.26	849.45
20.33	662.89	20.26	777.31	20.28	851.94

Appendix B: Mechanical Characteristics

20.36	661.65	20.32	781.04	20.30	859.40
20.38	664.14	20.38	781.04	20.34	869.35
20.41	666.62	20.45	778.56	20.40	873.08
20.45	671.60	20.51	773.58	20.48	868.10
20.50	675.33	20.56	767.36	20.56	859.40
20.56	676.57	20.59	758.66	20.60	851.94
20.62	672.84	20.63	757.41	20.63	846.96
20.62	657.92	20.64	752.44	20.64	843.23
20.70	662.89	20.66	752.44	20.66	843.23
20.74	661.65	20.68	754.93	20.68	843.23
20.76	660.41	20.70	758.66	20.73	851.94
20.78	657.92	20.73	764.88	20.75	856.91
20.81	661.65	20.78	771.10	20.80	859.40
20.84	666.62	20.84	774.83	20.88	856.91
20.89	670.36	20.91	772.34	20.95	849.45
20.95	671.60	20.98	767.36	21.00	841.99
21.00	670.36	21.04	762.39	21.03	835.77
21.05	669.11	21.06	754.93	21.05	832.04
21.11	670.36	21.10	751.20	21.07	829.55
21.14	659.16	21.11	747.46	21.09	830.79
21.19	659.16	21.15	747.46	21.11	837.01
21.22	651.70	21.17	747.46	21.14	844.47
21.23	649.21	21.19	748.71	21.19	850.69
21.25	650.46	21.22	753.68	21.27	848.21
21.27	652.94	21.25	758.66	21.35	840.74
21.30	657.92	21.30	762.39	21.40	830.79
21.35	664.14	21.37	763.63	21.43	824.58
21.41	666.62	21.47	759.90	21.46	820.84
21.47	664.14	21.50	748.71	21.48	819.60

Appendix B: Mechanical Characteristics

21.53	661.65	21.57	746.22	21.49	820.84
21.58	657.92	21.60	741.25	21.51	827.06
21.62	652.94	21.61	737.52	21.55	835.77
21.65	650.46	21.63	736.27	21.59	840.74
21.68	647.97	21.63	733.78	21.67	838.26
21.70	647.97	21.68	742.49	21.75	829.55
21.72	650.46	21.68	746.22	21.80	819.60
21.76	655.43	21.72	752.44	21.83	814.63
21.80	661.65	21.77	758.66	21.85	809.65
21.85	661.65	21.85	758.66	21.87	808.41
21.91	660.41	21.93	753.68	21.88	809.65
21.97	657.92	21.99	747.46	21.90	815.87
22.02	656.67	22.04	742.49	21.94	823.33
22.05	652.94	22.07	737.52	21.99	829.55
22.07	650.46	22.09	733.78	22.07	830.79
22.10	651.70	22.11	730.05	22.12	823.33
22.12	652.94	22.14	730.05	22.17	813.38
22.16	657.92	22.15	730.05	22.23	809.65
22.21	661.65	22.18	735.03	22.26	803.43
22.26	662.89	22.23	740.00	22.29	800.94
22.32	661.65	22.27	742.49	22.30	798.46
22.37	659.16	22.34	746.22	22.32	799.70
22.41	656.67	22.39	743.73	22.34	807.16
22.43	654.19	22.45	738.76	22.39	812.14
22.46	654.19	22.51	733.78	22.45	813.38
22.48	654.19	22.54	727.57	22.51	804.68
22.53	657.92	22.58	726.32	22.59	795.97
22.57	660.41	22.59	721.35	22.63	784.78
22.62	661.65	22.61	720.10	22.67	777.31

Appendix B: Mechanical Characteristics

22.67	659.16	22.63	722.59	22.70	772.34
22.72	659.16	22.65	727.57	22.71	771.10
22.76	656.67	22.68	732.54	22.72	772.34
22.79	654.19	22.74	740.00	22.74	778.56
22.82	654.19	22.81	740.00	22.76	787.26
22.86	655.43	22.89	736.27	22.81	792.24
22.88	657.92	22.95	731.30	22.89	794.73
22.92	660.41	22.99	726.32	22.97	787.26
22.97	666.62	23.00	718.86	23.03	777.31
23.03	666.62	23.03	717.62	23.05	772.34
23.08	662.89	23.05	716.37	23.08	767.36
23.14	659.16	23.07	717.62	23.10	767.36
23.17	654.19	23.10	721.35	23.12	768.61
23.20	651.70	23.13	726.32	23.14	774.83
23.22	650.46	23.18	728.81	23.18	782.29
23.25	651.70	23.25	730.05	23.24	786.02
23.27	654.19	23.30	727.57	23.29	784.78
23.32	659.16	23.36	725.08	23.35	783.53
23.36	662.89	23.41	720.10	23.39	778.56
23.43	665.38	23.44	716.37	23.41	772.34
23.47	664.14	23.47	715.13	23.46	772.34
23.52	661.65	23.49	715.13	23.47	767.36
23.56	659.16	23.51	716.37	23.52	773.58
23.59	657.92	23.54	720.10	23.55	778.56
23.61	656.67	23.58	725.08	23.60	783.53
23.65	657.92	23.64	730.05	23.65	787.26
23.69	660.41	23.69	728.81	23.71	788.51
23.74	660.41	23.75	726.32	23.75	786.02
23.81	662.89	23.81	721.35	23.80	781.05

Appendix B: Mechanical Characteristics

23.82	657.92	23.84	718.86	23.83	777.31
23.87	655.43	23.87	717.62	23.87	776.07
23.92	654.19	23.90	716.37	23.89	774.83
23.93	647.97	23.91	716.37	23.92	777.31
23.97	651.70	23.93	718.86	23.94	781.05
24.00	652.94	23.98	723.83	24.00	787.26
24.04	654.19	24.03	727.57	24.06	788.51
24.08	651.70	24.10	727.57	24.12	784.78
24.15	654.19	24.17	723.83	24.16	778.56
24.20	650.46	24.21	713.88	24.21	774.83
24.24	645.48	24.25	712.64	24.23	769.85
24.24	636.78	24.28	707.67	24.27	773.58
24.29	640.51	24.31	706.42	24.29	771.10
24.32	641.75	24.32	705.18	24.32	774.83
24.35	646.73	24.34	707.67	24.36	781.05
24.39	651.70	24.37	711.40	24.40	783.53
24.42	655.43	24.41	716.37	24.45	783.53
24.48	657.92	24.46	718.86	24.52	781.05
24.54	656.67	24.53	720.10	24.55	776.07
24.59	654.19	24.59	715.13	24.59	773.58
24.63	650.46	24.64	712.64	24.62	771.10
24.66	649.21	24.67	708.91	24.64	771.10
24.69	649.21	24.70	706.42	24.68	773.58
24.71	651.70	24.72	705.18	24.73	776.07
24.75	656.67	24.74	706.42	24.76	779.80
24.79	662.89	24.78	711.40	24.81	779.80
24.85	664.14	24.81	716.37	24.86	778.56
24.92	662.89	24.86	717.62	24.92	774.83
24.96	657.92	24.94	717.62	24.96	772.34

Appendix B: Mechanical Characteristics

25.00	655.43	24.99	715.13	24.99	767.36
25.03	651.70	25.03	711.40	25.05	772.34
25.05	652.94	25.06	710.15	25.04	767.36
25.08	655.43	25.09	707.67	25.06	772.34
25.10	659.16	25.11	708.91	25.11	778.56
25.14	664.14	25.14	711.40	25.16	779.80
25.19	667.87	25.17	715.13	25.22	778.56
25.26	667.87	25.22	720.10	25.27	774.83
25.32	664.14	25.27	722.59	25.31	768.61
25.37	659.16	25.35	720.10	25.34	766.12
25.40	656.67	25.41	715.13	25.36	764.88
25.42	654.19	25.44	710.15	25.38	766.12
25.44	654.19	25.47	706.42	25.43	773.58
25.47	657.92	25.49	705.18	25.47	778.56
25.50	664.14	25.52	705.18	25.52	779.80
25.54	667.87	25.54	707.67	25.58	778.56
25.62	674.09	25.57	711.40	25.64	777.31
25.67	667.87	25.61	721.35	25.67	771.10
25.72	664.14	25.66	722.59	25.71	769.85
25.76	661.65	25.71	722.59	25.73	766.12
25.79	660.41	25.78	720.10	25.77	767.36
25.80	659.16	25.83	715.13	25.79	768.61
25.82	661.65	25.87	712.64	25.83	773.58
25.86	666.62	25.90	708.91	25.88	776.07
25.92	670.36	25.93	706.42	25.93	776.07
25.95	669.11	25.96	706.42	25.98	774.83
26.03	670.36	25.98	707.67	26.02	772.34
26.07	666.62	26.01	712.64	26.07	768.61
26.11	664.14	26.06	720.10	26.09	763.63

Appendix B: Mechanical Characteristics

26.13	661.65	26.10	722.59	26.12	763.63
26.16	661.65	26.17	721.35	26.15	766.12
26.19	666.62	26.23	715.13	26.21	771.10
26.23	669.11	26.28	710.15	26.23	768.61
26.27	671.60	26.29	705.18	26.32	769.85
26.34	671.60	26.33	703.94	26.34	762.39
26.39	669.11	26.36	703.94	26.38	758.66
26.44	669.11	26.37	705.18	26.41	756.17
26.45	664.14	26.40	710.15	26.44	754.93
26.48	664.14	26.45	716.37	26.47	757.42
26.51	666.62	26.50	721.35	26.51	762.39
26.54	670.36	26.57	722.59	26.56	763.63
26.56	670.36	26.63	716.37	26.62	761.15
26.64	676.57	26.67	710.15	26.66	756.17
26.70	675.33	26.71	705.18	26.70	752.44
26.75	670.36	26.73	701.45	26.73	751.20
26.78	667.87	26.75	701.45	26.75	753.68
26.81	665.38	26.78	701.45	26.78	757.42
26.84	666.62	26.81	707.67	26.82	763.63
26.86	670.36	26.84	712.64	26.88	767.36
26.89	675.33	26.89	716.37	26.94	764.88
26.94	680.31	26.92	706.42	26.97	756.17
27.00	682.79	27.03	710.15	27.02	754.93
27.05	679.06	27.06	705.18	27.05	752.44
27.11	675.33	27.11	701.45	27.08	753.68
27.14	671.60	27.13	698.96	27.11	757.42
27.17	669.11	27.15	697.72	27.14	764.88
27.19	669.11	27.17	700.20	27.19	764.88
27.22	671.60	27.19	705.18	27.26	759.90

Appendix B: Mechanical Characteristics

27.25	677.82	27.24	710.15	27.30	757.42
27.30	682.79	27.30	711.40	27.32	751.20
27.36	684.04	27.40	715.13	27.36	751.20
27.41	680.31	27.44	705.18	27.38	752.44
27.47	676.57	27.47	697.72	27.42	757.42
27.50	670.36	27.50	691.50	27.47	761.15
27.53	667.87	27.52	687.77	27.53	756.17
27.56	669.11	27.55	689.01	27.58	749.95
27.58	670.36	27.57	692.74	27.62	744.98
27.61	676.57	27.59	698.96	27.64	743.73
27.66	682.79	27.63	705.18	27.67	744.98
27.71	685.28	27.71	707.67	27.70	751.20
27.78	681.55	27.78	702.69	27.74	754.93
27.82	674.09	27.82	697.72	27.79	757.42
27.87	671.60	27.86	692.74	27.85	754.93
27.88	667.87	27.88	690.25	27.90	754.93
27.91	667.87	27.90	686.52	27.93	747.47
27.93	671.60	27.92	691.50	27.97	744.98
27.98	679.06	27.96	698.96	27.99	743.73
28.02	682.79	27.99	707.67	28.02	746.22
28.07	684.04	28.05	708.91	28.06	751.20
28.12	681.55	28.11	708.91	28.10	754.93
28.18	680.31	28.17	705.18	28.16	756.17
28.20	677.82	28.21	701.45	28.22	751.20
28.23	677.82	28.26	696.47	28.26	744.98
28.27	679.06	28.28	693.99	28.29	741.25
28.30	681.55	28.31	692.74	28.32	738.76
28.34	685.28	28.34	693.99	28.34	740.00
28.37	675.33	28.37	697.72	28.37	744.98

Appendix B: Mechanical Characteristics

28.39	667.87	28.40	702.69	28.42	748.71
28.40	664.14	28.45	705.18	28.48	749.95
28.41	656.67	28.52	703.94	28.53	746.22
28.41	651.70	28.53	690.25	28.59	742.49
28.40	647.97	28.60	691.50	28.61	736.27
28.41	646.73	28.64	689.01	28.63	735.03
28.42	644.24	28.66	690.25	28.66	735.03
28.42	641.75	28.69	693.99	28.69	741.25
28.42	640.51	28.73	702.69	28.74	744.98
28.42	639.26	28.77	707.67	28.80	746.22
28.42	636.78	28.83	706.42	28.85	741.25
28.42	638.02	28.84	686.52	28.89	737.52
28.42	636.78	28.85	679.06	28.92	731.30
28.42	636.78	28.87	676.57	28.95	731.30
28.44	638.02	28.86	670.36	29.00	735.03
28.42	635.53	28.86	665.38	29.02	736.27
28.43	634.29	28.86	661.65	29.05	738.76
28.43	634.29	28.87	659.16	29.11	740.00
28.43	635.53	28.89	659.16	29.16	737.52
28.44	634.29	28.89	657.92	29.22	735.03
28.43	633.04	28.87	652.94	29.25	731.30

Appendix B: Mechanical Characteristics

s3	s1	q=sd	q=sd/2	p=(s1+s3)/2	p=(s1+2s3)/3
40.00	747.00	707.00	353.50	393.5	275.67
60.00	1090.00	1030.00	515.00	575	403.33
80.00	1275.00	1195.00	597.50	677.5	478.33

		cos A	sinA	x	y
0	0	1.000	0.000	747.00	0.00
1	0.261799	0.966	0.259	734.95	91.49
2	0.523599	0.866	0.500	699.64	176.75
3	0.785398	0.707	0.707	643.46	249.96
4	1.047198	0.500	0.866	570.25	306.14
5	1.308997	0.259	0.966	484.99	341.45
6	1.570796	0.000	1.000	393.50	353.50
7	1.832596	-0.259	0.966	302.01	341.45
8	2.094395	-0.500	0.866	216.75	306.14
9	2.356194	-0.707	0.707	143.54	249.96
10	2.617994	-0.866	0.500	87.36	176.75
11	2.879793	-0.966	0.259	52.05	91.49
12	3.141593	-1.000	0.000	40.00	0.00
0	0	1.000	0.000	1090.00	0.00
1	0.261799	0.966	0.259	1072.45	133.29
2	0.523599	0.866	0.500	1021.00	257.50
3	0.785398	0.707	0.707	939.16	364.16
4	1.047198	0.500	0.866	832.50	446.00
5	1.308997	0.259	0.966	708.29	497.45

Appendix B: Mechanical Characteristics

6	1.570796	0.000	1.000	575.00	515.00
7	1.832596	-0.259	0.966	441.71	497.45
8	2.094395	-0.500	0.866	317.50	446.00
9	2.356194	-0.707	0.707	210.84	364.16
10	2.617994	-0.866	0.500	129.00	257.50
11	2.879793	-0.966	0.259	77.55	133.29
12	3.141593	-1.000	0.000	60.00	0.00
0	0	1.000	0.000	1275.00	0.00
1	0.261799	0.966	0.259	1254.64	154.64
2	0.523599	0.866	0.500	1194.95	298.75
3	0.785398	0.707	0.707	1100.00	422.50
4	1.047198	0.500	0.866	976.25	517.45
5	1.308997	0.259	0.966	832.14	577.14
6	1.570796	0.000	1.000	677.50	597.50
7	1.832596	-0.259	0.966	522.86	577.14
8	2.094395	-0.500	0.866	378.75	517.45
9	2.356194	-0.707	0.707	255.00	422.50
10	2.617994	-0.866	0.500	160.05	298.75
11	2.879793	-0.966	0.259	100.36	154.64
12	3.141593	-1.000	0.000	80.00	0.00

Appendix B: Mechanical Characteristics

Mohr Failure Envelope												
n	1	2	3	4	5	6	7	8	9	10	x	y
Test no.	s_1	$(s_1)^2$	s_3	$(s_3)^2$	s_1+s_3	s_1s_3	$(s_1+s_3)s_1$	$(s_1+s_3)s_3$	$(n^*(2))-(1)^2$	$(n^*(4))-(3)^2$	0	31.91
1	747.00	558009	40.00	1600	787.00	29880	587889	31480	430658	2400	747	1296.87
2	1090.00	1188100	60.00	3600	1150.00	65400	1253500	69000			1090	1877.70
3	1275.00	1625625	80.00	6400	1355.00	102000	1727625	108400			1275	2190.98
3	3112.00	3371734.00	180.00	11600.00	3292.00	197280.00	3569014.00	208880.00				

s3	s1	q=sd	q=sd/2	p=(s1+s3)/2	p=(s1+2s3)/3
50.00	1080.00	1030.00	515.00	565	393.33
100.00	1240.00	1140.00	570.00	670	480.00
150.00	1600.00	1450.00	725.00	875	633.33

Appendix B: Mechanical Characteristics

		cos A	sinA	x	y
0	0	1.000	0.000	1080.00	0.00
1	0.261799	0.966	0.259	1062.45	133.29
2	0.523599	0.866	0.500	1011.00	257.50
3	0.785398	0.707	0.707	929.16	364.16
4	1.047198	0.500	0.866	822.50	446.00
5	1.308997	0.259	0.966	698.29	497.45
6	1.570796	0.000	1.000	565.00	515.00
7	1.832596	-0.259	0.966	431.71	497.45
8	2.094395	-0.500	0.866	307.50	446.00
9	2.356194	-0.707	0.707	200.84	364.16
10	2.617994	-0.866	0.500	119.00	257.50
11	2.879793	-0.966	0.259	67.55	133.29
12	3.141593	-1.000	0.000	50.00	0.00
0	0	1.000	0.000	1240.00	0.00
1	0.261799	0.966	0.259	1220.58	147.53
2	0.523599	0.866	0.500	1163.63	285.00
3	0.785398	0.707	0.707	1073.05	403.05
4	1.047198	0.500	0.866	955.00	493.63
5	1.308997	0.259	0.966	817.53	550.58
6	1.570796	0.000	1.000	670.00	570.00
7	1.832596	-0.259	0.966	522.47	550.58
8	2.094395	-0.500	0.866	385.00	493.63
9	2.356194	-0.707	0.707	266.95	403.05
10	2.617994	-0.866	0.500	176.37	285.00
11	2.879793	-0.966	0.259	119.42	147.53
12	3.141593	-1.000	0.000	100.00	0.00

Appendix B: Mechanical Characteristics

0	0	1.000	0.000	1600.00	0.00
1	0.261799	0.966	0.259	1575.30	187.64
2	0.523599	0.866	0.500	1502.87	362.50
3	0.785398	0.707	0.707	1387.65	512.65
4	1.047198	0.500	0.866	1237.50	627.87
5	1.308997	0.259	0.966	1062.64	700.30
6	1.570796	0.000	1.000	875.00	725.00
7	1.832596	-0.259	0.966	687.36	700.30
8	2.094395	-0.500	0.866	512.50	627.87
9	2.356194	-0.707	0.707	362.35	512.65
10	2.617994	-0.866	0.500	247.13	362.50
11	2.879793	-0.966	0.259	174.70	187.64
12	3.141593	-1.000	0.000	150.00	0.00

Mohr Failure Envelope												
n	1	2	3	4	5	6	7	8	9	10	x	y
Test no.	s_1	$(s_1)^2$	s_3	$(s_3)^2$	s_1+s_3	s_1s_3	$(s_1+s_3)s_1$	$(s_1+s_3)s_3$	$(n^*(2))- (1)^2$	$(n^*(4))- (3)^2$	0	167.68
1	1080.0 0	1166400	50.00	2500	1130.0 0	54000	1220400	56500	425600	15000	108 0	1180.0 0
2	1240.0 0	1537600	100.0 0	10000	1340.0 0	124000	1661600	134000			124 0	1329.9 8
3	1600.0 0	2560000	150.0 0	22500	1750.0 0	240000	2800000	262500			160 0	1667.4 2
3	3920.0 0	5264000.0 0	300.0 0	35000.0 0	4220.0 0	418000.0 0	5682000.0 0	453000.0 0				

Appendix B: Mechanical Characteristics

APPENDIX B (Mechanical Characterisations) Resilient Modulus Test

Testing sequence	Deviator stress (kPa)	confining stress (kPa)	Bulk stress (kPa)	CRB	100%OMC&7dHyd	90%OMC&7dHyd	80%OMC&7dHyd
0	50	100	150	132.35	435.80	415.05	585.80
1	75	150	225	174.37	529.05	537.66	665.19
2	100	200	300	210.75	625.88	633.09	768.99
3	125	250	375	242.34	719.67	714.76	867.57
4	150	300	450	275.82	817.54	795.07	976.01
5	100	200	300	203.33	632.82	610.89	756.09
6	50	150	200	143.10	448.90	419.57	575.26
7	75	225	300	188.42	577.96	539.52	703.97
8	100	300	400	233.31	700.07	653.25	841.57
9	125	375	500	273.34	815.60	764.37	974.00
10	150	450	600	309.69	929.94	869.94	1096.02
11	75	225	300	185.21	573.92	535.44	692.67
12	40	125	165	123.17	399.13	372.79	518.04
13	30	100	130	107.28	353.24	330.83	476.41
14	40	150	190	132.98	415.34	384.11	543.97
15	50	200	250	158.22	483.04	447.03	609.48
16	75	300	375	213.32	633.09	576.44	766.09
17	100	400	500	264.90	773.96	709.04	925.57
18	125	500	625	310.15	908.12	829.42	1079.36
19	75	300	375	210.61	630.25	569.17	756.08
20	30	125	155	114.03	369.65	335.98	488.19
21	20	100	120	96.89	321.37	292.44	439.91
22	30	150	180	124.24	388.40	351.17	515.80

Appendix B: Mechanical Characteristics

23	40	200	240	150.36	455.36	414.04	580.45
24	50	250	300	178.41	522.61	472.36	650.42
25	75	375	450	240.58	691.59	627.72	833.44
26	100	500	600	295.96	857.45	771.11	1019.02
27	50	250	300	176.16	525.75	465.63	636.73
28	30	180	210	134.13	413.99	366.39	531.53
29	50	300	350	194.34	566.93	505.26	701.64
30	75	450	525	265.08	759.22	676.93	910.53
31	50	300	350	193.67	567.59	503.19	695.91
32	30	180	210	133.86	413.80	366.70	532.18
33	40	250	290	168.62	502.26	442.10	624.96
34	30	210	240	145.50	441.36	390.04	562.32
35	40	280	320	182.13	529.15	470.60	664.84
36	50	350	400	216.39	621.03	552.65	758.32
37	75	525	600	288.87	826.88	695.18	989.29
38	40	280	320	179.61	527.30	460.99	655.40
39	20	150	170	114.83	367.99	317.01	479.74
40	30	245	275	159.87	471.56	414.72	592.26
41	40	325	365	199.18	571.52	501.80	705.95
42	50	400	450	235.29	663.13	584.54	808.48
43	30	245	275	160.49	473.43	415.60	594.37
44	20	185	205	129.22	399.69	346.21	513.90
45	30	275	305	173.85	504.80	441.03	630.75
46	40	370	410	219.90	618.55	545.75	761.84
47	50	450	500	255.55	717.32	627.01	865.78
48	30	275	305	172.67	505.04	437.54	626.07
49	20	225	245	147.17	434.45	381.42	553.25
50	30	335	365	199.35	565.02	496.62	698.18
51	40	450	490	249.20	698.63	572.77	844.92

Appendix B: Mechanical Characteristics

52	50	550	600	284.60	803.59	700.82	974.64
53	20	250	270	155.52	457.50	394.54	574.51
54	30	375	405	212.87	597.99	489.14	736.42
55	40	500	540	263.32	743.37	639.61	894.12
56	20	300	320	176.06	504.50	438.68	633.63
57	30	450	480	240.71	671.08	590.55	816.24
58	40	600	640	283.96	823.53	711.55	987.45
59	30	500	530	249.66	713.85	610.74	862.23
60	20	350	370	192.05	550.33	481.14	687.03
61	30	550	580	263.11	761.72	657.08	919.40
62	20	375	395	200.57	574.37	503.97	708.60
63	30	575	605	268.25	780.01	678.09	930.12
64	20	400	420	207.06	596.44	519.17	736.81
65	20	500	520	243.47	694.97	605.84	848.04

Testing sequence	Deviator stress (kPa)	confining stress (kPa)	Bulk stress (kPa)	CRB	100%OMC&14d Hyd	90%OMC&14d Hyd	80%OMC&14d Hyd
0	50	100	150	132.347	562.738	454.278	530.521
1	75	150	225	174.372	657.656	544.614	664.926
2	100	200	300	210.745	770.914	634.415	785.324
3	125	250	375	242.344	916.35	722.023	910.233
4	150	300	450	275.823	1008.365	798.19	1034.574
5	100	200	300	203.326	777.076	630.946	778.425
6	50	150	200	143.102	558.554	457.091	581.206
7	75	225	300	188.423	704.688	567.888	738.736
8	100	300	400	233.306	867.556	678.105	901.41
9	125	375	500	273.342	999.66	778.504	1049.974
10	150	450	600	309.688	1108.306	874.613	1186.766

Appendix B: Mechanical Characteristics

11	75	225	300	185.212	726.538	565.951	735.108
12	40	125	165	123.172	513.396	411.578	522.451
13	30	100	130	107.28	470.949	378.344	470.215
14	40	150	190	132.98	525.216	424.133	556.007
15	50	200	250	158.219	606.963	483.055	641.123
16	75	300	375	213.323	788.598	611.217	828.365
17	100	400	500	264.902	948.447	737.553	1009.174
18	125	500	625	310.145	1088.612	849.137	1174.975
19	75	300	375	210.613	791.525	609.992	823.429
20	30	125	155	114.031	480.954	385.464	492.521
21	20	100	120	96.889	434.699	348.025	442.393
22	30	150	180	124.243	491.722	398.689	528.246
23	40	200	240	150.359	580.799	450.762	614.98
24	50	250	300	178.408	652.897	514.641	700.435
25	75	375	450	240.584	852.545	662.989	918.114
26	100	500	600	295.963	1033.883	805.428	1116.324
27	50	250	300	176.164	661.303	514.882	697.794
28	30	180	210	134.129	531.374	416.389	558.511
29	50	300	350	194.343	718.184	552.281	762.546
30	75	450	525	265.083	928.472	724.474	1000.33
31	50	300	350	193.672	712.189	551.488	761.673
32	30	180	210	133.86	528.223	417.04	562.64
33	40	250	290	168.621	641.262	492.293	674.984
34	30	210	240	145.499	570.896	441.685	604.525
35	40	280	320	182.125	676.282	519.057	718.242
36	50	350	400	216.387	773.51	598.356	832.691
37	75	525	600	288.867	1004.476	775.142	1086.369
38	40	280	320	179.612	674.021	516.288	710.723
39	20	150	170	114.833	468.942	370.113	502.798

Appendix B: Mechanical Characteristics

40	30	245	275	159.872	598.14	463.271	644.535
41	40	325	365	199.179	719.516	553.178	771.798
42	50	400	450	235.285	823.881	634.445	890.113
43	30	245	275	160.488	602.723	464.852	644.067
44	20	185	205	129.218	507.462	400.544	546.527
45	30	275	305	173.852	647.903	493.47	687.717
46	40	370	410	219.895	773.749	592.925	833.592
47	50	450	500	255.549	883.894	681.902	955.308
48	30	275	305	172.674	639.778	492.775	685.347
49	20	225	245	147.171	563.82	429.741	598.02
50	30	335	365	199.346	714.225	547.388	764.8
51	40	450	490	249.203	863.148	661.381	930.674
52	50	550	600	284.604	982.152	756.156	1065.477
53	20	250	270	155.522	587.488	450.599	625.603
54	30	375	405	212.871	750.273	576.131	810.124
55	40	500	540	263.32	908.975	702.191	984.426
56	20	300	320	176.058	646.321	492.655	689.095
57	30	450	480	240.705	834.363	647.462	903.844
58	40	600	640	283.958	998.373	779.47	1078.188
59	30	500	530	249.658	881.582	679.653	943.574
60	20	350	370	192.045	695.017	538.287	748.305
61	30	550	580	263.114	893.587	727.419	1003.367
62	20	375	395	200.571	722.571	560.277	779.861
63	30	575	605	268.249	960.508	701.017	1032.092
64	20	400	420	207.056	754.628	582.668	806.071
65	20	500	520	243.465	864.247	672.319	929.463

Appendix B: Mechanical Characteristics

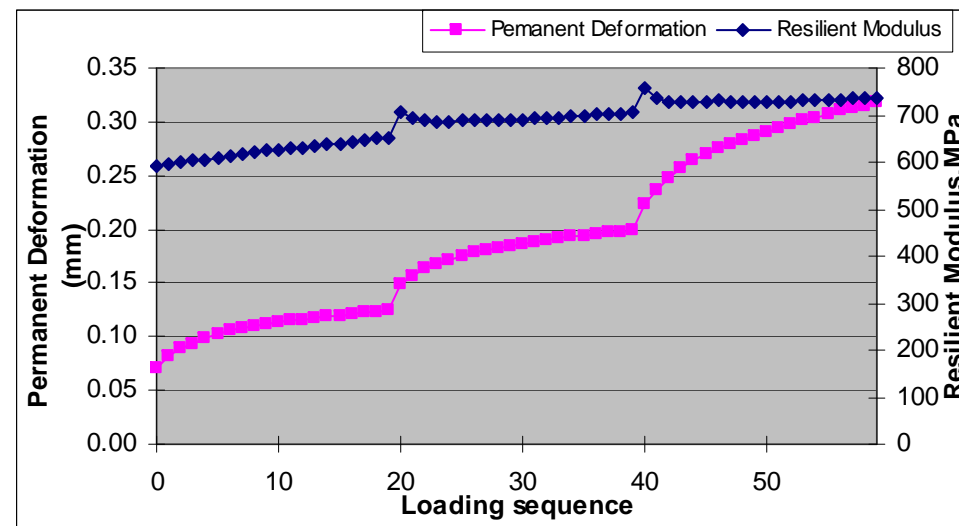
Testing sequence	Deviator stress (kPa)	confining stress (kPa)	Bulk stress (kPa)	CRB	100%OMC&30d Hyd	90%OMC&30d Hyd	80%OMC&30d Hyd
0	50	100	150	132.347	325.136	530.521	411.712
1	75	150	225	174.372	391.673	664.926	532.319
2	100	200	300	210.745	444.394	785.324	635.095
3	125	250	375	242.344	497.873	910.233	738.426
4	150	300	450	275.823	557.47	1034.574	830.385
5	100	200	300	203.326	429.184	778.425	615.796
6	50	150	200	143.102	308.949	581.206	444.847
7	75	225	300	188.423	387.471	738.736	582.434
8	100	300	400	233.306	467.097	901.41	718.948
9	125	375	500	273.342	549.124	1049.974	844.923
10	150	450	600	309.688	637.78	1186.766	968.707
11	75	225	300	185.212	382.593	735.108	575.216
12	40	125	165	123.172	269.956	522.451	389.007
13	30	100	130	107.28	237.064	470.215	335.837
14	40	150	190	132.98	281.612	556.007	414.218
15	50	200	250	158.219	327.818	641.123	486.62
16	75	300	375	213.323	422.777	828.365	651.154
17	100	400	500	264.902	525.229	1009.174	808.168
18	125	500	625	310.145	625.217	1174.975	955.919
19	75	300	375	210.613	421.565	823.429	646.909
20	30	125	155	114.031	243.933	492.521	358.807
21	20	100	120	96.889	214.307	442.393	314.412
22	30	150	180	124.243	261.413	528.246	385.644
23	40	200	240	150.359	306.598	614.98	458.119
24	50	250	300	178.408	353.675	700.435	539.383
25	75	375	450	240.584	470.072	918.114	725

Appendix B: Mechanical Characteristics

26	100	500	600	295.963	589.279	1116.324	906.911
27	50	250	300	176.164	351.035	697.794	535.261
28	30	180	210	134.129	277.046	558.511	413.058
29	50	300	350	194.343	383.352	762.546	590.406
30	75	450	525	265.083	519.481	1000.33	804.916
31	50	300	350	193.672	382.485	761.673	589.525
32	30	180	210	133.86	276.995	562.64	415.304
33	40	250	290	168.621	336.373	674.984	511.928
34	30	210	240	145.499	297.466	604.525	449.249
35	40	280	320	182.125	359.966	718.242	549.122
36	50	350	400	216.387	421.173	832.691	649.29
37	75	525	600	288.867	568.044	1086.369	885.075
38	40	280	320	179.612	354.234	710.723	544.639
39	20	150	170	114.833	241.297	502.798	360.123
40	30	245	275	159.872	318.345	644.535	484.411
41	40	325	365	199.179	387.726	771.798	598.434
42	50	400	450	235.285	454.281	890.113	704.107
43	30	245	275	160.488	318.486	644.067	483.526
44	20	185	205	129.218	266.625	546.527	399.006
45	30	275	305	173.852	342.623	687.717	522.308
46	40	370	410	219.895	424.498	833.592	652.768
47	50	450	500	255.549	493.797	955.308	766.225
48	30	275	305	172.674	340.424	685.347	521.525
49	20	225	245	147.171	295.383	598.02	445.39
50	30	335	365	199.346	389.486	764.8	593.81
51	40	450	490	249.203	484.17	930.674	742.578
52	50	550	600	284.604	558.216	1065.477	870.183
53	20	250	270	155.522	311.099	625.603	470.244
54	30	375	405	212.871	416.248	810.124	637.702

Appendix B: Mechanical Characteristics

55	40	500	540	263.32	513.901	984.426	791.44
56	20	300	320	176.058	349.939	689.095	530.927
57	30	450	480	240.705	475.555	903.844	723.063
58	40	600	640	283.958	579.05	1078.188	886.325
59	30	500	530	249.658	504.77	943.574	767.351
60	20	350	370	192.045	387.01	748.305	585.289
61	30	550	580	263.114	543.221	1003.367	816.827
62	20	375	395	200.571	406.764	779.861	613.428
63	30	575	605	268.249	553.367	1032.092	844.782
64	20	400	420	207.056	425.233	806.071	644.159
65	20	500	520	243.465	605.844	929.463	754.071

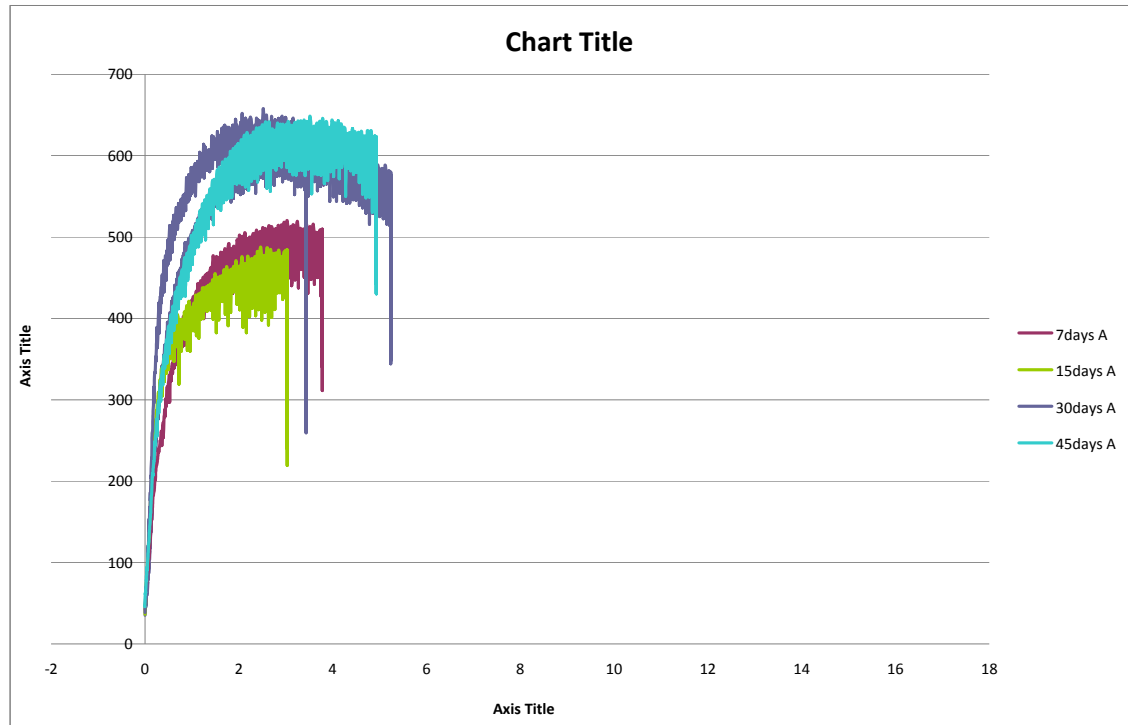


	Sample A OMC from part 1				
	Resilent modulus				
Loading Sequences	5A	7A	15A	30A	45A
0	160.606	154.027	153.79	153.583	144.271
1	93.912	86.364	80.58	76.456	67.75
2	115.767	111.151	106.426	106.614	86.989
3	140.363	132.453	134.045	131.933	110.422
4	109.502	104.251	107.174	104.189	88.718
5	148.556	140.971	145.447	142.131	122.394
6	174.832	166.103	169.468	167.942	148.18
7	139.921	134.848	137.317	133.975	126.419
8	196.862	193.176	194.518	196.4	177.791
9	239.932	231.594	229.208	243.087	217.549
10	136.446	130.722	122.094	128.621	133.177
11	165.779	157.848	152.578	159	154.835
12	247.99	237.173	234.712	249.573	228.665
13	172.11	171.737	155.577	167.411	176.402
14	205.168	201.137	189.364	201.536	200.914
15	293.909	287.158	280.057	299.038	280.132

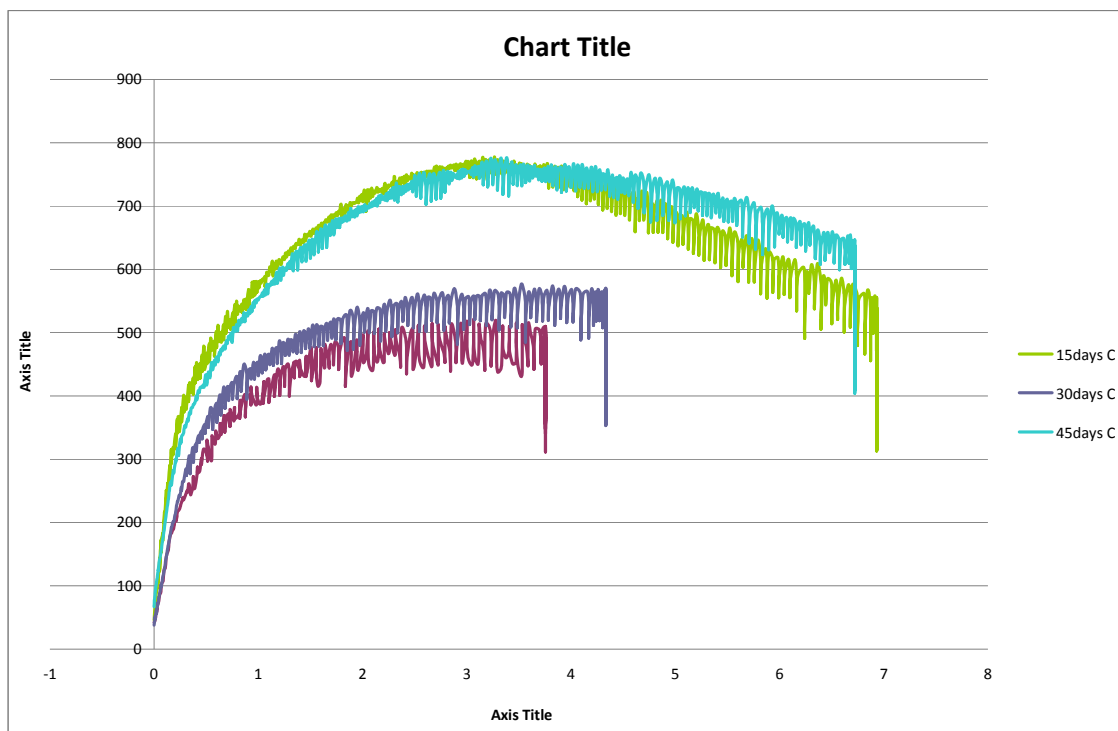
	Sample B back to 8%				
	Resilent modulus				
Loading Sequences	5B	7B	15B	30B	45B
0	97.657	83.11	102.758	72.079	97.015
1	61.214	55.077	68.014	32.385	60.625
2	77.207	63.638	81.676	45.974	74.179
3	84.399	60.259	92.097	59.125	78.213
4	64.836	50.041	68.95	37.524	63.802
5	92.12	61.03	93.14	62.104	82.861
6	94.147	0	103.925	73.022	
7	76.34	0	83.302	60.019	
8	105.395		118.934	94.034	
9			134.338		
10			93.333		
11			105.075		
12			142.417		
13			123.565		
14			136.831		
15			171.496		

Appendix B: Mechanical Characteristics

	Sample C the original omc				
	Resilent modulus				
Loading Sequences	5C	7C	15C	30C	45C
0	93.498	150.705	189.044	148.154	169.787
1	60.477	59.373	99.799	75.775	83.72
2	74.21	91.357	116.179	97.775	91.807
3	85.535	125.351	141.911	122.038	115.316
4	65.807	108.232	134.759	97.155	104.034
5	89.208	142.025	160.238	133	128.451
6	102.159	171.784	187.953	160.717	156.194
7	84.582	152.251	189.346	131.879	175.533
8	121.68	206.476	233.345	185.733	198.949
9	127.009	249.214	276.759	224.225	240.182
10	84.103	145.944	201.064	129.754	215.675
11	100.706	173.865	222.441	150.969	214.843
12	140.592	263.739	300.199	230.088	272.52
13	111.964	182.847	244.609	163.442	275.205
14	129.558	216.72	272.626	189.37	286.109
15	169.324	308.965	363.262	275.59	350.647



Appendix B: Mechanical Characteristics



Appendix B: Mechanical Characteristics

APPENDIX B (Mechanical Characterisations) Permanent Deformation Test

Testing sequence Mean and Std. Deviation data:				
Sequence	Axial permanent deform'n (mm)			
	7day Hyd	14 day Hyd	28 day Hyd	CRB
0	0.071	0.987	0.751	1.378
1	0.081	1.027	0.818	1.521
2	0.089	1.05	0.855	1.604
3	0.094	1.066	0.881	1.662
4	0.099	1.077	0.9	1.707
5	0.102	1.085	0.915	1.743
6	0.106	1.092	0.927	1.773
7	0.108	1.098	0.938	1.798
8	0.11	1.102	0.948	1.821
9	0.112	1.107	0.956	1.84
10	0.113	1.111	0.964	1.856
11	0.115	1.113	0.97	1.871
12	0.116	1.116	0.975	1.881
13	0.117	1.118	0.98	1.89
14	0.119	1.121	0.984	1.898
15	0.12	1.125	0.988	1.905
16	0.121	1.127	0.993	1.913
17	0.122	1.129	0.995	1.92
18	0.123	1.132	0.999	1.926
19	0.124	1.132	1.002	1.933
20	0.149	1.168	1.09	2.183
21	0.156	1.182	1.145	2.334
22	0.163	1.192	1.18	2.419
23	0.168	1.202	1.207	2.477
24	0.172	1.212	1.225	2.52
25	0.175	1.219	1.239	2.55
26	0.179	1.228	1.252	2.575
27	0.181	1.234	1.261	2.595
28	0.183	1.239	1.269	2.612
29	0.185	1.245	1.276	2.625
30	0.187	1.248	1.283	2.638
31	0.188	1.251	1.289	2.649
32	0.19	1.253	1.294	2.659
33	0.191	1.256	1.3	2.669
34	0.193	1.259	1.304	2.677
35	0.194	1.262	1.308	2.687
36	0.196	1.265	1.311	2.692
37	0.197	1.268	1.315	2.7
38	0.198	1.271	1.318	2.706
39	0.199	1.273	1.323	2.713

Appendix B: Mechanical Characteristics

40	0.224	1.304	1.402	2.853
41	0.237	1.322	1.465	2.996
42	0.248	1.335	1.509	3.117
43	0.257	1.351	1.539	3.201
44	0.264	1.359	1.56	3.261
45	0.27	1.366	1.576	3.308
46	0.275	1.371	1.59	3.347
47	0.279	1.375	1.602	3.38
48	0.283	1.38	1.613	3.408
49	0.287	1.384	1.624	3.433
50	0.291	1.389	1.634	3.456
51	0.295	1.393	1.64	3.476
52	0.298	1.397	1.65	3.495
53	0.301	1.4	1.658	3.51
54	0.304	1.404	1.665	3.527
55	0.307	1.406	1.673	3.54
56	0.31	1.408	1.681	3.552
57	0.313	1.41	1.686	3.563
58	0.315	1.411	1.692	3.574
59	0.318	1.41	1.698	3.584

Permanent Deformation				
5A	7A	15A	30A	45A
1.548	2.131	2.502	2.163	1.767
1.554	2.146	2.438	2.143	1.671
1.658	2.331	2.562	2.34	1.794
1.825	2.605	2.759	2.577	1.955
1.803	2.578	2.742	2.551	1.931
1.9	2.727	2.87	2.681	2.045
2.182	3.183	3.305	3.065	2.38
2.145	3.147	3.299	3.024	2.355
2.452	3.616	3.758	3.404	2.696
3.014	4.545	4.771	4.233	3.316
2.904	4.401	4.647	4.083	3.196
2.953	4.469	4.718	4.155	3.244
3.22	4.777	5.037	4.51	3.445
3.169	4.705	4.971	4.432	3.394
3.209	4.746	5.018	4.479	3.423
3.583	5.035	5.371	4.856	3.613

Appendix B: Mechanical Characteristics

Permanent Deformation				
5B	7B	15B	30B	45B
6.561	9.338	5.519	8.041	10.638
6.785	9.8	5.6	8.189	10.836
7.325	10.988	5.919	8.774	11.566
8.248	16.424	6.689	11.08	13.804
8.221	16.646	6.642	11.037	13.835
8.93	20.203	7.117	12.174	15.368
12.907	26.28	9.156	18.921	
13.189	26.28	9.053	19.288	
15.891		10.273	21.928	
17.861		13.308	26.382	
17.861		12.976	26.382	
		13.134	26.382	
		13.886		
		13.743		
		13.808		
		14.346		

Permanent Deformation				
5C	7C	15C	30C	45C
9.076	2.169	0.821	2.051	0.977
9.1	1.995	0.694	2.006	0.835
9.277	2.152	0.783	2.138	0.953
9.782	2.331	0.901	2.319	1.086
9.725	2.319	0.892	2.296	1.071
10.151	2.411	0.947	2.4	1.139
12.062	2.748	1.161	2.743	1.351
12.044	2.736	1.157	2.709	1.355
13.577	3.083	1.356	3.105	1.509
19.166	3.912	1.848	3.972	1.87
18.986	3.803	1.785	3.83	1.827
19.225	3.856	1.811	3.89	1.842
20.525	4.085	1.946	4.206	1.936
20.411	4.029	1.918	4.135	1.928
20.53	4.068	1.937	4.174	1.939
21.81	4.49	2.113	4.53	2.031

APPENDIX C: SHAKEDOWN CHARACTERISATION

APPENDIX C
(Shakedown Characterisation)
CRB with Various Stress Levels

5				6			
Permanent Deformation	Resilient Strain 10-3	Permanent strain10-3	Strain Rate	Permanent Deformation	Resilient Strain 10-3	Permanent strain10-3	Strain Rate
0.00000	0.68800	0.00000	0.00000	0.00000	0.67000	0.00000	0.00000
0.25400	0.72200	1.27100	0.00662	0.33300	0.85800	1.66310	0.01732
0.31900	0.71500	1.59750	0.00170	0.41400	0.85800	2.07110	0.00425
0.35900	0.71000	1.79380	0.00102	0.46500	0.85100	2.32440	0.00264
0.38600	0.70600	1.93010	0.00071	0.50000	0.84100	2.49780	0.00181
0.40600	0.69900	2.02850	0.00051	0.52400	0.83500	2.62220	0.00130
0.42000	0.69300	2.10130	0.00038	0.54500	0.83100	2.72290	0.00105
0.43200	0.69200	2.16010	0.00031	0.56100	0.83200	2.80630	0.00087
0.44300	0.69100	2.21430	0.00028	0.57600	0.82900	2.87930	0.00076
0.45200	0.69200	2.26210	0.00025	0.58800	0.82700	2.94220	0.00066
0.46100	0.69200	2.30510	0.00022	0.60000	0.82700	3.00070	0.00061
0.46900	0.69000	2.34720	0.00022	0.61100	0.82700	3.05280	0.00054
0.47700	0.68700	2.38380	0.00019	0.62000	0.82400	3.10140	0.00051
0.48300	0.68900	2.41730	0.00017	0.62900	0.82300	3.14450	0.00045
0.49000	0.67800	2.45170	0.00018	0.63700	0.82200	3.18460	0.00042
0.49500	0.67900	2.47600	0.00013	0.64500	0.82300	3.22270	0.00040
0.50000	0.68000	2.49840	0.00012	0.65100	0.82400	3.25630	0.00035
0.50400	0.68500	2.51890	0.00011	0.65800	0.82300	3.28860	0.00034
0.50900	0.68600	2.54370	0.00013	0.66400	0.82100	3.32100	0.00034
0.51300	0.68500	2.56700	0.00012	0.67000	0.82300	3.34870	0.00029
0.51800	0.68200	2.59040	0.00012	0.67600	0.81900	3.37750	0.00030
0.52200	0.68100	2.61100	0.00011	0.68100	0.81500	3.40600	0.00030
0.52700	0.67600	2.63330	0.00012	0.68500	0.82000	3.42250	0.00017
0.53100	0.67100	2.65410	0.00011	0.69000	0.81600	3.44850	0.00027

Appendix C: Shakedown Characteristics

0.53300	0.67300	2.66630	0.00006	0.69400	0.81700	3.46970	0.00022
0.53600	0.67600	2.67840	0.00006	0.69800	0.81900	3.48850	0.00020
0.53900	0.67700	2.69340	0.00008	0.70200	0.81900	3.50840	0.00021
0.54200	0.67800	2.70790	0.00008	0.70500	0.82400	3.52300	0.00015
0.54500	0.67700	2.72290	0.00008	0.70800	0.82500	3.54000	0.00018
0.54800	0.67800	2.73760	0.00008	0.71200	0.82700	3.55860	0.00019
0.55000	0.67600	2.75180	0.00007	0.71700	0.81800	3.58380	0.00026
0.55400	0.67000	2.77020	0.00010	0.72000	0.82300	3.59800	0.00015
0.55700	0.66800	2.78320	0.00007	0.72400	0.81800	3.62010	0.00023
0.55900	0.66800	2.79320	0.00005	0.72700	0.82000	3.63550	0.00016
0.56100	0.66900	2.80420	0.00006	0.73000	0.82000	3.65190	0.00017
0.56300	0.67100	2.81300	0.00005	0.73300	0.82100	3.66540	0.00014
0.56500	0.67100	2.82390	0.00006	0.73700	0.81200	3.68670	0.00022
0.56700	0.66900	2.83580	0.00006	0.73800	0.82000	3.68980	0.00003
0.56900	0.66900	2.84710	0.00006	0.74200	0.81300	3.70960	0.00021
0.57200	0.66800	2.85860	0.00006	0.74500	0.81100	3.72350	0.00014
0.57500	0.66000	2.87490	0.00008	0.74600	0.81700	3.73000	0.00007
0.57700	0.66000	2.88340	0.00004	0.74900	0.81200	3.74660	0.00017
0.57800	0.66200	2.89000	0.00003	0.75100	0.81400	3.75680	0.00011
0.58000	0.66300	2.89780	0.00004	0.75400	0.81400	3.76850	0.00012
0.58100	0.66400	2.90530	0.00004	0.75600	0.81300	3.78040	0.00012
0.58300	0.66600	2.91310	0.00004	0.75800	0.81800	3.78870	0.00009
0.58400	0.66400	2.92240	0.00005	0.76000	0.81600	3.80010	0.00012
0.58600	0.66300	2.93160	0.00005	0.76200	0.82000	3.80920	0.00009
0.58900	0.66000	2.94280	0.00006	0.76400	0.82000	3.82030	0.00012
0.59100	0.65200	2.95660	0.00007	0.76600	0.82100	3.82840	0.00008
0.59200	0.65400	2.96100	0.00002	0.76700	0.82300	3.83710	0.00009
0.59300	0.65600	2.96620	0.00003	0.77000	0.81700	3.85170	0.00015
0.59400	0.65800	2.97150	0.00003	0.77400	0.80600	3.87020	0.00019
0.59500	0.65900	2.97740	0.00003	0.77500	0.80700	3.87750	0.00008
0.59700	0.66000	2.98380	0.00003	0.77800	0.80600	3.88750	0.00010
0.59800	0.65800	2.99190	0.00004	0.77900	0.80800	3.89350	0.00006

Appendix C: Shakedown Characteristics

0.60000	0.65800	2.99950	0.00004	0.78100	0.80700	3.90260	0.00009
0.60200	0.65400	3.01040	0.00006	0.78200	0.80900	3.91000	0.00008
0.60400	0.64700	3.02100	0.00006	0.78400	0.80700	3.91860	0.00009
0.60500	0.65000	3.02460	0.00002	0.78500	0.80800	3.92720	0.00009
0.60600	0.65300	3.02830	0.00002	0.78700	0.80800	3.93450	0.00008
0.60700	0.65400	3.03330	0.00003	0.78800	0.80900	3.94200	0.00008
0.60800	0.65500	3.03830	0.00003	0.79000	0.81000	3.94980	0.00008
0.60900	0.65500	3.04460	0.00003	0.79100	0.81200	3.95600	0.00006
0.61000	0.65400	3.05150	0.00004	0.79300	0.81200	3.96470	0.00009
0.61100	0.65400	3.05720	0.00003	0.79500	0.81000	3.97310	0.00009
0.61400	0.64600	3.07050	0.00007	0.79600	0.81400	3.97790	0.00005
0.61500	0.64400	3.07720	0.00003	0.79800	0.81000	3.98900	0.00012
0.61600	0.64600	3.07960	0.00001	0.80000	0.80300	4.00130	0.00013
0.61700	0.64900	3.08290	0.00002	0.80200	0.80100	4.01000	0.00009
0.61700	0.65100	3.08660	0.00002	0.80300	0.80100	4.01640	0.00007
0.61800	0.65100	3.09100	0.00002	0.80400	0.80100	4.02170	0.00006
0.61900	0.65100	3.09660	0.00003	0.80600	0.80100	4.02870	0.00007
0.62100	0.65000	3.10300	0.00003	0.80700	0.80200	4.03440	0.00006
0.62200	0.65000	3.10900	0.00003	0.80800	0.80300	4.03980	0.00006
0.62400	0.64100	3.12150	0.00007	0.80900	0.80400	4.04540	0.00006
0.62500	0.64100	3.12610	0.00002	0.81000	0.80500	4.05150	0.00006
0.62600	0.64300	3.12840	0.00001	0.81100	0.80600	4.05660	0.00005
0.62600	0.64500	3.13090	0.00001	0.81200	0.80700	4.06220	0.00006
0.62700	0.64700	3.13420	0.00002	0.81400	0.80700	4.06920	0.00007
0.62800	0.64800	3.13750	0.00002	0.81500	0.80600	4.07600	0.00007
0.62900	0.64700	3.14250	0.00003	0.81700	0.80600	4.08260	0.00007
0.63000	0.64700	3.14790	0.00003	0.81800	0.80600	4.08910	0.00007
0.63100	0.64500	3.15470	0.00004	0.81900	0.80600	4.09500	0.00006
0.63300	0.63600	3.16690	0.00006	0.82100	0.80100	4.10550	0.00011
0.63400	0.63800	3.16860	0.00001	0.82200	0.80200	4.11010	0.00005
0.63400	0.64000	3.17060	0.00001	0.82300	0.80000	4.11720	0.00007
0.63500	0.64200	3.17320	0.00001	0.82500	0.79700	4.12610	0.00009

Appendix C: Shakedown Characteristics

0.63500	0.64300	3.17510	0.00001	0.82700	0.79300	4.13360	0.00008
0.63600	0.64600	3.17770	0.00001	0.82800	0.79400	4.13780	0.00004
0.63700	0.64400	3.18320	0.00003	0.82800	0.79400	4.14170	0.00004
0.63700	0.64400	3.18740	0.00002	0.82900	0.79600	4.14570	0.00004
0.63900	0.64100	3.19570	0.00004	0.83000	0.79700	4.14990	0.00004
0.64100	0.63200	3.20610	0.00005	0.83100	0.79700	4.15410	0.00004
0.64100	0.63500	3.20740	0.00001	0.83200	0.79900	4.15830	0.00004
0.64200	0.63700	3.20870	0.00001	0.83300	0.80000	4.16260	0.00004
0.64200	0.63900	3.21050	0.00001	0.83300	0.80100	4.16680	0.00004
0.64300	0.64000	3.21330	0.00001	0.83400	0.80200	4.17150	0.00005
0.64300	0.64100	3.21630	0.00002	0.83500	0.80200	4.17650	0.00005
0.64400	0.64100	3.22060	0.00002	0.83600	0.80200	4.18190	0.00006
0.64500	0.64100	3.22530	0.00002	0.83700	0.80100	4.18750	0.00006
0.64700	0.63300	3.23620	0.00006	0.83800	0.80100	4.19180	0.00004
0.64800	0.63000	3.24220	0.00003	0.83900	0.80200	4.19720	0.00006
0.64900	0.63300	3.24310	0.00000	0.84200	0.79600	4.20790	0.00011
0.64900	0.63400	3.24460	0.00001	0.84300	0.79200	4.21540	0.00008
0.64900	0.63600	3.24680	0.00001	0.84400	0.79000	4.22080	0.00006
0.65000	0.63800	3.24850	0.00001	0.84500	0.79100	4.22410	0.00003
0.65000	0.63800	3.25160	0.00002	0.84500	0.79100	4.22720	0.00003
0.65100	0.63700	3.25590	0.00002	0.84600	0.79300	4.23030	0.00003
0.65200	0.63600	3.26100	0.00003	0.84700	0.79400	4.23330	0.00003
0.65400	0.62700	3.27230	0.00006	0.84700	0.79600	4.23680	0.00004
0.65500	0.62700	3.27550	0.00002	0.84800	0.79700	4.24050	0.00004
0.65500	0.62900	3.27620	0.00000	0.84900	0.79700	4.24350	0.00003
0.65600	0.63000	3.27780	0.00001	0.85000	0.79900	4.24750	0.00004
0.65600	0.63200	3.27910	0.00001	0.85000	0.79900	4.25090	0.00004
0.65600	0.63400	3.28070	0.00001	0.85100	0.79900	4.25550	0.00005
0.65700	0.63400	3.28390	0.00002	0.85200	0.79900	4.26010	0.00005
0.65700	0.63400	3.28730	0.00002	0.85300	0.79800	4.26470	0.00005
0.65900	0.63000	3.29370	0.00003	0.85400	0.79800	4.26890	0.00004
0.66100	0.62100	3.30450	0.00006	0.85500	0.79800	4.27440	0.00006

Appendix C: Shakedown Characteristics

0.66100	0.62400	3.30450	0.00000	0.85700	0.79300	4.28280	0.00009
0.66100	0.62600	3.30510	0.00000	0.85800	0.79000	4.28940	0.00007
0.66100	0.62800	3.30620	0.00001	0.85900	0.78700	4.29530	0.00006
0.66200	0.62900	3.30760	0.00001	0.85900	0.78900	4.29730	0.00002
0.66200	0.63100	3.30850	0.00000	0.86000	0.79100	4.29970	0.00002
0.66200	0.63000	3.31200	0.00002	0.86000	0.79100	4.30230	0.00003
0.66300	0.63100	3.31560	0.00002	0.86100	0.79200	4.30490	0.00003
0.66500	0.62100	3.32710	0.00006	0.86200	0.79200	4.30860	0.00004
0.66600	0.61900	3.33190	0.00003	0.86200	0.79300	4.31160	0.00003
0.66600	0.62100	3.33190	0.00000	0.86300	0.79500	4.31430	0.00003
0.66700	0.62300	3.33290	0.00001	0.86300	0.79500	4.31740	0.00003
0.66700	0.62500	3.33340	0.00000	0.86400	0.79600	4.32080	0.00004
0.66700	0.62700	3.33480	0.00001	0.86500	0.79600	4.32430	0.00004
0.66700	0.62800	3.33710	0.00001	0.86600	0.79700	4.32810	0.00004
0.66800	0.62700	3.34000	0.00002	0.86700	0.79600	4.33260	0.00005
0.66900	0.62600	3.34500	0.00003	0.86700	0.79500	4.33670	0.00004
0.67100	0.61700	3.35600	0.00006	0.86800	0.79500	4.34110	0.00005
0.67200	0.61700	3.35790	0.00001	0.87000	0.78900	4.34960	0.00009
0.67200	0.62000	3.35790	0.00000	0.87100	0.78500	4.35660	0.00007
0.67200	0.62100	3.35920	0.00001	0.87200	0.78300	4.36240	0.00006
0.67200	0.62200	3.36010	0.00000	0.87300	0.78400	4.36410	0.00002
0.67200	0.62400	3.36040	0.00000	0.87300	0.78500	4.36590	0.00002
0.67200	0.62500	3.36210	0.00001	0.87400	0.78700	4.36800	0.00002
0.67300	0.62400	3.36550	0.00002	0.87400	0.78700	4.37090	0.00003
0.67400	0.62200	3.37040	0.00003	0.87500	0.78900	4.37350	0.00003
0.67600	0.61400	3.38120	0.00006	0.87500	0.79000	4.37620	0.00003
0.67700	0.61300	3.38380	0.00001	0.87600	0.79100	4.37950	0.00003
0.67700	0.61700	3.38480	0.00001	0.87600	0.79200	4.38190	0.00002
0.67700	0.61800	3.38670	0.00001	0.87700	0.79200	4.38440	0.00003
0.67800	0.61900	3.38850	0.00001	0.87700	0.79300	4.38730	0.00003
0.67800	0.62200	3.38940	0.00000	0.87800	0.79400	4.39060	0.00003
0.67800	0.62300	3.39010	0.00000	0.87900	0.79400	4.39430	0.00004

Appendix C: Shakedown Characteristics

0.67900	0.62200	3.39250	0.00001	0.87900	0.79300	4.39740	0.00003
0.67900	0.61900	3.39710	0.00002	0.88000	0.79300	4.40100	0.00004
0.68100	0.61000	3.40600	0.00005	0.88200	0.78700	4.41090	0.00010
0.68100	0.61100	3.40540	0.00000	0.88400	0.78300	4.41800	0.00007
0.68100	0.61400	3.40400	-0.00001	0.88500	0.78100	4.42290	0.00005
0.68100	0.61500	3.40300	-0.00001	0.88500	0.78200	4.42420	0.00001

7				8			
Permanent Deformation	Resilient Strain 10-3	Permanent strain10-3	Strain Rate	Permanent Deformation	Resilient Strain 10-3	Permanent strain10-3	Strain Rate
0.00000	0.69400	0.00000	0.00000	0.00000	0.81200	0.00000	0.00000
0.36800	0.93600	1.83830	0.03830	0.60000	1.06100	2.99970	0.06249
0.46600	0.93100	2.33180	0.01028	0.75600	1.06900	3.78040	0.01626
0.53100	0.92900	2.65330	0.00670	0.86000	1.06100	4.29870	0.01080
0.57800	0.93400	2.89040	0.00494	0.93800	1.04700	4.68840	0.00812
0.61700	0.93100	3.08390	0.00403	1.00000	1.04700	4.99820	0.00645
0.64800	0.93300	3.24160	0.00329	1.05100	1.04500	5.25730	0.00540
0.67600	0.93500	3.37760	0.00283	1.09400	1.04600	5.46980	0.00443
0.69900	0.93700	3.49540	0.00245	1.13000	1.04600	5.65170	0.00379
0.72000	0.93800	3.59950	0.00217	1.16300	1.04200	5.81740	0.00345
0.73900	0.93900	3.69650	0.00202	1.19300	1.03700	5.96380	0.00305
0.75700	0.94100	3.78500	0.00184	1.21900	1.04300	6.09450	0.00272
0.77400	0.93800	3.86960	0.00176	1.24500	1.04100	6.22550	0.00273
0.79000	0.93400	3.95040	0.00168	1.26900	1.03900	6.34330	0.00245
0.80400	0.94300	4.01940	0.00144	1.29200	1.03400	6.45840	0.00240
0.81800	0.94100	4.09100	0.00149	1.31200	1.03300	6.55980	0.00211
0.83200	0.93800	4.15840	0.00140	1.33000	1.03700	6.64790	0.00184
0.84400	0.94400	4.21840	0.00125	1.34800	1.03200	6.74240	0.00197
0.85600	0.94000	4.27840	0.00125	1.36700	1.02700	6.83710	0.00197
0.86700	0.94000	4.33570	0.00119	1.38500	1.02600	6.92580	0.00185
0.87800	0.93800	4.39090	0.00115	1.40100	1.02900	7.00480	0.00165

Appendix C: Shakedown Characteristics

0.88800	0.93900	4.44110	0.00105	1.41700	1.02300	7.08630	0.00170
0.89800	0.93900	4.49110	0.00104	1.43300	1.02300	7.16450	0.00163
0.90800	0.93900	4.53870	0.00099	1.44700	1.02400	7.23600	0.00149
0.91700	0.94100	4.58260	0.00091	1.46200	1.01700	7.31210	0.00159
0.92500	0.94100	4.62690	0.00092	1.47600	1.01600	7.37760	0.00136
0.93400	0.94100	4.67130	0.00093	1.48700	1.01800	7.43610	0.00122
0.94300	0.94400	4.71270	0.00086	1.50000	1.01800	7.50140	0.00136
0.95100	0.94100	4.75500	0.00088	1.51100	1.02600	7.55350	0.00109
0.95900	0.93900	4.79560	0.00085	1.52400	1.01700	7.61870	0.00136
0.96700	0.93500	4.83480	0.00082	1.53600	1.00800	7.68050	0.00129
0.97400	0.94000	4.86930	0.00072	1.54700	1.00600	7.73550	0.00115
0.98100	0.93600	4.90680	0.00078	1.55600	1.00700	7.78240	0.00098
0.98900	0.92900	4.94480	0.00079	1.56500	1.00700	7.82460	0.00088
0.99500	0.92300	4.97640	0.00066	1.57300	1.00300	7.86660	0.00087
1.00100	0.92100	5.00410	0.00058	1.58200	1.00100	7.90760	0.00085
1.00600	0.91900	5.02920	0.00052	1.59000	0.99900	7.94870	0.00086
1.01100	0.92000	5.05340	0.00050	1.59800	0.99400	7.98800	0.00082
1.01500	0.91800	5.07620	0.00048	1.60500	0.98900	8.02430	0.00076
1.01900	0.92000	5.09690	0.00043	1.61100	0.99200	8.05480	0.00064
1.02400	0.92000	5.11890	0.00046	1.61800	0.99200	8.08870	0.00071
1.02800	0.92200	5.14060	0.00045	1.62300	0.99900	8.11740	0.00060
1.03200	0.92100	5.16180	0.00044	1.63000	0.99300	8.15120	0.00070
1.03700	0.92200	5.18400	0.00046	1.63700	0.99000	8.18530	0.00071
1.04100	0.92100	5.20600	0.00046	1.64300	0.98900	8.21610	0.00064
1.04500	0.92400	5.22690	0.00044	1.65000	0.98600	8.25080	0.00072
1.05000	0.92200	5.24880	0.00046	1.65700	0.98700	8.28310	0.00067
1.05600	0.94600	5.28020	0.00065	1.66300	0.98600	8.31460	0.00066
1.05900	0.92500	5.29420	0.00029	1.66900	0.98800	8.34360	0.00060
1.06300	0.92800	5.31430	0.00042	1.67500	0.98700	8.37640	0.00068
1.06700	0.92800	5.33550	0.00044	1.68100	0.98400	8.40450	0.00059
1.07100	0.92900	5.35710	0.00045	1.68600	0.98600	8.43050	0.00054
1.07600	0.93100	5.37920	0.00046	1.69200	0.98400	8.46180	0.00065

Appendix C: Shakedown Characteristics

1.08000	0.93300	5.40090	0.00045	1.69800	0.98400	8.48830	0.00055
1.08500	0.93300	5.42390	0.00048	1.70400	0.97900	8.51970	0.00065
1.08900	0.93500	5.44700	0.00048	1.70900	0.97700	8.54640	0.00056
1.09400	0.93700	5.46940	0.00047	1.71300	0.98000	8.56550	0.00040
1.09800	0.93600	5.49150	0.00046	1.71900	0.97200	8.59380	0.00059
1.10300	0.93800	5.51440	0.00048	1.72300	0.97100	8.61600	0.00046
1.10700	0.94100	5.53740	0.00048	1.72800	0.96800	8.63770	0.00045
1.11200	0.93900	5.56050	0.00048	1.73200	0.96900	8.65950	0.00045
1.11600	0.94100	5.58210	0.00045	1.73500	0.97200	8.67470	0.00032
1.12100	0.94000	5.60550	0.00049	1.73800	0.97200	8.69190	0.00036
1.12500	0.93900	5.62660	0.00044	1.74200	0.97500	8.70890	0.00035
1.13000	0.93600	5.64770	0.00044	1.74500	0.97600	8.72750	0.00039
1.13400	0.93500	5.66780	0.00042	1.74900	0.97800	8.74710	0.00041
1.13700	0.93400	5.68720	0.00040	1.75300	0.97900	8.76730	0.00042
1.14100	0.93300	5.70530	0.00038	1.75700	0.98100	8.78740	0.00042
1.14500	0.93300	5.72320	0.00037	1.76200	0.98400	8.80780	0.00042
1.14800	0.93400	5.74060	0.00036	1.76600	0.98400	8.82920	0.00045
1.15200	0.93600	5.75810	0.00036	1.77000	0.98600	8.84980	0.00043
1.15500	0.93600	5.77680	0.00039	1.77400	0.98700	8.87180	0.00046
1.15900	0.93800	5.79500	0.00038	1.77900	0.98700	8.89510	0.00049
1.16300	0.93700	5.81350	0.00039	1.78400	0.98800	8.91790	0.00047
1.16600	0.93900	5.83190	0.00038	1.78800	0.98900	8.93830	0.00043
1.17000	0.93900	5.85040	0.00039	1.79300	0.98800	8.96340	0.00052
1.17400	0.93900	5.86880	0.00038	1.79700	0.98900	8.98630	0.00048
1.17800	0.94100	5.88810	0.00040	1.80200	0.99000	9.00850	0.00046
1.18100	0.94300	5.90660	0.00039	1.80600	0.99000	9.03050	0.00046
1.18500	0.94300	5.92500	0.00038	1.81100	0.98900	9.05350	0.00048
1.18900	0.94500	5.94350	0.00039	1.81500	0.98700	9.07410	0.00043
1.19300	0.94400	5.96260	0.00040	1.81900	0.98800	9.09360	0.00041
1.19600	0.94500	5.98180	0.00040	1.82300	0.98700	9.11360	0.00042
1.20000	0.94600	6.00080	0.00040	1.82600	0.98900	9.13200	0.00038
1.20400	0.94600	6.02030	0.00041	1.83000	0.98800	9.15070	0.00039

Appendix C: Shakedown Characteristics

1.20800	0.94700	6.03930	0.00040	1.83400	0.98700	9.16900	0.00038
1.21200	0.95400	6.05800	0.00039	1.83800	0.98600	9.18780	0.00039
1.21500	0.95300	6.07680	0.00039	1.84100	0.98700	9.20490	0.00036
1.21900	0.95400	6.09620	0.00040	1.84500	0.98700	9.22370	0.00039
1.22300	0.94900	6.11520	0.00040	1.84900	0.98800	9.24270	0.00040
1.22700	0.95000	6.13470	0.00041	1.85200	0.98800	9.26240	0.00041
1.23000	0.94900	6.15230	0.00037	1.85600	0.99000	9.28150	0.00040
1.23400	0.95000	6.17120	0.00039	1.86100	0.98700	9.30480	0.00049
1.23800	0.94800	6.19080	0.00041	1.86600	0.98300	9.32790	0.00048
1.24200	0.94600	6.20820	0.00036	1.86900	0.98500	9.34650	0.00039
1.24500	0.94400	6.22500	0.00035	1.87200	0.99100	9.36190	0.00032
1.24800	0.94200	6.24210	0.00036	1.87600	0.99300	9.38050	0.00039
1.25100	0.94100	6.25730	0.00032	1.88000	0.99300	9.40070	0.00042
1.25500	0.93900	6.27270	0.00032	1.88400	0.99400	9.41980	0.00040
1.25800	0.93800	6.28760	0.00031	1.88800	0.99700	9.43930	0.00041
1.26000	0.94000	6.30140	0.00029	1.89200	0.99600	9.45940	0.00042
1.26300	0.93800	6.31600	0.00030	1.89600	0.99600	9.47930	0.00041
1.26600	0.94100	6.32980	0.00029	1.90000	0.99600	9.49900	0.00041
1.26900	0.94000	6.34440	0.00030	1.90300	0.99500	9.51650	0.00036
1.27200	0.94100	6.35870	0.00030	1.90700	0.99300	9.53570	0.00040
1.27500	0.94300	6.37340	0.00031	1.91000	0.99400	9.55190	0.00034
1.27800	0.94200	6.38770	0.00030	1.91300	0.99400	9.56730	0.00032
1.28100	0.94100	6.40460	0.00035	1.91700	0.99400	9.58380	0.00034
1.28400	0.94200	6.42000	0.00032	1.92000	0.99200	9.60030	0.00034
1.28700	0.94200	6.43490	0.00031	1.92300	0.99200	9.61520	0.00031
1.29000	0.94200	6.44990	0.00031	1.92600	0.99000	9.63120	0.00033
1.29300	0.94000	6.46540	0.00032	1.92900	0.99100	9.64520	0.00029
1.29600	0.94200	6.48020	0.00031	1.93200	0.99300	9.65930	0.00029
1.29900	0.94100	6.49580	0.00033	1.93500	0.99300	9.67580	0.00034
1.30200	0.94200	6.51020	0.00030	1.93800	0.99200	9.69210	0.00034
1.30500	0.94200	6.52520	0.00031	1.94200	0.99400	9.70760	0.00032
1.30800	0.94300	6.54040	0.00032	1.94500	0.99300	9.72440	0.00035

Appendix C: Shakedown Characteristics

1.31100	0.94300	6.55450	0.00029	1.94800	0.99300	9.74090	0.00034
1.31400	0.94500	6.56890	0.00030	1.95100	0.99300	9.75670	0.00033
1.31700	0.94500	6.58330	0.00030	1.95500	0.99300	9.77320	0.00034
1.32000	0.94600	6.59820	0.00031	1.95800	0.99300	9.78950	0.00034
1.32300	0.94400	6.61360	0.00032	1.96100	0.99300	9.80700	0.00036
1.32600	0.94400	6.62800	0.00030	1.96500	0.99400	9.82250	0.00032
1.32900	0.94500	6.64330	0.00032	1.96800	0.99400	9.83990	0.00036
1.33200	0.94100	6.65880	0.00032	1.97100	0.99300	9.85700	0.00036
1.33500	0.94000	6.67350	0.00031	1.97500	0.99300	9.87340	0.00034
1.33700	0.93800	6.68680	0.00028	1.97800	0.99100	9.88880	0.00032
1.34000	0.93800	6.69980	0.00027	1.98100	0.98900	9.90390	0.00031
1.34300	0.93500	6.71270	0.00027	1.98400	0.98700	9.91790	0.00029
1.34500	0.93500	6.72480	0.00025	1.98600	0.98900	9.93120	0.00028
1.34700	0.93400	6.73630	0.00024	1.98900	0.98700	9.94500	0.00029
1.35000	0.93500	6.74750	0.00023	1.99200	0.98500	9.95860	0.00028
1.35200	0.93500	6.75840	0.00023	1.99400	0.98400	9.97110	0.00026
1.35400	0.93700	6.77000	0.00024	1.99700	0.98200	9.98420	0.00027
1.35600	0.93600	6.78210	0.00025	1.99900	0.98200	9.99570	0.00024
1.35900	0.93800	6.79350	0.00024	2.00200	0.98300	10.00750	0.00025
1.36100	0.93700	6.80520	0.00024	2.00400	0.98300	10.02050	0.00027
1.36300	0.93800	6.81740	0.00025	2.00700	0.98300	10.03250	0.00025
1.36600	0.93700	6.82930	0.00025	2.00900	0.98200	10.04510	0.00026
1.36800	0.93900	6.84090	0.00024	2.01100	0.98300	10.05740	0.00026
1.37100	0.93800	6.85260	0.00024	2.01400	0.98200	10.06920	0.00025
1.37300	0.93900	6.86410	0.00024	2.01600	0.98300	10.08130	0.00025
1.37500	0.93900	6.87570	0.00024	2.01900	0.98300	10.09450	0.00028
1.37800	0.94000	6.88760	0.00025	2.02100	0.98300	10.10660	0.00025
1.38000	0.94000	6.89880	0.00023	2.02400	0.98200	10.11930	0.00026
1.38200	0.94100	6.91070	0.00025	2.02600	0.98300	10.13210	0.00027
1.38400	0.94100	6.92230	0.00024	2.02900	0.98200	10.14540	0.00028
1.38700	0.94300	6.93450	0.00025	2.03200	0.98200	10.15820	0.00027
1.38900	0.94200	6.94650	0.00025	2.03400	0.98200	10.17120	0.00027

Appendix C: Shakedown Characteristics

1.39200	0.94400	6.95870	0.00025	2.03700	0.98100	10.18290	0.00024
1.39400	0.94500	6.97070	0.00025	2.03900	0.98000	10.19490	0.00025
1.39600	0.94500	6.98240	0.00024	2.04100	0.97600	10.20640	0.00024
1.39900	0.94300	6.99500	0.00026	2.04300	0.97800	10.21620	0.00020
1.40100	0.94500	7.00680	0.00025	2.04600	0.97700	10.22770	0.00024
1.40400	0.94600	7.01800	0.00023	2.04800	0.97200	10.23810	0.00022
1.40600	0.94300	7.03140	0.00028	2.05000	0.97700	10.24800	0.00021
1.40900	0.94000	7.04280	0.00024	2.05200	0.97600	10.25750	0.00020
1.41100	0.93900	7.05370	0.00023	2.05400	0.97400	10.26790	0.00022

9				10			
Permanent Deformation (mm)	Resilient Strain 10-3	Permanent strain10-3	Strain Rate	Permanent Deformation (mm)	Resilient Strain 10-3	Permanent strain10-3	Strain Rate
0.00000	1.09500	0.00000	0.00000	0.00000	0.78400	0.00000	0.00000
0.38000	1.16700	1.90090	0.07920	0.62000	1.10200	3.09990	0.03229
0.55100	1.18400	2.75270	0.03549	0.76900	1.10800	3.84700	0.00778
0.67500	1.19500	3.37470	0.02592	0.86600	1.10700	4.33130	0.00504
0.78200	1.20200	3.90870	0.02225	0.93700	1.13600	4.68740	0.00371
0.87000	1.20700	4.35180	0.01846	1.00100	1.13900	5.00520	0.00331
0.94800	1.20600	4.73910	0.01614	1.05500	1.14000	5.27280	0.00279
1.01700	1.20300	5.08470	0.01440	1.10000	1.13800	5.49830	0.00235
1.07900	1.19900	5.39710	0.01302	1.13900	1.13700	5.69390	0.00204
1.13500	1.20000	5.67320	0.01150	1.17400	1.13000	5.87040	0.00184
1.18500	1.20500	5.92700	0.01058	1.20500	1.12300	6.02620	0.00162
1.23200	1.20700	6.16120	0.00976	1.23300	1.11600	6.16310	0.00143
1.27700	1.21300	6.38370	0.00927	1.25700	1.10800	6.28700	0.00129
1.31900	1.21500	6.59360	0.00875	1.27900	1.10200	6.39460	0.00112
1.35900	1.21300	6.79690	0.00847	1.29800	1.09500	6.49090	0.00100
1.39800	1.21000	6.98920	0.00801	1.31500	1.09000	6.57710	0.00090
1.43500	1.20900	7.17260	0.00764	1.33100	1.08900	6.65290	0.00079
1.47000	1.20700	7.34760	0.00729	1.34400	1.09100	6.72120	0.00071

Appendix C: Shakedown Characteristics

1.50300	1.20400	7.51510	0.00698	1.35800	1.09300	6.78940	0.00071
1.53500	1.20400	7.67250	0.00656	1.37100	1.09600	6.85580	0.00069
1.56400	1.20200	7.82100	0.00619	1.38500	1.09500	6.92270	0.00070
1.59300	1.20100	7.96320	0.00593	1.39700	1.09400	6.98700	0.00067
1.62000	1.20300	8.09830	0.00563	1.41100	1.08500	7.05610	0.00072
1.64600	1.20300	8.22850	0.00543	1.42200	1.08800	7.10970	0.00056
1.67100	1.20400	8.35570	0.00530	1.43300	1.08700	7.16610	0.00059
1.69600	1.20800	8.48000	0.00518	1.44400	1.08200	7.22010	0.00056
1.72000	1.20800	8.60030	0.00501	1.45400	1.07800	7.27100	0.00053
1.74400	1.20700	8.71770	0.00489	1.46400	1.07400	7.31800	0.00049
1.76700	1.20900	8.83500	0.00489	1.47100	1.07800	7.35650	0.00040
1.79000	1.20800	8.94820	0.00472	1.47900	1.08000	7.39480	0.00040
1.81200	1.20500	9.06030	0.00467	1.48700	1.08300	7.43290	0.00040
1.83400	1.20500	9.16880	0.00452	1.49400	1.08400	7.47130	0.00040
1.85500	1.20300	9.27480	0.00442	1.50200	1.08600	7.50930	0.00040
1.87600	1.20400	9.37790	0.00430	1.51000	1.08600	7.54900	0.00041
1.89600	1.20400	9.48070	0.00428	1.51800	1.08400	7.58980	0.00042
1.91600	1.20200	9.58150	0.00420	1.52600	1.08200	7.63090	0.00043
1.93600	1.20200	9.68050	0.00413	1.53400	1.07700	7.66890	0.00040
1.95700	1.19800	9.78350	0.00429	1.54100	1.07400	7.70540	0.00038
1.97500	1.20100	9.87540	0.00383	1.54800	1.06900	7.74050	0.00037
1.99500	1.20200	9.97250	0.00405	1.55500	1.06600	7.77290	0.00034
2.01300	1.19700	10.06520	0.00386	1.56000	1.07000	7.79820	0.00026
2.03000	1.19600	10.15180	0.00361	1.56400	1.07600	7.82160	0.00024
2.04700	1.19400	10.23450	0.00345	1.57000	1.07800	7.84920	0.00029
2.06300	1.19200	10.31700	0.00344	1.57500	1.07900	7.87670	0.00029
2.08000	1.19200	10.39790	0.00337	1.58100	1.08100	7.90450	0.00029
2.09500	1.19200	10.47510	0.00322	1.58600	1.08200	7.93200	0.00029
2.11000	1.19100	10.55190	0.00320	1.59200	1.08100	7.96190	0.00031
2.12500	1.19000	10.62750	0.00315	1.59900	1.07800	7.99280	0.00032
2.14000	1.18700	10.69980	0.00301	1.60500	1.07400	8.02340	0.00032
2.15400	1.18600	10.76890	0.00288	1.61000	1.07100	8.05190	0.00030

Appendix C: Shakedown Characteristics

2.16700	1.18500	10.83600	0.00280	1.61600	1.06800	8.07970	0.00029
2.18000	1.18200	10.90090	0.00270	1.62100	1.06300	8.10650	0.00028
2.19300	1.18100	10.96420	0.00264	1.62600	1.06500	8.12800	0.00022
2.20500	1.18100	11.02360	0.00248	1.62900	1.07100	8.14590	0.00019
2.21700	1.18000	11.08380	0.00251	1.63300	1.07400	8.16460	0.00019
2.22800	1.17900	11.14130	0.00240	1.63700	1.07600	8.18590	0.00022
2.24000	1.17800	11.19870	0.00239	1.64100	1.07800	8.20680	0.00022
2.25100	1.17900	11.25540	0.00236	1.64600	1.07900	8.22860	0.00023
2.26200	1.17800	11.31120	0.00233	1.65000	1.07900	8.25170	0.00024
2.27300	1.18100	11.36690	0.00232	1.65600	1.07500	8.27800	0.00027
2.28400	1.18000	11.42190	0.00229	1.66100	1.07000	8.30420	0.00027
2.29500	1.18000	11.47650	0.00228	1.66600	1.06900	8.32970	0.00027
2.30600	1.18000	11.53040	0.00225	1.67100	1.06600	8.35360	0.00025
2.31700	1.18100	11.58390	0.00223	1.67500	1.06100	8.37690	0.00024
2.32800	1.18000	11.63940	0.00231	1.67900	1.06200	8.39680	0.00021
2.33900	1.18000	11.69340	0.00225	1.68200	1.06800	8.40780	0.00011
2.35000	1.17800	11.74760	0.00226	1.68500	1.06800	8.42340	0.00016
2.36000	1.17800	11.79970	0.00217	1.68800	1.07300	8.44020	0.00018
2.37000	1.17700	11.85010	0.00210	1.69100	1.07500	8.45640	0.00017
2.38000	1.17600	11.90000	0.00208	1.69500	1.07500	8.47480	0.00019
2.39000	1.17400	11.94890	0.00204	1.70000	1.07200	8.49800	0.00024
2.40000	1.17500	11.99870	0.00208	1.70400	1.06900	8.52060	0.00024
2.41000	1.17500	12.04790	0.00205	1.70900	1.06400	8.54410	0.00024
2.41900	1.17500	12.09610	0.00201	1.71300	1.06200	8.56410	0.00021
2.42900	1.17600	12.14620	0.00209	1.71700	1.05900	8.58440	0.00021
2.43900	1.17400	12.19610	0.00208	1.72100	1.05400	8.60540	0.00022
2.44900	1.17300	12.24440	0.00201	1.72500	1.05300	8.62290	0.00018
2.45800	1.17200	12.29200	0.00198	1.72700	1.06000	8.63300	0.00011
2.46800	1.17100	12.33950	0.00198	1.72900	1.06200	8.64590	0.00013
2.47700	1.17000	12.38650	0.00196	1.73200	1.06400	8.66120	0.00016
2.48700	1.17100	12.43310	0.00194	1.73500	1.06600	8.67680	0.00016
2.49600	1.17000	12.47850	0.00189	1.73900	1.06500	8.69310	0.00017

Appendix C: Shakedown Characteristics

2.50500	1.17000	12.52260	0.00184	1.74200	1.06400	8.70950	0.00017
2.51300	1.16700	12.56620	0.00182	1.74600	1.06100	8.72910	0.00020
2.52200	1.16700	12.60880	0.00177	1.75000	1.05700	8.74810	0.00020
2.53000	1.16400	12.65140	0.00178	1.75300	1.05300	8.76690	0.00020
2.53800	1.16300	12.69220	0.00170	1.75700	1.04900	8.78480	0.00019
2.54700	1.16400	12.73250	0.00168	1.76100	1.04400	8.80340	0.00019
2.55500	1.16300	12.77270	0.00168	1.76400	1.04400	8.81800	0.00015
2.56200	1.16400	12.81120	0.00160	1.76600	1.05000	8.82790	0.00010
2.57000	1.16200	12.84970	0.00160	1.76700	1.05300	8.83730	0.00010
2.57700	1.16100	12.88750	0.00157	1.77000	1.05600	8.84850	0.00012
2.58500	1.16100	12.92470	0.00155	1.77200	1.05800	8.86140	0.00013
2.59200	1.16300	12.95970	0.00146	1.77500	1.05700	8.87690	0.00016
2.59900	1.16200	12.99590	0.00151	1.77800	1.06000	8.88890	0.00013
2.60600	1.16300	13.02960	0.00140	1.78100	1.05800	8.90510	0.00017
2.61300	1.16200	13.06430	0.00145	1.78400	1.05600	8.92220	0.00018
2.62000	1.16100	13.09850	0.00143	1.78800	1.05000	8.93990	0.00018
2.62600	1.16000	13.13160	0.00138	1.79100	1.04800	8.95650	0.00017
2.63300	1.16000	13.16390	0.00135	1.79500	1.04300	8.97350	0.00018
2.64000	1.15900	13.19920	0.00147	1.79700	1.04500	8.98480	0.00012
2.64600	1.15600	13.23230	0.00138	1.79900	1.04900	8.99340	0.00009
2.65300	1.15600	13.26640	0.00142	1.80000	1.05400	9.00160	0.00009
2.66000	1.15500	13.29810	0.00132	1.80200	1.05600	9.01230	0.00011
2.66600	1.15500	13.33140	0.00139	1.80500	1.05700	9.02450	0.00013
2.67300	1.15500	13.36360	0.00134	1.80700	1.05800	9.03610	0.00012
2.67900	1.15700	13.39650	0.00137	1.81000	1.05600	9.04960	0.00014
2.68600	1.15500	13.42950	0.00138	1.81300	1.05200	9.06500	0.00016
2.69200	1.15500	13.46190	0.00135	1.81600	1.04900	9.08000	0.00016
2.69900	1.15300	13.49410	0.00134	1.81900	1.04500	9.09460	0.00015
2.70500	1.15500	13.52610	0.00133	1.82200	1.04000	9.10950	0.00016
2.71200	1.15400	13.55830	0.00134	1.82500	1.03600	9.12340	0.00014
2.71800	1.15300	13.59020	0.00133	1.82700	1.03800	9.13250	0.00009
2.72400	1.15300	13.62230	0.00134	1.82700	1.04500	9.13690	0.00005

Appendix C: Shakedown Characteristics

2.73100	1.15300	13.65410	0.00133	1.82800	1.05100	9.14070	0.00004
2.73700	1.15100	13.68610	0.00133	1.83000	1.05300	9.14800	0.00008
2.74300	1.15100	13.71640	0.00126	1.83200	1.05400	9.15770	0.00010
2.74900	1.15200	13.74660	0.00126	1.83400	1.05200	9.16970	0.00013
2.75500	1.15100	13.77690	0.00126	1.83600	1.05000	9.18180	0.00013
2.76100	1.15100	13.80580	0.00120	1.83900	1.04800	9.19400	0.00013
2.76700	1.15100	13.83450	0.00120	1.84100	1.04600	9.20610	0.00013
2.77300	1.15200	13.86330	0.00120	1.84400	1.04300	9.21820	0.00013
2.77900	1.15200	13.89270	0.00123	1.84600	1.04100	9.22970	0.00012
2.78400	1.15100	13.92150	0.00120	1.84800	1.03800	9.24160	0.00012
2.79000	1.15100	13.95050	0.00121	1.85100	1.03500	9.25410	0.00013
2.79600	1.15100	13.97950	0.00121	1.85300	1.03200	9.26560	0.00012
2.80100	1.15200	14.00690	0.00114	1.85500	1.03000	9.27590	0.00011
2.80700	1.15300	14.03460	0.00115	1.85700	1.03100	9.28510	0.00010
2.81300	1.15000	14.06610	0.00131	1.85700	1.03800	9.28720	0.00002
2.81900	1.15100	14.09590	0.00124	1.85800	1.04300	9.29080	0.00004
2.82500	1.15000	14.12510	0.00122	1.85900	1.04700	9.29670	0.00006
2.83100	1.15100	14.15310	0.00117	1.86100	1.04800	9.30450	0.00008
2.83600	1.14900	14.18060	0.00115	1.86300	1.04500	9.31450	0.00010
2.84100	1.15000	14.20680	0.00109	1.86500	1.04300	9.32570	0.00012
2.84700	1.15300	14.23380	0.00112	1.86700	1.04200	9.33660	0.00011
2.85200	1.15600	14.25920	0.00106	1.86900	1.04000	9.34730	0.00011
2.85700	1.15400	14.28560	0.00110	1.87200	1.03800	9.35830	0.00011
2.86200	1.15100	14.31120	0.00107	1.87400	1.03500	9.36930	0.00011
2.86700	1.14900	14.33730	0.00109	1.87600	1.03300	9.38000	0.00011
2.87200	1.14800	14.36180	0.00102	1.87800	1.02900	9.39190	0.00012
2.87700	1.14700	14.38630	0.00102	1.88000	1.02700	9.40200	0.00011
2.88200	1.14800	14.41020	0.00100	1.88200	1.02500	9.41140	0.00010
2.88600	1.14800	14.43240	0.00092	1.88400	1.02300	9.42020	0.00009
2.89100	1.14700	14.45610	0.00099	1.88400	1.03100	9.42200	0.00002
2.89600	1.14800	14.47880	0.00095	1.88500	1.03900	9.42300	0.00001
2.90000	1.14800	14.50150	0.00095	1.88500	1.04300	9.42720	0.00004

Appendix C: Shakedown Characteristics

2.90500	1.14700	14.52410	0.00094	1.88700	1.04200	9.43430	0.00007
2.90900	1.14500	14.54690	0.00095	1.88900	1.04100	9.44320	0.00009
2.91400	1.14300	14.56950	0.00094	1.89100	1.03800	9.45330	0.00011
2.91800	1.14400	14.59100	0.00090	1.89300	1.03600	9.46410	0.00011
2.92300	1.14300	14.61270	0.00090	1.89500	1.03400	9.47390	0.00010
2.92700	1.14300	14.63420	0.00090	1.89700	1.03100	9.48400	0.00011
2.93100	1.14200	14.65650	0.00093	1.89900	1.03000	9.49280	0.00009
2.93500	1.14200	14.67740	0.00087	1.90000	1.02700	9.50240	0.00010
2.94000	1.14200	14.69990	0.00094	1.90200	1.02500	9.51240	0.00010
2.94400	1.14300	14.72160	0.00090	1.90400	1.02300	9.52110	0.00009
2.94900	1.14200	14.74360	0.00092	1.90600	1.02100	9.52980	0.00009
2.95300	1.14200	14.76580	0.00092	1.90700	1.02000	9.53690	0.00007

11				13			
Permanent Deformation	Resilient Strain 10-3	Permanent strain10-3	Strain Rate	Permanent Deformation	Resilient Strain 10-3	Permanent strain10-3	Strain Rate
0.000000	1.080000	0.000000	0.000000	0.000000	0.980000	0.000000	0.000000
1.562000	1.302000	7.810900	0.081364	1.676000	1.246000	8.382400	0.043658
1.978000	1.272000	9.891100	0.021669	2.153000	1.251000	10.763700	0.012403
2.259000	1.277000	11.295900	0.014633	2.478000	1.259000	12.389300	0.008467
2.497000	1.285000	12.482900	0.012365	2.721000	1.264000	13.605500	0.006334
2.671000	1.285000	13.354200	0.009076	2.923000	1.262000	14.616300	0.005265
2.840000	1.280000	14.200900	0.008820	3.086000	1.243000	15.431200	0.004244
2.970000	1.263000	14.852400	0.006786	3.214000	1.231000	16.070100	0.003328
3.079000	1.247000	15.393500	0.005636	3.330000	1.225000	16.651200	0.003027
3.174000	1.236000	15.869700	0.004960	3.437000	1.227000	17.186800	0.002790
3.255000	1.231000	16.276000	0.004232	3.543000	1.223000	17.715500	0.002754
3.341000	1.249000	16.706600	0.004485	3.642000	1.235000	18.210600	0.002579
3.427000	1.239000	17.136600	0.004479	3.739000	1.235000	18.697200	0.002534
3.494000	1.243000	17.469300	0.003466	3.823000	1.225000	19.115300	0.002178

Appendix C: Shakedown Characteristics

3.554000	1.236000	17.771900	0.003152	3.892000	1.209000	19.457700	0.001783
3.607000	1.237000	18.037000	0.002761	3.956000	1.206000	19.781000	0.001684
3.656000	1.229000	18.278100	0.002511	4.016000	1.199000	20.082400	0.001570
3.702000	1.213000	18.512100	0.002438	4.073000	1.217000	20.363100	0.001462
3.747000	1.206000	18.736300	0.002335	4.133000	1.217000	20.664300	0.001569
3.793000	1.199000	18.963500	0.002367	4.194000	1.192000	20.970600	0.001595
3.850000	1.154000	19.250000	0.002984	4.244000	1.177000	21.218000	0.001289
3.889000	1.166000	19.446200	0.002044	4.285000	1.160000	21.426500	0.001086
3.928000	1.162000	19.640600	0.002025	4.328000	1.164000	21.640100	0.001112
3.963000	1.165000	19.812600	0.001792	4.369000	1.165000	21.844400	0.001064
3.994000	1.166000	19.967700	0.001616	4.405000	1.170000	22.023500	0.000933
4.027000	1.160000	20.132600	0.001718	4.442000	1.166000	22.211100	0.000977
4.053000	1.159000	20.265300	0.001382	4.478000	1.155000	22.390900	0.000936
4.079000	1.142000	20.394800	0.001349	4.506000	1.142000	22.529600	0.000722
4.100000	1.123000	20.499500	0.001091	4.529000	1.141000	22.645800	0.000605
4.119000	1.109000	20.593500	0.000979	4.555000	1.127000	22.774800	0.000672
4.134000	1.105000	20.672200	0.000820	4.578000	1.135000	22.891700	0.000609
4.148000	1.102000	20.741700	0.000724	4.601000	1.148000	23.005400	0.000592
4.166000	1.074000	20.828000	0.000899	4.629000	1.135000	23.143300	0.000718
4.176000	1.098000	20.880000	0.000542	4.659000	1.104000	23.297000	0.000801
4.189000	1.096000	20.944900	0.000676	4.674000	1.124000	23.369500	0.000378
4.202000	1.097000	21.009600	0.000674	4.692000	1.120000	23.459400	0.000468
4.215000	1.093000	21.074100	0.000672	4.712000	1.099000	23.561400	0.000531
4.227000	1.087000	21.134000	0.000624	4.728000	1.096000	23.641800	0.000419
4.239000	1.085000	21.196500	0.000651	4.741000	1.104000	23.705700	0.000333
4.254000	1.070000	21.272300	0.000790	4.757000	1.103000	23.786400	0.000420
4.264000	1.075000	21.320000	0.000497	4.774000	1.077000	23.870900	0.000440
4.278000	1.059000	21.388100	0.000709	4.782000	1.093000	23.909800	0.000203
4.288000	1.053000	21.441000	0.000551	4.794000	1.092000	23.967900	0.000303
4.297000	1.043000	21.486500	0.000474	4.804000	1.095000	24.020200	0.000272
4.307000	1.029000	21.533100	0.000485	4.816000	1.098000	24.077600	0.000299
4.315000	1.016000	21.573200	0.000418	4.828000	1.095000	24.140600	0.000328

Appendix C: Shakedown Characteristics

4.322000	1.005000	21.611600	0.000400	4.840000	1.084000	24.201900	0.000319
4.329000	1.005000	21.646300	0.000361	4.851000	1.077000	24.253000	0.000266
4.335000	1.005000	21.677200	0.000322	4.858000	1.076000	24.289200	0.000189
4.340000	1.014000	21.700300	0.000241	4.867000	1.075000	24.336400	0.000246
4.340000	1.089000	21.698700	- 0.000017	4.875000	1.078000	24.373600	0.000194
4.353000	1.078000	21.763100	0.000671	4.886000	1.071000	24.428800	0.000287
4.362000	1.082000	21.808500	0.000473	4.895000	1.064000	24.473800	0.000234
4.363000	1.125000	21.814900	0.000067	4.901000	1.058000	24.507200	0.000174
4.386000	1.068000	21.932000	0.001220	4.907000	1.062000	24.536200	0.000151
4.396000	1.066000	21.980800	0.000508	4.914000	1.067000	24.568400	0.000168
4.407000	1.057000	22.033700	0.000551	4.919000	1.069000	24.596100	0.000144
4.410000	1.087000	22.050700	0.000177	4.929000	1.063000	24.644400	0.000252
4.420000	1.059000	22.098800	0.000501	4.937000	1.054000	24.683700	0.000205
4.428000	1.054000	22.138700	0.000416	4.942000	1.053000	24.711800	0.000146
4.435000	1.055000	22.173500	0.000363	4.947000	1.055000	24.733600	0.000114
4.441000	1.057000	22.202800	0.000305	4.953000	1.055000	24.762800	0.000152
4.448000	1.051000	22.242200	0.000410	4.959000	1.061000	24.796300	0.000174
4.456000	1.046000	22.281600	0.000410	4.966000	1.056000	24.827700	0.000164
4.447000	1.119000	22.236900	- 0.000466	4.973000	1.051000	24.863400	0.000186
4.458000	1.107000	22.289400	0.000547	4.979000	1.048000	24.894800	0.000164
4.470000	1.087000	22.351100	0.000643	4.984000	1.052000	24.920100	0.000132
4.473000	1.116000	22.367000	0.000166	4.989000	1.052000	24.947100	0.000141
4.497000	1.057000	22.483600	0.001215	4.995000	1.052000	24.975600	0.000148
4.508000	1.042000	22.537500	0.000561	5.001000	1.059000	25.002600	0.000141
4.514000	1.038000	22.569800	0.000336	5.008000	1.051000	25.042300	0.000207
4.518000	1.043000	22.588800	0.000198	5.014000	1.052000	25.071400	0.000152
4.525000	1.034000	22.623000	0.000356	5.022000	1.041000	25.108100	0.000191
4.530000	1.032000	22.649300	0.000274	5.026000	1.042000	25.131700	0.000123
4.536000	1.020000	22.680800	0.000328	5.030000	1.045000	25.151500	0.000103
4.542000	1.006000	22.711600	0.000321	5.035000	1.043000	25.174200	0.000118

Appendix C: Shakedown Characteristics

4.548000	0.994000	22.739000	0.000285	5.039000	1.046000	25.195200	0.000109
4.550000	0.996000	22.751200	0.000127	5.046000	1.041000	25.228500	0.000173
4.555000	0.986000	22.775600	0.000254	5.051000	1.040000	25.254900	0.000138
4.539000	1.100000	22.694900	- 0.000841	5.057000	1.032000	25.284100	0.000152
4.539000	1.165000	22.697100	0.000023	5.061000	1.030000	25.305600	0.000112
4.553000	1.140000	22.762800	0.000684	5.065000	1.034000	25.324900	0.000101
4.570000	1.110000	22.849800	0.000906	5.069000	1.033000	25.343700	0.000098
4.590000	1.051000	22.949900	0.001043	5.072000	1.034000	25.361700	0.000094
4.598000	1.039000	22.991400	0.000432	5.076000	1.039000	25.381800	0.000105
4.605000	1.031000	23.023700	0.000336	5.083000	1.031000	25.414100	0.000168
4.606000	1.050000	23.030200	0.000068	5.089000	1.026000	25.444800	0.000160
4.611000	1.045000	23.054600	0.000254	5.091000	1.024000	25.456400	0.000060
4.615000	1.047000	23.075400	0.000217	5.094000	1.028000	25.469400	0.000068
4.619000	1.050000	23.097100	0.000226	5.098000	1.031000	25.488600	0.000100
4.625000	1.046000	23.123700	0.000277	5.101000	1.034000	25.502600	0.000073
4.629000	1.049000	23.145300	0.000225	5.104000	1.037000	25.520400	0.000093
4.636000	1.036000	23.177700	0.000338	5.109000	1.029000	25.546800	0.000137
4.624000	1.115000	23.119900	- 0.000602	5.114000	1.016000	25.568500	0.000113
4.630000	1.117000	23.148200	0.000295	5.116000	1.015000	25.579300	0.000056
4.638000	1.118000	23.188000	0.000415	5.118000	1.020000	25.587500	0.000043
4.646000	1.111000	23.231200	0.000450	5.120000	1.018000	25.600900	0.000070
4.650000	1.128000	23.248000	0.000175	5.122000	1.021000	25.611800	0.000057
4.660000	1.111000	23.297900	0.000520	5.126000	1.020000	25.631100	0.000101
4.682000	1.031000	23.408600	0.001153	5.130000	1.008000	25.652400	0.000111
4.685000	1.029000	23.426700	0.000189	5.133000	1.004000	25.665300	0.000067
4.688000	1.037000	23.440900	0.000148	5.134000	1.008000	25.671100	0.000030
4.691000	1.038000	23.457300	0.000171	5.136000	1.011000	25.680900	0.000051
4.696000	1.035000	23.478200	0.000218	5.138000	1.013000	25.690000	0.000047
4.700000	1.032000	23.497800	0.000204	5.142000	1.008000	25.708200	0.000095
4.701000	1.040000	23.504800	0.000073	5.146000	1.001000	25.729400	0.000110

Appendix C: Shakedown Characteristics

4.706000	1.032000	23.528500	0.000247	5.149000	0.997000	25.742700	0.000069
4.698000	1.085000	23.487500	- 0.000427	5.150000	1.000000	25.748800	0.000032
4.715000	1.010000	23.575900	0.000921	5.151000	1.002000	25.755900	0.000037
4.708000	1.073000	23.537600	- 0.000399	5.153000	1.002000	25.766400	0.000055
4.700000	1.128000	23.501400	- 0.000377	5.156000	0.999000	25.778900	0.000065
4.723000	1.047000	23.613800	0.001171	5.157000	1.002000	25.787100	0.000043
4.730000	1.029000	23.649300	0.000370	5.161000	0.998000	25.806000	0.000098
4.735000	1.021000	23.673400	0.000251	5.164000	0.991000	25.819900	0.000072
4.738000	1.018000	23.689200	0.000165	5.166000	0.992000	25.827600	0.000040
4.739000	1.021000	23.696300	0.000074	5.167000	0.993000	25.834600	0.000036
4.742000	1.021000	23.710400	0.000147	5.169000	0.995000	25.842500	0.000041
4.745000	1.013000	23.727100	0.000174	5.170000	0.998000	25.849200	0.000035
4.747000	1.017000	23.734600	0.000078	5.171000	1.000000	25.855700	0.000034
4.749000	1.022000	23.742900	0.000086	5.174000	0.995000	25.871900	0.000084
4.751000	1.016000	23.757000	0.000147	5.178000	0.988000	25.890400	0.000096
4.737000	1.087000	23.686900	- 0.000730	5.180000	0.985000	25.899200	0.000046
4.758000	1.009000	23.788700	0.001060	5.181000	0.989000	25.903100	0.000020
4.743000	1.099000	23.715200	- 0.000766	5.182000	0.990000	25.910000	0.000036
4.749000	1.097000	23.744400	0.000304	5.183000	0.993000	25.916700	0.000035
4.766000	1.027000	23.832200	0.000915	5.184000	0.997000	25.922000	0.000028
4.772000	1.012000	23.861500	0.000305	5.187000	0.995000	25.933900	0.000062
4.776000	1.007000	23.880500	0.000198	5.190000	0.993000	25.950300	0.000085
4.779000	1.002000	23.893400	0.000134	5.193000	0.983000	25.965500	0.000079
4.781000	1.001000	23.906300	0.000134	5.194000	0.985000	25.970300	0.000025
4.782000	1.006000	23.909400	0.000032	5.195000	0.986000	25.975900	0.000029
4.784000	1.007000	23.918900	0.000099	5.197000	0.987000	25.983900	0.000042
4.786000	1.007000	23.928300	0.000098	5.198000	0.988000	25.991300	0.000039
4.787000	1.010000	23.934700	0.000067	5.199000	0.991000	25.997000	0.000030

Appendix C: Shakedown Characteristics

4.789000	1.015000	23.944600	0.000103	5.202000	0.985000	26.011500	0.000076
4.790000	1.017000	23.951900	0.000076	5.206000	0.978000	26.029100	0.000092
4.790000	1.077000	23.950300	- 0.000017	5.208000	0.971000	26.039400	0.000054
4.797000	1.009000	23.985100	0.000363	5.208000	0.976000	26.042100	0.000014
4.785000	1.089000	23.924400	- 0.000632	5.209000	0.978000	26.046600	0.000023
4.802000	1.015000	24.009700	0.000889	5.211000	0.981000	26.052700	0.000032
4.805000	1.013000	24.022900	0.000137	5.212000	0.982000	26.058800	0.000032
4.808000	1.006000	24.041300	0.000192	5.213000	0.981000	26.065900	0.000037
4.810000	1.001000	24.050800	0.000099	5.216000	0.983000	26.078700	0.000067
4.812000	1.003000	24.059500	0.000091	5.220000	0.967000	26.098000	0.000101
4.813000	1.002000	24.067200	0.000080	5.220000	0.966000	26.102400	0.000023
4.816000	0.997000	24.080100	0.000134	5.221000	0.971000	26.106500	0.000021
4.818000	0.997000	24.090500	0.000108	5.223000	0.971000	26.112700	0.000032
4.819000	0.998000	24.096200	0.000059	5.223000	0.975000	26.117200	0.000023
4.822000	0.990000	24.112000	0.000165	5.224000	0.977000	26.122000	0.000025
4.823000	0.989000	24.115700	0.000039	5.227000	0.973000	26.134700	0.000066
4.818000	1.022000	24.090300	- 0.000265	5.230000	0.965000	26.151500	0.000087
4.831000	0.961000	24.155000	0.000674	5.232000	0.960000	26.159100	0.000040
4.833000	0.968000	24.165800	0.000112	5.232000	0.964000	26.161300	0.000011
4.832000	0.984000	24.159700	- 0.000064	5.233000	0.967000	26.165800	0.000023
4.838000	0.958000	24.187900	0.000294	5.234000	0.969000	26.169300	0.000018
4.841000	0.946000	24.207100	0.000200	5.235000	0.972000	26.173100	0.000020
4.844000	0.934000	24.218400	0.000118	5.236000	0.971000	26.180500	0.000039
4.844000	0.944000	24.217900	- 0.000005	5.239000	0.970000	26.193400	0.000067

Appendix C: Shakedown Characteristics

14				15			
Permanent Deformation	Resilient Strain 10-3	Permanent strain10-3	Strain Rate	Permanent Deformation	Resilient Strain 10-3	Permanent strain10-3	Strain Rate
0	1.028	0	0	0.00000	0.97700	0.00000	0.00000
2.02	1.312	10.0983	0.105190625	0.30800	1.31600	1.53830	0.51277
2.519	1.292	12.5954	0.026011458	0.48100	1.40100	2.40280	0.28817
2.831	1.272	14.1535	0.016230208	0.60400	1.42300	3.02180	0.20633
3.113	1.294	15.564	0.014692708	0.70500	1.40900	3.52320	0.16713
3.314	1.296	16.5707	0.010486458	0.78200	1.40700	3.90870	0.12850
3.481	1.253	17.4033	0.008672917	0.84800	1.40600	4.24230	0.11120
3.658	1.287	18.2906	0.009242708	0.90800	1.41200	4.53810	0.09860
3.788	1.247	18.9389	0.006753125	0.97100	1.40100	4.85620	0.10603
3.883	1.205	19.413	0.004938542	1.02100	1.51100	5.10580	0.08320
4.011	1.357	20.0542	0.006679167	1.07600	1.47100	5.38130	0.09183
4.158	1.278	20.7878	0.007641667	1.12400	1.44300	5.61750	0.07873
4.257	1.256	21.2872	0.005202083	1.16500	1.42600	5.82260	0.06837
4.343	1.246	21.7145	0.004451042	1.20300	1.41900	6.01260	0.06333
4.42	1.237	22.0994	0.004009375	1.23800	1.41200	6.19000	0.05913
4.488	1.233	22.4392	0.003539583	1.27200	1.40400	6.36050	0.05683
4.555	1.227	22.7725	0.003471875	1.29000	1.47500	6.45220	0.03057
4.617	1.218	23.0865	0.003270833	1.31300	1.47100	6.56420	0.03733
4.676	1.221	23.379	0.003046875	1.32900	1.55400	6.64580	0.02720
4.733	1.211	23.664	0.00296875	1.36300	1.54700	6.81600	0.05673
4.785	1.202	23.9236	0.002704167	1.41200	1.47200	7.06180	0.08193
4.832	1.196	24.1599	0.002461458	1.45600	1.42300	7.28180	0.07333
4.876	1.198	24.3791	0.002283333	1.49100	1.40400	7.45480	0.05767
4.918	1.194	24.5895	0.002191667	1.52100	1.39400	7.60440	0.04987
4.959	1.194	24.7948	0.002138542	1.54800	1.39300	7.74200	0.04587
5.001	1.176	25.0063	0.002203125	1.57400	1.39200	7.87250	0.04350
5.036	1.18	25.1797	0.00180625	1.60100	1.38800	8.00460	0.04403
5.069	1.18	25.3427	0.001697917	1.62600	1.38300	8.12970	0.04170

Appendix C: Shakedown Characteristics

5.101	1.172	25.5039	0.001679167	1.65100	1.37800	8.25600	0.04210
5.131	1.167	25.6551	0.001575	1.67500	1.37900	8.37300	0.03900
5.161	1.15	25.8059	0.001570833	1.69800	1.37800	8.48790	0.03830
5.191	1.14	25.9538	0.001540625	1.72100	1.37800	8.60390	0.03867
5.214	1.153	26.0704	0.001214583	1.74300	1.37900	8.71500	0.03703
5.241	1.156	26.2056	0.001408333	1.76700	1.37300	8.83390	0.03963
5.268	1.145	26.341	0.001410417	1.78900	1.37600	8.94360	0.03657
5.294	1.147	26.4712	0.00135625	1.81100	1.37600	9.05720	0.03787
5.319	1.153	26.5967	0.001307292	1.83500	1.37100	9.17270	0.03850
5.345	1.148	26.7264	0.001351042	1.85400	1.37600	9.27060	0.03263
5.37	1.155	26.8521	0.001309375	1.87500	1.37600	9.37560	0.03500
5.396	1.145	26.9806	0.001338542	1.89800	1.36900	9.48930	0.03790
5.419	1.148	27.0933	0.001173958	1.91700	1.37800	9.58410	0.03160
5.441	1.148	27.2035	0.001147917	1.93700	1.37300	9.68680	0.03423
5.462	1.148	27.3092	0.001101042	1.95600	1.37600	9.78040	0.03120
5.483	1.143	27.417	0.001122917	1.97600	1.37600	9.88090	0.03350
5.505	1.144	27.5253	0.001128125	1.99600	1.37800	9.97990	0.03300
5.527	1.147	27.6365	0.001158333	2.01400	1.38500	10.06860	0.02957
5.55	1.144	27.751	0.001192708	2.03300	1.38200	10.16570	0.03237
5.575	1.142	27.8738	0.001279167	2.05400	1.38200	10.26790	0.03407
5.597	1.144	27.9872	0.00118125	2.07200	1.39100	10.36000	0.03070
5.623	1.136	28.1145	0.001326042	2.09000	1.40000	10.44830	0.02943
5.644	1.137	28.2188	0.001086458	2.11100	1.39900	10.55310	0.03493
5.662	1.144	28.3097	0.000946875	2.13100	1.39900	10.65370	0.03353
5.683	1.142	28.4139	0.001085417	2.15000	1.40500	10.74970	0.03200
5.704	1.138	28.519	0.001094792	2.16900	1.40500	10.84530	0.03187
5.722	1.134	28.6092	0.000939583	2.18900	1.40700	10.94440	0.03303
5.738	1.131	28.6877	0.000817708	2.20900	1.40200	11.04330	0.03297
5.752	1.132	28.7607	0.000760417	2.22800	1.40300	11.13970	0.03213
5.767	1.126	28.8373	0.000797917	2.24700	1.40300	11.23420	0.03150
5.784	1.122	28.9212	0.000873958	2.26500	1.41000	11.32270	0.02950
5.801	1.112	29.0034	0.00085625	2.28700	1.39300	11.43320	0.03683

Appendix C: Shakedown Characteristics

5.815	1.11	29.0772	0.00076875	2.30200	1.40900	11.51130	0.02603
5.831	1.094	29.1562	0.000822917	2.32200	1.41700	11.60770	0.03213
5.846	1.085	29.23	0.00076875	2.34100	1.40200	11.70360	0.03197
5.859	1.079	29.2932	0.000658333	2.35800	1.40900	11.78790	0.02810
5.87	1.076	29.3524	0.000616667	2.37500	1.41200	11.87710	0.02973
5.884	1.066	29.421	0.000714583	2.39400	1.41100	11.97130	0.03140
5.894	1.062	29.4719	0.000530208	2.41200	1.41500	12.05760	0.02877
5.905	1.066	29.5241	0.00054375	2.43000	1.41500	12.14860	0.03033
5.914	1.063	29.5678	0.000455208	2.44700	1.41800	12.23300	0.02813
5.923	1.054	29.6138	0.000479167	2.46500	1.41700	12.32670	0.03123
5.933	1.037	29.6663	0.000546875	2.48400	1.41600	12.41850	0.03060
5.934	1.078	29.6699	3.75E-05	2.50000	1.42400	12.50170	0.02773
5.944	1.081	29.7195	0.000516667	2.52000	1.41900	12.59940	0.03257
5.953	1.073	29.7665	0.000489583	2.53700	1.42000	12.68400	0.02820
5.965	1.058	29.824	0.000598958	2.55400	1.42400	12.76770	0.02790
5.974	1.054	29.8702	0.00048125	2.57300	1.41300	12.86730	0.03320
5.983	1.051	29.9146	0.0004625	2.59000	1.42200	12.95120	0.02797
5.991	1.044	29.9571	0.000442708	2.60800	1.42400	13.03970	0.02950
6	1.037	30.0014	0.000461458	2.62600	1.42600	13.12950	0.02993
6.008	1.033	30.041	0.0004125	2.64400	1.42500	13.22130	0.03060
6.016	1.028	30.0796	0.000402083	2.66100	1.43200	13.30290	0.02720
6.024	1.021	30.1184	0.000404167	2.67900	1.43100	13.39320	0.03010
6.03	1.02	30.1492	0.000320833	2.69600	1.43100	13.48060	0.02913
6.035	1.025	30.1737	0.000255208	2.71400	1.43100	13.56960	0.02967
6.042	1.019	30.2084	0.000361458	2.73100	1.43400	13.65450	0.02830
6.047	1.017	30.2339	0.000265625	2.74800	1.44200	13.73840	0.02797
6.05	1.03	30.2491	0.000158333	2.76600	1.43100	13.82880	0.03013
6.056	1.031	30.2786	0.000307292	2.78200	1.43800	13.91000	0.02707
6.062	1.025	30.3083	0.000309375	2.79900	1.43100	13.99720	0.02907
6.068	1.025	30.3385	0.000314583	2.81600	1.43400	14.07980	0.02753
6.076	1.008	30.3784	0.000415625	2.83100	1.44800	14.15580	0.02533
6.08	1.004	30.4023	0.000248958	2.85000	1.44300	14.24760	0.03060

Appendix C: Shakedown Characteristics

6.086	1	30.4301	0.000289583	2.86600	1.45200	14.32980	0.02740
6.09	1.004	30.4492	0.000198958	2.88500	1.43700	14.42250	0.03090
6.093	1.008	30.466	0.000175	2.90100	1.44500	14.50420	0.02723
6.1	1.003	30.4999	0.000353125	2.91800	1.44100	14.59060	0.02880
6.103	1.004	30.5164	0.000171875	2.93700	1.43500	14.68330	0.03090
6.108	0.996	30.5394	0.000239583	2.95400	1.43800	14.76790	0.02820
6.112	0.996	30.5603	0.000217708	2.96900	1.44000	14.84370	0.02527
6.117	0.987	30.5863	0.000270833	2.98600	1.44000	14.92870	0.02833
6.121	0.982	30.6031	0.000175	3.00400	1.43700	15.01840	0.02990
6.124	0.981	30.6184	0.000159375	3.02000	1.43700	15.09980	0.02713
6.128	0.976	30.6412	0.0002375	3.03700	1.43800	15.18700	0.02907
6.131	0.977	30.6543	0.000136458	3.05400	1.44000	15.26770	0.02690
6.135	0.97	30.6741	0.00020625	3.06900	1.44500	15.34540	0.02590
6.138	0.968	30.6891	0.00015625	3.08700	1.44300	15.43280	0.02913
6.142	0.969	30.7091	0.000208333	3.10400	1.44100	15.52110	0.02943
6.145	0.973	30.7234	0.000148958	3.12100	1.43700	15.60700	0.02863
6.145	0.981	30.7233	-1.04167E-06	3.13600	1.44600	15.68030	0.02443
6.148	0.993	30.7389	0.0001625	3.15300	1.44100	15.76630	0.02867
6.15	0.988	30.7515	0.00013125	3.17000	1.44000	15.84990	0.02787
6.153	0.989	30.7646	0.000136458	3.18700	1.43800	15.93420	0.02810
6.156	0.988	30.7793	0.000153125	3.20400	1.43900	16.01810	0.02797
6.159	0.981	30.7967	0.00018125	3.21700	1.44400	16.08690	0.02293
6.162	0.979	30.8102	0.000140625	3.23500	1.43700	16.17370	0.02893
6.165	0.979	30.8246	0.00015	3.25100	1.43500	16.25250	0.02627
6.169	0.973	30.8434	0.000195833	3.26600	1.43400	16.33070	0.02607
6.171	0.978	30.8543	0.000113542	3.28100	1.43800	16.40450	0.02460
6.175	0.97	30.8733	0.000197917	3.29700	1.43800	16.48490	0.02680
6.177	0.969	30.8869	0.000141667	3.31500	1.42700	16.57520	0.03010
6.18	0.967	30.8988	0.000123958	3.32900	1.43000	16.64700	0.02393
6.182	0.972	30.9096	0.0001125	3.34500	1.43200	16.72540	0.02613
6.184	0.969	30.921	0.00011875	3.36000	1.43500	16.80150	0.02537

Appendix C: Shakedown Characteristics

6.186	0.975	30.929	8.33333E-05	3.37700	1.43100	16.88260	0.02703
6.189	0.962	30.9464	0.00018125	3.39100	1.43600	16.95720	0.02487
6.19	0.971	30.9511	4.89583E-05	3.40900	1.42600	17.04560	0.02947
6.194	0.963	30.9685	0.00018125	3.42400	1.43100	17.11770	0.02403
6.197	0.953	30.9861	0.000183333	3.43700	1.43500	17.18710	0.02313
6.199	0.952	30.9942	8.4375E-05	3.45100	1.44000	17.25610	0.02300
6.201	0.952	31.0069	0.000132292	3.46700	1.44100	17.33540	0.02643
6.203	0.952	31.0144	7.8125E-05	3.48100	1.44200	17.40670	0.02377
6.204	0.954	31.0221	8.02083E-05	3.49700	1.44100	17.48540	0.02623
6.206	0.957	31.028	6.14583E-05	3.51200	1.44300	17.56010	0.02490
6.209	0.952	31.0441	0.000167708	3.52700	1.44700	17.63540	0.02510
6.21	0.956	31.0498	5.9375E-05	3.54200	1.44400	17.71100	0.02520
6.211	0.961	31.0552	5.625E-05	3.55900	1.44000	17.79480	0.02793
6.213	0.96	31.0645	9.6875E-05	3.57300	1.44300	17.86330	0.02283
6.216	0.961	31.0789	0.00015	3.58700	1.44800	17.93390	0.02353
6.217	0.963	31.0836	4.89583E-05	3.60200	1.44100	18.01220	0.02610
6.22	0.956	31.0975	0.000144792	3.61700	1.44600	18.08730	0.02503
6.221	0.956	31.1037	6.45833E-05	3.63400	1.44200	18.16850	0.02707
6.223	0.953	31.1137	0.000104167	3.64800	1.44600	18.23910	0.02353
6.223	0.958	31.1169	3.33333E-05	3.66300	1.44600	18.31690	0.02593
6.225	0.956	31.1269	0.000104167	3.67800	1.44900	18.38980	0.02430
6.226	0.962	31.1277	8.33333E-06	3.69300	1.44500	18.46650	0.02557
6.228	0.961	31.1406	0.000134375	3.70800	1.44600	18.54160	0.02503
6.23	0.957	31.1507	0.000105208	3.72300	1.44600	18.61670	0.02503
6.232	0.957	31.1604	0.000101042	3.73900	1.44700	18.69290	0.02540
6.234	0.956	31.1686	8.54167E-05	3.75400	1.44600	18.76960	0.02557
6.235	0.96	31.1745	6.14583E-05	3.76900	1.44300	18.84570	0.02537
6.236	0.965	31.1777	3.33333E-05	3.78400	1.44300	18.91920	0.02450
6.237	0.972	31.1871	9.79167E-05	3.79900	1.44600	18.99410	0.02497
6.239	0.967	31.1937	6.875E-05	3.81300	1.44700	19.06670	0.02420
6.241	0.961	31.204	0.000107292	3.82800	1.44800	19.14110	0.02480
6.243	0.954	31.2156	0.000120833	3.84300	1.44800	19.21680	0.02523

Appendix C: Shakedown Characteristics

6.244	0.955	31.2195	4.0625E-05	3.85800	1.45100	19.28810	0.02377
6.246	0.949	31.2323	0.000133333	3.87200	1.45100	19.36200	0.02463
6.248	0.948	31.2387	6.66667E-05	3.88900	1.44500	19.44410	0.02737

5		6		7		8		9	
n	pd	n	pd	n	pd	n	pd	n	pd
0	0	0	0	0	0	0	0	0	0
10	1.28008	10	1.706813	10	2.157181	10	2.620893	10	3.089242
100	1.677742	100	2.313113	100	3.022877	100	3.797573	100	4.62841
1000	2.198938	1000	3.134785	1000	4.235985	1000	5.502538	1000	6.934444
2000	2.385505	2000	3.43516	2000	4.688841	2000	6.15242	2000	7.831887
3000	2.501894	3000	3.62404	3000	4.975867	3000	6.567599	3000	8.409777
10000	2.882046	10000	4.248334	10000	5.935923	10000	7.972965	10000	10.38942
20000	3.126571	20000	4.655409	20000	6.570514	20000	8.914619	20000	11.734
30000	3.279117	30000	4.911383	30000	6.972727	30000	9.516199	30000	12.59982
50000	3.481941	50000	5.254002	50000	7.514689	50000	10.33222	50000	13.78213
80000	3.67962	80000	5.590315	80000	8.050475	80000	11.14471	80000	14.96773
100000	3.777364	100000	5.757441	100000	8.318061	100000	11.55252	100000	15.56579
200000	4.097851	200000	6.309119	200000	9.207319	200000	12.91694	200000	17.58029
300000	4.297786	300000	6.656021	300000	9.770944	300000	13.7886	300000	18.87748
350000	4.376331	350000	6.792856	350000	9.994164	350000	14.13522	350000	19.39539
400000	4.44553	400000	6.913659	400000	10.19164	400000	14.44251	400000	19.8555
500000	4.563618	500000	7.120346	500000	10.5304	500000	14.97099	500000	20.64887

Appendix C: Shakedown Characteristics

10		11		12		13		14	
n	pd	n	pd	n	pd	n	pd	n	pd
0	0	0	0	0	0	0	0	0	0
10	11.62338	10	13.95467	10	16.46197	10	19.13696	10	21.97154
100	12.45297	100	15.05144	100	17.8755	100	20.92027	100	24.18093
1000	13.34177	1000	16.23441	1000	19.41041	1000	22.86977	1000	26.61248
2000	13.62154	2000	16.6084	2000	19.89777	2000	23.49145	2000	27.39126
3000	13.78791	3000	16.83116	3000	20.18852	3000	23.86292	3000	27.85733
10000	14.294	10000	17.51035	10000	21.07711	10000	25.00093	10000	29.28855
20000	14.59375	20000	17.91374	20000	21.60633	20000	25.68055	20000	30.14563
30000	14.77199	30000	18.154	30000	21.92203	30000	26.08664	30000	30.65858
50000	14.99965	50000	18.46129	50000	22.32635	50000	26.6074	50000	31.31725
80000	15.21222	80000	18.74861	80000	22.70495	80000	27.09572	80000	31.93578
100000	15.3142	100000	18.88658	100000	22.88693	100000	27.33069	100000	32.2337
200000	15.63534	200000	19.32167	200000	23.46159	200000	28.07364	200000	33.17698
300000	15.8263	300000	19.58082	300000	23.8044	300000	28.51757	300000	33.7415
350000	15.89952	350000	19.68025	350000	23.93604	350000	28.68818	350000	33.95863
400000	15.96321	400000	19.76679	400000	24.05067	400000	28.83679	400000	34.14785
500000	16.07022	500000	19.91226	500000	24.24344	500000	29.08686	500000	34.46641

Appendix C: Shakedown Characteristics

15	
n	pd
0	0
10	3.770938
20	4.983871
30	5.871679
40	6.599262
100	9.617721
200	12.90904
300	15.47092
400	17.7377
500	19.89057
600	22.04148
700	24.27993
800	26.69146
900	29.36781
1000	32.41441
1100	35.9574
1200	40.15118
1300	45.18724
1400	51.30488
1500	58.80453

Appendix C: Shakedown Characteristics

APPENDIX C (Shakedown Characterisation) HCTCRB with Various Stress Levels

8				10			
Permanent Deformation	Resilient Strain 10-3	Permanent strain10-3	Strain Rate	Permanent Deformation	Resilient Strain 10-3	Permanent strain10-3	Strain Rate
0.00000	0.80500	0.00000	0.00000	0.00000	0.93500	0.00000	0.00000
0.36600	0.83500	1.82790	0.01904	0.30000	0.91000	1.49960	0.01562
0.42100	0.81800	2.10730	0.00291	0.34900	0.88600	1.74560	0.00256
0.45100	0.81100	2.25610	0.00155	0.37600	0.87100	1.87890	0.00139
0.47100	0.80700	2.35530	0.00103	0.39300	0.86200	1.96640	0.00091
0.48600	0.80400	2.42800	0.00076	0.40600	0.85800	2.02920	0.00065
0.49700	0.80200	2.48570	0.00060	0.41500	0.85700	2.07520	0.00048
0.50400	0.81400	2.51810	0.00034	0.42300	0.84900	2.11270	0.00039
0.51100	0.81300	2.55600	0.00039	0.42900	0.84700	2.14390	0.00033
0.51900	0.80800	2.59440	0.00040	0.43400	0.84400	2.17220	0.00029
0.52400	0.80800	2.62170	0.00028	0.43900	0.84000	2.19610	0.00025
0.53000	0.80700	2.64770	0.00027	0.44400	0.83700	2.21890	0.00024
0.53400	0.80400	2.67170	0.00025	0.44800	0.83800	2.23840	0.00020
0.53900	0.80200	2.69370	0.00023	0.45200	0.83500	2.25800	0.00020
0.54300	0.79600	2.71690	0.00024	0.45500	0.83300	2.27500	0.00018
0.54700	0.79600	2.73450	0.00018	0.45800	0.83000	2.29060	0.00016
0.55100	0.79100	2.75500	0.00021	0.46000	0.82800	2.30170	0.00012
0.55500	0.78700	2.77300	0.00019	0.46200	0.82700	2.31200	0.00011
0.55800	0.78100	2.79090	0.00019	0.46500	0.82400	2.32420	0.00013
0.56000	0.78000	2.80180	0.00011	0.46700	0.82300	2.33360	0.00010
0.56200	0.78100	2.81170	0.00010	0.46900	0.82100	2.34330	0.00010
0.56500	0.77900	2.82270	0.00011	0.47000	0.82000	2.35130	0.00008
0.56600	0.77800	2.83160	0.00009	0.47200	0.81900	2.35990	0.00009
0.56800	0.77700	2.83960	0.00008	0.47400	0.81800	2.36820	0.00009

Appendix C: Shakedown Characteristics

0.57000	0.77600	2.84960	0.00010	0.47500	0.81600	2.37520	0.00007
0.57200	0.77300	2.86010	0.00011	0.47600	0.81600	2.38220	0.00007
0.57300	0.77300	2.86710	0.00007	0.47800	0.81300	2.38980	0.00008
0.57500	0.77200	2.87470	0.00008	0.48000	0.81100	2.39830	0.00009
0.57600	0.77100	2.88180	0.00007	0.48100	0.81200	2.40350	0.00005
0.57800	0.77100	2.88830	0.00007	0.48200	0.81200	2.41160	0.00008
0.57900	0.77000	2.89460	0.00007	0.48400	0.80900	2.41960	0.00008
0.58000	0.76900	2.90140	0.00007	0.48500	0.80800	2.42720	0.00008
0.58200	0.76800	2.90890	0.00008	0.48600	0.80700	2.43220	0.00005
0.58400	0.76500	2.91790	0.00009	0.48700	0.80600	2.43730	0.00005
0.58600	0.76100	2.92800	0.00011	0.48800	0.80500	2.44150	0.00004
0.58700	0.75900	2.93550	0.00008	0.48900	0.80500	2.44540	0.00004
0.58800	0.75800	2.94010	0.00005	0.49000	0.80400	2.44990	0.00005
0.58900	0.75900	2.94380	0.00004	0.49100	0.80300	2.45410	0.00004
0.59000	0.75900	2.94800	0.00004	0.49200	0.80200	2.45770	0.00004
0.59000	0.75900	2.95160	0.00004	0.49200	0.80100	2.46230	0.00005
0.59100	0.76000	2.95530	0.00004	0.49300	0.80100	2.46540	0.00003
0.59200	0.75900	2.95930	0.00004	0.49400	0.80000	2.46960	0.00004
0.59300	0.75800	2.96380	0.00005	0.49500	0.79900	2.47370	0.00004
0.59300	0.75800	2.96710	0.00003	0.49500	0.79900	2.47720	0.00004
0.59400	0.75800	2.97100	0.00004	0.49600	0.79700	2.48160	0.00005
0.59500	0.75700	2.97450	0.00004	0.49700	0.80000	2.48400	0.00003
0.59600	0.75700	2.97810	0.00004	0.49800	0.79800	2.49040	0.00007
0.59600	0.75700	2.98130	0.00003	0.49900	0.79800	2.49410	0.00004
0.59700	0.75600	2.98560	0.00004	0.50000	0.79500	2.50040	0.00007
0.59800	0.75500	2.98950	0.00004	0.50100	0.79300	2.50480	0.00005
0.59900	0.75200	2.99700	0.00008	0.50100	0.79400	2.50630	0.00002
0.60100	0.75000	3.00280	0.00006	0.50200	0.79400	2.50930	0.00003
0.60200	0.74700	3.00980	0.00007	0.50200	0.79300	2.51180	0.00003
0.60300	0.74700	3.01350	0.00004	0.50300	0.79300	2.51470	0.00003
0.60300	0.74700	3.01580	0.00002	0.50300	0.79300	2.51630	0.00002
0.60400	0.74700	3.01760	0.00002	0.50400	0.79200	2.51830	0.00002

Appendix C: Shakedown Characteristics

0.60400	0.74700	3.02000	0.00003	0.50400	0.79000	2.52180	0.00004
0.60400	0.74800	3.02240	0.00003	0.50500	0.79400	2.52310	0.00001
0.60500	0.74600	3.02550	0.00003	0.50600	0.79200	2.52770	0.00005
0.60500	0.74700	3.02750	0.00002	0.50700	0.79000	2.53340	0.00006
0.60600	0.74800	3.02930	0.00002	0.50700	0.78900	2.53730	0.00004
0.60600	0.74700	3.03230	0.00003	0.50800	0.78800	2.53930	0.00002
0.60700	0.74600	3.03460	0.00002	0.50800	0.78800	2.54050	0.00001
0.60700	0.74700	3.03640	0.00002	0.50900	0.78900	2.54290	0.00002
0.60800	0.74700	3.03900	0.00003	0.50900	0.78700	2.54540	0.00003
0.60800	0.74700	3.04090	0.00002	0.51000	0.78700	2.54800	0.00003
0.60900	0.74500	3.04360	0.00003	0.51000	0.78600	2.54970	0.00002
0.61000	0.74400	3.04940	0.00006	0.51000	0.78600	2.55200	0.00002
0.61100	0.74100	3.05510	0.00006	0.51100	0.78500	2.55440	0.00003
0.61200	0.73900	3.05980	0.00005	0.51200	0.78400	2.55760	0.00003
0.61300	0.73700	3.06520	0.00006	0.51200	0.78200	2.56050	0.00003
0.61300	0.73700	3.06610	0.00001	0.51300	0.78400	2.56300	0.00003
0.61300	0.74000	3.06480	- 0.00001	0.51300	0.78300	2.56720	0.00004
0.61300	0.74100	3.06500	0.00000	0.51400	0.78300	2.56970	0.00003
0.61300	0.74100	3.06690	0.00002	0.51400	0.78500	2.57030	0.00001
0.61400	0.74100	3.06830	0.00001	0.51400	0.78500	2.57230	0.00002
0.61400	0.74100	3.07010	0.00002	0.51500	0.78400	2.57430	0.00002
0.61400	0.74000	3.07230	0.00002	0.51500	0.78400	2.57500	0.00001
0.61500	0.73900	3.07510	0.00003	0.51500	0.78400	2.57640	0.00001
0.61600	0.73800	3.08010	0.00005	0.51600	0.78400	2.57790	0.00002
0.61700	0.73500	3.08580	0.00006	0.51600	0.78400	2.57950	0.00002
0.61800	0.73300	3.08990	0.00004	0.51600	0.78300	2.58190	0.00003
0.61900	0.73100	3.09450	0.00005	0.51700	0.78200	2.58340	0.00002
0.61900	0.73000	3.09680	0.00002	0.51700	0.78200	2.58460	0.00001
0.62000	0.73000	3.09850	0.00002	0.51700	0.78200	2.58720	0.00003
0.62000	0.72900	3.10040	0.00002	0.51800	0.78000	2.59050	0.00003
0.62000	0.72900	3.10240	0.00002	0.51800	0.78000	2.59220	0.00002

Appendix C: Shakedown Characteristics

0.62100	0.72800	3.10440	0.00002	0.51900	0.78100	2.59440	0.00002
0.62100	0.72800	3.10600	0.00002	0.52000	0.77900	2.59760	0.00003
0.62100	0.72800	3.10700	0.00001	0.52000	0.77800	2.59980	0.00002
0.62200	0.72800	3.10820	0.00001	0.52000	0.77800	2.60100	0.00001
0.62200	0.72800	3.10910	0.00001	0.52100	0.77800	2.60280	0.00002
0.62200	0.72700	3.11080	0.00002	0.52100	0.77700	2.60510	0.00002
0.62200	0.72800	3.11150	0.00001	0.52200	0.77700	2.60760	0.00003
0.62300	0.72700	3.11410	0.00003	0.52200	0.77600	2.61010	0.00003
0.62300	0.72700	3.11600	0.00002	0.52200	0.77500	2.61180	0.00002
0.62400	0.72600	3.11970	0.00004	0.52300	0.77600	2.61390	0.00002
0.62500	0.72300	3.12430	0.00005	0.52300	0.77400	2.61660	0.00003
0.62600	0.72100	3.12910	0.00005	0.52400	0.77300	2.62020	0.00004
0.62600	0.72000	3.13170	0.00003	0.52400	0.77300	2.62140	0.00001
0.62600	0.72000	3.13250	0.00001	0.52500	0.77300	2.62480	0.00004
0.62700	0.72000	3.13330	0.00001	0.52600	0.77200	2.62810	0.00003
0.62700	0.72100	3.13390	0.00001	0.52600	0.77100	2.62970	0.00002
0.62700	0.72100	3.13400	0.00000	0.52600	0.77200	2.63060	0.00001
0.62700	0.72100	3.13580	0.00002	0.52600	0.77100	2.63190	0.00001
0.62700	0.72100	3.13650	0.00001	0.52700	0.77100	2.63310	0.00001
0.62800	0.72100	3.13810	0.00002	0.52700	0.77100	2.63420	0.00001
0.62800	0.72100	3.13870	0.00001	0.52700	0.77100	2.63510	0.00001
0.62800	0.72100	3.14000	0.00001	0.52700	0.77100	2.63640	0.00001
0.62800	0.72100	3.14040	0.00000	0.52700	0.77100	2.63740	0.00001
0.62800	0.72100	3.14150	0.00001	0.52800	0.77100	2.63840	0.00001
0.62800	0.72100	3.14250	0.00001	0.52800	0.77100	2.63960	0.00001
0.62900	0.72000	3.14400	0.00002	0.52800	0.77000	2.64100	0.00001
0.62900	0.72000	3.14630	0.00002	0.52800	0.76900	2.64200	0.00001
0.63000	0.71900	3.15010	0.00004	0.52900	0.76900	2.64400	0.00002
0.63100	0.71500	3.15500	0.00005	0.52900	0.77000	2.64560	0.00002
0.63100	0.71400	3.15750	0.00003	0.53000	0.76800	2.65040	0.00005
0.63200	0.71400	3.15910	0.00002	0.53100	0.76700	2.65400	0.00004
0.63200	0.71400	3.15980	0.00001	0.53100	0.76600	2.65710	0.00003

Appendix C: Shakedown Characteristics

0.63200	0.71500	3.15900	- 0.00001	0.53200	0.76600	2.65820	0.00001
0.63200	0.71400	3.16100	0.00002	0.53200	0.76700	2.65920	0.00001
0.63200	0.71400	3.16110	0.00000	0.53200	0.76600	2.66010	0.00001
0.63200	0.71500	3.16220	0.00001	0.53200	0.76500	2.66130	0.00001
0.63300	0.71400	3.16300	0.00001	0.53200	0.76600	2.66220	0.00001
0.63300	0.71500	3.16360	0.00001	0.53300	0.76600	2.66280	0.00001
0.63300	0.71500	3.16420	0.00001	0.53300	0.76500	2.66390	0.00001
0.63300	0.71500	3.16490	0.00001	0.53300	0.76600	2.66500	0.00001
0.63300	0.71500	3.16570	0.00001	0.53300	0.76400	2.66620	0.00001
0.63300	0.71500	3.16600	0.00000	0.53300	0.76500	2.66710	0.00001
0.63300	0.71600	3.16700	0.00001	0.53400	0.76400	2.66830	0.00001
0.63400	0.71500	3.16830	0.00001	0.53400	0.76400	2.66930	0.00001
0.63400	0.71300	3.17230	0.00004	0.53400	0.76300	2.67130	0.00002
0.63500	0.71100	3.17610	0.00004	0.53500	0.76400	2.67430	0.00003
0.63600	0.70900	3.18050	0.00005	0.53600	0.76200	2.67850	0.00004
0.63700	0.70800	3.18270	0.00002	0.53600	0.76100	2.68160	0.00003
0.63700	0.70800	3.18270	0.00000	0.53700	0.76100	2.68350	0.00002
0.63600	0.70900	3.18210	- 0.00001	0.53700	0.76100	2.68420	0.00001
0.63700	0.71000	3.18300	0.00001	0.53700	0.76100	2.68530	0.00001
0.63700	0.71000	3.18270	0.00000	0.53700	0.76100	2.68560	0.00000
0.63700	0.70900	3.18380	0.00001	0.53700	0.76000	2.68690	0.00001
0.63700	0.70900	3.18440	0.00001	0.53800	0.76000	2.68780	0.00001
0.63700	0.71000	3.18500	0.00001	0.53800	0.76000	2.68840	0.00001
0.63700	0.70900	3.18570	0.00001	0.53800	0.76000	2.68900	0.00001
0.63700	0.70900	3.18630	0.00001	0.53800	0.76000	2.68990	0.00001
0.63700	0.71000	3.18660	0.00000	0.53800	0.76000	2.69060	0.00001
0.63700	0.71000	3.18660	0.00000	0.53800	0.76000	2.69170	0.00001
0.63800	0.71000	3.18760	0.00001	0.53900	0.75900	2.69280	0.00001
0.63800	0.70900	3.18890	0.00001	0.53900	0.75800	2.69470	0.00002
0.63800	0.71000	3.19020	0.00001	0.53900	0.75800	2.69620	0.00002

Appendix C: Shakedown Characteristics

0.63900	0.70700	3.19420	0.00004	0.54000	0.75800	2.69920	0.00003
0.64000	0.70400	3.19820	0.00004	0.54100	0.75700	2.70290	0.00004
0.64000	0.70300	3.20130	0.00003	0.54100	0.75600	2.70550	0.00003
0.64100	0.70200	3.20300	0.00002	0.54100	0.75600	2.70720	0.00002
0.64100	0.70300	3.20300	0.00000	0.54200	0.75600	2.70770	0.00001
0.64100	0.70300	3.20300	0.00000	0.54200	0.75600	2.70810	0.00000
0.64100	0.70400	3.20300	0.00000	0.54200	0.75600	2.70890	0.00001
0.64100	0.70400	3.20290	0.00000	0.54200	0.75600	2.70920	0.00000
0.64100	0.70500	3.20330	0.00000	0.54200	0.75600	2.70990	0.00001
0.64100	0.70500	3.20380	0.00001	0.54200	0.75600	2.71090	0.00001
0.64100	0.70500	3.20420	0.00000	0.54200	0.75500	2.71160	0.00001
0.64100	0.70600	3.20430	0.00000	0.54200	0.75500	2.71250	0.00001
0.64100	0.70400	3.20530	0.00001	0.54300	0.75600	2.71290	0.00000
0.64100	0.70500	3.20510	0.00000	0.54300	0.75500	2.71410	0.00001
0.64100	0.70500	3.20580	0.00001	0.54300	0.75400	2.71480	0.00001
0.64100	0.70500	3.20650	0.00001	0.54300	0.75400	2.71590	0.00001
0.64200	0.70400	3.20760	0.00001	0.54300	0.75400	2.71720	0.00001
0.64200	0.70500	3.20950	0.00002	0.54400	0.75300	2.72190	0.00005
0.64300	0.70200	3.21390	0.00005	0.54500	0.75200	2.72500	0.00003
0.64400	0.69900	3.21770	0.00004	0.54600	0.75100	2.72810	0.00003
0.64400	0.69800	3.22060	0.00003	0.54600	0.75000	2.72980	0.00002
0.64400	0.69800	3.22030	0.00000	0.54600	0.75000	2.73000	0.00000
0.64400	0.69800	3.22060	0.00000	0.54600	0.75100	2.73030	0.00000
0.64400	0.70000	3.22010	- 0.00001	0.54600	0.75000	2.73080	0.00001
0.64400	0.70000	3.22020	0.00000	0.54600	0.75000	2.73110	0.00000
0.64400	0.70000	3.22040	0.00000	0.54600	0.75000	2.73160	0.00001
0.64400	0.70000	3.22070	0.00000	0.54600	0.75000	2.73220	0.00001
0.64400	0.70000	3.22090	0.00000	0.54600	0.74900	2.73250	0.00000
0.64400	0.70000	3.22110	0.00000	0.54700	0.74900	2.73280	0.00000
0.64400	0.70100	3.22140	0.00000	0.54700	0.75000	2.73340	0.00001
0.64400	0.70100	3.22190	0.00001	0.54700	0.75000	2.73370	0.00000

Appendix C: Shakedown Characteristics

0.64400	0.70100	3.22220	0.00000	0.54700	0.74900	2.73420	0.00001
0.64400	0.70100	3.22210	0.00000	0.54700	0.74900	2.73530	0.00001
0.64500	0.70100	3.22290	0.00001	0.54700	0.75000	2.73690	0.00002
0.64500	0.70100	3.22380	0.00001	0.54800	0.74800	2.74110	0.00004

12				14			
Permanent Deformation	Resilient Strain 10 ⁻³	Permanent strain10 ⁻³	Strain Rate	Permanent Deformation	Resilient Strain 10 ⁻³	Permanent strain10 ⁻³	Strain Rate
0.00000	0.73700	0.00000	0.00000	0.00000	0.98700	0.00000	0.00000
0.15500	0.82000	0.77330	0.01611	0.42500	1.02000	2.12490	0.04427
0.18100	0.81900	0.90490	0.00274	0.50700	1.01500	2.53410	0.00853
0.19600	0.81900	0.98030	0.00157	0.55500	1.01000	2.77530	0.00503
0.20600	0.81700	1.03220	0.00108	0.58900	1.00700	2.94280	0.00349
0.21400	0.81500	1.07140	0.00082	0.61400	1.00700	3.07220	0.00270
0.22100	0.81500	1.10260	0.00065	0.63500	1.00300	3.17330	0.00211
0.22600	0.81400	1.12770	0.00052	0.65200	1.00100	3.25820	0.00177
0.22900	0.81500	1.14670	0.00040	0.66600	0.99800	3.32960	0.00149
0.23300	0.81400	1.16480	0.00038	0.67800	0.99500	3.39060	0.00127
0.23600	0.81400	1.17960	0.00031	0.68900	0.99300	3.44320	0.00110
0.23900	0.81300	1.19310	0.00028	0.69900	0.98800	3.49470	0.00107
0.24100	0.81200	1.20490	0.00025	0.70700	0.98700	3.53410	0.00082
0.24300	0.81100	1.21590	0.00023	0.71400	0.98700	3.57030	0.00075
0.24500	0.80900	1.22680	0.00023	0.72100	0.98300	3.60440	0.00071
0.24700	0.80800	1.23660	0.00020	0.72700	0.98000	3.63630	0.00066
0.24900	0.80700	1.24470	0.00017	0.73300	0.97700	3.66470	0.00059
0.25100	0.80600	1.25330	0.00018	0.73800	0.98100	3.69190	0.00057
0.25200	0.80500	1.26050	0.00015	0.74300	0.98100	3.71530	0.00049
0.25400	0.80400	1.26830	0.00016	0.74700	0.98500	3.73290	0.00037
0.25500	0.80300	1.27410	0.00012	0.75100	0.98300	3.75370	0.00043
0.25600	0.80200	1.28140	0.00015	0.75500	0.98100	3.77320	0.00041
0.25700	0.80200	1.28620	0.00010	0.75800	0.97700	3.79160	0.00038

Appendix C: Shakedown Characteristics

0.25800	0.80100	1.29240	0.00013	0.76200	0.97500	3.80840	0.00035
0.26000	0.80000	1.29830	0.00012	0.76500	0.97500	3.82390	0.00032
0.26100	0.80000	1.30360	0.00011	0.76800	0.97300	3.84050	0.00035
0.26200	0.79700	1.31000	0.00013	0.77100	0.97500	3.85670	0.00034
0.26300	0.79700	1.31470	0.00010	0.77400	0.97400	3.87060	0.00029
0.26400	0.79600	1.31890	0.00009	0.77700	0.97200	3.88540	0.00031
0.26500	0.79600	1.32330	0.00009	0.78000	0.97100	3.89820	0.00027
0.26500	0.79500	1.32750	0.00009	0.78200	0.97100	3.91120	0.00027
0.26600	0.79400	1.33190	0.00009	0.78500	0.97200	3.92320	0.00025
0.26700	0.79400	1.33580	0.00008	0.78700	0.97100	3.93540	0.00025
0.26800	0.79300	1.33950	0.00008	0.78900	0.97000	3.94680	0.00024
0.26900	0.79400	1.34280	0.00007	0.79200	0.96900	3.95780	0.00023
0.26900	0.79400	1.34720	0.00009	0.79400	0.96800	3.96790	0.00021
0.27000	0.79400	1.35090	0.00008	0.79500	0.96800	3.97720	0.00019
0.27100	0.79400	1.35460	0.00008	0.79700	0.96800	3.98710	0.00021
0.27200	0.79400	1.35830	0.00008	0.79900	0.96400	3.99700	0.00021
0.27200	0.79400	1.36230	0.00008	0.80100	0.96700	4.00450	0.00016
0.27300	0.79400	1.36470	0.00005	0.80300	0.96400	4.01400	0.00020
0.27300	0.79500	1.36730	0.00005	0.80400	0.96300	4.02250	0.00018
0.27400	0.79400	1.36980	0.00005	0.80600	0.96300	4.02900	0.00014
0.27500	0.79200	1.37360	0.00008	0.80800	0.96000	4.03770	0.00018
0.27500	0.79300	1.37540	0.00004	0.80900	0.95900	4.04510	0.00015
0.27600	0.79200	1.37890	0.00007	0.81000	0.95900	4.05210	0.00015
0.27600	0.79100	1.38130	0.00005	0.81200	0.95700	4.05860	0.00014
0.27700	0.79000	1.38370	0.00005	0.81300	0.95400	4.06620	0.00016
0.27700	0.79000	1.38660	0.00006	0.81500	0.95200	4.07300	0.00014
0.27800	0.78900	1.38950	0.00006	0.81600	0.95700	4.07840	0.00011
0.27800	0.78700	1.39220	0.00006	0.81700	0.95800	4.08500	0.00014
0.27900	0.78700	1.39410	0.00004	0.81800	0.95600	4.08990	0.00010
0.27900	0.78600	1.39680	0.00006	0.81900	0.95600	4.09580	0.00012
0.28000	0.78500	1.39920	0.00005	0.82000	0.95400	4.10060	0.00010
0.28100	0.78400	1.40260	0.00007	0.82100	0.95400	4.10510	0.00009

Appendix C: Shakedown Characteristics

0.28100	0.78300	1.40490	0.00005	0.82200	0.95100	4.11050	0.00011
0.28100	0.78400	1.40640	0.00003	0.82300	0.95000	4.11540	0.00010
0.28200	0.78400	1.40890	0.00005	0.82400	0.95000	4.12080	0.00011
0.28200	0.78400	1.41070	0.00004	0.82500	0.95000	4.12580	0.00010
0.28200	0.78300	1.41220	0.00003	0.82600	0.95000	4.13090	0.00011
0.28300	0.78300	1.41470	0.00005	0.82700	0.95200	4.13550	0.00010
0.28300	0.78300	1.41680	0.00004	0.82800	0.95100	4.14090	0.00011
0.28400	0.78300	1.41850	0.00004	0.82900	0.95100	4.14590	0.00010
0.28400	0.78200	1.42110	0.00005	0.83000	0.95100	4.15120	0.00011
0.28500	0.78100	1.42350	0.00005	0.83100	0.95000	4.15580	0.00010
0.28500	0.78000	1.42580	0.00005	0.83200	0.95000	4.16090	0.00011
0.28600	0.78200	1.42750	0.00004	0.83300	0.94900	4.16600	0.00011
0.28600	0.78100	1.43050	0.00006	0.83400	0.95100	4.16990	0.00008
0.28600	0.78000	1.43230	0.00004	0.83500	0.95000	4.17410	0.00009
0.28700	0.78000	1.43470	0.00005	0.83600	0.94900	4.17890	0.00010
0.28700	0.78000	1.43700	0.00005	0.83700	0.94900	4.18320	0.00009
0.28800	0.78100	1.43830	0.00003	0.83700	0.94900	4.18730	0.00009
0.28800	0.78000	1.44160	0.00007	0.83800	0.94700	4.19200	0.00010
0.28800	0.78100	1.44230	0.00001	0.83900	0.94500	4.19610	0.00009
0.28900	0.78100	1.44450	0.00005	0.84000	0.94300	4.20060	0.00009
0.28900	0.78000	1.44620	0.00004	0.84100	0.94300	4.20460	0.00008
0.28900	0.78000	1.44750	0.00003	0.84200	0.94100	4.20900	0.00009
0.29000	0.77900	1.44860	0.00002	0.84300	0.93900	4.21300	0.00008
0.29000	0.77800	1.45070	0.00004	0.84400	0.93600	4.21770	0.00010
0.29100	0.77700	1.45270	0.00004	0.84400	0.93500	4.22050	0.00006
0.29100	0.77700	1.45340	0.00001	0.84500	0.93200	4.22510	0.00010
0.29100	0.77700	1.45480	0.00003	0.84500	0.93900	4.22660	0.00003
0.29100	0.77500	1.45740	0.00005	0.84600	0.94100	4.23110	0.00009
0.29200	0.77400	1.45910	0.00004	0.84700	0.94100	4.23380	0.00006
0.29200	0.77400	1.45990	0.00002	0.84700	0.94100	4.23680	0.00006
0.29300	0.77300	1.46250	0.00005	0.84800	0.94000	4.23980	0.00006
0.29300	0.77300	1.46350	0.00002	0.84900	0.93900	4.24280	0.00006

Appendix C: Shakedown Characteristics

0.29300	0.77300	1.46510	0.00003	0.84900	0.94000	4.24470	0.00004
0.29300	0.77200	1.46650	0.00003	0.84900	0.93800	4.24730	0.00005
0.29400	0.77200	1.46810	0.00003	0.85000	0.93800	4.24950	0.00005
0.29400	0.77200	1.46900	0.00002	0.85100	0.93800	4.25270	0.00007
0.29400	0.77100	1.47110	0.00004	0.85100	0.93900	4.25470	0.00004
0.29400	0.77100	1.47240	0.00003	0.85200	0.93900	4.25850	0.00008
0.29500	0.77000	1.47430	0.00004	0.85200	0.94000	4.26130	0.00006
0.29500	0.77000	1.47530	0.00002	0.85300	0.93900	4.26430	0.00006
0.29500	0.77000	1.47680	0.00003	0.85400	0.94000	4.26750	0.00007
0.29600	0.76900	1.47840	0.00003	0.85400	0.94100	4.27010	0.00005
0.29600	0.76900	1.47980	0.00003	0.85500	0.93900	4.27400	0.00008
0.29600	0.76900	1.48130	0.00003	0.85500	0.94000	4.27650	0.00005
0.29700	0.76800	1.48350	0.00005	0.85600	0.94000	4.27920	0.00006
0.29700	0.76800	1.48570	0.00005	0.85700	0.93900	4.28270	0.00007
0.29700	0.76900	1.48610	0.00001	0.85700	0.93900	4.28500	0.00005
0.29800	0.76900	1.48850	0.00005	0.85800	0.93800	4.28800	0.00006
0.29800	0.77000	1.48870	0.00000	0.85800	0.93700	4.29100	0.00006
0.29800	0.76900	1.49110	0.00005	0.85900	0.93600	4.29420	0.00007
0.29800	0.76900	1.49250	0.00003	0.85900	0.93500	4.29650	0.00005
0.29900	0.76900	1.49330	0.00002	0.86000	0.93600	4.29890	0.00005
0.29900	0.76900	1.49350	0.00000	0.86000	0.93500	4.30150	0.00005
0.29900	0.76800	1.49570	0.00005	0.86100	0.93500	4.30460	0.00006
0.29900	0.76700	1.49680	0.00002	0.86100	0.93300	4.30720	0.00005
0.30000	0.76700	1.49800	0.00003	0.86200	0.93300	4.31060	0.00007
0.30000	0.76700	1.49880	0.00002	0.86300	0.93100	4.31270	0.00004
0.30000	0.76700	1.49900	0.00000	0.86300	0.92800	4.31560	0.00006
0.30000	0.76700	1.50070	0.00004	0.86400	0.92600	4.31870	0.00006
0.30000	0.76600	1.50180	0.00002	0.86400	0.93300	4.32130	0.00005
0.30000	0.76600	1.50240	0.00001	0.86500	0.93200	4.32420	0.00006
0.30100	0.76500	1.50390	0.00003	0.86500	0.93200	4.32590	0.00004
0.30100	0.76400	1.50540	0.00003	0.86600	0.93000	4.32810	0.00005
0.30100	0.76400	1.50630	0.00002	0.86600	0.93000	4.32940	0.00003

Appendix C: Shakedown Characteristics

0.30200	0.76400	1.50760	0.00003	0.86600	0.92700	4.33210	0.00006
0.30200	0.76300	1.50900	0.00003	0.86700	0.92600	4.33430	0.00005
0.30200	0.76400	1.50930	0.00001	0.86700	0.92600	4.33550	0.00002
0.30200	0.76300	1.51100	0.00004	0.86700	0.92700	4.33680	0.00003
0.30200	0.76300	1.51180	0.00002	0.86800	0.92800	4.33900	0.00005
0.30300	0.76200	1.51330	0.00003	0.86800	0.92900	4.34080	0.00004
0.30300	0.76200	1.51420	0.00002	0.86900	0.92900	4.34320	0.00005
0.30300	0.76300	1.51500	0.00002	0.86900	0.92900	4.34530	0.00004
0.30300	0.76200	1.51640	0.00003	0.86900	0.93000	4.34730	0.00004
0.30300	0.76300	1.51740	0.00002	0.87000	0.93000	4.34910	0.00004
0.30400	0.76200	1.51840	0.00002	0.87000	0.92800	4.35190	0.00006
0.30400	0.76200	1.51990	0.00003	0.87100	0.92800	4.35420	0.00005
0.30400	0.76100	1.52190	0.00004	0.87100	0.92900	4.35610	0.00004
0.30500	0.76100	1.52330	0.00003	0.87200	0.93000	4.35770	0.00003
0.30500	0.76200	1.52470	0.00003	0.87200	0.92900	4.36010	0.00005
0.30500	0.76100	1.52580	0.00002	0.87200	0.92800	4.36220	0.00004
0.30600	0.76100	1.52780	0.00004	0.87300	0.92700	4.36490	0.00006
0.30600	0.76100	1.52860	0.00002	0.87300	0.92700	4.36640	0.00003
0.30600	0.76200	1.52970	0.00002	0.87400	0.92700	4.36880	0.00005
0.30600	0.76100	1.53100	0.00003	0.87400	0.92700	4.37060	0.00004
0.30600	0.76100	1.53160	0.00001	0.87500	0.92600	4.37320	0.00005
0.30600	0.76100	1.53190	0.00001	0.87500	0.92500	4.37590	0.00006
0.30700	0.76200	1.53260	0.00001	0.87600	0.92500	4.37770	0.00004
0.30700	0.76100	1.53320	0.00001	0.87600	0.92300	4.38030	0.00005
0.30700	0.76000	1.53450	0.00003	0.87700	0.92200	4.38290	0.00005
0.30700	0.76000	1.53440	0.00000	0.87700	0.92000	4.38470	0.00004
0.30700	0.76000	1.53630	0.00004	0.87700	0.91700	4.38730	0.00005
0.30700	0.76000	1.53650	0.00000	0.87800	0.92000	4.38920	0.00004
0.30800	0.75900	1.53830	0.00004	0.87800	0.92300	4.39080	0.00003
0.30800	0.75900	1.53870	0.00001	0.87900	0.92300	4.39270	0.00004
0.30800	0.75800	1.54040	0.00004	0.87900	0.92400	4.39250	0.00000
0.30800	0.75800	1.54100	0.00001	0.87900	0.92200	4.39400	0.00003

Appendix C: Shakedown Characteristics

0.30800	0.75700	1.54230	0.00003	0.87900	0.92000	4.39590	0.00004
0.30900	0.75700	1.54280	0.00001	0.88000	0.91900	4.39760	0.00004
0.30900	0.75700	1.54400	0.00003	0.88000	0.91900	4.39860	0.00002
0.30900	0.75600	1.54510	0.00002	0.88000	0.92000	4.40000	0.00003
0.30900	0.75700	1.54550	0.00001	0.88000	0.92000	4.40130	0.00003
0.30900	0.75600	1.54680	0.00003	0.88100	0.92000	4.40290	0.00003
0.30900	0.75600	1.54740	0.00001	0.88100	0.92100	4.40400	0.00002
0.31000	0.75600	1.54830	0.00002	0.88100	0.92100	4.40550	0.00003
0.31000	0.75600	1.54880	0.00001	0.88200	0.92100	4.40750	0.00004
0.31000	0.75600	1.55010	0.00003	0.88200	0.92200	4.40870	0.00002
0.31000	0.75500	1.55130	0.00003	0.88200	0.92300	4.41030	0.00003
0.31000	0.75600	1.55240	0.00002	0.88300	0.92200	4.41270	0.00005
0.31100	0.75600	1.55350	0.00002	0.88300	0.92200	4.41400	0.00003
0.31100	0.75400	1.55530	0.00004	0.88300	0.92200	4.41610	0.00004
0.31100	0.75400	1.55680	0.00003	0.88400	0.92200	4.41790	0.00004
0.31100	0.75500	1.55740	0.00001	0.88400	0.92100	4.41980	0.00004
0.31200	0.75500	1.55890	0.00003	0.88400	0.92000	4.42080	0.00002
0.31200	0.75400	1.56030	0.00003	0.88500	0.91900	4.42290	0.00004
0.31200	0.75400	1.56110	0.00002	0.88500	0.91700	4.42470	0.00004
0.31200	0.75400	1.56170	0.00001	0.88500	0.91500	4.42640	0.00004
0.31200	0.75500	1.56210	0.00001	0.88600	0.91400	4.42810	0.00004
0.31200	0.75500	1.56220	0.00000	0.88600	0.91400	4.42970	0.00003
0.31300	0.75500	1.56280	0.00001	0.88600	0.91300	4.43150	0.00004
0.31300	0.75400	1.56340	0.00001	0.88700	0.91200	4.43300	0.00003
0.31300	0.75500	1.56400	0.00001	0.88700	0.91100	4.43450	0.00003
0.31300	0.75400	1.56470	0.00001	0.88700	0.91100	4.43560	0.00002
0.31300	0.75500	1.56440	- 0.00001	0.88800	0.91000	4.43820	0.00005
0.31300	0.75400	1.56550	0.00002	0.88800	0.91000	4.43960	0.00003
0.31300	0.75400	1.56660	0.00002	0.88800	0.91400	4.44150	0.00004
0.31300	0.75400	1.56700	0.00001	0.88900	0.91400	4.44300	0.00003
0.31400	0.75300	1.56770	0.00001	0.88800	0.91700	4.44070	-

Appendix C: Shakedown Characteristics

							0.00005
0.31400	0.75300	1.56870	0.00002	0.88900	0.91600	4.44270	0.00004
0.31400	0.75200	1.56960	0.00002	0.88900	0.91500	4.44400	0.00003

16				18			
Permanent Deformation	Resilient Strain 10-3	Permanent strain10-3	Strain Rate	Permanent Deformation	Resilient Strain 10-3	Permanent strain10-3	Strain Rate
0.00000	1.00600	0.00000	0.00000	0.00000	0.92500	0.00000	0.00000
0.50400	1.18100	2.52000	0.05250	0.83600	1.28600	4.17780	0.04352
0.59200	1.16500	2.95750	0.00911	1.02400	1.29400	5.11810	0.00979
0.64200	1.15300	3.20980	0.00526	1.14600	1.28800	5.72780	0.00635
0.67800	1.15800	3.38860	0.00373	1.23900	1.28000	6.19300	0.00485
0.70600	1.14600	3.52930	0.00293	1.31300	1.27300	6.56340	0.00386
0.72800	1.14800	3.63840	0.00227	1.37400	1.26400	6.87220	0.00322
0.74600	1.14800	3.72840	0.00188	1.42400	1.26300	7.11820	0.00256
0.76100	1.14600	3.80580	0.00161	1.46300	1.25100	7.31610	0.00206
0.77200	1.15400	3.86210	0.00117	1.49500	1.24100	7.47360	0.00164
0.78400	1.15000	3.91810	0.00117	1.51800	1.23500	7.58820	0.00119
0.79300	1.15000	3.96580	0.00099	1.56300	1.30200	7.81740	0.00239
0.80200	1.14700	4.01030	0.00093	1.59800	1.26800	7.99240	0.00182
0.81000	1.14200	4.05210	0.00087	1.62700	1.26200	8.13550	0.00149
0.81800	1.13800	4.08870	0.00076	1.65200	1.25400	8.25960	0.00129
0.82500	1.13600	4.12310	0.00072	1.67400	1.25200	8.36890	0.00114
0.83100	1.13300	4.15510	0.00067	1.69400	1.25000	8.47200	0.00107
0.83700	1.12900	4.18360	0.00059	1.71300	1.24800	8.56670	0.00099
0.84200	1.12500	4.21060	0.00056	1.73100	1.24700	8.65590	0.00093
0.84700	1.12300	4.23530	0.00051	1.74800	1.24200	8.74040	0.00088
0.85200	1.12000	4.25840	0.00048	1.76300	1.23900	8.81660	0.00079
0.85600	1.11700	4.28020	0.00045	1.77800	1.23000	8.89010	0.00077
0.86000	1.11100	4.30090	0.00043	1.79000	1.22100	8.95180	0.00064

Appendix C: Shakedown Characteristics

0.86400	1.10800	4.31990	0.00040	1.80100	1.21000	9.00560	0.00056
0.86800	1.10500	4.33850	0.00039	1.81000	1.18800	9.05050	0.00047
0.87100	1.10200	4.35540	0.00035	1.82600	1.27100	9.12800	0.00081
0.87400	1.09900	4.37150	0.00034	1.83900	1.24000	9.19470	0.00069
0.87700	1.09800	4.38570	0.00030	1.85000	1.23500	9.25050	0.00058
0.88000	1.09700	4.39980	0.00029	1.86000	1.23000	9.30210	0.00054
0.88300	1.09600	4.41270	0.00027	1.87000	1.23000	9.34950	0.00049
0.88500	1.09500	4.42480	0.00025	1.87900	1.22700	9.39750	0.00050
0.88800	1.09100	4.43760	0.00027	1.88800	1.22700	9.44100	0.00045
0.89000	1.08900	4.44980	0.00025	1.89700	1.22800	9.48440	0.00045
0.89200	1.08100	4.46080	0.00023	1.90500	1.22400	9.52730	0.00045
0.89400	1.11600	4.47010	0.00019	1.91300	1.22600	9.56530	0.00040
0.89600	1.10300	4.48100	0.00023	1.92100	1.22100	9.60320	0.00039
0.89800	1.09900	4.48980	0.00018	1.92800	1.21700	9.63750	0.00036
0.89900	1.10000	4.49700	0.00015	1.93400	1.20900	9.66820	0.00032
0.90100	1.10100	4.50450	0.00016	1.93900	1.19900	9.69610	0.00029
0.90200	1.10200	4.51100	0.00014	1.94300	1.18500	9.71500	0.00020
0.90300	1.10600	4.51400	0.00006	1.95200	1.25800	9.76070	0.00048
0.90400	1.11100	4.51770	0.00008	1.96000	1.22600	9.79870	0.00040
0.90600	1.10500	4.52810	0.00022	1.96600	1.22000	9.82840	0.00031
0.90700	1.10500	4.53670	0.00018	1.97100	1.22000	9.85520	0.00028
0.90900	1.10300	4.54470	0.00017	1.97600	1.22000	9.87970	0.00026
0.91100	1.10200	4.55280	0.00017	1.98100	1.21800	9.90520	0.00027
0.91200	1.10000	4.56070	0.00016	1.98600	1.21500	9.93160	0.00027
0.91300	1.09900	4.56730	0.00014	1.99100	1.21700	9.95520	0.00025
0.91500	1.09700	4.57470	0.00015	1.99600	1.21800	9.97770	0.00023
0.91600	1.09600	4.58220	0.00016	2.00000	1.21500	10.00180	0.00025
0.91800	1.09300	4.58940	0.00015	2.00500	1.21200	10.02390	0.00023
0.91900	1.09100	4.59600	0.00014	2.01000	1.20200	10.04890	0.00026
0.92100	1.08800	4.60380	0.00016	2.01500	1.19000	10.07250	0.00025
0.92200	1.08600	4.61030	0.00014	2.01700	1.18300	10.08640	0.00014
0.92300	1.08300	4.61730	0.00015	2.02000	1.15600	10.09800	0.00012

Appendix C: Shakedown Characteristics

0.92500	1.08100	4.62360	0.00013	2.02500	1.23900	10.12460	0.00028
0.92600	1.07900	4.62960	0.00012	2.02900	1.21200	10.14670	0.00023
0.92700	1.07700	4.63560	0.00013	2.03300	1.20600	10.16590	0.00020
0.92800	1.07600	4.64150	0.00012	2.03600	1.20500	10.18080	0.00016
0.92900	1.07900	4.64610	0.00010	2.03900	1.20300	10.19720	0.00017
0.93000	1.07600	4.65170	0.00012	2.04200	1.20400	10.21180	0.00015
0.93100	1.07400	4.65690	0.00011	2.04500	1.20300	10.22660	0.00015
0.93200	1.07100	4.66190	0.00010	2.04800	1.20100	10.24230	0.00016
0.93400	1.06600	4.66770	0.00012	2.05100	1.20000	10.25700	0.00015
0.93400	1.08900	4.67130	0.00008	2.05400	1.19900	10.27090	0.00014
0.93500	1.08500	4.67520	0.00008	2.05700	1.19700	10.28350	0.00013
0.93600	1.07900	4.67870	0.00007	2.06000	1.19100	10.29800	0.00015
0.93600	1.08200	4.68240	0.00008	2.06200	1.18400	10.30890	0.00011
0.93700	1.08300	4.68410	0.00004	2.06400	1.17500	10.31970	0.00011
0.93700	1.08400	4.68610	0.00004	2.06600	1.14600	10.32820	0.00009
0.93700	1.09000	4.68550	- 0.00001	2.06800	1.23100	10.34240	0.00015
0.93800	1.09000	4.68850	0.00006	2.07200	1.20400	10.36130	0.00020
0.93800	1.08900	4.69210	0.00007	2.07400	1.19700	10.37250	0.00012
0.93900	1.08600	4.69710	0.00010	2.07700	1.19700	10.38260	0.00011
0.94000	1.08600	4.70080	0.00008	2.07900	1.19600	10.39260	0.00010
0.94100	1.08500	4.70540	0.00010	2.08100	1.19700	10.40270	0.00011
0.94200	1.08500	4.70890	0.00007	2.08300	1.19700	10.41300	0.00011
0.94300	1.08400	4.71320	0.00009	2.08500	1.19600	10.42350	0.00011
0.94300	1.08300	4.71700	0.00008	2.08700	1.19400	10.43420	0.00011
0.94400	1.08100	4.72050	0.00007	2.08900	1.19200	10.44460	0.00011
0.94500	1.08000	4.72490	0.00009	2.09100	1.18700	10.45280	0.00009
0.94600	1.07800	4.72840	0.00007	2.09300	1.18200	10.46270	0.00010
0.94700	1.07700	4.73250	0.00009	2.09400	1.17600	10.47190	0.00010
0.94800	1.07300	4.73770	0.00011	2.09600	1.14900	10.47930	0.00008
0.94800	1.07100	4.74170	0.00008	2.09800	1.20900	10.48850	0.00010
0.94900	1.06800	4.74670	0.00010	2.10000	1.20200	10.50250	0.00015

Appendix C: Shakedown Characteristics

0.95000	1.06600	4.74980	0.00006	2.10200	1.19300	10.51140	0.00009
0.95100	1.06500	4.75360	0.00008	2.10400	1.19000	10.52070	0.00010
0.95100	1.06600	4.75700	0.00007	2.10500	1.19100	10.52660	0.00006
0.95200	1.06700	4.76020	0.00007	2.10700	1.19100	10.53470	0.00008
0.95300	1.06500	4.76400	0.00008	2.10800	1.19000	10.54180	0.00007
0.95400	1.06300	4.76770	0.00008	2.11000	1.19100	10.55000	0.00009
0.95400	1.05700	4.77060	0.00006	2.11200	1.18900	10.55970	0.00010
0.95500	1.05500	4.77470	0.00009	2.11300	1.19000	10.56640	0.00007
0.95500	1.07400	4.77550	0.00002	2.11500	1.18800	10.57340	0.00007
0.95600	1.08400	4.77950	0.00008	2.11600	1.18400	10.58070	0.00008
0.95600	1.07200	4.78170	0.00005	2.11800	1.17600	10.59010	0.00010
0.95600	1.07400	4.78230	0.00001	2.11900	1.17000	10.59640	0.00007
0.95700	1.07600	4.78300	0.00001	2.12100	1.14600	10.60290	0.00007
0.95700	1.07600	4.78510	0.00004	2.12200	1.18900	10.60870	0.00006
0.95600	1.08200	4.78200	- 0.00006	2.12500	1.19900	10.62270	0.00015
0.95700	1.08000	4.78510	0.00006	2.12600	1.18500	10.63000	0.00008
0.95800	1.07900	4.78820	0.00006	2.12700	1.18500	10.63660	0.00007
0.95800	1.07700	4.79030	0.00004	2.12800	1.18200	10.64180	0.00005
0.95900	1.07600	4.79370	0.00007	2.13000	1.18200	10.64770	0.00006
0.95900	1.07600	4.79670	0.00006	2.13100	1.18200	10.65380	0.00006
0.96000	1.07300	4.80050	0.00008	2.13200	1.18300	10.65980	0.00006
0.96100	1.07400	4.80300	0.00005	2.13300	1.18300	10.66570	0.00006
0.96100	1.07300	4.80570	0.00006	2.13400	1.18400	10.67090	0.00005
0.96200	1.07100	4.80870	0.00006	2.13600	1.18100	10.67850	0.00008
0.96200	1.06900	4.81170	0.00006	2.13700	1.17800	10.68330	0.00005
0.96300	1.07000	4.81640	0.00010	2.13800	1.17000	10.69040	0.00007
0.96400	1.05900	4.82150	0.00011	2.13900	1.16500	10.69490	0.00005
0.96500	1.05800	4.82510	0.00007	2.14000	1.14500	10.70040	0.00006
0.96600	1.05600	4.82790	0.00006	2.14100	1.15300	10.70500	0.00005
0.96600	1.05700	4.83100	0.00006	2.14300	1.20800	10.71600	0.00011
0.96700	1.05800	4.83290	0.00004	2.14400	1.18200	10.72160	0.00006

Appendix C: Shakedown Characteristics

0.96700	1.05300	4.83650	0.00008	2.14600	1.17900	10.72870	0.00007
0.96800	1.04700	4.83900	0.00005	2.14600	1.17700	10.73220	0.00004
0.96800	1.04400	4.83880	0.00000	2.14700	1.17700	10.73620	0.00004
0.96900	1.04000	4.84450	0.00012	2.14800	1.17700	10.74100	0.00005
0.96900	1.04100	4.84730	0.00006	2.14900	1.17700	10.74650	0.00006
0.96900	1.08200	4.84670	- 0.00001	2.15000	1.18000	10.75080	0.00004
0.97000	1.07000	4.85060	0.00008	2.15100	1.17600	10.75660	0.00006
0.97000	1.07100	4.85200	0.00003	2.15200	1.17600	10.76150	0.00005
0.97000	1.07300	4.85230	0.00001	2.15300	1.17300	10.76550	0.00004
0.97100	1.07300	4.85330	0.00002	2.15400	1.16900	10.76940	0.00004
0.97000	1.07700	4.85110	- 0.00005	2.15500	1.16500	10.77400	0.00005
0.97000	1.07900	4.85240	0.00003	2.15600	1.15000	10.77960	0.00006
0.97100	1.07700	4.85420	0.00004	2.15600	1.12600	10.78250	0.00003
0.97100	1.07800	4.85660	0.00005	2.15800	1.20700	10.79130	0.00009
0.97200	1.07600	4.85880	0.00005	2.16000	1.17900	10.79880	0.00008
0.97200	1.07400	4.86160	0.00006	2.16100	1.17600	10.80360	0.00005
0.97300	1.07300	4.86440	0.00006	2.16100	1.17400	10.80710	0.00004
0.97300	1.07400	4.86600	0.00003	2.16200	1.17300	10.80990	0.00003
0.97400	1.07100	4.86900	0.00006	2.16300	1.17300	10.81450	0.00005
0.97400	1.07000	4.87150	0.00005	2.16400	1.17200	10.81940	0.00005
0.97500	1.06800	4.87360	0.00004	2.16500	1.17300	10.82280	0.00004
0.97500	1.06800	4.87560	0.00004	2.16600	1.17300	10.82780	0.00005
0.97600	1.06500	4.87790	0.00005	2.16600	1.17400	10.83200	0.00004
0.97700	1.06300	4.88300	0.00011	2.16700	1.17100	10.83690	0.00005
0.97700	1.05500	4.88680	0.00008	2.16800	1.16800	10.84110	0.00004
0.97800	1.05400	4.88990	0.00006	2.16900	1.16100	10.84520	0.00004
0.97900	1.05300	4.89280	0.00006	2.17000	1.15400	10.84880	0.00004
0.97900	1.05500	4.89490	0.00004	2.17100	1.12900	10.85270	0.00004
0.97900	1.05300	4.89740	0.00005	2.17200	1.19700	10.85810	0.00006
0.98000	1.05000	4.89950	0.00004	2.17300	1.17800	10.86600	0.00008

Appendix C: Shakedown Characteristics

0.98000	1.04700	4.90130	0.00004	2.17400	1.17300	10.87130	0.00006
0.98100	1.04200	4.90370	0.00005	2.17500	1.17100	10.87500	0.00004
0.98100	1.03800	4.90560	0.00004	2.17600	1.16900	10.87790	0.00003
0.98100	1.04000	4.90420	- 0.00003	2.17600	1.16900	10.88050	0.00003
0.98200	1.05900	4.90960	0.00011	2.17700	1.16800	10.88340	0.00003
0.98200	1.08700	4.91090	0.00003	2.17700	1.17000	10.88690	0.00004
0.98200	1.06100	4.91080	0.00000	2.17800	1.17100	10.89080	0.00004
0.98200	1.06200	4.91040	- 0.00001	2.17900	1.17100	10.89450	0.00004
0.98200	1.06400	4.90990	- 0.00001	2.18000	1.17000	10.89790	0.00004
0.98200	1.06500	4.90990	0.00000	2.18000	1.16600	10.90110	0.00003
0.98200	1.06700	4.90820	- 0.00004	2.18100	1.16000	10.90510	0.00004
0.98200	1.06700	4.90940	0.00002	2.18200	1.15200	10.90890	0.00004
0.98200	1.06800	4.91040	0.00002	2.18300	1.12800	10.91270	0.00004
0.98200	1.06600	4.91230	0.00004	2.18300	1.19500	10.91660	0.00004
0.98300	1.06700	4.91430	0.00004	2.18500	1.17600	10.92430	0.00008
0.98300	1.06800	4.91560	0.00003	2.18600	1.16800	10.92900	0.00005
0.98300	1.06700	4.91730	0.00004	2.18600	1.16900	10.93100	0.00002
0.98400	1.06600	4.91960	0.00005	2.18700	1.16800	10.93480	0.00004
0.98400	1.06300	4.92230	0.00006	2.18700	1.16600	10.93700	0.00002
0.98500	1.06300	4.92380	0.00003	2.18800	1.16800	10.93800	0.00001
0.98500	1.06200	4.92480	0.00002	2.18800	1.17000	10.93920	0.00001
0.98500	1.06100	4.92730	0.00005	2.18800	1.17200	10.94130	0.00002
0.98600	1.05800	4.92970	0.00005	2.18900	1.17100	10.94330	0.00002
0.98700	1.05400	4.93400	0.00009	2.18900	1.17000	10.94680	0.00004
0.98700	1.04700	4.93720	0.00007	2.19000	1.17100	10.94880	0.00002
0.98800	1.04300	4.94050	0.00007	2.19100	1.16500	10.95300	0.00004
0.98900	1.04200	4.94280	0.00005	2.19100	1.15800	10.95580	0.00003
0.98900	1.04100	4.94480	0.00004	2.19200	1.14200	10.95910	0.00003

Appendix C: Shakedown Characteristics

0.98900	1.03700	4.94650	0.00004	2.19200	1.16700	10.96190	0.00003
0.99000	1.03200	4.94880	0.00005	2.19400	1.19000	10.96960	0.00008
0.99000	1.07900	4.94990	0.00002	2.19500	1.17100	10.97490	0.00006
0.99000	1.06100	4.95230	0.00005	2.19600	1.17100	10.97850	0.00004
0.99100	1.06800	4.95290	0.00001	2.19600	1.17000	10.97970	0.00001
0.99000	1.05500	4.95210	- 0.00002	2.19700	1.16800	10.98310	0.00004
0.99000	1.05600	4.95200	0.00000	2.19700	1.16900	10.98530	0.00002
0.99000	1.05600	4.95140	- 0.00001	2.19800	1.16800	10.98790	0.00003
0.99000	1.05900	4.95020	- 0.00002	2.19800	1.17000	10.98920	0.00001

20				22			
Permanent Deformation	Resilient Strain 10-3	Permanent strain10-3	Strain Rate	Permanent Deformation	Resilient Strain 10-3	Permanent strain10-3	Strain Rate
0.00000	0.88000	0.00000	0.00000	0.00000	1.08000	0.00000	0.00000
0.50200	1.25400	2.51240	0.10468	0.49100	1.30700	2.45470	0.05114
0.62100	1.25000	3.10460	0.02468	0.61200	1.29800	3.05820	0.01257
0.69500	1.24800	3.47340	0.01537	0.68500	1.29100	3.42700	0.00768
0.74800	1.25000	3.74010	0.01111	0.73700	1.27500	3.68590	0.00539
0.79000	1.24700	3.95200	0.00883	0.77200	1.24700	3.85910	0.00361
0.82500	1.25100	4.12290	0.00712	0.79600	1.22000	3.97930	0.00250
0.85600	1.25500	4.27920	0.00651	0.81300	1.19500	4.06390	0.00176
0.88300	1.25200	4.41670	0.00573	0.82500	1.17000	4.12520	0.00128
0.90800	1.24700	4.53810	0.00506	0.83400	1.14700	4.16900	0.00091
0.92900	1.24100	4.64630	0.00451	0.84000	1.12500	4.20110	0.00067
0.94800	1.24000	4.74020	0.00391	0.84500	1.10500	4.22490	0.00050
0.96600	1.23100	4.82820	0.00367	0.84900	1.09000	4.24280	0.00037
0.98000	1.23300	4.89850	0.00293	0.85300	1.15000	4.26620	0.00049
0.99400	1.22400	4.96850	0.00292	0.86300	1.21900	4.31550	0.00103
1.00400	1.21500	5.02230	0.00224	0.88200	1.29200	4.41060	0.00198

Appendix C: Shakedown Characteristics

1.01500	1.19500	5.07560	0.00222	0.91300	1.34600	4.56690	0.00326
1.02100	1.17400	5.10400	0.00118	0.94500	1.34000	4.72580	0.00331
1.02900	1.17900	5.14250	0.00160	0.96900	1.33300	4.84440	0.00247
1.03500	1.16200	5.17400	0.00131	0.99000	1.33600	4.95130	0.00223
1.04000	1.17800	5.20050	0.00110	1.01000	1.33900	5.04790	0.00201
1.04400	1.17700	5.22230	0.00091	1.02900	1.33800	5.14250	0.00197
1.04900	1.16400	5.24530	0.00096	1.04600	1.33300	5.23240	0.00187
1.05300	1.15500	5.26310	0.00074	1.06300	1.33000	5.31580	0.00174
1.05600	1.14300	5.28080	0.00074	1.07900	1.32700	5.39320	0.00161
1.05900	1.13000	5.29720	0.00068	1.09300	1.32400	5.46590	0.00151
1.06200	1.11800	5.31080	0.00057	1.10600	1.32000	5.53180	0.00137
1.06400	1.10800	5.32180	0.00046	1.11900	1.31600	5.59260	0.00127
1.06600	1.09900	5.33230	0.00044	1.13000	1.31100	5.65100	0.00122
1.06800	1.12100	5.34190	0.00040	1.14100	1.30200	5.70430	0.00111
1.07100	1.15500	5.35540	0.00056	1.15000	1.29400	5.75210	0.00100
1.07500	1.19000	5.37480	0.00081	1.15900	1.28400	5.79530	0.00090
1.08100	1.22700	5.40480	0.00125	1.16600	1.26500	5.83040	0.00073
1.09000	1.25800	5.45060	0.00191	1.17200	1.24400	5.85810	0.00058
1.09900	1.28700	5.49740	0.00195	1.17600	1.22400	5.87910	0.00044
1.11000	1.29500	5.55230	0.00229	1.17900	1.20400	5.89570	0.00035
1.12100	1.28100	5.60310	0.00212	1.18200	1.18400	5.90900	0.00028
1.12900	1.27400	5.64480	0.00174	1.18400	1.16400	5.91960	0.00022
1.13600	1.27300	5.68110	0.00151	1.18600	1.14500	5.92790	0.00017
1.14300	1.27500	5.71550	0.00143	1.18700	1.12500	5.93500	0.00015
1.15000	1.27700	5.74930	0.00141	1.18800	1.10900	5.93970	0.00010
1.15700	1.27800	5.78260	0.00139	1.18900	1.16000	5.94480	0.00011
1.16300	1.28300	5.81440	0.00132	1.19100	1.22100	5.95720	0.00026
1.16900	1.28600	5.84620	0.00132	1.19600	1.28000	5.98090	0.00049
1.17500	1.28700	5.87640	0.00126	1.20400	1.32300	6.02160	0.00085
1.18200	1.28300	5.90930	0.00137	1.21300	1.32800	6.06540	0.00091
1.18800	1.28000	5.94170	0.00135	1.22000	1.31300	6.09990	0.00072
1.19500	1.27700	5.97410	0.00135	1.22600	1.31600	6.12990	0.00062

Appendix C: Shakedown Characteristics

1.20100	1.27400	6.00720	0.00138	1.23200	1.32000	6.15780	0.00058
1.20800	1.26900	6.04060	0.00139	1.23800	1.31600	6.19030	0.00068
1.21400	1.26700	6.07070	0.00125	1.24500	1.31300	6.22400	0.00070
1.22000	1.26400	6.09990	0.00122	1.25100	1.30900	6.25680	0.00068
1.22500	1.26300	6.12630	0.00110	1.25800	1.30700	6.28860	0.00066
1.23000	1.26600	6.14880	0.00094	1.26400	1.30400	6.31850	0.00062
1.23500	1.26500	6.17440	0.00107	1.27000	1.29900	6.34830	0.00062
1.23900	1.26600	6.19580	0.00089	1.27500	1.29500	6.37540	0.00056
1.24400	1.26400	6.21890	0.00096	1.28000	1.29100	6.39970	0.00051
1.24800	1.26500	6.24120	0.00093	1.28500	1.28400	6.42300	0.00049
1.25200	1.26300	6.26180	0.00086	1.28900	1.27700	6.44530	0.00046
1.25700	1.26200	6.28350	0.00090	1.29300	1.26700	6.46470	0.00040
1.26100	1.26100	6.30400	0.00085	1.29600	1.25000	6.48060	0.00033
1.26500	1.25600	6.32370	0.00082	1.29900	1.23100	6.49340	0.00027
1.26900	1.25300	6.34410	0.00085	1.30100	1.21200	6.50340	0.00021
1.27200	1.25100	6.36100	0.00070	1.30200	1.19400	6.51130	0.00016
1.27600	1.24600	6.38090	0.00083	1.30400	1.17500	6.51790	0.00014
1.28000	1.24200	6.39940	0.00077	1.30500	1.15700	6.52400	0.00013
1.28300	1.24000	6.41640	0.00071	1.30600	1.13900	6.52830	0.00009
1.28600	1.23900	6.43150	0.00063	1.30700	1.12000	6.53260	0.00009
1.28900	1.23700	6.44660	0.00063	1.30700	1.10200	6.53620	0.00007
1.29200	1.23300	6.46150	0.00062	1.30800	1.14300	6.53880	0.00005
1.29500	1.23000	6.47450	0.00054	1.30900	1.20100	6.54410	0.00011
1.29700	1.22700	6.48700	0.00052	1.31100	1.25600	6.55530	0.00023
1.30000	1.22300	6.49870	0.00049	1.31500	1.30400	6.57430	0.00040
1.30200	1.21600	6.51010	0.00048	1.31900	1.31900	6.59520	0.00044
1.30400	1.20800	6.51860	0.00035	1.32200	1.30600	6.61040	0.00032
1.30600	1.19800	6.52800	0.00039	1.32500	1.30500	6.62340	0.00027
1.30700	1.18800	6.53570	0.00032	1.32700	1.30800	6.63730	0.00029
1.30800	1.17900	6.54170	0.00025	1.33000	1.30600	6.65150	0.00030
1.31000	1.16800	6.54880	0.00030	1.33400	1.30400	6.67000	0.00039
1.31100	1.15900	6.55380	0.00021	1.33800	1.30100	6.68830	0.00038

Appendix C: Shakedown Characteristics

1.31200	1.15100	6.55840	0.00019	1.34100	1.29900	6.70600	0.00037
1.31200	1.14200	6.56230	0.00016	1.34500	1.29600	6.72300	0.00035
1.31300	1.13400	6.56650	0.00017	1.34800	1.29200	6.73920	0.00034
1.31400	1.12600	6.57070	0.00017	1.35100	1.28800	6.75510	0.00033
1.31500	1.12400	6.57430	0.00015	1.35400	1.28300	6.76980	0.00031
1.31600	1.13200	6.57770	0.00014	1.35700	1.27700	6.78420	0.00030
1.31600	1.16000	6.58120	0.00015	1.35900	1.27000	6.79660	0.00026
1.31700	1.19100	6.58670	0.00023	1.36200	1.26200	6.80780	0.00023
1.31800	1.22300	6.59240	0.00024	1.36300	1.24400	6.81740	0.00020
1.32000	1.24100	6.60250	0.00042	1.36500	1.22700	6.82440	0.00015
1.32300	1.26300	6.61470	0.00051	1.36600	1.20800	6.83060	0.00013
1.32600	1.27800	6.63070	0.00067	1.36700	1.19000	6.83620	0.00012
1.32900	1.27700	6.64470	0.00058	1.36800	1.17200	6.84030	0.00009
1.33200	1.26600	6.65880	0.00059	1.36900	1.15500	6.84500	0.00010
1.33400	1.25700	6.67090	0.00050	1.37000	1.13800	6.84810	0.00006
1.33600	1.25400	6.68070	0.00041	1.37000	1.12100	6.84920	0.00002
1.33800	1.25600	6.68800	0.00030	1.37100	1.10200	6.85320	0.00008
1.33900	1.25800	6.69430	0.00026	1.37100	1.13700	6.85310	0.00000
1.34000	1.25900	6.70150	0.00030	1.37100	1.19500	6.85560	0.00005
1.34200	1.26200	6.70840	0.00029	1.37200	1.24800	6.86220	0.00014
1.34300	1.26500	6.71570	0.00030	1.37500	1.29600	6.87390	0.00024
1.34500	1.26600	6.72390	0.00034	1.37800	1.31400	6.88900	0.00031
1.34700	1.26300	6.73490	0.00046	1.37900	1.30100	6.89680	0.00016
1.34900	1.26000	6.74710	0.00051	1.38100	1.29800	6.90340	0.00014
1.35200	1.25700	6.75950	0.00052	1.38200	1.30300	6.90860	0.00011
1.35400	1.25300	6.77250	0.00054	1.38400	1.30100	6.91780	0.00019
1.35700	1.25100	6.78480	0.00051	1.38600	1.29800	6.93010	0.00026
1.35900	1.25000	6.79620	0.00047	1.38800	1.29600	6.94230	0.00025
1.36100	1.24800	6.80720	0.00046	1.39100	1.29400	6.95340	0.00023
1.36300	1.24700	6.81710	0.00041	1.39300	1.29000	6.96590	0.00026
1.36500	1.24600	6.82670	0.00040	1.39600	1.28500	6.97880	0.00027
1.36700	1.24700	6.83460	0.00033	1.39800	1.27900	6.99070	0.00025

Appendix C: Shakedown Characteristics

1.36800	1.24700	6.84180	0.00030	1.40000	1.27300	7.00170	0.00023
1.37000	1.24800	6.84970	0.00033	1.40200	1.26700	7.01180	0.00021
1.37300	1.24000	6.86450	0.00062	1.40400	1.26000	7.02150	0.00020
1.37500	1.23900	6.87350	0.00038	1.40600	1.25200	7.02950	0.00017
1.37600	1.23900	6.88080	0.00030	1.40700	1.23400	7.03620	0.00014
1.37800	1.23600	6.88960	0.00037	1.40800	1.21600	7.04160	0.00011
1.38000	1.23300	6.89900	0.00039	1.40900	1.19700	7.04650	0.00010
1.38100	1.23000	6.90750	0.00035	1.41000	1.17900	7.05010	0.00008
1.38300	1.22600	6.91550	0.00033	1.41100	1.16100	7.05340	0.00007
1.38500	1.22400	6.92250	0.00029	1.41100	1.14300	7.05640	0.00006
1.38600	1.22400	6.92900	0.00027	1.41200	1.12400	7.05840	0.00004
1.38700	1.22200	6.93580	0.00028	1.41200	1.10600	7.06110	0.00006
1.38800	1.22200	6.94240	0.00027	1.41300	1.09100	7.06290	0.00004
1.39000	1.21800	6.94980	0.00031	1.41300	1.14500	7.06360	0.00001
1.39100	1.21600	6.95540	0.00023	1.41300	1.20200	7.06650	0.00006
1.39200	1.21100	6.96190	0.00027	1.41400	1.25300	7.07230	0.00012
1.39400	1.20500	6.96760	0.00024	1.41600	1.29500	7.08130	0.00019
1.39500	1.19800	6.97290	0.00022	1.41800	1.30000	7.08870	0.00015
1.39500	1.18900	6.97730	0.00018	1.41800	1.28700	7.09230	0.00007
1.39600	1.17900	6.98100	0.00015	1.41900	1.28800	7.09500	0.00006
1.39700	1.16900	6.98470	0.00015	1.41900	1.29100	7.09670	0.00004
1.39800	1.15800	6.98810	0.00014	1.42100	1.28800	7.10340	0.00014
1.39800	1.14900	6.99120	0.00013	1.42200	1.28700	7.11180	0.00018
1.39900	1.13900	6.99420	0.00013	1.42400	1.28500	7.12110	0.00019
1.39900	1.12900	6.99720	0.00012	1.42600	1.28200	7.12930	0.00017
1.40000	1.12000	6.99930	0.00009	1.42800	1.28300	7.13870	0.00020
1.40000	1.11100	7.00140	0.00009	1.42900	1.27700	7.14680	0.00017
1.40100	1.10100	7.00360	0.00009	1.43100	1.27600	7.15430	0.00016
1.40100	1.09200	7.00530	0.00007	1.43200	1.26700	7.16190	0.00016
1.40100	1.08800	7.00650	0.00005	1.43400	1.26500	7.16860	0.00014
1.40100	1.11500	7.00660	0.00000	1.43500	1.25500	7.17480	0.00013
1.40200	1.14600	7.00770	0.00005	1.43600	1.24500	7.18100	0.00013

Appendix C: Shakedown Characteristics

1.40200	1.17500	7.00980	0.00009	1.43700	1.22600	7.18560	0.00010
1.40300	1.20800	7.01300	0.00013	1.43800	1.20900	7.18940	0.00008
1.40300	1.23200	7.01750	0.00019	1.43900	1.19100	7.19340	0.00008
1.40500	1.25200	7.02370	0.00026	1.43900	1.17400	7.19600	0.00005
1.40700	1.26300	7.03290	0.00038	1.44000	1.15600	7.19900	0.00006
1.40800	1.25500	7.04240	0.00040	1.44000	1.13900	7.20120	0.00005
1.40800	1.25100	7.04160	- 0.00003	1.44100	1.12100	7.20320	0.00004
1.40900	1.24600	7.04580	0.00017	1.44100	1.10300	7.20520	0.00004
1.41000	1.24400	7.04850	0.00011	1.44100	1.08900	7.20690	0.00004
1.41100	1.24300	7.05400	0.00023	1.44100	1.14200	7.20700	0.00000
1.41200	1.24100	7.06020	0.00026	1.44200	1.19900	7.20930	0.00005
1.41300	1.24100	7.06500	0.00020	1.44300	1.25500	7.21280	0.00007
1.41400	1.24100	7.06800	0.00012	1.44400	1.29100	7.21950	0.00014
1.41400	1.24300	7.07020	0.00009	1.44500	1.29700	7.22390	0.00009
1.41500	1.24300	7.07460	0.00018	1.44500	1.28500	7.22500	0.00002
1.41600	1.24000	7.08120	0.00027	1.44500	1.28800	7.22580	0.00002
1.41800	1.23900	7.08760	0.00027	1.44500	1.28800	7.22720	0.00003
1.41900	1.23600	7.09560	0.00033	1.44600	1.28700	7.23080	0.00008
1.42000	1.23600	7.10140	0.00024	1.44800	1.28500	7.23760	0.00014
1.42200	1.23400	7.10810	0.00028	1.44900	1.28200	7.24470	0.00015
1.42300	1.23100	7.11650	0.00035	1.45100	1.27900	7.25270	0.00017
1.42500	1.22900	7.12400	0.00031	1.45200	1.27600	7.25980	0.00015
1.42600	1.23000	7.12860	0.00019	1.45300	1.27100	7.26590	0.00013
1.42700	1.22600	7.13540	0.00028	1.45400	1.26800	7.27200	0.00013
1.42800	1.22600	7.14090	0.00023	1.45600	1.26300	7.27780	0.00012
1.42900	1.22300	7.14740	0.00027	1.45700	1.25700	7.28350	0.00012
1.43100	1.21800	7.15570	0.00035	1.45800	1.25300	7.28840	0.00010
1.43200	1.21600	7.16150	0.00024	1.45900	1.24300	7.29350	0.00011
1.43300	1.21400	7.16650	0.00021	1.45900	1.22700	7.29710	0.00008
1.43400	1.21100	7.17180	0.00022	1.46000	1.21000	7.30050	0.00007
1.43500	1.20900	7.17570	0.00016	1.46100	1.18700	7.30340	0.00006

Appendix C: Shakedown Characteristics

1.43600	1.20700	7.18040	0.00020	1.46100	1.16900	7.30550	0.00004
1.43700	1.20600	7.18490	0.00019	1.46200	1.15100	7.30770	0.00005
1.43800	1.20300	7.18880	0.00016	1.46200	1.13100	7.31020	0.00005
1.43900	1.20100	7.19370	0.00020	1.46200	1.11400	7.31170	0.00003
1.44000	1.20100	7.19750	0.00016	1.46300	1.09600	7.31320	0.00003
1.44000	1.20000	7.20030	0.00012	1.46300	1.07900	7.31450	0.00003
1.44100	1.19800	7.20450	0.00017	1.46300	1.12700	7.31460	0.00000
1.44200	1.19400	7.20870	0.00017	1.46300	1.18400	7.31640	0.00004
1.44200	1.18900	7.21210	0.00014	1.46400	1.24000	7.31860	0.00005

24				26			
Permanent Deformation	Resilient Strain 10-3	Permanent strain10-3	Strain Rate	Permanent Deformation	Resilient Strain 10-3	Permanent strain10-3	Strain Rate
0.00000	1.24700	0.00000	0.00000	0.00000	1.15600	0.00000	0.00000
0.73500	1.49100	3.67270	0.07651	0.25100	1.39500	1.25450	0.41817
0.93000	1.47700	4.65140	0.02039	0.37700	1.43800	1.88410	0.20987
1.05600	1.45700	5.28070	0.01311	0.47600	1.44300	2.37810	0.16467
1.15000	1.45400	5.74880	0.00975	0.55300	1.44100	2.76630	0.12940
1.22600	1.45100	6.12950	0.00793	0.61400	1.43500	3.06960	0.10110
1.28700	1.43500	6.43580	0.00638	0.66500	1.42600	3.32380	0.08473
1.33600	1.41200	6.68130	0.00511	0.70700	1.41400	3.53400	0.07007
1.37200	1.38000	6.86220	0.00377	0.74400	1.40800	3.72120	0.06240
1.39800	1.35100	6.99190	0.00270	0.77600	1.39900	3.88120	0.05333
1.41700	1.32300	7.08680	0.00198	0.80500	1.39200	4.02600	0.04827
1.43100	1.29700	7.15410	0.00140	0.83100	1.38600	4.15510	0.04303
1.44100	1.27000	7.20530	0.00107	0.85400	1.38700	4.26970	0.03820
1.44900	1.24400	7.24380	0.00080	0.87600	1.38100	4.38110	0.03713
1.45400	1.22100	7.27190	0.00059	0.89600	1.37700	4.48230	0.03373
1.45900	1.19800	7.29360	0.00045	0.91600	1.37400	4.57800	0.03190
1.46200	1.17600	7.31100	0.00036	0.93300	1.37100	4.66730	0.02977
1.46500	1.15600	7.32410	0.00027	0.95000	1.36700	4.75160	0.02810

Appendix C: Shakedown Characteristics

1.46700	1.13500	7.33450	0.00022	0.96600	1.36500	4.83040	0.02627
1.46900	1.12400	7.34300	0.00018	0.98100	1.36000	4.90650	0.02537
1.47100	1.18100	7.35310	0.00021	0.99600	1.35600	4.97780	0.02377
1.47500	1.24600	7.37440	0.00044	1.01000	1.35000	5.04940	0.02387
1.48400	1.26400	7.41990	0.00095	1.02300	1.34900	5.11360	0.02140
1.49600	1.37500	7.47850	0.00122	1.03500	1.34700	5.17370	0.02003
1.52000	1.44100	7.59800	0.00249	1.04700	1.34300	5.23340	0.01990
1.55300	1.45700	7.76380	0.00345	1.05800	1.33900	5.29070	0.01910
1.58500	1.46400	7.92510	0.00336	1.06900	1.33500	5.34540	0.01823
1.61300	1.46200	8.06590	0.00293	1.08000	1.33200	5.39820	0.01760
1.63900	1.45400	8.19650	0.00272	1.09000	1.33000	5.44910	0.01697
1.66400	1.44300	8.31850	0.00254	1.10000	1.32600	5.49840	0.01643
1.68600	1.42800	8.43080	0.00234	1.10900	1.32300	5.54640	0.01600
1.70800	1.42000	8.53770	0.00223	1.11800	1.32100	5.59240	0.01533
1.72600	1.42300	8.62960	0.00191	1.12700	1.31300	5.63620	0.01460
1.74300	1.42000	8.71400	0.00176	1.13500	1.31300	5.67730	0.01370
1.75700	1.39800	8.78550	0.00149	1.14400	1.31000	5.71940	0.01403
1.76800	1.37200	8.84080	0.00115	1.15200	1.30600	5.75900	0.01320
1.77700	1.34600	8.88290	0.00088	1.15900	1.30000	5.79740	0.01280
1.78300	1.32100	8.91530	0.00067	1.16700	1.29700	5.83480	0.01247
1.78800	1.29600	8.93950	0.00050	1.17400	1.29200	5.87030	0.01183
1.79200	1.27500	8.95830	0.00039	1.18100	1.28900	5.90500	0.01157
1.79500	1.25400	8.97320	0.00031	1.18800	1.28600	5.93900	0.01133
1.79700	1.23100	8.98550	0.00026	1.19400	1.28500	5.97110	0.01070
1.79900	1.21000	8.99480	0.00019	1.20000	1.28300	6.00230	0.01040
1.80100	1.18900	9.00280	0.00017	1.20700	1.28000	6.03320	0.01030
1.80200	1.16700	9.00930	0.00014	1.21300	1.27800	6.06340	0.01007
1.80300	1.14700	9.01480	0.00011	1.21800	1.27700	6.09090	0.00917
1.80400	1.12700	9.01910	0.00009	1.22400	1.27500	6.11920	0.00943
1.80500	1.16200	9.02290	0.00008	1.22900	1.27400	6.14730	0.00937
1.80600	1.22400	9.02910	0.00013	1.23500	1.27300	6.17340	0.00870
1.80800	1.28000	9.04080	0.00024	1.24000	1.27100	6.19920	0.00860

Appendix C: Shakedown Characteristics

1.81200	1.33600	9.06220	0.00045	1.24500	1.26900	6.22410	0.00830
1.82000	1.39400	9.09890	0.00076	1.25000	1.26600	6.24840	0.00810
1.83100	1.43600	9.15650	0.00120	1.25400	1.26400	6.27230	0.00797
1.84500	1.43500	9.22380	0.00140	1.25900	1.26100	6.29550	0.00773
1.85600	1.44700	9.28170	0.00121	1.26400	1.26000	6.31800	0.00750
1.86700	1.43600	9.33730	0.00116	1.26800	1.25700	6.33910	0.00703
1.87800	1.42500	9.39100	0.00112	1.27200	1.25400	6.36100	0.00730
1.88900	1.41400	9.44350	0.00109	1.27600	1.25300	6.38110	0.00670
1.89900	1.39800	9.49320	0.00104	1.28000	1.24900	6.40100	0.00663
1.90800	1.39700	9.53960	0.00097	1.28400	1.24700	6.42060	0.00653
1.91600	1.39100	9.58210	0.00089	1.28800	1.24400	6.43900	0.00613
1.92400	1.37800	9.61920	0.00077	1.29200	1.24300	6.45770	0.00623
1.93000	1.35500	9.64930	0.00063	1.29500	1.24000	6.47580	0.00603
1.93400	1.33400	9.67120	0.00046	1.29900	1.23700	6.49370	0.00597
1.93800	1.31200	9.68930	0.00038	1.30200	1.23600	6.51090	0.00573
1.94100	1.28700	9.70390	0.00030	1.30500	1.23300	6.52720	0.00543
1.94300	1.26600	9.71510	0.00023	1.30900	1.23000	6.54360	0.00547
1.94500	1.24500	9.72410	0.00019	1.31200	1.22800	6.55980	0.00540
1.94600	1.22300	9.73170	0.00016	1.31500	1.22600	6.57530	0.00517
1.94800	1.20700	9.73780	0.00013	1.31800	1.22400	6.59050	0.00507
1.94900	1.18900	9.74370	0.00012	1.32100	1.22400	6.60510	0.00487
1.95000	1.16800	9.74820	0.00009	1.32400	1.22100	6.61940	0.00477
1.95000	1.14900	9.75170	0.00007	1.32700	1.21800	6.63340	0.00467
1.95100	1.12800	9.75530	0.00007	1.32900	1.21600	6.64720	0.00460
1.95200	1.13000	9.75760	0.00005	1.33200	1.21500	6.66080	0.00453
1.95200	1.19700	9.75970	0.00004	1.33500	1.21100	6.67430	0.00450
1.95300	1.25200	9.76500	0.00011	1.33700	1.20900	6.68710	0.00427
1.95500	1.30000	9.77560	0.00022	1.34000	1.20800	6.69930	0.00407
1.95800	1.35500	9.79190	0.00034	1.34200	1.20500	6.71210	0.00427
1.96400	1.40200	9.81910	0.00057	1.34500	1.20300	6.72380	0.00390
1.97100	1.41500	9.85540	0.00076	1.34700	1.20100	6.73530	0.00383
1.97700	1.42200	9.88650	0.00065	1.34900	1.19900	6.74680	0.00383

Appendix C: Shakedown Characteristics

1.98300	1.41500	9.91510	0.00060	1.35200	1.19700	6.75790	0.00370
1.98900	1.40900	9.94670	0.00066	1.35400	1.19500	6.76850	0.00353
1.99500	1.39700	9.97650	0.00062	1.35600	1.19200	6.77950	0.00367
2.00100	1.38600	10.00500	0.00059	1.35800	1.19200	6.78980	0.00343
2.00700	1.37900	10.03480	0.00062	1.36000	1.19000	6.79980	0.00333
2.01200	1.37600	10.06050	0.00054	1.36200	1.18700	6.81020	0.00347
2.01700	1.37000	10.08320	0.00047	1.36400	1.18500	6.81970	0.00317
2.02000	1.34900	10.10180	0.00039	1.36600	1.18200	6.82850	0.00293
2.02300	1.32800	10.11680	0.00031	1.36700	1.18100	6.83740	0.00297
2.02600	1.30400	10.12840	0.00024	1.36900	1.17900	6.84570	0.00277
2.02800	1.28300	10.13820	0.00020	1.37100	1.17700	6.85490	0.00307
2.02900	1.26200	10.14600	0.00016	1.37300	1.17500	6.86320	0.00277
2.03000	1.24100	10.15230	0.00013	1.37400	1.17300	6.87210	0.00297
2.03200	1.22000	10.15750	0.00011	1.37600	1.17200	6.88000	0.00263
2.03300	1.20000	10.16270	0.00011	1.37800	1.17000	6.88800	0.00267
2.03300	1.18100	10.16630	0.00007	1.37900	1.17100	6.89560	0.00253
2.03400	1.16300	10.16940	0.00006	1.38100	1.17000	6.90360	0.00267
2.03500	1.14400	10.17260	0.00007	1.38200	1.16900	6.91070	0.00237
2.03500	1.12300	10.17560	0.00006	1.38400	1.16800	6.91840	0.00257
2.03600	1.11400	10.17790	0.00005	1.38500	1.16600	6.92520	0.00227
2.03600	1.17200	10.17960	0.00004	1.38600	1.16400	6.93210	0.00230
2.03600	1.23200	10.18250	0.00006	1.38800	1.16000	6.93940	0.00243
2.03800	1.28700	10.18810	0.00012	1.38900	1.15900	6.94600	0.00220
2.04000	1.33700	10.19810	0.00021	1.39000	1.15600	6.95200	0.00200
2.04300	1.38300	10.21410	0.00033	1.39200	1.15400	6.95830	0.00210
2.04700	1.40400	10.23640	0.00046	1.39300	1.15200	6.96470	0.00213
2.05100	1.40600	10.25620	0.00041	1.39400	1.14900	6.97120	0.00217
2.05500	1.40800	10.27270	0.00034	1.39500	1.14600	6.97620	0.00167
2.05800	1.40100	10.29160	0.00039	1.39600	1.14500	6.98160	0.00180
2.06200	1.39100	10.31110	0.00041	1.39700	1.14600	6.98690	0.00177
2.06600	1.37700	10.33070	0.00041	1.39900	1.14400	6.99270	0.00193
2.07000	1.36900	10.34940	0.00039	1.40000	1.13800	6.99830	0.00187

Appendix C: Shakedown Characteristics

2.07400	1.36800	10.36760	0.00038	1.40100	1.13900	7.00280	0.00150
2.07700	1.36500	10.38340	0.00033	1.40200	1.13600	7.00860	0.00193
2.07900	1.34400	10.39630	0.00027	1.40300	1.13600	7.01430	0.00190
2.08100	1.32200	10.40680	0.00022	1.40400	1.13400	7.01910	0.00160
2.08300	1.30000	10.41600	0.00019	1.40500	1.13200	7.02470	0.00187
2.08500	1.28000	10.42330	0.00015	1.40600	1.12900	7.02990	0.00173
2.08600	1.25900	10.42890	0.00012	1.40700	1.12800	7.03440	0.00150
2.08700	1.24000	10.43360	0.00010	1.40800	1.12600	7.03940	0.00167
2.08800	1.22100	10.43770	0.00009	1.40900	1.12400	7.04420	0.00160
2.08800	1.20200	10.44110	0.00007	1.40900	1.12500	7.04700	0.00093
2.08900	1.18300	10.44470	0.00008	1.41000	1.12400	7.05050	0.00117
2.09000	1.16400	10.44770	0.00006	1.41100	1.12300	7.05490	0.00147
2.09000	1.14200	10.45080	0.00006	1.41200	1.12100	7.05900	0.00137
2.09100	1.12300	10.45370	0.00006	1.41300	1.11900	7.06330	0.00143
2.09100	1.10400	10.45530	0.00003	1.41400	1.11800	7.06760	0.00143
2.09100	1.14700	10.45610	0.00002	1.41400	1.11700	7.07120	0.00120
2.09100	1.20800	10.45720	0.00002	1.41500	1.11500	7.07520	0.00133
2.09200	1.26200	10.45980	0.00005	1.41600	1.11400	7.07870	0.00117
2.09300	1.31300	10.46470	0.00010	1.41600	1.11100	7.08210	0.00113
2.09500	1.36400	10.47490	0.00021	1.41700	1.11100	7.08600	0.00130
2.09800	1.39400	10.48900	0.00029	1.41800	1.10900	7.08950	0.00117
2.10000	1.39200	10.50210	0.00027	1.41900	1.10700	7.09320	0.00123
2.10200	1.40100	10.51240	0.00021	1.41900	1.10600	7.09640	0.00107
2.10500	1.39100	10.52300	0.00022	1.42000	1.10500	7.09940	0.00100
2.10700	1.38400	10.53700	0.00029	1.42100	1.10300	7.10320	0.00127
2.11000	1.37300	10.55010	0.00027	1.42100	1.10100	7.10580	0.00087
2.11300	1.36100	10.56420	0.00029	1.42200	1.09900	7.10910	0.00110
2.11500	1.35600	10.57650	0.00026	1.42300	1.09600	7.11260	0.00117
2.11800	1.35500	10.58760	0.00023	1.42300	1.09600	7.11540	0.00093
2.11900	1.34000	10.59750	0.00021	1.42400	1.09400	7.11880	0.00113
2.12100	1.31900	10.60590	0.00017	1.42400	1.09300	7.12070	0.00063
2.12200	1.30000	10.61190	0.00013	1.42500	1.09100	7.12360	0.00097

Appendix C: Shakedown Characteristics

2.12400	1.28000	10.61760	0.00012	1.42500	1.09000	7.12670	0.00103
2.12400	1.26000	10.62230	0.00010	1.42600	1.08700	7.12950	0.00093
2.12500	1.24100	10.62640	0.00009	1.42600	1.08700	7.13200	0.00083
2.12600	1.22000	10.62970	0.00007	1.42700	1.08600	7.13450	0.00083
2.12700	1.20200	10.63290	0.00007	1.42700	1.08500	7.13730	0.00093
2.12700	1.18100	10.63610	0.00007	1.42800	1.08400	7.13960	0.00077
2.12800	1.16100	10.63890	0.00006	1.42800	1.08200	7.14190	0.00077
2.12800	1.14200	10.64160	0.00006	1.42900	1.08000	7.14460	0.00090
2.12900	1.12400	10.64340	0.00004	1.42900	1.08000	7.14720	0.00087
2.12900	1.10600	10.64550	0.00004	1.43000	1.08200	7.14920	0.00067
2.12900	1.12900	10.64650	0.00002	1.43000	1.08500	7.15140	0.00073
2.12900	1.18900	10.64690	0.00001	1.43100	1.08700	7.15420	0.00093
2.13000	1.24500	10.64790	0.00002	1.43100	1.08900	7.15620	0.00067
2.13000	1.29600	10.65020	0.00005	1.43200	1.09200	7.15880	0.00087
2.13100	1.34300	10.65660	0.00013	1.43200	1.09600	7.16190	0.00103
2.13300	1.38000	10.66630	0.00020	1.43300	1.09900	7.16500	0.00103
2.13500	1.37900	10.67610	0.00020	1.43400	1.10400	7.16790	0.00097
2.13600	1.38900	10.68210	0.00013	1.43400	1.10700	7.17100	0.00103
2.13800	1.38300	10.68860	0.00014	1.43500	1.11100	7.17410	0.00103
2.14000	1.37700	10.69790	0.00019	1.43500	1.11400	7.17740	0.00110
2.14200	1.36600	10.70760	0.00020	1.43600	1.11900	7.18100	0.00120
2.14300	1.35600	10.71730	0.00020	1.43700	1.12400	7.18520	0.00140
2.14500	1.35000	10.72660	0.00019	1.43800	1.12900	7.18950	0.00143
2.14700	1.34600	10.73480	0.00017	1.43900	1.13300	7.19320	0.00123
2.14800	1.33600	10.74230	0.00016	1.44000	1.13700	7.19810	0.00163
2.15000	1.31800	10.74800	0.00012	1.44100	1.14100	7.20290	0.00160
2.15100	1.29800	10.75350	0.00011	1.44100	1.15100	7.20750	0.00153
2.15200	1.27900	10.75800	0.00009	1.44300	1.16300	7.21450	0.00233
2.15200	1.25900	10.76140	0.00007	1.44400	1.16800	7.22100	0.00217
2.15300	1.23900	10.76490	0.00007	1.44500	1.17300	7.22700	0.00200
2.15400	1.21900	10.76790	0.00006	1.44700	1.17700	7.23420	0.00240
2.15400	1.20200	10.77060	0.00006	1.44800	1.18100	7.24190	0.00257

Appendix C: Shakedown Characteristics

2.15500	1.18200	10.77330	0.00006	1.45000	1.18400	7.25000	0.00270
2.15500	1.16300	10.77550	0.00005	1.45200	1.18800	7.25800	0.00267
2.15600	1.14300	10.77810	0.00005	1.45300	1.19500	7.26490	0.00230
2.15600	1.12600	10.78040	0.00005	1.45500	1.20000	7.27340	0.00283
2.15600	1.10700	10.78250	0.00004	1.45600	1.20500	7.28230	0.00297
2.15700	1.08900	10.78380	0.00003	1.45800	1.21000	7.29110	0.00293

APPENDIX D: FINITE ELEMENT ANALYSIS

APPENDIX D

(Finite Element Analysis)

Pavement Diagrams

conventional diagram							
				thickness	modulus (MPa)	poisson	unit weight
Asphalt	Surfacing	Isotropic	Isotropic	30	3000	0.3	2400
HCTCRB	Base	Anisototic	Isotropic	150	750	0.35	2120
CLS	Subbase	Anisototic	Isotropic	200	350	0.35	1820
PS	Subgrade	Anisototic	Isotropic	1000	150	0.35	1800

[illegible]

Appendix D: Finite Element Analysis

AC												
Thickness	Sxx (kPa)		Syy (kPa)		Sxy (kPa)		Exx (micro strain)		Eyy (micro strain)		Exy (micro strain)	
	top	bottom	top	bottom	top	bottom	top	bottom	top	bottom	top	bottom
30	-1.76E+03	-6.71E+02	-7.49E+02	-7.37E+02	-9.15E-01	-8.69E+00	-4.36E+02	-1.08E+02	1.37E+00	-1.36E+02	-7.93E-01	-7.53E+00
40	-1.88E+03	-4.30E+02	-7.48E+02	-7.05E+02	-2.27E+00	-1.18E+01	-5.53E+02	-7.29E+01	-6.09E+01	-1.92E+02	-1.97E+00	-1.03E+01
60	-1.84E+03	8.13E+01	-7.47E+02	-6.27E+02	-3.24E+00	-1.54E+01	-5.37E+02	8.98E+01	-6.54E+01	-2.17E+02	-2.81E+00	-1.34E+01
90	-1.70E+03	4.18E+02	-7.47E+02	-5.14E+02	-2.71E+00	-1.56E+01	-4.91E+02	1.91E+02	-7.94E+01	-2.13E+02	-2.35E+00	-1.35E+01
120	-1.56E+03	5.36E+02	-7.48E+02	-4.24E+02	-1.98E+00	-1.31E+01	-4.46E+02	2.21E+02	-9.33E+01	-1.95E+02	-1.72E+00	-1.14E+01
150	-1.45E+03	5.66E+02	-7.49E+02	-3.56E+02	-1.50E+00	-1.02E+01	-4.07E+02	2.24E+02	-1.05E+02	-1.75E+02	-1.30E+00	-8.88E+00
180	-1.35E+03	5.61E+02	-7.49E+02	-3.04E+02	-1.21E+00	-8.33E+00	-3.77E+02	2.17E+02	-1.14E+02	-1.57E+02	-1.05E+00	-7.22E+00
210	-1.28E+03	5.41E+02	-7.49E+02	-2.64E+02	-1.02E+00	-6.45E+00	-3.52E+02	2.07E+02	-1.22E+02	-1.42E+02	-8.87E-01	-5.59E+00
240	-1.22E+03	5.15E+02	-7.49E+02	-2.33E+02	-9.05E-01	-5.31E+00	-3.31E+02	1.95E+02	-1.28E+02	-1.29E+02	-7.85E-01	-4.60E+00
270	-1.17E+03	4.88E+02	-7.49E+02	-2.08E+02	-8.26E-01	-4.24E+00	-3.14E+02	1.83E+02	-1.33E+02	-1.18E+02	-7.16E-01	-3.68E+00
300	-1.12E+03	4.61E+02	-7.49E+02	-1.88E+02	-7.72E-01	-3.56E+00	-2.99E+02	1.73E+02	-1.38E+02	-1.09E+02	-6.69E-01	-3.09E+00

Appendix D: Finite Element Analysis

AC				
Thickness	top		bottom	
	q	p	q	p
30	7.49E+02	2.30E+02	7.37E+02	6.93E+02
40	7.48E+02	2.23E+02	7.05E+02	5.22E+02
60	7.47E+02	2.09E+02	6.27E+02	1.55E+02
90	7.47E+02	1.89E+02	5.14E+02	1.08E+02
120	7.48E+02	1.69E+02	4.24E+02	2.16E+02
150	7.49E+02	1.50E+02	3.56E+02	2.59E+02
180	7.49E+02	1.30E+02	3.04E+02	2.72E+02
210	7.49E+02	1.10E+02	2.64E+02	2.72E+02
240	7.49E+02	8.97E+01	2.33E+02	2.66E+02
270	7.49E+02	6.98E+01	2.08E+02	2.56E+02
300	7.49E+02	4.98E+01	1.88E+02	2.45E+02

Appendix D: Finite Element Analysis

Base												
Thickness	Sxx (kPa)		Syy (kPa)		Sxy (kPa)		Exx (micro strain)		Eyy (micro strain)		Exy (micro strain)	
	top	bottom	top	bottom	top	bottom	top	bottom	top	bottom	top	bottom
30	-3.74E+02	2.65E+02	-7.18E+02	-3.39E+02	-1.11E+01	-7.88E+00	1.42E+01	5.24E+02	-6.04E+02	-5.64E+02	-4.00E+01	-2.84E+01
40	-2.12E+02	2.39E+02	-6.79E+02	-3.16E+02	-1.55E+01	-7.01E+00	3.46E+01	4.67E+02	-8.06E+02	-5.33E+02	-5.59E+01	-2.52E+01
60	-8.54E+01	2.31E+02	-5.97E+02	-2.84E+02	-1.57E+01	-5.77E+00	1.65E+02	4.41E+02	-7.56E+02	-4.87E+02	-5.65E+01	-2.08E+01
90	7.24E+00	2.14E+02	-4.86E+02	-2.46E+02	-1.34E+01	-4.44E+00	2.36E+02	3.99E+02	-6.51E+02	-4.27E+02	-4.82E+01	-1.60E+01
120	4.79E+01	1.95E+02	-4.01E+02	-2.16E+02	-1.06E+01	-3.40E+00	2.51E+02	3.61E+02	-5.57E+02	-3.79E+02	-3.80E+01	-1.22E+01
150	6.62E+01	1.78E+02	-3.38E+02	-1.93E+02	-8.54E+00	-2.74E+00	2.46E+02	3.28E+02	-4.81E+02	-3.41E+02	-3.08E+01	-9.86E+00
180	7.38E+01	1.63E+02	-2.90E+02	-1.75E+02	-6.60E+00	-2.20E+00	2.33E+02	2.99E+02	-4.21E+02	-3.10E+02	-2.38E+01	-7.93E+00
210	7.61E+01	1.50E+02	-2.53E+02	-1.61E+02	-5.41E+00	-1.83E+00	2.19E+02	2.75E+02	-3.72E+02	-2.84E+02	-1.95E+01	-6.60E+00
240	7.57E+01	1.38E+02	-2.24E+02	-1.49E+02	-4.31E+00	-1.53E+00	2.05E+02	2.53E+02	-3.34E+02	-2.62E+02	-1.55E+01	-5.49E+00
270	7.38E+01	1.27E+02	-2.01E+02	-1.38E+02	-3.60E+00	-1.30E+00	1.92E+02	2.34E+02	-3.02E+02	-2.44E+02	-1.30E+01	-4.69E+00
300	7.12E+01	1.17E+02	-1.82E+02	-1.30E+02	-2.96E+00	-1.11E+00	1.80E+02	2.17E+02	-2.76E+02	-2.28E+02	-1.07E+01	-4.00E+00

Appendix D: Finite Element Analysis

Base				
Thickness	top		bottom	
	q	p	q	p
30	7.18E+02	4.89E+02	3.39E+02	6.40E+01
40	6.79E+02	3.67E+02	3.16E+02	5.41E+01
60	5.97E+02	2.56E+02	2.84E+02	5.96E+01
90	4.86E+02	1.57E+02	2.46E+02	6.06E+01
120	4.01E+02	1.02E+02	2.16E+02	5.81E+01
150	3.38E+02	6.84E+01	1.93E+02	5.45E+01
180	2.90E+02	4.73E+01	1.75E+02	5.04E+01
210	2.53E+02	3.35E+01	1.61E+02	4.63E+01
240	2.24E+02	2.41E+01	1.49E+02	4.23E+01
270	2.01E+02	1.76E+01	1.38E+02	3.85E+01
300	1.82E+02	1.31E+01	1.30E+02	3.49E+01

Appendix D: Finite Element Analysis

Various thickness of base course												
			Trial 1	Trial 2	Trial 3	Trial 4	Trial 5	Trial 6	Trial 7	Trial 8	Trial 9	Trial 10
			thickness	thickness	thickness	thickness	thickness	thickness	thickness	thickness	thickness	thickness
Surfacing	Isotropic	Isotropic	30	30	30	30	30	30	30	30	30	30
Base	Anisototic	Isotropic	175	200	225	250	275	300	325	350	375	400
Subbase	Anisototic	Isotropic	200	200	200	200	200	200	200	200	200	200
Subgrade	Anisototic	Isotropic	1000	1000	1000	1000	1000	1000	1000	1000	1000	1000

AC												
Thickness	Sxx (kPa)		Syy (kPa)		Sxy (kPa)		Exx (micro strain)		Eyy (micro strain)		Exy (micro strain)	
	top	bottom	top	bottom	top	bottom	top	bottom	top	bottom	top	bottom
150	-1.76E+03	-6.71E+02	-7.49E+02	-7.37E+02	-9.15E-01	-8.69E+00	-4.36E+02	-1.08E+02	1.37E+00	-1.36E+02	-7.93E-01	-7.53E+00
175	-1.84E+03	-8.40E+02	-7.49E+02	-7.35E+02	-1.02E+00	-9.22E+00	-5.40E+02	-2.06E+02	-6.53E+01	-1.61E+02	-8.87E-01	-7.99E+00
200	-1.80E+03	-8.31E+02	-7.49E+02	-7.36E+02	-9.30E-01	-8.87E+00	-5.27E+02	-2.03E+02	-6.93E+01	-1.62E+02	-8.06E-01	-7.69E+00
225	-1.77E+03	-8.20E+02	-7.49E+02	-7.37E+02	-8.60E-01	-8.60E+00	-5.15E+02	-2.00E+02	-7.26E+01	-1.64E+02	-7.45E-01	-7.45E+00
250	-1.74E+03	-8.09E+02	-7.49E+02	-7.38E+02	-8.08E-01	-8.40E+00	-5.06E+02	-1.96E+02	-7.55E+01	-1.65E+02	-7.00E-01	-7.28E+00
275	-1.72E+03	-7.98E+02	-7.49E+02	-7.38E+02	-7.69E-01	-8.24E+00	-4.97E+02	-1.92E+02	-7.81E+01	-1.66E+02	-6.66E-01	-7.14E+00
300	-1.69E+03	-7.87E+02	-7.49E+02	-7.38E+02	-7.38E-01	-8.11E+00	-4.90E+02	-1.88E+02	-8.03E+01	-1.67E+02	-6.40E-01	-7.03E+00
325	-1.67E+03	-7.76E+02	-7.49E+02	-7.39E+02	-7.15E-01	-8.02E+00	-4.83E+02	-1.85E+02	-8.23E+01	-1.69E+02	-6.20E-01	-6.95E+00
350	-1.66E+03	-7.66E+02	-7.49E+02	-7.39E+02	-6.97E-01	-7.94E+00	-4.77E+02	-1.82E+02	-8.41E+01	-1.70E+02	-6.04E-01	-6.88E+00
375	-1.64E+03	-7.57E+02	-7.49E+02	-7.39E+02	-6.82E-01	-7.87E+00	-4.72E+02	-1.78E+02	-8.57E+01	-1.71E+02	-5.91E-01	-6.82E+00
400	-1.63E+03	-7.48E+02	-7.49E+02	-7.39E+02	-6.70E-01	-7.82E+00	-4.67E+02	-1.75E+02	-8.71E+01	-1.72E+02	-5.80E-01	-6.78E+00

Appendix D: Finite Element Analysis

Base												
Thickness	Sxx (kPa)		Syy (kPa)		Sxy (kPa)		Exx (micro strain)		Eyy (micro strain)		Exy (micro strain)	
	top	bottom	top	bottom	top	bottom	top	bottom	top	bottom	top	bottom
150	-3.74E+02	2.65E+02	-7.18E+02	-3.39E+02	-1.11E+01	-7.88E+00	1.42E+01	5.24E+02	-6.04E+02	-5.64E+02	-4.00E+01	-2.84E+01
175	-3.14E+02	2.29E+02	-7.15E+02	-3.02E+02	-1.16E+01	-6.50E+00	-8.44E+01	4.47E+02	-8.07E+02	-5.09E+02	-4.18E+01	-2.34E+01
200	-3.15E+02	2.18E+02	-7.17E+02	-2.75E+02	-1.12E+01	-5.43E+00	-8.48E+01	4.19E+02	-8.09E+02	-4.68E+02	-4.03E+01	-1.96E+01
225	-3.14E+02	2.07E+02	-7.18E+02	-2.52E+02	-1.09E+01	-4.62E+00	-8.32E+01	3.93E+02	-8.11E+02	-4.32E+02	-3.93E+01	-1.66E+01
250	-3.14E+02	1.96E+02	-7.19E+02	-2.33E+02	-1.07E+01	-3.99E+00	-8.24E+01	3.70E+02	-8.13E+02	-4.01E+02	-3.84E+01	-1.44E+01
275	-3.12E+02	1.85E+02	-7.20E+02	-2.16E+02	-1.05E+01	-3.44E+00	-7.98E+01	3.48E+02	-8.14E+02	-3.75E+02	-3.78E+01	-1.24E+01
300	-3.11E+02	1.76E+02	-7.21E+02	-2.02E+02	-1.03E+01	-2.96E+00	-7.82E+01	3.29E+02	-8.16E+02	-3.52E+02	-3.72E+01	-1.07E+01
325	-3.09E+02	1.67E+02	-7.21E+02	-1.90E+02	-1.02E+01	-2.59E+00	-7.53E+01	3.11E+02	-8.17E+02	-3.31E+02	-3.69E+01	-9.34E+00
350	-3.08E+02	1.59E+02	-7.21E+02	-1.79E+02	-1.01E+01	-2.30E+00	-7.35E+01	2.95E+02	-8.18E+02	-3.13E+02	-3.64E+01	-8.27E+00
375	-3.06E+02	1.51E+02	-7.22E+02	-1.70E+02	-1.00E+01	-2.02E+00	-7.16E+01	2.81E+02	-8.20E+02	-2.97E+02	-3.61E+01	-7.29E+00
400	-3.04E+02	1.44E+02	-7.22E+02	-1.62E+02	-9.98E+00	-1.81E+00	-6.88E+01	2.67E+02	-8.21E+02	-2.83E+02	-3.59E+01	-6.50E+00

Appendix D: Finite Element Analysis

Base				
Thickness	top		bottom	
	q	p	q	p
150	7.18E+02	4.89E+02	3.39E+02	6.40E+01
175	7.15E+02	4.47E+02	3.02E+02	5.23E+01
200	7.17E+02	4.49E+02	2.75E+02	5.39E+01
225	7.18E+02	4.48E+02	2.52E+02	5.37E+01
250	7.19E+02	4.49E+02	2.33E+02	5.31E+01
275	7.20E+02	4.48E+02	2.16E+02	5.16E+01
300	7.21E+02	4.47E+02	2.02E+02	5.00E+01
325	7.21E+02	4.46E+02	1.90E+02	4.80E+01
350	7.21E+02	4.46E+02	1.79E+02	4.61E+01
375	7.22E+02	4.45E+02	1.70E+02	4.41E+01
400	7.22E+02	4.44E+02	1.62E+02	4.20E+01

Appendix D: Finite Element Analysis

Various stiffness of AC												
			Trial 1	Trial 2	Trial 3	Trial 4	Trial 5	Trial 6	Trial 7	Trial 8	Trial 9	Trial 10
			modulus (MPa)	modulus (MPa)	modulus (MPa)	modulus (MPa)	modulus (MPa)	modulus (MPa)	modulus (MPa)	modulus (MPa)	modulus (MPa)	modulus (MPa)
Surfacing	Isotropic	Isotropic	1000	1500	2000	2500	3000	3500	4000	4500	5000	5500
Base	Anisotropic	Isotropic	750	750	750	750	750	750	750	750	750	750
Subbase	Anisotropic	Isotropic	350	350	350	350	350	350	350	350	350	350
Subgrade	Anisotropic	Isotropic	150	150	150	150	150	150	150	150	150	150

AC												
Modulus	Sxx (kPa)		Syy (kPa)		Sxy (kPa)		Exx (micro strain)		Eyy (micro strain)		Exy (micro strain)	
	top	bottom	top	bottom	top	bottom	top	bottom	top	bottom	top	bottom
750	-8.71E+02	-6.13E+02	-7.49E+02	-7.42E+02	-7.74E-01	-5.35E+00	-6.67E+02	-3.58E+02	-4.56E+02	-5.81E+02	-2.68E+00	-1.85E+01
1000	-1.01E+03	-6.57E+02	-7.49E+02	-7.41E+02	-7.52E-01	-5.91E+00	-6.22E+02	-3.09E+02	-2.90E+02	-4.18E+02	-1.96E+00	-1.54E+01
1500	-1.23E+03	-7.03E+02	-7.49E+02	-7.40E+02	-7.26E-01	-6.81E+00	-5.54E+02	-2.34E+02	-1.34E+02	-2.66E+02	-1.26E+00	-1.18E+01
2000	-1.43E+03	-7.13E+02	-7.49E+02	-7.39E+02	-7.43E-01	-7.53E+00	-5.04E+02	-1.80E+02	-6.23E+01	-1.97E+02	-9.66E-01	-9.79E+00
2500	-1.60E+03	-7.00E+02	-7.49E+02	-7.38E+02	-8.08E-01	-8.14E+00	-4.66E+02	-1.40E+02	-2.29E+01	-1.59E+02	-8.40E-01	-8.47E+00
3000	-1.76E+03	-6.71E+02	-7.49E+02	-7.37E+02	-9.15E-01	-8.69E+00	-4.36E+02	-1.08E+02	1.37E+00	-1.36E+02	-7.93E-01	-7.53E+00
3500	-1.90E+03	-6.30E+02	-7.49E+02	-7.35E+02	-1.06E+00	-9.18E+00	-4.12E+02	-8.19E+01	1.74E+01	-1.21E+02	-7.87E-01	-6.82E+00
4000	-2.04E+03	-5.81E+02	-7.49E+02	-7.34E+02	-1.23E+00	-9.65E+00	-3.91E+02	-6.06E+01	2.86E+01	-1.10E+02	-8.03E-01	-6.27E+00
4500	-2.17E+03	-5.26E+02	-7.49E+02	-7.32E+02	-1.43E+00	-1.01E+01	-3.74E+02	-4.28E+01	3.66E+01	-1.03E+02	-8.29E-01	-5.83E+00
5000	-2.29E+03	-4.65E+02	-7.48E+02	-7.31E+02	-1.65E+00	-1.05E+01	-3.59E+02	-2.77E+01	4.26E+01	-9.67E+01	-8.60E-01	-5.47E+00
5500	-2.41E+03	-4.02E+02	-7.48E+02	-7.29E+02	-1.89E+00	-1.09E+01	-3.46E+02	-1.48E+01	4.72E+01	-9.21E+01	-8.94E-01	-5.16E+00

Appendix D: Finite Element Analysis

Base												
Modulus	Sxx (kPa)		Syy (kPa)		Sxy (kPa)		Exx (micro strain)		Eyy (micro strain)		Exy (micro strain)	
	top	bottom	top	bottom	top	bottom	top	bottom	top	bottom	top	bottom
750	-5.87E+02	2.45E+02	-7.31E+02	-3.67E+02	-5.66E+00	-8.67E+00	-2.26E+02	5.18E+02	-4.86E+02	-5.84E+02	-2.04E+01	-3.12E+01
1000	-5.45E+02	2.49E+02	-7.29E+02	-3.61E+02	-6.67E+00	-8.51E+00	-1.78E+02	5.19E+02	-5.10E+02	-5.80E+02	-2.40E+01	-3.06E+01
1500	-4.82E+02	2.54E+02	-7.25E+02	-3.53E+02	-8.26E+00	-8.28E+00	-1.07E+02	5.20E+02	-5.45E+02	-5.73E+02	-2.97E+01	-2.98E+01
2000	-4.36E+02	2.59E+02	-7.23E+02	-3.47E+02	-9.45E+00	-8.11E+00	-5.51E+01	5.21E+02	-5.71E+02	-5.69E+02	-3.40E+01	-2.92E+01
2500	-4.02E+02	2.62E+02	-7.20E+02	-3.43E+02	-1.04E+01	-7.98E+00	-1.62E+01	5.23E+02	-5.89E+02	-5.66E+02	-3.74E+01	-2.87E+01
3000	-3.74E+02	2.65E+02	-7.18E+02	-3.39E+02	-1.11E+01	-7.88E+00	1.42E+01	5.24E+02	-6.04E+02	-5.64E+02	-4.00E+01	-2.84E+01
3500	-3.52E+02	2.68E+02	-7.15E+02	-3.36E+02	-1.17E+01	-7.79E+00	3.87E+01	5.25E+02	-6.15E+02	-5.62E+02	-4.22E+01	-2.80E+01
4000	-3.34E+02	2.70E+02	-7.13E+02	-3.33E+02	-1.22E+01	-7.71E+00	5.88E+01	5.26E+02	-6.24E+02	-5.60E+02	-4.40E+01	-2.78E+01
4500	-3.18E+02	2.72E+02	-7.10E+02	-3.31E+02	-1.26E+01	-7.64E+00	7.56E+01	5.27E+02	-6.31E+02	-5.59E+02	-4.55E+01	-2.75E+01
5000	-3.05E+02	2.73E+02	-7.08E+02	-3.29E+02	-1.30E+01	-7.58E+00	8.97E+01	5.27E+02	-6.36E+02	-5.57E+02	-4.67E+01	-2.73E+01
5500	-2.93E+02	2.75E+02	-7.06E+02	-3.27E+02	-1.33E+01	-7.52E+00	1.02E+02	5.27E+02	-6.41E+02	-5.56E+02	-4.78E+01	-2.71E+01

Appendix D: Finite Element Analysis

Base				
Modulus	top		bottom	
	q	p	q	p
750	7.31E+02	6.35E+02	3.67E+02	4.13E+01
1000	7.29E+02	6.06E+02	3.61E+02	4.52E+01
1500	7.25E+02	5.63E+02	3.53E+02	5.16E+01
2000	7.23E+02	5.32E+02	3.47E+02	5.67E+01
2500	7.20E+02	5.08E+02	3.43E+02	6.07E+01
3000	7.18E+02	4.89E+02	3.39E+02	6.40E+01
3500	7.15E+02	4.73E+02	3.36E+02	6.67E+01
4000	7.13E+02	4.60E+02	3.33E+02	6.90E+01
4500	7.10E+02	4.49E+02	3.31E+02	7.10E+01
5000	7.08E+02	4.39E+02	3.29E+02	7.26E+01
5500	7.06E+02	4.31E+02	3.27E+02	7.41E+01

Appendix D: Finite Element Analysis

Various stiffness of base course												
			Trial 1	Trial 2	Trial 3	Trial 4	Trial 5	Trial 6	Trial 7	Trial 8	Trial 9	Trial 10
			modulus (MPa)	modulus (MPa)	modulus (MPa)	modulus (MPa)	modulus (MPa)	modulus (MPa)	modulus (MPa)	modulus (MPa)	modulus (MPa)	modulus (MPa)
Surfacing	Isotropic	Isotropic	3000	3000	3000	3000	3000	3000	3000	3000	3000	3000
Base	Anisotropic	Isotropic	1000	1500	2000	2500	3000	3500	4000	4500	5000	5500
Subbase	Anisotropic	Isotropic	350	350	350	350	350	350	350	350	350	350
Subgrade	Anisotropic	Isotropic	150	150	150	150	150	150	150	150	150	150

AC												
Modulus	Sxx (kPa)		Syy (kPa)		Sxy (kPa)		Exx (micro strain)		Eyy (micro strain)		Exy (micro strain)	
	top	bottom	top	bottom	top	bottom	top	bottom	top	bottom	top	bottom
350	-1.98E+03	-2.76E+01	-7.49E+02	-7.34E+02	-1.59E+00	-9.05E+00	-5.03E+02	8.70E+01	3.01E+01	-2.19E+02	-1.38E+00	-7.84E+00
750	-1.76E+03	-6.71E+02	-7.49E+02	-7.37E+02	-9.15E-01	-8.69E+00	-4.36E+02	-1.08E+02	1.37E+00	-1.36E+02	-7.93E-01	-7.53E+00
1000	-1.71E+03	-8.29E+02	-7.49E+02	-7.36E+02	-9.81E-01	-8.69E+00	-4.22E+02	-1.56E+02	-4.75E+00	-1.16E+02	-8.50E-01	-7.53E+00
1500	-1.65E+03	-9.83E+02	-7.49E+02	-7.35E+02	-1.16E+00	-8.63E+00	-4.03E+02	-2.03E+02	-1.27E+01	-9.52E+01	-1.01E+00	-7.48E+00
2000	-1.60E+03	-1.05E+03	-7.49E+02	-7.34E+02	-1.28E+00	-8.46E+00	-3.88E+02	-2.22E+02	-1.92E+01	-8.67E+01	-1.11E+00	-7.33E+00
2500	-1.55E+03	-1.07E+03	-7.49E+02	-7.34E+02	-1.35E+00	-8.25E+00	-3.74E+02	-2.30E+02	-2.51E+01	-8.32E+01	-1.17E+00	-7.15E+00
3000	-1.51E+03	-1.08E+03	-7.49E+02	-7.34E+02	-1.39E+00	-8.02E+00	-3.61E+02	-2.33E+02	-3.07E+01	-8.22E+01	-1.20E+00	-6.95E+00
3500	-1.47E+03	-1.08E+03	-7.49E+02	-7.35E+02	-1.40E+00	-7.80E+00	-3.49E+02	-2.32E+02	-3.58E+01	-8.24E+01	-1.22E+00	-6.76E+00
4000	-1.43E+03	-1.07E+03	-7.49E+02	-7.35E+02	-1.41E+00	-7.59E+00	-3.38E+02	-2.30E+02	-4.06E+01	-8.35E+01	-1.22E+00	-6.57E+00
4500	-1.40E+03	-1.06E+03	-7.49E+02	-7.35E+02	-1.41E+00	-7.38E+00	-3.27E+02	-2.27E+02	-4.51E+01	-8.49E+01	-1.22E+00	-6.40E+00
5000	-1.37E+03	-1.05E+03	-7.49E+02	-7.36E+02	-1.40E+00	-7.19E+00	-3.18E+02	-2.23E+02	-4.93E+01	-8.65E+01	-1.21E+00	-6.23E+00
5500	-1.34E+03	-1.04E+03	-7.49E+02	-7.36E+02	-1.39E+00	-7.01E+00	-3.09E+02	-2.19E+02	-5.32E+01	-8.83E+01	-1.20E+00	-6.08E+00

Appendix D: Finite Element Analysis

Base												
Modulus	Sxx (kPa)		Syy (kPa)		Sxy (kPa)		Exx (micro strain)		Eyy (micro strain)		Exy (micro strain)	
	top	bottom	top	bottom	top	bottom	top	bottom	top	bottom	top	bottom
350	-2.68E+02	2.31E+01	-7.14E+02	-3.84E+02	-1.10E+01	-8.55E+00	2.93E+02	5.76E+02	-1.43E+03	-9.93E+02	-8.46E+01	-6.60E+01
750	-3.74E+02	2.65E+02	-7.18E+02	-3.39E+02	-1.11E+01	-7.88E+00	1.42E+01	5.24E+02	-6.04E+02	-5.64E+02	-4.00E+01	-2.84E+01
1000	-4.47E+02	3.88E+02	-7.17E+02	-3.21E+02	-1.09E+01	-7.51E+00	-5.37E+01	4.92E+02	-4.18E+02	-4.65E+02	-2.95E+01	-2.03E+01
1500	-5.94E+02	5.93E+02	-7.17E+02	-2.97E+02	-1.05E+01	-6.96E+00	-1.22E+02	4.41E+02	-2.32E+02	-3.61E+02	-1.88E+01	-1.25E+01
2000	-7.33E+02	7.66E+02	-7.17E+02	-2.80E+02	-9.98E+00	-6.59E+00	-1.53E+02	4.02E+02	-1.41E+02	-3.04E+02	-1.35E+01	-8.89E+00
2500	-8.65E+02	9.16E+02	-7.17E+02	-2.67E+02	-9.55E+00	-6.32E+00	-1.68E+02	3.72E+02	-8.82E+01	-2.67E+02	-1.03E+01	-6.82E+00
3000	-9.88E+02	1.05E+03	-7.18E+02	-2.56E+02	-9.17E+00	-6.11E+00	-1.76E+02	3.48E+02	-5.43E+01	-2.40E+02	-8.25E+00	-5.50E+00
3500	-1.10E+03	1.17E+03	-7.19E+02	-2.48E+02	-8.83E+00	-5.94E+00	-1.80E+02	3.27E+02	-3.12E+01	-2.20E+02	-6.81E+00	-4.59E+00
4000	-1.21E+03	1.28E+03	-7.20E+02	-2.40E+02	-8.52E+00	-5.81E+00	-1.81E+02	3.10E+02	-1.47E+01	-2.04E+02	-5.75E+00	-3.92E+00
4500	-1.31E+03	1.39E+03	-7.20E+02	-2.34E+02	-8.25E+00	-5.70E+00	-1.81E+02	2.95E+02	-2.52E+00	-1.91E+02	-4.95E+00	-3.42E+00
5000	-1.41E+03	1.49E+03	-7.21E+02	-2.28E+02	-8.00E+00	-5.61E+00	-1.79E+02	2.82E+02	6.68E+00	-1.80E+02	-4.32E+00	-3.03E+00
5500	-1.50E+03	1.58E+03	-7.22E+02	-2.23E+02	-7.77E+00	-5.52E+00	-1.77E+02	2.71E+02	1.38E+01	-1.71E+02	-3.82E+00	-2.71E+00

Appendix D: Finite Element Analysis

Base				
Modulus	top		bottom	
	q	p	q	p
350	7.14E+02	4.16E+02	3.84E+02	1.13E+02
750	7.18E+02	4.89E+02	3.39E+02	6.40E+01
1000	7.17E+02	5.37E+02	3.21E+02	1.51E+02
1500	7.17E+02	6.35E+02	2.97E+02	2.97E+02
2000	7.17E+02	7.28E+02	2.80E+02	4.17E+02
2500	7.17E+02	8.16E+02	2.67E+02	5.22E+02
3000	7.18E+02	8.98E+02	2.56E+02	6.15E+02
3500	7.19E+02	9.75E+02	2.48E+02	6.99E+02
4000	7.20E+02	1.05E+03	2.40E+02	7.76E+02
4500	7.20E+02	1.12E+03	2.34E+02	8.48E+02
5000	7.21E+02	1.18E+03	2.28E+02	9.14E+02
5500	7.22E+02	1.24E+03	2.23E+02	9.77E+02